FIT CONDITION AND FIT-UP BEHAVIOR – IMPACT ON DESIGN AND CONSTRUCTION OF STEEL I-GIRDER BRIDGES

A Dissertation
Presented to
The Academic Faculty

by

Thanh Van Nguyen

In Partial Fulfillment
of the Requirements for the Degree
Doctor of Philosophy in the
School of Civil and Environmental Engineering

Georgia Institute of Technology
December 2015

FIT CONDITION AND FIT-UP BEHAVIOR – IMPACT ON DESIGN AND CONSTRUCTION OF STEEL I-GIRDER BRIDGES

Approved by:

Dr. Donald W. White, Advisor
School of Civil and Environmental Engineering
Georgia Institute of Technology

Dr. Abdul-Hamid Zureick
School of Civil and Environmental Engineering
Georgia Institute of Technology

Dr. Barry Goodno
School of Civil and Environmental Engineering
Georgia Institute of Technology

Dr. Richard W. Neu
School of Mechanical Engineering
Georgia Institute of Technology

Dr. Kenneth M. Will
School of Civil and Environmental Engineering
Georgia Institute of Technology

Date Approved: October 20, 2015

To my parents and my older brother

ACKNOWLEDGEMENTS

I would like to dedicate this dissertation to my parents and my older brother. Their support and endurance throughout the years were the ultimate motivation for me in completing my doctoral studies.

I would like to express my deepest gratitude for the guidance provided by my advisor, Professor Donald W. White. I was fortunately picked up by him in the last semester of my Master's studies and given an opportunity to begin my doctoral studies. His patience and guidance were truly appreciated. I hold the utmost respect for and look up to Professor White.

I would also like to extend my thanks to the other members of my doctoral committee, including Professors Abdul Zureick, Kenneth Will, Barry Goodno, and Richard Neu. Their comments and suggestions were greatly helpful.

The financial support of the National Cooperative Highway Research Program is gratefully acknowledged. Similarly, I would like to thank Mike Grubb from M.A. Grubb & Associates, Domenic Coletti and Dr. Brandon Chavel from HDR Engineering, Inc., for the valuable input provided in various topics of this thesis.

Lastly, I would like to thank Dr. Cagri Ozgur and Dr. Andres Sanchez for their prior research and contributions related to this research.

TABLE OF CONTENTS

LIST OF TABLES

Page

LIST OF FIGURES

Page

SUMMARY

Tighter constraints on right-of-way, particularly in urban environments, have led to a significantly increased utilization of skewed and/or curved alignments in highway bridge construction. Due to the relative ease of configuring the structure to the roadway geometry, steel I-girder bridges are often a preferred option for these cases. However, challenging attributes of the framing arrangements combined with current practices for detailing of the cross-frames and erecting these bridges can result in problems during and after construction.

This research studies various factors and methods and proposes improved design, detailing and erection guidelines to facilitate the fit-up of skewed and/or curved steel I-girder bridges. Substantial progress has been made in answering many of the questions associated with this research in prior NCHRP Report 725 research as well as in subsequent efforts by an ad hoc Task Group of the AASHTO/National Steel Bridge Alliance (NSBA) Steel Bridge Collaboration on Skewed and/or Curved Steel I-Girder Bridge Fit. However, the focus of these efforts was predominantly on sufficiency of different methods of analysis and on synthesis of broad observations and experiences with respect to fit-up.

This research provides quantitative data to aid engineers in the selection of various attributes to facilitate fit-up during I-girder bridge construction. Concepts and procedures for explicit calculation of locked-in forces due to cross-frame detailing are developed and discussed. Fit-up forces are evaluated and discussed for a suite of bridge cases analyzed in this research. Bridge cases with difficult fit-up are highlighted. Recommendations for erection procedures are provided to facilitate fit-up. The research investigates and

recommends beneficial staggered cross-frame framing arrangements that are applicable to straight skewed bridges, framing arrangements with liberal offsets around bearing lines at interior pier in continuous spans bridges, and the use of staggered versus lean-on cross-frame arrangements in straight skewed bridges. The research also addresses the impacts of cross-frame detailing methods, that is, the "fit condition" of the structure, on cross-frame forces, girder elevations, girder layovers, girder stresses, and vertical reactions in the completed bridges.

CHAPTER 1

INTRODUCTION

1.1. Background

The "fit" or "fit condition" of a skewed and/or curved I-girder bridge refers to the geometry in which the cross-frames are detailed to attach to the girders. A fit condition is selected to offset, or compensate for (to different extents), the tendency of the I-girders to twist in these bridge types. The selected fit condition corresponds to a specific targeted outcome of when the girder webs will be approximately plumb in the field. "Fit-up" refers to the assembly of the structural steel during the bridge erection. It is desirable that the "fit-up" of the structural steel should be manageable, without the need for excessive jacking or pulling forces from the erector. The "fit condition" and the "fit-up" of the structural steel are interrelated, but these terms refer to different attributes of the construction.

Table 1 summarizes the three most common fit conditions considered in skewed and/or curved I-girder bridges. Alternate names for each potential fit condition, which are generally more familiar to Fabricators/Detailers, are also provided in the table; the names are used interchangeably in practice.

Steel Dead Load Fit (SDLF) gives approximately plumb girder webs once the erection of the steel is completed. This is the most customary form of detailing for skewed and/or curved I-girder bridges. Total Dead Load Fit (TDLF) gives approximately plumb girder webs once the bridge is subjected to its Total Dead Load (TDL). The term "Total Dead Load," typically is assumed to include either all dead loads that are present when the bridge is opened to traffic, or the as-constructed dead loads, taken as the weight of the structural

steel plus the weight of the concrete deck, but not including the weight of the barrier rails. The later of these definitions is the preferred definition (NSBA 2014b). This definition is employed in this research. Future wearing surface loads and their effects generally are not considered as a part of the TDL. No-Load Fit (NLF) corresponds to detailing of the cross-frames so that they fit-up with the girders in their No-Load (NL) undeflected geometry. In this case, the girder webs will not be plumb once the bridge is subjected to its dead loads, except at non-skewed bearing lines.

Table 1. Common Fit Conditions.

Condition	**Alternate Name**	**Description**
No-Load Fit (NLF)	Fully-Cambered Fit	The cross-frames are detailed to fit to the girders in the fabricated fully-cambered and plumb position of the girders under zero load.
Steel Dead Load Fit (SDLF)	Erected Fit	The cross-frames are detailed to fit to the girders in an ideal plumb position where the girders are assumed deflected under the self-weight of the structural steel at the completion of the steel erection.
Total Dead Load Fit (TDLF)	Final Fit	The cross-frames are detailed to fit to the girders in an ideal plumb position where the girders are assumed deflected under the total as-constructed dead loads.

There are two key sets of values used by detailers in calculating the geometry of the cross-frames for SDLF or TDLF detailing:

(1) The vertical Total Dead Load (TDL) and/or Steel Dead Load (SDL) deflections provided on the design plans (Both TDL and SDL deflections are required for SDLF detailing while only the TDL deflections are required for TDLF detailing), and

(2) The associated major-axis bending rotations at the girder connection plates under the targeted load condition.

The girder camber profiles provided on the engineering plans are commonly set as the negative of the TDL vertical deflections. These camber values are referred to herein as the TDL camber. Although not actually applied to the girders, the corresponding negative of the SDL vertical deflections is referred to in this work as the girder SDL camber. These values are used along with the TDL camber in setting the geometry (i.e., the "drops") of the cross-frames for SDLF detailing.

1.2. Problem Statement and Research Objectives

Tighter constraints on right-of-way, particularly in urban environments, have led to a significantly increased utilization of skewed and/or curved alignments in highway bridge construction. Due to the relative ease of configuring the structure to the roadway geometry, steel I-girder bridges are often a preferred option for these cases. However, challenging attributes of the framing arrangements combined with current practices for detailing the cross-frames and erecting these bridges can result in problems during and after construction. Some of the problems encountered have included:

- Girders and cross-frames that are difficult to fit-up during erection, requiring un-planned contractor operations such as substantial force fitting of connections, field drilling and field welding,
- Erected girders with webs that are significantly out of plumb, although out-of-plumbness of girder webs is not necessarily indicative of a structural problem, as discussed in NSBA (2014b) and NCHRP Report 725,
- Locked-in stresses in the cross-frames and girders that were not appropriately accounted for in design,
- Bearings rotated beyond tolerable design limits, and
- Deck joints and barrier rails that are significantly out-of-alignment between the approach and the end of the bridge.

In certain instances, these problems have resulted in construction delays, rework, cost overruns, disputes and litigation. These problems can be avoided by developing a better understanding of the ways in which framing arrangements, cross-frame detailing practices and erection procedures affect the overall constructed bridge geometry as well as the fit-up during the erection of the steel.

Substantial progress has been made in answering many of the questions associated with this research via the completion of NCHRP Report 725 as well as subsequent efforts by an ad hoc Task Group of the AASHTO/National Steel Bridge Alliance (NSBA) Steel Bridge Collaboration on Skewed and/or Curved Steel I-Girder Bridge Fit. NCHRP Report 725 provided a substantive literature review of this area and conducted numerous targeted studies related to ensure fit-up. However, the NCHRP Report 725 project focused predominantly on the sufficiency of different methods of analysis and did not provide a

comprehensive evaluation of the questions related to this research. The subsequent AASHTO/NSBA Steel Bridge Collaboration Task Group effort provided an intensive focus on the various attributes and practices associated with fit-up, and produced a white paper on this topic. However, the focus of this effort was predominantly on broad recommendations and a synthesis of the best information on the various behavioral phenomena, and how that behavior might influence the decision to specify a particular fit condition for a skewed and/or curved I-girder bridge.

The objective of this research is to provide quantitative data and corresponding improved design, detailing and erection guidelines to facilitate the fit-up of skewed and/or curved steel I-girder bridges. These guidelines will provide a clear understanding of the implications of various

- Framing arrangements,
- Cross-frame detailing methods, and
- Erection procedures

on the

- Ease of fit-up during the steel erection,
- Achievement of the targeted constructed geometry, and
- Generation of locked-in stresses in the cross-frames and girders.

1.3. Summary of Research Contributions

This study achieves the following important research contributions:

- Clearly explain the behavior of curved and/or curved skewed I-girder bridges with respect to fit condition and fit-up considerations.
- Develop concepts and procedures for including cross-frame detailing effects directly in the structural analysis.
- Quantify the influence of various framing arrangements on skewed and/or curved I-girder bridge responses.
- Provide improved cross-frame framing arrangements to alleviate transverse nuisance stiffness due to skew.
- Assess the level of fit-up forces at cross-frame and girder splice connections to predict fit-up difficulty.
- Evaluate the influence of erection schemes on fit responses and provide recommendations on erection procedures.
- Assess the influence of detailing methods on the erection of steel I-girder bridges and on the responses within these bridges in their completed condition.
- Provide guidance for the selection of detailing methods.
- Quantify the influence of line girder versus refined analysis camber calculations on straight skewed bridges.
- Evaluate the influence of various tolerances on fit responses.

1.4. Organization

Chapter 2 provides an overview of the analytical studies conducted in this research. This is followed by Chapter 3, which highlights the concepts and procedures for including cross-frame detailing effects directly in a structural analysis. Chapter 4 provides an overview of the behavior of each of major bridge types or bridge classifications considered in this work: straight skewed, radially curved-supported, and curved and skewed I-girder bridges. Chapter 5 summarizes the results from the evaluations of fit-up forces. Chapter 6 presents findings on the influence of cross-frame detailing methods on various responses in completed bridges. Chapter 7 studies the influence of cross-frame arrangements on fit responses and gives recommendations on how to alleviate nuisance transverse stiffness effects due to skew. Chapter 8 discusses and gives recommendations on erection procedures. Chapter 9 provides detailed evaluation of straight skewed bridge responses associated with the use of Line Girder Analysis (LGA) camber versus 3D Finite Element Analysis (FEA) camber. Chapter 10 investigates the sensitivities of the completed bridge responses to various factors. Finally, Chapter 11 provides conclusions and recommendations.

CHAPTER 2

ANALYTICAL STUDIES

2.1. Simulation Modeling (3D FEA) of I-Girder Bridges

At the present time (2015), simulation of many types of physical responses can be readily performed using 3D Finite Element Analysis (FEA). The availability of these tools provides substantial promise for detailed analytical studies to address the outstanding questions in this research. However, the accuracy of results from 3D FEA simulations depends on the accuracy of the capture of the following attributes:

- Geometry details,
- Boundary conditions – loads and displacements,
- Assumed initial conditions, e.g., any lack-of-fit between components in the No-Load (NL) condition,
- The interconnection between various components (e.g., dimensional tolerances in girder splice and cross-frame to girder connections, and the composite action between the steel girders and the concrete slab).

In this research, 3D FEA is used to calculate all the bridge responses. All of the 3D FEA studies are conducted using the ABAQUS 6.12 platform (Dassault Systemes, 2014). The research utilizes an ABAQUS input file generator that allows accelerated generation of the 3D FEA models. The following are modeling specifics selected in ABAQUS for this research:

- The girder webs are modeled using the S4R shell elements throughout the depths between the mid-thicknesses of the girder flanges. The S4R element is a 4-node

quadrilateral displacement-based shell element with reduced integration and a large-strain formulation. This research utilizes the FEA mesh density recommended by the NCHRP Report 725 research, which demonstrated that the use of 12 S4R shell elements through the web depth is sufficient for the types of studies to be conducted in this research. The number of the S4R elements is selected along the girder lengths such that an element aspect ratio close to 1.0 is achieved.

- A 2-node shear-deformable beam element, B31, which is compatible with the S4R shell element, is used to model the flanges, stiffeners, and chords of V or inverted-V cross-frames to which the diagonals are connected. The cross-frame chords in this case are modeled as moment connected to the girder webs.
- A truss element, T3D2, is used to model the cross-frames everywhere except in the case of the chords mentioned above. The cross-frame elements are connected to their exact physical work points on the girder webs. The connections of the cross-frames at the girder webs are modeled using multi-point constraints. This is to eliminate the need to adjust the FEA discretization through the depth of the girder webs to place the nodes at the work points.
- The axial stiffness of single-angle and flange-connected tee cross-frame members is taken as 0.65 of the nominal EA/L of these members. This modeling practice accounts for the additional flexibility associated with the eccentric one-sided connections at the member ends, as specified in the 7th Edition AASHTO LRFD Specifications. This modeling of the reduced stiffness of single-angle and flange-connected tee cross-frame members was not employed in the NCHRP Report 725 research.

- Separate line girder analyses (LGA) are conducted in this research to obtain LGA cambers for straight skewed bridges. These analyses are conducted by running the corresponding 3D FEA model but with the cross-frame elements removed and the girder lateral displacements restrained. The LGA cambers also can be obtained by analyzing the girders using ordinary beam elements. The LGA cambers obtained from the above 3D FEA model and from a beam element model are the same for all practical purposes. The usage of the 3D FEA model to conduct the LGA solutions is simply a matter of convenience in this research, since the same girder models employed in the 3D FEA system simulations could be easily re-used to obtain the LGA solutions.
- Grid-analysis is conducted in this research to illustrate the incorporation of cross-frame detailing method effects via initial fixed-end forces, as discussed in Chapter 3. For this portion of the research, the girders are modeled using a grid analysis capability developed in this research using an Euler-Bernoulli frame element. The girder section properties are specified including the use of the equivalent St. Venant torsion constant for the I-girders from the NCHRP Report 725 research, which accounts approximately for the contribution of warping to the torsional stiffness. The cross-frames are modeled using equivalent beam elements based on two methods: Euler-Bernoulli beam elements with the cross-section properties determined by the flexural analogy, as discussed in Section 3.2.3 of the NCHRP Report 725, and the Timoshenko beam approach recommended by the NCHRP Report 725. The equivalent beam cross-frame properties were calculated for each of these two beam elements using the methods recommended in the NCHRP Report

725. The Timoshenko beam element derivation is explained in (McGuire et. al. 2000). It is shown that for the bridge cases studied in Chapter 3, the bridge responses are essentially the same with the cross-frames modeled based on Euler-Bernoulli beam with the flexural analogy and Timoshenko beam. This is largely because the cross-frames are effectively rigid relative to the stiffness of the girders in the example bridges studied in this section.

- In this research, the lack-of-fit due to SDLF and TDLF detailing is accounted for directly in the 3D FEA simulations via cross-frame initial strains. These initial strains are calculated in ABAQUS by imposing the vertical deflections associated with the girder dead load cambers (i.e., the corresponding lack-of-fit of the cross-frames in the bridge reference no-load geometry is equal to the TDL camber for TDLF and it is equal to the SDL camber for SDLF; the cross-frames are detailed to fit to the girder elevations after the SDL displacements have occurred, for SDLF, and after the TDL displacements have occurred, for TDLF). The TDL camber is taken simply as the negative of the TDL girder vertical deflections; similarly, the term "SDL camber" is used in this research to refer to the negative of the SDL deflections used in the calculation of the cross-frame initial strains for SDLF detailing. Special-purpose tools were developed and used to facilitate the calculation of initial strains in the 3D FEA software and for including these initial strains in the bridge 3D FEA simulations.
- The cambers used for SDLF or TDLF detailing are calculated from a LGA for the straight skewed bridges, unless noted otherwise. For the curved and curved and skewed bridges, the girder cambers are calculated in all cases using the 3D FEA

models. When TDLF detailing is used on a straight skewed bridge, the TDL cambers used for fabrication of the girders are calculated directly from a LGA, neglecting any contribution of the bridge deck to the resistance of vertical displacements. When SDLF detailing is employed, the correct total cambers to be fabricated into the girders are calculated as the SDL camber from an LGA for SDL plus the Concrete Dead Load (CDL) camber, taken as the negative of the girder displacements in the bridge system as calculated from 3D FEA (neglecting the contribution of the bridge deck to the resistance of vertical displacements). For the unusual case of NLF detailing on a sharply skewed straight I-girder bridge, the TDL girder cambers used for fabricating the girders are determined directly from 3D FEA.

- In all cases, the girder cambers are calculated by the common practice of building a model of the structure (or girder) and then simply "turning gravity on." The influence of the SDLF or TDLF detailing effects on the girder vertical displacements is not considered in calculating the girder cambers.
- The girder cambers are accounted for explicitly in the structural analysis simulations by modeling the no-load geometry of the steel girders using their cambered no-load profiles. Given the specified cambers, from whatever the source and method that they may be determined, the 3D FEA procedures provide a unified rigorous approach for determining the locked-in force effects associated with the SDLF or TDLF detailing.
- Superelevation, grade and vertical curve are neglected in this research. The effects of these attributes on the gravity load responses usually is assumed negligible in

bridge design practice, based on the assumption that the angles with the horizontal associated with these attributes of the geometry are small.

- The weight of steel is modeled using a weight density of 490 pcf. In the above LGA calculations, the weights of un-modeled cross-frames are included by adding vertical concentrated loads at their work points on the girder webs.
- The concrete deck weight is modeled on the noncomposite I-girders as distributed line loads applied at the centerlines of the top flanges. This weight is calculated based on the tributary widths between the girders and from the deck overhangs.
- Construction equipment loads are not considered in the direct calculations considered in this research.
- The influence of staged concrete deck placement is neglected in this research. Where TDL responses are evaluated, the calculations are performed using the idealization that the entire concrete deck is placed prior to any participation of the deck in resisting load. This results in an upper-bound estimate of the TDL deflections and the corresponding fit-condition and fit-up effects.
- The bridges are assumed to float on the bearings to minimize the impact of bearing restraints on the system responses in all cases. This is a common recommended approach for highly skewed and/or curved I-girder bridges (NHI 2011). The bridge is restrained laterally only by small lateral stiffnesses from the bridge bearings, thus avoiding undesirable restraint in the lateral or longitudinal directions. The physical bearing details are designed to restrain large movements during potential extreme events.

- The bridges are analyzed using a geometrically nonlinear elastic analysis in all cases. This allows for the capture of second-order amplification of the physical response in any situations where these effects may be important.
- All of the test simulation models are based on the assumption of linear elastic material behavior in this research.

This research utilizes an ABAQUS input file generator that allows accelerated generation of the 3D FEA models. Python scripts and Excel macros have been developed to expedite the extraction of stresses, displacements, and reactions from the FEA results.

2.2. Design of Analytical Studies

2.2.1. Selection of Base Steel I-Girder Bridge Designs

This research identified a suite of 21 base steel I-girder bridge designs targeted to address the key research questions. NHCRP Report 725 compiled and developed a suite of existing and parametric study bridge designs encompassing a spectrum of span arrangements, span lengths, curvature, bridge widths and skew angles encountered in practice. This research leveraged the NCHRP Report 725 research to maximize the number of cases that could be studied feasibly in the current research. In selecting a set of 21 base I-girder bridge designs, emphasis was placed (in the order listed below) on cases where:

1) Fit-up problems might exist,
2) The bridge may be useful in identifying the boundaries where fit-up problems start to occur and how key response parameters vary as a function of the bridge geometry,

3) Quality field response measurements and observations from existing bridges were available, particularly measurements and observations during intermediate construction stages,

4) Detailed erection plans were available (for existing bridges).

The 21 steel I-girder bridges studied in this research are designated by the letters A to U. In addition, the bridges are named as follows using the naming convention from NCHRP Report 725 research (e.g., EISCR1):

- The first letter in the bridge name indicates whether the structure is an Existing bridge (E) or a New design (N) conducted by HDR, Inc., as part of the NCHRP Report 725 research, based on targeted overall geometry parameters.
- The second letter in the bridge name indicates that the bridge is an I-girder bridge type (NCHRP Report 725 also studied tub-girder bridges; however, these bridge types are not within the scope of this research).
- The third letter indicates whether the bridge is a Simple span (S) or a Continuous span (C).
- The fourth letter indicates whether the bridge is Curved (C) or Straight (S).
- The fifth letter in the bridge name indicates whether the bridge has "Radial" (R) or "Skewed" (S) supports.
- Finally, the number at the end of the bridge name is simply a unique designator assigned to the bridge as part of a given category based on the above parameters.

The base plan geometries for the bridges selected using the above criteria are shown and the key characteristics of these bridges are summarized in the following sub-sections.

The rectangles shown on the bridge plans indicate the bearing support lines. In addition, a scale is shown for each of the bridge plans. The curved radially-supported bridges are discussed first, followed by straight skewed cases, and finally, the bridges that are both curved and skewed

2.2.1.1. Curved Radially-Supported Bridges

The following seven curved radially-supported bridges were evaluated in this research. The curved radially-supported bridges are designated from (A) through (G) in the overall list of bridges. These bridges are listed in the order of:

1) Simple-span bridges,
2) Continuous-span bridges, and
3) Increasing maximum span length of the curved spans (within each of the simple-span and continuous-span bridge sub-groups).

The key geometry parameters shown for each of these bridges are:

L_s = span lengths along the curve between the bearing lines at the centerline of the bridge;

w_g = out-to-out width between the fascia girders in the radial direction orthogonal to the girder tangents;

R = radius of curvature to the centerline of the bridge;

n_g = number of girders in the bridge cross-section;

L_s/D = bridge span to girder depth ratios.

Descriptions of Bridges (A) through (G) follow:

(A) EISCR1 (L_s = 90 ft; w_g = 17.5 ft; R = 200 ft; n_g = 3; L_s/R = 0.45; L_s/w_g = 5.1; L_s/D = 23.5)

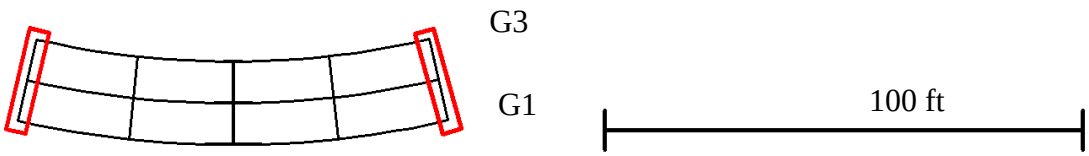

Figure 1. Bridge (A) EISCR1.

This is a very basic simple-span curved radially-supported bridge that was tested at the FHWA Turner Fairbank Research Center in 2005-2006 (Jung and White, 2008). This bridge was designed to a number of extreme limits of the AASHTO LRFD Specifications and is useful as a benchmark and demonstration case for horizontally curved radially-supported bridge responses.

(B) NISCR2 (L_s = 150 ft; w_g= 24 ft; R = 438 ft; n_g = 4; L_s/R = 0.34; L_s/w_g = 6.2; L_s/D = 22.1)

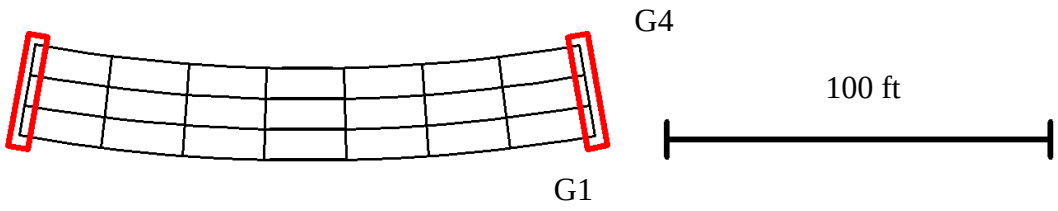

Figure 2. Bridge (B) EISCR2.

This bridge was used in NCHRP Report 725 to provide a substantive illustration of the behavior of curved radially-supported I-girder bridges, including the influence of NLF, SDLF and TLDF detailing. For this bridge, NCHRP Report 725 showed that the maximum cross-frame diagonal forces are increased by 50 % and 100 % relative to the NLF total dead load forces when SDLF and TDLF detailing are used, respectively. This

result is consistent with the findings of this research. This increase in the cross-frame responses is believed to be relatively large compared to that of many bridges.

(C) NISCR7 (L_s = 150 ft; w_g = 74 ft; R = 280 ft; n_g = 9; L_s/R = 0.54; L_s/w_g = 2.0; L_s/D = 24.3)

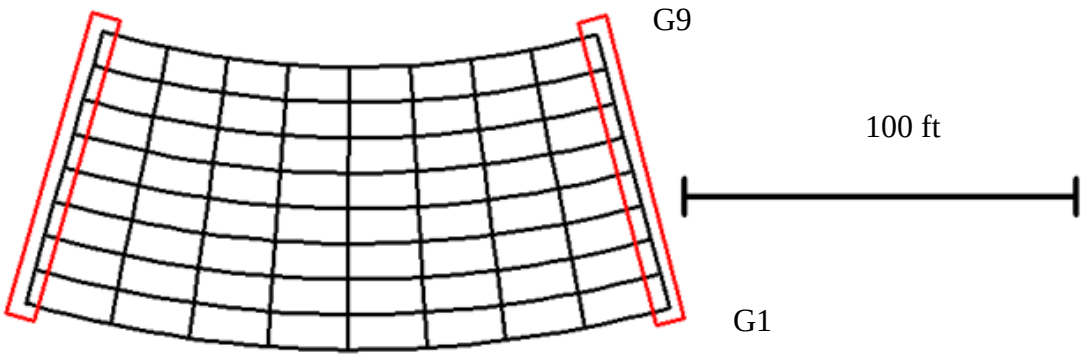

Figure 3. Bridge (C) NISCR7.

This bridge has greater interaction between the girders and cross-frames compared to bridge (B) NISCR2 since it is a wider and more sharply curved radially-supported I-girder bridge. In this research, it is observed that the cross-frame members with the largest forces are not in the exterior bay of this bridge (the bay between the outside girder and the adjacent interior girder).

(D) NISCR10 (L_s = 225 ft; w_g = 74 ft; R = 705 ft; n_g = 9; L_s/R = 0.32; L_s/w_g = 3.0; L_s/D = 23.7)

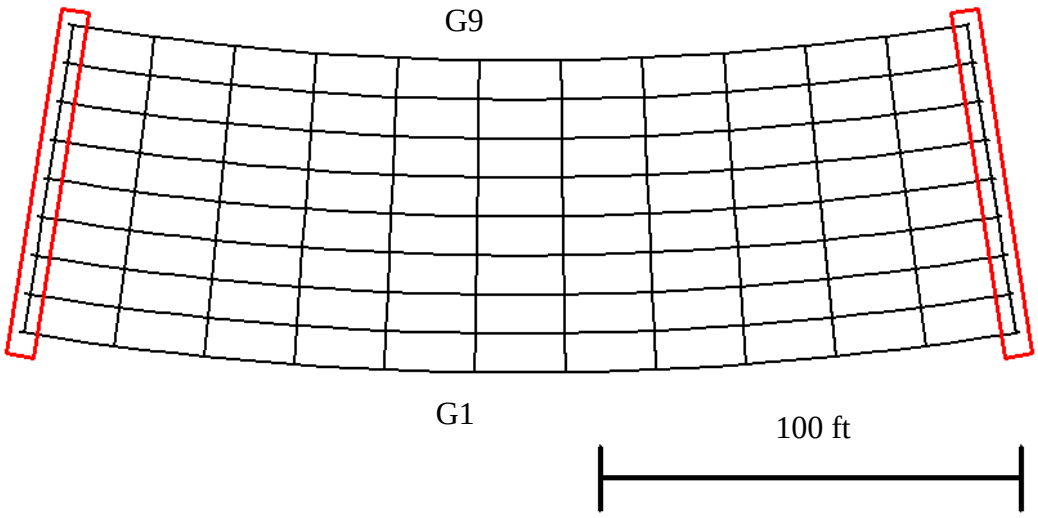

Figure 4. Bridge (D) NISCR10.

This is an intermediate-span wide bridge with a more moderate horizontal curvature compared to bridge (C) NISCR7. The cross-frame members with the largest forces are not in the bay between the outside girder and the adjacent interior girder in this bridge as well.

(E) EICCR11, Ford City Bridge, Ford City, PA (L_s = 322, 417 and 322 ft; w_g = 40.4 ft; R = ∞,∞,411 ft, i.e., the bridge is straight in spans 1 and 2, and 411 ft in span 3; n_g = 4; L_s/R = 0, 0, and 0.80; L_s/w_g = 8.0, 10.3, and 8.1; L_s/D = 23.0, 29.8, 23.5)

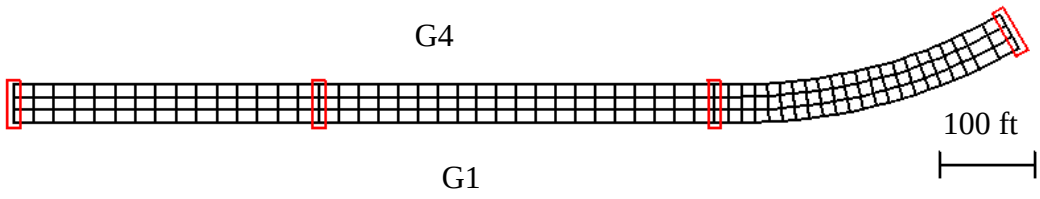

Figure 5. Bridge (E) EICCR11.

As discussed in NCHRP Report 725, this bridge represents an extreme geometry that exhibited relatively large fit-up forces in the field. The erection of the curved span involved drop-in segments. The cross-frames in this bridge were mistakenly detailed for SDLF based on concrete dead load deflections. Fortunately, this was essentially SDLF detailing since the steel and concrete dead load deflections are approximately equal for this structure. This bridge has been studied extensively in prior research by Chavel and Earls (2006a & b).

(F) NICCR12 (L_s = 350, 350 and 280 ft; w_g = 74 ft; R = 909 ft; n_g = 9; L_s/R = 0.39, 0.39, and 0.31; L_s/w_g = 4.7, 4.7 and 3.8; L_s/D = 25, 25, 20)

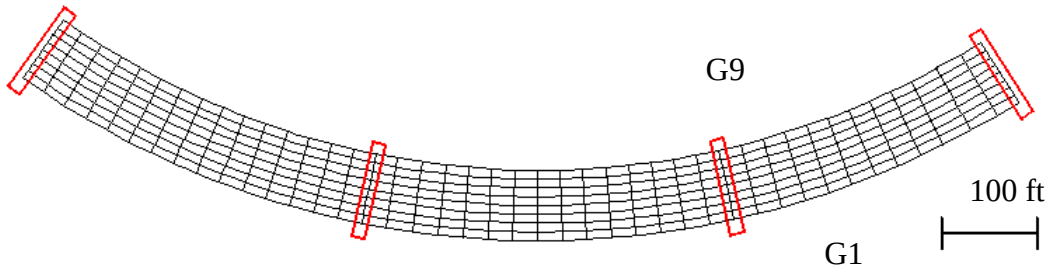

Figure 6. Bridge (E) NICCR12.

This case represents an extremely long-span, relatively wide bridge with significant horizontal curvature and radial supports. Shoring towers were used to install the long field segments.

(G) EICCR4 (L_s = 219, 260, 211 ft, 162 ft, 256 ft, and 190 ft; w_g = 36.7 ft; R = 968, 3 @ 1108 ft, 968 ft, and ∞, n_g = 4; L_s/R = 0.198, 0.235, 0.190, 0.146, 0.264, 0; L_s/w_g = 6.0, 7.1, 5.7, 4.4, 7.0, and 5.2; L_s/D = 26.5, 31.5, 25.6, 19.6, 31.0 ,23.0)

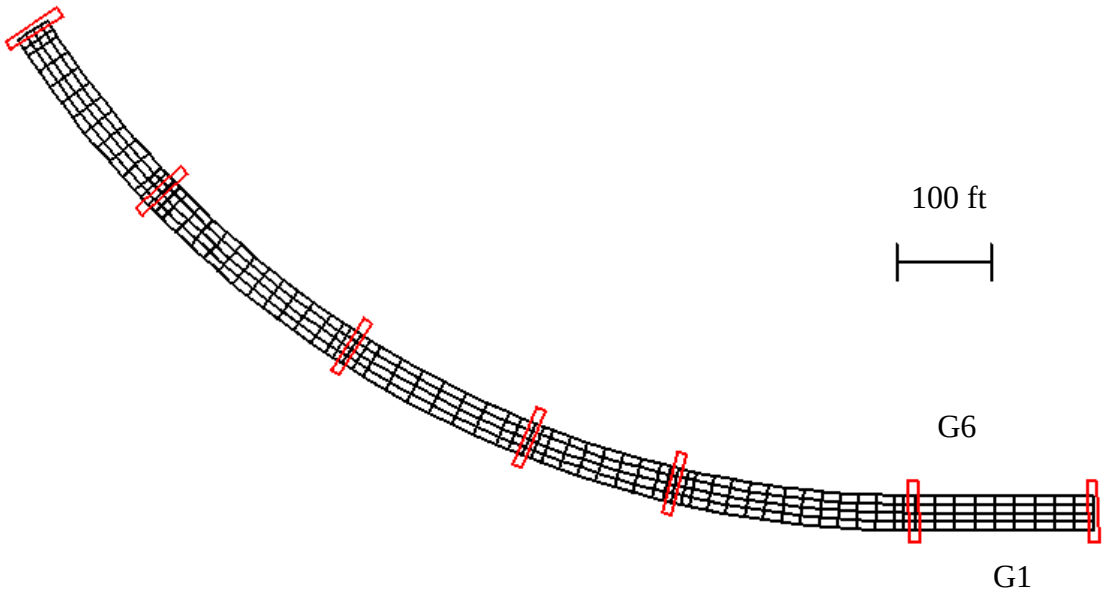

Figure 7. Bridge (G) EICCR4.

This is the existing Ramp GG of the John F. Kennedy Memorial Highway, I-95 Express Toll Lanes and I-695 Interchange, Baltimore Co., MD. It has relatively long spans as well as a relatively narrow bridge cross-section. It represents a successful implementation of SDLF detailing.

2.2.1.2. Straight Skewed Bridges

The following six straight skewed bridges were evaluated in this research. Similar to the presentation of the curved radially-supported bridges, simple-span bridges are shown first followed by continuous-span bridges. Within each of these sub-groups, the bridges are listed in the order of increasing maximum span length. The key geometry parameters shown for each bridge, not already defined in Section 2.2.1 for the curved radially-supported bridges, are:

L_{max} = maximum fascia girder length, reported for the bridges with non-parallel skew;

L_{min} = minimum fascia girder length, reported for the bridges with non-parallel skew;

θ = bearing line skew angle, defined as zero for a bearing line having zero skew (one value shown for all the bearing lines for bridges with parallel skew);

L_s = span length between the bearing lines along the centerline of the bridge;

$$I_s = \frac{w_g \times \tan\theta}{L_s} \qquad \text{Eq. (1)}$$

= Maximum value of the skew index for each span

The straight skewed bridges are designated from (H) through (M) in the overall list of bridges. Multiple framing arrangements are considered for all of these bridges except for bridge (L) NISCS16. Overview plan sketches are shown here for only the original or base framing arrangements. The alternative framing arrangements for the straight skewed bridges are discussed and shown in Section 2.2.3.1. The designations within the parentheses with a number included after the letter indicate that different framing arrangements are considered subsequently for the given bridge geometry.

Descriptions of Bridges (H) through (M) follow:

(H1) EISSS57 (L_s = 137 ft; L_{max} = 211 ft; L_{min} = 63 ft; w_g = 61.0 ft; θ = 69.5° and -4.4°, non-parallel skew; n_g = 7; I_s = 1.19; L_{max}/w_g = 3.5; L_{min}/w_g = 1.0; L_s/D = 18.3)

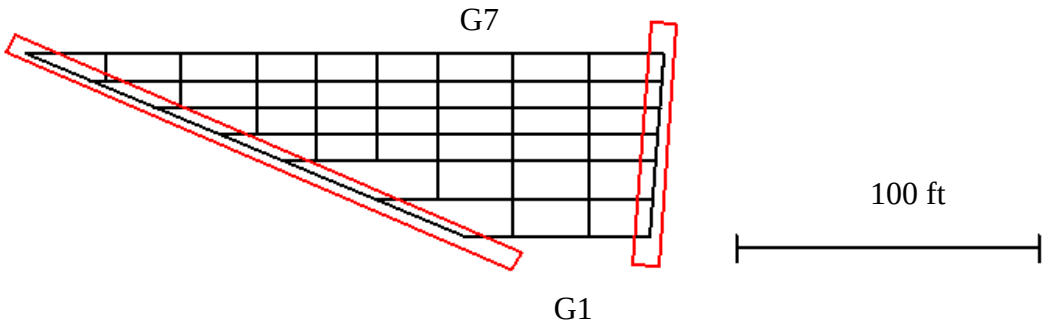

Figure 8. Bridge (H1) EISSS57.

This is an existing bridge with an extreme non-parallel skew, erected over a rail yard in Fort Worth, TX. The characteristics of this bridge have been discussed as an example of those that may cause potential fit-up issues in various workshop and seminar venues. This bridge's geometry is slightly simplified from the existing bridge in Fort Worth: (1) the girder spacing is assumed constant along the length of the girders, whereas some of the girders were slightly splayed in the existing bridge; (2) the bridge deck is assumed to be straight, whereas the bridge deck in the existing bridge was slightly curved, causing variable width overhangs.

(I1) NISSS14 (L_s = 150 ft; w_g = 74 ft; θ= 70º, parallel skew; n_g = 9; I_s = 1.36; L_s/w_g = 2.0; L_s/D = 25)

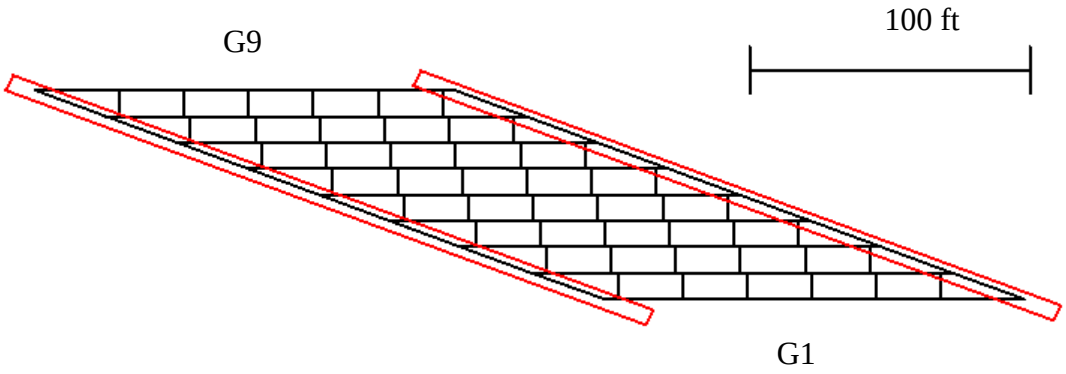

Figure 9. Bridge (I1) NISSS14.

This is a relatively short bridge that had the largest skew index of all the simple-span bridges studied in the NCHRP Report 725 research. This framing arrangement has relatively high nuisance transverse stiffness due to small offsets from the first intermediate cross-frames to the skewed bearing lines, small stagger distances between the cross-frames, and a large number of cross-frames.

(J1) NISSS54 (L_s = 300 ft; w_g = 74 ft; θ = 70°, parallel skew; n_g = 9; I_s = 0.68; L_s/w_g = 4.1; L_s/D = 25)

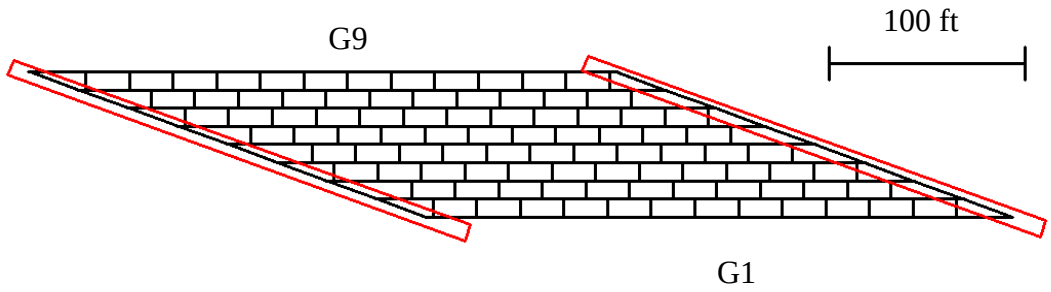

Figure 10. Bridge (J1) NISSS54.

This bridge has a long span and a high skew index, making it particularly sensitive to any variation in attributes that affect erection fit-up. In addition, this bridge has been used extensively as an example case in NCHRP Report 725.

(K1) EICSS12, US 82 Mainline Underpass at 19th Street WB, Lubbock, TX (L_s = 150 and 139 ft; w_g = 41.0 ft; θ = 59.6°, parallel skew; n_g = 6; I_s = 0.47 and 0.50; L_s/w_g = 3.7 and 3.4; L_s/D = 33.3, 30.8)

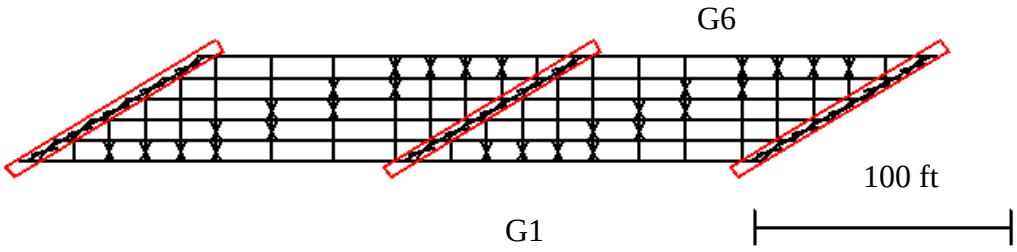

Figure 11. Bridge (K1) EICSS12.

This two-span continuous bridge, constructed in Lubbock, TX, was studied extensively by Romage (2008) and others. This bridge served as an evaluation and demonstration case for the use of lean-on bracing systems in straight skewed I-girder bridges (Helwig

and Yura, 2012). The cross-frames with diagonals are marked by an ′X′ on the above plan. The rest of the cross-frames have only top and bottom chords.

(L) NICSS16 (L_s = 120, 150 and 150 ft; w_g = 74 ft; θ = 70°, parallel skew; n_g = 9; I_s = 1.69, 1.36, and 1.36; L_s/w_g = 1.6, 2.0, and 2.0; L_s/D = 20, 25, 25)

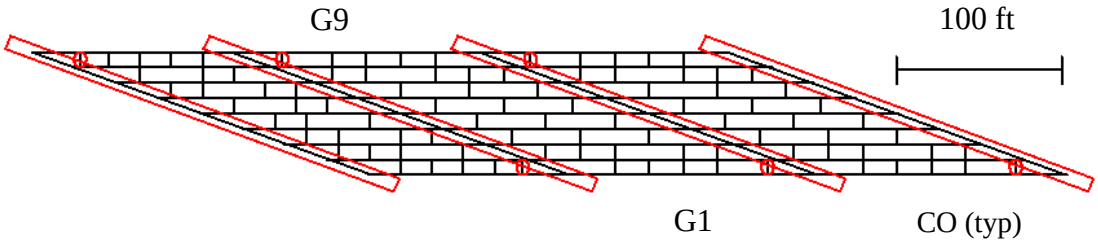

Figure 12. Bridge (L) NICSS16.

This three-span continuous bridge had the largest skew index of all the bridges studied in the NCHRP Report 725 research. The framing plan shown is a modification of the bridge (L) NISCS16 original framing plan, which is not studied in this research. The original plan had undesirable features such as very close offsets between the intermediate cross-frames and the bearing lines, and very small stagger spacing between cross-frames. The issues associated with these features are addressed by the studies of bridge (I1) NISSS14.

The framing plan shown here provides larger offsets of the first intermediate cross-frames from the bearing lines except on the first interior girder at the acute corners. At these locations, providing an offset that satisfies the 1.5D and 0.4L_b rules discussed in Section 7.1 would make the unbraced lengths on the fascia girders at the acute corners quite large. Instead, small offset distances are used at these locations and the diagonals are removed in these first intermediate cross-frames to alleviate the nuisance transverse stiffness effects. The cross-frames highlighted by an oval and labeled on the plan view

as “CO” (for “chords only”) do not contain any diagonals. Furthermore, the intermediate cross-frames are all equally-spaced except for the offsets adjacent to the skewed bearing lines. Every other cross-frame is intentionally omitted within the interior of the bridge plan. In addition to reducing the cross-frame forces caused by nuisance transverse stiffness effects, this results in a significant reduction in the overall number of cross-frames employed in the bridge.

(M1) EICSS2, I-235 EB over E. University Ave., Polk Co., IA (L_s = 239, 257, and 220 ft; L_{max} = 259, 255, and 220 ft; L_{min} = 241,183, and 220 ft; w_g = 66.6 ft; θ = 58°, 61.8°, 38°, and 38°; n_g = 8; I_s = 0.52, 0.48, and 0.24; L_{max}/w_g = 3.9, 3.8, and 3.3; L_{min}/w_g = 3.6, 2.7, and 3.3; L_s/D = 26, 28, 23.8)

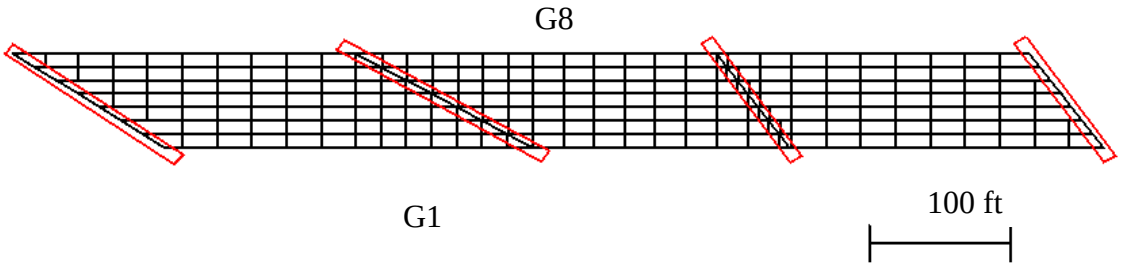

Figure 13. Bridge (M1) EICSS2.

This three-span continuous bridge, constructed in Polk Co., IA, had substantial difficulty with the installation of its cross-frames during the steel erection. This bridge was built using phased construction. The bridge was built in two phases. In the first phase, the first four girder lines and the cross-frames between these girder lines were installed, and then the concrete deck was placed on the girders associated with this phase. In the second phase, the other four girder lines and the cross-frames between these girder lines were installed and then the concrete deck was placed on the girders associated with the second phase. The phased construction made the installation of the

cross-frames in-between the phases difficult. The intermediate cross-frames framing directly into the bearing locations at the interior piers create a large transverse (nuisance) stiffness, and are subject to high differential deflections.

2.1.1.3. Curved and Skewed Bridges

Seven bridges having combined horizontal curvature and skew were evaluated in this research. Similar to the curved radially-supported and straight skewed bridge presentations, the simple-span bridges are shown first followed by continuous-span bridges. The bridges are presented in the order of increasing maximum span length within each of these sub-groups. The curved and skewed bridges are designated from (N) through (U).

Multiple framing arrangements are considered for five of these bridges. Overview plan sketches are shown here for the original framing arrangements. The alternative framing arrangements for the curved and skewed bridges are discussed and shown in Section 2.2.3.2. The designations in the parentheses that have numbers included after the letter indicate that different framing arrangements are considered subsequently for the given bridge geometry.

Descriptions of Bridges (N) through (U) follow:

(N) NISCS14 (L_s = 150 ft; L_{max} = 192 ft; L_{min} = 126 ft; w_g = 74 ft; R = 280 ft; θ = 53.7° and 0°; n_g = 9; L_s/R = 0.54; L_s/w_g = 2.0; $(L_{min} - L_{max})/(L_{min} + L_{max})$ = -0.21; L_s/D = 25)

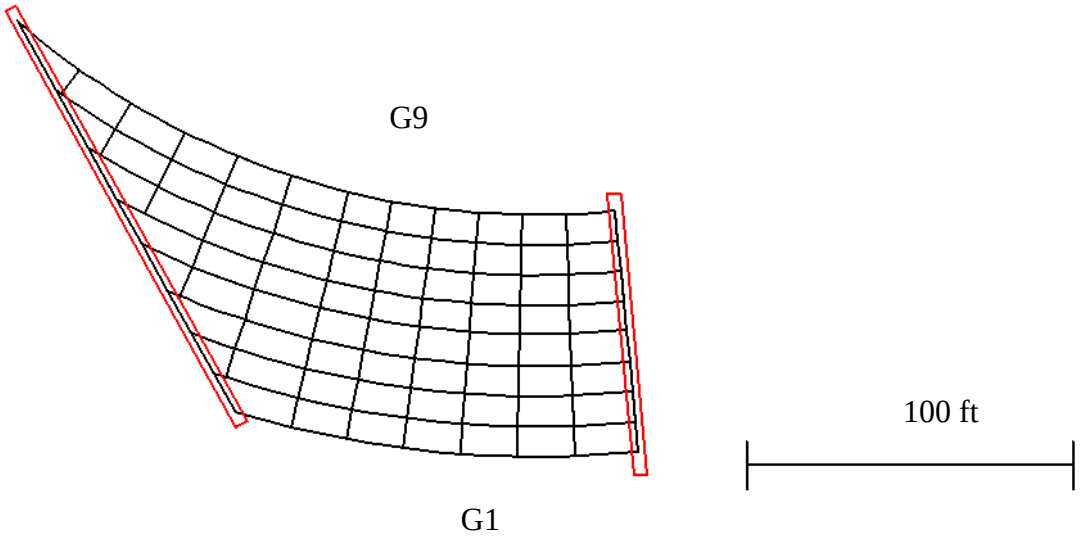

Figure 14. Bridge (N) NISCS14.

This bridge is similar to (C) NISCR7 in terms of span length, bridge width, and radius of curvature. The orientation of the skew at the left end of this bridge makes the inside girder (i.e., the girder on the inside of the curve) longer than the outside girder. The orientation of the skew at the left end tends to counteract the bridge horizontal curvature effects to some extent.

(O1) NISCS15 (L_s = 150 ft; L_{max} = 195 ft; L_{min} = 103 ft; w_g = 74 ft; R = 280 ft; θ = -35° and 0°; n_g = 9; L_s/R = 0.54; L_s/w_g = 2.0; $(L_{max} - L_{min})/(L_{max} + L_{min})$ = 0.31; L_s/D = 20)

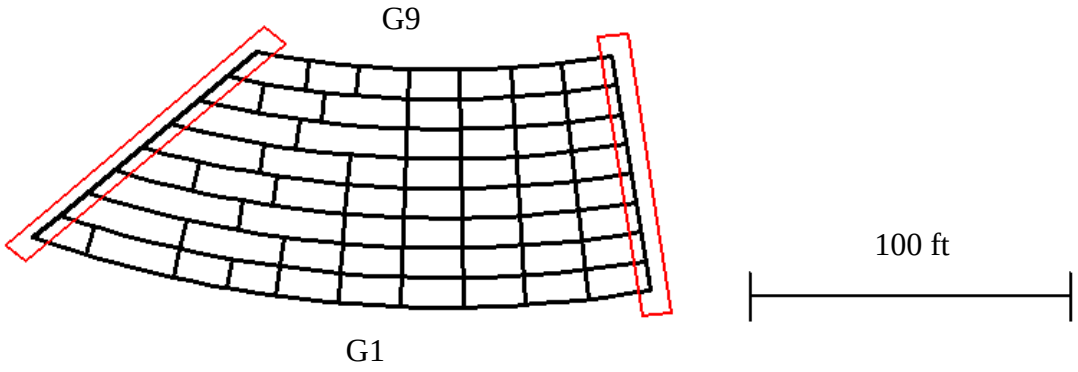

Figure 15. Bridge (O1) NISCS15.

This bridge is similar to (C) NISCR7 and (N) NISCS14 in terms of span length, bridge width, and radius of curvature. However, the orientation of the skew at the left end makes the girders on the inside of the curve significantly shorter than the outside girders. The effects of the skew at the left-hand end tend to be additive with the horizontal curvature effects.

(P) EISCS3, SR 8002 Ramp A-1, King of Prussia, PA (L_s = 153 ft; L_{max} = 164 ft; L_{min} = 140 ft; w_g = 30.6 ft; R = 279 ft; θ = 52.4° and 0°; n_g = 6; L_s/R = 0.55; L_s/w_g = 5.0; $(L_{min} - L_{max})/(L_{min} + L_{max})$ = -0.08; L_s/D = 27)

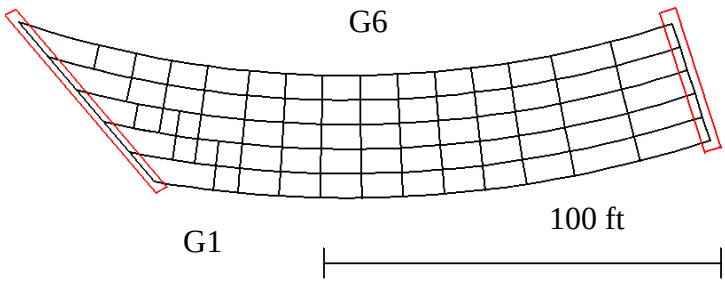

Figure 16. Bridge (P) EISCS3.

This is an existing bridge that required a holding crane until four girders were erected. This bridge has been studied extensively in prior research by Chavel and Earls (2003) and Chavel (2008). The orientation of the skew at the left end of this bridge tends to counteract the bridge horizontal curvature effects to some extent.

(Q1) NISCS38 (L_s = 300 ft; L_{max} = 366 ft; L_{min} = 249 ft; w_g = 74 ft; R = 730 ft; θ = 62.6° and 0°; n_g = 9; L_s/R = 0.41; L_s/w_g = 4.1; $(L_{min} - L_{max})/(L_{min} + L_{max})$ = -0.19; L_s/D = 23)

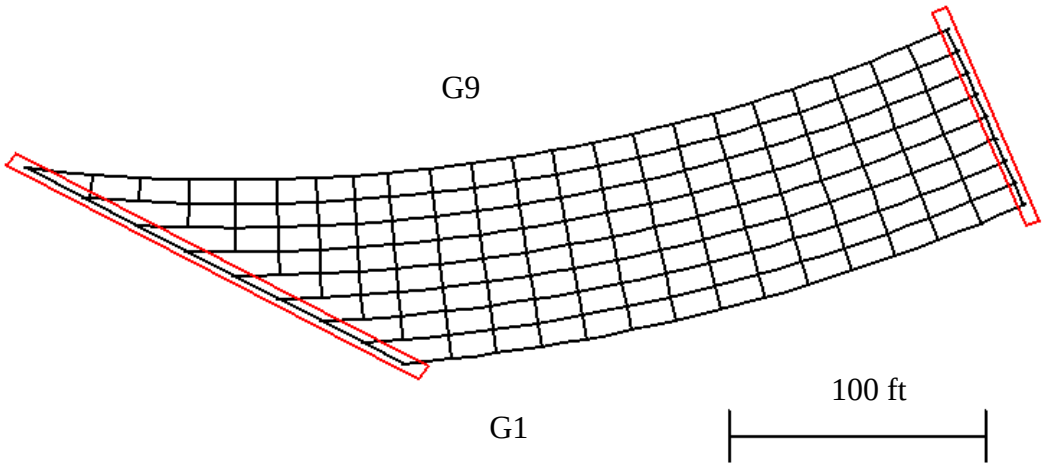

Figure 17. Bridge (Q1) NISCS38.

This is a longer-span curved and skewed bridge similar to (N) NISCS14. Phased construction is studied on this bridge for the framing plan shown above. The second

phase, which includes the four inside girders, has a span length of 330 ft with a width of 27.75 ft. This is the critical phase of the construction. The deflections of this phase are large and the system is near the point of instability during its deck placement.

(R1) NISCS39 (L_s = 300 ft; L_{max} = 340 ft; L_{min} = 258 ft; w_g = 74 ft; R = 730 ft; θ = -35° and 0°; n_g = 9; L_s/R = 0.41; L_s/w_g = 4.1; $(L_{max} - L_{min})/(L_{max} + L_{min})$ = 0.14 ; L_s/D =23)

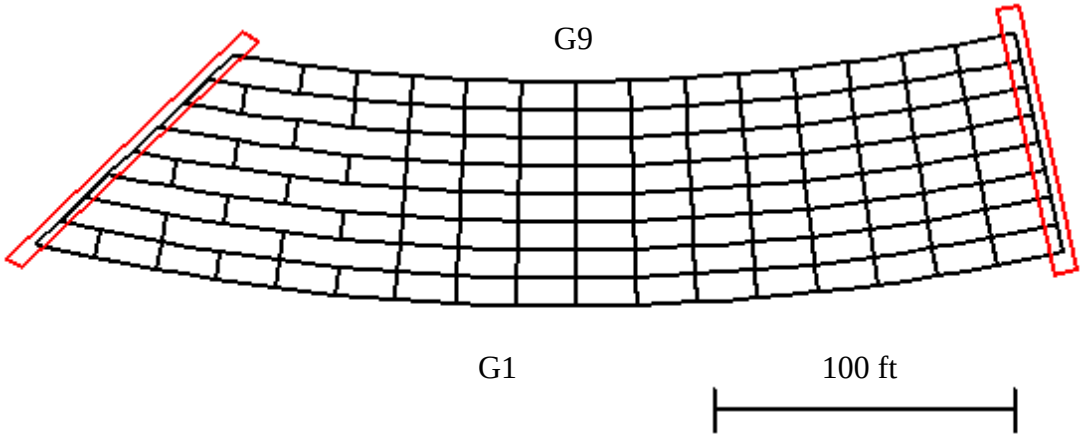

Figure 18. Bridge (R1) NISCS39.

This is a longer-span curved and skewed bridge similar to (O1) NISCS15. The skew orientation makes the outside girder (i.e., the girder on the outside of the curve) significantly longer than the inside girder.

(S) XICCS7 (L_s = 160, 210 and 160 ft; L_{max} = 185, 214 and 191 ft; L_{min} = 136, 205 and 126 ft; w_g = 33.0 ft; R =700 ft; θ = 0, -60, -60 and 0°; n_g = 4; L_s/R = 0.26, 0.31 and 0.27; L_s/w_g = 4.8, 6.4 and 4.8; $(L_{min} - L_{max})/(L_{min} + L_{max})$ = -0.15, $(L_{max} - L_{min})/(L_{max} + L_{min})$ = 0.02 and 0.21; L_s/D = 20.8, 27.4, 20.8)

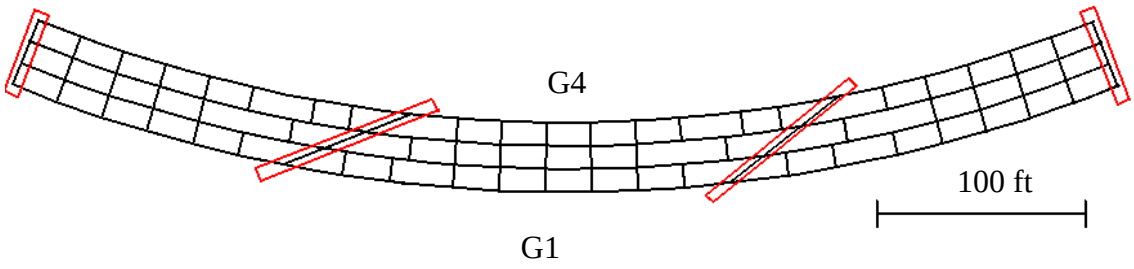

Figure 19. Bridge (X) XICCS7.

This is a significantly curved and skewed I-girder bridge. This bridge is presented as a design example in the NHI Course "Analysis and Design of Skewed and Curved Steel Bridges with LRFD" (NHI 2011).

(T1) EICCS27, SR 386 over SR6 and Ramp F, Sumner Co., TN (L_s = 279 ft, 224 ft, and 236 ft; L_{max} = 279, 239 and 231 ft; L_{min} = 268, 214 and 217 ft; w_g = 79.9 ft; R = 2546 ft; θ= -53.1, -59.4, -64.4 and -69.7°; n_g = 8; L_s/R = 0.11, 0.09 and 0.09; L_s/w_g = 3.5, 2.8 and 3.0; $(L_{min} - L_{max})/(L_{min} + L_{max})$ = -0.02, -0.03 and -0.01; L_s/D = 37.2, 29.8, 31.5)

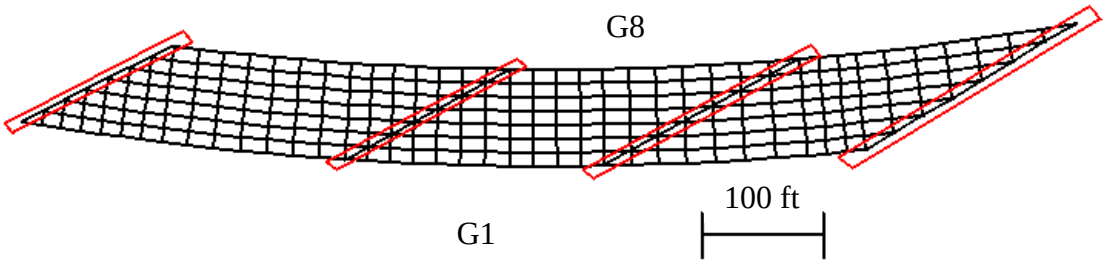

Figure 20. Bridge (T1) EICCS27.

This is an existing bridge in which a number of bolts connecting the cross-frames to the connection plates sheared off after the erection of the steel and before the completion of the structure. The intermediate cross-frames frame directly into the

bearing locations at the interior piers, creating a large (nuisance) transverse stiffness. These cross-frames are subject to high differential deflections.

(U1) EICCS28, Corridor X and I-65 Interchange Ramp NW65X, Jefferson County, AL (*L_s* = 326, 160 and 235 ft; *L_{max}* = 369, 165 and 258 ft; *w_g* = 52.0 ft; *R* = 1255 ft; θ= 0, 47, 54.5 and 0°; *n_g* = 7; *L_s*/*R* = 0.26, 0.13 and 0.19; *L_s*/*w_g* = 6.3, 3.1 and 4.5; *L_s*/*D* = 32.6, 16, 23.5)

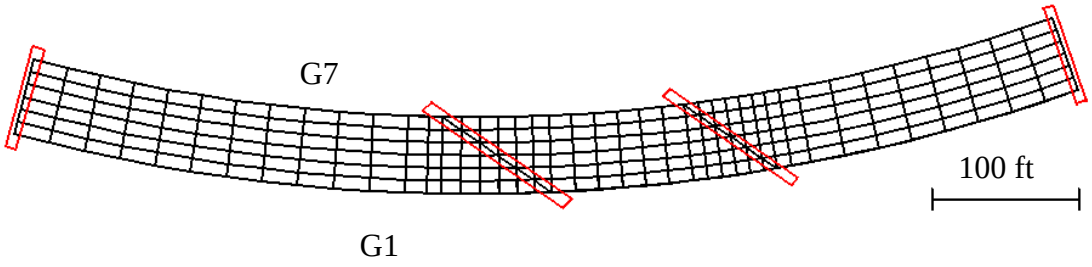

Figure 21. Bridge (U1) EICCS28.

This is an existing bridge which suffered substantial delays during construction due to erection difficulty resulting from a combination of high span length to girder depth ratios, poor span balance, long spans, a tight horizontal curve, sharp skew of the interior bearing lines, substantial transverse (nuisance) stiffness paths and detailing of the cross-frames for TDLF. For the above framing arrangement, the bearing at the first pier from the left on the inside fascia girder experiences significant uplift at the end of the erection and after the deck is placed (in the structural analysis conducted in this research). For this and other reasons, this framing arrangement is considered infeasible to build.

2.2.2 Summary

To succinctly convey the main geometry parameters of the above selected bridges, Table 2 summarizes the span length *L_s*, width *w_g*, radius of curvature *R*, skew angle θ,

subtended angle between the bearing lines L_s/R, length-to-width ratio L_s/w_g or maximum L_{ooc}/w_g, skew index I_s, and the span length-to-depth ratio L_s/D for all of the bridges. These parameters do not capture all of the parametric influences on the bridge responses, but they are certainly some of the most important parameters. It should be noted that the maximum span-to-depth ratio may have a significant impact in some bridges, since if this ratio is large, the bridge may exhibit relatively large displacements during the different stages of construction and in the completed bridge. In straight skewed bridges, the displacements are significantly influenced by the span length and skew index. In curved bridges, the span length and subtended angle between the bearing lines have significant impact on the displacements. In addition, in curved bridges with large length-to-width ratios, the lateral and vertical displacements can be amplified.

Table 2. Summary of the selected 21 I-girder bridges studied in this research.

Bridge Type	**Bridge Letter**	**Bridge Name**	L_s **(ft)**	w_g **(ft)**	R **(ft)**	θ **(deg)**	L_s/R	L_s/w_g ***or*** L_{max}/w_g^*	I_s	L_s/D
Radially-Curved	A	EISCR1	90	17.5	200	0,0	0.45	5.1	0	23.5
	B	NISCR2	150	24	438	0,0	0.34	6.2	0	22.1
	C	NISCR7	150	74	280	0,0	0.54	2.0	0	24.3
	D	NISCR10	225	74	705	0,0	0.32	3.0	0	23.7
	E	EICCR11	310,417, 322	40.3	∞, ∞, 411	0,0, 0,0	0.78	8.0,10.3, 8.1	0	23,29.8, 23.5
	F	NICCR12	350,350, 280	74	909	0,0, 0,0	0.31,0.39	4.7,4.7, 3.8	0	25,25, 20
	G	EICCR4	219,260, 211,162, 256,190	36.7	968, 3@1108, 968,∞	0,0, 0,0, 0,0	0.20,0.24, 0.19,0.15, 0.27,0	6.0,7.1, 5.7,4.4, 7.0,5.2	0	26.5,31.5, 25.6,19.6, 31.0,23.0

Table 2(Continued). Summary of the selected 21 I-girder bridges studied in this research.

Bridge Type	**Bridge Letter**	**Bridge Name**	L_s **(ft)**	w_g **(ft)**	R **(ft)**	θ **(deg)**	L_s/R	L_s/w_g **or** L_{max}/w_g^*	I_s	L_s/D
Straight-Skewed	H	EISSS57	137	61	N/A	69,-4	N/A	3.5	1.19	18.3
	I	NISSS14	150	74	N/A	70,70	N/A	2.0	1.36	25
	J	NISSS54	300	74	N/A	70,70	N/A	4.1	0.68	25
	K	EICSS12	150,139	41	N/A	59.6,59.6, 59.6	N/A	3.7,3.4	0.47,0.50	33.3,30.8
	L	NICSS16	120,150, 150	74	N/A	70,70, 70,70	N/A	1.6,2.0, 2.0	1.69,1.36, 1.36	20,25, 25
	M	EICSS2	239,257, 220	66.6	N/A	58,62, 38,38	N/A	0.48,0.49, 0.23	0.52,0.48, 0.24	26,28, 23.8

Table 2(Continued). Summary of the selected 21 I-girder bridges studied in this research.

Bridge Type	**Bridge Letter**	**Bridge Name**	L_s **(ft)**	w_g **(ft)**	R **(ft)**	θ **(deg)**	L_s/R	L_s/w_g **or** L_{max}/w_g*	I_s	L_s/D
Curved and Skewed	N	NISCS14	150	74	280	53.7,0	0.54	2.0	0.53	25
	O	NISCS15	150	74	280	-35,0	0.54	2.0	0.27	20
	P	EISCS3	153	74	279	52.4,0	0.55	5.0	0.24	27
	Q	NISCS38	300	74	730	62.6,0	0.41	4.1	0.39	23
	R	NISCS39	300	74	730	-35,0	0.41	4.1	0.15	23
	S	XICCS7	160,210, 160	33	700	0,60, 60,0	0.23,0.30, 0.23	4.8,6.4, 4.8	0.31,0.27, 0.30	20.8,27.4, 20.8
	T	EICCS27	279,224, 236	79.9	2546	-53.1,-59.4, -64.4,-69.7	0.11,0.09, 0.09	3.5,2.8, 3.0	0.48,0.70, 0.94	37.2,29.8, 31.5
	U	EICCS28	326,160, 235	52	1255	0,54.5, 47,0	0.26,0.13, 0.19	6.3,3.1, 4.5	0.28,0.44, 0.15	32.6,16, 23.5

* For the straight skewed and curved and skewed bridges, this table reports the maximum fascia girder length (along its arc for curved girders), divided by the width between the fascia girders perpendicular to the girders.

2.2.3. Variation of the Framing Arrangements

In this research, the framing arrangements were studied for all 21 of the base bridge designs discussed in Section 2.2.1. In a number of these bridges, it was apparent that specific improvements in the cross-frame framing arrangements were possible based on the NCHRP Report 725 research and other more recent developments and findings. These improvements relate particularly to the alleviation of significant nuisance transverse stiffness (undesirable transverse stiffness associated with combination of the skew and the cross-frame framing arrangement, leading to large cross-frame forces) via the application of the following guidelines:

1) Provide generous offsets between intermediate cross-frames and skewed supports and avoid large discrepancies in girder unbraced lengths to the extent practicable at skewed bearing lines.
2) Provide cross-frames along skewed bearing lines and avoid framing of intermediate cross-frames directly into bearing locations at interior piers.
3) In straight skewed bridges, stagger the intermediate cross-frames such that common work points on the cross-frames are oriented along lines parallel to the skew, in parallel skew cases, and roughly along lines that fan between the skew angles of the adjacent bearing lines in spans with non-parallel skew.
4) Keep the intermediate cross-frames contiguous within the main portion of the span in curved bridges.

These and other recommendations for improved cross-frame framing arrangements are discussed in Chapter 7.

In this research, the bridge girders and cross-frames were not redesigned given the changes in the framing layouts. The modified base bridges, with the varied framing arrangements, are expected to provide a reasonable first-level estimate of the effect of changes in the framing on the primary factors to be investigated in this research: ease of fit-up during erection of the steel, achievement of the targeted constructed geometry, and generation of locked-in stresses in the cross-frames and girders. It is emphasized that the base designs are actual bridges in service, or bridges that have been designed specifically to satisfy the design criteria of the AASHTO LRFD Specifications.

2.2.3.1.Alternative Framing Arrangements for the Straight Skewed Bridges

Alternative framing arrangements for the straight skewed bridges studied in this research are shown below. The simple-span bridges are shown first followed by the continuous-span bridges. In addition, the bridges are listed in the order of increasing maximum span length within each sub-group.

(H2) EISSS57 (L_s = 137 ft; L_{max} = 211 ft; L_{min} = 63 ft; w_g = 61.0 ft; θ = 69.5° and -4.4°, non-parallel skew; n_g = 7; I_s = 1.19; L_{max}/w_g = 3.5; L_{min}/w_g = 1.0; L_s/D = 18.3)

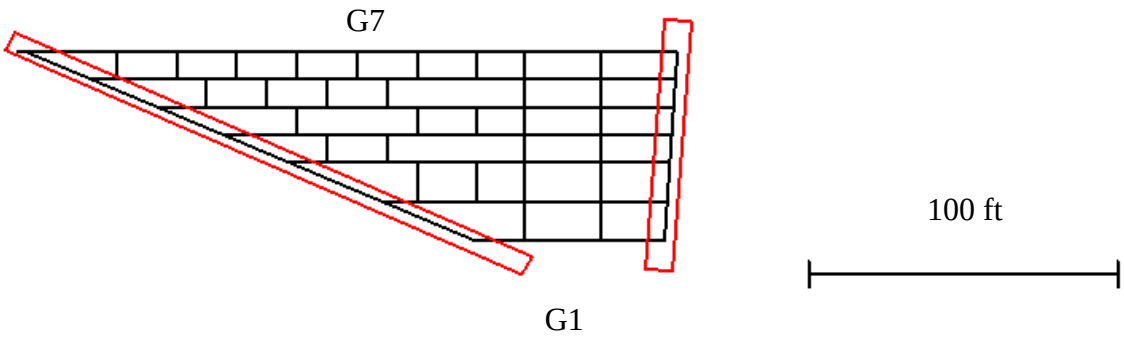

Figure 22. Bridge (H2) EISSS57.

Compared to bridge (H1) (Figure 8), the framing arrangement of bridge (H2) employs slightly larger offsets from the left highly-skewed bearing line, as well as staggered cross-frames near this bearing line. The cross-frames are kept contiguous near the right bearing line.

(I2) NISSS14 (L_s = 300 ft; w_g = 74 ft; θ = 70°, parallel skew; n_g = 9; I_s = 1.36; L_s/w_g = 4.1; L_s/D = 25)

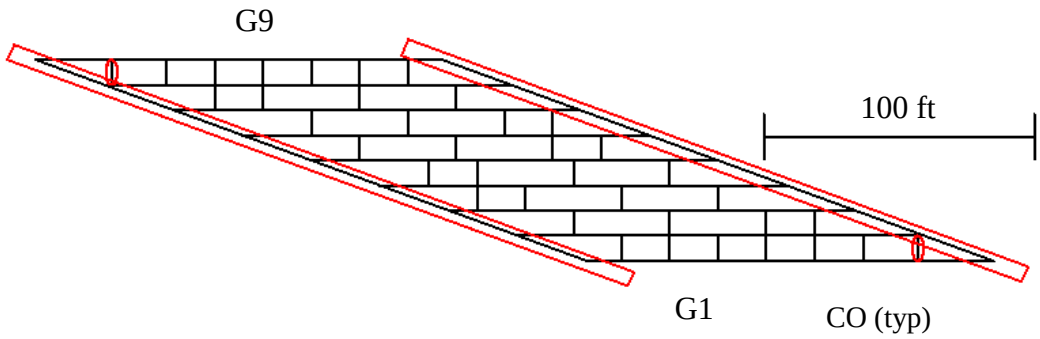

Figure 23. Bridge (I2) NISSS14.

The cross-frames are all equally-spaced in this framing arrangement except for the offsets adjacent to the skewed bearing lines. Seven intermediate cross-frames are attached between the fascia girder and the first interior girder on each side of the bridge. However, compared to bridge (I1) (Figure 9), almost every other cross-frame is intentionally omitted within the interior of the bridge plan. This results in a significant reduction in the overall number of cross-frames being employed in the bridge. The cross-frames that are not omitted are kept in the bridge plan so that the unbraced lengths on the interior girders are equally-spaced except for the unbraced lengths adjacent to the skewed bearing lines.

The diagonal members of the first intermediate cross-frames adjacent to the skewed bearing lines at the acute corner in the exterior bays are removed to alleviate a nuisance

stiffness problem (i.e., the unwanted transverse stiffness caused by the position of these cross-frames and the sharp skew of the bearing lines). The cross-frames highlighted by an oval and labeled on this plan view as "CO" (for "chords only") do not contain any diagonals. This is to allow for a small offset of these cross-frames relative to the skewed bearing lines (i.e., the highlighted cross-frames do not intersect exactly at the skewed bearing lines) without inducing large cross-frame forces from nuisance transverse stiffness effects.

(J2) NISSS54 (L_s = 300 ft; w_g = 74 ft; θ = 70°, parallel skew; n_g = 9; I_s = 0.68; L_s/w_g = 4.1; L_s/D = 25)

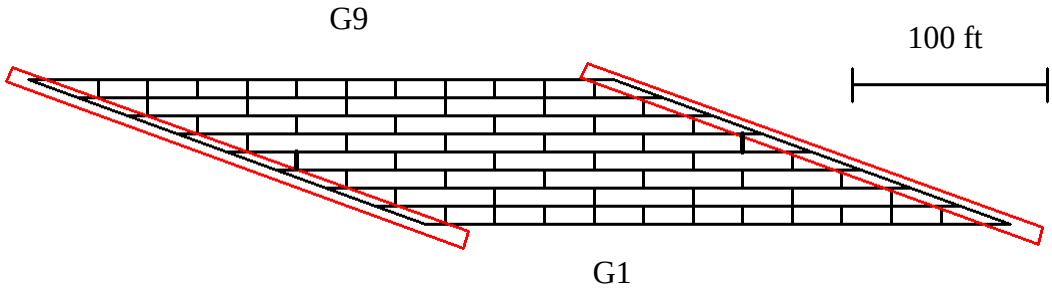

Figure 24. Bridge (J2) NISSS54.

The considerations in selecting the framing arrangement for bridge (J2) NISSS54 are similar to the considerations for bridge (I2) NISSS14 (Figure 23). However, all the cross-frames have diagonal members in this alternative framing plan. Compared to bridge (J1) (Figure 10), the framing arrangement of bridge (J2) results in a significantly reduced number of cross-frames in the bridge system. Not only does this provide cost savings by reducing the large cross-frame forces caused by nuisance transverse stiffness effects; significant savings are achieved by the sheer reduction in the number of cross-frames in the bridge.

(K2 and K3) EICSS12, US 82 Mainline Underpass at 19th Street WB, Lubbock, TX (L_s = 150 and 139 ft; w_g = 41.0 ft; θ = 59.6°, parallel skew; n_g = 6; I_s = 0.47 and 0.50; L_s/w_g = 3.7 and 3.4; L_s/D = 33.3, 30.8)

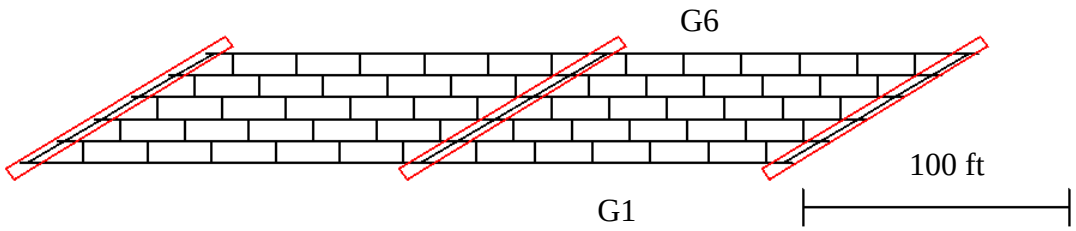

Figure 25. Bridge (K2) EICSS12.

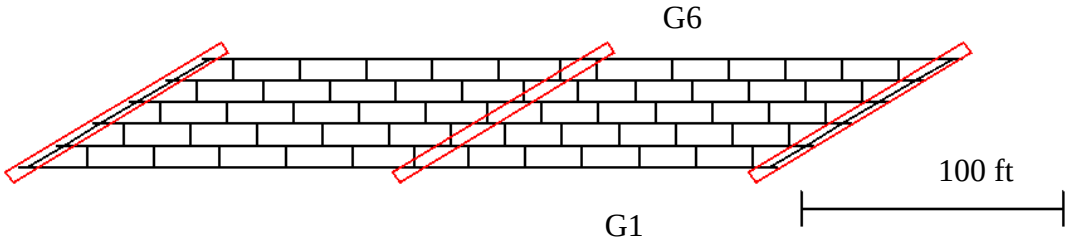

Figure 26. Bridge (K3) EICSS12.

The framing arrangements of bridge cases (K1), and (K2) and (K3) EICSS12 are studied to understand the effectiveness of staggered cross-frames versus lean-on cross-frames with respect to fit-up. Compared to bridge (K1) (Figure 11), bridge (K2) provides a larger offset of the intermediate cross-frames relative to the skewed bearing lines at the interior pier and at the abutments. Skewed bearing line cross-frames are used at the interior pier for bridge (K2). In addition, bridge (K2) employs a staggered cross-frame arrangement within the span.

The considerations for bridge (K3) are similar to bridge (K2). Bridge (K3) does not use any skewed bearing line cross-frames at the interior pier, but provides an intermediate

cross-frame normal to the girder on one or both of its sides at each of the bearings at the interior pier.

(M2) EICSS2, I-235 EB over E. University Ave., Polk Co., IA (L_s = 239, 257 and 220 ft; L_{max} = 259, 255 and 220 ft; L_{min} = 241,183 and 220 ft; w_g = 66.6 ft; θ = 58°, 61.8°, 38° and 38°; n_g = 8; I_s = 0.52, 0.48, and 0.24; L_{max}/w_g = 3.9, 3.8 and 3.3; L_{min}/w_g = 3.6, 2.7 and 3.3; L_s/D = 26, 28, 23.8)

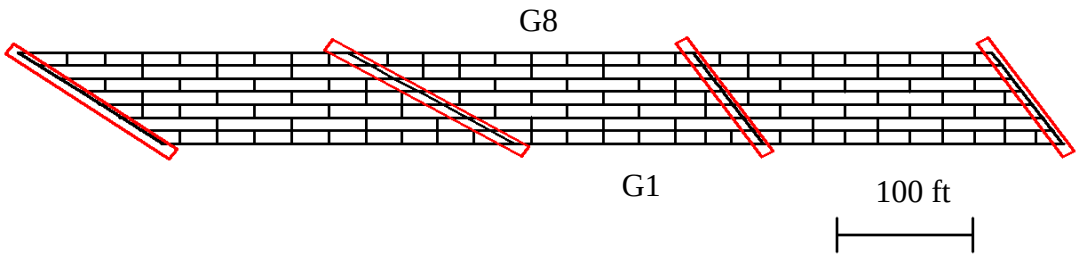

Figure 27. Bridge (M2) EICSS2.

The considerations for bridge (M2) EICSS2 are similar to the considerations for bridge cases (I2) NISSS14 (Figure 23) and (J2) NISSS54 (Figure 24). Because the center span has a non-parallel skew, a number of cross-frames were taken out to ensure that the offsets from the bearing lines are greater than the recommended minimums. In addition, cross-frames are provided at the skewed bearing lines at the interior piers, and the intermediate cross-frames are offset from the skewed bearing lines at the interior piers and at the abutments.

2.2.3.2.Alternative Framing Arrangements for the Curved and Skewed Bridges

Alternative framing arrangements for the curved and skewed bridges studied in this research are shown below. The simple-span bridges are shown first followed by the

continuous-span bridges. In addition, the bridges are listed in the order of increasing maximum span length within each sub-group.

(O2) NISCS15 (L_s = 150 ft; L_{max} = 195 ft; L_{min} = 103 ft; w_g = 74 ft; R = 280 ft; θ = -35° and 0°; n_g = 9; L_s/R = 0.54; L_s/w_g = 2.0; $(L_{max} - L_{min})/(L_{max} + L_{min})$ = 0.31; L_s/D = 20)

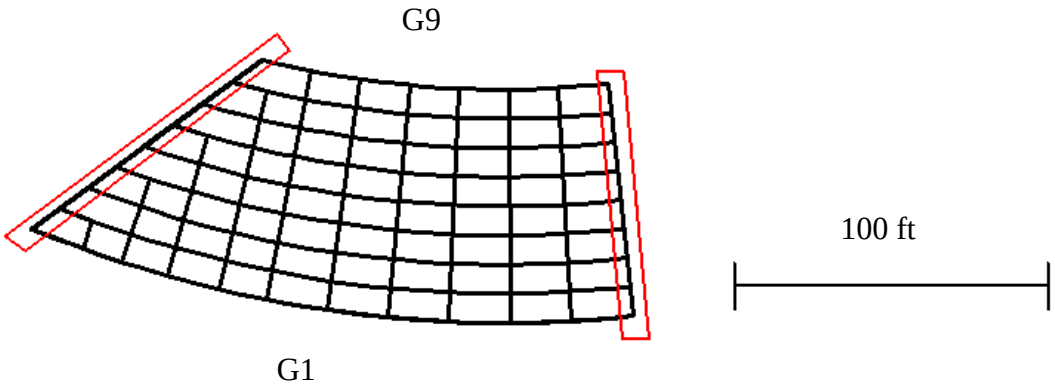

Figure 28. Bridge (O2) NISCS15.

The framing arrangement of bridge (O2) NISCS 15 has contiguous cross-frames instead of staggered cross-frames near the skewed bearing line as in bridge (O1) (Figure 15). The first intermediate cross-frames exceed the recommended minimum offset distance from the left skewed bearing line (see Section 7.1). By using a contiguous cross-frame arrangement, the overall rotations and deflections of bridge (O2) are reduced because of the increased engagement of the girders in developing the overall width of the structural system. However, at the skewed bearing line, uplift occurs at the support for the girder on the inside of the curve as well as for the adjacent interior girder. Uplift is encountered both at the end of the steel erection and in the completed structure. The uplift is resisted by using a tie-down device.

(Q2) NISCS38 (L_s = 300 ft; L_{max} = 366 ft; L_{min} = 249 ft; w_g = 74 ft; R = 730 ft; θ = 62.6° and 0°; n_g = 9; L_s/R = 0.41; L_s/w_g = 4.1; $(L_{min} - L_{max})/(L_{min} + L_{max})$ = -0.19; L_s/D = 23)

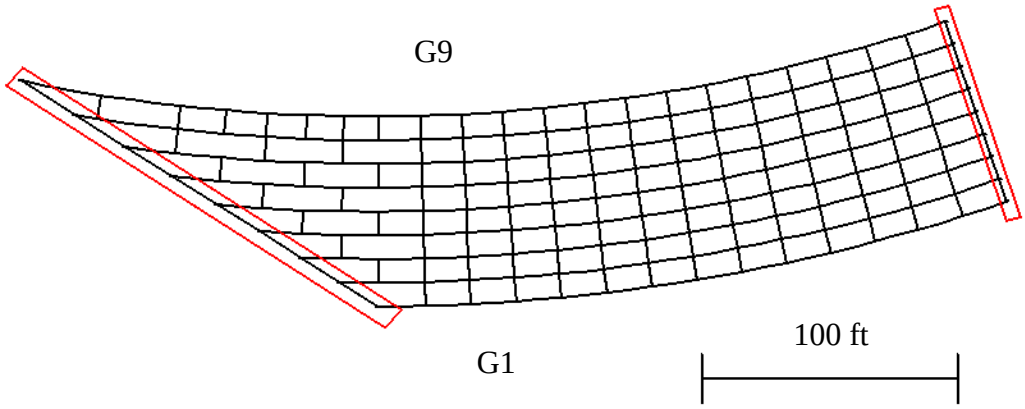

Figure 29. Bridge (Q2) NISCS38.

The framing arrangement of bridge (Q2) NISCS38 has staggered cross-frames near the left-hand skewed bearing line. The first intermediate cross-frames are offset at a minimum distance from the skewed bearing line. Studying bridge cases (Q1) (Figure 17) and (Q2) provides a better understanding of the influence of contiguous versus staggered cross-frame arrangements in curved and skewed bridges where the skew orientation makes the inside girder (i.e., the girder on the inside of the curve) longer.

(R2) NISCS39 (L_s = 300 ft; L_{max} = 340 ft; L_{min} = 258 ft; w_g = 74 ft; R = 730 ft; θ = -35^o and 0^o; n_g = 9; L_s/R = 0.41; L_s/w_g = 4.1; $(L_{max} - L_{min})/(L_{max} + L_{min})$ = 0.14; L_s/D = 23)

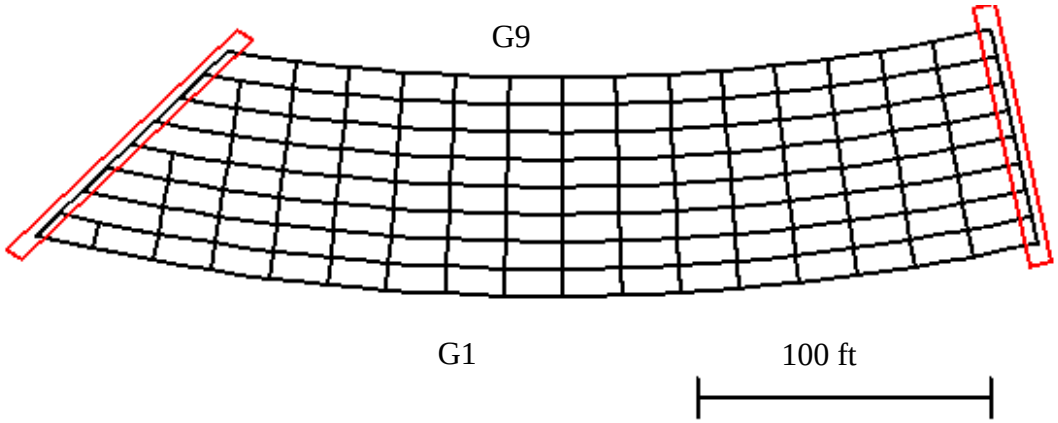

Figure 30. Bridge (R2) NISCS39.

Bridge cases (R1) (Figure 18), (R2) NISCS39, (O1) (Figure 15) and (O2) NISCS15 (Figure 28) have a skew orientation that makes the outside girder significantly longer. Bridge (R2) uses a contiguous cross-frame arrangement adjacent to the skewed bearing line. Due to increased development of the girders by the contiguous cross-frames, bridge (R2) experiences significant uplift at the girder on the inside of the curve as well as at the adjacent interior girder at the skewed bearing line. The magnitude of the uplift force, 457 kip, is too large to be offset by a typical tie-down device or a counter-weight. This framing arrangement is considered infeasible to build.

(T2) EICCS27, SR 386 over SR6 and Ramp F, Sumner Co., TN (L_s = 279 ft, 224 ft, and 236 ft; L_{max} = 279, 239 and 231 ft; L_{min} = 268, 214 and 217 ft; w_g = 79.9 ft; R = 2546 ft; θ= -53.1, -59.4, -64.4 and -69.7°; n_g = 8; L_s/R = 0.11, 0.09 and 0.09; L_s/w_g = 3.5, 2.8 and 3.0; $(L_{min} - L_{max})/(L_{min} + L_{max})$ = -0.02, -0.03 and -0.01; L_s/D = 37.2, 29.8, 31.5)

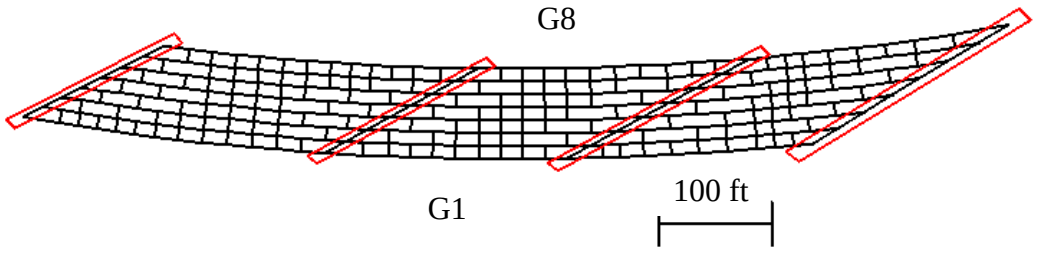

Figure 31. Bridge (T2) EICCS27.

Bridge (T2) has staggered cross-frames near the skewed bearing lines while using cross-frames along the skewed bearing lines both at the interior piers and at the abutments. In addition, intermediate cross-frames are offset by more than the recommended minimum distance from the skewed bearing lines, discussed further in Section 7.1.

(U2) EICCS28, Corridor X and I-65 Interchange Ramp NW65X, Jefferson County, AL (*L_s* = 326, 160 and 235 ft; L_{max} = 369, 165 and 258 ft; w_g = 52.0 ft; R = 1255 ft; θ= 0, 47, 54.5 and 0°; n_g = 7; L_s/R = 0.26, 0.13 and 0.19; L_s/w_g = 6.3, 3.1 and 4.5; L_s/D = 32.6, 16, 23.5)

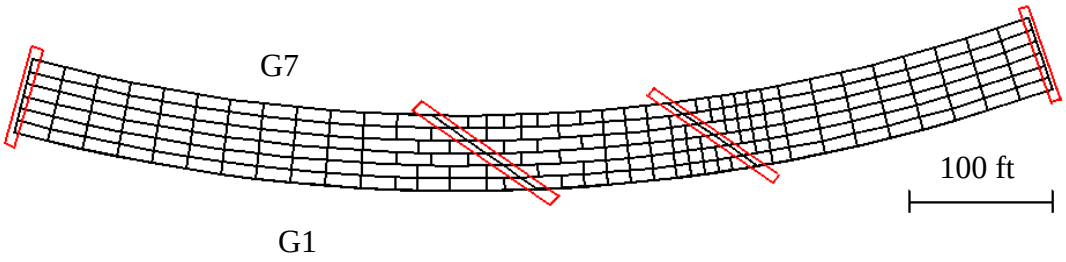

Figure 32. Bridge (U2) EICCS28.

Significant uplift (at the inside girder at the first interior pier from the left-hand abutment) and high cross-frame forces were experienced in bridge (U1) EICCS28 (Figure 21). Bridge (U2) alleviates the uplift at this support as well as the large forces in the adjacent cross-frame members by staggering the cross-frames near the first interior pier from the left abutment. The cross-frames are offset by the recommended minimum distance, and bearing line cross-frames are used along the skew at the interior piers. The cross-frames near the second interior pier from the left-hand abutment have relatively low forces whether these cross-frames are staggered or contiguous.

2.2.4. Variation of the Cross-Frame Detailing Methods

In this research, the three main types of cross-frame detailing, No-Load Fit (NLF), Steel Dead Load Fit (SDLF) and Total Dead Load Fit (TDLF), are varied and applied to the 21 base designs and their framing variations.

It is necessary to study NLF detailing for all the cases since this is the base case from which the SDLF and TDLF effects are measured. It should be noted that SDLF and TDLF detailing of the cross-frames generally results in significant changes to the dead load cross-frame internal forces as well as the dead load flange lateral bending stresses in the girders. The research did not conduct any full redesign of the base bridges and their framing variations to account for the modified internal forces from the detailing of the cross-frames. In all cases, it is emphasized that the base bridge were analyzed for design, and for setting the girder cambers, using the current customary practice within the bridge design industry, which is to analyze the bridge structural system dead load effects by simply "turning gravity on," without considering the locked-in force effects associated with the cross-frame detailing (i.e., assuming NLF detailing). The simulation studies conducted in this research

include the initial lack-of-fit effects associated with SDLF and TDLF detailing directly and rigorously in the corresponding structural analysis.

It is important to note that, in this research, the cambers used for SDLF or TDLF detailing are calculated from a line girder analysis (LGA) for the straight bridges and from 3D FEA for the curved bridges, unless noted otherwise. In straight skewed bridges, the use of cambers from LGA gives the closest match to the ideal zero girder layovers and internal stresses under the targeted dead load conditions. The use of cambers from an accurate 2D Grid or 3D FEA gives non-zero girder layovers and flange lateral bending stresses. However, these layovers and stresses are small compared to the overall dead load responses under the targeted conditions. Therefore, the ultimate recommendation from this researchis that the engineer should not mix the methods of analysis being applied to a given bridge. That is, if a refined analysis is employed for the overall bridge design (i.e., grid analysis or 3D FEA), the cambers also should be calculated based on the refined analysis. The influence of camber calculations (accurate refined analysis versus LGA) in straight skewed bridges is discussed in Chapter 9.

The specific procedures used for LGA and 3D FEA, including the incorporation of the effects of the detailing methods considered in this research in the structural analysis simulations, are discussed in Chapter 3.

2.2.5. Selection of Erection Schemes

Erection schemes were selected for the 21 bridges listed in Sections 2.2.1 and 2.2.3. The research analyzed the erection stages for both the base design and alternate framing arrangements. For the existing bridges, the erection schemes followed the as-built scheme, if available. This allowed for an evaluation of the as-built scheme fit-up difficulty and

comparison with available field observations for bridge cases such as (E) EICCR11, (M1) EICSS2, and (U1) EICCS28. For existing bridges whose erection schemes were unavailable and for the parametric bridges, the erection schemes were devised so that the fit-up forces were manageable. These erection schemes are not necessarily the "optimum" schemes, but they provide for feasible and practical erection of the bridge.

Detailed erection plans with numerous stages were developed for all 21 bridges. When developing the erection plans, the locations of the field splices, the segment length that can be lifted in the field, and girder stability during erection (particularly important for curved girders) were considered. The research then selected what were expected to be the most critical erection stages, i.e., stages that were expected to experience potential fit-up difficulty, for detailed simulation.

For straight skewed bridges, when erecting girder by girder, the later stages have a higher skew index. As a result, the collateral effects due to the skew are more substantial during the later stages. For curved bridges, substantial vertical support from shoring towers and/or cranes is often necessary in the early stages. The later stages often involve less vertical support from shoring towers and/or cranes, and thus have higher fit-up forces. Due to these characteristics, the critical erection stages are often the last few stages for both straight and curved bridges.

For continuous-span bridges, or simple-span bridges with long span lengths, a sufficient number of stages were selected to illustrate the bridge behavior as the erection progresses. For a number of curved bridges, two erection methods were selected to investigate the effects of erecting from the inside to the outside of the curve and vice versa.

Support uplift often is more apt to occur during erection. In all cases, the analyses conducted allowed the girders to uplift at any support locations that did not have a tie-down.

Unless noted otherwise, the shoring and crane elevations are modeled at the no-load elevations for all the curved radially-supported and curved and skewed bridges studied in this research. This idealization of the shoring and crane elevations is applied regardless of the cross-frame detailing method. For straight skewed bridges, the shoring and crane elevations are modeled at the steel dead load elevations (i.e., the steel dead load elevations in the completed bridge system) in all cases, unless noted otherwise. The rationale for these assumptions is as follows:

- The girder fabricated geometries are of course the no-load geometry.
- In addition, the girder splices are commonly detailed for the no-load geometry.
- In cases where the girders can be installed sequentially along the length of the bridge, without the need for any drop-in segments, the field section that is being installed can be knifed-in to the splice with the previous field section, as long as attention is paid to the orientation of the splice and vertical clearances between the field section that is being installed and permanent support locations. However, for cases involving drop-in segments, the completion of the second girder splice of the drop-in segment can be greatly facilitated by having the steel on both sides of the splice in the approximate non-load geometry.

- The cross-frame fit-up forces in horizontally curved bridge units tend to be minimized, as an approximate target, by hold points and temporary supports that are located at the no-load elevations.

- For straight skewed bridges, the fit-up of the cross-frames often can be achieved most easily by allowing the girders to deflect under their self-weight. Particularly when Steel Dead Load Fit (SDLF) detailing is employed, the resulting girder elevations will be very close to their Steel Dead Load (SDL) elevations in the completed bridge. This condition is of course achieved approximately by locating the girder hold and temporary support points at the final SDL elevations of the completed bridge.

Erection simulations for straight skewed bridges with NLF detailing are not considered in this research. This is because the sharp skews associated with the bridges considered in this work would cause high girder layovers and large rotation demands on the bearings if NLF detailing was used.

2.2.6. Post-Processing of Analysis Results

Data from these studies were collected, synthesized, and analyzed to quantify the influence of the various parameters on the three primary factors investigated in this research: ease of fit-up during erection of the steel, achievement of the targeted constructed geometry, and generation of locked-in stresses in the cross-frames and girders. This includes the development of force summary tables for each analysis case, and tabulation of the summary results of the girder layovers, the girder vertical displacements, the girder elevation profiles, the girder major-axis bending stresses, the girder flange lateral bending stresses, and the cross-frame forces. Various graphs and plots of the data are provided to

allow effective visualization of the responses. The tables, graphs and plots were generated automatically to the maximum extent possible via advanced programming tools utilized within the NCHRP Report 725 research plus some additional refinements to those tools.

CHAPTER 3

CONCEPTS AND PROCEDURES FOR INCLUDING CROSS-FRAME DETAILING EFFECTS DIRECTLY IN THE STRUCTURAL ANALYSIS

Cross-frame detailing methods can have a significant influence on the bridge responses in the completed bridge as well as during construction. In straight skewed bridges, SDLF and TDLF detailing effects are beneficial, i.e., they are subtractive relative to the dead load effects on the cross-frame forces and girder flange lateral bending stresses. However, in curved radially-supported bridges, SDLF and TDLF detailing effects tend to be additive with the dead load effects on the cross-frame forces and flange lateral bending stresses. In addition, in curved and skewed bridges, SDLF and TDLF detailing effects can either increase or decrease the cross-frame forces and flange lateral bending stresses depending on many complex factors. This section presents general procedures for including cross-frame detailing effects directly in the structural analysis.

Section 3.1 discusses the initial lack-of-fit associated with the cross-frame detailing methods in curved and/or skewed I-girder bridges. Section 3.2 then addresses the calculation of initial strains and initial fixed-end forces via the software GT-LOFT, a "Lack of Fit analysis Tool" developed as part of this research. Examples are provided illustrating the inclusion of the detailing effects via initial strains in 3D FEA (Section 3.3) and via initial fixed-end forces in a grid analysis (Section 3.4). The examples consider both a representative straight skewed bridge and a representative curved radially-supported bridge.

3.1. Calculation of the Initial Lack-of-Fit due to SDLF or TDLF Detailing

When the cross-frames are detailed for either SDLF or TDLF, they do not fit up with the girders in their cambered, plumb, no-load (NL) geometry. This initial lack-of-fit between the cross-frames and the girders consists of two components: the lack-of-fit due to the girder vertical displacements and the lack-of-fit due to the girder major-axis bending rotations. These components are referred to as the vertical and the rotational lack-of-fit displacements in the following discussions.

3.1.1. Initial Vertical Lack-of-Fit Displacements

Figure 33 illustrates a cross-frame, detailed for SDLF or TDLF within the span of a curved and/or skewed I-girder bridge. The girders are assumed to be in their idealized cambered, plumb, NL geometry in this sketch. As a simplification, the geometric factors involving superelevation, grade and vertical curve are not shown. Therefore, the targeted final girder elevations under the TDL, measured for instance as the elevations at the top of the girder webs, fall within a single horizontal plane. The cross-frame in Figure 33 is assumed to be attached to the connection plate on the left-hand girder. However, it does not fit up with the work points at the connection plate on the right-hand girder. This is because the cross-frame is detailed to fit to the girders in an idealized plumb SDL or TDL condition. The cross-frame initial vertical lack-of-fit displacement may be calculated as follows:

- For SDLF detailing, the initial vertical lack-of-fit displacement is equal to the difference between the negative of the girder SDL vertical deflections on each side of the cross-frame, referred to as the differences in the girder SDL cambers in this research.

- For TDLF detailing, the initial vertical lack-of-fit displacement is equal the difference in the negative of the girder TDL deflections on each side of the cross-frame. That is, the initial vertical lack of fit is equal to the difference in the girder TDL cambers.

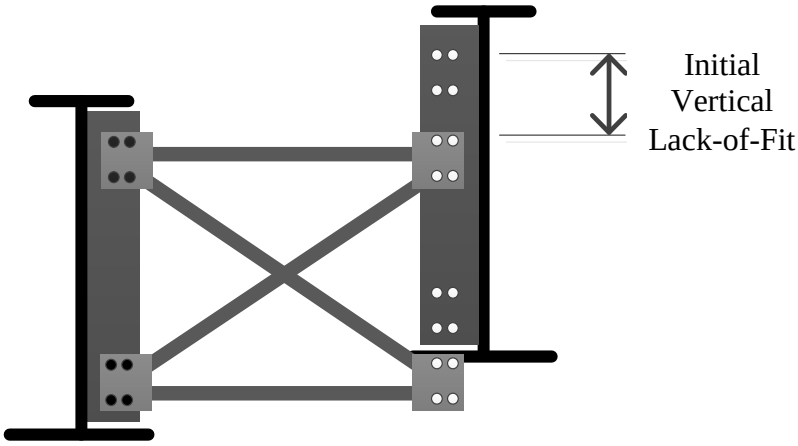

Figure 33: Illustration of the initial vertical lack-of-fit. The girders are in their idealized fully-cambered, plumb, NL geometry and the cross-frame is in its unstressed geometry detailed for SDLF or TDLF. The cross-frame is connected only to the left-hand girder.

The initial vertical lack-of-fit displacement characterize the shear racking deformation that the cross-frame must be subjected to if vertical displacement compatibility is maintained with the girders in their fully-cambered NL geometry.

3.1.2. Initial Rotational Lack-of-Fit Displacements

Figure 34 shows a representative elevation view of a girder in a simply-supported curved and/or skewed bridge. The girder height is exaggerated for purposes of illustration. The dashed lines show the girder in its final, ideal (flat) TDL geometry with a plumb girder web. The solid lines show the girder in its idealized fully-cambered, plumb, NL geometry. The connection plates and cross-frames are not shown for clarity. It is assumed that the

girder is attached to skewed bearing-line cross-frames at its ends. In the following, the skewed end cross-frames are used to explain the mechanics of the initial rotational lack-of-fit for the case of TDLF detailing. The behavior for SDLF detailing is similar.

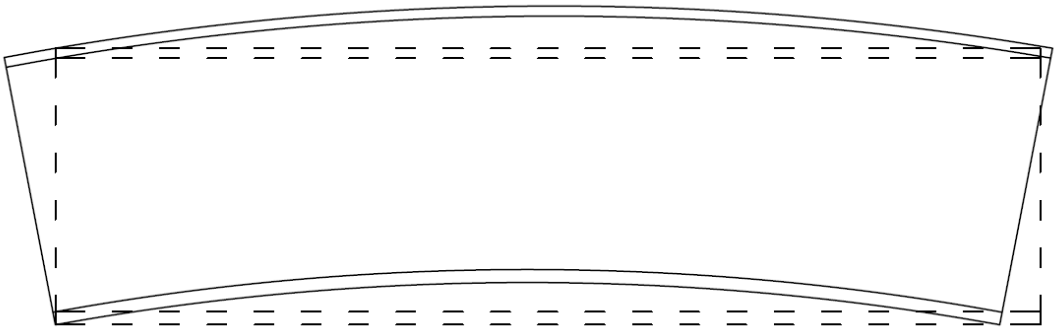

Figure 34. Illustration of the major-axis bending rotation due TDL cambers. The dashed lines show the girder in its final, ideally TDL elevations with plumb girder web. The solid lines show the girder in its idealized fully-cambered, plumb, NL geometry. The girder is assumed fixed in the longitudinal direction at the bottom flange on the left-hand end.

With TDLF detailing, the end cross-frames fit to the vertically-oriented connection plates on the targeted TDL geometry of the girders, shown by the dashed lines. When the bridge is in the NL geometry, the girders are cambered upwards and the end connection plates are no longer vertical. The girder end major-axis bending rotations in the NL geometry can be calculated from the TDL cambers by assuming that the girder cross-sections (and the end connection plates) are perpendicular to the flanges. The girder TDL cambers, as well as the girder TDL major-axis bending camber rotations, are often different for different bridge girders.

As stated above, the end cross-frames are detailed such that they fit exactly to the girders in their final deflected (flat) TDL positions without any forcing. However, the end cross-frames have to deform to maintain compatibility with the work points at the girder connection plates in the fully-cambered NL geometry. The change in the vertical

displacements at the girder ends is zero in going from the final TDL configuration to the fully-cambered NL configuration. However, the girder ends experience a major-axis bending rotation in going from the flat TDL geometry to the fully-cambered NL geometry. The corresponding displacements imposed on the end cross-frames at their connections to the girders are the rotational lack-of-fit displacements. Note that if the end cross-frames are perpendicular to the girders, and if the girder camber rotations on each side of the cross-frames are the same, the rotational lack-of-fit at the end cross-frames is zero. In this case, the cross-frames are subjected simply to rigid-body rotation due to the major-axis bending camber rotations at the girder ends. However, if the end cross-frames or skewed and/or the end girders have different major-axis bending camber rotations, the cross-frames are subjected to non-zero rotational lack-of-fit displacements to maintain compatibility with the girder workpoints.

The initial rotational lack-of-fit displacements characterize the deformations that the cross-frames must be subjected to if rotational compatibility is maintained with the girders in their fully-cambered NL geometry.

In general, both the girder TDL cambers and the girder TDL major-axis bending camber rotations are different on each side of an intermediate cross-frame. The difference in the girder cambers between the sides of a cross-frame is the vertical lack-of-fit. In addition, intermediate cross-frames also generally have a rotational lack-of-fit whenever they have a non-zero TDL camber rotations and a non-zero skew relative to the girders, and/or when the girders have a different major-axis bending camber rotation at opposite sides of a cross-frame.

The cross-frame vertical and rotational lack-of-fit displacements are calculated generally by performing a position vector analysis on the work points at the cross-frame to girder connections. For this purpose, the girders are assumed fixed in the longitudinal direction at the bottom flange at their left-hand ends in the elevation views in this work. Because the total length along the girder centroid is unchanged (assuming zero axial load within the girder), the distance from the fixed point on the bottom flange to the bottom flange at the opposite end of the girder is shorter in the no-load condition compared to the targeted TDL condition (see Figure 34). The girders generally shift longitudinally as the girder TDL vertical deflections and major-axis rotations occur. These longitudinal displacements are included in a position vector analysis to determine the total displacements of the work points on the girders at the cross-frame connections. Given typical girder length-to-depth ratios, the above longitudinal movements are commonly an order of magnitude smaller than the corresponding girder maximum vertical deflections. Therefore, although there is some lack-of-fit of the cross-frames associated with these movements, the predominant lack-of-fit effects are the vertical and rotational lack-of-fit discussed above.

The total initial lack-of-fit is the summation of the initial vertical lack-of-fit and initial rotational lack-of-fit. For cross-frames at different locations in a bridge, the contribution of each of the components to the total initial lack-of-fit varies as discussed below:

- At skewed bearing line cross-frames, where the vertical deflections are zero, the initial rotational lack-of-fit is the only lack-of-fit component.
- For intermediate cross-frames that frame normal to the girder tangents, the initial vertical lack-of-fit is the dominant component.

- For skewed intermediate cross-frames, the initial vertical and rotational lack-of-fit are both significant components.

3.2. Calculation of Initial Strains and Initial Fixed End Forces due to the Lack-of-Fit from SDLF or TDLF Detailing

Various methods are possible to account for the influence of cross-frame detailing methods. However, many of these methods are approximate and may not always properly capture the effects. The most accurate and direct approach is to either include the initial strains or stresses due to the above vertical and rotational initial lack-of-fit displacements in a 3D FEA model, or the corresponding fixed-end forces due to these displacements in a grid analysis model. Any 3D FEA software that is already capable of modeling thermal loading has the capability to include the initial strains due to the initial lack-of-fit. In addition, the corresponding fixed-end forces can be calculated for the beam elements representing the cross-frames in any grid analysis software. The negative of these forces can be applied to the nodes at the ends of the cross-frames in a grid analysis to model the initial lack-of-fit effects.

3.2.1. Calculation of the Initial Strains in 3D FEA Software

Generally speaking, any matrix analysis software where the structure is modeled in three dimensions may be referred to as a three-dimensional finite element analysis (3D FEA). The NCHRP Report 725 research and this research adopt the more restrictive definition of 3D FEA stated by AASHTO/NSBA G13.1 (2011). According to G13.1, an analysis method is classified as 3D FEA if:

1) The superstructure is modeled fully in three dimensions,
2) The individual girder flanges are modeled using beam, shell, or solid type elements,

3) The girder webs are modeled using shell or solid type elements,
4) The cross-frames or diaphragms are modeled using truss, beam, shell, or solid type elements as appropriate, and
5) The concrete deck is modeled using shell or solid elements (when considering the response of the composite structure).

The cross-frame initial strains can be obtained directly from 3D FEA software, by imposing the vertical deflections associated with the girder dead load cambers. The procedure is as follows:

- A specified displacement analysis can be run in which the girders are displaced from the configuration where the they are in their desired, plumb final dead load configuration to the configuration where the girders are "locked" in their no-load, plumb, and fully-cambered geometry. In this work, the nodal vertical displacements (from the corresponding camber profiles) are applied to the bottom flange nodes of the girders throughout the girder lengths.
- The cross-frames are subjected to the initial strains associated with the corresponding initial lack-of-fit by maintaining compatibility with the girder displaced configurations at the cross-frame connection points.
- For SDLF detailing, the above nodal displacements are the negative of the SDL displacements, which are referred to as the SDL cambers in this work.
- For TDLF detailing, the above nodal displacements are obtained from the girder TDL camber profiles. That is, for TDLF detailing, the nodal displacements are the TDL cambers (i.e., the negative of the girder TDL vertical displacements).

- By definition, the girders are restrained from any lateral displacements in this 3D FEA solution. Only the girder vertical displacement effects, and the corresponding girder major-axis bending rotations, are considered.

It should be noted that the above initial strains are simply a computational device to account for the initial lack-of-fit. Therefore, even if the corresponding initial stress is larger than the material yield strength, the material behavior should be assumed to be linear elastic.

One should note that in the above specified displacement analysis, the elastic modulus for the cross-frame members should be set to a value significantly smaller than the physical elastic modulus (1000 times smaller is used in this research). This avoids local web deformations in the girders due to potentially large "initial" stresses and the corresponding longitudinal force components introduced to the girders from cross-frame members.

The initial strains for SDLF and TDLF detailing of the bridge cases studied in this research are calculated using the 3D FEA ABAQUS software. Special-purpose tools were developed and used to facilitate the calculation of the initial strains in the 3D FEA software and for including these initial strains in the simulations of the bridge cases.

3.2.2. Calculation of the Initial Strains for 3D FEA using GT-LOFT

Running the above displacement analysis in a 3D FEA software system to obtain the initial strains due to the cross-frame detailing methods can be time consuming, and not all bridge programs are capable of easily running such an analysis. Therefore, the GT-LOFT software tool was developed as part of this research to facilitate the calculation of cross-frame initial strains, which can then be specified in the cross-frame elements of the bridge

analysis software (assuming the software has capabilities for directly modeling initial strains, such as for modeling thermal deformations). The tool utilizes an Excel spreadsheet to specify the bridge inputs and MATLAB to calculate the initial strains. Based on the bridge inputs, the tool determines the spatial position of the work points on the girders in the final plumb targeted dead load geometry and in the plumb fully-cambered geometry. The tool assumes that the connection plates are effectively rigid and are normal to the girder flanges. The influence of connection plates that are not normal to the flanges, typically plates that are desired to be vertical in the final girder geometry (including any effects of grade and/or vertical curve), is assumed to be small. Also, any superelevation is assumed to have a negligible effect on the bridge structural actions.

The calculation of the initial strains depends on the cross-frame type and the element formulation. The discussions below give the initial engineering strain calculations, suitable for use in a geometrically linear (i.e., first-order) elastic analysis, as well as rotated engineering strains and log strains, suitable for use in a geometrically nonlinear analysis in which the cross-frame element formulation is based on either of these strain measures. The geometrically nonlinear versions of the B31 (beam) and T3D2 (truss) elements utilized in ABAQUS are based on log strain. The tool uses a right-handed Cartesian coordinate system for straight skewed bridges and a cylindrical coordinate system for horizontally curved bridges. For straight bridges, the girders span in the positive direction of the X-axis and the non-skewed cross-frames are considered to frame between the girders in the positive direction of the Y-axis. The coordinate origin is at the start of Girder 1 which is the bottom girder on the plan view for straight bridges. For curved bridges, $\theta = 0$ is taken

at the intersection of ray from the center of curvature to the centerline of the bridge cross-section.

The initial strain calculation varies depending on whether the analysis being conducted is geometrically linear (first-order) or geometrically nonlinear (second-order), and if the analysis is second-order, the strain measure upon which the elements used to model the cross-frame members are based. Geometrically linearly (first-order) elements are based on engineering strain, whereas common geometrically nonlinear element formulations are often based on rotated engineering strain or log strain. For X-type cross-frames, the cross-frame initial strains are calculated for these different cases as follows:

(1) Initial engineering strain:

$$\varepsilon = \frac{L' - L_o}{L_o} \qquad \text{Eq. (2a)}$$

where:

$$L' = \frac{L_x L_{xo} + L_y L_{yo} + L_z L_{zo}}{L_o} \qquad \text{Eq. (2b)}$$

= Projection of the cross-frame member length corresponding to the girder fully-cambered geometries onto the targeted dead load orientation of the member; the member length being projected here is the length that the cross-frame members must be stretched or compressed to in order to connect to the girders in their fully-cambered geometries.

L_o = Cross-frame member length in the targeted dead load condition.

L_x, L_y, L_z = Cross-frame member length components in the fully-cambered geometry of the bridge system, corresponding to the global X, Y, and Z directions, respectively; for curved bridges, the lengths in the R, θ, Z coordinates are transformed to a global X, Y, Z system for this calculation.

L_{xo}, L_{yo}, L_{zo} = Cross-frame member length components in the targeted dead load geometry of the bridge system, corresponding to the X, Y, and Z global directions, respectively.

(2) Initial rotated engineering strains:

$$\varepsilon = \frac{L - L_o}{L_o} \qquad \text{Eq. (3)}$$

where,

L = Cross-frame member length in the fully-cambered geometry of the bridge system

(3) Initial log strains:

$$\varepsilon = \ln \frac{L}{L_o} \qquad \text{Eq. (4)}$$

For V or inverted-V cross-frames, when the girders are in their plumb fully-cambered position, the positions of the chord middle node where the diagonals frame in cannot be found by kinematics alone. GT-LOFT has a built-in matrix analysis that solves for the engineering initial strains based on the displacements calculated at each of the cross-frame work points on the girders. For the rotated engineering or log initial strains, the tool

calculates the location of the chord middle node in the geometry corresponding to the fully-cambered girder profiles from a geometric linear structural analysis and then solves for the rotated engineering and log initial strains via Eqs. (3) and (4). Benchmarking studies show that there is negligible error associated with the determination of the middle node displacements by this simpler geometrically linear analysis, followed by calculation of the rotated engineering or log initial strains.

The Excel spreadsheet has three input worksheets: General, Cross-Frames, and Section Changes. In the General sheet, the user specifies the negative of the girder SDL vertical displacements (defined as the "SDL cambers") for SDLF detailing and the negative of the girder TDL vertical displacements (the TDL cambers) for TDLF detailing. In addition, the user specifies the girder depths, the girder lengths, the girder spacing, the distance from each girder bearing radial line (i.e., the line perpendicular to the girder tangent at each bearing) to the coordinate origin (or simply the distance along the X axis to each bearing for straight skewed bridges), the number of girders, and the elastic modulus.

GT-LOFT presently addresses only circular horizontal curves. The user specifies the location of the bearing at the start of each girder as a distance along the girder arc from the radial line corresponding to $\theta = 0$. The cross-frame connection workpoint positions are then specified as a distance along the girder arc from bearing at the start of the girder. The elastic modulus and the coefficient of thermal expansion are used by the tool to convert the calculated initial strains into initial stresses and equivalent temperature changes respectively, to facilitate input into programs that may support only a thermal strain analysis.

In the Cross-Frames sheet, the user provides the positions of cross-frames along the girders, the cross-frame types (X, V, and Inverted-V), the offsets of the chords from the top and bottom of the web, and the cross-frame member cross-section properties. The cross-frame properties are used for the matrix analysis to determine the V or Inverted-V type cross-frame initial strains.

GT-LOFT applies the cambers at the bottom of the girder webs to perform its calculations. The vertical displacements due to the camber are essentially the same at the top of the girder webs; however, the bottom of the webs is a more convenient reference for ultimately determining the position of the cross-frame to girder connection work points, for reasons explained in the discussions below. The camber profile curve may be defined using 11 to 21 camber points for the span under consideration. GT-LOFT fits a piecewise cubic hermite interpolating polynomial function to these points to represent the camber profiles and the associated major-axis bending rotations at the cross-frame locations. This function generates a smooth curve with continuous first derivatives for the camber profiles. The camber profiles pass through the specified camber points and the girder simply-supported ends, where the second derivative of the interpolated vertical displacements is zero. For continuous spans, the cambers for each span should be specified into the adjacent span up to the approximate inflection point location, typically taken as $0.20L$ or $0.25L$ in the adjacent span, where L is the adjacent span length. This practice allows the interpolating functions to be ended where the second derivative of the vertical displacements is approximately zero.

In addition to the above camber profile curve, GT-LOFT calculates the longitudinal position of the points along the bottom flange at the cross-frame connection locations as

explained below. The lengths along the girder bottom flange projected onto the girder longitudinal axis change due to the major-axis bending rotations associated with the cambers, as shown in Figure 34 for TDLF. To account for this change, GT-LOFT provides the sheet Section Changes, for input of girder dimensions. The tool assumes that the total length along the girder centroidal axis is unchanged and that the connection plates are perpendicular to the flanges. All the girders are assumed as fixed longitudinally at the bottom flange at the girder left-hand ends in the elevation views of the members. As such, the longitudinal positions of the bottom flange at the cross-frame locations are calculated in the fully-cambered geometry as follows:

$$\bar{X} = X - d_0\,\phi_0 + d_{CF}\,\phi_{CF} - \sum_{i=1}^{n}(d_i - d_{i-1})\,\phi_i \qquad \text{Eq. (5)}$$

where:

$\bar{X}$ = Longitudinal position of the bottom flange at a cross-frame location, in the plumb fully-cambered geometry.

X = Longitudinal position of the bottom flange at the cross-frame location, in the plumb targeted dead load condition.

d_i = Distance from the girder centroid to the bottom flange at *i*th section change location, location 0 corresponding to the starting end of the girder.

d_{CF} = Distance from the centroid to the bottom flange at the cross-frame location under consideration.

n = The number of section changes between the girder start and the cross-frame location. The girders are assumed to be prismatic between the locations where there is a section change.

ϕ_i = Major-axis bending rotation due to the camber, in the fully-cambered geometry, at the *i*th section change location.

ϕ_{CF} = Major-axis bending rotation due to the camber, in the fully-cambered geometry, at the cross-frame location under consideration.

The term $d_1\phi_1$ in Eq. (5) gives the shift in the girder centroid at the starting end of the girder, along the girder axis, due to the major-axis bending rotation at that point, ϕ_1. The term $d_{CF}\phi_{CF}$ gives the shift in the position along the bottom of the web relative to the girder centroid due to the major-axis bending rotation ϕ_{CF} at that location. The term $\sum_{i=1}^{n}(d_i - d_{i-1})\,\phi_i$ gives the shift in the longitudinal coordinate of the girder centroid from all the section change locations between the starting end of the girder and the cross-frame that is being considered.

Given the above calculations, the longitudinal and vertical coordinates can be determined for the bottom of the web at each of the cross-frame connection locations in the targeted SDL or TDL geometry, as well as in the fully-cambered geometry. In addition, the girder camber rotations can be determined at each of the connection locations. Given this information, the longitudinal and vertical positions of all the cross-frame connection work points can be calculated. Given these work point positions in the targeted geometry and in the fully-cambered geometry, the desired strains can be determined from Eqs.

(2)_through (4) and the work point vertical and longitudinal camber displacements can be computed.

For curved bridges, the above calculations are applied along the arc of the girder and the cross-frame work point coordinates are maintained along the girder arc, both in the plumb targeted dead load condition and in the plumb fully-cambered positions of the girders. That is, the *R* coordinates of the cross-frame connection work points are not allowed to change.

3.2.3. Calculation of Initial Fixed-End Forces for 2D Grid Analysis using GT-LOFT

In a 2D Grid analysis, the cross-frames are represented by equivalent beam elements. In addition, in a 2D Grid analysis, the depth of the superstructure is not considered. The girders, cross-frames and bearings are all modeled at a common elevation. There are various forms of 2D Grid analysis, some of which use a reduced degree of freedom set (the vertical displacement and rotations about two axes within the plane of the bridge model). In the work presented here, it is assumed that three translational and three rotational degrees of freedom (dofs) are tracked at each node of the grid model. The discussions below focus on the calculation of the fixed-end forces in the cross-frame equivalent beam elements associated with the lack-of-fit from SDLF or TDLF detailing. It is assumed that the 2D Grid analysis is a geometrically linear (i.e., first-order) elastic analysis. To calculate the equivalent beam element fixed-end forces, GT-LOFT resolves the displacements at the cross-frame work points, calculated as discussed in Section 3.2.2, into beam element end displacements and rotations using the assumption that the nodes of the 2D Grid model are at the mid-height of the cross-frame at each of the cross-frame ends.

One should note that the equivalent beam element end rotations associated with the lack-of-fit calculation are nonzero only within the plane of the girder web. This is because the girder webs are taken as plumb in both the NL and the targeted SDL or TDL geometry. Figure 35 shows an elevation view of a representative cross-frame and its equivalent beam element. Specifically, the equivalent beam element end displacements and rotations are calculated by GT-LOFT as follows:

$$u_{Ii} = \frac{u_{Ai} + u_{Bi}}{2} \qquad \text{Eq. (6)}$$

$$u_{IIi} = \frac{u_{Ci} + u_{Di}}{2} \qquad \text{Eq. (7)}$$

$$\phi_I = \frac{u_B - u_A}{h} \qquad \text{Eq. (8)}$$

$$\phi_{II} = \frac{u_D - u_C}{h} \qquad \text{Eq. (9)}$$

where:

u_{Ii} = Displacement in the *i*th direction at the equivalent beam element end I.

u_{IIi} = Displacement in the *i*th direction at the equivalent beam element end II.

u_{Ai} = Displacement in the *i*th direction at the cross-frame workpoint *A*, similar for workpoints *B*, *C* and *D*

u_A = Displacement tangent to the girder longitudinal axis at cross-frame workpoint *A*, similar for workpoints *B*, *C* and *D*

ϕ_I = Rotation of the equivalent beam element about the axis normal the girder web ϕ at the element end I.

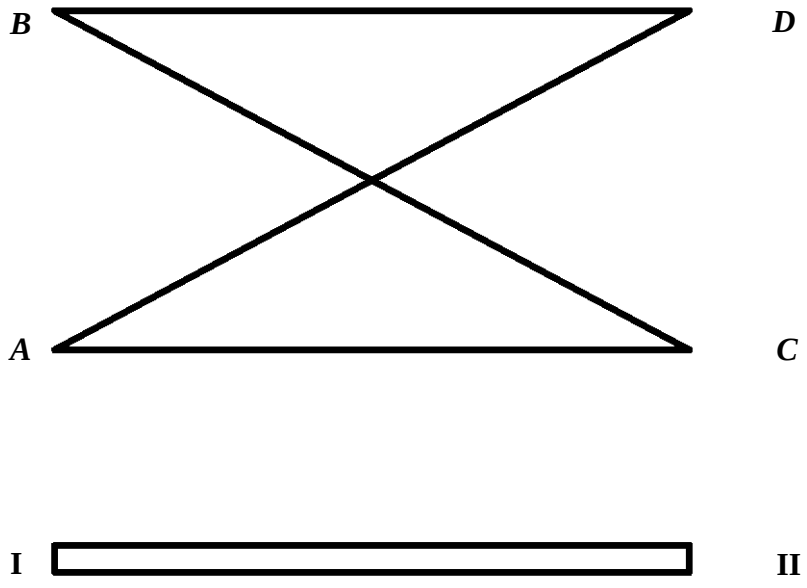

Figure 35. Illustration of a representative cross-frame (top) and its equivalent beam element (bottom). The cross-frame work points are labeled A through D. The ends of the equivalent beam element are labeled I and II.

ϕ_{II} = Rotation of the equivalent beam element about the axis normal the girder web at the element end II.

i = X, Y, and Z directions in the right-handed Cartesian coordinate system for straight bridges. R, θ, and Z directions in the cylindrical coordinate system for curved bridges.

h = Depth of the cross-frame, taken as the distance between the cross-frame top and bottom chords.

The element end displacements and rotations are calculated in the global coordinate system, which is an XYZ Cartesian system for straight skewed bridges and an RθZ cylindrical coordinate system for horizontally curved bridges with or without skew. In straight skewed bridges, the cross-frame end vertical displacements and the rotations about the Y-axis (the axis normal to the girder webs) have the greatest impact on the cross-frame equivalent beam fixed-end forces. In curved bridges, the cross-frame end vertical

displacements and the rotations about the R-axis (again, the axis normal to the girder webs) have the greatest impact on the cross-frame equivalent beam fixed-end forces.

The above element end displacements and rotations are used to calculate the initial fixed-end forces as follows:

$$f_{initial} = k_{equivalent} d_{equivalent} \qquad \text{Eq. (10)}$$

where:

$k_{equivalent}$ = Stiffness of the equivalent beam element in the bridge global coordinates (12x12 matrix).

$d_{equivalent}$ = End displacements and rotations of the equivalent beam element in the bridge global coordinates, calculated based on the displacements of the cross-frame work points from the targeted SDL or TDL geometry to the fully-cambered geometry, using the above assumption that girder webs are plumb under the no-load and the targeted SDL or TDL geometries (12x1 vector).

$f_{initial}$ = Initial fixed-end forces of the equivalent beam element, calculated in the bridge global coordinates (12x1 vector).

The above calculation applies to all cross-frame types (X, V, and inverted V) and to geometrically linear (first-order) analysis. Depending on the element formulation, the above element stiffness $k_{equivalent}$ varies. GT-LOFT provides the calculations of initial fixed-end forces for the following equivalent beam element formulations:

- The Euler-Bernoulli beam element based on the traditional flexural analogy or shear analogy approximations,
- The Timoshenko beam element, which is recommended in NCHRP Report 725, and
- An "exact" equivalent beam element (Sanchez, 2011).

GT-LOFT calculates the moment of inertia for bending within the plane of the cross-frame for the equivalent Euler-Bernoulli beam element based either on the flexural analogy or shear analogy as explained in Sections 3.2.3.1 and 3.2.3.2 of NCHRP Report 725. GT-LOFT calculates the moment of inertia and the shear area for bending within the plane of the cross-frame for the equivalent Timoshenko beam element via the calculations presented in Section 3.2.3.3 of the NCHRP Report 725. For both the equivalent Euler-Bernoulli and Timoshenko beam elements, the area *A*, the torsional constant *J*, and the moment of inertia for out-of-plane bending of the cross-frame are taken as the sum of the corresponding values of the cross-frame top and bottom chords.

The cross-frame initial fixed-end forces calculated above appear in the global matrix equations for a 2D Grid analysis as follows:

$$F = F_{initial} + K\,D \qquad \text{Eq. (11)}$$

where:

K = Global stiffness matrix of the bridge system.

D = Vector of the global nodal displacements in the bridge system.

$F_{initial}$ = Global vector of equivalent beam element nodal initial fixed-end forces, assembled from the individual element $f_{initial}$ vectors.

F = Global nodal forces applied to the 2D Grid model of the bridge system.

One can subtract $F_{initial}$ from both sides of Eq. (11) to observe that the overall global effect of the lack-of-fit induced by the SDLF or TDLF detailing is generated by applying the negative of $F_{initial}$ at the nodal degrees of freedom in the global 2D Grid analysis model. The force vector $-F_{initial}$ causes global nodal displacements D, which offset the dead load torsional rotations of the girders. It should be emphasized that the actual cross-frame "locked-in" forces are calculated as

$$f_{locked\text{-}in} = f_{initial} + k_{equivalent}\, d \qquad \text{Eq. (12)}$$

where $f_{initial}$ is the element fixed-end force vector calculated in Eq. (10), $k_{equivalent}$ is the equivalent beam element stiffness matrix, and d is the element displacements associated with the global nodal displacements D caused by $-F_{initial}$. The total cross-frame dead load force is equal to the above force plus the cross-frame forces caused by the global dead load nodal forces F.

3.3. Examples Showing Inclusion of the Detailing Effects via Initial Strains in 3D FEA

This section illustrates the inclusion of the initial strains due to the detailing effects, calculated by GT-LOFT, in the analyses of a straight skewed bridge NISSS4, not studied in the previously considered bridge cases, and a curved radially-supported bridge (B) NISCR2. These two bridges were selected because they are relatively small simple-span bridges. In addition, the number of cross-frames are relatively low, thus facilitating the

illustration of calculating the initial strains. Complete sets of results showing the responses of bridge NISSS4 and bridge (B) NISCR2 are shown in Appendices A and B, respectively. These results are with SDLF and TDLF detailing effects included via the initial strains calculated by GT-LOFT. Since the geometric nonlinearity in bridge NISSS4 and bridge (B) NISCR2 is insignificant, Appendices A and B effectively show the same results as obtained from a geometrically linear (first-order) elastic analysis and using the initial engineering strains from GT-LOFT.

The initial strains for SDLF and TDLF detailing calculated by GT-LOFT are identical for all practical purposes to the initial strains for SDLF and TDLF detailing calculated by 3D FEA using the procedure discussed in Section 3.2.1. Correspondingly, the bridge responses are identical for all practical purposes using the initial strains from GT-LOFT and the initial strains from the procedure described in Section 3.2.1.

3.3.1. Straight Skewed Bridge Example – NISSS4

Figure 36 shows the framing plan for straight skewed bridge NISSS4. This bridge has a span length of 150 ft and a severe parallel skew of 70 degrees. All the girders have the same prismatic section (1.125 in. x 16 in. top flanges and 2 in. x 18 in. bottom flanges) throughout the bridge length. The intermediate cross-frames are X type, and the end cross-frames are inverted-V type. All cross-frame members are L6x6x1. The girders are 72 in. deep and are designated G1 to G4, starting at the bottom and proceeding to the top of the plan view as shown in Figure 36.

Figure 37 shows the SDL and TDL LGA cambers, determined as explained in Section 2.1. Tables 3 and 4 show the initial engineering strains and the initial log strains calculated by GT-LOFT for SDLF detailing. The initial rotated engineering strains are not shown

since they are essentially equal to the initial log strains. Tables 5 and 6 show the initial engineering strains and the initial log strains calculated by GT-LOFT for TDLF detailing. In these tables, the columns indicate the bays between the designated girders, i.e. column G1-G2 indicates the bay between G1 and G2. The rows indicate the cross-frames in the order from left to right in the plan view, i.e. row 1 indicates cross-frames on the left-hand skewed bearing line.

One can observe from these tables that the initial strains are much higher for the diagonals than the chords. This is because the diagonals have higher initial vertical and rotational lack-of-fit. The bottom chords have very low initial strains. In addition, the initial strains for TDLF detailing are higher than the initial strains for SDLF detailing. This is because the TDL cambers are larger than the SDL cambers (see Figure 37). The intermediate cross-frame top chords and bottom chords have zero initial engineering strains. These members are perpendicular to the girder webs and the offsets from the bottom flanges to the bottom chords are all the same. The chord lengths projected onto the member orientation in the targeted DL condition are the same as the chords lengths in the targeted DL condition. Figures 38 and 39 show the girder layovers and twists from a geometrically linear analysis using the initial engineering strains versus from a geometrically nonlinear analysis using the initial log strains under SDL and TDL. One can see that, with the calculated initial strains included in the structural analysis, the girder webs are essentially plumb under SDL for SDLF detailing and under TDL for TDLF detailing. The difference in layovers between the geometrically linear analysis with initial engineering strains and the geometrically nonlinear analysis with initial log strains are

negligible for bridge NISSS4. Appendix A provides detailed results and a brief discussion of other responses for bridge NISSS4.

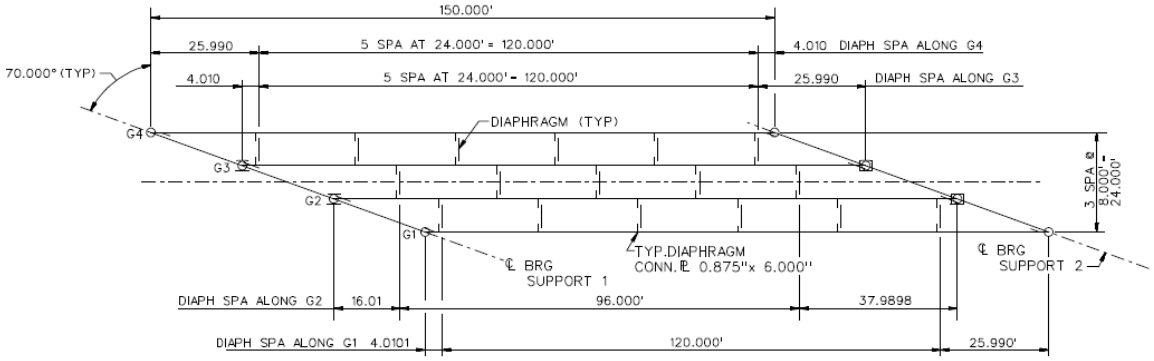

Figure 36. Bridge NISSS4 framing plan.

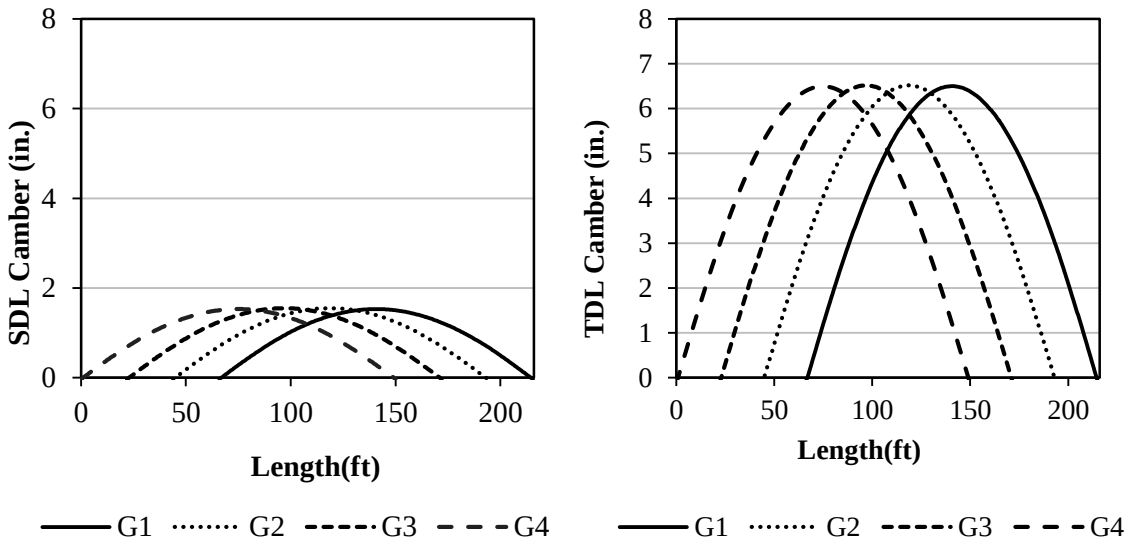

Figure 37. Bridge NISSS4 SDL cambers (left) and TDL cambers (right) from LGA.

Table 3. Bridge NISSS4 SDLF initial engineering strains based on LGA cambers and obtained from GT-LOFT (x10^6, '--' indicates that the value is not available because there is no cross-frame member that location).

CF #	Bottom Chords			Top Chords 1			Top Chords 2		
	G1-G2	G2-G3	G3-G4	G1-G2	G2-G3	G3-G4	G1-G2	G2-G3	G3-G4
1	0.21	-1.54	0.25	-525.38	-539.60	-512.99	530	503.92	518.76
2	0.00	0.00	0.00	0.00	0.00	0.00	--	--	--
3	0.00	0.00	0.00	0.00	0.00	0.00	--	--	--
4	0.00	0.00	0.00	0.00	0.00	0.00	--	--	--
5	0.00	0.00	0.00	0.00	0.00	0.00	--	--	--
6	0.00	0.00	0.00	0.00	0.00	0.00	--	--	--
7	0.00	-1.54	0.00	0.00	503.92	0.00	--	-539.60	--
8	1.14	--	-6.54	515.62	--	533.77	-513.70	--	-506.34

Table 3 (Continued). Bridge NISSS4 SDLF initial engineering strains based on LGA cambers and obtained from GT-LOFT (x10^6,'--' indicates that the value is not available because there is no cross-frame member that location).

CF #	Diagonals 1			Diagonals 2		
	G1-G2	G2-G3	G3-G4	G1-G2	G2-G3	G3-G4
1	579.28	572.62	566.17	-579.28	-572.64	-566.17
2	3246.63	2753.10	3195.80	-3248.61	-2754.60	-3197.73
3	2220.20	1514.25	2250.37	-2221.19	-1514.80	-2251.37
4	760.12	-0.06	823.97	-760.32	-0.06	-824.18
5	-822.04	-1514.80	-787.19	821.82	1514.25	786.98
6	-2236.28	-2754.60	-2271.19	2235.28	2753.10	2270.19
7	-3189.21	-572.64	-3266.02	3187.28	572.62	3264.09
8	-564.84	--	-570.80	564.85	--	570.72

Table 4. Bridge NISSS4 SDLF initial log strains based on LGA cambers and obtained from GT-LOFT ($x10^6$, '--' indicates that the value is not available because there is no cross-frame member that location).

CF #	Bottom Chords			Top Chords 1			Top Chords 2		
	G1-G2	G2-G3	G3-G4	G1-G2	G2-G3	G3-G4	G1-G2	G2-G3	G3-G4
1	0.21	-1.54	0.25	-525.52	-539.75	-513.12	530.12	503.79	518.62
2	24.89	17.91	24.12	24.91	17.95	24.13	--	--	--
3	11.66	5.44	11.98	11.71	5.51	12.02	--	--	--
4	1.40	0.04	1.64	1.46	0.13	1.70	--	--	--
5	1.63	5.44	1.50	1.69	5.51	1.56	--	--	--
6	11.82	17.91	12.19	11.86	17.95	12.24	--	--	--
7	23.99	-1.54	25.16	24.01	503.79	25.17	--	-539.75	--
8	1.14	--	-6.54	515.48	--	533.63	-513.84	--	-506.47

Table 4(Continued). Bridge NISSS4 SDLF initial log strains based on LGA cambers and obtained from GT-LOFT ($x10^6$, '--' indicates that the value is not available because there is no cross-frame member that location).

CF #	Diagonals 1			Diagonals 2		
	G1-G2	G2-G3	G3-G4	G1-G2	G2-G3	G3-G4
1	579.23	572.57	566.12	-579.34	-572.69	-566.22
2	3254.25	2758.56	3203.19	-3240.75	-2748.88	-3190.12
3	2223.74	1515.89	2254.01	-2217.49	-1513.03	-2247.58
4	760.52	-0.05	824.44	-759.87	-0.05	-823.66
5	-821.51	-1513.03	-786.71	822.29	1515.89	787.41
6	-2232.53	-2748.88	-2267.34	2238.87	2758.56	2273.88
7	-3181.63	-572.69	-3258.12	3194.64	572.57	3271.76
8	-564.89	--	-570.85	564.80	--	570.67

Table 5. Bridge NISSS4 TDLF initial engineering strains based on LGA cambers and obtained from GT-LOFT (x10^6, '--' indicates that the value is not available because there is no cross-frame member that location)

CF #	Bottom Chords			Top Chords 1			Top Chords 2		
	G1-G2	G2-G3	G3-G4	G1-G2	G2-G3	G3-G4	G1-G2	G2-G3	G3-G4
1	0.83	-6.11	0.99	-2085.5	-2142.0	-2036.3	2104.9	2000.3	2059.2
2	0.00	0.00	0.00	0.00	0.00	0.00	--	--	--
3	0.00	0.00	0.00	0.00	0.00	0.00	--	--	--
4	0.00	0.00	0.00	0.00	0.00	0.00	--	--	--
5	0.00	0.00	0.00	0.00	0.00	0.00	--	--	--
6	0.00	0.00	0.00	0.00	0.00	0.00	--	--	--
7	0.00	-6.11	0.00	0.00	2000.3	0.00	--	-2142.0	--
8	4.52	--	-25.96	2046.8	--	2118.86	-2039.2	--	-2009.9

Table 5(Continued). Bridge NISSS4 TDLF initial engineering strains based on LGA cambers and obtained from GT-LOFT (x10^6, '--' indicates that the value is not available because there is no cross-frame member that location).

CF #	Diagonals 1			Diagonals 2		
	G1-G2	G2-G3	G3-G4	G1-G2	G2-G3	G3-G4
1	2299.51	2273.08	2247.46	-2427.01	-242.75	-2458.12
2	12880.04	10924.60	12678.23	-12911.38	-10948.19	-12708.70
3	8812.08	6011.36	8931.71	-8827.78	-6019.90	-8947.47
4	3018.05	-0.87	3271.57	-3021.24	-0.87	-3274.93
5	-3266.40	-6019.90	-3128.03	3263.03	6011.36	3124.70
6	-8887.55	-10948.19	-9026.30	8871.79	10924.60	9010.56
7	-12674.86	-2273.22	-12979.75	12644.48	2273.08	12949.29
8	-2242.22	--	-2265.89	2242.20	--	2265.52

Table 6. Bridge NISSS4 TDLF initial log strains based on LGA cambers and obtained from GT-LOFT (x106, '--' indicates that the value is not available because there is no cross-frame member that location).

CF #	Bottom Chords			Top Chords 1			Top Chords 2		
	G1-G2	G2-G3	G3-G4	G1-G2	G2-G3	G3-G4	G1-G2	G2-G3	G3-G4
1	0.83	-6.11	0.99	-2087.75	-2144.32	-2038.45	2102.71	1998.38	2057.16
2	392.22	282.17	380.02	392.81	283.19	380.51	--	--	--
3	183.83	85.73	188.80	184.80	86.98	189.70	--	--	--
4	22.11	0.63	25.90	23.05	2.08	26.86	--	--	--
5	25.75	85.73	23.69	26.72	86.98	24.66	--	--	--
6	186.28	282.17	192.18	187.19	283.19	193.17	--	--	--
7	378.00	-6.11	396.41	378.50	1998.38	396.90	--	-2144.32	--
8	4.52	--	-25.96	2044.72	--	2116.62	-2041.29	--	-2012.00

Table 6(Continued). Bridge NISSS4 TDLF initial log strains based on LGA cambers and obtained from GT-LOFT (x10^6, '--' indicates that the value is not available because there is no cross-frame member that location).

CF #	Diagonals 1			Diagonals 2		
	G1-G2	G2-G3	G3-G4	G1-G2	G2-G3	G3-G4
1	2298.70	2272.27	2246.69	-2300.37	-2273.98	-2248.28
2	12996.65	11008.54	12791.44	-12783.75	-10855.77	-12585.12
3	8866.89	6036.85	8987.94	-8768.16	-5991.59	-8886.40
4	3024.40	-0.80	3278.98	-3014.06	-0.80	-3266.63
5	-3258.12	-5991.59	-3120.37	3270.41	6036.85	3131.49
6	-8827.18	-10855.77	-8964.30	8927.36	11008.54	9067.56
7	-12551.89	-2273.98	-12851.45	12757.10	2272.27	13066.69
8	-2242.99	--	-2266.59	2241.45	--	2264.67

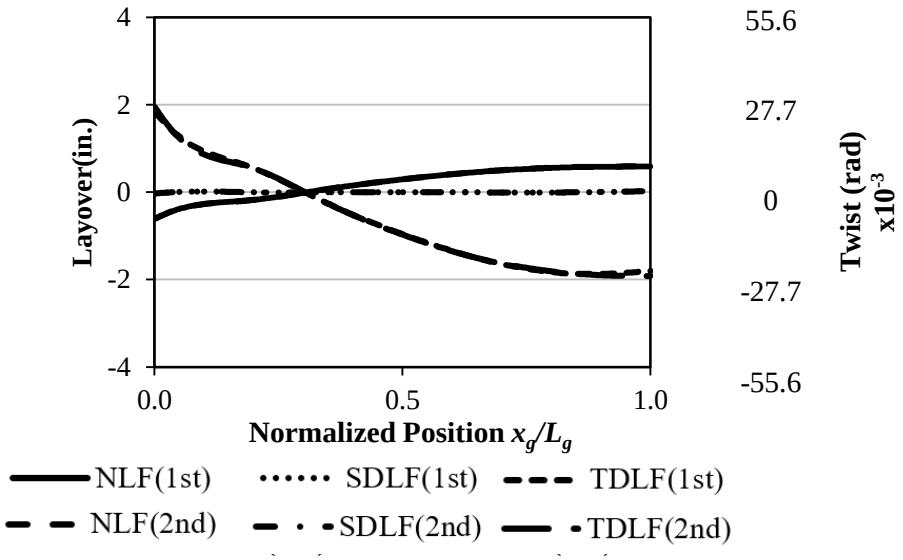

Figure 38. Layovers of a fascia girder G1 of bridge NISSS4 under SDL. The (1st-order) layovers are from a geometrically linear 3D FEA using the initial engineering strains. The (2nd-order) layovers are from a geometrically nonlinear 3D FEA using the initial log strains.

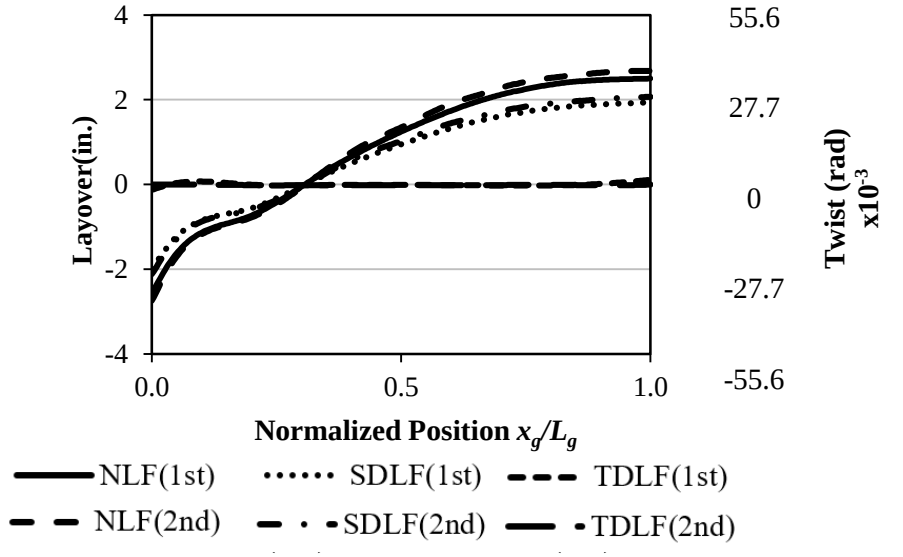

Figure 39. Layovers of a fascia girder G1 of bridge NISSS4 under TDL. The (1st-order) layovers are from a geometrically linear 3D FEA using the initial engineering strains. The (2nd-order) layovers are from a geometrically nonlinear 3D FEA using the initial log strains.

3.3.2. Curved Radially-Supported Bridge Example – NISCR2

Figure 40 shows the framing plan for the curved radially-supported bridge (B) NISCR2. This bridge has a span length of 150 ft and centerline radius of curvature of 438 ft. All of the girders have four section changes along the span. The intermediate cross-frames are X type, and the end cross-frame are inverted-V type. All the cross-frame members are L6x6x3/4. A detailed description of this bridge is provided in Appendix B. The girders are 84 in. deep and are designated G1 to G4, where G1 and G4 are the girders on the outside and the inside of the curve as shown in Figure 40.

Figure 41 shows the SDL and TDL 3D FEA cambers for bridge (B) NISCR2. These cambers have a significant influence on the calculation of the initial strains. Tables 7 and 8 show the initial engineering and log strains calculated by GT-LOFT for SDLF detailing. The initial rotated engineering strains are not shown since they essentially equal to the initial log strains. Tables 9 and 10 show the initial engineering and log strains calculated by GT-LOFT for TDLF detailing. In these tables, the columns indicate the bays between the designated girders, i.e. column G1-G2 indicates the bay between G1 and G2. The rows indicate the cross-frames in the order from left to right, i.e. row 1 indicates cross-frames on the left-hand bearing line.

One can observe from these tables that the initial strains are much higher for the diagonals than the chords. The top and bottom chords have relatively low initial strains with respect to the diagonals. This is because the diagonals have higher initial vertical and rotational lack-of-fit. In addition, the initial strains for TDLF detailing are higher than the initial strains for SDLF detailing. This is because the TDL cambers are larger than the SDL cambers (see Figure 41). The intermediate cross-frame top and bottom chords have close

to zero initial engineering strains. The slightly non-zero values of these strains are due to the fact that the girders toward the outside of the curve have larger deflections and rotations than the girders toward the inside of the curve, and the cross-frame connection work point camber displacements are forced to maintain constant *R*.

Figures 42 and 43 show the girder layovers and twists from a geometrically linear analysis using the initial engineering strains versus from a geometrically nonlinear analysis using the log strains. These figures correspond to SDL and TDL respectively. One can see that, with the initial strains calculated by GT-LOFT included in the analysis, the girder webs are approximately plumb under SDL for SDLF detailing and under TDL for TDLF detailing. The difference in layovers between the geometrically linear analysis with initial engineering strains and the geometrically nonlinear analysis with initial log strains are negligible for bridge (B) NISCR2. Appendix B provides detailed results and a brief discussion for other responses for this bridge.

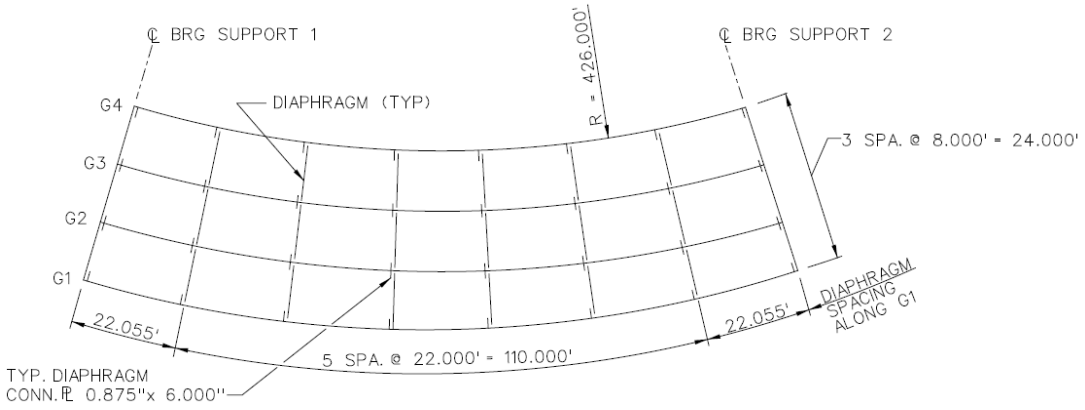

Figure 40. Bridge (C) NISCR2 framing plan

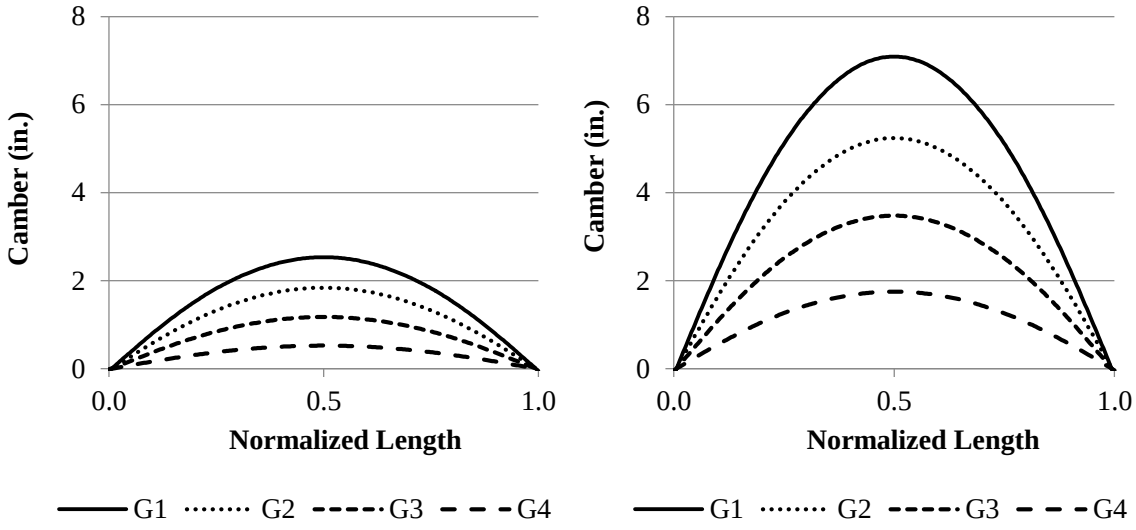

Figure 41. Bridge (C) NISCR2 SDL cambers (left) and TDL 3D FEA cambers (right) based on 3D FEA.

Table 7. Bridge (C) NISCR2 SDLF initial engineering strains based on 3D FEA cambers and obtained from GT-LOFT (x10^6, '--' indicates that the value is not available because there is no cross-frame member that location).

CF #	Bottom Chords			Top Chords 1			Top Chords 2		
	G1-G2	G2-G3	G3-G4	G1-G2	G2-G3	G3-G4	G1-G2	G2-G3	G3-G4
1	0.000	0.000	0.000	0.250	0.417	0.226	-0.250	-0.366	-0.226
2	-0.001	-0.001	-0.001	-0.047	-0.034	-0.020	--	--	--
3	-0.004	-0.003	-0.002	-0.032	-0.023	-0.014	--	--	--
4	-0.009	-0.006	-0.004	-0.019	-0.013	-0.009	--	--	--
5	-0.018	-0.012	-0.008	-0.008	-0.006	-0.004	--	--	--
6	-0.028	-0.019	-0.013	-0.002	-0.001	-0.001	--	--	--
7	-0.037	-0.026	-0.017	0.000	0.000	0.000	--	--	--
8	-0.072	-0.058	0.039	0.269	0.421	0.248	-0.269	-0.366	-0.248

Table 7(Continued). Bridge (C) NISCR2 SDLF initial engineering strains based on 3D FEA cambers and obtained from GT-LOFT (x10^6)

CF #	Diagonals 1			Diagonals 2		
	G1-G2	G2-G3	G3-G4	G1-G2	G2-G3	G3-G4
1	18.59	12.03	6.03	19.52	13.38	6.86
2	-1555	-1517	-1493	1555	1514	1493
3	-2707	-2631	-2597	2707	2631	2597
4	-3314	-3221	-3179	3314	3221	3179
5	-3310	-3217	-3179	3310	3217	3179
6	-2703	-2628	-2597	2703	2628	2597
7	-1555	-1514	-1493	1555	1514	1493
8	19.24	12.38	6.03	20.21	13.76	6.93

Table 8. Bridge (C) NISCR2 SDLF initial log strains based on 3D FEA cambers and obtained from GT-LOFT (x10^6, '--' indicates that the value is not available because there is no cross-frame member that location).

CF #	Bottom Chords			Top Chords 1			Top Chords 2		
	G1-G2	G2-G3	G3-G4	G1-G2	G2-G3	G3-G4	G1-G2	G2-G3	G3-G4
1	0.002	0.002	0.002	0.250	0.417	0.226	-0.250	-0.366	-0.226
2	5.241	4.966	4.828	5.586	5.310	5.241	--	--	--
3	15.9	15.0	14.7	16.1	15.2	14.9	--	--	--
4	23.9	22.6	22.0	23.9	22.6	22.1	--	--	--
5	23.9	22.6	22.1	23.8	22.5	22.0	--	--	--
6	16.0	15.2	14.9	15.9	15.0	14.6	--	--	--
7	5.517	5.207	5.138	5.207	4.966	4.793	--	--	--
8	0.306	0.284	0.466	0.269	0.421	0.248	-0.269	-0.366	-0.248

Table 8(Continued). Bridge (C) NISCR2 SDLF initial log strains based on 3D FEA cambers and obtained from GT-LOFT (x10^6)

CF #	Diagonals 1			Diagonals 2		
	G1-G2	G2-G3	G3-G4	G1-G2	G2-G3	G3-G4
1	18.59	12.03	6.03	19.52	13.38	6.86
2	-1555	-1514	-1493	1555	1514	1493
3	-2703	-2628	-2593	2707	2631	2600
4	-3307	-3214	-3172	3314	3221	3183
5	-3307	-3214	-3172	3314	3221	3179
6	-2697	-2624	-2590	2703	2631	2597
7	-1548	-1510	-1490	1552	1510	1490
8	19.24	12.38	6.03	20.21	13.76	6.93

Table 9. Bridge (C) NISCR2 TDLF initial engineering strains based on 3D FEA cambers and obtained from GT-LOFT (x106, '--' indicates that the value is not available because there is no cross-frame member that location).

CF #	Bottom Chords			Top Chords 1			Top Chords 2		
	G1-G2	G2-G3	G3-G4	G1-G2	G2-G3	G3-G4	G1-G2	G2-G3	G3-G4
1	-0.002	-0.002	-0.001	0.001	0.001	0.001	-0.001	-0.001	-0.001
2	-0.011	-0.008	-0.006	-0.345	-0.254	-0.171	--	--	--
3	-0.032	-0.021	-0.017	-0.241	-0.173	-0.122	--	--	--
4	-0.071	-0.049	-0.038	-0.144	-0.102	-0.074	--	--	--
5	-0.135	-0.094	-0.070	-0.064	-0.043	-0.034	--	--	--
6	-0.208	-0.146	-0.108	-0.021	-0.012	-0.012	--	--	--
7	-0.279	-0.194	-0.146	-0.002	0.000	-0.002	--	--	--
8	-0.417	-0.306	-0.022	0.001	0.001	0.001	-0.001	-0.001	-0.001

Table 9(Continued). Bridge (C) NISCR2 TDLF initial engineering strains based on 3D FEA cambers and obtained from GT-LOFT ($x10^6$)

CF #	Diagonals 1			Diagonals 2		
	G1-G2	G2-G3	G3-G4	G1-G2	G2-G3	G3-G4
1	0.05	0.04	0.02	0.06	0.04	0.02
2	-4000	-3862	-3793	4000	3862	3793
3	-6931	-6724	-6621	6931	6724	6621
4	-8483	-8207	-8103	8483	8207	8103
5	-8483	-8207	-8103	8483	8207	8103
6	-6931	-6690	-6621	6931	6690	6621
7	-3966	-3862	-3793	3966	3862	3793
8	0.06	0.04	0.02	0.06	0.04	0.02

Table 10. Bridge (C) NISCR2 TDLF initial log strains based on 3D FEA cambers and obtained from GT-LOFT ($x10^6$, '--' indicates that the value is not available because there is no cross-frame member that location).

CF #	Bottom Chords			Top Chords 1			Top Chords 2		
	G1-G2	G2-G3	G3-G4	G1-G2	G2-G3	G3-G4	G1-G2	G2-G3	G3-G4
1	0.020	0.017	0.023	0.001	0.001	0.001	-0.001	-0.001	-0.001
2	34.8	32.6	31.7	36.9	34.8	34.3	--	--	--
3	104.8	98.3	95.9	106.2	99.7	97.6	--	--	--
4	157.2	147.2	144.1	157.9	147.9	144.5	--	--	--
5	157.6	147.6	144.5	157.2	147.2	143.8	--	--	--
6	105.9	99.3	97.2	104.5	97.9	95.5	--	--	--
7	36.2	34.1	33.9	34.4	32.3	31.5	--	--	--
8	2.307	1.952	3.072	0.001	0.001	0.001	-0.001	-0.001	-0.001

Table 10(Continued). Bridge (C) NISCR2 TDLF initial log strains based on 3D FEA cambers and obtained from GT-LOFT ($x10^6$).

CF #	Diagonals 1			Diagonals 2		
	G1-G2	G2-G3	G3-G4	G1-G2	G2-G3	G3-G4
1	0.05	0.04	0.02	0.06	0.04	0.02
2	-3966	-3862	-3793	4000	3862	3793
3	-6931	-6690	-6621	6966	6724	6655
4	-8448	-8207	-8103	8517	8241	8138
5	-8448	-8172	-8103	8517	8241	8138
6	-6897	-6690	-6586	6931	6724	6621
7	-3966	-3828	-3793	3966	3862	3793
8	0.06	0.04	0.02	0.06	0.04	0.02

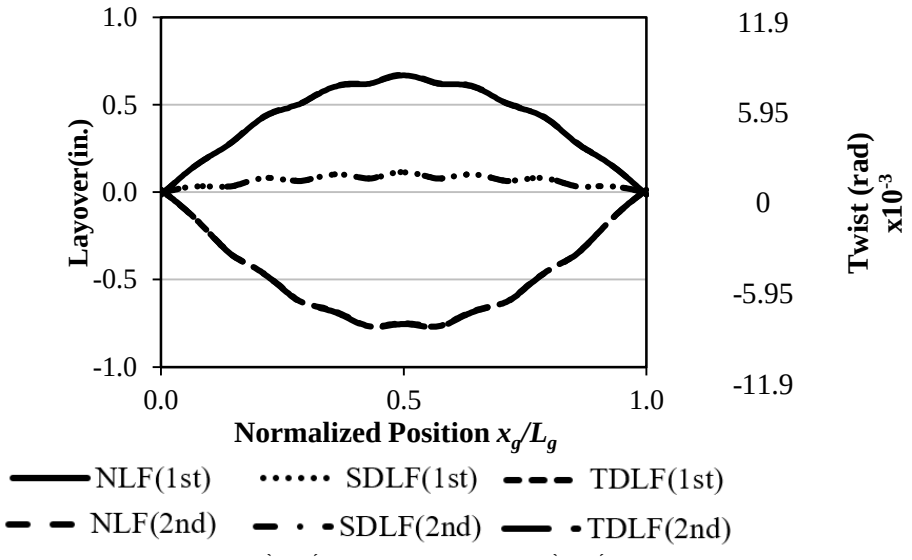

Figure 42. Layovers of the outside girder G1 of bridge (C) NISCR2 under SDL. The (1st-order) layovers are from a geometrically linear 3D FEA using the initial engineering strains. The (2nd-order) layovers are from a geometrically nonlinear 3D FEA using the initial log strains.

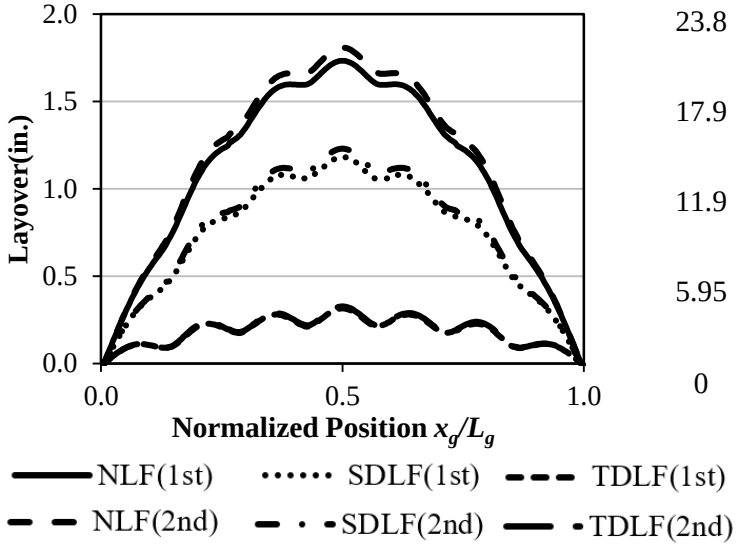

Figure 43. Layovers of the outside girder G1 of bridge (C) NISCR2 under TDL. The (1st-order) layovers are from a geometrically linear 3D FEA using the initial engineering strains. The (2nd-order) layovers are from a geometrically nonlinear 3D FEA using the initial log strains.

3.4. Illustration of the Inclusion of the Detailing Effects via Fixed-End Forces in 2D Grid Analysis

This section provides example illustration of the inclusion of the fixed-end forces due to the detailing effects, calculated by GT-LOFT, in a 2D Grid analysis of the straight skewed bridge NISSS4 and the curved radially-supported bridge (B) NISCR2. These two bridges were selected for this section for the same reasons explained in Section 3.3. This allows for comparisons of the 3D FEA and 2D Grid analysis. Complete sets of results showing the responses for bridge NISSS4 and Bridge (B) NISCR2 are shown in Appendices C and D respectively

A 2D Grid analysis was developed in MATLAB to illustrate the incorporation of cross-frame detailing effects via initial fixed-end forces. The important aspects of the grid analysis conducted in section are as follows:

- The girders are modeled using Euler-Bernoulli beam elements.
- Equivalent St. Venant torsion constants, J_{eq}, are used for the I-girders as specified in the NCHRP 725 report. These constants account approximately for the contribution of warping to the girder torsional stiffness. A different value is calculated for each unbraced length. It is assumed that the warping is fixed at both ends in intermediate girder unbraced lengths and that the warping is free at the free end and fixed at the other end for end unbraced lengths.
- Each girder unbraced length is modeled by a single element for straight bridge NISSS4 and by two elements for the curved bridge NISCR2.
- The cross-frames are modeled using two approaches: an equivalent Euler-Bernoulli beam element with properties determined by the flexural analogy and equivalent

Timoshenko beam element with properties determined as recommended in NCHRP Report 725. It is found that the responses for the example bridges used in this section are approximately the same for the two approaches. The results in this section are provided with the cross-frames modeled using the Timoshenko beam element.

3.4.1. Straight Skewed Bridge Example - NISSS4

The framing plan of bridge NISSS4 is shown in Section 3.3.1, Figure 36 . The primary bridge characteristics are discussed in this section. The SDL and TDL cambers used below are LGA cambers determined using the grid model by removing the equivalent cross-frame elements and restraining the girder lateral displacements. These LGA cambers are effectively the same as the LGA cambers determined from 3D FEA (shown in Figure 37).

Tables 11 and 12 show the initial fixed-end forces calculated by GT-LOFT for SDLF and TDLF detailing. In these tables, the columns indicate the initial fixed-end forces (dofs 1 to 3) and moments (dofs 4 to 6). These initial fixed-end forces and moments are shown in two groups corresponding to the beam element ends I and II. These forces and moments correspond to the global right-handed Cartesian coordinate system used for straight skewed bridges in GT-LOFT. The rows indicate the cross-frames in the order from left to right, i.e. row 1 indicates the cross-frames on the left-hand skewed bearing line.

It is important to note that the initial fixed-end forces and moments in any equivalent beam element are in static equilibrium, as shown in Figure 44 for the second equivalent beam element from the left skewed bearing line between girders 1 and 2.

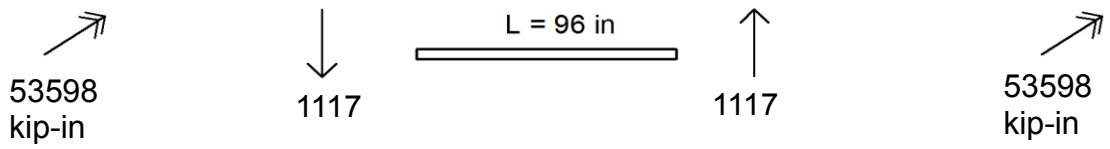

Figure 44. Illustration of static equilibrium of initial fixed-end forces and moments in the second equivalent beam element from the left skewed bearing line between Girders 1 and 2 of Bridge NISSS4.

The following are important observations from Tables 11 and 12:

- The largest fixed-end force values are in the columns corresponding to dof 3 (the vertical fixed-end forces) and dof 4 (the fixed-end moments about the X-axis). This is because, in determining the fixed-end forces, the equivalent beam element is subjected to vertical lack-of-fit displacements while the end rotations about the X-axis are restrained to enforce plumb girder webs in both the final targeted dead load position and in the initially-plumb cambered positions of the girders.

- The initial fixed-end forces in the X and Y axis directions, shown in the columns corresponding to dofs 1 and 2 in Tables 11 and 12, are zero or quite small compared to the values discussed above.

- For the skewed cross-frames, to maintain compatibility between the cross-frames and the girders, the columns corresponding to dof 5 (the initial fixed-end moments about the Y-axis) are comparable to the moments about the X-axis.

- The initial fixed-end forces are larger for TDLF detailing than SDLF detailing because the displacements and rotations subjected to the equivalent beam element are larger.

Figures 45 and 46 show the girder layovers and twists from a geometrically linear 2D Grid analysis using the initial engineering fixed-end forces, calculated by GT-LOFT. These figures correspond to SDL and TDL respectively. The symbols on the curves correspond to the cross-frame locations. One can see that, with the calculated initial fixed-end forces included in the grid analysis, the girder webs are essentially plumb under SDL for SDLF detailing and under TDL for TDLF detailing. It can been seen that the girder layovers and twists from Figures 45 and 46 closely match with those from Figures 38 and 39.

Table 11. Bridge NISSS4 SDLF initial fixed end forces based on LGA cambers and obtained from GT-LOFT.

Between	CF #	Equivalent Element End I Global DOF						Equivalent Element End II Global DOF					
		1 (kip)	2 (kip)	3 (kip)	4 (kip*in)	5 (kip*in)	6 (kip*in)	1 (kip)	2 (kip)	3 (kip)	4 (kip*in)	5 (kip*in)	6 (kip*in)
G1-G2	**1**	0	0	-73	-3498	-9619	0	0	0	73	-3498	-9619	0
	2	0	0	-1117	-53598	0	5	0	0	1117	-53598	0	5
	3	0	0	-766	-36769	-1	8	0	0	766	-36769	1	8
	4	0	0	-262	-12595	-1	10	0	0	262	-12595	1	10
	5	0	0	262	12595	-1	10	0	0	-262	12595	1	10
	6	0	0	766	36769	-1	8	0	0	-766	36769	1	8
	7	0	0	1117	53598	0	5	0	0	-1117	53598	0	5
	8	0	0	73	3498	9619	0	0	0	-73	3498	9619	0
G2-G3	**1**	0	0	-73	-3498	-9619	0	0	0	73	-3498	-9619	0
	2	0	0	-967	-46396	-1	7	0	0	967	-46396	1	7
	3	0	0	-527	-25287	-1	10	0	0	527	-25287	1	10
	4	0	0	0	0	-1	11	0	0	0	0	1	11
	5	0	0	527	25287	-1	10	0	0	-527	25287	1	10
	6	0	0	967	46396	-1	7	0	0	-967	46396	1	7
	7	0	0	73	3498	9619	0	0	0	-73	3498	9619	0

Table 11 (Continued). Bridge NISSS4 SDLF initial fixed end forces based on LGA cambers and obtained from GT-LOFT.

Between	CF #	Equivalent Element End I Global DOF						Equivalent Element End II Global DOF					
		1 (kip)	2 (kip)	3 (kip)	4 (kip*in)	5 (kip*in)	6 (kip*in)	1 (kip)	2 (kip)	3 (kip)	4 (kip*in)	5 (kip*in)	6 (kip*in)
G3-G4	**1**	0	0	-73	-3498	-9619	0	0	0	73	-3498	-9619	0
	2	0	0	-1117	-53598	0	5	0	0	1117	-53598	0	5
	3	0	0	-766	-36769	-1	8	0	0	766	-36769	1	8
	4	0	0	-262	-12595	-1	10	0	0	262	-12595	1	10
	5	0	0	262	12595	-1	10	0	0	-262	12595	1	10
	6	0	0	766	36769	-1	8	0	0	-766	36769	1	8
	7	0	0	1117	53598	0	5	0	0	-1117	53598	0	5
	8	0	0	73	3498	9619	0	0	0	-73	3498	9619	0

Table 12. Bridge NISSS4 TDLF initial fixed end forces based on LGA cambers and obtained from GT-LOFT.

Between	CF #	Equivalent Element End I Global DOF						Equivalent Element End II Global DOF					
		1 (kip)	2 (kip)	3 (kip)	4 (kip*in)	5 (kip*in)	6 (kip*in)	1 (kip)	2 (kip)	3 (kip)	4 (kip*in)	5 (kip*in)	6 (kip*in)
G1-G2	**1**	0	0	-289	-13885	-38185	0	0	0	289	-13885	-38185	0
	2	0	0	-4434	-212827	-2	19	0	0	4434	-212827	2	19
	3	0	-1	-3042	-146036	-3	34	0	1	3042	-146036	3	34
	4	0	-1	-1042	-50028	-4	39	0	1	1042	-50028	4	39
	5	0	-1	1042	50028	-4	39	0	1	-1042	50028	4	39
	6	0	-1	3042	146036	-3	34	0	1	-3042	146036	3	34
	7	0	0	4434	212827	-2	19	0	0	-4434	212827	2	19
	8	0	0	289	13885	38185	0	0	0	-289	13885	38185	0
G2-G3	**1**	0	0	-289	-13885	-38185	0	0	0	289	-13885	-38185	0
	2	0	-1	-3839	-184254	-3	27	0	1	3839	-184254	3	27
	3	0	-1	-2093	-100441	-4	38	0	1	2093	-100441	4	38
	4	0	-1	0	0	-4	43	0	1	0	0	4	43
	5	0	-1	2093	100441	-4	38	0	1	-2093	100441	4	38
	6	0	-1	3839	184254	-3	27	0	1	-3839	184254	3	27
	7	0	0	-289	-13885	-38185	0	0	0	289	-13885	-38185	0

Table 12 (Continued). Bridge NISSS4 TDLF initial fixed end forces based on LGA cambers and obtained from GT-LOFT.

Between	CF #	Equivalent Element End I Global DOF						Equivalent Element End II Global DOF					
		1 (kip)	2 (kip)	3 (kip)	4 (kip*in)	5 (kip*in)	6 (kip*in)	1 (kip)	2 (kip)	3 (kip)	4 (kip*in)	5 (kip*in)	6 (kip*in)
G3-G4	**1**	-1	4	-295	-14134	-38868	0	1	-4	295	-14207	-39068	0
	2	0	0	-2775	-133199	-2	16	0	0	2775	-133199	2	16
	3	0	-1	-1954	-93808	-3	32	0	1	1954	-93808	3	32
	4	0	-1	-716	-34348	-4	41	0	1	716	-34348	4	41
	5	0	-1	683	32806	-4	41	0	1	-683	32806	4	41
	6	0	-1	1972	94635	-3	34	0	1	-1972	94635	3	34
	7	0	0	2834	136043	-2	16	0	0	-2834	136043	2	16
	8	-3	9	298	14564	40051	0	3	-9	-298	14005	38513	0

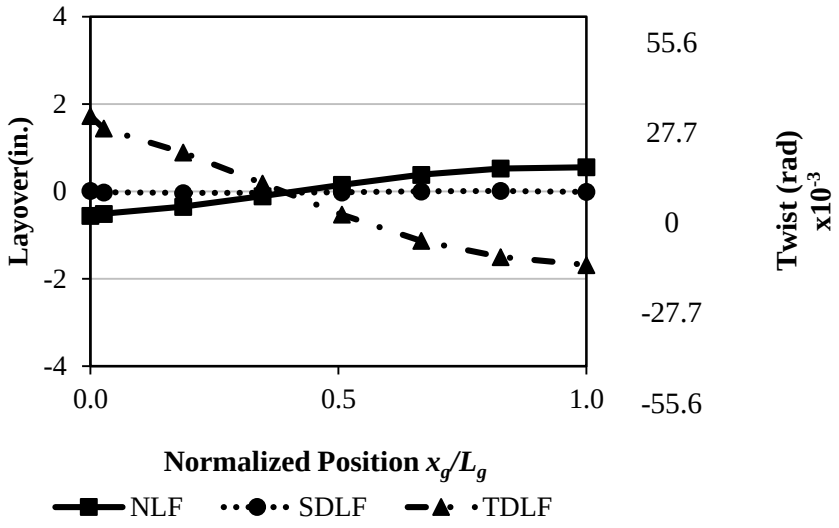

Figure 45. Layovers of a fascia girder G1 of bridge NISSS4 under SDL. These are layovers are from a geometrically linear grid analysis using the initial engineering strains.

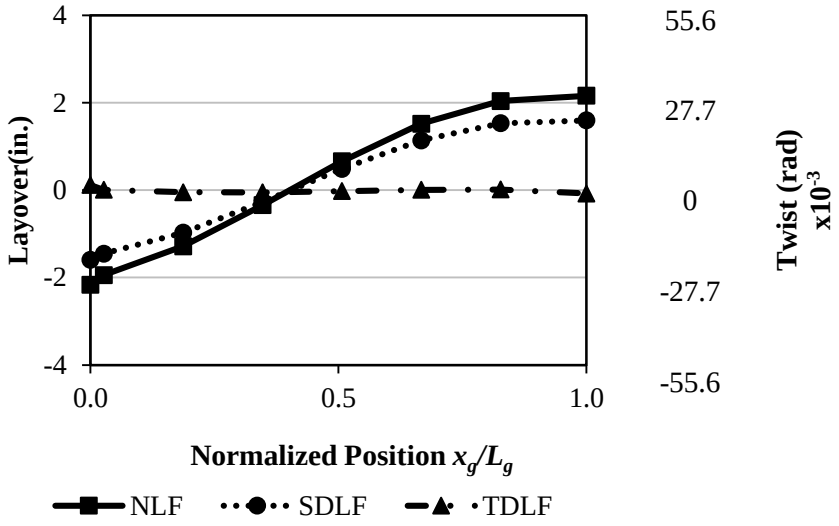

Figure 46. Layovers of a fascia girder G1 of bridge NISSS4 under TDL. These are layovers are from a geometrically linear grid analysis using the initial engineering strains.

3.4.2. Curved Radially-Supported Bridge Example – NISCR2

The framing plan of Bridge (B) NISCR2 is shown in Section 3.3.2, Figure 40. The primary bridge characteristics are discussed in this section. The SDL and TDL cambers used below are obtained from a 2D Grid analysis. The grid analysis cambers from the grid model are approximately the same as the 3D FEA cambers (shown in Figure 41).

Tables 13 and 14 show the initial fixed-end forces calculated by GT-LOFT for SDLF and TDLF detailing respectively. In these tables, the columns indicate the initial fixed-end forces, dofs 1 to 3, and moments, dofs 4 to 6. These initial fixed-end forces and moments are shown in two groups corresponding to ends I and II of the cross-frames. These forces and moments are calculated in the tool's cylindrical coordinate system. The rows indicate the cross-frames in the order from left to right, i.e. row 1 indicates cross-frames on the left-hand skewed bearing line.

The following are important observations from Tables 13 and 14:

- The largest values are in the columns corresponding to dof 3 (the vertical fixed-end forces) and dof 5 (the fixed-end moments about the θ axis). This is because, in determining the fixed-end forces, the equivalent beam element is subjected to vertical displacement while the end rotations about the θ axis are restrained to enforce plumb girder webs in both the final targeted dead load position and in the plumb fully-cambered positions of the girders.
- The initial fixed-end forces in the R and θ axis directions, indicated in the columns corresponding to dofs 1 and 2 in Tables 13 and 14, are zero.

- The initial fixed-end forces are larger for TDLF detailing than SDLF detailing since the displacements and rotations subjected to the equivalent beam element are larger.

Figures 47 and 48 show the girder layovers and twists from a geometrically linear 2D Grid analysis using the initial engineering fixed end forces, calculated by GT-LOFT. These figures correspond to the SDL and TDL conditions respectively. The symbols on the curves correspond to the cross-frame nodes. One can see that, with the calculated initial fixed-end forces included in the grid analysis, the girder webs are essentially plumb under SDL for SDLF detailing and under TDL for TDLF detailing. It can been seen that the girder layovers and twists from Figures 47 and 48 closely match with those from Figures 42 and 43.

Table 13. Bridge NISCR2 SDLF initial fixed end forces based on 3D FEA cambers and obtained from GT-LOFT.

Between	CF #	Equivalent Element End I Global DOF						Equivalent Element End II Global DOF					
		1 (kip)	2 (kip)	3 (kip)	4 (kip*in)	5 (kip*in)	6 (kip*in)	1 (kip)	2 (kip)	3 (kip)	4 (kip*in)	5 (kip*in)	6 (kip*in)
G1-G2	**1**	0	0	0	0	0	0	0	0	0	0	0	0
	2	0	0	508	0	24367	0	0	0	-508	0	24367	0
	3	0	0	883	0	42376	0	0	0	-883	0	42376	0
	4	0	0	1081	0	51878	0	0	0	-1081	0	51878	0
	5	0	0	1081	0	51878	0	0	0	-1081	0	51878	0
	6	0	0	883	0	42375	0	0	0	-883	0	42375	0
	7	0	0	508	0	24367	0	0	0	-508	0	24367	0
	8	0	0	0	0	0	0	0	0	0	0	0	0
G2-G3	**1**	0	0	0	0	0	0	0	0	0	0	0	0
	2	0	0	453	0	21749	0	0	0	-453	0	21749	0
	3	0	0	787	0	37771	0	0	0	-787	0	37771	0
	4	0	0	963	0	46226	0	0	0	-963	0	46226	0
	5	0	0	963	0	46226	0	0	0	-963	0	46226	0
	6	0	0	787	0	37772	0	0	0	-787	0	37772	0
	7	0	0	453	0	21749	0	0	0	-453	0	21749	0
	8	0	0	0	0	0	0	0	0	0	0	0	0

Table 13 (Continued). Bridge NISCR2 SDLF initial fixed end forces based on 3D FEA cambers and obtained from GT-LOFT.

Between	CF #	Equivalent Element End I Global DOF						Equivalent Element End II Global DOF					
		1 (kip)	2 (kip)	3 (kip)	4 (kip*in)	5 (kip*in)	6 (kip*in)	1 (kip)	2 (kip)	3 (kip)	4 (kip*in)	5 (kip*in)	6 (kip*in)
G3-G4	**1**	0	0	0	0	0	0	0	0	0	0	0	0
	2	0	0	411	0	19718	0	0	0	-411	0	19718	0
	3	0	0	714	0	34290	0	0	0	-714	0	34290	0
	4	0	0	874	0	41969	0	0	0	-874	0	41969	0
	5	0	0	874	0	41969	0	0	0	-874	0	41969	0
	6	0	0	714	0	34290	0	0	0	-714	0	34290	0
	7	0	0	411	0	19718	0	0	0	-411	0	19718	0
	8	0	0	0	0	0	0	0	0	0	0	0	0

Table 14. Bridge NISCR2 TDLF initial fixed end forces based on 3D FEA cambers and obtained from GT-LOFT.

Between	CF #	Equivalent Element End I Global DOF						Equivalent Element End II Global DOF					
		1 (kip)	2 (kip)	3 (kip)	4 (kip*in)	5 (kip*in)	6 (kip*in)	1 (kip)	2 (kip)	3 (kip)	4 (kip*in)	5 (kip*in)	6 (kip*in)
G1-G2	**1**	0	0	-8	-1	-375	0	0	0	8	1	-375	0
	2	0	0	1256	-1	60296	0	0	0	-1256	1	60296	0
	3	0	0	2182	-1	104755	0	0	0	-2182	1	104755	0
	4	0	0	2671	0	128186	0	0	0	-2671	0	128186	0
	5	0	0	2671	0	128186	0	0	0	-2671	0	128186	0
	6	0	0	2182	1	104755	0	0	0	-2182	-1	104755	0
	7	0	0	1256	1	60296	0	0	0	-1256	-1	60296	0
	8	0	0	-8	1	-395	0	0	0	8	-1	-395	0
G2-G3	**1**	0	0	-5	-1	-222	0	0	0	5	1	-222	0
	2	0	0	1154	-1	55410	0	0	0	-1154	1	55410	0
	3	0	0	2005	-1	96242	0	0	0	-2005	1	96242	0
	4	0	0	2454	0	117801	0	0	0	-2454	0	117801	0
	5	0	0	2454	0	117801	0	0	0	-2454	0	117801	0
	6	0	0	2005	1	96242	0	0	0	-2005	-1	96242	0
	7	0	0	1154	1	55410	0	0	0	-1154	-1	55410	0
	8	0	0	-4	1	-203	0	0	0	4	-1	-203	0

Table 14 (Continued). Bridge NISCR2 TDLF initial fixed end forces based on 3D FEA cambers and obtained from GT-LOFT.

Between	CF #	Equivalent Element End I Global DOF						Equivalent Element End II Global DOF					
		1 (kip)	2 (kip)	3 (kip)	4 (kip*in)	5 (kip*in)	6 (kip*in)	1 (kip)	2 (kip)	3 (kip)	4 (kip*in)	5 (kip*in)	6 (kip*in)
G3-G4	**1**	0	0	-8	-1	-396	0	0	0	8	1	-396	0
	2	0	0	1089	-1	52289	0	0	0	-1089	1	52289	0
	3	0	0	1895	-1	90963	0	0	0	-1895	1	90963	0
	4	0	0	2320	0	111355	0	0	0	-2320	0	111355	0
	5	0	0	2320	0	111355	0	0	0	-2320	0	111355	0
	6	0	0	1895	1	90963	0	0	0	-1895	-1	90963	0
	7	0	0	1089	1	52289	0	0	0	-1089	-1	52289	0
	8	0	0	-9	1	-409	0	0	0	9	-1	-409	0

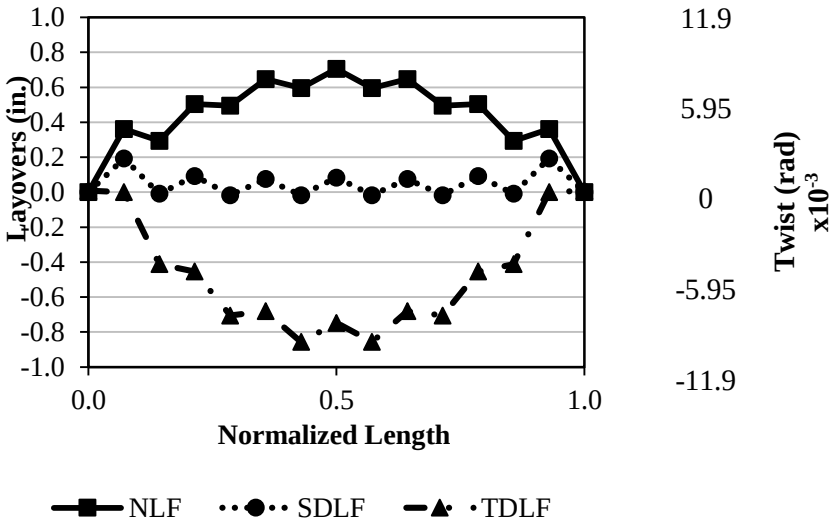

Figure 47. Layovers of a fascia girder G1 of bridge NISCR2 under SDL. These are layovers are from a geometrically linear grid analysis using the initial engineering strains.

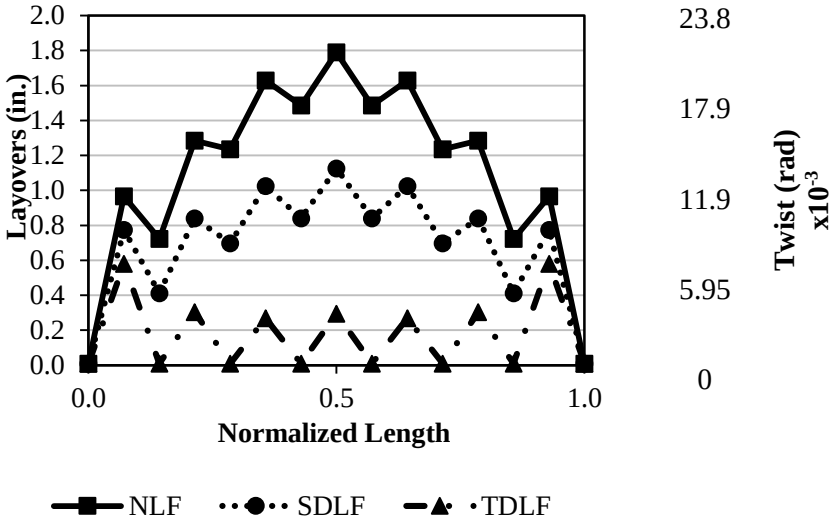

Figure 48. Layovers of a fascia girder G1 of bridge NISCR2 under TDL. These are layovers are from a geometrically linear grid analysis using the initial engineering strains.

CHAPTER 4

BEHAVIOR OF CURVED AND/OR SKEWED I-GIRDER BRIDGES

Understanding the behavior of straight skewed, curved, and curved and skewed I-girder bridges is important to understanding the implications of various framing arrangements, cross-frame detailing methods, and erection procedures on the ease of fit-up, achievement of the targeted constructed geometry, and generation of locked-in stresses in the cross-frame and girders of these structures. The key pertinent behavior of each of these bridge types is summarized in Sections 4.1, 4.2, and 4.3 respectively.

4.1. Behavior of Straight-Skewed I-Girder Bridges

In straight skewed bridges, the girders deflect only vertically under their self-weight, as long as the cross-frames are not connected to the girders in a manner such that they are engaged and can transfer internal shears and moments. This is illustrated by Figure 49, but with the cross-frames not shown. If all the girders are theoretically placed on their vertical supports, just the top chords of all the cross-frames are attached to the girders (such that there is no shear and moment transfer via the cross-frames), and the girders are allowed to deflect under the full steel self-weight, the resulting girder vertical deflections are exactly equal to the Steel Dead Load (SDL) deflections obtained from a Line Girder Analysis (LGA).

If the SDL cambers are set based on the above deflections, and then the cross-frames are detailed for Steel Dead Load Fit (SDLF) using these cambers, the cross-frames will theoretically fit exactly to the girders in the above SDL geometry without any forcing. That is, the SDLF detailing creates locked-in internal forces that cancel out the dead load cross-frame forces that would exist if the cross-frames were detailed for No-Load Fit (NLF).

These statements apply to all straight I-girder bridges with either parallel skew or non-parallel skew. However, they do not apply to curved I-girder bridges, as explained in Section 4.2. Chapter 9 provides a detailed explanation of this behavior in straight skewed bridges.

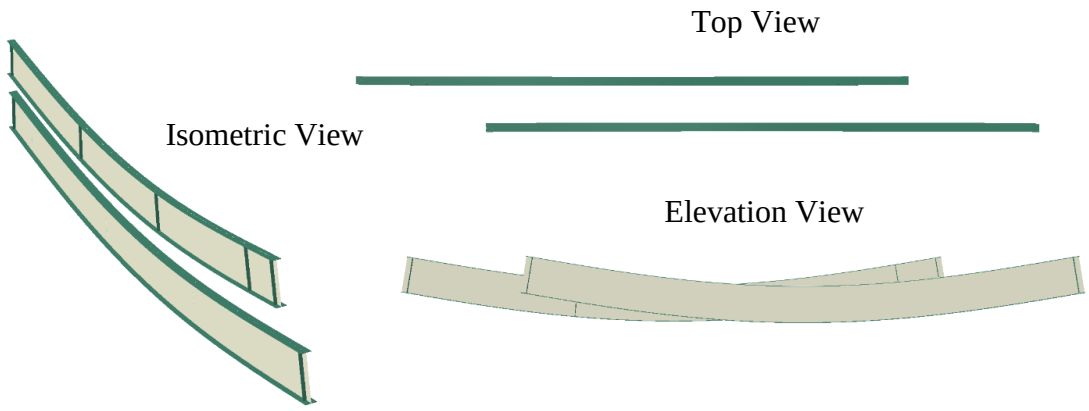

Figure 49. Magnified girder deflections for two straight I-girders, simply-supported at their ends on skewed bearing lines, and subjected to the self-weight of the structural steel prior to interconnecting the girders by the cross-frames (cross-frames not shown).

After the cross-frames are connected to the girders, the interconnected girders deflect as a 3D system under all subsequent loads. The cross-frames brace the girders, but they also serve as an additional transverse load path in the system. As a result, the girders deflect vertically and simultaneously twist under the dead loads. This is illustrated using a simple two-girder system in Figure 50.

This behavior is different from the behavior of a straight non-skewed bridge. In a straight non-skewed bridge, the girders deflect predominantly in a vertical fashion. This is because there are no significant differential vertical deflections between the girders and there is no significant interaction between the girders and the cross-frames (aside from aspects such as eccentric overhang bracket loads during the concrete deck placement).

However, in a straight skewed bridge, there are significant differential vertical deflections between the girders at each of the intermediate cross-frames, since these cross-frames connect to different positions within the span of each of the girders. In addition, to maintain compatibility between the cross-frames and the girders at sharply-skewed abutment bearing lines, the girders have to twist substantially at the skewed abutments.

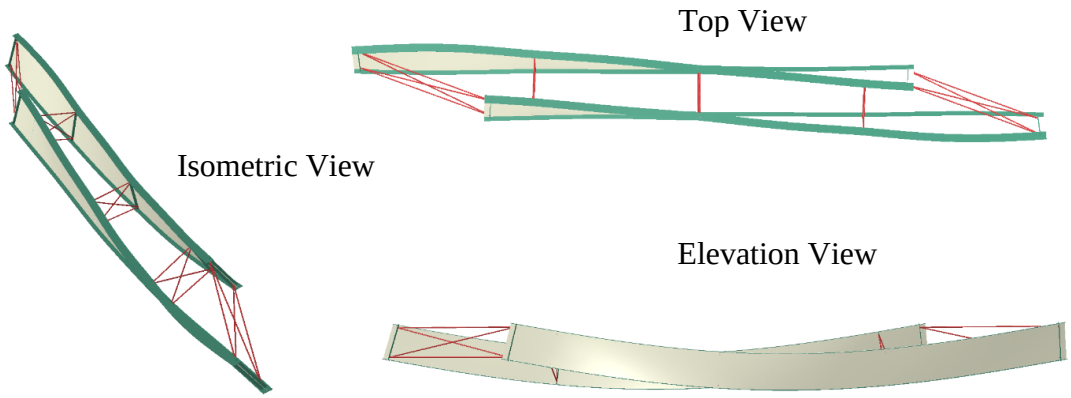

Figure 50. Magnified girder deflections for two straight I-girders, simply-supported on skewed bearing lines at their ends, and subjected to vertical load after interconnecting the girders by cross-frames.

4.2. Behavior of Curved Radially-Supported Bridges

The fundamental behavior of horizontally curved radially-supported I-girder bridges is substantially different from that of straight skewed I-girder bridges. Figure 51 shows the magnified deflections under vertical load in a simply-supported bridge of this type after all of the steelwork has been completed. By comparing to Figure 49, one can immediately observe that the deflections are entirely different in a curved radially-supported bridge. Essential behavior differences compared to straight skewed bridges are discussed below.

The bridge cross-section in horizontally curved bridges is subjected to substantial internal torsional moments due to the fact that the resultant of the bridge vertical loads

within the spans has an eccentricity relative to a straight chord between the supports. In a straight bridge, the total internal torsion tends to be relatively small and the twisting of the girders is induced predominantly by the compatibility of deformations between the girders and the cross-frames. That is, if the girders are not interconnected by the cross-frames, there is no tendency for them to twist under the primary vertical loads. In a curved bridge, the total internal torsion is due to the eccentricity of the resultant of the vertical loads. This torsion is independent of the interconnection of the girders by the cross-frames.

The predominant resistance to the above internal torsion in horizontally curved I-girder bridges is developed by interconnecting the girders by the cross-frames across the entire bridge width. If the girders in Figure 50 were connected together *only* by the cross-frames at the *ends of the span*, the individual girder twist rotations and the coupled vertical displacements would be excessive. Curved I-girders, and curved I-girder bridge units, generally cannot be erected without providing some type of intermediate vertical support within the spans, typically via holding cranes or temporary shoring at critical stages of the erection. The individual girders as well as the partially completed bridge cross-sections tend to "torsionally over-rotate" during the steel erection compared to their behavior within the completed steel superstructure.

In a straight skewed bridge detailed for SDLF, the girders inherently do not transfer load to the cross-frames under the SDL conditions since the cross-frames are not needed to restrain the girders from twisting. Horizontally curved bridges are different. Regardless of the detailing method used (NLF, SDLF, TDLF, etc.), vertical forces ("V-loads") are applied to the girders by the cross-frames, producing a shift in the internal vertical loads toward the girders on the outside of the horizontal curve. Associated radial forces are

applied to the girders from the cross-frames that restrain the tendency of the girders to twist excessively on their own. The cross-frames provide these restoring forces to the individual girders via the system behavior of the bridge, thus preventing excessive individual girder out-of-plane rotations.

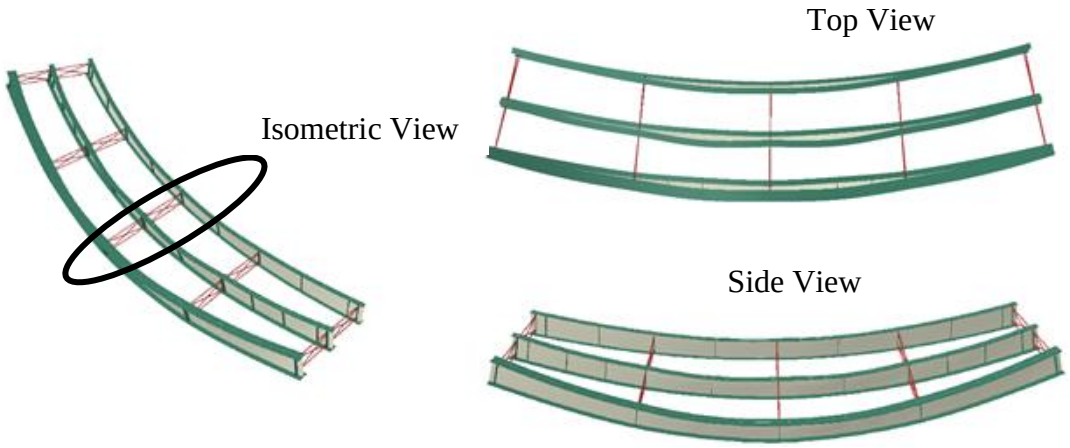

Figure 51. Magnified girder deflections in a representative horizontally curved I-girder bridge, simply-supported on radial bearing lines at its ends, and subjected to vertical load after interconnecting all the girders by cross-frames.

Due to the above behavioral effects, the locked-in internal forces due to SDLF and TDLF detailing of the cross-frames tend to be additive with the other internal dead load force effects. This behavior can be explained conceptually by considering the actions at a contiguous cross-frame line near mid-span in the representative curved radially-supported bridge shown in Figure 51. Figure 52 illustrates the behavior at the highlighted cross-frame line in the curved bridge from Figure 51. If the cross-frames in this bridge were detailed for NLF, then the girders are plumb and the cross-frames fit between the girders without any forcing in the fully-cambered no-load geometry. Therefore, once the TDL is applied to this bridge, the overall bridge cross-section twists and the girders will be "laid over" within the bridge span. These layovers are not a structural concern, generally, as long as

overall global stability of the bridge system is ensured, since they are within the span and do not have any significant influence on the bearings or the overall roadway alignment. For simplicity, the sketch in Figure 52 shows the girders in a configuration without any superelevation or cross-slope at the completion of the bridge and under the TDL, assuming NLF detailing of the cross-frames (see the middle sketch in Figure 52). The girder at the left of Figure 52 is on the outside of the curve and is subjected to larger dead load deflection because of the behavior resulting for horizontal curvature. Therefore it has larger vertical camber than the adjacent interior girder and is at a higher elevation in the no-load condition.

If TDLF detailing of the cross-frames is used on a curved radially-supported bridge such as in the above example, the cross-frames are built in a geometry such that they twist the girders substantially in the direction opposite from the direction which they want to roll under dead loads. This is illustrated by the sketch at the bottom of Figure 36. In this case, this additional "pulling" (or "twisting") of the girders in the direction opposite from that which they want to roll tends to increase the internal forces in the cross-frames.

TDLF detailing also twists the girders substantially in the direction opposite from that which they roll under dead loads in a straight skewed bridge. However, in this case, the detailing relieves the TDL effects in the cross-frames. This is because the TDL twist rotations in a straight skewed bridge are imposed on the girders via the compatibility of deformations with the cross-frames. Conversely, in a curved radially-supported bridge, the intermediate cross-frames restrain or resist the tendency of the curved girders to twist and deflect excessively, which would occur if they were restrained from twisting only at the bearing lines. The intermediate cross-frames tie the girders into the overall structural system, and force the girders to work together to resist torsion via differential major-axis

bending of the girders across the bridge cross-section. Therefore, the additional pulling or twisting of the girders in the opposite direction from that which they want to roll adds to the other dead load cross-frame forces in a curved radially-supported bridge, since the other dead load forces *and* the additional forces associated with the TDLF detailing are both restraining or resisting the tendency of the individual girders to twist and deflect excessively.

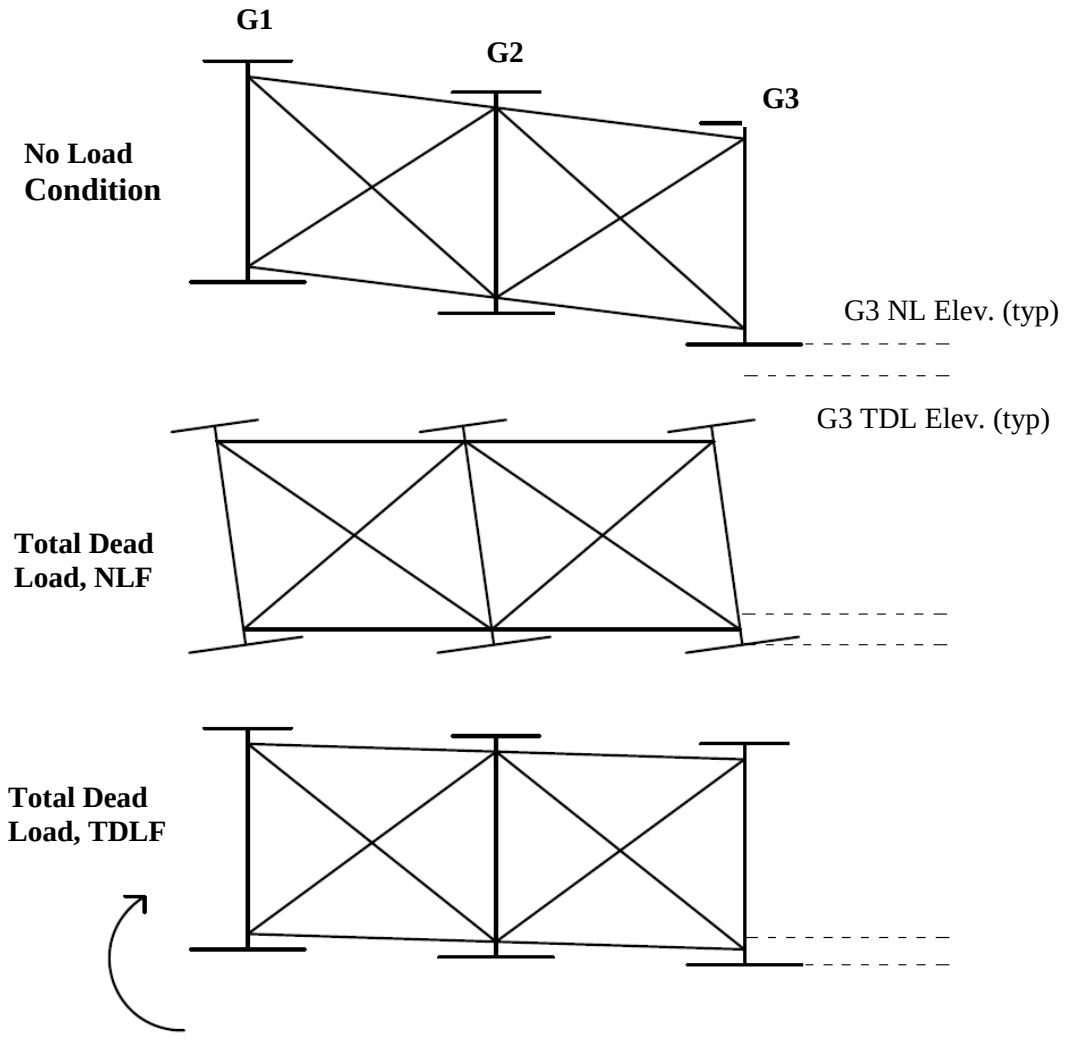

Figure 52. The behavior at the highlighted cross-frame line in the curved radially-supported bridge from Figure 51.

It should be noted that Figure 51 does not include the initial vertical camber that is fabricated into the girders. If the initial vertical camber were included in Figure 51, the bridge would essentially be in a flat geometry under the TDL when NLF detailing is used, as shown in the center sketch of Figure 52. Figure 51shows the magnified displacements on the bridge geometry, neglecting the influence of the vertical camber. When TDLF detailing is used, the girders are twisted in the direction opposite from the direction they tend to roll under dead loads. Because twist rotations and vertical deflections are coupled in curved bridges, the final girder elevations are somewhat higher when TDLF detailing is used.

4.3. Behavior of Curved and Skewed Bridges

Horizontally curved I-girder bridges with skewed supports generally include a combination of all of the effects discussed in the above sections. The curvature and the skew can induce responses that are either additive or subtractive to one another, depending on the overall bridge geometry. A skewed abutment, combined with the framing arrangement of the cross-frames, can cause girder twist rotations that are in the same direction as the twist due to the horizontal curvature. However, a similar skewed abutment with a skew angle that is the negative of the above case, in combination with the framing of the cross-frames, can induce girder twist rotations that are in the opposite direction from those due to the horizontal curvature. Therefore, it is imperative that curved and skewed bridges be considered on a case-by-case basis.

CHAPTER 5

EVALUATION OF FIT-UP

Cross-frame fit-up forces are the forces required to physically bring a cross-frame and a girder that the cross-frame is being connected to together and complete the connection during the erection of the steel. These forces are influenced by the bridge type (straight skewed, curved radially-supported, or curved and skewed), bridge parameters such as span length and radius of curvature, detailing methods, framing arrangements, and erection procedures.

A major focus of this research is on the ease of fit-up of the cross-frames during erection. In this work, cross-frame fit-up is estimated by calculating the forces induced at the cross-frame top and bottom connections, for the second girder the cross-frame is connected to, as the cross-frame is installed. The first and second connections made to a given girder are denoted as connections A and B. In cases involving V or inverted-V type cross-frames, the first connection is assumed to be made to the joint where the diagonal attaches to the girder. In cases involving X-type cross-frames, the first connection is typically made at the top chord in these studies. The connection forces are zero prior to making a given connection, and they assume a non-zero value as a function of the geometry and boundary conditions at a given stage once the connection is completed. In this research, extensive parametric analyses are conducted to evaluate the cross-frame fit-up forces by sequentially installing cross-frames at selected critical stages.

The fit-up force calculations performed in this research are accurate to the extent that the nominal assumptions generally employed in bridge design are satisfied. That is, the simulations to determine fit-up forces are based on the following assumptions:

(1) No yielding of the steel occurs during erection,

(2) No incidental restraints from friction, etc. at temporary or permanent supports,

(3) The girder geometries, support elevations, etc. are as specified in the bridge plans, and

(4) Negligible play in the connections between the various bridge components.

There are various factors that can influence the actual bridge erection but cannot be accounted for in any detailed way within a practical engineering erection analysis, such as:

- Tolerances and the associated "play" at bolted connections,
- Adjustments of the crane and support elevations by the erector,
- Tolerances on support elevations, and
- Changes in the geometry of the steel due to thermal movements, etc.

These factors can cause differences between the actual fit-up forces encountered in the field compared to the erection analysis estimates. Connection tolerances and adjustment of crane and temporary support elevations can indeed make the fit-up forces somewhat smaller than the calculated estimates, as discussed subsequently in Section 8.2.1. However, the calculated fit-up forces determined in this research are believed to be reasonable engineering estimates associated with the nominal design representation of the structures.

As noted in Section 2.2.5, for the curved radially-supported and curved and skewed bridges studied in this research, the shoring and crane holding elevations are modeled at

the no-load elevations. Conversely, for the straight skewed bridges, the final steel dead load elevations are used for the shoring and crane holding elevations. These elevations have been observed to be good targets that tend to facilitate the fit-up of the cross-frames.

This research focuses on the maximum of the cross-frame fit-up forces to make the connections at selected critical stages. Discussions of how critical stages were selected in this research are provided in Chapter 8. All the cross-frame connections within the selected critical stages are parametrically evaluated to determine the maximum fit-up forces. The sub-sections below provide some discussion of whether the fit-up forces are large for a significant number of cross-frames or only for a small number of cross-frames. However, the key fit-up force estimate is of course the maximum one. The distribution of the final steel and total dead load cross-frame forces in the completed bridges is discussed in Section 6.4. The cross-frame fit-up forces are of course indirectly related to the final cross-frame dead load forces.

5.1. Cross-Frame Fit-Up in Curved Radially-Supported Bridges

For the evaluation of the fit-up forces, all three detailing methods – No-Load Fit (NLF), Steel Dead Load Fit (SDLF) and Total Dead Load Fit (TDLF) – are considered for the curved radially-supported bridges. NLF detailing generally provides the lowest fit-up forces for these bridge types. This is because, as explained in Section 4.2, SDLF and TDLF detailing effects tend to be additive with the internal force effects in these bridge types. Evaluating the SDLF and TDLF fit-up forces (i.e., the fit-up forces when the cross-frames are detailed for SDLF and TDLF) for the study bridges provides insight into when SDLF and TDLF fit-up may become prohibitive.

The following are trends in the values of the cross-frame fit-up forces in the curved radially-supported bridge cases studied in this research:

- The cross-frame fit-up forces for NLF detailing are generally very low for radial bearing-line cross-frames. This is because the girder deflections, girder differential deflections, and girder layovers are all practically zero at these locations. However, SDLF and TDLF detailing tend to give a minor increase in the fit-up forces for these radial bearing-line cross-frames. This is due to the deformation in the system caused by force-fitting the cross-frames at the other locations and due to the lack-of-fit from the differential major-axis rotations of the girders (note that the differential vertical deflections are still zero).

- The cross-frame fit-up forces for all detailing methods are generally largest near mid-span where the differential deflections and the differences in the girder layovers are also largest. The specific cross-frame connections with the largest fit-up forces are not necessarily the same for each of the detailing methods.

- The latter stages where the holding cranes often have been released often have larger cross-frame fit-up forces due to the bridge cross-section rotations and deflections and the increasing stiffness of the partially completed bridge system as more girders are installed.

Table 15 provides a synthesis of the maximum fit-up forces during the steel erection, calculated for all the curved radially-supported bridges studied in this research. In parallel to the presentation of the bridges in Chapter 2, the simple-span bridges are shown first followed by continuous-span bridges. They are presented in the order of increasing

maximum span length within each of these sub-groups. One can observe several basic trends in this data. However, some of the values require detailed inspection of the bridge geometry, framing arrangement, and erection procedure to fully understand their origins. The base overall bridge geometry parameters shown in Table 1 are listed in these tables along with the maximum fit-up force values to assist the reader in inspecting the results.

Erectors commonly use come-alongs and other local equipment, as necessary, to make the connections between the cross-frames and the girders. A typical come-along capacity is taken as 20 kips (some erectors indicate that 12 kips is more typical). A calculated fit-up force significantly more than 40 kips is considered difficult and is shown by dark shading in Table 15. The selection of this value is based on the judgment of the research, considering the fact that various factors in the field, including connection tolerances as well as manipulation of crane, temporary tower, or support elevations, can typically result in some reduction in these forces. Maximum fit-up forces between 30 and 40 kips are shown by light shading in Table 15.

The most significant trends shown in Table 15 are as follows (exceptions are discussed further below):

(1) In most cases, the fit-up forces for NLF detailing are small and manageable.

(2) In general, because of the additive SDLF and TDLF detailing effects on the internal dead load forces in curved radially-supported bridges, SDLF and TDLF detailing tend to increase the maximum fit-up forces in these bridges. However, the fit-up force increase caused by SDLF detailing typically is not prohibitive.

(3) In most cases, the fit-up forces for TDLF detailing are significantly larger.

(4) For the curved radially-supported bridges, the largest of the maximum fit-up forces correspond to cases with a combination of longer spans with a narrow bridge cross-section (large L_s/w_g) and a tight curve (large L_s/R).

(5) Higher differential deflections tend to lead to higher fit-up forces. However, the fit-up forces are significantly reduced when temporary supports such as shoring towers or holding cranes are used.

A few of the bridge cases do not follow the above trends. The critical erection stages for TDLF detailing are shown for each of the bridge cases in the subsequent figures in this section. In many cases, the critical stages are the same stages for NLF, SDLF, and TDLF detailing. As shown in Figure 53, Bridge (D) NISCR10 uses a shoring tower during its construction to allow the girder splices to be made in the air, resulting in a significant reduction in the displacements during the erection. Correspondingly, the fit-up forces are reduced for this bridge. Bridge (B) NISCR2, with Erection Scheme 2A (shown in Figure 54), has high maximum fit-up forces regardless of the method of cross-frame detailing. This is due to the specific erection procedure used for this bridge – erection of the girders from the inside to the outside of the curve – and the fact that this bridge has a relatively large L_s/w_g of 6.2 and a tight horizontal curve (L_s/R = 0.34). The large fit-up forces for this bridge are occurring in spite of the relatively short span length (L_s = 150 ft). The large forces shown for Scheme 2A indicate that this is not a feasible erection scheme. It is necessary to add additional vertical support on the outside girder of the partially completed bridge cross-section, to reduce its vertical deflections. Erection Scheme 2B (Figure 54) does this by placing an additional holding crane on the outside girder of the partially completed bridge cross-section. The NLF and TDLF fit-up forces for NISCR2 Scheme 2B

are reduced to 40.4 kip and 50.5 kip, respectively, which are close to the 40 kip threshold where fit-up is considered to become difficult.

The SDLF fit-up forces for all the curved radially-supported bridges except for bridge (E) EICCR11 (Figure 55), which is the most extreme case considered here, involving a highly curved large span and a relatively narrow bridge cross-section, and bridge (B) NISCR2 Scheme 2A (Figure 54) are below 40 kips and thus are considered manageable. Bridge (E) EICCR11 is discussed further in Section 5.4.

In all cases in Table 15, except for bridge (B) NISCR2 with Erection Schemes 2A and 2B and bridge (E) EICCR11, the fit-up forces for the NLF cases are small and manageable. The maximum TDLF fit-up forces for bridges (A) EISCR1, (D) NISCR10, and (G) EICCR4 (i.e., the maximum calculated fit-up forces when TDLF detailing is used) are below 40 kips. These results are discussed further below:

- Bridge (A) EISCR1 (Figure 56) is a short span and its maximum girder differential deflection under SDL is low (0.42 in).
- Bridge (D) NISCR10 (Figure 53) has a longer span of 225 ft, but its span to radius ratio L_s/R is smaller (0.32). Furthermore, the erection of bridge (D) NISCR10 involved the use of a shoring tower within the span.
- The bridge (G) EICCR4 (Figure 57) maximum span length is 350 ft, but its maximum L_s/R is relatively low (0.26). In addition, the erection of Bridge (G) EICCR4 used shoring towers, which helped reduce the fit-up forces.

Table 15. Maximum cross-frame fit-up forces of the curved radially-supported bridges studied in this research (Fit-up forces below 30 kips are unshaded, between 30 and 40 kips are shown by a light shading, and above 40 kips are shown by a dark shading).

Bridge	**Framing Plan**	**Shoring Towers**	L_s **(ft)**	w_g **(ft)**	R **(ft)**	n_g	L_s/R	L_s/w_g	**Differential Deflections (in.)**		**Cross-Frame Fit-Up Force (in.)**		
									SDL	**TDL**	**NLF**	**SDLF**	**TDLF**
(A) EISCR1	Figure 1	0	90	17.5	200	3	0.45	5.1	**0.42**	**1.67**	**3.3**	**7.4**	**22.3**
(B) NISCR2, Scheme 1	Figure 2	0	150	24.0	438	4	0.34	6.2	**0.68**	**1.83**	**16.6**	**28.7**	**54.0**
(B) NISCR2, Scheme 2A	"	"	"	"	"	"	"	"	"	"	**84.4**	**82.5**	**80.2**
(B) NISCR2, Scheme 2B	"	"	"	"	"	"	"	"	"	"	**40.4**	**19.4**	**50.5**
(C) NISCR7	Figure 3	0	150	74.0	280	9	0.54	2.0	**0.42**	**1.19**	**21.3**	**35.9**	**75.3**
(D) NISCR10	Figure 4	1	225	74.0	705	9	0.32	3.0	**0.47**	**0.78**	**18.6**	**20.4**	**21.8**
(E) EICCR11	Figure 5	3 (in curved span)	322,417, 322	40.4	∞, ∞, 411	4	0, 0, 0.80	8.0, 10.3, 8.1	**3.10**	**5.41**	**37.5**	**86.3**	**130.0**
(F) NICCR12	Figure 6	3	350,350, 280	74.0	909	9	0.39, 0.39, 0.31	4.7, 4.7, 3.8	**0.96**	**1.72**	**28.4**	**38.6**	**57.4**
(G) EICCR4	Figure 7	2	219,260, 211,162, 256,190	36.7	968,3@1108, 968,∞	4	0.20,0.24, 0.19,0.15, 0.26,0	6.0,7.1, 5.7,4.4, 7.0,5.2	**0.35**	**1.09**	**12.3**	**12.6**	**16.0**

Notes:
(1) Bridge (B) NISCR2 Schemes 2A and 2B involved erection from the inside to the outside of the curve.
(2) Bridge cases (E) EICCR11 and (G) EICCR4 involved drop-in segments.

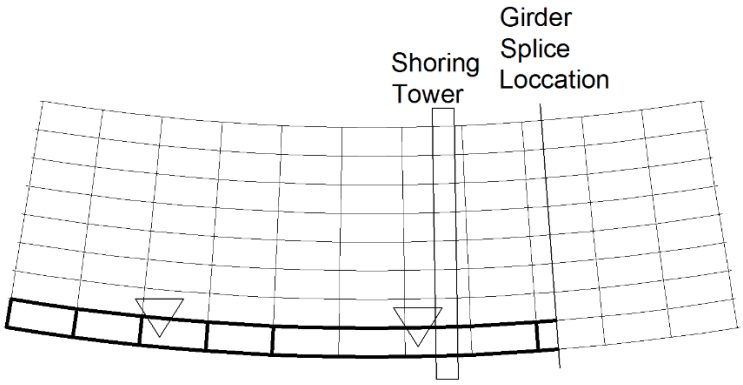

Figure 53. Critical erection stage of Bridge (D) NISCR10 for TDLF detailing. The darker lines show portions of the bridge that are already completed. The two triangles are the pick points of the lifting crane.

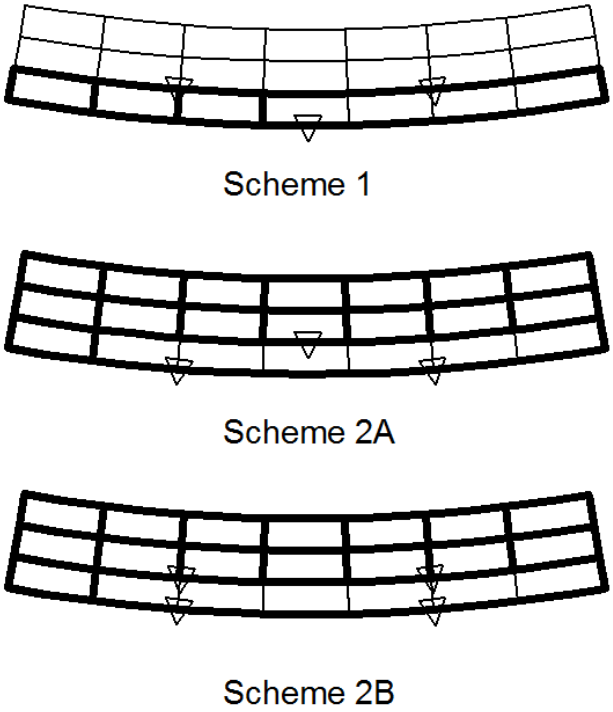

Figure 54. Critical erection stages of Erection Schemes 1 (outside to inside, one holding crane), 2A (inside to outside, one holding crane) and 2B (inside to outside, two holding cranes) of Bridge (B) NISCR2 for TDLF detailing. The darker lines show portions of the bridge that are already completed. The triangles denote the pick points of the lifting crane and of the holding crane.

The maximum TDLF fit-up forces for bridges (B) NISCR2 Schemes 1, 2A, and 2B, (C) NISCR7 (Figure 58), (E) EICCR11, and (F) NICCR12 (Figure 59) are significantly larger than 40 kips. Specific explanations of the TDLF fit-up forces for these bridges are as follows:

- For bridge (B) NISCR2, its L_s/R is reasonably high (0.34).
- For bridge (C) NISCR7, its L_s/R (0.54) is even larger than bridge (B) NISCR2, leading to larger TDLF fit-up forces than bridge (B) NISCR2 Schemes 1 and 2B.
- Both bridge (B) NISCR2 Scheme 1 and bridge (C) NISCR7 did not use shoring towers.
- Bridge (E) EICCR11 is a large bridge with long spans, a narrow bridge cross-section, and the highest L_s/R (0.78) of all bridge cases studied. The site conditions limited the locations of the shoring towers. In addition the use of drop-in segments was required on this bridge. For bridge (E) EICCR11, not only is the TDLF fit-up unmanageable, but SDLF fit-up also is prohibitive.
- Bridge (F) NICCR12 has the longest span of all bridge cases considered (350 ft). However, a single shoring tower is provided at the mid-spans of this bridge, which leads to some reduction in the calculated maximum fit-up forces. In addition, the maximum L_s/R is relatively high (0.39) for this structure.

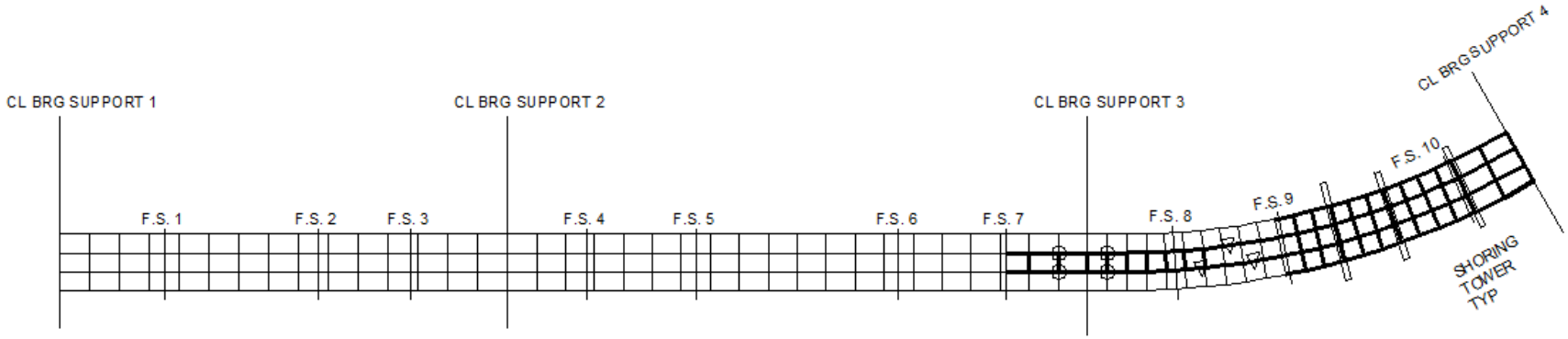

Figure 55. Critical erection stage of Bridge (E) EICCR11 for TDLF detailing. The darker lines show portions of the bridge that are already completed. The triangles denote the pick points of the lifting crane and of the holding crane. The four circles are the pier brackets.

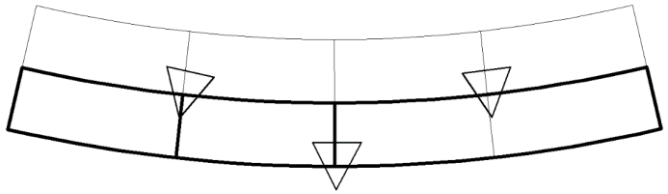

Figure 56. Critical erection stage of Bridge (A) EISCR1 for TDLF detailing. The darker lines show portions of the bridge that are already completed. The triangles denote the pick points of the lifting crane and of the holding crane.

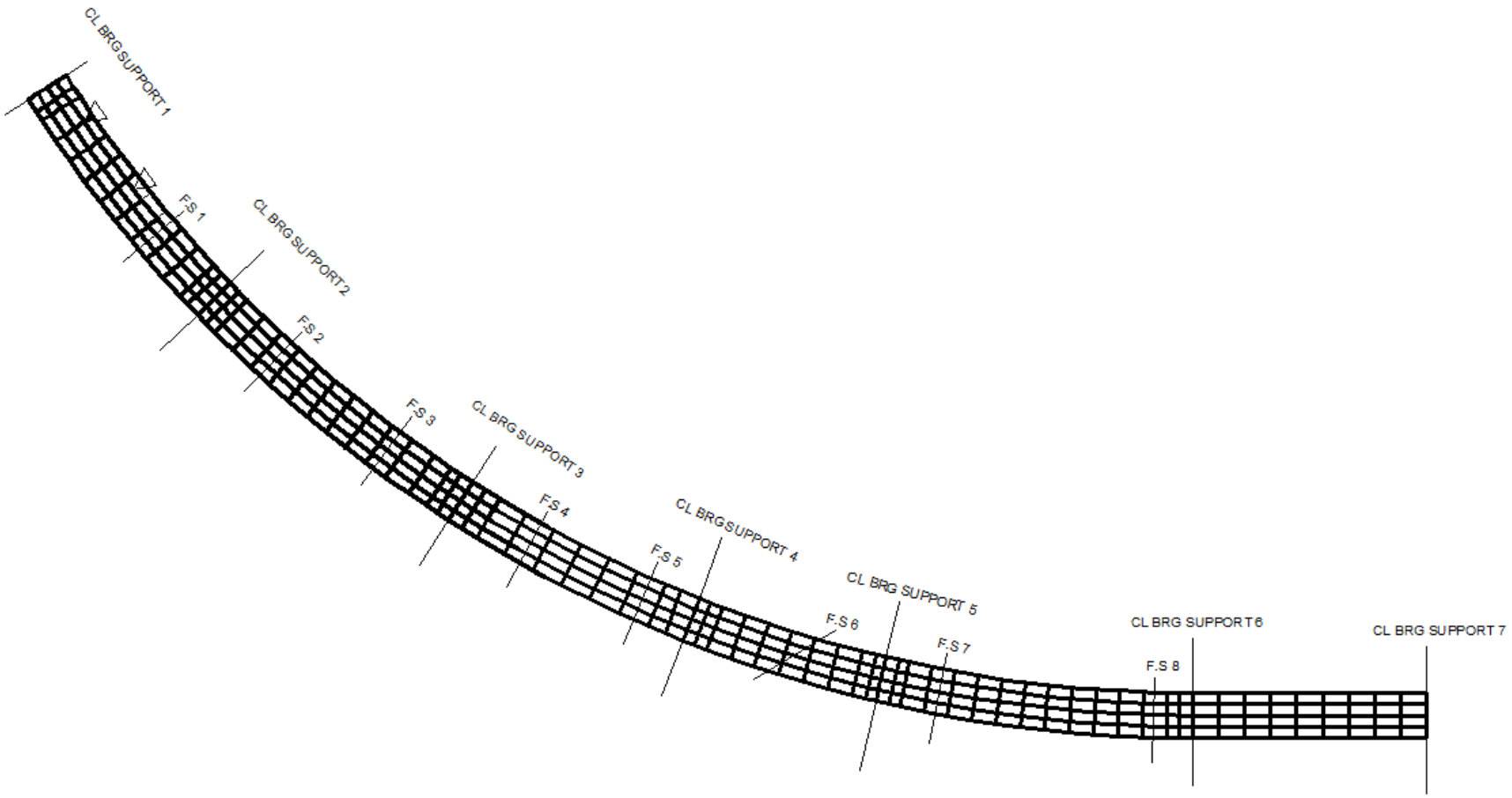

Figure 57. Critical erection stage of Bridge (G) EICCR4 for TDLF detailing (see Span 1). The darker lines show portions of the bridge that are already completed. The two triangles denote the pick points of the lifting crane.

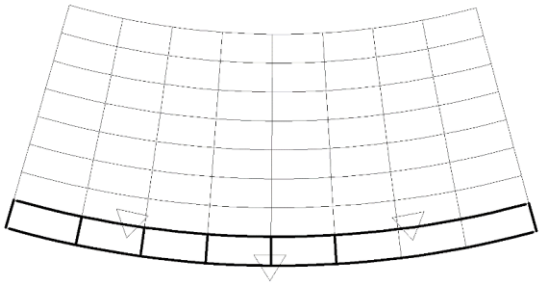

Figure 58. Critical erection stage of Bridge (C) NISCR7 for TDLF detailing. The darker lines show portions of the bridge that are already completed. The triangles denote the pick points of the lifting crane and of the holding crane.

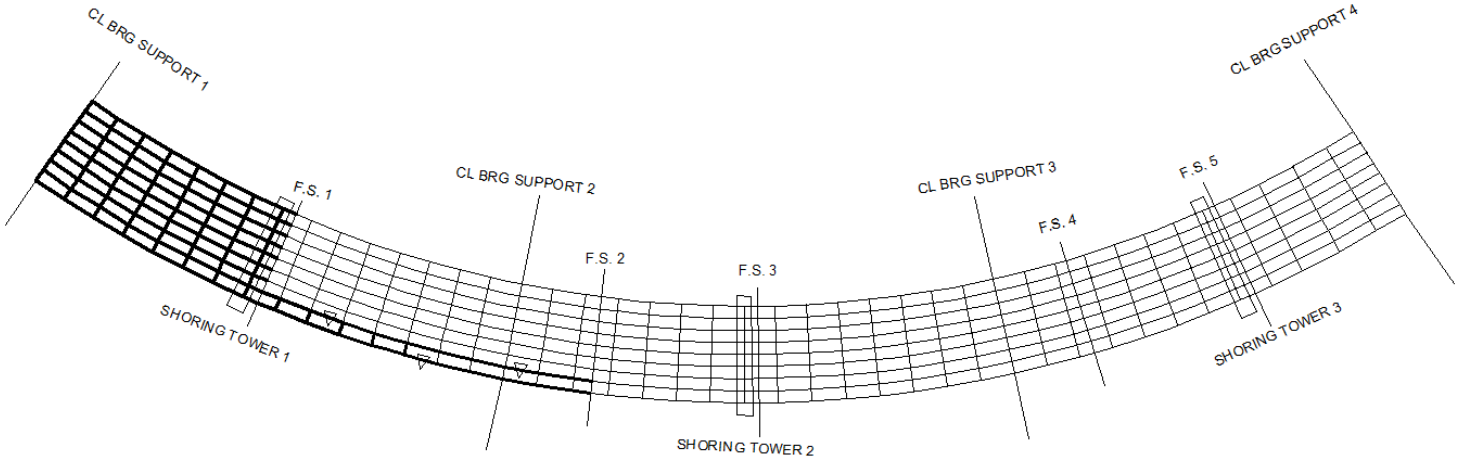

Figure 59. Critical erection stage of Bridge (F) NICCR12 for TDLF detailing. The darker lines show portions of the bridge that are already completed. The triangles denote the pick points of the lifting crane and of the holding crane.

5.2. Cross-Frame Fit-Up in Straight Skewed Bridges

For straight skewed bridges, only cases with SDLF and TDLF detailing were considered for the evaluation of the fit-up forces. This is for the following reasons:

- SDLF detailing provides the lowest fit-up forces for straight skewed bridges
- Studying the fit-up forces with TDLF detailing provides insights into when TDLF detailing could become prohibitive.
- The cases with NLF detailing were not studied for the evaluation of fit-up forces in straight skewed bridges because NLF fit-up can be more difficult than SDLF in straight skewed bridges.
- Furthermore, more importantly, the bearing rotation demands and girder layovers under TDL can be excessive if a straight skewed bridge with sharp skew were detailed using a NLF. (The studies on curved radially-supported bridges and bridges having both skew and horizontal curvature consider NLF detailing in addition to SDLF and TDLF detailing.)

In contrast, the results of all three detailing methods are provided for all the bridge cases in the evaluation of the bridge responses in the final SDL and TDL conditions. This is because the current common practice in design is to analyze the bridge neglecting any internal forces induced by the detailing method, i.e., bridges are commonly analyzed assuming NLF detailing is used.

The following are trends in the values of cross-frame fit-up forces in the straight skewed bridge cases studied in this research (these trends are distinctly different from the trends in curved radially-supported bridges):

- The cross-frame fit-up forces for all detailing methods are generally largest near the skewed bearing line and along the transverse load path between the obtuse corners (in bridges with parallel skew). For non-parallel skewed bridges, the cross-frame fit-up forces tend to be largest near the skewed bearing line and between the interior girders. These observations similar to the distribution of the cross-frame forces in the completed structure in straight skewed bridges discussed in Section 6.7.2.

- For erection stages where the splice connection has not been made (i.e. the steel is not yet at the SDL elevation profile), the cross-frame fit-up forces for SDLF and TDLF detailing are generally larger at the crane and shoring tower locations which can have temporary lateral bracing. In these cases, the cross-frame fit-up forces for TDLF detailing tend to be larger than those for SDLF detailing since the crane and shoring tower elevations are set at the SDL elevations for the straight skewed bridges in this research. The partially-erected bridge system is deflecting under its self-weight, but the total dead loads are of course not yet in place.

- The specific cross-frame connections with the largest fit-up forces are not necessarily the same for SDLF and TDLF detailing.

- In straight skewed bridges, holding cranes do not have as significant of an effect on the bridge deflection as in curved bridges. Holding cranes are often only needed during the installation of the first few girders for stability. In parallel-skewed bridges, most of the bridge cases are installed in the same sequence for each of their girders and cross-frames. Therefore, the latter erection stages where the holding

cranes often have been released generally have the same range of cross-frame fit-up forces as in the other erection stages. In non-parallel straight skewed bridges, the erection stages with the longer girders often have higher cross-frame fit-up forces due to higher differential deflections at these stages.

Table 16 provides a synthesis of the maximum fit-up forces during the steel erection, calculated for all the straight skewed bridges studied by the research. As indicated in Chapter 2, the simple-span bridges are shown first followed by continuous-span bridges. The bridges are presented in the order of increasing maximum span length within each of these sub-groups. Some of the values require detailed inspection of the bridge geometry, framing arrangement, and erection scheme to fully understand their origins and significance. The base overall bridge geometry parameters shown in Table 2 are listed in these tables along with the maximum fit-up force values. A calculated fit-up force significantly more than 40 kips is considered difficult and is shown by dark shading in Table 16. Maximum fit-up forces between 30 and 40 kips are shown by light shading.

The most significant trends shown in Table 16 are as follows:

(1) The maximum fit-up forces are generally low when SDLF detailing is used. These forces are only a fraction of the forces encountered when TDLF detailing is used. However, TDLF detailing is never prohibitive on the straight skewed bridges considered in this researchuntil the spans become relatively long (larger than about 200 ft).

(2) The maximum fit-up forces tend to be larger for longer span bridges with sharper skew of the bearing lines.

Table 16. Maximum cross-frame fit-up forces of the straight skewed bridges studied in this research (Fit-up forces below 30 kips are unshaded, between 30 and 40 kips are shown by a light shading, and above 40 kips are shown by a dark shading).

Bridge	Framing Plan	Shoring Towers	L_{max} (ft)	L_{min} (ft)	w_g (ft)	θ (deg)	n_g	I_s	L_{max}/w_g	L_{min}/w_g	Differential Deflections (in.)		Max fit-up forces (kip)	
											SDL	TDL	SDLF	TDLF
(H1) EISSS57	Figure 8	0	211	63	61	69.5, -4.4	7	0.77	3.5	1.0	**1.00**	**2.95**	**5.0**	**15.0**
(H2) EISSS57	Figure 22	"	"	"	"	"	"	"	"	"	**1.09**	**3.19**	**5.0**	**14.2**
(I1) NISSS14	Figure 9	0	150	150	74	70	9	1.36	2.0	2.0	**0.97**	**4.33**	**3.6**	**15.3**
(I2) NISSS14	Figure 23	"	"	"	"	"	"	"	"	"	**0.98**	**4.37**	**2.5**	**7.5**
(J1) NISSS54	Figure 10	1	300	300	74	70	9	0.68	4.1	4.1	**2.07**	**4.56**	**9.2**	**73.5**
(J2) NISSS54	Figure 24	"	"	"	"	"	"	"	"	"	**1.98**	**4.49**	**8.4**	**47.9**
(K1) EICSS12	Figure 11	0	150, 139	150, 139	41	59.6	6	0.47, 0.50	3.7, 3.4	3.7, 3.4	**0.38**	**1.67**	**0.6**	**6.3**
(K2) EICSS12	Figure 25	"	"	"	"	"	"	"	"	"	**0.36**	**1.62**	**0.4**	**7.7**
(K3) EICSS12	Figure 26	"	"	"	"	"	"	"	"	"	**0.36**	**1.60**	**1.2**	**17.0**
(L) NICSS16	Figure 12	0	120, 150, 150	120, 150, 150	74	70	9	1.69, 1.36, 1.36	1.6, 2.0, 2.0	1.6, 2.0, 2.0	**0.53**	**2.81**	**0.8**	**36.9**
(M1) EICSS2	Figure 13	0	259, 255, 220	241, 183 ,220	66.6	58, 61.8, 38,38	8	0.48, 0.49, 0.23	3.9, 3.8, 3.3	3.6, 2.7, 3.3	**0.77**	**2.39**	**4.9**	**46.9**
(M2) EICSS2	Figure 27	"	"	"	"	"	"	"	"	"	**0.74**	**2.49**	**0.8**	**2.8**

Notes: Bridge cases (M1) and (M2) EICSS2 involved phased construction.

(3) Higher differential deflections tend to lead to higher fit-up forces. For the same order of differential deflections, the fit-up forces tend to be higher for curved radially-supported bridges than for straight skewed bridges (see Table 15).

As noted above, for the straight skewed bridges in Table 15, the SDLF fit-up forces are low and are only a fraction of the TDLF fit-up forces. This is because the cross-frame internal forces are minimal under SDL for SDLF detailing. The locked-in forces due to SDLF detailing approximately cancel with the SDL internal force effects determined via 3D FEA. Stated alternately, the SDLF cross-frame geometries are such that the cross-frames fit up with the girders, with negligible to small forcing, in the deflected (stressed) condition of the girders under the self-weight of the partially and fully erected steel.

The fit-up forces are evaluated for the base and alternate framing arrangements of the straight skewed bridges. The alternate framing plans stagger the cross-frames in a way that tends to alleviate the nuisance transverse stiffness effects. The erection schemes (installation order of girders and cross-frame and support requirements) are the same for the base and the alternate framing arrangements for each of the bridge cases. The figures shown below illustrate the erection schemes using the base framing arrangement. The following are further details regarding the behavior of the fit-up forces in for the straight skewed bridges from Table 16 (The critical erection stages for TDLF detailing are shown for each of the bridge cases in the subsequent figures in this section. In many cases, the critical stages are the same stages for SDLF and TDLF detailing):

- For bridge (H1) EISSS57 (Figure 60), a non-parallel straight skewed simple-span bridge, the alternate framing arrangement (H2) only slightly decreases the TDLF fit-up forces.

- For bridges (I1) NISSS14 (Figure 61) and (J1) NISSS54 (Figure 62), which are parallel skewed simple-span bridges, the alternate framing arrangements (I2) and (J2) significantly decrease the TDLF fit-up forces. However, for bridge (J2) NISSS54, the TDLF fit-up force remains high due to its 300 ft span and high skew index.

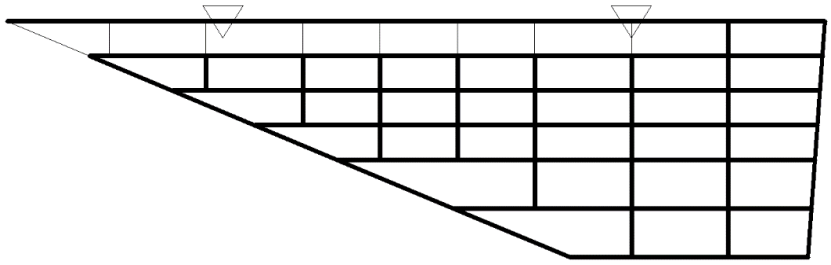

Figure 60. Critical erection stage of Bridge (H1) EISSS57 for TDLF detailing. The darker lines show portions of the bridge that are already completed. The two triangles denote the pick points of the lifting crane.

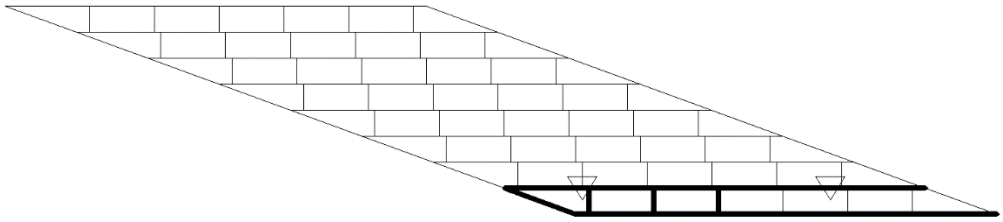

Figure 61. Critical erection stage of Bridge (I1) NISSS14 for TDLF detailing. The darker lines show portions of the bridge that are already completed. The two triangles denote the pick points of the lifting crane.

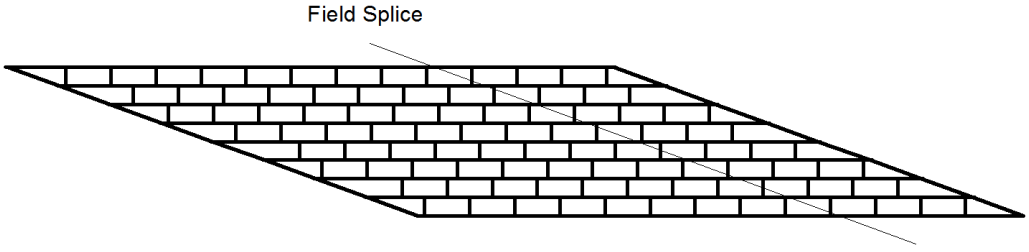

Figure 62. Critical erection stage of Bridge (J1) NISSS54 for TDLF detailing.

- Bridge (K1) EICSS12 (Figure 63) employs a lean-on system (Helwig and Yura, 2012). The alternate framing arrangement (K2) employs a staggered cross-frame system plus larger offsets of the intermediate cross-frames from the bearing lines. The arrangement (K3) employs a staggered cross-frame system with no bearing line cross-frames at the interior pier location and cross-frames connected directly into the bearing positions. Bridge (K1) with a lean-on framing arrangement has the lowest TDLF fit-up forces compared to bridge cases (K2) and (K3). It is important to note that the difference in TDLF fit-up forces between Bridge case (K1) (6.3 kip) and (K2) (7.7 kip) is small. Bridge (K3), with cross-frames connected directly into the bearing locations, has the highest TDLF fit-up forces. Framing cross-frames directly into the bearing locations results in an increased displacement incompatibility between the adjacent girders at the interior bearing line. For these cross-frames, the girder vertical displacement is zero on the side connected to the bearing and non-zero on the other side. Section 7.4 provides additional discussion of the effects of lean-on versus staggered cross-frame framing arrangements on the completed bridge responses.
- Bridge cases (M1) and (M2) EICSS2 (Figure 64) involved phased construction. With the exception of the cross-frames within the closure region between the phases, the SDLF fit-up forces are low.
- The TDLF fit-up forces are high for bridge (M1) EICSS2, due to the high transverse stiffness caused by the contiguous cross-frame arrangement and the framing of the cross-frames into the girders close into the bearing locations (i.e., small offsets). The closure cross-frames are installed after the decks of the two phases are assumed

placed. This means the closure cross-frames are installed under TDL conditions. As a result, the closure fit-up forces are significant if these cross-frames are detailed for SDLF. Conversely, the TDLF closure fit-up forces are relatively low. An alternate fit-up option for this bridge would be to detail the main bridge cross-frames for SDLF, and detail the closure region cross-frames to fit to the geometry under TDL. However, the girders are not plumb under TDL for SDLF detailing of the main bridge cross-frames. Detailing the closure region cross-frames to fit to this TDL geometry would involve additional detailed calculations that are different than the routine calculations commonly conducted for TDLF. A suggested option for the cross-frames in the closure region, to facilitate ease of fit-up, is to use chords without diagonals between the phases during the deck placement, where needed, and to then field weld or field drill bolt holes to fit the cross-frame diagonals to the completed geometry.

- The fit-up forces on bridge (M2) EICSS2 were reduced substantially due to the modifications in the framing arrangement. In general, the fit-up forces in the closure region for these bridges can be high, depending on the attributes of the framing plans. These forces are not shown in Table 16.

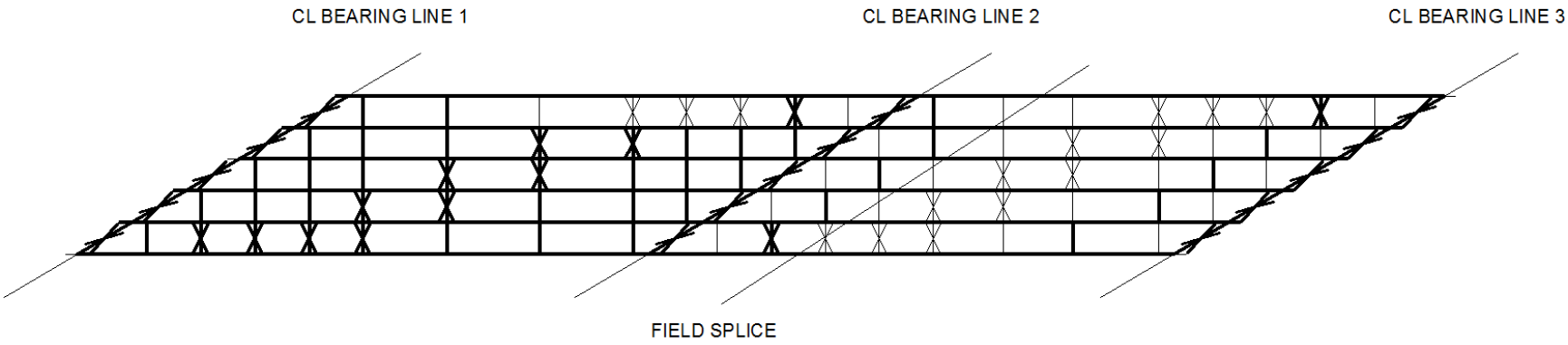

Figure 63. Critical erection stage of Bridge (K1) EICSS12 for TDLF detailing. The darker lines show portions of the bridge that are already completed.

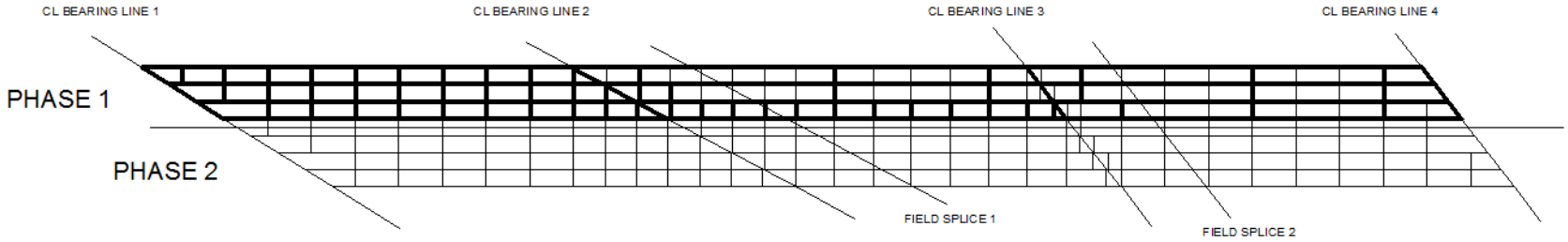

Figure 64. Critical erection stage of Bridge (M1) EICSS2 for TDLF detailing. The darker lines show portions of the bridge that are already completed.

5.3. Cross-Frame Fit-Up in Curved and Skewed Bridges

For the evaluation of the fit-up forces, all three main detailing methods were considered for the curved and skewed bridges examined in this research. For curved radially-supported bridges, NLF detailing generally provides the lowest fit-up forces. This is because SDLF and TDLF detailing effects tend to be additive with the internal force effects in these bridge types. For straight skewed bridges, SDLF detailing provides the lowest fit-up forces, while TDLF detailing makes the fit-up during steel erection difficult in some longer-span cases with a high skew index. For curved and skewed bridges, there is a complex combination of effects from the skew and curvature.

The following are trends in the values of cross-frame fit-up forces in the curved and skewed bridge cases studied in this research (these trends of course related to the trends observed for the curved radially-supported bridges and straight skewed bridges):

- The cross-frame fit-up forces for NLF detailing are generally very low for radial bearing-line cross-frames. This is because the girder deflections, girder differential deflections, and girder layovers are practically zero at these locations. However, SDLF and TDLF detailing tend to give a minor increase in the fit-up forces for these radial bearing-line cross-frames. This is due to the deformation in the system caused by force-fitting the cross-frames at the other locations and due to the lack-of-fit from the differential major-axis rotations of the girders (note that the differential deflections are still zero).

- The cross-frame fit-up forces are generally slightly higher at the skewed bearing lines than at the radial bearing lines. However, the cross-frame fit-up forces for all the detailing methods tend to be largest near mid-span where the differential deflections and the difference in girder layovers are also largest. The specific cross-frame connections

- The latter stages where the holding cranes often have been released often have larger cross-frame fit-up forces due to larger bridge cross-section rotations and deflections.

- The orientation of the skew can make one fascia girder substantially longer than the other fascia girder. In these cases, the cross-frame fit-up forces tend to be substantially larger for the erection stages involving the longer girders in the bridge.

Table 17 provides a synthesis of the maximum fit-up forces during the steel erection, calculated for all the curved and skewed bridges studied in this research. As indicated in Chapter 2, the simple-span bridges are shown first followed by continuous-span bridges. They are presented in the order of increasing maximum span length within each of these sub-groups. Some of the values require detailed inspection of the bridge geometry, framing arrangement, and erection scheme to fully understand their origins and significance. The base overall bridge geometry parameters shown in Table 2 are listed in Table 17 along with the maximum fit-up force values. A calculated fit-up force significantly more than 40 kips is considered difficult and is shown by dark shading in the table. Maximum fit-up forces between 30 and 40 kips are shown by light shading.

Table 17. Maximum cross-frame fit-up forces of the curved and skewed bridges studied in this research (Fit-up forces below 30 kips are unshaded, between 30 and 40 kips are shown by a light shading, and above 40 kips are shown by a dark shading).

Bridge	Framing Plan	Shoring Towers	L_s (ft)	w_g (ft)	R (ft)	θ (deg)	L_s/R	L_s/w_g or L_{ooc}/w_g	I_s	Differential Deflections (in.)		Max fit-up forces (kip)		
										SDL	TDL	NLF	SDLF	TDLF
(N) NISCS14	Figure 14	0	150	74	280	53.7,0	0.54	2.0	0.53	**0.49**	**1.52**	**35.3**	**34.9**	**34.8**
(O1) NISCS15 Scheme 1	Figure 15	0	150	74	280	-35,0	0.54	2.0	0.27	**1.04**	**2.23**	**79.3**	**81.0**	**81.8**
(O1) NISCS15 Scheme 2A	"	"	"	"	"	"	"	"	"	"	"	**40.8**	**39.2**	**64.5**
(O1) NISCS15 Scheme 3	"	"	"	"	"	"	"	"	"	"	"	**82.0**	**32.6**	**93.8**
(O1) NISCS15 Scheme 4	"	"	"	"	"	"	"	"	"	"	"	**9.9**	**38.5**	**71.2**
(O2) NISCS15 Scheme 2A	Figure 28	0	"	"	"	"	"	"	"	**0.66**	**1.40**	**141.0**	**147.1**	**155.8**
(O2) NISCS15 Scheme 2B	"	"	"	"	"	"	"	"	"	"	"	**88.1**	**58.7**	**50.1**
(O2) NISCS15 Scheme 2C	"	"	"	"	"	"	"	"	"	"	"	**61.1**	**51.0**	**78.4**
(O2) NISCS15 Scheme 4	"	1	"	"	"	"	"	"	"	"	"	**6.5**	**40.0**	**50.3**

Table 5 (Continued). Maximum cross-frame fit-up forces of the curved and skewed bridges studied in this research. (Fit-up forces below 30 kips are unshaded, between 30 and 40 kips are shown by a light shading, and above 40 kips are shown by a dark shading).

Bridge	Framing Plan	Shoring Towers	L_s (ft)	w_g (ft)	R (ft)	θ (deg)	L_s/R	L_s/w_g or L_{ooc}/w_g	I_s	Differential Deflections (in.)		Max fit-up forces (kip)		
										SDL	TDL	NLF	SDLF	TDLF
(P) EISCS3 Scheme 1	Figure 16	0	153	31	279	52.4,0	0.55	5.0	0.24	**0.40**	**0.83**	**23.4**	**14.9**	**16.8**
(P) EISCS3 Scheme 2	"	0	"	"	"	"	"	"	"	**"**	**"**	**45.7**	**33.0**	**20.5**
(Q1) NISCS38	Figure 17	2	300	74	730	62.6,0	0.41	4.1	0.39	**1.06**	**2.26**	**22.4**	**21.6**	**26.2**
(Q2) NISCS38	Figure 29	2	"	"	"	"	"	"	"	**1.00**	**2.15**	**20.1**	**18.5**	**15.7**
(R1) NISCS39	Figure 18	2	300	74	730	-35,0	0.41	4.1	0.15	**1.84**	**3.25**	**16.9**	**61.2**	**103.9**
(R2) NISCS39	Figure 30	NA	"	"	"	"	"	"	"	**1.67**	**2.85**	**NA**	**NA**	**NA**

Notes: (1) For bridge cases (O1) and (O2) NISCS15, Scheme 1 uses one holding crane until 3 outside girders are installed. Scheme 2A uses two holding cranes until 4 outside girders are installed. Scheme 2B is similar to Scheme 2A, but the holding cranes are retained until all girders are installed. Scheme 2C is similar to Scheme 2B, but the cross-frames are installed sequentially in the opposite direction along the span. The erection is from the inside to the outside of the curve for Scheme 3. Two holding cranes are used for Scheme 3. Scheme 4 uses one shoring tower.

Table 5 (Continued). Maximum cross-frame fit-up forces of the curved and skewed bridges studied in this research. (Fit-up forces below 30 kips are unshaded, between 30 and 40 kips are shown by a light shading, and above 40 kips are shown by a dark shading).

Bridge	**Framing Plan**	**Shoring Towers**	L_s **(ft)**	w_g **(ft)**	R **(ft)**	θ **(deg)**	L_s/R	L_s/w_g **or** L_{ooc}/w_g	I_s	**Differential Deflections (in.)**		**Max fit-up forces (kip)**		
										SDL	**TDL**	**NLF**	**SDLF**	**TDLF**
(T1) EICCS27	Figure 20	4	279, 224, 236	79.9	2546	-53.1,-59.4, -64.4,-69.7	0.11, 0.09, 0.09	3.5, 2.8, 3.0	0.48, 0.70, 0.94	**1.67**	**5.90**	**15.2**	**14.2**	**46.2**
(T2) EICCS27	Figure 31	4	"	"	"	"	"	"	"	**1.65**	**5.85**	**9.0**	**9.6**	**28.8**
(U1) EICCS28	Figure 21	NA	326, 160, 235	52	1255	0, 54.5, 47,0	0.26, 0.13, 0.19	6.3, 3.1, 4.5	0.28, 0.44, 0.15	**1.82**	**3.25**	**NA**	**NA**	**NA**
(U2) EICCS28	Figure 32	5	"	"	"	"	"	"	"	**2.09**	**3.75**	**6.1**	**19.6**	**33.0**

Notes:

(1) Bridge (P) EISCS3 erection is from the inside to the outside of the curve.

(2) Bridge cases (R2) NISCS39 and (U1) EICCS28 were not feasible for construction.

It can be observed from Table 17 that there is no simple general trend for curved and skewed bridges. The tendencies related to the skew and the horizontal curvature combine and/or offset each other in complex ways in these types of structures. Other than this fact, the most important points shown in Table 17 are as follows:

(1) The fit-up forces are highly dependent on the erection method. In tightly curved and sharply skewed bridges, the use of shoring towers is advisable to reduce the deflections and help reduce the fit-up forces due to the extreme geometries.

(2) For bridges that are highly curved but not sharply skewed, the fit-up forces tend to follow the trend for curved radially-supported bridges. For bridges that are sharply skewed but not tightly curved, the fit-up forces tend to follow the trend for straight skewed bridges.

(3) The skew orientation has a significant influence on the fit-up forces in the highly curved bridges. When the skew orientation makes the girder on the inside of the curve longer, the effects of the skew tend to relieve the effects of the curvature. The fit-up forces for all three detailing methods are lower in these cases. When the skew orientation makes the girder on the outside of the curve longer, the effects of the skew tend to be additive with the effects of the curvature. The fit-up forces for all three detailing methods are higher in these cases.

(4) The maximum fit-up forces tend to be larger for cases involving a combination of longer maximum fascia girder span length with a tighter curve (larger L_s/R).

(5) Higher differential deflections tend to lead to higher fit-up forces. However, fit-up forces are significantly decreased when shoring towers are used.

The fit-up forces were evaluated for both the base and alternate framing arrangements of the curved and skewed bridges, except for Bridge (R2) NISCS39 which experienced significant uplift at the end skewed bearing support and Bridge (T1) EICCS28 which experienced high cross-frame forces and significant uplift at an interior skewed bearing support. The alternate framing plans typically stagger the cross-frames near skewed bearing lines for the base contiguous framing arrangements and make these cross-frame lines contiguous for cases where the base bridge designs used staggered framing arrangements in these regions. The goal was to study the effects of different framing arrangements on bridges with different combinations of skew and curvature. The erection schemes (installation order of the girders and cross-frame and support requirements) are the same for the base and the alternate framing arrangements for each of the bridge cases, except Bridge (R2) and Bridge (T1). The following are further details of the fit-up forces reported in Table 17 (The critical erection stages for TDLF detailing are shown for each of the bridge cases in the subsequent figures in this section. In many cases, the critical stages are the same stages for NLF, SDLF, and TDLF detailing):

- Bridge (N) NISCS14 (Figure 65) has a span length of 150 ft. The skew effects relieve the curvature effects in this bridge; the maximum fit-up forces for this bridge are slightly below the 40 kip threshold.
- Bridge cases (O1) and (O2) NISCS15 (Figures 66 and 67) also have a span length of 150 ft, but the skew effects are additive with the curvature effects. It can be seen from Table 17 that for all the cases except Erection Scheme 4 for bridge cases (O1) and (O2), the fit-up forces varied from relatively large to very large. For this bridge, Erection Scheme 1 involves erection from the outside to the inside of the curve with

one holding crane on the outside girder until the next two adjacent girders of the bridge cross-section were installed. Erection Scheme 2A is similar to Erection Scheme 1 but has two holding cranes on the outside girder until the next three adjacent girders of the bridge cross-section are installed. Erection Scheme 2B is similar to Scheme 2A but holding cranes are retained until all girders of the bridge cross-section are installed. For Erection Schemes 1, 2A, and 2B, the cross-frames are installed sequentially from the skewed bearing line to the radial bearing line. Erection Scheme 2C is similar to Erection Scheme 2B but the cross-frames are installed sequentially from the radial bearing line to the skewed bearing line.

- As shown by Table 17, for the same framing arrangement, generally the maximum fit-up forces are reduced the most by the scheme that has more vertical support (i.e., the scheme that has more holding cranes and in which the holding cranes were left in place until a larger number of girders and cross-frames were installed). For bridge (O1) NISCS15, Erection Scheme 3 - erecting from the inside to the outside of the curve - significantly increases the maximum fit-up forces. For bridge cases (O1) and (O2) NISCS15, Erection Scheme 4 uses a shoring tower across the full width of the bridge cross-section until all the girders are erected. As a result, the maximum fit-up forces for bridge cases (O1) and (O2) NISCS15 Erection Scheme 4 are significantly smaller than for the other erection schemes.
- For bridge (P) EISCS3 (Figure 68), the skew effects relieved the curvature effects. For Erection Scheme 1 where the girders were erected from the outside to the inside, the maximum fit-up forces were relatively low. Bridge (P) EISCS3 and bridge (N) NISCS14 (Figure 65) have a skew index of 0.24 and 0.53, respectively.

The maximum fit-up forces were lower for bridge (P) than for bridge (N). For Erection Scheme 2 on bridge (P), where the girders were erected from the inside to the outside, the maximum NLF fit-up force was slightly above the 40-kip threshold.

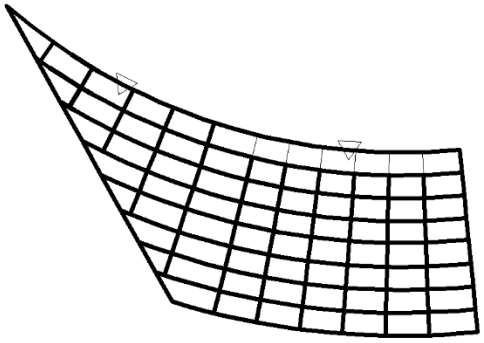

Figure 65. Critical erection stage of Bridge (N) NISCS14. The darker lines show portions of the bridge that are already completed. The triangles denote the pick points of the lifting.

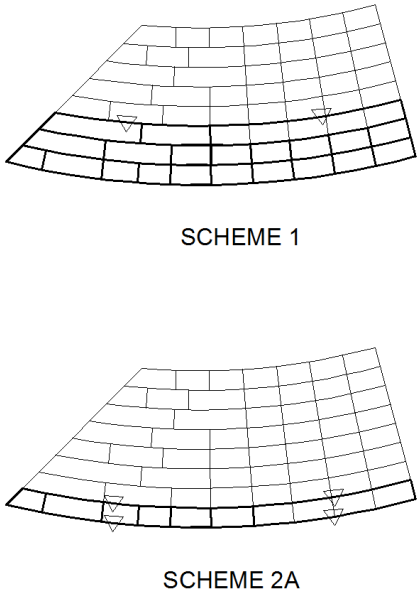

Figure 66. Critical erection stages of erection schemes 1 and 2A of bridge cases (O1) and (O2) NISCS15 for TDLF detailing. The darker lines show portions of the bridge that are already completed. The triangles denote the pick points of the lifting and holding cranes.

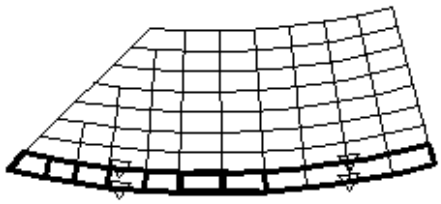

SCHEME 2B

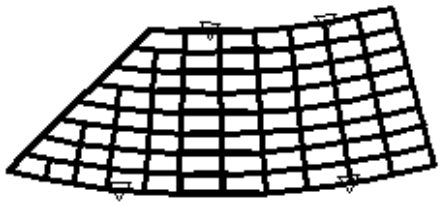

SCHEME 2C

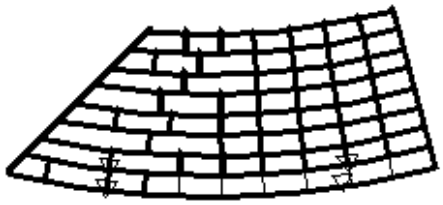

SCHEME 3

SCHEME 4

Figure 67. Critical erection stages of erection schemes 2B, 2C, 3 and 4 of bridge cases (O1) and (O2) NISCS15 for TDLF detailing. The darker lines show portions of the bridge that are already completed. The triangles denote the pick points of the lifting and holding cranes.

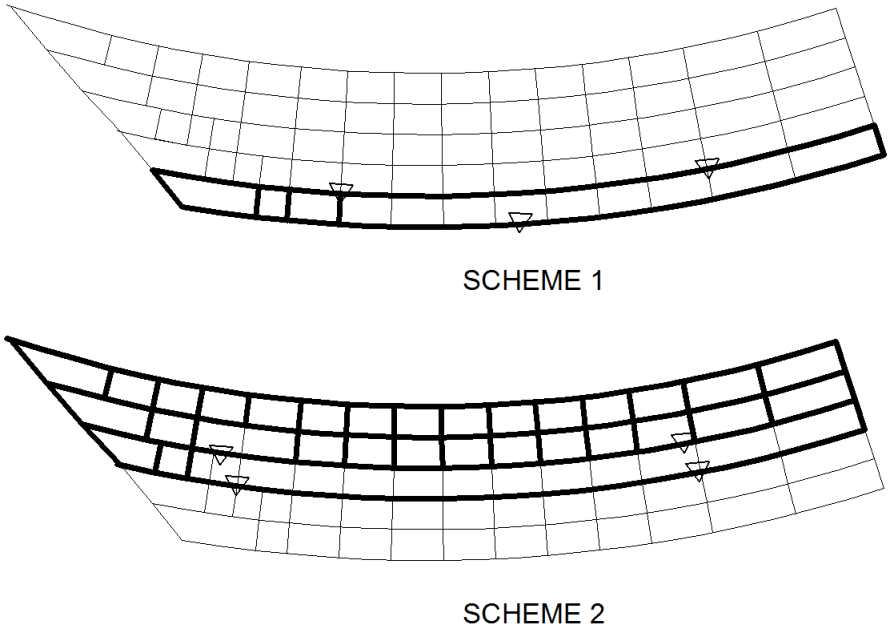

Figure 68. Critical erection stages of erection schemes 1 and 2 of Bridge (P) EISCS3 for TDLF detailing. The darker lines show portions of the bridge that are already completed. The two triangles denote the pick points of the lifting and holding cranes.

- For bridge cases (Q1) and (Q2) NISCS38 (Figure 69), the skew effects again relieved the curvature effects. However, the span length is 300 ft at the centerline of this bridge, and the maximum fascia girder span length is 365 ft. Two shoring towers were used to erect this bridge. By using this approach, the maximum fit-up forces were manageable. Phased construction was initially considered for the bridge case (Q1). However, the studies showed that phased construction was not feasible for this case. Phased construction was not considered for bridge case (Q2).
- Bridge (R1) NISCS39 (Figure 70) also has a span length of 300 ft but its skew effects were additive to its curvature effects. Two shoring towers are used to erect this bridge.

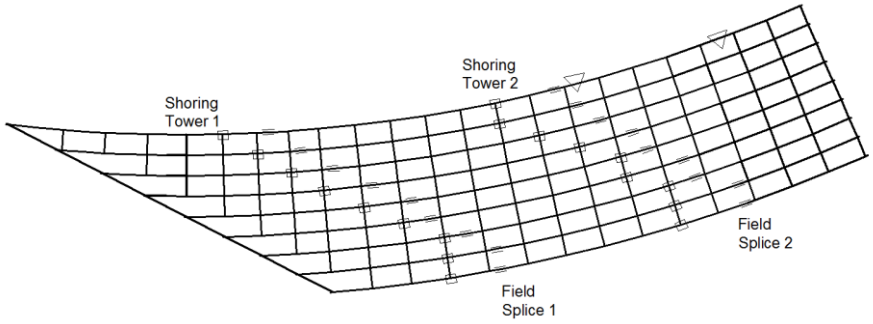

Figure 69. Critical erection stage of bridge (Q1) NISCS38. The two triangles are the pick points of the lifting crane.

- Bridge (R2) NISCS39 used a contiguous framing arrangement. This bridge experiences significant uplift at the obtuse corner associated with the skewed end bearing line. The required capacity of tie-downs and the magnitude of counter-weights to resist the uplift are impractical. As such, the results for this framing arrangement are studied only for the final constructed geometry. The bridge effectively is not buildable, unless it is substantially shored during the construction, and even then, the uplift at the obtuse corner is impractical in the bridge's final constructed condition. Erection studies are not conducted and the fit-up forces are not provided for this case.
- Bridge (S) XICCS7 (Figure 71) has a relatively low L_s/R ratio. The use of a shoring tower and skewed bearing line cross-frames at the interior piers, combined with offsetting the intermediate cross-frames from the bearing lines, help to make the fit-up forces for this bridge the lowest of all the curved and skewed bridge cases studied

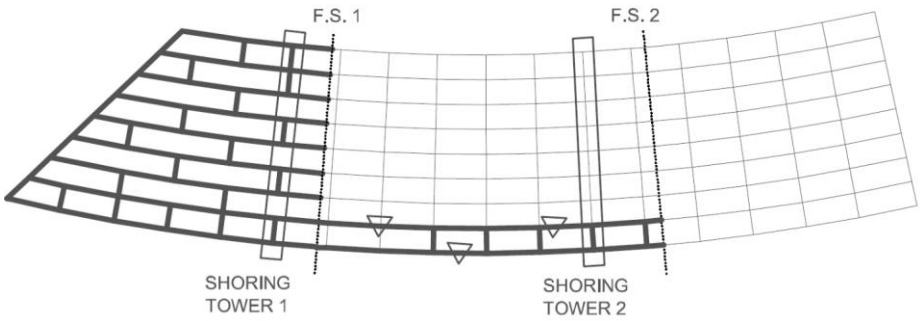

Figure 70. Critical erection stage of Bridge (R1) NISCS39 for TDLF detailing. The darker lines show portions of the bridge that are already completed. The two triangles denote the pick points of the lifting and holding cranes.

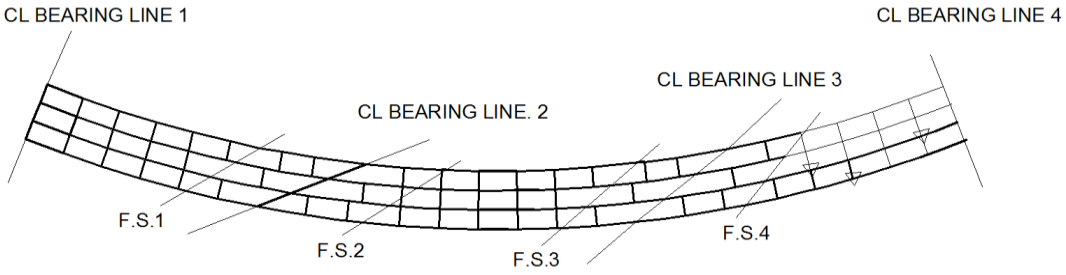

Figure 71. Critical erection stage of Bridge (S) XICCS7. The darker lines show portions of the bridge that are already completed. The two triangles denote the pick points of the lifting and holding cranes.

- Bridge cases (T1) and (T2) EICCS27 (Figure 72) have the lowest L_s/R ratio of the curved and skewed bridges studied in this research. This bridge behaves much like a straight skewed bridge. The SDLF fit-up force is the lowest for bridge case (T1) and is only slightly larger than the NLF fit-up force for bridge case (T2). The TDLF fit-up forces for bridge case (T1) are relatively large because of the contiguous cross-frames and intermediate cross-frames framing into the bearing locations. The maximum fit-up forces for bridge case (T2) are significantly reduced because the cross-frames are staggered throughout the spans and the intermediate cross-frames

framing into the bearing locations are eliminated. Four shoring towers are used for the erection of cases (T1) and (T2), all positioned at the no-load elevations. The spans in this bridge have multiple field splices. Span 1 has three field sections and two shoring towers are selected for that span. Span 3 has two field sections, and one shoring tower is selected for that span. Span 2 involves the use of a drop-in segment and needs one shoring tower to limit its deflections. After making the field splices within the spans of this bridge, the shoring towers in the corresponding spans could be moved toward the middle of the span to reduce the number of shoring towers. However, it is felt that it is more efficient to maintain the towers at their original locations throughout the erection. Two lifting cranes with a spreader beam and holding cranes were used for this bridge.

- Bridge case (U1) EICCS28 experiences high cross-frame forces and significant uplift at an interior bearing location due to the use of contiguous framing arrangement in all spans with intermediate cross-frames framing into the interior bearing locations, poor span balance, long spans, tight curvature and sharp skew. As such, the results for this framing arrangement are studied only for the final constructed geometry. Erection studies are not conducted and the fit-up forces are not provided for this case.
- For bridge case (U2) EICCS28 (Figure 73), the cross-frames are staggered near the skewed bearing lines and skewed bearing line cross-frames are used along with offsetting of the intermediate cross-frames from the bearing lines. Due to the large span lengths and large number of field sections, five shoring towers are selected to

facilitate the installation of the girders and cross-frames. Using this approach, the maximum fit-up forces for this case are relatively low.

5.4. Girder Splice Fit-Up

Girder splice fit-up forces are the forces required to physically bring two adjacent field sections together and complete the splice connection during the erection of the steel. In this research, girder splice fit-up is examined by calculating the following quantities (induced at the splice connections as the girder field sections are installed):

- The major axis bending moments,
- The equivalent flange forces, and
- The flange lateral bending moments.

The following are important considerations regarding fit-up and girder splices:

- For the cases where the girder field sections are installed sequentially from one end of the bridge to the other, generally the erector can simply knife the field sections in at the splice to the portion of the structure that is already erected. That is, the erector can generally adjust the position and orientation of the field section being erected, so that it will fit properly with the previously erected field section to which the new section is being spliced.
- The erector needs to ensure that the girder end at the splice, in the portion of the structure that is already erected, is at an orientation and/or elevation such that there is no interference of the field section being knifed in with the abutments or piers.

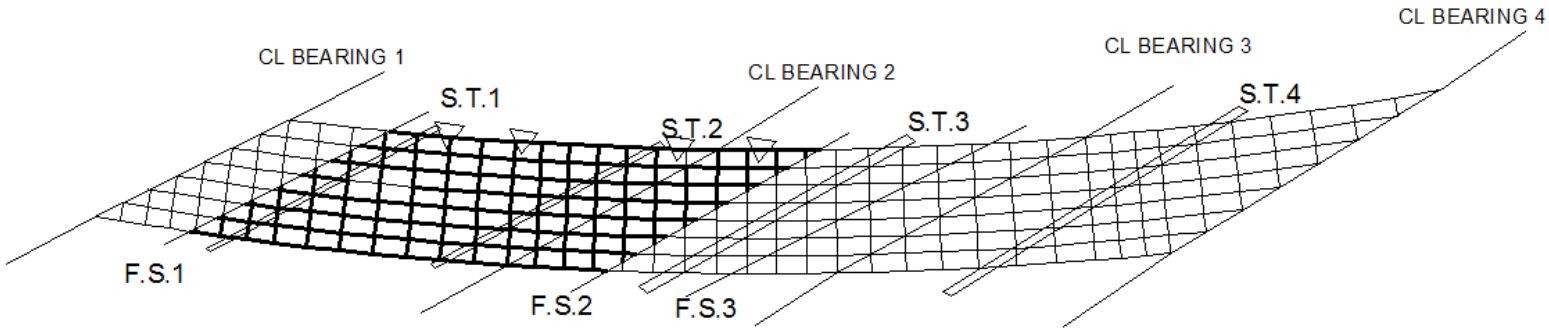

Figure 72. Critical erection stage of Bridge (T1) EICCS27for TDLF detailing. The darker lines show portions of the bridge that is already completed. The triangles denote the pick points of the lifting crane.

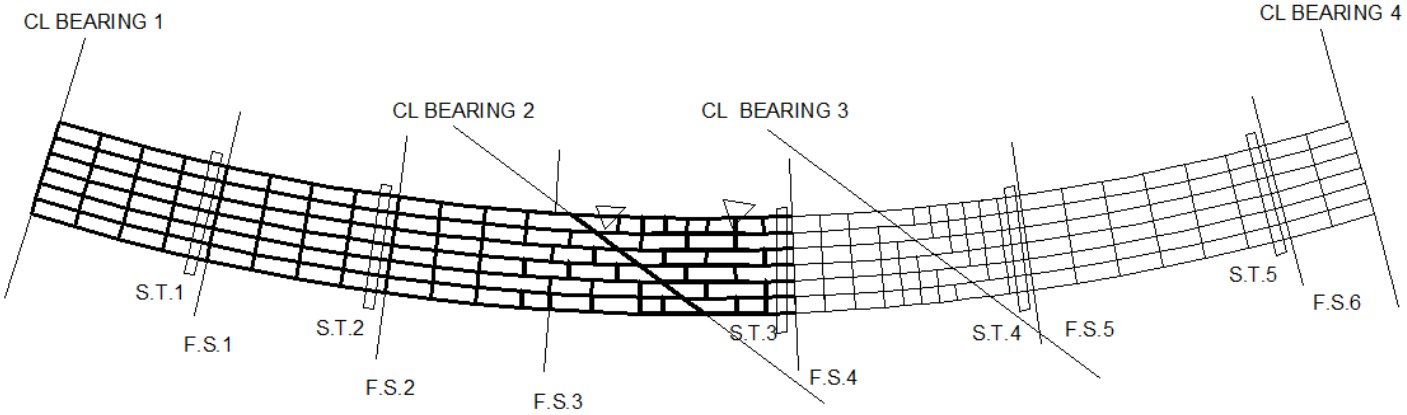

Figure 73. Critical erection stage of Bridge (U2) EICCS28 for TDLF detailing. The darker lines show portions of the bridge that is already completed. The two triangles denote the pick points of the lifting crane.

- When interference of the field section and the abutments or piers occurs, the erector can adjust the elevations of shoring towers and/or cranes to higher elevations, remove a bearing, etc., to resolve the interference. In addition, the erector can avoid the interference by adjusting the locations and/or heights of the shoring towers (either in the back spans or in the cantilever spans)such that the cantilever tips deflect to higher elevations and/or the slope at the tips are positive to the horizontal line.
- Curved girders are also likely to be twisted at the cantilevered end due to the effects of the curvature. Lifting to adjust the orientation of the web is more problematic for curved bridges since the girders typically are interconnected by cross-frames and are working together as a structural system; therefore, much larger forces are required to raise the bridge elevations.

Erecting the girders in the above fashion is not always feasible due to reasons such as site constraints. An example case of this is bridge (E) EICCR11 in which the erection site constraint was a waterway. The following describes the erection stages for the actual field section installation in this bridge:

- Girder field sections were installed from the right abutment (Support 4 in Figure 74) and the second pier (Support 3 in Figure 74).
- The field section between Field Splices F.S.8 and F.S.9 was then dropped in. The first splice connection at F.S.8 could be knifed in with relative ease. However, the second splice connection at F.S.9 was difficult.

Table 18 shows the predicted major-axis bending moments, flange lateral bending moments, and equivalent flange forces developed at the second splice at the time that this

connection is made (for girders 2, 4, and 1). Stages 12, 15, and 16 involved the installation of the drop-in field sections between F.S.8 and F.S.9 for girders 2, 4, and 1, respectively. The following are observations from Table 18:

- Stage 12 (shown only the curved span in Figure 75) is the critical stage for bridge (E) EICCR11.
- The cross-frames of this bridge were designed and fabricated approximately for SDLF. This led to delays and fit-up difficulty as observed in the field. It is evident from Table 5 that NLF detailing would have substantially alleviated the problems that occurred in erecting this bridge.
- The SDLF and TDLF detailing effects tend to increase the predicted major-axis bending moments, flange lateral bending moments, and equivalent flange forces developed at the second splice connection. This is consistent with the field observations that the field splice fit-up was very difficult for the approximation of the SDLF detailing condition used in this bridge.
- It should be reiterated that Bridge (E) EICCR11 is an extreme case involving longer-spans and significantly larger L_s/R and L_s/w_g than the other bridges studied in this research.
- The major-axis and flange lateral bending moments and the equivalent flange forces for NLF detailing are relatively low, but they are not ideally zero. This is due to the deflections of the bridge system in spite of the shoring towers, cranes, and pier brackets which were all set at the no-load elevations.

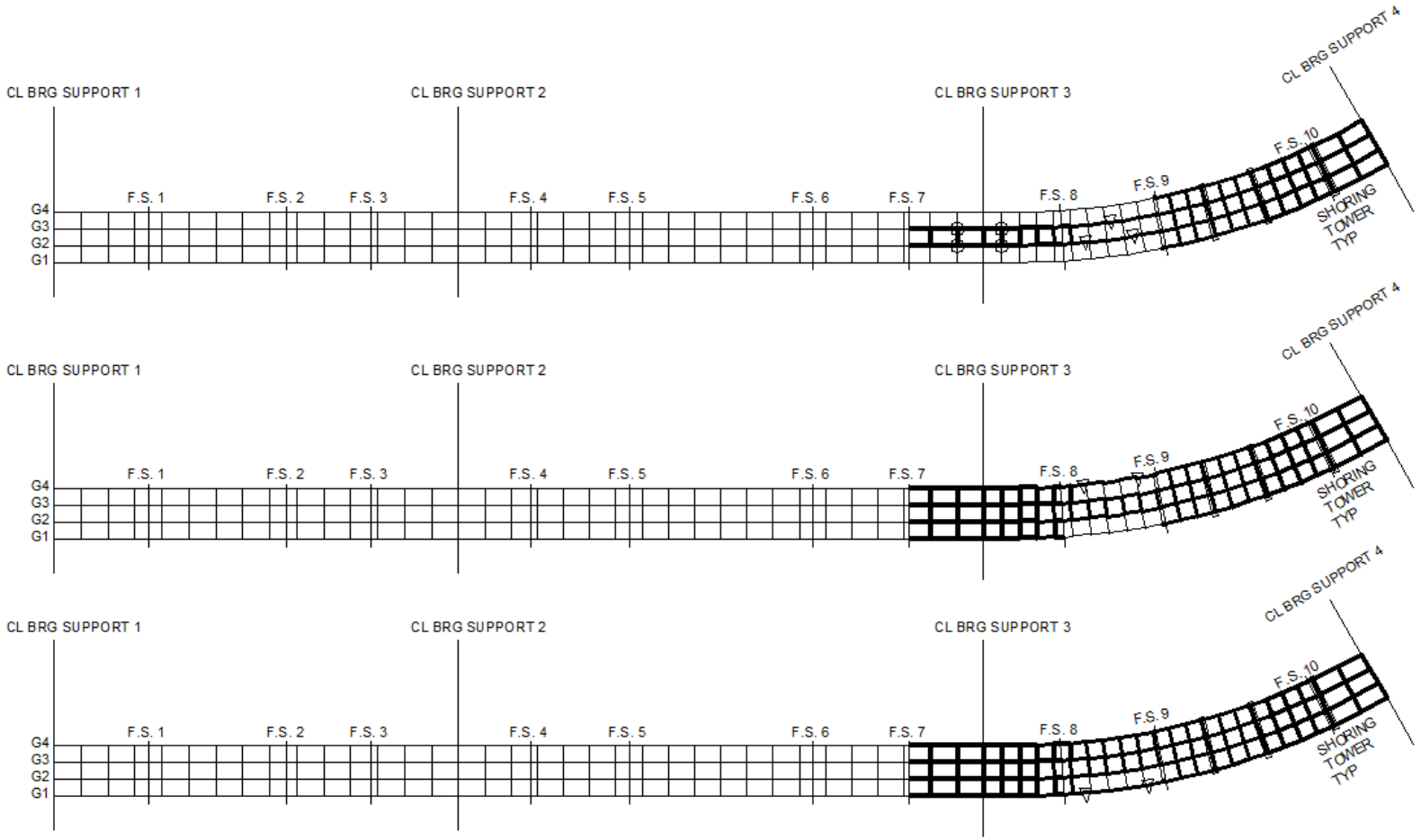

Figure 74. Erection stages involving field splice connections of drop-in segments in bridge (E) EICCR11.

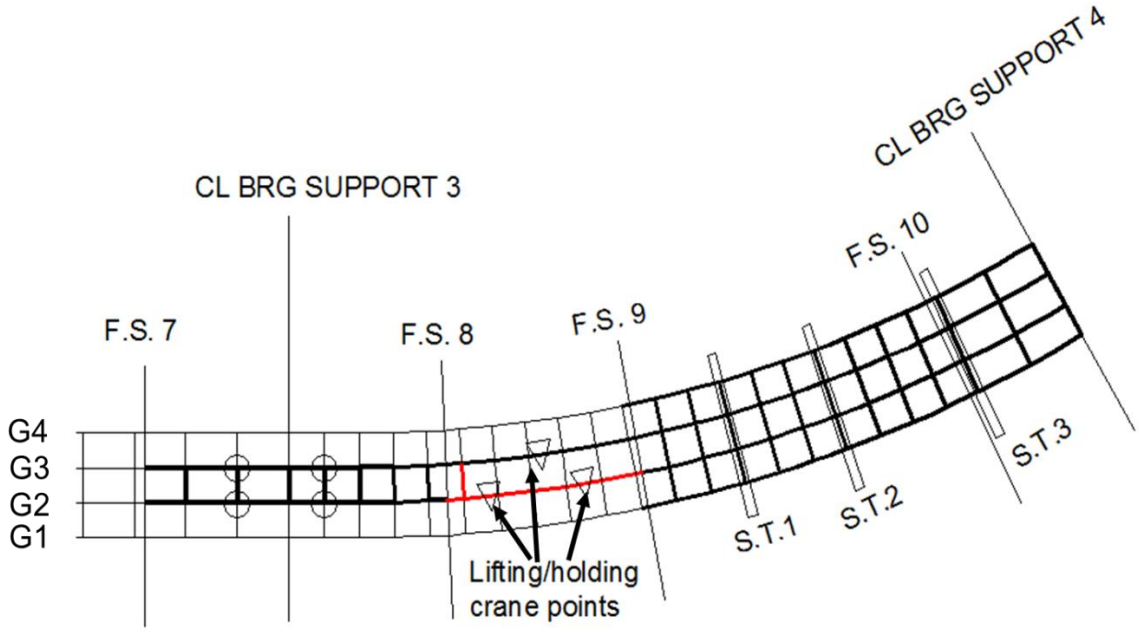

Figure 75. Critical stage of bridge (E) EICCR11, involving field splice connection of drop-in segments of girder line 2 (showing only the curved span).

Table 18. Predicted major-axis bending moments, equivalent flange forces, and flange lateral bending moments and at the second field splice connections at F.S.9 for G2, G4, and G1 for bridge (E) EICCR11.

Stage	Detailing Method	M (kip*ft)	Equivalent Flange Force (kip)	Top Flange M_ℓ (kip*ft)	Bottom Flange M_ℓ (kip*ft)
12	NLF	315	23	4.8	4.8
	SDLF	7566	540	43.5	9.5
	TDLF	11267	805	103.1	17.2
15	NLF	212	15	5.3	5.4
	SDLF	2694	192	34.3	2.8
	TDLF	1454	104	32.4	13.0
16	NLF	639	46	0.2	1.8
	SDLF	8986	642	103.9	12.3
	TDLF	12443	889	161.0	15.7

The curved and skewed bridge cases (T1) and (T2) EICCS27 (shown in Figure 76 for bridge (T1)) also involved the use of drop-in segments. From Table 19 one can observe that values of the predicted major-axis bending moments, flange lateral bending moments, and equivalent flange forces at the second field splice connection of the inside girder are much lower for both bridge cases (T1) and (T2) than bridge case (E). This is because bridge cases (T1) and (T2) have the smallest L_s/R ratio of the bridges studied and four shoring towers were used for the erection of cases (T1) and (T2), all positioned at the no-load elevations. The values for bridge case (T2) are significantly reduced because the cross-frames are staggered throughout the spans and the intermediate cross-frames framing into the bearing locations are eliminated. The SDLF and TDLF detailing effects tend to increase the predicted major-axis bending moments, flange lateral bending moments, and equivalent flange forces developed at the second splice connection for bridge cases (T1) and (T2).

Shoring towers and holding and lifting cranes should be set at the no-load elevations to facilitate girder splice fit-up of drop-in segments. This is because the girders, and the girder splices, are detailed for NLF by customary practice. For straight skewed bridges, shoring towers and holding and lifting cranes should be set at the SDL elevations to facilitate cross-frame fit-up. For straight skewed bridge cases that involve drop-in segments, the elevations can be adjusted temporarily to higher elevations to facilitate the girder splice fit-up.

Table 19. Predicted major-axis bending moments, equivalent flange forces, and flange lateral bending moments and at the second field splice connection of the inside girder for bridge cases (T1) and (T2) EICCS27.

Bridge Case	Detailing Method	M (kip*ft)	Equivalent Flange Force (kip)	Top Flange M_ℓ (kip*ft)	Bottom Flange M_ℓ (kip*ft)
(T1) EICCS27	NLF	31	0.3	0.1	0.2
	SDLF	113	1.2	1.1	1.2
	TDLF	508	5.6	4.8	4.2
(T2) EICCS27	NLF	6	0.1	0.4	0.3
	SDLF	20	0.2	1.1	0.8
	TDLF	61	0.7	3.5	2.5

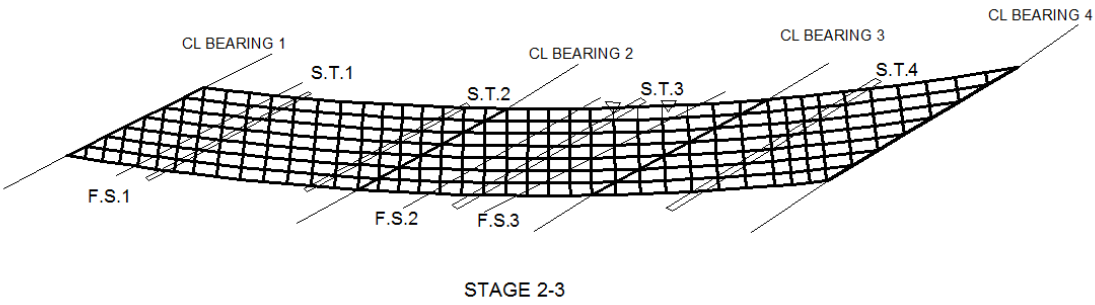

Figure 76. Erection stage involving field splice connections of drop-in segments in bridge (T1) EICCS27.

CHAPTER 6

INFLUENCE OF DETAILING METHODS ON COMPLETED BRIDGE RESPONSES

Cross-frame detailing methods can have a significant influence on the responses in completed bridge systems. This section provides a major synthesis of the broad effects of different types of detailing on the responses for the three major bridge types considered in this research – curved radially-supported, straight skewed and curved and skewed. Data from the parametric studies conducted in this research is summarized and analyzed to explain the trends, and recommendations for simplified handling of the effects of the different cross-frame detailing methods are provided.

It can be argued that, ultimately, the simplest way of handling the effects of SDLF or TDLF cross-frame detailing on bridge responses is to directly model the corresponding fabricated lack-of-fit between the cross-frames and the girders. This approach gives the most accurate calculation of the reductions in cross-frame forces and girder flange lateral bending stresses in cases where the detailing results in a reduction of these forces and stresses, and it gives the most accurate calculation of increases in these responses in cases where increases occur. The basic structural analysis methods for handling lack-of-fit are fundamental, and are taught in common undergraduate Strength of Materials and Structural Analysis courses. The handling of lack-of-fit is very similar to the handling of the effects of temperature change within the structural system.

Nevertheless, within a design production environment, it is essential that the lack-of-fit calculations be handled in an automated or semi-automated fashion to avoid undue manual and potentially error prone calculation burdens on the design engineer. Although

the calculations are relatively basic and straightforward, they require a detailed understanding and, manually, they can become somewhat tedious. Chapter 3 aims to provide the necessary details of the processes for handling the lack-of-fit due to SDLF and TDLF detailing of the cross-frames. It is hoped that bridge engineers and software providers will recognize the value of these calculations, and that handling of lack-of-fit from the detailing of the cross-frames in curved and/or skewed I-girder bridges will eventually become as common place as other important considerations such as handling of temperature effects and staged deck placement or general staged construction effects. Until this milestone is reached, and even then, for certain design situations, simplified methods are needed for accounting for these effects in design, where they are important. In addition, the influences of SDLF and TDLF detailing generally need to be better understood by bridge professionals. This section aims to address these needs in a thorough fashion.

Abbreviations and definitions of terms central to discussion of the influence of detailing methods on completed bridge responses are summarized in Section 6.1. Section 6.2 provides a synthesis of the wide range of facts and attributes pertaining to curved and/or skewed I-girder bridge fit. It is important to understand these facts and attributes to facilitate a complete understanding of the data summarized from related analytical studies. Recommended procedures for including the results from a dead load fit refined analysis (DLF RA) in LRFD load combinations (i.e., the locked-in stresses and forces obtained from a refined analysis that includes the lack-of-fit associated with SDLF or TDLF detailing of the cross-frames) are discussed in Section 6.3. This is followed by Section 6.4 which summarizes key questions pertaining to the influence of the fit decision on completed bridge responses. These questions are addressed in Sections 6.5 to 6.10. The specific

influences of SDLF and TDLF detailing on the bridge responses is summarized in these sections. In addition, these sections provide recommendations for handling DLF detailing effects using simple approximate scale factors on the dead load results from a No-Load Fit Refined Analysis (NLF RA), i.e., a refined analysis that does not include the lack-of-fit effects from DLF detailing of the cross-frames. These sections address the following six specific combinations of bridge types and methods of setting the cambers and detailing of the cross-frames:

- Curved radially-supported bridges with cambers set based on NLF RA,
- Straight bridges with parallel skew and cambers set based on Line Girder Analysis (LGA),
- Straight bridges with parallel skew and cambers set based on NLF RA,
- Straight bridges with non-parallel skew and cambers set based on LGA,
- Straight bridges with non-parallel skew and cambers set based on NLF RA, and
- Curved and skewed bridges with cambers set based on NLF RA.

In each of these sections, key results and data from the studies conducted in this research are presented first, followed by a summary of the influences of SDLF and TDLF on the different bridge responses and recommendations for the use and handling of the SDLF and TDLF detailing effects.

6.1. Abbreviations and Definitions

The area of skewed and curved I-girder bridge fit is littered with numerous subtle and ambiguous definitions and terms. Therefore, it is essential to provide clear definitions of all the terms to be able engage in any rigorous evaluation of the procedures.

6.1.1 Abbreviations

The following abbreviations are used in the discussions below to help make the discussions as concise as possible:

CDL	=	Concrete Dead Load
CF	=	Cross-Frame
DL	=	Dead Load
LGA	=	Line Girder Analysis
NL	=	No Load, i.e., zero load
NLF	=	No-Load Fit
RA	=	Refined Analysis
SDL	=	Steel Dead Load, i.e., self-weight of all the structural steel including the girders and the CFs
SDLF	=	Steel Dead Load Fit
TDL	=	Total Dead Load, taken as the weight of the structural steel plus the weight of the concrete bridge deck, but not including any additional DC2 and DW loads
TDLF	=	Total Dead Load Fit

6.1.2. Definitions

The following terms are used in the discussions below:

CF detailing = Determination of the cross-frame (CF) fabricated geometry such that the CF connection work points match with corresponding work points on the girders in a particular assumed undeflected or deflected geometry, with the girders assumed to be plumb and without any forcing or deformation of the CFs. Also referred to as fit.

CF drop = The difference in the vertical elevation between the top of the girder webs on each side of a CF, considered under NL or under a targeted DL condition. For SDLF and TDLF detailing, the detailer calculates the drops by subtracting the vertical DL deflections (i.e., the girder SDL or TDL cambers) provided on the design plans from the girder fully-cambered NL geometry. Alternatively, some detailers start from the targeted TDL elevations and add the appropriate deflections (the TDL minus the SDL deflections for SDLF, or the TDL deflections for NLF) to determine the geometry in the targeted fit condition. The goal is for the CF connection work points to match with the corresponding work points on the girders in the targeted fit condition. It is important to note that, generally, there are two major contributors to the detailing of the CFs. The CF drops are one contributor. The other contributor, particularly at skewed CF

lines, is the corresponding girder connection plate rotated positions in the targeted DL geometry.

CF initial lack-of-fit forces = The CF member forces required to theoretically resolve the lack-of-fit in the undeformed NL geometry due to SDLF or SDLF detailing, if the girders were held artificially in their fully-cambered NL geometry and the CFs were then deformed (subjected to their initial strains) such that their connection work points are matched with the corresponding work points on the girders. The actual CF locked-in forces due to the lack-of-fit are generally much smaller than the CF initial lack-of-fit forces, since deformations are induced in the girders and the rest of the structure when the CF lack-of-fit is resolved by enforcing compatibility at the CF-to-girder connections. As such, although the locked-in forces due to SDLF or TDLF detailing are directly related to the CF lack-of-fit, the CF lack-of-fit on its own is not sufficient to estimate the locked-in forces. The locked-in forces also depend on the compliance of the structure in resisting the removal of the lack-of-fit displacements by enforcing compatibility at the CF-to-girder connections.

CF initial strains = The strains induced in the CF members by theoretically resolving the lack-of-fit in the undeformed NL geometry due to SDLF or TDLF detailing, if the girders were held artificially in their fully-cambered NL geometry and the CFs were then

deformed such that the CF connection work points are matched with the corresponding work points on the girders.

CF initial fixed-end forces = The forces induced in an equivalent beam representation of the CFs by theoretically resolving the lack-of-fit in the undeformed NL geometry due to SDLF or TDLF detailing, if the girders were held artificially in their fully-cambered NL geometry and the CFs were then deformed such that the CF connection work points are matched with the corresponding work points on the girders.

CF lack-of-fit = The difference in the position between the work points of the CF connections and the corresponding work points on the girders in the undeformed geometry of the structure under zero load, typically measured/calculated as the displacement incompatibility between the CF and the girder on one side of the CFs with the CF connection work points attached to the girder work points on other side of the CFs. It should be noted that for CFs that are not normal (perpendicular) to the girders, there are generally two contributions to the initial lack-of-fit: (1) the difference in the vertical elevation between the work points on the connected girders, typically referred to as the CF drop, and (2) the major-axis bending rotational orientation of the connection plates at the girder work points (see Section 3.1). The NL geometry defines the reference state of the corresponding

conservative elastic system at which the strain energy is equal to zero. Hence, the NL configuration serves as the most appropriate basis for calculation of the lack-of-fit and its effects on the structure.

Dead Load Fit (DLF) = Dead Load Fit (DLF) detailing.

DL condition = The fit condition under a given DL, typically either the SDL condition or the TDL condition.

DLF detailing = A method of detailing in which the CF fabricated geometry is set such that the CF connection work points match with corresponding work points on the girders in a particular dead load (DL) deflected position, with the girders assumed to be plumb and without any forcing or deformation of the CFs.

DLF Refined Analysis (RA) = A refined analysis (RA) that includes initial strains in the CF members (for 3D FEA) or initial fixed-end forces in the CF elements (using accurate grid analysis methods) to account for any fabricated lack-of-fit between the CFs and the girders in the undeformed geometry of the structure.

DLF RA Cambers = Girder cambers calculated using a DLF Refined Analysis (RA). This calculation of the girder cambers would generally require an iterative solution, since DLF detailing generally has some influence on the girder vertical displacements, and in turn, the girder displacements influence the DLF RA cambers and the

DLF RA cambers influence the girder vertical displacements. This process is neither recommended nor required for sufficiency of DLF detailing.

Fit = In curved and/or skewed I-girder bridges, the process of determining the geometry in which the CFs are detailed to attach to the girders.

Fit-up = The process of assembling the structural steel during the bridge erection. It is desirable that the fit-up of the structural steel should be manageable, without the need for excessive jacking or pulling forces from the erector.

Fit-up forces = The forces required to physically bring the components together and complete a connection during the erection of the steel. These forces are influenced by initial lack-of-fit effects from SDLF or TDLF detailing of the CFs, but generally, they are distinctly different from the forces associated with the initial lack-of-fit between the girders and the CFs in the initial fabricated NL geometry.

Fit condition = The undeflected or deflected geometry of the girders that the CFs are detailed to attach to without any forcing or deformation of the CFs. The fit condition is selected to offset, or compensate for (to different extents), the tendency of the I-girders to twist in curved and/or skewed bridges (with due consideration of the impact on the bridge constructability and the impact on the

internal forces in the structure). The selected fit condition corresponds to a specific targeted outcome of when the girder webs will be approximately plumb in the field.

Fit choice = Fit decision.

Fit decision = The selection of a fit condition; also referred to as the fit choice.

Lack-of-fit = CF lack-of-fit.

Lack-of-fit analysis = A structural analysis in which locked-in forces are determined based on the initial lack-of-fit between the connection points within the structure. The designer can conduct a lack-of-fit analysis without any applied DL on the structure to calculate the specific locked-in forces in the structure, or the SDL or TDL may be included in the analysis to determine the total force effects in the structure for the selected SDL or TDLcondition.

Layover = The lateral deflection of the girder top flange relative to its bottom flange associated with twisting.

LGA cambers = Camber profiles determined based on a Line Girder Analysis (LGA). LGA cambers are applicable only for straight skewed bridges. Furthermore, it is explained in this research that Refined Analysis (RA) cambers are the preferred cambers for use in design.

Locked-in forces = The internal forces induced into the structural system by the CF lack-of-fit. These internal forces would remain if the structure's

DL were theoretically removed. In straight skewed bridges, the locked-in forces in the CFs due to SDLF or TLDF detailing are predominantly opposite in sign to the corresponding DL effects. In curved radially-supported bridges, the locked-in forces in the CFs due to SDLF or TDLF detailing are predominantly additive with the corresponding DL effects. The locked-in forces are never "removed" by the corresponding SDL or TDL forces; however, when they are opposite in sign to these forces, they reduce these forces. In addition, it should be noted that the locked-in forces in the CFs generally are substantially smaller than the corresponding CF initial lack-of-fit forces. This is due to the overall compliance of the structural system that is invoked when resolving the lack-of-fit. Therefore, just the lack-of-fit itself is not a good indicator of the magnitude of the locked-in forces in a bridge structure.

NL condition = The undeformed plumb geometry of the girders under No Load; also referred to as the fully-cambered condition.

No-Load Fit (NLF) = The process of conducting NLF detailing; also referred to as "fully-cambered fit."

NLF detailing = A method of detailing in which the CF fabricated geometry is set such that the CF connection work points match with corresponding work points on the girders, without any forcing or deformation of the CFs and with the girders assumed erected

in their undeformed fully-cambered (plumb) geometry under zero load (i.e., under NL); also referred to as "fully-cambered fit."

NLF Refined Analysis (RA) = A refined analysis that does not include any accounting for DLF.

NLF RA Cambers = Girder cambers calculated using a NLF Refined Analysis (RA). NLF RA cambers are the recommended standard camber calculation.

Nuisance transverse stiffness = Undesired transverse stiffness associated with a combination of the bridge skew and CF framing arrangement that can result in excessively large CF forces, and potentially difficult CF installation, particularly near skewed support lines. Nuisance transverse stiffness effects can be reduced, when CFs are provided along a skewed support line, by offsetting the first intermediate CF placed perpendicular to the girders adjacent to that support, where practicable, by a distance greater than or equal to the minimum indicated in AASHTO LRFD Article C6.7.4.2, and by providing discontinuous (staggered) CF lines in the vicinity of the skewed supports.

Refined Analysis (RA) = A structural analysis in which the 3D actions of the interconnected bridge system are accounted for. In all the discussions provided in this study, it is assumed that the RA is an *accurate* RA. That is, it is assumed that the analysis provides

an accurate calculation of the true 3D bridge system responses. NCHRP Report 725 provides guidelines for when simplified methods of analysis, such as grid methods, may be considered to be sufficiently accurate. In this research, refined 3D FEA models, as described in Section 2.1, are employed to represent the "gold standard" RA.

Refined Analysis (RA) cambers = Girder cambers (SDL or TDL) determined using an accurate refined analysis of the interconnected 3D bridge system in which the bridge model is fully assembled and then the gravity loads are simply "turned on."

SDL camber = The negative of the girder SDL deflections.

SDL condition = The hypothetical geometry in which the girders are assumed to be plumb but subjected to the Steel Dead Load (SDL) vertical deflections; also referred to as the "erected condition."

Steel Dead Load Fit (SDLF) = The process of conducting SDLF detailing; also referred to as "erected fit."

SDLF detailing = A method of detailing in which the CF fabricated geometry is set such that the CF connection work points match with corresponding work points on the girders, without any forcing or deformation of the CFs and with the girders deformed into the plumb hypothetical position obtained by subtracting the SDL vertical deflections calculated at the completion of the steel

erection, and the associated girder major-axis rotations, from the fully-cambered geometry of the girders; also referred to as "erected fit." Detailers work with the girder SDL cambers or SDL deflections specified on the engineering drawings to set the CF drops associated with this method of detailing. They also consider the relative major-axis bending rotational orientation of the girder connection plates associated with the CF drops. The girders are assumed to be displaced from their initially fabricated fully-cambered and plumb position to the targeted *plumb* SDL position. Any twisting of the girders associated with their 3D interactions with the CFs and the overall structural system are not considered in these calculations.

Targeted DL condition = The DL condition for which the CFs are detailed and in which it is desired for the girders to be approximately plumb, selected considering the impact on constructability and on the internal forces generated in the structure, i.e., the SDL condition for SDLF and the TDL condition for TDLF; also referred to as the targeted fit condition and the targeted DL geometry.

Targeted DL geometry = Targeted DL condition.

Targeted fit condition = Targeted DL condition.

Targeted elevation = The desired final elevation of the girders under the TDL, taken as a flat horizontal plane in the absence of considering the

superelevation, cross-slope, vertical curve and grade; also referred to as the targeted TDL elevation.

Targeted TDL elevation = Targeted elevation.

TDL camber = The negative of the girder TDL deflections; also referred to as the total camber. This is the nominal camber used for fabrication of the girders. The actual fabricated girder camber is typically larger than the nominal camber since the AWS D1.5 Specification has a zero tolerance for under-camber.

TDL condition = The hypothetical geometry in which the girders are assumed to be plumb but subjected to the total deal load (TDL) vertical deflections; also referred to as the "final condition."

Total camber = TDL camber.

Total Dead Load Fit (TDLF) = The process of conducting TDLF detailing; also referred to as "final fit."

TDLF detailing = A method of detailing in which the CF fabricated geometry is set such that the CF connection work points match with the corresponding work points on the girders, without any forcing or deformation of the CFs and with the girders deformed into the plumb hypothetical position obtained by subtracting the TDL vertical deflections calculated at the completion of the concrete deck placement, and the associated major-axis rotations, from the fully-cambered geometry of the girders (or put alternately,

with the girders deflected into their final targeted elevations); also referred to as "final fit." Detailers work solely with the girder total cambers or the TDL deflections specified on the engineering drawings to set the CF drops associated with this method of detailing. They also consider the relative major-axis bending rotational orientation of the girder connection plates associated with the CF drops. The girders are assumed to be displaced from their initially fabricated (cambered and plumb) position to the targeted *plumb* TDL position. Any twisting of the girders associated with their 3D interactions with the CFs, slab, and overall structural system are not considered in these calculations.

6.2 Facts and Attributes of Curved and/or Skewed I-Girder Bridge Fit

There are numerous facts and attributes associated with skewed and/or curved I-girder bridge fit. It is important to clearly understand these facts and attributes as a starting point for any rigorous assessment of the procedures.

6.2.1. General

The following are general facts and attributes about curved and/or skewed I-girder bridge fit:

- SDLF and TDLF detailing give approximately plumb webs in the targeted DL condition.

- Except in unusual cases involving substantial global displacement amplification of a slender I-girder bridge unit in its noncomposite condition during the deck placement, due to stability effects as discussed in AASHTO LRFD Article 6.10.3.4.2, deviation from the ideal plumb condition due to the deflection of the structure is typically taken to have a negligible influence on the structural resistance.
- Twisting of the girders and of the structural system in skewed and/or curved I-girder bridges is not necessarily indicative of a structural problem or deficiency; it is a natural, predictable, and controllable response to gravity loading in these types of structures. If this were not the case, essentially all of these bridges would be deficient under the design live loads (since they twist under live load).
- Since the structural displacements in skewed and/or curved bridges involve twisting of the girders and of the bridge system, the girders can be plumb only under one loading condition. In fact, generally speaking, due to the elastic deformation of the CFs and the elastic torsional deformation of the girders, all the girders being perfectly plumb at all locations is physically impossible except in certain very specific cases.
- The magnitude of the TDLF detailing effects on the responses is generally larger than the magnitude of the SDLF detailing effects. For SDLF or TDLF detailing, the pattern of the effects on the responses typically is similar under the respective targeted SDL and TDL conditions. There are slight differences in some cases due to geometric nonlinearity of the bridge system.
- The locked-in forces in the bridge structural system due to SDLF or TDLF depend generally on both the lack-of-fit in the NL fully-cambered geometry associated with the DLF detailing as well as the overall compliance of the structural system in resisting

the removal of the lack-of-fit displacements by enforcing compatibility at the CF-to-girder connections.

6.2.2. Straight skewed bridges with the CFs detailed based on Line Girder Analysis (LGA) cambers

The following are specific facts and attributes about straight skewed bridge fit where the CFs are detailed based on LGA:

- In straight skewed bridges, SDLF using LGA cambers results theoretically in zero CF forces, zero flange lateral bending stresses, and perfectly plumb girders in the SDL condition. This is accomplished by detailing the CFs to fit between the girders in their theoretical deflected position under the self-weight of the structural steel, but with the CFs conceptually disengaged such that they do not transfer any internal forces. If the girders are allowed deflect conceptually under the SDL with the CFs disengaged, the girder vertical deflections, major-axis bending stresses, and reactions are theoretically identical to the values determined from LGA for the SDL. In turn, for SDLF, the CF connection work points match with the corresponding work points on the SDL deflected geometry of the girders.
- The above result, i.e., girder responses identical to the values determined from LGA for the SDL, is accomplished in the 3D bridge system via the lack-of-fit introduced between the CFs and the girders in their undeformed (NL) geometry by the SDLF detailing of the CFs.
- Based on the assumptions that:
    1) All the bridge components stay elastic,

2) Any play in the CF-to-girder and girder splice connections has a negligible influence on the bridge response, and

3) There is no incidental restraint (friction forces, etc.) at the bridge supports,

the bridge is a conservative elastic structural system. As such, the bridge responses in the completed condition and at any stage of erection are unique and independent of the prior sequence of the erection. These are the assumptions commonly made by the Design Engineer when analyzing a bridge. This fact explains why the above two different conceptual models for SDLF (i.e., disengaging the CFs from the girders and then connecting them once the girders are deflected to their SDL profiles, versus forcing the girders and CFs to fit together under zero load, then applying the SDL) produce the same end result. This does not mean that the erector can neglect the influence of play in the structural connections on the bridge geometry.

- In straight skewed bridges, TDLF using LGA cambers results in theoretically zero CF forces, zero flange lateral bending stresses, and perfectly plumb girders in the TDL condition, based on the idealization that the deck forms and the bridge deck in its early condition during concrete placement do not provide any interconnection between the girders in resisting the TDL.
- Similar to the above behavior for SDLF detailing, TDLF detailing of the CFs based on LGA cambers theoretically produces zero CF forces and girder responses identical to the values determined from LGA for the TDL condition in straight skewed bridges.
- The above behavior for SDLF and TDLF is the same regardless of whether the bridge has parallel or non-parallel skew of its bearing lines. SDLF and TDLF detailing of the

CFs causes the complete behavior of the individual girders to be theoretically exactly equal to the behavior from the LGA in the targeted DL condition. However, the behavior of the interconnected 3D bridge system clearly can be very different for parallel skew versus non-parallel skew.

- The physical straight skewed bridge responses do not match up exactly with the above theoretical results for various reasons including:
    1) For TDLF, the additional torsional loading on the fascia girders from eccentric overhang bracket loads. These torsional loads may be calculated separately from the other TDL effects; however, they are included in the DLF RA results presented in this research.
    2) For SDLF and TDLF, minute lack-of-symmetry of the girders associated with one-sided web stiffeners and connection plates, etc., such that the girders exhibit some minor lateral deflections when they are conceptually disengaged from the CFs.
    3) For SDLF and TDLF, secondary bending of the CF members due to any rotational continuity between the CF members and the girders, as well as secondary bending of the CF members due to connection eccentricities for single angle and flange-connected tees.
    4) As discussed in Section 2.1, in the DLF RA (3D FEA simulation) studies conducted in this research, the CF chord to which the diagonals are connected in V and inverted-V CFs is modeled as being moment connected to the girder connection plates. Although one would expect that this assumption results in some secondary bending within the 3D FEA bridge models, it is apparent from the research results that this assumption also has a measurable effect on the axial forces in the CF

members in cases where the CF member axial forces are relatively small due to improved CF framing arrangements.

5) As discussed in Section 2.1, the influence of secondary bending within single angle and flange-connected Tee-section members on the member axial stiffnesses is included in the 3D FEA analyses conducted in this research by reducing the member axial stiffnesses by 0.65 as specified in Article 4.6.3.3.4 of the 7th Edition AASHTO LRFD Specifications.

6) For SDLF and TDLF, specific lateral constraint conditions at guided and fixed bearings. As discussed at length in NHI (2011), it is common to obtain large lateral forces at bearing locations in 3D FEA models, particularly when rigid constraints are assumed in the directions of bearing fixity. As discussed in Section 2.1, the bridges in this research are assumed to be "floated" on the bearings in the lateral directions to eliminate these potentially large lateral forces. As such, the lateral forces at the bearings are negligible in the 3D FEA studies conducted in this research.

7) Various attributes of the physical bridge behavior, including incidental contributions from deck forms and early concrete deck stiffness (for TLDF), incidental lateral or rotational restraint at bearings, play in the CF and girder splice connections within connection tolerances, over-camber of the girders within camber tolerances, variations in the concrete deck thickness within construction tolerances, factors that affect the specific geometry of the steel, such as field temperature, deviations from ideal support elevations within construction

tolerances, etc. For engineering design, bridges are commonly analyzed without directly accounting for these factors.

- It is desirable to understand the potential impact of the above effects on the deviation from the ideal theoretical results.
- It is important to note that the LGA calculations give a theoretically "exact" determination of the girder responses ONLY in straight skewed bridges and ONLY in the targeted DL condition. It is desirable to understand the magnitude of the errors produced by using LGA calculations for other DL conditions.
- In straight skewed bridges detailed for SDLF based on LGA cambers, the TDL responses are theoretically equal to the LGA responses under the SDL plus the CDL responses obtained from a NLF RA. Alternatively, the TDL responses may be calculated directly from a DLF RA.
- In straight skewed bridges detailed for TDLF based on LGA cambers, the SDL responses are theoretically equal to the LGA responses under the TDL minus the CDL responses obtained from a NLF RA. Alternatively, the SDL responses may be calculated directly from a DLF RA.
- Based on the above, for straight skewed bridges, theoretically the most accurate girder TDL cambers that should be fabricated into the girders to achieve the targeted elevations under the TDL (when the CFs are detailed based on the LGA cambers) are:
  1) For TDLF, the negative of the girder TDL vertical deflections obtained from the LGA.
  2) For SDLF, the negative of the girder SDL vertical deflections obtained from the LGA plus the negative of the CDL vertical deflections obtained from a NLF RA.

- Although TDLF and SDLF detailing based on the above LGA deflections (or the corresponding girder cambers) is theoretically the most accurate approach, this is not recommended for reasons discussed in the next section, which addresses the use of RA cambers in straight skewed bridges.
- It is important to note that since the girder LGA vertical displacements generally differ substantially from the girder NLF RA displacements, the bridge responses from a NLF RA generally will differ substantially from the theoretical (and actual) bridge responses associated with SDLF or TDLF detailing based on the LGA cambers. Detailing for SDLF or TLDF based on LGA cambers results in the girder responses in the targeted DL condition theoretically being exactly the responses from the corresponding LGA (LGA girder vertical deflections, zero flange lateral bending, LGA major-axis bending stresses and LGA girder vertical reactions).
- It is desirable to understand the errors associated with applying a NLF RA to predict the responses in straight skewed bridges detailed for SDLF or TDLF using LGA cambers. These errors are due to neglecting the lack-of-fit associated with the DLF detailing in the structural analysis, and are expected to vary as a function of the "nuisance transverse stiffness" effects in a given bridge. That is, a bridge that has substantial transverse stiffness, compared to the vertical stiffnesses of the girders in their longitudinal direction, will tend to have larger deviation of the NLF RA responses from the correct theoretical (and actual) results that include the influence of the SDLF or TDLF detailing. These errors are different from the errors associated with attempts to apply LGA to predict bridge responses in DL conditions other than the targeted condition; however, they can be of comparable significance.

- It should be noted that, given the specified girder SDL or TDL cambers arrived at by any method, including fabrication over-camber, etc., DLF RA produces the correct theoretical responses by properly accounting for the lack-of-fit in the initial undeformed (NL) geometry associated with the SDLF or TLDF detailing.

6.2.3 Straight skewed bridges with the CFs detailed based on Refined Analysis (RA) cambers

The following are specific facts and attributes about straight skewed bridge fit where the CFs are detailed based on Refined Analysis (RA):

- In straight skewed bridges, if SDLF and TDLF detailing are conducted using RA cambers, which can be dramatically different from the LGA cambers because of the 3D action of the interconnected bridge system, the CF lack-of-fit can be dramatically different from that associated with the LGA cambers.
- In straight skewed bridges, SDLF and TDLF detailing based on RA cambers still gives approximately plumb webs, small flange lateral bending stresses, and small CF forces in the targeted DL condition; however, these responses are no longer theoretically zero. This is due to the overall elastic deformations of the CFs and the elastic torsional deformations of the girders in the structural system. There is only one set of cambers and corresponding CF drops that gives theoretically exactly plumb webs, zero flange lateral bending stresses and zero CF forces in the targeted DL condition for straight skewed bridges – the LGA cambers. If the CF members truly have zero force and the girder flanges truly have zero lateral bending, then the girders can only respond in the manner assumed in the LGA.

- In straight skewed bridges, SDLF and TDLF detailing based on RA cambers tends to have only a small impact on the girder vertical displacements, as opposed to SDLF and TDLF detailing based on LGA cambers, in which the girder vertical displacements are actually modified from the values obtained from a NLF RA to those associated with LGA (via the initial lack-of-fit and the resulting locked-in forces). Since DLF detailing based on RA cambers has a small effect on the girder vertical displacements, the change in the girder major-axis bending stresses and reactions from the values obtained from a NLF RA tends to be relatively small.
- The relatively small changes in the vertical displacements in straight skewed bridges, when DLF detailing based on RA cambers is employed, is because the resulting targeted DL elevations are essentially the "natural" deflected elevations of the girders under the targeted DL in the 3D structural system. As such, the girders are subjected predominantly just to twist rotations to move them from their deflected out-of-plumb geometry in the 3D system to their approximately plumb targeted DL geometry, via the DLF detailing effects. The girder twisting is accomplished with relative ease when the straight girders are in this "natural" deflected geometry.
- It is desirable to understand the potential impact of SDLF and TDLF detailing based on RA cambers on the magnitude of the small girder layovers, CF forces, and girder flange lateral bending stresses in straight skewed bridges. Stated alternately, what are the consequences of using a NLF RA (which neglects the lack-of-fit associated with the CF detailing) to calculate the girder layovers, CF forces and girder flange lateral bending stresses, when the CFs are detailed for SDLF or TDLF based on RA cambers?

- It is desirable to understand the potential impact of SDLF and TDLF detailing based on RA cambers on the SDL and TDL girder major-axis bending stresses and vertical reactions, which are generally more substantial non-zero values.
- It is important to note that the girder layovers, the CF forces and the girder flange lateral bending stresses associated with SDLF or TLDF detailing based on the RA cambers are substantially reduced relative to the values obtained from a NLF RA. For instance, in certain cases with severe nuisance transverse stiffness effects, some of the CF forces can be tremendous in a NLF RA. In addition, in a bridge with sharply skewed abutments, the twist rotations of the girders at the abutment bearings can be several times larger than the corresponding girder major-axis bending rotations. The SDLF or TDLF detailing effects can reduce these forces and rotations to only a small fraction of their NLF based values.
- In parallel with the above facts, it should be emphasized that a NLF RA will tend to significantly over-predict the CF forces, girder flange lateral bending stresses, and girder twist rotations in a straight skewed bridge.
- It is desirable to understand the reductions in the girder layovers, CF forces and girder flange lateral bending stresses due to SDLF and TDLF detailing based on RA cambers.
- The overall behavior of straight bridges with non-parallel skew can be significantly different from that of straight bridges with parallel skew. Although the overall aspects of the behavior for SDLF and TDLF detailing using LGA cambers are the same regardless of the parallel or non-parallel nature of the skews, additional elastic system deformation characteristics come into play when a straight bridge with non-parallel skew is detailed using RA cambers.

- It is desirable to understand the behavior for SDLF and TDLF using RA cambers in straight bridges with non-parallel skew.
- An important question that may be asked is the following: Is it better to perform SDLF or TDLF detailing of straight skewed bridges using LGA cambers, or is it better to use RA cambers? Some of the considerations in answering this question are as follows:
    1) LGA cambers give the theoretical result of zero girder layover, zero CF forces, and zero girder flange lateral bending stress under the targeted DL condition.
    2) RA cambers result generally in larger DL displacements on some of the girders in the bridge cross-section (typically the fascia girders in straight bridges with parallel skew or the longer fascia girder in bridges with non-parallel skew, due to additional vertical loads distributed to those girders), and smaller displacements on other girders (e.g., the innermost girders in bridges with parallel skew, due to the transverse stiffness developed by the CFs in the short direction between the obtuse corners of the bridge plan); however, these displacements are offset by the calculated RA girder cambers, and therefore the final targeted elevations can be achieved with good accuracy.
    3) Similarly, if LGA cambers are employed, the vertical displacements are offset by the calculated cambers, and therefore the final targeted elevations can be achieved with good accuracy with that approach as well (theoretically, this approach gives the best accuracy); however, a "mixture" of SDL LGA deflections and RA CDL deflections must be considered in this case to achieve the best results.
    4) RA cambers tend to be smaller in many of the girders in a multi-girder bridge, since they are associated with the smaller girder vertical displacements of the

interconnected 3D structural system; however, in some bridges with extreme nuisance transverse stiffness effects, the differential RA cambers between the interior and the fascia girders can be large.

5) RA cambers match more closely with the displacements obtained from ordinary NLF RA models in which a model of the bridge is built, gravity is simply "turned on," and the lack-of-fit associated with SDLF or TDLF detailing is neglected.
6) SDLF or TDLF detailing with RA cambers does not require any "mixing and matching" of separate solutions from LGA and RA to achieve the best accuracy; however, a DLF RA gives a correct rigorous solution for the effect of the lack-of-fit associated with the detailing of the CFs, regardless of what this lack-of-fit is and regardless of what method or assumptions are used to detail the CFs.
7) RA better accommodates the consideration of staged concrete deck placement and its influence on the CDL deflections and the resulting appropriate cambers, in cases where the consideration of staged concrete deck placement may be important.
8) In the limit that TDLF based on LGA cambers is applied to bridges where the skew is close to zero, the application of the dead load to each girder based on the tributary deck widths (which is the recommended practice for sharply skewed bridges (NHI 2011)) combined with TDLF detailing, results in each of the individual girders behaving essentially as assumed in the LGA within the targeted TDL condition. Therefore, for instance, if a fascia girder is subjected to unusually heavy loads that are included in the TDL (due to a large overhang, a heavy wall placed at or near the fascia girder, etc.), the fascia girder will be designed to support this load entirely on its own without any help from the remainder of the girders in the bridge cross-

section. Furthermore, the cross-frames between this girder and the remainder of the bridge cross-section will be detailed with an initial lack-of-fit such that they do not transfer any of these large dead loads to the rest of the bridge, aside from the restraint of any eccentric torsion applied to the fascia girder. (The loads from eccentric torsion on the fascia girder are calculated separately from the basic LGA solution.) The vertical deflection of this fascia girder will tend to be substantially larger than the other bridge girders; however, this girder's camber will also be substantially larger, such that theoretically, the girder elevations will be as targeted. Although it can be argued that this is correct and acceptable design behavior (assuming that the concrete deck does not provide a significant path for the heavy load to be transferred to the rest of the bridge system), the response of the bridge designed in this way is not as efficient as it would be if TDLF RA cambers are used, in which case the entire bridge structural system is engaged in resisting the heavy load on the fascia girder.

9) RA is generally required for tightly curved bridge geometries; therefore, the use of RA cambers for straight skewed bridges results in calculations that are consistent and more uniform across all I-girder bridge geometries.

- The use of LGA for setting the girder cambers in sharply skewed straight bridges is generally discouraged based on the above considerations.
- It is desirable to understand the consequences of using LGA versus RA cambers more quantitatively.
- It should be noted that large DC2 loads, such as heavy walls, planters, etc. are not commonly included in the TDL considered for TDLF detailing.

6.2.4 Curved bridge geometries, with and without skew

The following are specific facts and attributes about horizontally curved bridge fit, for bridges with and without skew:

- For all curved and curved and skewed bridge geometries, generally the CF forces and the girder flange lateral bending stresses are significant due to the horizontal curvature. They never approach theoretical zero values as a function of the DLF detailing, as in straight skewed bridges, except in the limit that the radius of curvature becomes infinite and when LGA cambers are employed. In curved and skewed bridges, the magnitudes of these bridge responses can be increased or decreased compared to a similar curved radially-supported bridge depending on the skew orientation.
- For bridges having significant horizontal curvature, with or without skew, the design analysis typically should be an accurate RA. NCHRP Report 725 provides guidance regarding various simplifications, such as the use of grid analysis methods, and when these simplifications are sufficient. An accurate RA should always be used to calculate the girder cambers on a highly curved bridge.
- For curved geometries, with and without skew, SDLF and TDLF detailing result in approximately plumb webs in the targeted DL condition. However, the webs will never be perfectly plumb. This is due to the overall elastic deformations of the CFs and the elastic torsional deformations of the girders in the structural system.
- It is desirable to understand the magnitude of the girder layovers in typical curved I-girder bridge systems resulting from the above elastic deformations.

6.2.5 Curved radially-supported bridges

The following are specific facts and attributes about curved radially-supported bridges and fit:

- For curved radially-supported geometries, both SDLF and TDLF detailing tend to increase the CF forces and the girder flange lateral bending stresses. This is due to the fact that horizontally curved girders tend to twist and deflect excessively if they are restrained only at their ends (whereas straight girders conceptually do not twist at all if they are not engaged with the CFs).
- Due to the above fact, a NLF RA generally tends to under-predict the CF forces and girder flange lateral bending stresses in curved radially-supported bridges.
- It is desirable to understand the typical increases in the CF forces and the girder flange lateral bending stresses from the values obtained from a NLF RA due to SDLF and TDLF detailing effects. Stated alternately, it desirable to determine if any simple scale factors should be applied to the results of a NLF RA to account in a simple way for SDLF and TDLF detailing effects on the CF forces and the girder flange lateral bending stresses in curved radially-supported bridges.
- The girder displacements are generally reduced and the resulting elevations of the girders are increased in curved radially-supported bridges due to SDLF and TDLF detailing effects. This behavior is due to the coupling between twisting and vertical deflections in curved girders and bridge units. For example, a curved I-girder cannot be twisted about a chord through its ends without also changing its vertical displacements and vertical elevations within the span.

- It is desirable to understand the impact of the above elevation changes due to SDLF and TDLF detailing in horizontally curved bridges. Stated alternately, it is desirable to determine if any simple scale factors should be applied to the results of NLF RA to account in a simple way for SDLF and TDLF detailing effects on the girder vertical displacements.
- In curved radially-supported bridges, the impact of SDLF and TDLF detailing on the girder major-axis bending stresses and the support vertical reactions tends to be relatively small. However, there is some minor effect. The girder major-axis bending stresses and vertical reactions on the girder at the outside of the curve generally tend to be increased by the DLF detailing, since the major-axis bending of the girders is in effect used as a reaction to twist the girders back in the direction opposite to the one that that they want to roll.
- It is desirable to understand the impact of SDLF and TDLF detailing on the girder major-axis bending stresses and support vertical reactions in curved radially-supported bridges. Stated alternately, it is desirable to determine if simple scale factors can be applied to the results of NLF RA to account in a simple way for SDLF and TDLF detailing effects on the girder major-axis bending stresses and support vertical reactions.

6.2.6 Curved and skewed bridges

The following are specific facts and attributes about fit in curved and skewed bridges:

- In curved and skewed bridges, the separate effects of DLF detailing on the bridge responses discussed above (the DLF effects associated with skew and the DLF effects

associated with horizontal curvature) are observed, generally, in the limit that the horizontal curvature or the skew become small respectively.

- In curved and skewed bridges where both the curvature and the skew are significant, the separate DLF detailing effects associated with the skew and the curvature interact in complex ways:
  1) In simply-supported spans where the skew tends to make the girder on the outside of the curve longer, a number of the DLF detailing effects associated with the horizontal curvature tend to be amplified by the effects associated with the skew.
  2) In simply-supported spans where the skew tends to make the girder on the inside of the curve longer, a number of the DLF detailing effects associated with the horizontal curvature tend to be offset by the effects associated with the skew.
- The above results parallel the dramatically different overall behavior of straight skewed versus curved radially-supported bridges, and the combinations of these dramatically different behavior attributes when the bridge is curved and skewed.
- It is desirable to determine when a NLF RA gives sufficient predictions of the responses in curved and skewed I-girder bridges, and whether simple scale factors can be applied to the responses in cases where NLF RA may under-predict the magnitude of the responses.

6.3 Recommended Application of DLF RA to Curved and/or Skewed I-Girder Bridges

In bridges with large skew and tight curvature, where the effects of SDLF and TDLF are significant and cannot be captured accurately by a simplified methods, it is recommended that a DLF RA be performed to determine the bridge responses. In these

cases, recommendations for the application of DLF RA are provided in the bold italicized text below (the recommendations in the subsequent sections are also highlighted in bold italics):

- ***When a DLF RA is employed for curved and/or skewed I-girder bridges with the CFs detailed for SDLF based on NLF RA cambers, it is recommended that the locked-in force effects from the lack-of-fit be determined by a separate structural analysis and that the EL (miscellaneous locked-in force) load factor of 1.0 be applied to these effects for combination with other loadings. Per AASHTO LRFD recommendations, the resulting net factored DL to be considered for construction is 1.4 DC + 1.0 EL and the resulting net factored DL for STRENGH I is 1.25 DC + 1.0 EL.***
- ***When a DLF RA is employed for curved and/or skewed I-girder bridges with the CFs detailed for TDLF based on NLF RA cambers, it is recommended that the locked-in force effects from the lack-of-fit be determined by a separate structural analysis. When the locked-in force effects are additive to the effects of the DC loads, it is recommended that the EL (miscellaneous locked-in force) load factor of 1.0 be applied to these effects for combination with other loadings. When the locked-in force effects are of opposite sign to the DC loads, it is recommended that the EL (miscellaneous locked-in force) load factor of 0.85 be applied to these effects for combination with other loadings. Per AASHTO LRFD recommendations, the resulting net factored DL is 1.4 DC + 1.0 EL for construction load combinations and 1.25 DC + 1.0 EL for STRENGH I when the locked-in force effects are additive with the effects of the DC loads, and the resulting net factored DL is 1.4 DC + 0.85 EL for***

construction load combinations and 1.25 DC + 0.85 EL when the locked-in force effects are of opposite sign to the effects of the DC loads.

- The EL load factor of 1.0 is considered justified when a DLF RA is employed for SDLF and for TLDF where the effects are additive to the DC load effects because the lack-of-fit of the CFs in the NL geometry of the bridge is directly accounted for in the structural analysis.
- The EL load factor of 0.85 is intended to account for additional uncertainties and variabilities associated with TDLF, such as incidental participation of deck forms and early concrete stiffness in the structural resistance, and larger potential play in the CF connections due to the larger CF forces associated with TDLF. It is suggested that a value between 0.85 and 1.0 may be used if considered justified based on the judgment of the engineer of record.
- Although the girder deflections are changed slightly from the NLF RA values when a DLF RA is conducted in some cases, it is sufficient to use the vertical deflections from the NLF RA for setting the girder cambers (and the CF drops) in curved and/or skewed I-girder bridges. Use of the DLF RA deflections for setting the girder cambers would require an iterative approach, for instance, starting with a NLF RA, then modifying the girder cambers based on the results from the subsequent DLF RA, then feeding these results back into another DLF RA, etc. Although this type of iterative process results in girder layovers that are closer to zero (Ozgur 2011), any improvements achieved by this process are unjustified. The sufficiency of this approach is discussed in the following summaries of the *Elevation* results for the different bridge geometries.

6.4 Summary of Questions Pertaining to the Influence of the Fit Decision on Dead Load Responses in Completed Curved and/or Skewed I-Girder Bridge Systems

In lieu of accounting for the SDLF and TDLF detailing effects directly within a structural analysis, one can use the results from a NLF RA with simple approximate adjustment factors in certain curved and/or skewed bridges. As mentioned in the above discussions, for the development of these adjustment factors, the following questions need to be answered:

1) What is the influence of various incidental effects on the deviation of the responses from the ideal theoretical results in straight skewed bridges detailed for SDLF or TLDF using LGA cambers?
2) What magnitude of errors are produced by applying LGA for the calculation of all the responses in straight skewed bridges detailed for SDLF or TDLF using LGA cambers?
3) What magnitude of errors are produced by applying a NLF RA to predict the responses in straight skewed bridges detailed for SLDF or TDLF using LGA cambers?
4) What is the impact of SDLF and TDLF detailing based on RA cambers on the magnitude of the supposedly small girder layovers, CF forces and girder flange lateral bending stresses in straight skewed bridges?
5) What is the impact of SDLF and TDLF detailing based on RA cambers on the major-axis bending stresses and vertical reactions in straight skewed bridges?
6) Given that the reductions are not generally to zero values, to what extent are the girder layovers, CF forces and girder flange lateral bending stresses in straight skewed bridges reduced due to SDLF and TDLF detailing based on RA cambers?
7) What effects do the RA cambers have in straight bridges with non-parallel skew? Are there any significant differences in the effects compared to those in straight bridges

with parallel skew? How do the RA camber effects compare to the LGA camber effects in straight bridges with non-parallel skew?

8) What are the quantitative consequences of SDLF or TDLF detailing based on LGA cambers versus RA cambers in straight skewed bridges?
9) Given that the reductions are not generally to zero values, to what extent are the girder layovers reduced in curved radially-supported bridges by SLDF and TDLF detailing?
10) By what extent are the worst-case CF forces, girder flange lateral bending stresses, girder elevations, major-axis bending stresses, and support vertical reactions increased in curved radially-supported bridges by the effects of SDLF and TDLF detailing?
11) Given that the reductions are not generally to zero values, to what extent are the girder layovers reduced in curved and skewed bridges by SLDF and TDLF detailing?
12) What is the largest magnitude of the deviations from the targeted elevations due to SDLF and TDLF detailing in curved and skewed I-girder bridges?
13) By what extent are the worst-case CF forces, girder flange lateral bending stresses, girder elevations, major-axis bending stresses, and support vertical reactions increased in curved and skewed bridges by the effects of SDLF and TDLF detailing?

6.5 Curved Radially-Supported Bridges with Cambers Set Based on NLF RA

Section 6.5.1 provides quantitative results on the influence of SDLF and TDLF detailing on bridge responses in curved radially-supported bridges with cambers set based on NLF RA. The influence of SDLF and TDLF is discussed on the responses in the following order: girder vertical displacements, girder elevations, girder layovers, CF forces, girder stresses, and vertical reactions. Section 6.5.2 then summarizes the influences

on the key bridge responses and provides recommendations for handling of these effects. The recommendations are highlighted in bold italicized text.

6.5.1 Quantitative Results

6.5.1.1 Girder Vertical Displacements

For curved radially-supported bridges, SDLF and TDLF detailing tend to reduce the vertical displacements of all the girders, thus resulting in an overall tendency for higher final elevations of the steel within the spans. The twisting of the girders induced by SDLF and TDLF detailing, combined with the overall three-dimensional action of the curved spans, causes an upward movement of all of the girders. This effect is illustrated in Figure 77 which shows the vertical displacements of the girder on the outside of the curve for Bridge (C) NISCR7 under TDL. The horizontal axis of this plot is the normalized position along the girder length, x_g/L_g, where x_g is the position along the curved axis of the girder and L_g is the total distance from bearing-to-bearing along the length of the girder.

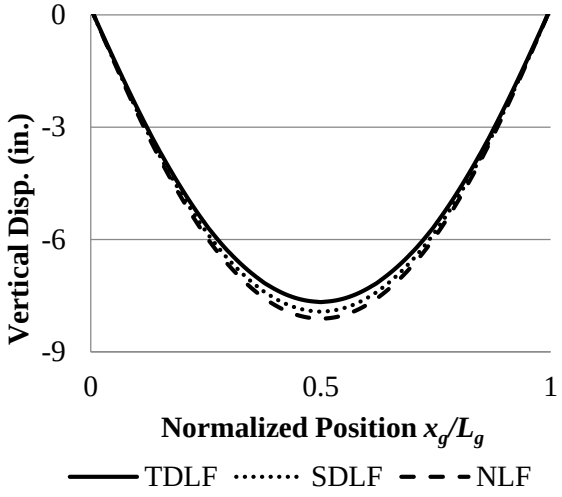

Figure 77. Bridge (C) NISCR7 vertical displacements under TDL for the girder on the outside of the curve.

Table 20 shows the maximum vertical displacements and the changes in the vertical displacements relative to those associated with NLF detailing for the curved radially-supported bridges studied in this research. One should note that Table 20 reports the absolute maximum downward displacement in the bridges. As such, the data in this table is useful for understanding the overall trends in the behavior of the bridges, but not necessarily the specific changes that occur at different positions in the individual girders. In some of the cases for the bridges considered in this research, the location of the maximum displacement can change as a function of the CF detailing method.

Table 20. Maximum vertical displacement under TDL with NLF, SDLF and TDLF detailing, and corresponding change in the maximum vertical displacement relative to the results from NLF RA, for the curved radially-supported bridges studied in this research (excluding Bridge (E), the largest changes due to SDLF and TDLF are highlighted by dark shading).

Bridge	**NLF**	**SDLF**		**TDLF**	
	Disp. (in.)	Disp. (in.)	Change (in.)	Disp. (in.)	Change (in.)
(A) EISCR1	-4.7	-4.5	0.2	-3.9	0.8
(B) NISCR2	-7.1	-6.6	0.5	-5.9	1.2
(C) NISCR7	-8.1	-7.9	0.2	-7.7	0.4
(D) NISCR10	-11.7	-11.4	0.3	-11.3	0.4
(E) EICCR11	-19.4	-16.8	2.6	-15.5	3.9
(F) NICCR12	-18.0	-16.8	**1.2**	-16.0	**2.0**
(G) EICCR4	-9.6	-9.5	0.1	-9.3	0.3

From Table 20, it can be observed that SDLF and TDLF detailing reduce the maximum vertical displacements in all of the cases. The largest decreases in the maximum TDL vertical displacement are 2.6 inches for SDLF detailing and 3.9 inches for TDLF detailing. These decreases occur in Bridge (E) EICCR11, which is significantly more extreme than

the other bridges considered. In all other cases, the largest decreases in the maximum TDL vertical displacement are 1.2 inches for SDLF detailing and 2.0 inches for TDLF detailing.

6.5.1.2 Girder Elevations

The girder cambers for the curved radially-supported bridges are based on NLF RA in this research. The total girder cambers are taken as the negative of the vertical deflections obtained from the NLF RA for the corresponding TDL, using the common engineering practice of building a model of the bridge and "turning gravity on." That is, any changes in the deflections due to SDLF or TDLF detailing effects are not included in the calculation of the cambers. The vertical elevations under TDL for NLF detaling are zero (assuming no superelevation, etc., as a simplification).

The negative of the SDL deflections is used in a similar fashion to the TDL cambers in setting the drops between each side of the CFs when SDLF detailing is employed. As such, the phrase "SDL camber" is used in this research to refer to the negative of the SDL deflections. These deflections, in addition to the TDL cambers, affect the final girder elevations when SDLF detailing is employed. Similar to the calculation of the TDL cambers, for the curved radially-supported bridges, the SDL cambers are calculated without considering the influence of the SDLF detailing effects on the girder vertical displacements.

Since the SDLF and TDLF detailing effects tend to reduce the vertical displacements as discussed above, the vertical elevations of the girders are somewhat higher than the targeted elevations (i.e., the "zero" elevation level) when SDLF or TDLF detailing is employed. The deviation from the targeted vertical elevations, when the bridge is detailed for SDLF or TDLF detailing, is equal to the displacement caused by the SDLF and TDLF

detailing effects alone. Figure 78 shows the vertical elevations of the girder on the outside of the curve for Bridge (C) NISCR7 under TDL. The maximum vertical elevation for this bridge, under TDL for TDLF detailing, is 0.44 inches.

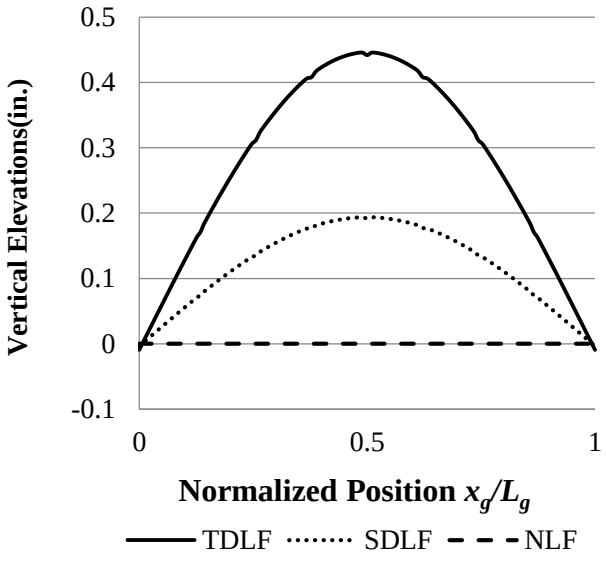

Figure 78. Bridge (C) NISCR7 TDL vertical elevation of the girder on the outside of the curve

Considering the complete set of curved radially-supported bridges studied in this research, the largest deviation from the targeted elevation under TDL for TDLF detailing, is 6.7 inches for Bridge (E) EICCR11 and the smallest is 0.4 inches for Bridge (G) EICCR4 (see Table 21). It is apparent that the geometry parameters for Bridge (E) are so different from the other bridges (L_s = 329 ft, L_s/R = 0.80 and L_s/w_g = 8.1 on its curved span) that this bridge should be considered as an outlier. Bridge (F) NICCR12 has the second largest deviation, 2.1 inches, from the targeted elevation under TDL for TDLF. This bridge has the longest curved spans considered (350 ft) of all the bridges studied. It is apparent that for tightly curved bridges with L_s values larger than about 250 ft, and if TDLF detailing were to be used (which is not recommended), consideration should be given to these

deviations from the targeted elevations. For extreme cases where SDLF is employed, consideration should be given to specifying a somewhat thicker concrete haunch than might normally be specified to compensate for these increases in the overall girder elevations. It is important to note the final elevation deviation values in Table 21 do not exactly match values of the maximum displacement change due to detailing methods in Table 20. This is because the cambers are based on NLF RA for all three detailing methods. The location of the maximum displacement in a given bridge may change due to the detailing method.

Table 21. Maximum final elevation deviation from the targeted elevation line, for the curved radially-supported bridges studied in this research (excluding Bridge (E), the largest final girder elevations with SDLF and TDLF detailing under TDL are highlighted by dark shading).

Bridge	NLF (in.)	SDLF (in.)	TDLF (in.)
(A) EISCR1	0.0	0.2	0.8
(B) NISCR2	0.0	0.5	1.2
(C) NISCR7	0.0	0.2	0.4
(D) NISCR10	0.0	0.3	0.4
(E) EICCR11	0.0	4.0	6.7
(F) NICCR12	0.0	**1.4**	**2.1**
(G) EICCR4	0.0	0.1	0.4

6.5.1.3 Girder Layovers

For curved radially-supported bridges, the girders and the bridge cross-section both tend to roll towards the outside of the curve under the action of the DL. The SDLF and TDLF detailing effects twist the girders in the opposite direction from these DL rotations. As shown in Figure 79 for Bridge (C) NISCR7, the maximum layover (i.e., the difference between the radial deflections of the top and bottom flanges) of the girder on the inside of

the curve is 0.02 inches for TDLF, and 0.53 inches for NLF. TDLF detailing is effective in making the inside girder nearly plumb under TDL. The girder layovers at the CF locations on the inside girder are essentially zero for TDLF. The girder layovers of the inside girder in-between the CF locations are slightly non-zero.

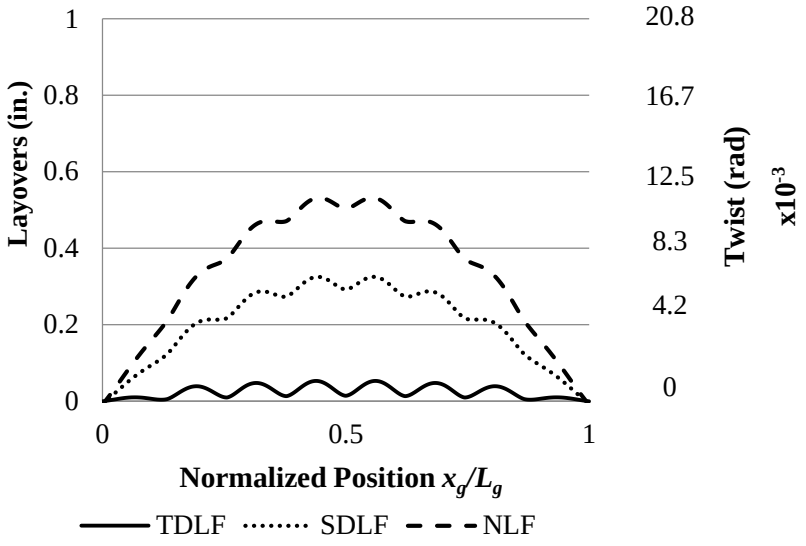

Figure 79. TDL layover and twist of the girder on the inside of the curve in Bridge (C) NISCR7.

As shown in Figure 80, for Bridge (C) NISCR7, the maximum layover of the girder on the outside of the curve is 0.42 inches for TDLF, and 0.87 inches for NLF. The girders are 74 in deep in NISCR7. Therefore, it can be stated that TDLF detailing also is reasonably effective in making the outside girder nearly plumb under TDL. The girders that are located further toward the outside of the curve are less plumb than the inside girders due to the elastic deformation of the CFs.

Considering the complete set of curved radially-supported bridges studied in this research, the largest girder layovers are 0.9 inches under SDL for SDLF detailing (see Table 22) and 1.2 inches under TDL for TDLF detailing (see Table 23). These layovers

occur on the outside girder of Bridge (E) EICCR11 which is an outlier with D = 168 in, L_s = 322 ft, L_s/R = 0.80 and L_s/w_g = 8.1 on its curved span. Other than Bridge (E) and Bridge (A) which has a limited number of CFs and CF spacing at the maximum limits permitted by the AASHTO LRFD Specifications, the largest girder layovers are 0.3 inches under SDL for SDLF detailing and 0.4 inches under TDL for TDLF detailing, corresponding to Bridge (F) NICCR12. The largest girder twist rotations are 0.0024 rad. under SDL for SDLF and 0.0048 rad. under TDL for TDLF, corresponding to Bridge (C) NICCR7.

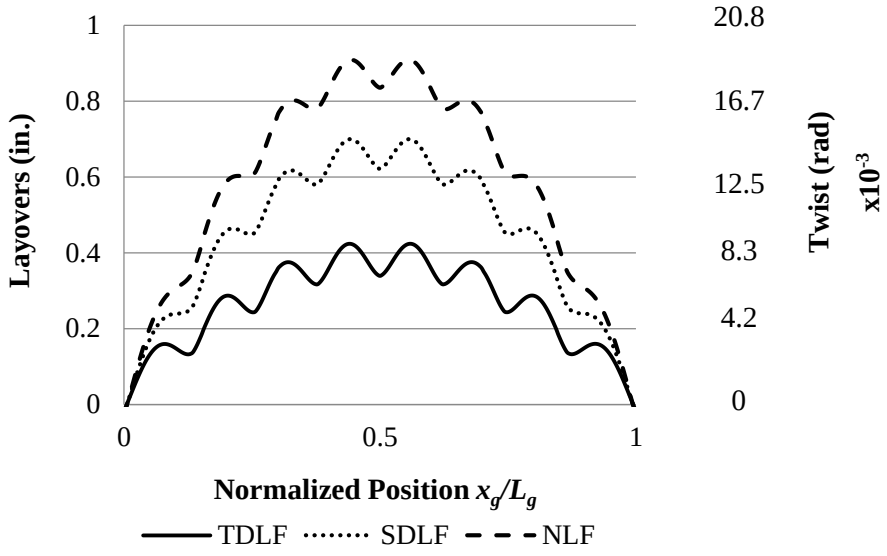

Figure 80. TDL layover and twist of the girder on the outside of the curve in Bridge (C) NISCR7.

Table 22. Maximum magnitudes of girder layovers and twists under SDL in the curved radially-supported bridges studied in this research (LO1 and LO2 are the maximum girder layovers with NLF and SDLF, respectively. $\phi 1$ and $\phi 2$ are the maximum girder twists with SDLF and SDLF detailing, respectively. Excluding the results for Bridge (E), the largest girder layover and twists with SDLF are highlighted by dark shading).

Bridge	Girder Depth (in.)	NLF		SDLF	
		LO1 (in.)	$\phi 1$ (rad) x10^{-3}	LO2 (in.)	$\phi 2$ (rad) x10^{-3}
(A) EISCR1	48	0.3	6.3	0.1	2.1
(B) NISCR2	84	0.7	8.3	0.1	1.2
(C) NISCR7	84	0.4	4.8	0.2	**2.4**
(D) NISCR10	120	0.6	5.0	0.2	1.7
(E) EICCR11	168	3.4	20.2	0.9	5.4
(F) NICCR12	168	1.5	8.9	**0.3**	1.8
(G) EICCR4	99	0.3	3.0	0.1	1.0

Table 23. Maximum magnitudes of girder layovers and twists under TDL in the curved radially-supported bridges studied in this research (LO1 and LO3 are the maximum girder layovers with NLF and TDLF, respectively. $\phi 1$ and $\phi 3$ are the maximum girder twists with NLF and TDLF detailing, respectively. Excluding the results for bridges (A) and (E), the largest girder layover and twists with TDLF are highlighted by dark shading).

Bridge	Girder Depth (in.)	NLF		TDLF	
		LO1 (in.)	$\phi 1$ (rad) x10^{-3}	LO3 (in.)	$\phi 3$ (rad) x10^{-3}
(A) EISCR1	48	1.1	22.9	0.4	8.3
(B) NISCR2	84	1.9	22.6	0.3	3.6
(C) NISCR7	84	0.9	10.7	**0.4**	**4.8**
(D) NISCR10	120	1	8.3	0.3	2.5
(E) EICCR11	168	6	35.7	1.2	7.1
(F) NICCR12	168	2.8	16.7	**0.4**	2.4
(G) EICCR4	99	1.1	11.1	0.1	1.0

6.5.1.4 Cross-Frame Forces

For curved radially-supported bridges, the effects of SDLF and TDLF detailing often do not have much influence on the CF chord forces. However, the influence on the CF diagonal forces is substantial. Table 24 summarizes the average and maximum magnitudes of the CF chord forces in the curved radially-supported bridges studied in this research, and Table 25 gives these values for the CF diagonals. The cells for Bridge (A) EISCR1 are shaded grey in the tables to highlight the fact that this FHWA test bridge had only three intermediate CF lines and subtended angles between the CFs, L_b/R, slightly larger than the permitted AASHTO LRFD maximum. Also, the cells for Bridge (E) EICCR11 are shaded grey, highlighting the aspect that this bridge is largely an outlier as discussed in the previous sections. The largest F2/F1 and F3/F1 ratios in the tables are highlighted by dark shading. These ratios compare the responses under SDL for SDLF to the corresponding responses under SDL for NLF, and the responses under TDL for TDLF to the corresponding responses under TDL for NLF. Clearly, the differences between the DLF and NLF values are relatively small for the chords, as shown in Table 24, excluding Bridges (A) and (E). The largest ratio of 1.29 between the SDL/SDLF maximums corresponds to Bridge (G) EICCR4, where the chord forces themselves are relatively small. However, Table 13 shows that both the average and the maximum ratios of the diagonal forces are substantially increased for all the bridges with the exception of Bridge (F) NICCR12. The increases in both the average and the maximum values are close to a multiple of 2.0 in the majority of the bridges. There is no clear correlation between the specific maximum and average values as a function of the different bridge geometry parameters (e.g., L_s, L_s/R, L_s/w_g, L_s/D, simple- or continuous-span, etc.)

Table 24. Average and maximum magnitudes of the CF chord forces in each of the curved radially-supported bridges studied in this research (F1, F2, and F3 are the average CF forces with NLF, SDLF, and TDLF detailing, respectively. Excluding bridges (A) and (E), the largest F2/F1, F2-F1, F3/F1, and F3-F1 for the average and maximum forces are highlighted by dark shading).

	Bridge	SDL				TDL			
		NLF	SDLF			NLF	TDLF		
		F1 (kip)	F2 (kip)	F2/F1	F2 – F1 (kip)	F1 (kip)	F3 (kip)	F3/F1	F3 – F1 (kip)
Avg	(A) EISCR1	4.5	5.1	1.13	0.6	26.4	29.4	1.11	3.0
	(B) NISCR2	6.5	6.4	**0.98**	-0.1	19.6	18.6	0.95	-1.0
	(C) NISCR7	18.1	16.4	0.91	-1.7	41.9	38.5	0.92	-3.4
	(D) NISCR10	11	10.2	0.93	-0.8	23.1	21.2	0.92	-1.9
	(E) EICCR11	9.1	11.6	1.27	2.5	18.2	20.2	1.11	2.0
	(F) NICCR12	10.9	10.4	0.95	-0.5	20.6	18.7	0.91	-1.9
	(G) EICCR4	1.1	1.04	0.92	-0.1	4.2	4.11	**0.98**	-0.1
Max	(A) EISCR1	18.9	23.9	1.26	5.0	96.0	113.9	1.19	17.9
	(B) NISCR2	19.0	17.5	0.92	-1.5	49.1	47.8	0.97	-1.3
	(C) NISCR7	59.0	55.1	0.93	-3.9	151.5	142.1	0.94	-9.4
	(D) NISCR10	41.8	40.9	0.98	-0.9	95.3	92.5	0.97	-2.8
	(E) EICCR11	45.8	76.2	1.66	30.4	91.0	100.8	1.11	9.8
	(F) NICCR12	56.8	58.4	1.03	1.6	108.4	102.7	0.95	-5.7
	(G) EICCR4	4.1	5.3	**1.29**	1.2	18.3	22.2	**1.21**	3.9

Table 25. Average and maximum magnitudes of the CF diagonal forces in each of the curved radially-supported bridges studied in this research (F1, F2, and F3 are the average CF forces with NLF, SDLF, and TDLF detailing, respectively. Excluding bridges (A) and (E), the largest F2/F1, F2-F1, F3/F1, and F3-F1 for the average and maximum forces are highlighted by dark shading).

	Bridge	SDL				TDL			
		NLF	SDLF			NLF	TDLF		
		F1 (kip)	F2 (kip)	F2/F1	F2 – F1 (kip)	F1 (kip)	F3 (kip)	F3/F1	F3 – F1 (kip)
Avg	(A) EISCR1	4.0	6.5	1.63	2.5	21.5	31.2	1.45	9.7
	(B) NISCR2	5.6	12.1	2.16	6.5	17.1	33.8	1.98	16.7
	(C) NISCR7	6.3	15.7	**2.49**	9.4	20.2	42.0	**2.08**	21.8
	(D) NISCR10	7.5	11.2	1.49	3.7	19.4	24.9	1.28	5.5
	(E) EICCR11	5.7	13.2	2.32	7.5	13.5	25.0	1.85	11.5
	(F) NICCR12	10.2	12.5	1.23	2.3	21.2	25.0	1.18	3.8
	(G) EICCR4	1.7	3.1	1.82	1.4	5.5	10.4	1.89	4.9
Max	(A) EISCR1	8.4	14.3	1.70	5.9	46.9	69.3	1.48	22.4
	(B) NISCR2	11.6	26.6	**2.29**	15.0	36.1	67.0	**1.86**	30.9
	(C) NISCR7	16	34	2.13	18.0	55.7	98.2	1.76	42.5
	(D) NISCR10	21.9	29.5	1.35	7.6	62.4	73.6	1.18	11.2
	(E) EICCR11	22.9	75.9	3.31	53.0	53.9	92.9	1.72	39.0
	(F) NICCR12	50.3	54.0	1.07	3.7	98.1	86.6	0.88	-11.5
	(G) EICCR4	7.3	10.9	1.49	3.6	22.1	35.3	1.60	13.2

The reasons for the behavior shown in Tables 24 and 25 are as follows:

- When SDLF or TDLF detailing is used, the CF geometry pulls the girders back further in the direction opposite from which they want to roll such that the girders

are approximately plumb under SDL or TDL, respectively (this behavior is explained in detail previously in Section 4.2).

- Because TDLF detailing pulls the girders back further than SDLF detailing, TDLF detailing increases the CF member forces more than SDLF detailing. However, it appears from Tables 24 and 25 that the ratios for SDL/SDLF are about the same as the ratios for TDL/TDLF. That is, the increase in magnitude of the TDLF effects relative to the SDLF effects is roughly the same as the ratio of the TDL to the SDL.
- The majority of the critical intermediate CFs in the bridges summarized in Tables 24 and 25 are X-type. The primary nature of the SDLF and TDLF effects on the cross-frames is a shear-racking action as shown in Figure 81. The girders tend to stay relatively parallel to each other, as they are twisted in the opposite direction from the one they want to roll by the DLF actions. Therefore, the CF actions associated with the DLF effects are similar to those of a simply-supported beam subjected to equal end rotations and equal end moments. Figure 81a shows the statical relationships for an X-type CF of equal width/depth associated with this behavior. The CF is subjected to a shear force V and the corresponding couple forces at the cross-frame connections are $V/2$ on each side of the CF. The corresponding forces in the CF diagonals are shown by the dashed arrows. One can observe that the above external actions on the X-type CF are resisted without inducing any force in the CF top and bottom chords. Figure 81b shows the same behavior for an X-type CF that has a width/depth of two. It should be noted that this result does not extend to V or inverted-V type CFs. For these CF types, the chords also must resist forces due to the above actions. The CFs in Bridge (A)

EISCR1 are V-type. From Tables 24 and 25, one can observe that the F2 – F1 for the chords is comparable to the F2 – F1 for the diagonals, corresponding to the SDLF actions. In addition, the F3 – F1 for the chords is comparable to the F3 – F1 for the diagonals, corresponding to the TDLF actions. However, the total chord forces are larger than the diagonal forces. Therefore, the DLF effects get washed out to some extent in the F2/F1 and F3/F1 ratios for the chords in Bridge (A) EISCR1.

In addition to the effect on the average and maximum CF member forces, it is useful to understand the frequency distribution of the changes in the CF member forces due to SDLF and TDLF detailing. Also, rather than consider the change normalized by the NLF member force, it is informative to evaluate the change normalized by the member yield load, which is an upper-bound estimate of the member load capacity. Figure 82 shows this frequency distribution for all the CF chords and Figure 83 shows this distribution for all the CF diagonals in Bridge (C) NISCR7. The horizontal axes in these plots correspond to sub-ranges of -12 to -10 %, -10 to -8 %, etc. The axis labels show the values at the middle of each sub-range. The change in the CF chord forces relative to the results from NLF RA, normalized by the member yield loads, is less than 0.6 % in all cases for TDLF and SDLF detailing. However, the increase in the CF diagonal forces is as large as 12.3 % for TDLF detailing and as large as 6.2 % for SDLF detailing.

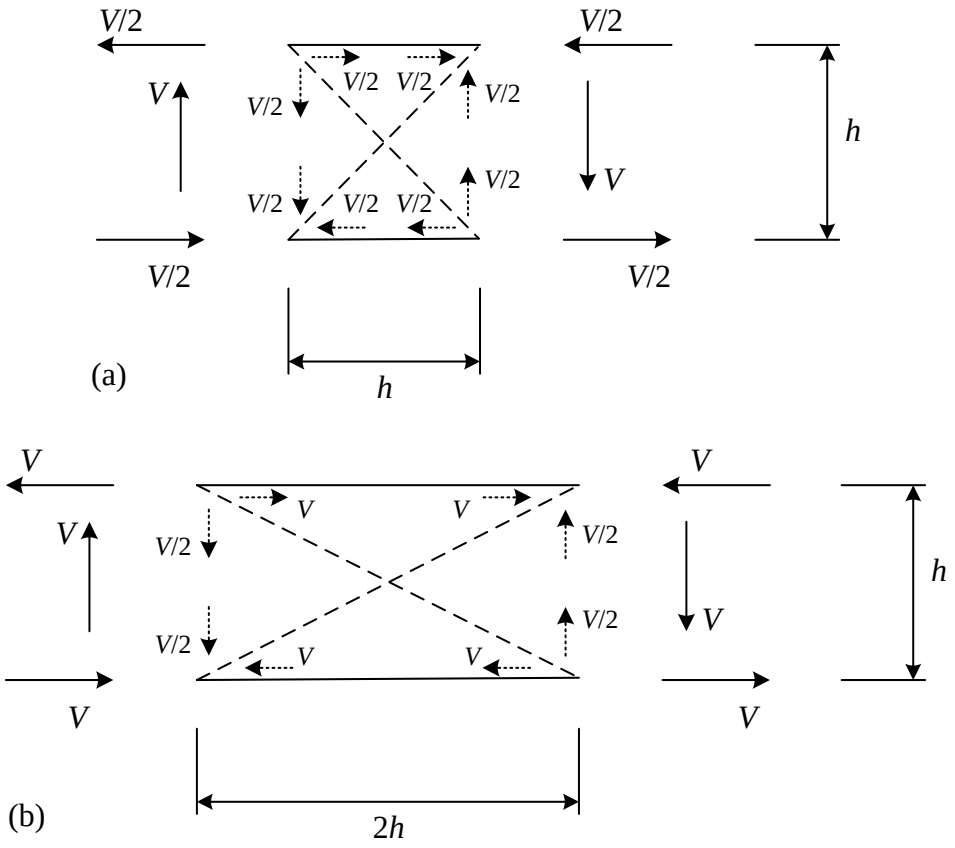

Figure 81. Statical behavior of X-type CFs associated with the DLF effects in horizontally-curved bridges.

Figure 84 shows the frequency distribution for all the CF chords and Figure 85 shows this distribution for all the CF diagonals in all the curved-radially supported bridges studied in this research. Table 26 shows a summary of the statistics for the percent change in the CF forces, normalized by the member yield load, due to SDLF or TDLF detailing in all the curved radially-supported bridges.

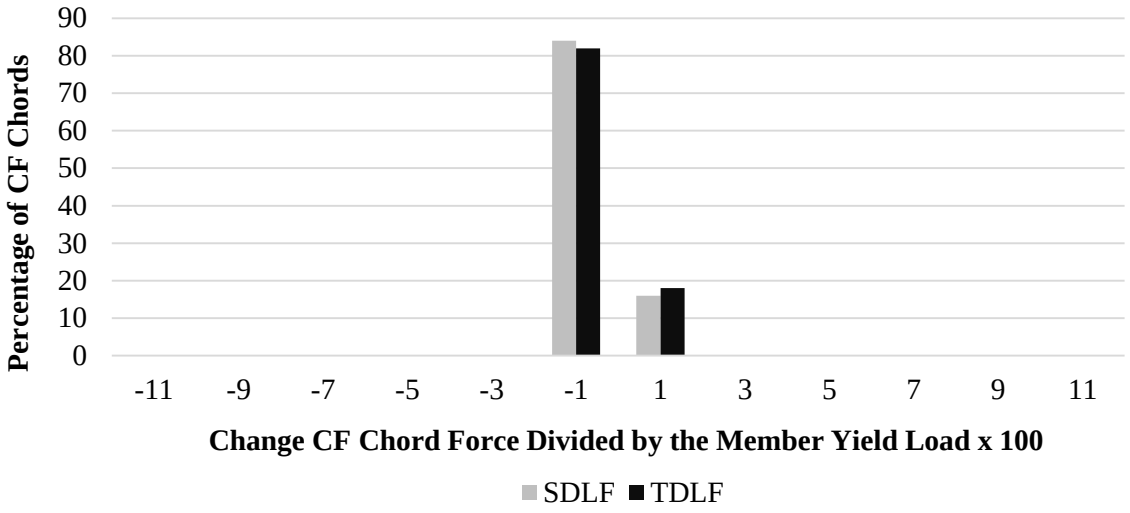

Figure 82. Frequency distribution for the change in the magnitude of the CF chord forces, normalized by the member yield load, due to SDLF or TDLF detailing in Bridge (C) NISCR7.

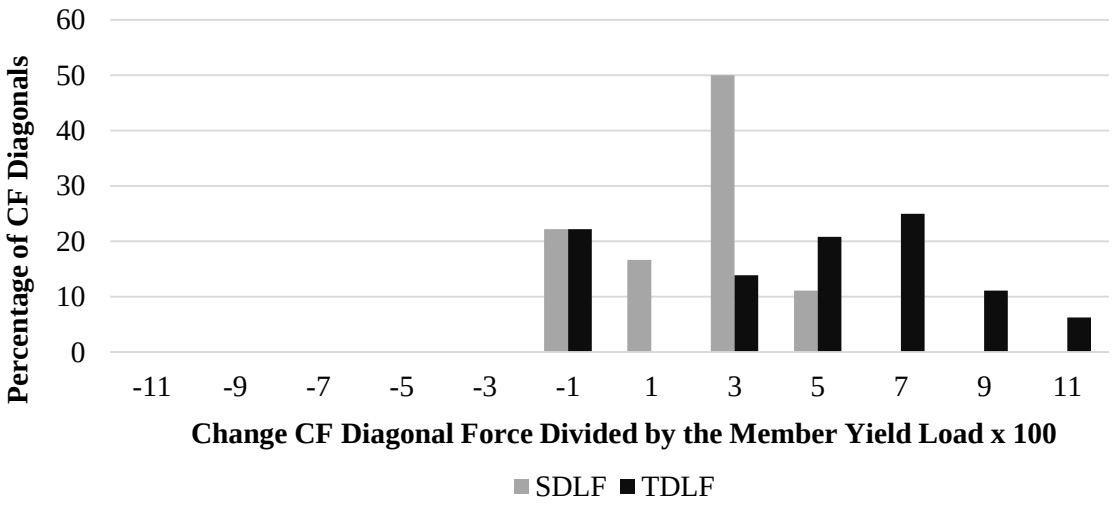

Figure 83. Frequency distribution for the change in the magnitude of the CF diagonal forces, normalized by the member yield load, due to SDLF or TDLF detailing in Bridge (C) NISCR7.

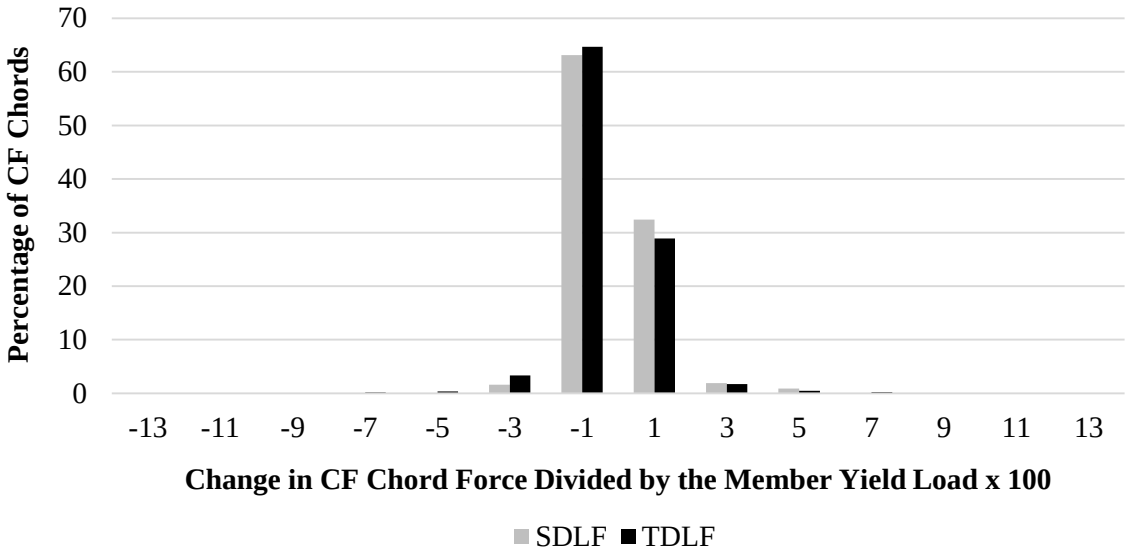

Figure 84. Frequency distribution for the change in the magnitude of the CF chord forces, relative to the member yield load, due to SDLF and TDLF detailing in all the curved-radially supported bridges studied in this research.

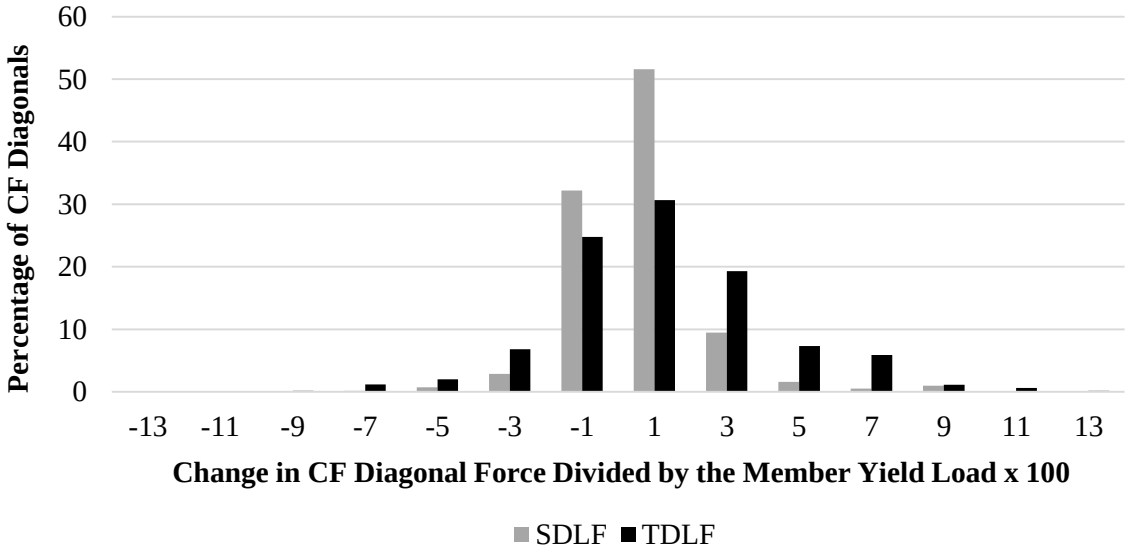

Figure 85. Frequency distribution for the change in the magnitude of the CF diagonal forces, relative to the member yield load, due to SDLF or TDLF detailing in all the curved-radially supported bridges.

- SDLF and TDLF detailing have a wide range of effects on the individual CF member forces. However, the force effects from SDLF and TDLF detailing are relatively small compared to the member yield loads in the all the curved radially-supported bridges studied.
- SDLF and TDLF detailing tend to increase the CF member forces in general, especially the diagonal forces.
- The largest percentage increase in any individual CF member force, normalized by the member yield load, is 9.5 and 12.9 % for SDLF and TDLF detailing, respectively (these results are 5.1 and 12.3 % excluding Bridge (E) EICCR11).

Table 26. Summary statistics for the percent change in the magnitude of the CF forces divided by the member yield load (change in member force divided by the member yield load x 100), due to SDLF or TDLF detailing, summed over all the curved-radially supported bridges.

	Chords		Diagonals	
	SDLF	TDLF	SDLF	TDLF
Average	-0.09	-0.22	0.54	1.16
Median	-0.06	-0.17	0.35	0.95
Max	5.15	10.2	9.52	12.9
Min	-4.10	-11.1	-7.02	-12.9
COV	-1.97	-2.97	4.22	9.14

The following should be noted regarding the tables and figures presented above as well as in subsequent sections presenting CF forces for other groups of completed bridges:

- The results are presented as the magnitude (absolute value) of the CF forces.
- The average CF member forces and the maximum CF member force in each bridge are useful to understand the broad trends in the behavior; however, these results do

not capture the detailed variations in the CF forces throughout the bridge system due to DLF detailing.

- In many of the cases for the bridges considered in this research, the location of the maximum CF force can change substantially as a function of the DLF detailing.
- The frequency distribution plots provide specific insight into the number of individual CF chords and diagonals that are significantly affected by the DLF detailing.
- The changes in the CF chord and diagonal member forces are normalized by the member yield load for the frequency distribution plots since:
    - If the changes are normalized relative to the NLF force, the percentage changes can be very large in situations where the NLF CF member force is small.
    - If the changes are not normalized at all and are presented as absolute forces in kips, the results are skewed by the size of the bridge.
    - By normalizing by the member yield load, the results are skewed by any conservatism in the design of the CF members; however, the bridge designs utilized in this research are based on representative current design practices.

Based on the above, results, it would appear that a potential coarse approximation of the SDLF and TDLF effects on the CF members in curved radially-supported bridges is to scale the CF SDL forces by a factor of 2.0 to account for SDLF effects and to scale the CF TDL forces also by a factor of 2.0 to account for TDLF effects, with the exception that the chord forces do not need to be scaled for X-type CFs. For Bridge (B) NISCR2, Figures 3-

72 through 3-77 of the NCHRP 725 report show that relative to the NLF SDLF, SDLF increases the diagonal forces by 2x, and relative to the NLF TDL forces, TDLF increase the diagonal forces by 2x. These figures of the NCHRP 725 report show that DLF detailing has little influence on the chord forces in this bridge. Therefore, the above findings are consistent with the targeted studies on Bridge (B) NISCR2 presented in the NCHRP 725 report.

In addition to the above results, it is useful to gain a more detailed perspective of how the specific CF forces are impacted by the SDLF and TDLF detailing effects. The above figures are intended to provide this perspective by plotting all the CF forces in Bridge (C) NISCR7. It should be noted that the CFs are all X-type in this bridge. Figures 86 and 87 show the gold standard DLF RA calculation of the CF forces in this bridge under the SDL and TDL. These calculations include the locked-in forces from SDLF and TDLF, respectively. The vertical axis of these plots is the axial force magnitude in kips. The horizontal axis corresponds to the CF number or identifier. The CF identifiers are not shown on the horizontal axis since generally, the number of CFs is too large to do so. The CFs are numbered starting with the bearing line CF in the bay between Girders G1 and G2 at bottom left corner of the bridge plan and progressing along the length of the bridge to the CF on the opposite bearing line. The numbering then continues from left to right in the second bay between girders G2 and G3, then the third bay, on so on.

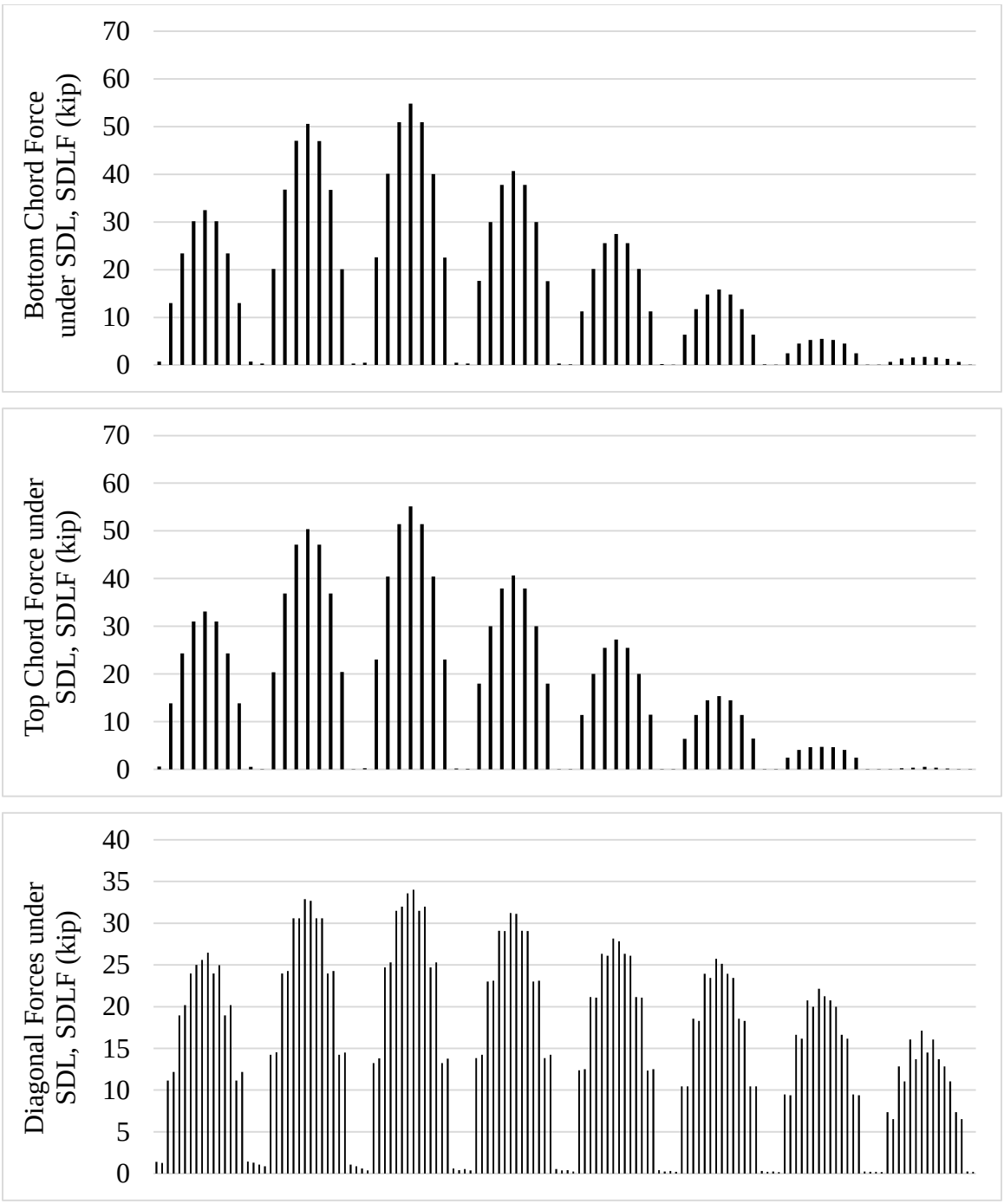

Figure 86. Magnitude of CF member forces from DLF RA, Bridge (C) NISCR7 under SDL, SDLF detailing.

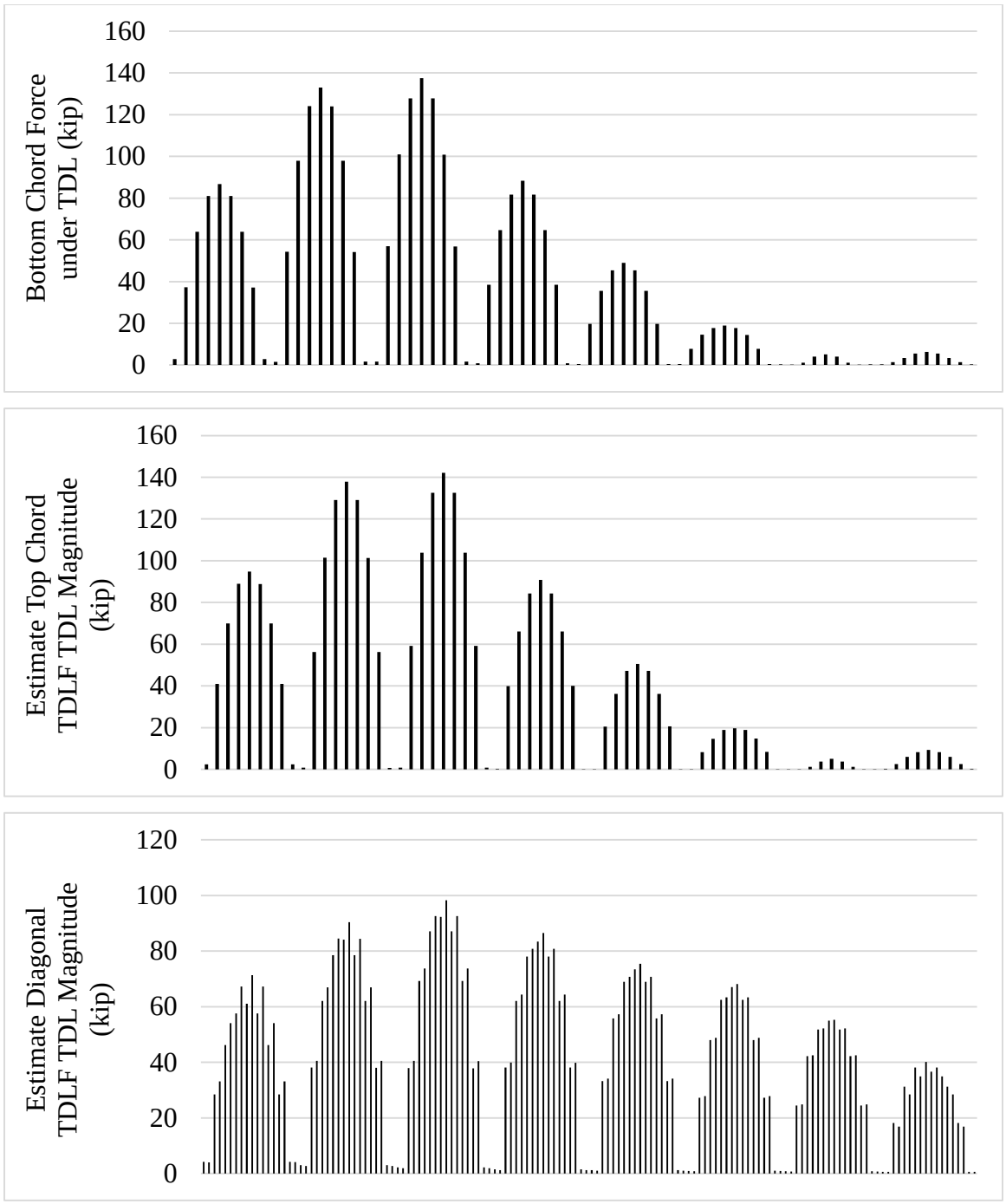

Figure 87. Magnitude of CF member forces from DLF RA, Bridge (C) NISCR7 under TDL, TDLF detailing.

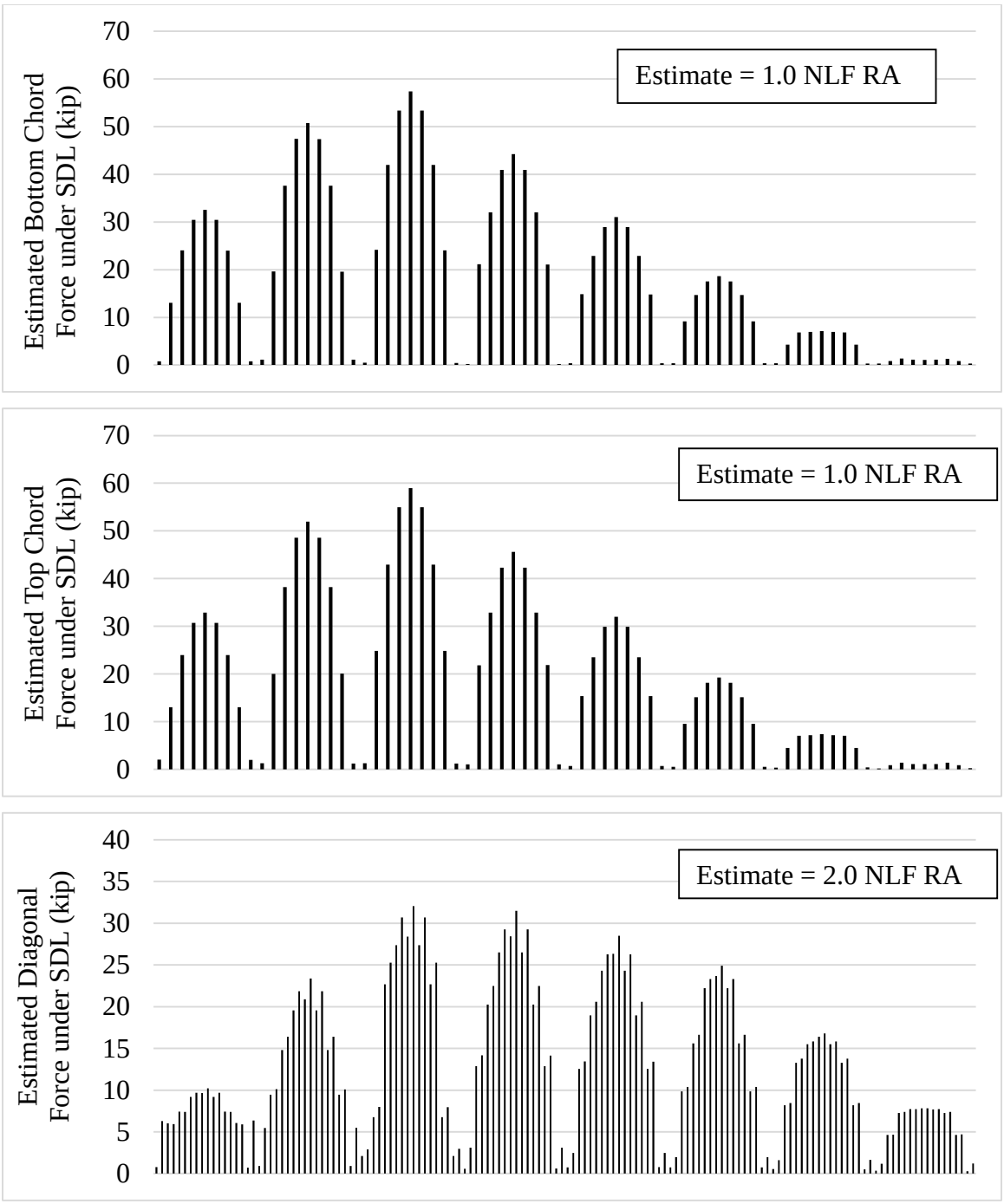

Figure 88. Estimated magnitude of CF member forces based on scaling of NLF RA results, assuming SDLF detailing, Bridge (C) NISCR7 under SDL.

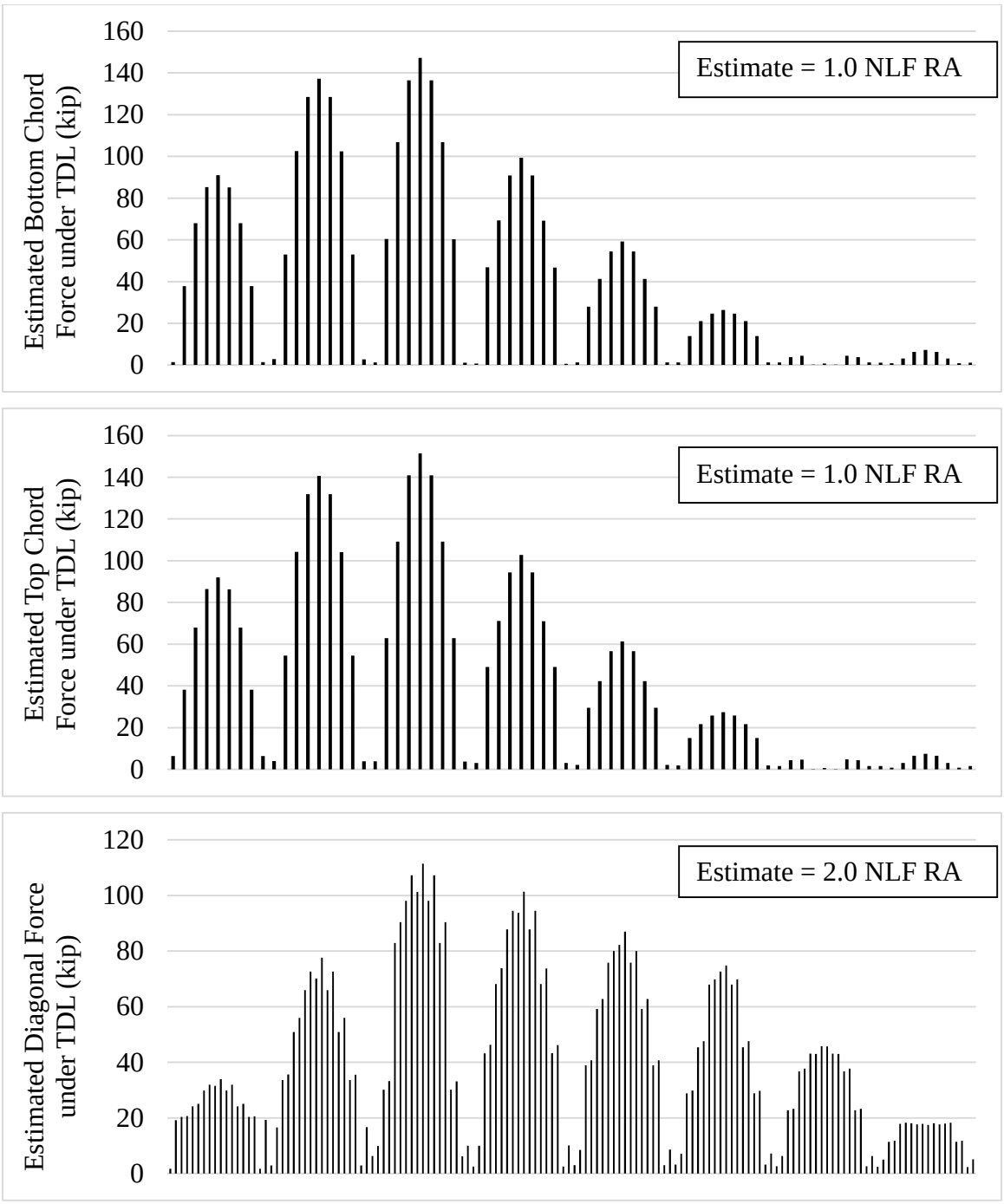

Figure 89. Estimated magnitude of CF member forces based on scaling of NLF RA results, assuming TDLF detailing, Bridge (C) NISCR7 under TDL.

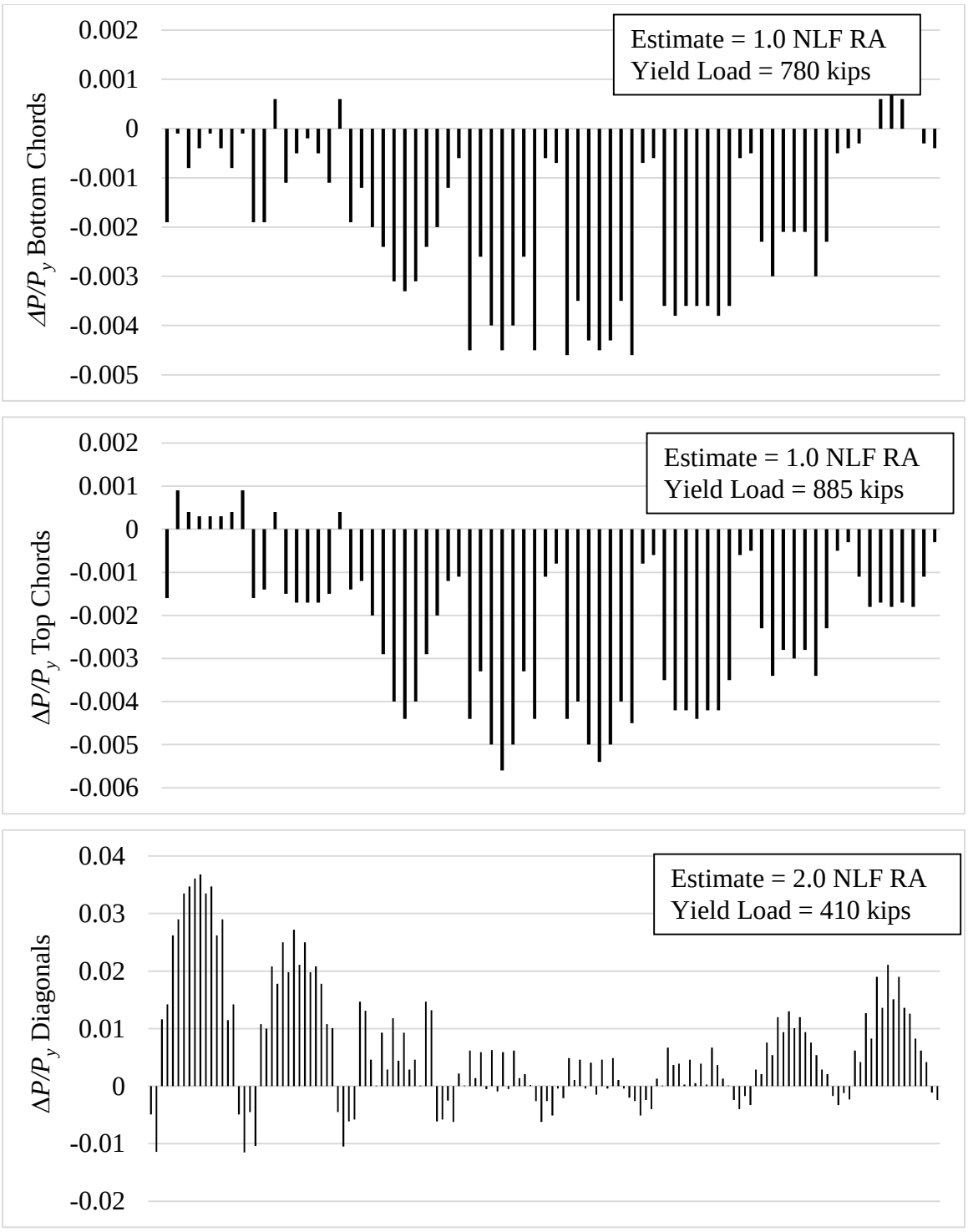

Figure 90. Difference between the magnitude of the DLF RA forces and the values estimated by scaling the NLF RA results, divided by the member yield load ($\Delta P/P_y$), Bridge (C) NISCR7 under SDL, SDLF detailing.

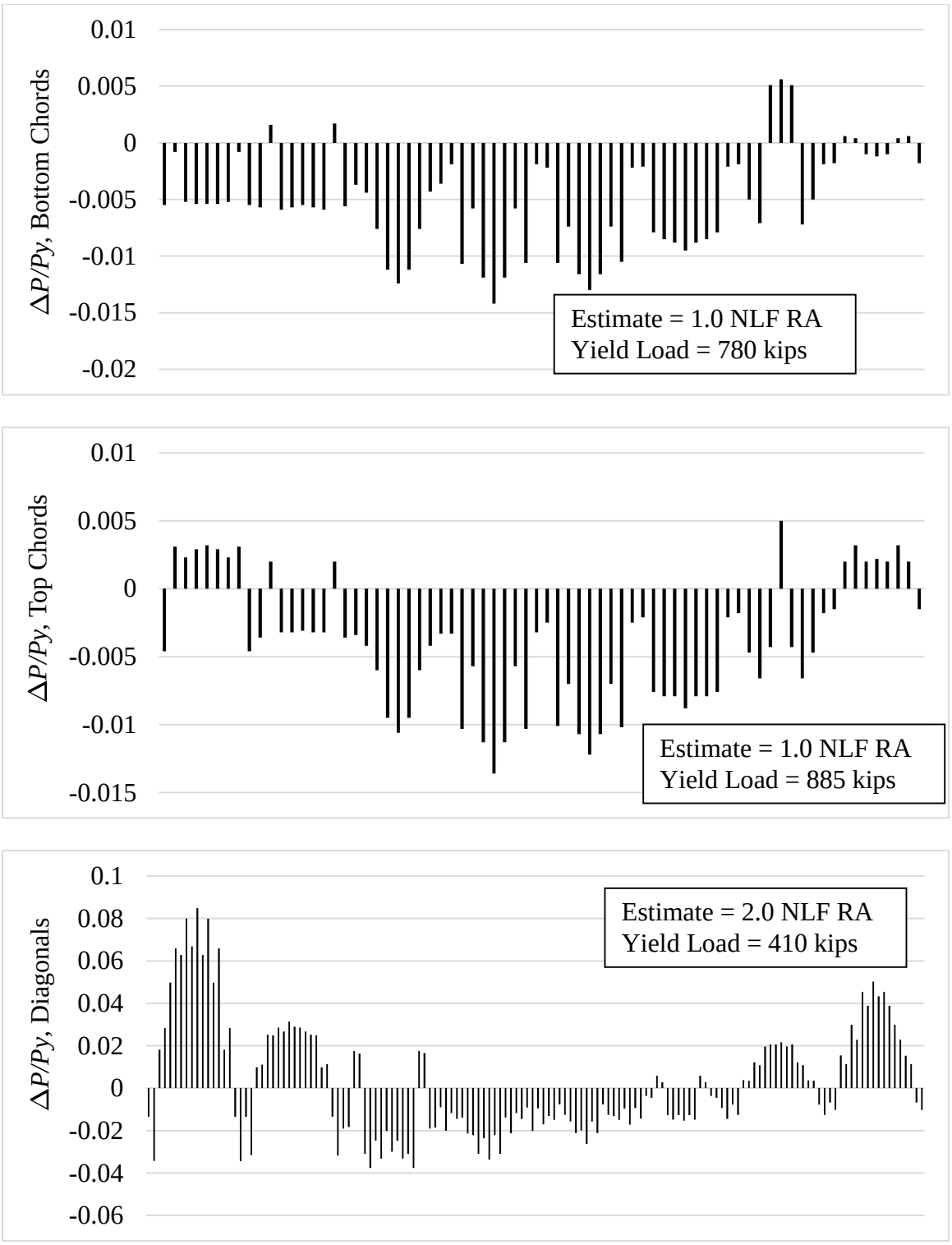

Figure 91. Difference between the magnitude of the DLF RA forces and the values estimated by scaling the NLF RA results, divided by the member yield load ($\Delta P/P_y$), Bridge (C) NISCR7 under TDL, TDLF detailing.

Given this ordering of the CFs, one can observe that the vertical bars in Figure 86 are arranged in eight groups. Each group corresponds to a different bay between the girders. The first group corresponds to the CFs in the bay between Girders G1 and G2 on the outside of the curve, the second group corresponds to the second bay between Girders G2 and G3, etc. The TDL/TDLF results have a very similar pattern to the SDL/SDLF results; however, the TDL/TDLF forces are generally larger.

One can observe that the largest CF forces in this relatively wide curved radially-supported bridge are at the middle of the span and in bay 3 between Girders G3 and G4. The maximum chord forces are 55.1 kips for SDL/SDLF and 151.5 kips for TDL/TDLF. These values are also reported for Bridge (C) NISCR7. The maximum diagonal forces are 34.0 and 98.2 kips for SDL/SDLF and TDL/TDLF in these figures, which are reported in Table 13 for Bridge (C). The fact that the cross-frame forces are not maximum in the bay on the outside of the curve is consistent with estimates that can be generated using the V-load Method. However, the detailed variation of the CF forces across the width of the bridge depends on the elasticity of the bridge system.

Figures 88 and 89 show the approximation of the SDL/SDLF and TDL/TDLF CF forces suggested at the conclusion of the above discussion of Table 26. By comparing the top two plots of these figures to the corresponding plots in Figures 86 and 87, one can observe that taking the unscaled results from a NLF RA, which does not include the lack-of-fit associated with the DLF detailing, gives a reasonable approximation of the chord forces from the DLF RA. Furthermore, by comparing the bottom plots in Figures 88 and 89 to the corresponding plots in Figures 86 and 87, on can observe that the maximum diagonal forces are predicted reasonably well by scaling the NLF RA forces by a factor of

2.0. The maximum diagonal force estimate for SDL/SDLF is 32.0 kips versus a force of 34.0 kips from the DLF RA and the maximum diagonal force estimate for TDL/TDLF is 111.4 kips versus 98.2 kips from the DLF RA. However, the actual maximum forces particularly in bay 1 and in bay 8 are somewhat underestimated. For instance, in bay 1, the maximum force estimate for SDL/SDLF is 10 kips whereas the corresponding maximum force from the DLF RA is 26 kips. This under-estimate of the diagonal forces in bay 1 is not a problem if a single section is selected for all of the different CF diagonals, which is often the case in design. That is, a significant amount of repetition in CF member sizes would be expected throughout the bridge.

Figures 90 and 91 show the differences between the CF forces from DLF RA and the above coarse estimates obtained by scaling the diagonal forces from NLF RA by the factor 2.0, ΔP, divided by the yield load for all the members, P_y. The yield load for each of the chords and for the diagonals is reported in these figures. One can observe that the largest under-prediction of the DLF RA results for the chords is approximately $0.001P_y$ for SDL/SDLF and $0.005P_y$ for TDL/TDLF, whereas the largest over-prediction is approximately $-0.0055P_y$ for SDL/SDLF and $-0.014P_y$ for TDL/TDLF. For the diagonals, the results are less conservative, with the largest under-prediction of the DLF/RA results being $0.036P_y$ for SDL/SDLF and $0.081P_y$ for TDL/TDLF and the largest over-prediction being $-0.011P_y$ for SDL/SDLF and $-0.039P_y$ for TDL/TLDF.

Figures 92 and 93 show the $\Delta P/P_y$ results for the above NLF RA estimate of the DLF RA results for SDL/SDLF and TDL/TLDF in Bridge (B) NISCR2, and Figures 94 and 95 show the corresponding results for Bridge (G) EICCR4. The largest under-predictions for these bridges is $0.015P_y$ for the diagonals and SDL/SDLF and $0.019P_y$ for the diagonals

and TDL/TDLF for Bridge (B), and $0.012P_y$ for the diagonals for SDL/SDLF and $0.014P_y$ for the diagonals and TDL/TDLF for Bridge (G).

In summary, it is found that the suggested estimate of 2x the CF forces from NLF RA, with the exception that the chord forces in X-type CFs do not need to be scaled, limits the under-prediction to less than $0.05P_y$ for SDL/SDLF and less than $0.10P_y$ in all the bridges studied for TDL/TDLF.

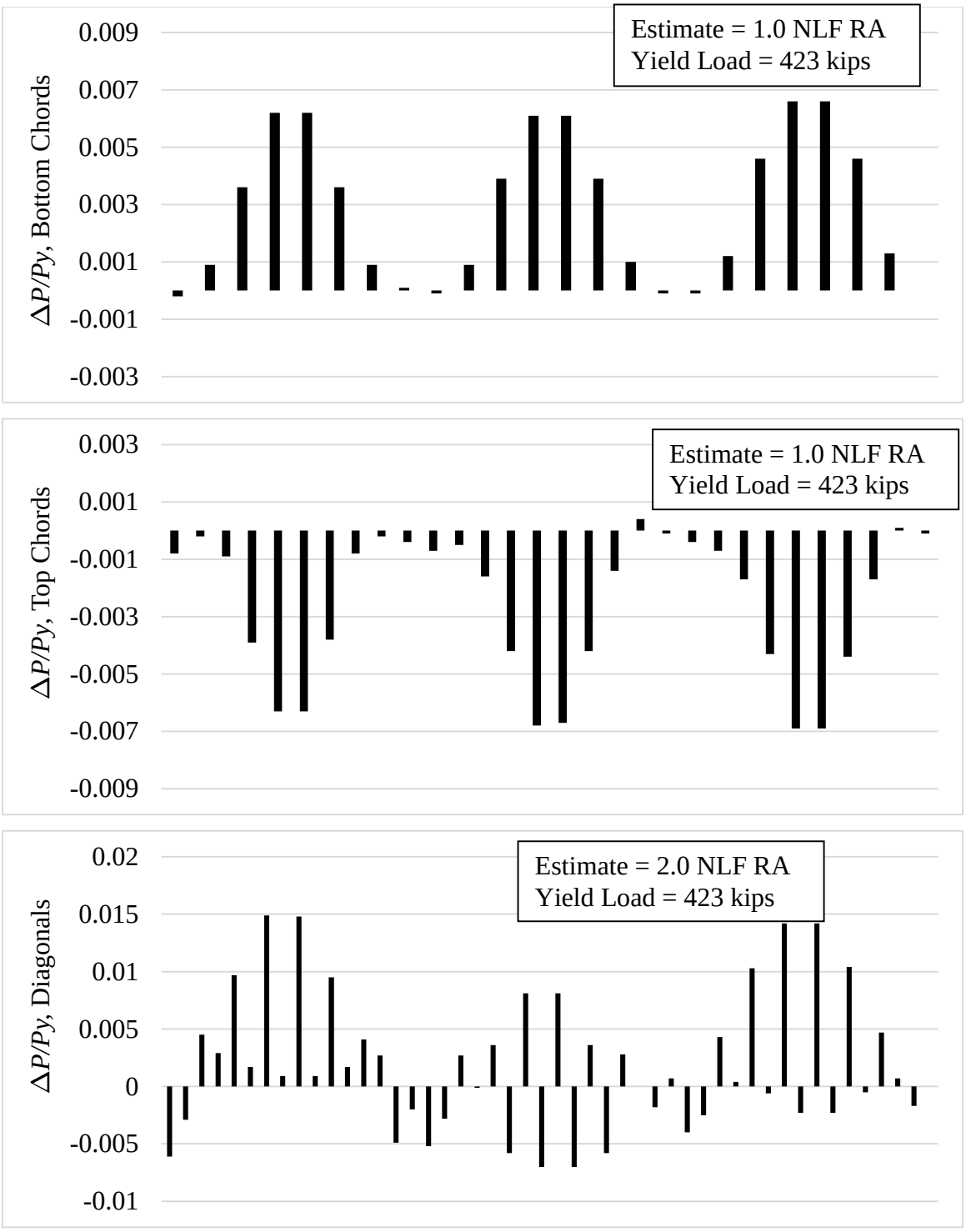

Figure 92. Difference between the magnitude of the DLF RA forces and the values estimated by scaling the NLF RA results, divided by the member yield load ($\Delta P/P_y$), Bridge (B) NISCR2 under SDL, SDLF detailing.

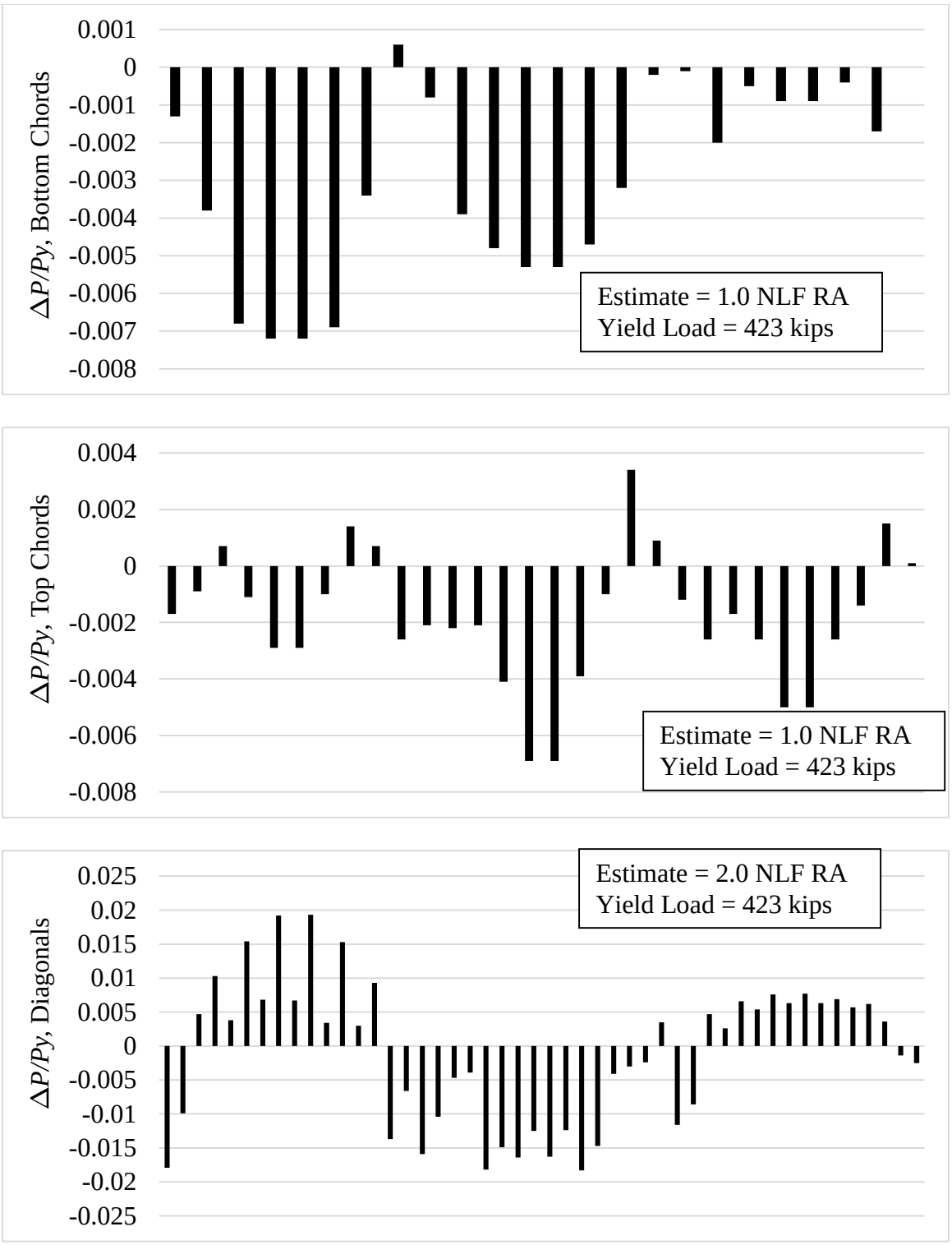

Figure 93. Difference between the magnitude of the DLF RA forces and the values estimated by scaling the NLF RA results, divided by the member yield load ($\Delta P/P_y$), Bridge (B) NISCR2 under TDL, TDLF detailing.

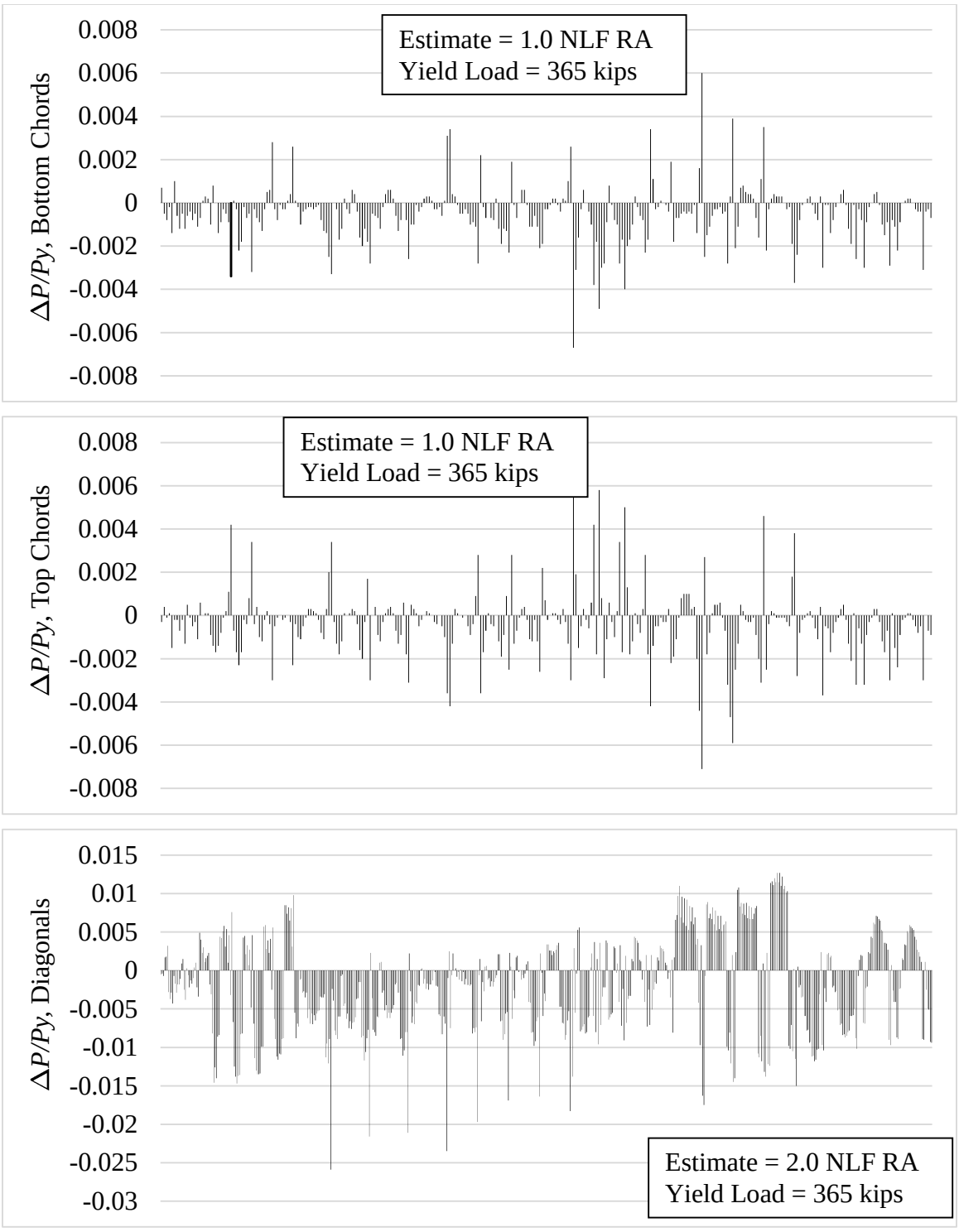

Figure 94. Difference between the magnitude of the DLF RA forces and the values estimated by scaling the NLF RA results, divided by the member yield load ($\Delta P/P_y$), Bridge (G) EICCR4 under SDL, SDLF detailing.

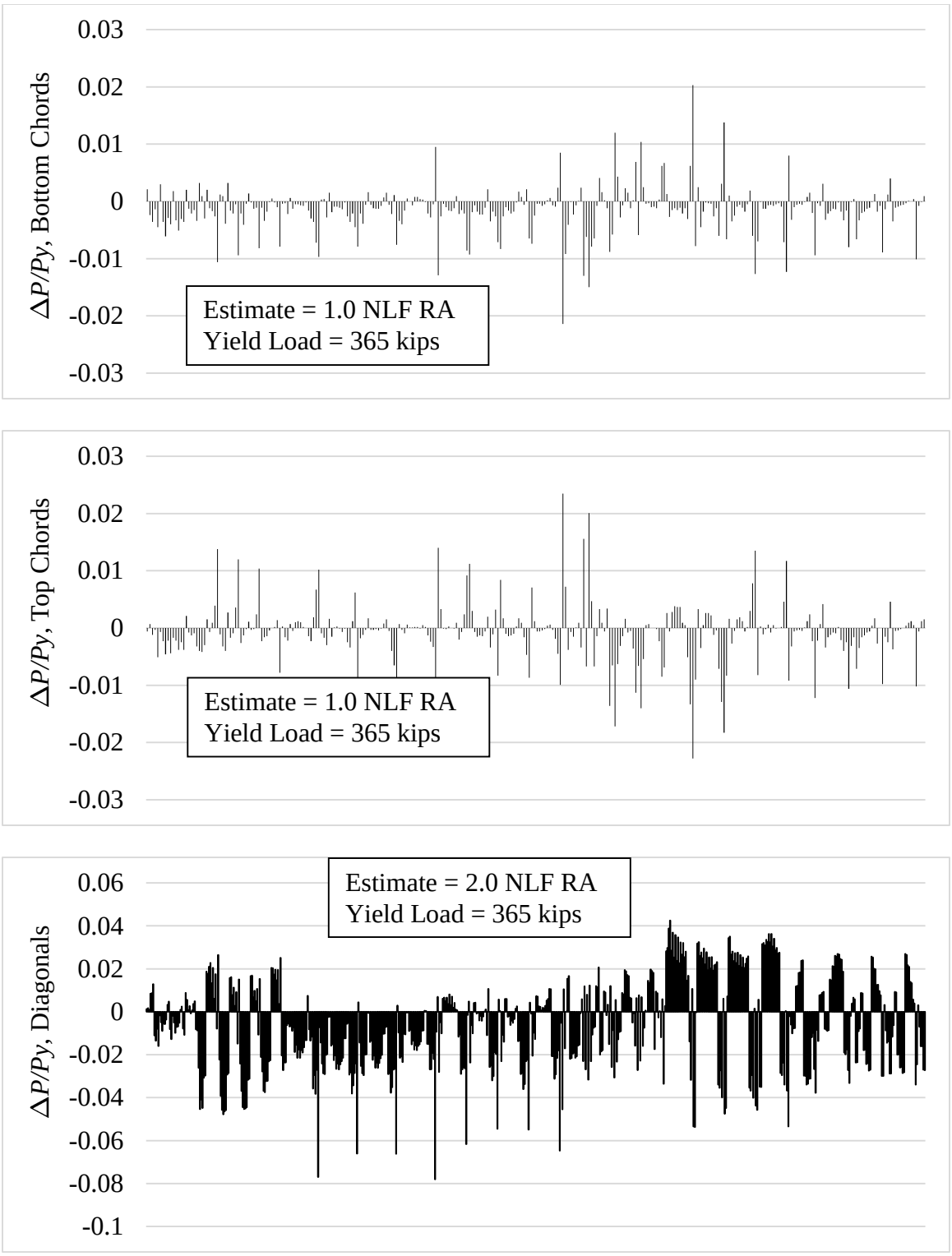

Figure 95. Difference between the magnitude of the DLF RA forces and the values estimated by scaling the NLF RA results, divided by the member yield load ($\Delta P/P_y$), Bridge (G) EICCR4 under TDL, TDLF detailing.

6.5.1.5 Girder Stresses

The SDLF and TDLF detailing effects tend to increase the maximum girder major-axis bending and flange lateral bending stresses in curved radially-supported bridges. However, the increase in the major-axis bending stress tends to be insignificant, and the increase in the flange lateral bending stress is relatively small. Figures 96 and 97 show a typical result, taken from Bridge (C) NISCR7, and Table 27 gives a summary of the results for the curved radially-supported bridge cases studied in this research. From Table 27, the largest increase in the maximum girder major-axis bending stresses 31 % under the SDL for SDLF detailing and 10 % under the TDL for TDLF detailing. The governing case for SDL/SDLF is the fascia girder on the inside of the curve in Bridge (C) NISCR7 and the governing case for TDL/TDLF is the fascia girder on the inside of the curve in Bridge (B) NISCR2. It can be observed that the increase for TDL/TDLF on Bridge (C), for the girder on the inside of the curve, is only 1.08. The corresponding increase under the TDL for SDLF (not shown in the table) is 1.05. The largest increase in f_b in the girder on the outside of the curve is only 1.02 under the TDL for SDLF. The above 31 % increase for SDL/SDLF is largely due to the fact that the value of the maximum f_b for the girder on the inside of the curve is very small, only 1.3 ksi, for Bridge (C) NISCR7. Therefore, it can be argued that, based on the minor increase in the major-axis bending stresses under the TDL for SDLF, the influence of SDLF on the major-axis bending stresses may be neglected.

The maximum increases in the TDL maximum flange lateral bending stresses relative to NLF detailing are 25 % under the SDL for SDLF detailing and 22 % under the TDL for TDLF detailing. Furthermore, the increase in the flange lateral bending stress is close to 20 % both for SDL/SDLF and TDL/TDLF for a large number of the bridges and on the fascia

girders both on the inside and the outside of the curve. These flange lateral bending stresses tend to come from the significant overall bridge cross-section twist rotations in these types of bridges. The behavior is analogous to support settlement on a continuous-span beam subjected to transverse load. If one considers the girder flanges as effective continuous-span beams in their lateral bending direction, spanning across the CF locations, these effective beams in essence experience some "support settlement" at the CF locations due to the overall twisting of the structure in relatively narrow, tightly curved bridges.

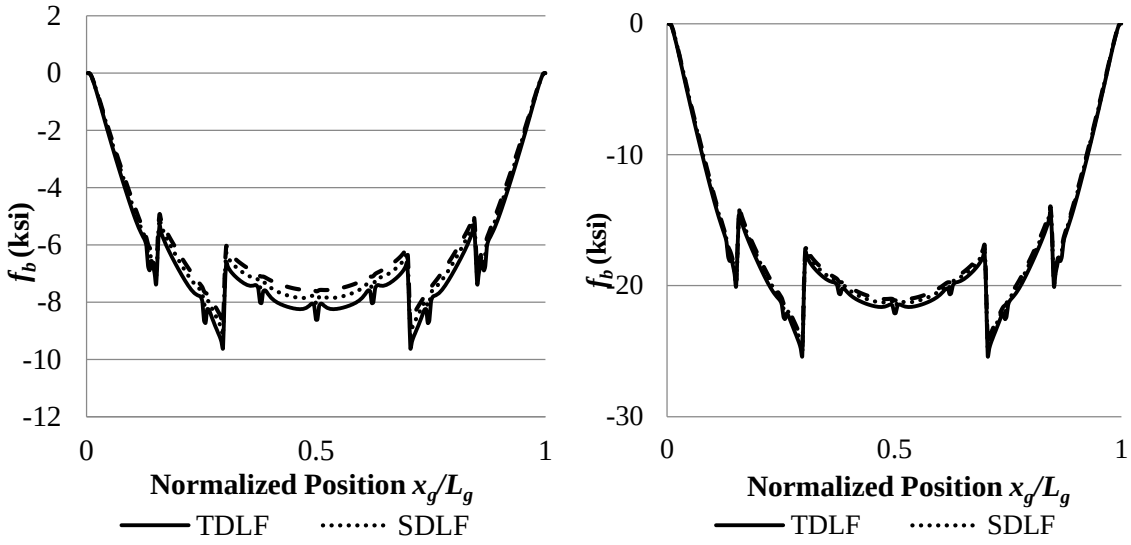

Figure 96. SDL (left) and TDL (right) top flange major-axis bending stresses in the girder on the outside for Bridge (C) NISCR7.

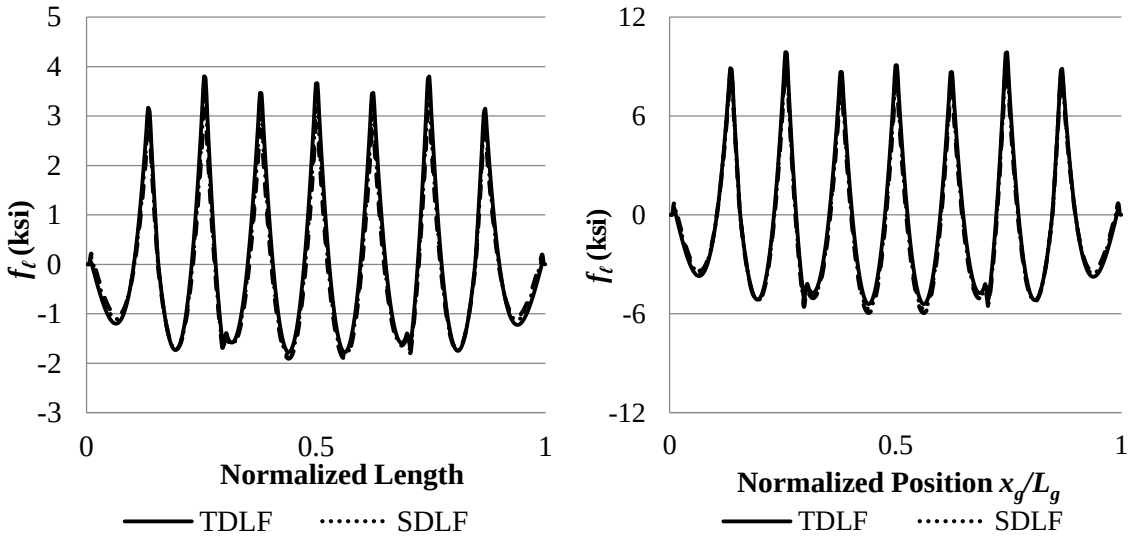

Figure 97. SDL (left and) TDL (right) top flange lateral bending stresses in the girder on the outside for Bridge (C) NISCR7.

Table 27. Maximum magnitudes of major-axis bending stresses and top flange lateral bending stresses on the girder on the outside and inside of the curve in the curved radially-supported bridges studied in this research. (f_{b1}, f_{b2} and f_{b3} are the maximum major-axis bending stresses, and $f_{\ell 1}$, $f_{\ell 2}$ and $f_{\ell 3}$ are the maximum girder flange lateral bending stresses for NLF, SDLF, and TDLF detailing, respectively; the largest f_{b2}/f_{b1}, $f_{\ell 2}/f_{\ell 1}$ under SDL for SDLF and f_{b3}/f_{b1} and $f_{\ell 3}/f_{\ell 1}$ under TDL for TDLF are highlighted by dark shading).

Girder	Bridge	SDL						TDL					
		NLF		SDLF				NLF		TDLF			
		f_{b1} (ksi)	$f_{\ell 1}$ (ksi)	f_{b2} (ksi)	$\frac{f_{b2}}{f_{b1}}$	$f_{\ell 2}$ (ksi)	$\frac{f_{\ell 2}}{f_{\ell 1}}$	f_{b1} (ksi)	$f_{\ell 1}$ (ksi)	f_{b3} (ksi)	$\frac{f_{b3}}{f_{b1}}$	$f_{\ell 3}$ (ksi)	$\frac{f_{\ell 3}}{f_{\ell 1}}$
Outside Girder	(A) EISCR1	4.4	2.7	4.5	1.02	3.1	1.15	21.2	12.8	21.2	1.00	15.4	1.20
	(B) NISCR2	8.3	2.2	8.3	1.00	2.7	1.23	23.4	7.7	23.2	0.99	7.9	1.03
	(C) NISCR7	8.8	3.1	9.1	1.03	3.4	1.10	24.6	8.9	25.4	1.03	9.9	1.11
	(D) NISCR10	11.2	2.0	11.2	1.00	2.0	1.00	26.1	4.9	26.1	1.00	4.9	1.00
	(E) EICCR11	13.6	2.7	15.1	1.11	2.5	0.93	28.8	6.2	29.3	1.02	5.3	0.85
	(F) NICCR12	12.0	1.9	12.5	1.04	1.6	0.84	23.1	4.8	23.8	1.03	3.3	0.69
	(G) EICCR4	6.7	1.2	6.8	1.01	1.3	1.08	21.6	5.0	21.9	1.01	5.1	1.02

Table 27(Continued). Maximum magnitudes of major-axis bending stresses and top flange lateral bending stresses on the girder on the outside and inside of the curve in the curved radially-supported bridges studied in this research. (f_{b1}, f_{b2} and f_{b3} are the maximum major-axis bending stresses, and $f_{\ell 1}$, $f_{\ell 2}$ and $f_{\ell 3}$ are the maximum girder flange lateral bending stresses for NLF, SDLF, and TDLF detailing, respectively; the largest f_{b2}/f_{b1}, $f_{\ell 2}/f_{\ell 1}$ under SDL for SDLF and f_{b3}/f_{b1} and $f_{\ell 3}/f_{\ell 1}$ under TDL for TDLF are highlighted by dark shading).

Girder	Bridge	SDL						TDL					
		NLF		SDLF				NLF		TDLF			
		f_{b1} (ksi)	$f_{\ell 1}$ (ksi)	f_{b2} (ksi)	$\frac{f_{b2}}{f_{b1}}$	$f_{\ell 2}$ (ksi)	$\frac{f_{\ell 2}}{f_{\ell 1}}$	f_{b1} (ksi)	$f_{\ell 1}$ (ksi)	f_{b3} (ksi)	$\frac{f_{b3}}{f_{b1}}$	$f_{\ell 3}$ (ksi)	$\frac{f_{\ell 3}}{f_{\ell 1}}$
Inside Girder	(A) EISCR1	0.3	0.4	0.3	1.00	0.5	**1.25**	5.3	4.7	5.6	1.06	5.7	1.21
	(B) NISCR2	0.5	0.6	0.5	1.00	0.2	0.33	2.9	3.0	3.2	**1.10**	0.7	0.23
	(C) NISCR7	1.3	0.6	1.7	**1.31**	0.7	1.17	8.7	3.4	9.4	1.08	4.1	1.21
	(D) NISCR10	4.9	1.2	4.9	1.00	1.4	1.17	17.1	4.3	17.2	1.01	4.9	1.14
	(E) EICCR11	9.2	1.9	10.0	1.09	1.0	0.53	26.3	5.3	27.7	1.05	1.9	0.36
	(F) NICCR12	7.4	1.1	7.0	0.95	0.8	0.73	16.1	3.4	15.2	0.94	1.5	0.44
	(G) EICCR4	4.9	0.8	4.8	0.98	0.9	1.13	16.9	1.8	16.6	0.98	2.2	**1.22**

6.5.1.6 Vertical Reactions

In simply-supported curved radially-supported bridges, the loads tend to shift from the inside to the outside of the curve in the bridge cross-section due to the curvature effects, resulting in higher vertical reactions in the outside girders and lower vertical reactions in the inside girders. This is not always the case in continuous-span curved radially-supported bridges, particularly for the interior pier reactions on the girders toward the inside of the curve.

For Bridge (C) NISCR7, the vertical reactions are approximately the same at each bearing for each of the girders due to the bridge symmetry about the CF line at the mid-span. With NLF detailing, the vertical reactions under TDL are 227 kips for Girder 1, the outside girder, and 60 kips for Girder 9, the inside girder. With the exception of one case at the completion of the steel erection and the removal of temporary in Bridge (E) EICCR11, uplift was not encountered for any of the curved radially-supported studied in this research. Although the bridges studied in this research have relatively extreme geometries, their proper design for combined dead and live load is such that uplift is not encountered under the dead load conditions. Avoiding uplift at the bearings tends to be more of a problem for sharply skewed bridges and in certain cases where sharp skew is combined with a tight horizontal curve. These types of cases are discussed subsequently.

SDLF and TDLF detailing effects twist the girders in the direction opposite to the direction the girders tend to roll under the DL. These effects tend to increase the reactions on both the inside and outside fascia girders of Bridge (C) NISCR7. This is due to the complex elastic interactions of the structural system with the lack-of-fit displacements in resolving the initial lack-of-fit (i.e., the resistance of the bridge to the enforcement of

compatibility between the CFs and the girders). For Bridge (C), the reactions on Girder 1, on the outside of the curve, are increased by 3 kips under the SDL for SDLF and 5 kips under the TDL for TDLF. The reactions for Girder 9, on the inside of the curve, are increased by 2 kips under the SDL for SDLF and by 4 kips under the TDL due to TDLF detailing. However, the reactions on Girder 4, an interior girder, are decreased by 3 kips under the SDL for SDLF and 7 kips under the TDL due to TDLF detailing. The total net change in vertical reactions at all bearings is zero when SDLF or TDLF detailing is employed, since DLF detailing does not and/or subtract any vertical load from the bridge.

From Table 29, it can be observed that the largest increase in any of the reactions is 17 % for SDL/SDLF and 9 % for TDL/TDLF detailing for the curved radially-supported studied in this research. However, the 17 % increase is actually only 2 kips, at one of the bearings on Bridge (C) NISCR7 where the DL reaction is relatively small. The next largest increase in any of the reactions under SDL due to SDLF is 6 %.

Checking the influence of SDLF or TDLF on the potential uplift at a bearing that has a relatively small DL reaction, due to a potential reduction in the bearing reaction, may be more of a concern than checking the increase in the reaction forces due to the DLF detailing effects. It is observed that a simple conservative estimate of the potential reduction in a bearing reaction, for the multi-girder curved radially-supported bridges considered in this research, is 10 % of the largest SDL reaction for SDLF and 10 % of the largest TDL reaction for TDLF.

Table 28. Bridge (C) NISCR7 vertical reactions (kips) (G1 and G9 are the outside girder and the inside girder of the curve, respectively).

Girder	Detailing Method	SDL Support 1	SDL Support 2	TDL Support 1	TDL Support 2
G1	NLF	79	79	227	227
	SDLF	82	82	229	229
	TDLF	85	85	232	232
G2	NLF	72	73	212	212
	SDLF	73	73	212	212
	TDLF	73	73	212	212
G3	NLF	65	65	198	198
	SDLF	65	65	197	197
	TDLF	65	65	197	197
G4	NLF	38	38	120	120
	SDLF	35	35	117	117
	TDLF	31	31	113	113
G5	NLF	32	32	109	109
	SDLF	31	31	107	107
	TDLF	29	29	106	106
G6	NLF	29	29	102	101
	SDLF	28	28	101	101
	TDLF	27	27	100	100
G7	NLF	23	23	85	85
	SDLF	22	22	85	85
	TDLF	22	22	85	85
G8	NLF	18	18	76	76
	SDLF	19	19	76	76
	TDLF	20	20	77	77
G9	NLF	11	11	60	60
	SDLF	13	13	62	62
	TDLF	15	15	64	64

Table 29. Summary of maximum percentage increase in the vertical reaction at each of the girder bearings due to SDLF and TDLF detailing in the curved radially-supported bridges (The largest percentage increases by SDLF and TDLF detailing are highlighted by dark shading).

Bridge	SDLF under SDL	TDLF under TDL
(A) EISCR1	5	4
(B) NISCR2	5	8
(C) NISCR7	**17 (2 kips)**	7
(D) NISCR10	6	5
(E) EICCR11	6	**9 (70 kips)**
(F) NICCR12	4	7
(G) EICCR4	1	2

6.5.2 Summary and Recommendations – Curved Radially-Supported Bridges with Cambers Set Based on NLF RA

The influence of SDLF and TDLF detailing on the responses in completed curved radially-supported bridge systems may be summarized as follows. Recommendations pertaining to these quantitative results are highlighted in bold italicized text.

Girder Elevations

- With the exception of the Ford City bridge (Bridge (E) EICCR11), which is significantly more extreme than the other bridges considered, the deviations from the targeted elevations are small (less than or equal to 2.1 inches for TLDF detailing) for all the curved radially-supported bridges studied in this research, based on the use of NLF RA.
- The above maximum deviation from the targeted girder elevations is due to the lack of consideration of the lack-of-fit from the DLF detailing in a NLF RA.

- ***It is recommended that NLF RA is sufficient for calculation of the cambers in curved radially-supported bridges. There is no need to consider any change in the girder vertical displacements and elevations due to the change in the internal forces, and the change in the vertical deflections in the structural system, associated with the DLF detailing.***

Girder Layovers

- With the exception of the Ford City Bridge (EICCR11), and not considering the FHWA test bridge (Bridge (A) EISCR1), which has a limited number of CFs and CF spacing at the maximum limits permitted by the AASHTO LRFD Specifications, the largest layovers are 0.3 inches (0.0024 rad) under SDL for SLDF detailing and 0.4 inches (0.0048 rad) under TDL for TDLF detailing in the bridges studied.
- The match with the calculated/expected non-zero layovers under TDL for SDLF, and under SDL for TDLF, is similar.
- ***It is recommended that the girder layovers may be assumed to be negligible in the targeted DL condition in curved radially-supported bridges. There is no need to consider any change in the girder layovers due to the change in the internal forces, and the change in the elastic deformations in the system, associated with the DLF detailing. The fascia girders should be checked separately for twist rotation between the CF locations due to eccentric overhang bracket loads.***
- ***For curved radially-supported bridges detailed for SDLF, the girder layovers under the TDL may be estimated as the CDL layovers obtained from a NLF RA.***

- ***For curved radially-supported bridges detailed for TDLF, the girder layovers under the SDL may be estimated as the negative of the CDL layovers obtained from a NLF RA.***

Cross-Frame Forces

- The effect of SDLF and TDLF detailing on the chord forces in X-type CFs is negligible in curved radially-supported bridges.
- The effect of SDLF detailing on other CF forces can be estimated accurately to conservatively by multiplying the CF forces obtained from a NLF RA by a factor of 2.0.
- The overall statistics for the percent change in the individual CF member forces relative the member yield load, due to SDLF and TDLF detailing, indicate a wide range (dispersion) of the individual CF member force effects. However, the force effects from SDLF and TDLF detailing are relatively small compared to the member yield loads in all the bridges studied. The mean, median, maximum and minimum change in the individual CF member forces are all somewhat larger in magnitude for TDLF detailing compared to SDLF detailing. For SDLF and TDLF detailing, the largest percentage increase in any individual CF member force, normalized by the member yield load, is 5.1 and 12.3 % respectively in the bridges studied, when Bridge (E) EICCR11 is excluded. These maximums occur for different bridge cases.
- ***In lieu of a DLF RA, it is recommended that the influence of SDLF detailing on the CF SDL forces in curved radially-supported bridges may be addressed by scaling the factored CF SDL forces from a NLF RA by the multiplier 2.0, with the exception that the chord member forces in X-type CFs need not be scaled.***

- ***In lieu of a DLF RA, it is recommended that the influence of TDLF detailing on the CF TDL forces in curved radially-supported bridges may be addressed by scaling the factored CF TDL forces from a NLF RA by the multiplier 2.0, with the exception that the chord member forces in X-type CFs need not be scaled. Since the TDL forces tend to be significantly larger, this recommendation amplifies the recommendation that, due to potential fit-up difficulty during the steel erection, TDLF detailing should not be employed for curved I-girder bridges.***
- With the use of the above scale factors, the maximum difference between the magnitudes of the individual DLF RA CF member forces versus the scaled NLF RA results, normalized by the member yield load, is reduced to 3.7 and 8.5 %, and the corresponding average difference is reduced to -0.5 and -1.2 % for SDLF under SDL and TDLF under TDL, respectively, for the curved radially-supported bridges studied in this research, excluding bridge (E) EICCR11.

Girder Stresses

- In curved radially-supported bridges, both the maximum girder major-axis bending (f_b) and flange lateral bending (f_ℓ) stresses generally are increased due to the DLF detailing effects.
- Under TDL, the largest percentage increase in the maximum f_b for the fascia girder on the outside of the curve is 2 % for SDLF detailing and 3 % for TDLF detailing for the bridges studied. The corresponding largest increases for the fascia girder on the inside of the curve are 5 % and 10 % for SDLF and TDLF detailing, respectively.
- The largest percentage increase in the maximum f_ℓ for the fascia girders on the outside of the curve is 23 % under SDL for SDLF detailing and 20 % for under TDL for TDLF

detailing. The corresponding values for the fascia girders on the inside of the curve are 25 % and 22 % for SDLF and TDLF detailing, respectively.

- ***It is recommended that the influence of SDLF detailing on the girder f_b stresses may be neglected in curved radially-supported bridges.***
- ***In lieu of a DLF RA, it is recommended that the influence of SDLF detailing on the girder f_ℓ stresses in curved radially-supported bridges may be addressed by scaling the* factored SDL *f_ℓ values obtained from a NLF RA by the multiplier 1.2.***
- ***In lieu of a DLF RA, it is recommended that the influence of TDLF detailing on the girder f_b and f_ℓ stresses in curved radially-supported bridges may be addressed by scaling the* factored TDL *f_b and f_ℓ values from a NLF RA by the multipliers 1.1 and 1.2, respectively.***

Vertical Reactions

- With the exception of one case at the completion of the steel erection and the removal of temporary supports in the Ford City Bridge (EICCR11), uplift was not encountered for any of the curved radially-supported bridges studied in this research.
- DLF detailing increases the reactions on some of the girders and decreases them on others. The net total change in the vertical reactions is zero.
- In single-span horizontally curved radially-supported bridges with simple supports, DLF detailing tends to increase the smaller reactions at the bearings toward the inside of the curve.
- The largest increase in the reactions is 6 % under SDL due to SDLF detailing and 9 % under TDL due to TDLF detailing for the curved radially-supported bridges studied.

- ***It is recommended that the influence of SDLF detailing on any potential increases in the girder vertical reactions may be neglected in curved radially-supported bridges.***
- ***In lieu of a DLF RA, it is recommended that the influence of TDLF detailing on the girder reactions may be addressed by scaling the reactions from a NLF RA by the multiplier 1.1.***
- ***For simply-supported horizontally-curved bridges on radial supports, DLF tends to have a relieving influence on potential uplift at bearings having the smaller reactions, and therefore the influence of DLF detailing on any uplift at the bearings may be neglected.***
- ***For continuous-span horizontally-curved bridges, a DLF RA should be considered in cases where there are any particular concerns about potential uplift at lightly-loaded bearings.***

The above recommendations are considered applicable for curved radially-supported bridges with L_s/R up to 0.5 and L_s up to 300 ft. These limits are different from those listed in the tables for recommended fit conditions discussed subsequently in Section 11.1. The limits here are aimed at ensuring sufficient accuracy of the structural analysis whereas the limits discussed in Section 11.1 address broader questions of ensuring reliable fit-up of the structural steel. For bridges that exceed these limits, it is recommended that DLF RA be considered. Chapter 3 explains the details of several procedures for conducting a DLF RA.

6.6 Straight Bridges with Parallel Skew and Cambers Set Based on LGA

Straight bridges with a difference in the skew angles at the ends of all the spans less than or equal to $\Delta\theta = 20^o$ may be considered as parallel skew bridges. The use of LGA for

setting the girder cambers in sharply skewed straight bridges is generally discouraged based on the considerations discussed in Section 6.2.3.

Section 6.6.1 provides quantitative results on the influence of SDLF and TDLF detailing on the responses in straight bridges with parallel skew and cambers set based on LGA. The influence of SDLF and TDLF is discussed on the responses in the following order: girder vertical displacements, girder elevations, girder layovers, CF forces, girder stresses, and vertical reactions. Section 6.6.2 then summarizes the influences on the key bridge responses, and provides recommendations for handling of these effects. The recommendations are highlighted in bold italicized text.

6.6.1 Quantitative Results

6.6.1.1 Girder Vertical Displacements

For straight skewed bridges with a parallel skew arrangement of the bearing lines, SDLF and TDLF detailing with cambers set based on LGA tend to reduce the vertical displacement of the fascia girders and increase the vertical displacement of the interior girders relative to the results from a NLF RA. The increase or decrease in the vertical displacements can be significant for bridges with long span and high skew index, such as Bridge (J1) NISSS54 (see Figure 98). (It should be noted that the analyses conducted here are 3D FEA for all the bridge cases. The only usage of LGA is for the determination of the girder cambers.) The maximum TDL displacement difference between the TDLF and NLF detailing is 3.7 inches on the innermost girder and 3.5 inches on the fascia girder. This occurs due to the fact that, when the CFs are detailed for TDLF, the effect of the TDLF detailing is to force the girders to deflect in the manner calculated by LGA under the TDL condition. However this effect is accomplished only under the targeted TDL condition. It

should be noted that, it is assumed that the concrete deck does not participate in resisting any of the DL in the studies conducted in this research. Similarly, when the CFs are detailed for SDLF, the effect of the SDLF detailing is to force the girders to deflect in the manner calculated by LGA under the SDL condition (but only under this condition).

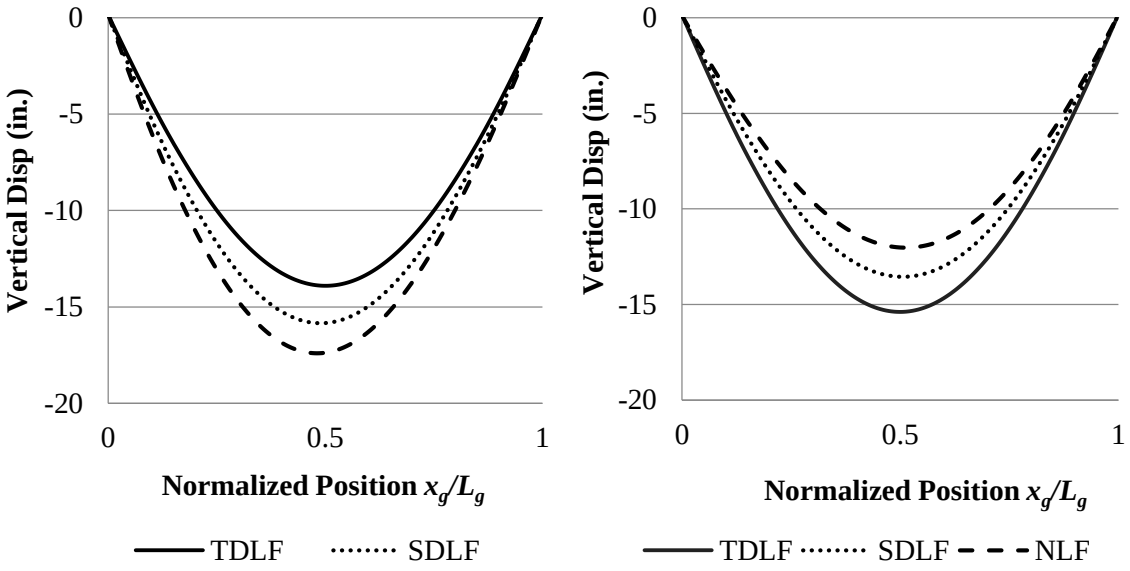

Figure 98. Bridge (J1) NISSS54 fascia girder (left) and innermost girder (right) vertical displacements under TDL from 3D FEA with the CFs detailed based on LGA cambers.

In bridges where the framing arrangement is improved to reduce the nuisance transverse stiffness effects, the girders in the bridge 3D system deflect in a fashion closer to that of the LGA model, and the changes in the vertical displacements due to the DLF detailing are smaller. For example, Bridge (J2) greatly reduces the nuisance transverse stiffness effects. For the maximum TDL vertical displacement, the largest decrease in the fascia girder displacement in this bridge is 2.6 inches and the largest increase in the innermost girder displacement is 0.8 inches due to TDLF detailing based on LGA cambers (again taking the downward direction as positive, which is the opposite of the sign convention used in the tables).

Table 30. Maximum vertical displacements under TDL of fascia girders and changes in maximum vertical displacements relative to NLF detailing for the straight skewed bridges studied in this research based on the use of LGA cambers (The largest changes by SDLF and TDLF under TDL are highlighted by dark shading).

Bridge	NLF	SDLF		TDLF	
	Disp. (in.)	Disp. (in.)	Change (in.)	Disp. (in.)	Change (in.)
(I1) NISSS14	-8.4	-8.2	0.2	-7.1	1.3
(I2) NISSS14	-8.4	-8.1	0.3	-7.2	1.2
(J1) NISSS54	-17.4	-15.8	**1.6**	-13.9	**3.5**
(J2) NISSS54	-16.5	-15.5	1.0	-13.9	2.6
(K1) EICSS12	-4.5	-4.4	0.1	-3.8	0.7
(K2) EICSS12	-4.5	-4.4	0.1	-3.9	0.6
(K3) EICSS12	-4.5	-4.4	0.1	-3.9	0.6
(L) NICSS16	-4.9	-4.8	0.1	-4.2	0.7
(M1) EICSS2	-12.2	-12.4	-0.2	-12.8	-0.6
(M2) EICSS2	-13.1	-12.9	0.2	-12.0	1.1

Table 31. Maximum vertical displacements under TDL of innermost girders and changes in maximum vertical displacements relative to NLF detailing for the straight skewed bridges studied in this research based on the use of LGA cambers (The largest changes by SDLF and TDLF under TDL are highlighted by dark shading).

Bridge	NLF	SDLF		TDLF	
	Disp. (in.)	Disp. (in.)	Change (in.)	Disp. (in.)	Change (in.)
(I1) NISSS14	-4.4	-5.2	-0.8	-7.9	-3.5
(I2) NISSS14	-6.9	-7.1	-0.2	-7.8	-0.9

(J1) NISSS54	-11.7	-13.4	**-1.7**	-15.4	**-3.7**
(J2) NISSS54	-14.1	-14.4	-0.3	-14.9	-0.8
(K1) EICSS12	-3.8	-3.9	-0.1	-4.0	-0.2
(K2) EICSS12	-3.8	-3.9	-0.1	-4.0	-0.2
(K3) EICSS12	-3.8	-3.8	-0	-4.0	-0.2
(L) NICSS16	-4.7	-4.7	-0	-4.6	-0.1
(M1) EICSS2	-9.4	-9.7	-0.3	-10.3	-0.9
(M2) EICSS2	-10.3	-10.1	0.2	-9.5	0.8

6.6.1.2 Girder Elevations

When a straight skewed bridge is designed using LGA, it is common that the CFs are detailed based on LGA cambers. The TDL LGA girder cambers are taken as the negative of the TDL girder vertical deflections calculated from a LGA. With TDLF detailing, the corresponding TDL girder elevations are theoretically zero (neglecting superelevation, etc.). Similarly, the SDL LGA cambers are taken as the negative of the SDL girder displacements calculated from a LGA. As noted previously, in this work the term "SDL camber" is simply a phrase used to indicate the negative of the calculated SDL displacements used for setting the drops between the girders for SDLF detailing of the CFs. The bridge girders are always fabricated based on the TDL cambers.

The actual responses corresponding to the above are always slightly different from the above theoretical ideals due to various factors that are not accounted for in the CF detailing, as discussed in Section 6.2.2. However, the use of LGA cambers gives the closest capture of these ideals. In addition, it is essential to recognize that the above findings apply ONLY to the targeted DL conditions. For example, one cannot use solely a LGA to determine the TDL girder deflections for a bridge that has been detailed for SDLF without encountering

some deviation from the targeted final girder elevations. The correct calculation of the girder TDL deflections in this case, if the SDLF detailing is based on LGA cambers, is to sum the girder SDL deflections obtained from a LGA with the Concrete Dead Load (CDL) deflections obtained from a 3D FEA. (It should be noted that if the corresponding CF initial lack-of-fit effects are included in an accurate 2D Grid analysis or 3D FEA, the influence of the girder cambers and CF drops, whatever they are, are directly and integrally incorporated within the RA without any mixing and matching of analysis methods.)

Figure 99 shows the TDL results, with SDLF detailing, for the final girder elevations, on the fascia girder and on the middle girder on Bridge (J1) NISSS54. It is important to note that for SDLF detailing, the total girder cambers are set by summing the girder SDL deflections from LGA with the CDL deflections from 3D FEA. The CFs are detailed to fit to the ideal girder SDL elevations based on the application of the SDL deflections obtained from the LGA to the above initial fully-cambered girder profiles. In this case, the largest deviation from the targeted elevations under TDL is 0.4 inches for Bridge (J1). Figure 100 shows similar results to Figure 99 but for Bridge (I1) NISSS14. One can observe that that the corresponding largest deviation from the targeted elevations under TDL is 0.1 inches for Bridge (I1).

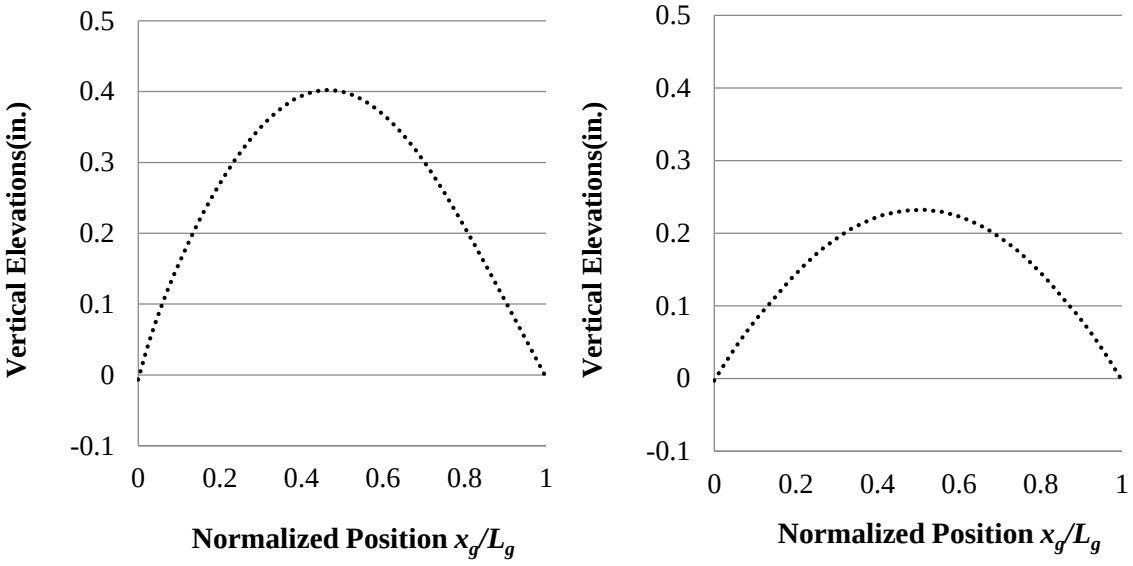

Figure 99. Bridge (J1) NISSS54 fascia girder (left) and middle girder (right) vertical elevations under TDL with SDLF based on LGA. The TDL girder cambers set based on the LGA SDL girder cambers plus the negative of the 3D FEA CDL girder displacements for SDLF detailing.

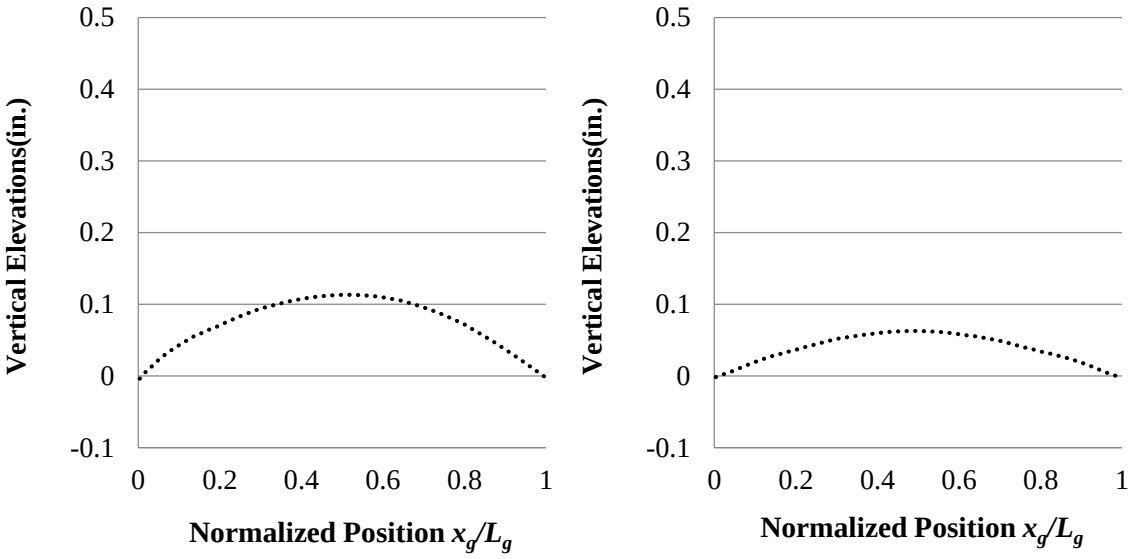

Figure 100. Bridge (I1) NISSS54 fascia girder (left) and middle girder (right) vertical elevations under TDL with SDLF based on LGA. The TDL girder cambers set based on the LGA SDL girder cambers plus the negative of the 3D FEA CDL girder displacements for SDLF detailing.

Figure 101 shows the vertical elevations for the fascia and middle girders of Bridge (J1) NISSS54, under TDL, if the CFs were detailed based on LGA and the girder TDL cambers are set *entirely* based on LGA. One can observe that the elevations match accurately with the targeted zero final elevations for TDLF in this situation. However, these good results apply *ONLY* to the use of TDLF and for the TDL condition.

If NLF detailing is used, and if the girder cambers are set based on the LGA results for the TDL, the girder final elevations are substantially in error from the targeted elevations. These errors are equal to the differences between the LGA girder deflections and the 3D FEA girder deflections. If SDLF detailing is used, and if the girder cambers are set based on the LGA results for the TDL, the elevation errors are smaller. However, these errors are still substantial, equal to the differences between the LGA girder deflections and the 3D FEA girder deflections under the CDL. Bridge cases (J1) and (J2) NISSS54 and (M1) EICSS2 show substantial final elevation errors for SDLF and NLF detailing if the cambers are based entirely on LGA and the CFs are detailed using the LGA cambers. These are cases with long span lengths and a high skew index. For the other straight skewed bridge cases studied in this research, the associated largest final elevation errors are 1.3 in for NLF detailing and 0.8 for SDLF detailing.

It is apparent from the above results that it is possible to "mix and match" the TDL cambers from LGA and RA results to obtain the desired targeted girder elevations while also achieving the close capture of the ideal responses (approximately zero CF forces, approximately zero girder flange lateral bending and approximately plumb girders under the targeted condition). However, this mixing and matching of analysis results can be awkward for the design engineer, and furthermore, it can be highly prone to errors.

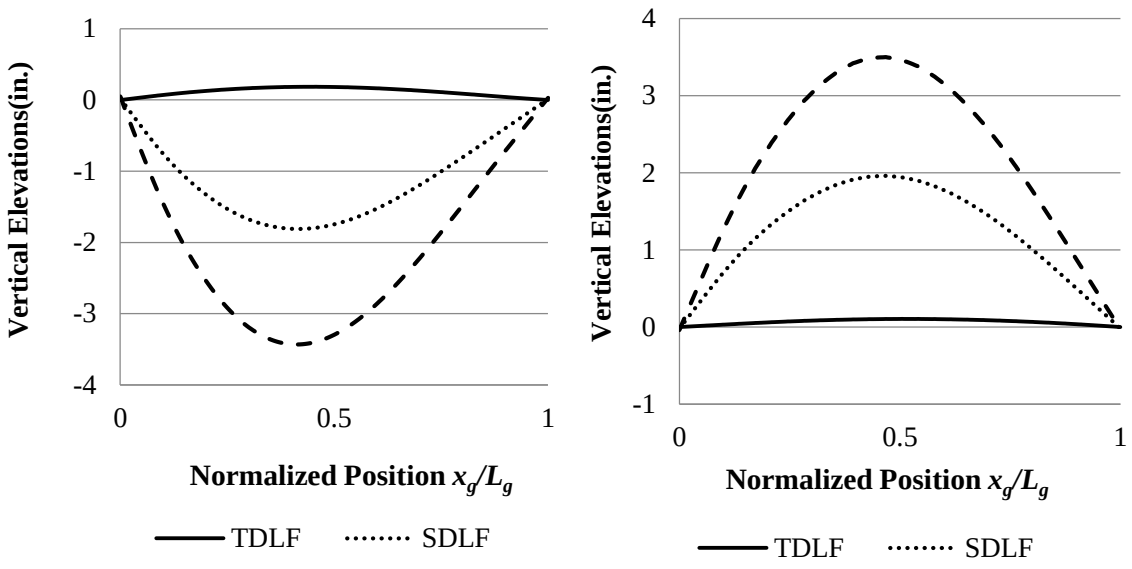

Figure 101. Bridge (J1) NISSS54 fascia girder (left) and middle girder (right) vertical elevations under TDL with the CFs detailed based on LGA and the TDL girder cambers set entirely based on LGA (not recommended), showing substantial elevation errors for SDLF and NLF detailing cases

Table 32. Maximum elevation deviations under TDL (The largest final girder elevations with NLF, SDLF and TDLF detailing under TDL are highlighted by dark shading).

Bridge	NLF	SDLF	TDLF
(I1) NISSS14	**3.5**	**2.7**	0.1
(I2) NISSS14	1.2	1.0	0.1
(J1) NISSS54	**3.5**	2.0	0.2
(J2) NISSS54	2.5	1.5	**0.3**
(K1) EICSS12	0.8	0.6	0.1
(K2) EICSS12	0.6	0.5	0.1
(K3) EICSS12	0.7	0.6	0.1
(L) NICSS16	1.0	0.8	0.1
(M1) EICSS2	3.0	2.0	0.1
(M2) EICSS2	0.9	0.6	0.3

6.6.1.3 Girder Layovers

For straight bridges with parallel skew, the CFs theoretically fit to the girders under TDL with zero force, when the CFs are detailed for TDLF using LGA. In this case, the girders are nearly ideally plumb under TDL with TDLF detailing based on LGA for Bridge (J1) NISSS54 (see Figure 102).

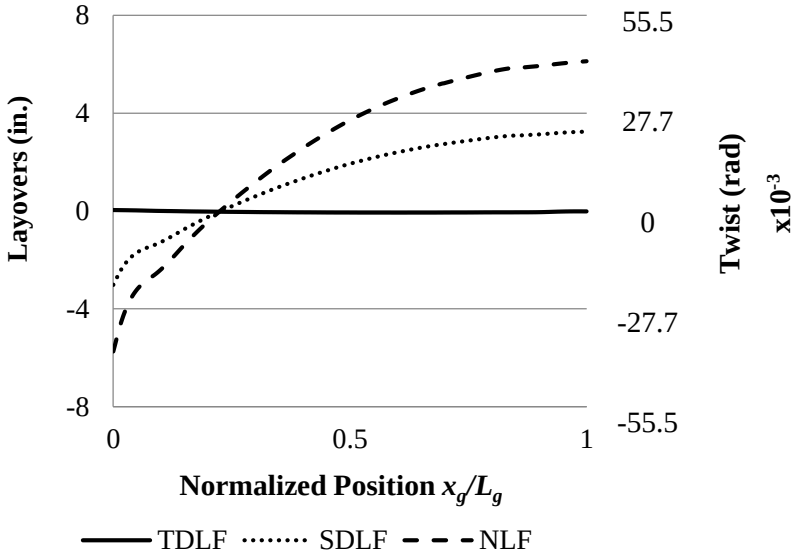

Figure 102. TDL fascia girder layovers Bridge (J1) NISSS54 for detailing based on LGA.

Considering the complete set of straight skewed bridges studied in this research, the largest corresponding girder layovers are 0.1 inches under SDL for SDLF detailing and 0.6 inches under TDL for TDLF detailing. The largest girder layovers are not ideally zero under the targeted condition due to a number a reasons, as discussed in Section 6.2.2. By comparison to the results in Section 6.5.1.3, it can be observed that SDLF and TDLF detailing are more effective in making the girders nearly plumb for straight skewed bridges than curved radially-supported bridges. This is due to the tendency for larger forces, and larger elastic deformations in the CFs of the curved bridges studied in this research.

One can observe that, for straight skewed bridges, the layovers under SDL with TDLF detailing are approximately equal in magnitude but opposite in sign to the layovers under TDL with SDLF detailing. With SDLF detailing, the layovers are theoretically zero under SDL (when LGA cambers are employed). The layovers with SDLF detailing under TDL are therefore theoretically equal to the layovers due to the CDL determined from a NLF RA. With TDLF detailing, the layovers are ideally zero under TDL. The layovers with TDLF detailing under SDL are thus theoretically equal in magnitude but opposite in sign to the layovers due to the CDL determined from a NLF RA. It should be emphasized that LGA can be a very erroneous predictor of the CDL displacements. This is because the girders are interconnected by their CFs and are thus behaving as a three-dimensional structural system under the action of the CDL.

Table 33. Maximum magnitudes of girder layovers and twists in the straight bridges with parallel skew studied in this research with CFs detailed entirely based on LGA cambers. (LO1, LO2, and LO3 are maximum girder layovers with NLF, SDLF, and TDLF detailing, respectively. $\phi 1$, $\phi 2$, and $\phi 3$ are the maximum girder twists with NLF, SDLF, and TDLF detailing, respectively. The largest girder layovers and twists with SDLF under SDL and TDLF under TDL are highlighted by dark shading).

Load Cond.	Bridge	Girder Depth (in.)	NLF		SDLF		TDLF	
			LO1 (in.)	$\phi 1$ (rad) x10^{-3}	LO2 (in.)	$\phi 2$ (rad) x10^{-3}	LO3 (in.)	$\phi 3$ (rad) x10^{-3}
SDL	(I1) NISSS14	72	0.7	9.7	0.0	0.0	2.6	36.1
	(I2) NISSS14	"	0.7	9.7	**0.1**	**1.4**	2.3	31.9
	(J1) NISSS54	144	2.8	19.4	**0.1**	0.7	3.3	22.9
	(J2) NISSS54	"	2.7	18.8	**0.1**	0.7	3.3	22.9
	(K1) EICSS12	54	0.2	3.7	0.0	0.0	0.7	13.0
	(K2) EICSS12	"	0.2	3.7	0.0	0.0	0.7	13.0
	(K3) EICSS12	"	0.2	3.7	0.0	0.0	0.7	13.0
	(L) NICSS16	72	0.4	5.6	0.0	0.0	1.6	22.2
	(M1) EICSS2	98.4	0.8	8.1	0.0	0.0	1.6	16.3
	(M2) EICSS2	"	0.8	8.1	0.0	0.0	1.6	16.3
TDL	(I1) NISSS14	72	3.3	45.8	2.6	36.1	0.3	4.2
	(I2) NISSS14	"	3.2	44.4	2.5	34.7	**0.6**	**8.3**
	(J1) NISSS54	144	6.1	42.4	3.3	22.9	0.1	0.7
	(J2) NISSS54	"	6.3	43.8	3.4	23.6	0.1	0.7
	(K1) EICSS12	54	1.0	18.5	0.8	14.8	0.1	1.9
	(K2) EICSS12	"	1.0	18.5	0.8	14.8	0.1	1.9
	(K3) EICSS12	"	1.0	18.5	0.8	14.8	0.1	1.9
	(L) NICSS16	72	2.3	31.9	1.9	26.4	0.4	5.6
	(M1) EICSS2	98.4	2.5	25.4	1.7	17.3	0.1	1.0
	(M2) EICSS2	"	2.5	25.4	1.7	17.3	0.3	3.0

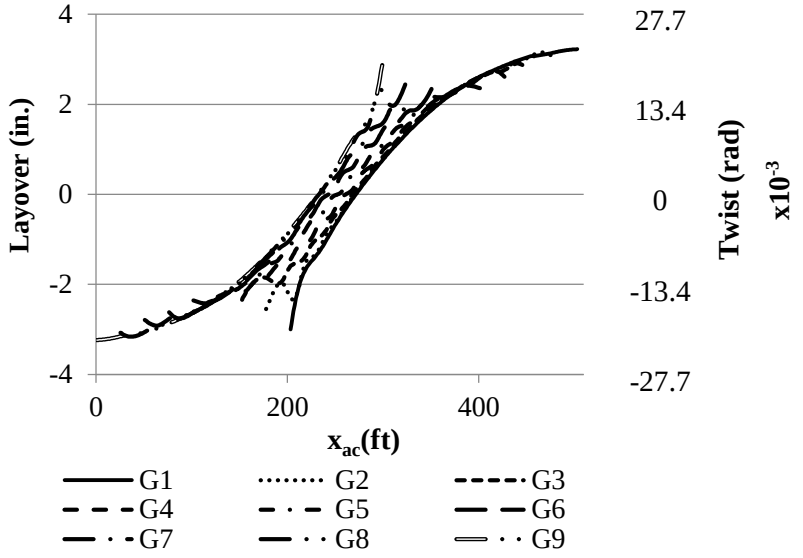

Figure 103. TDL girder layovers and twists of Bridge (J1) NISSS54 with SDLF detailing based on LGA cambers.

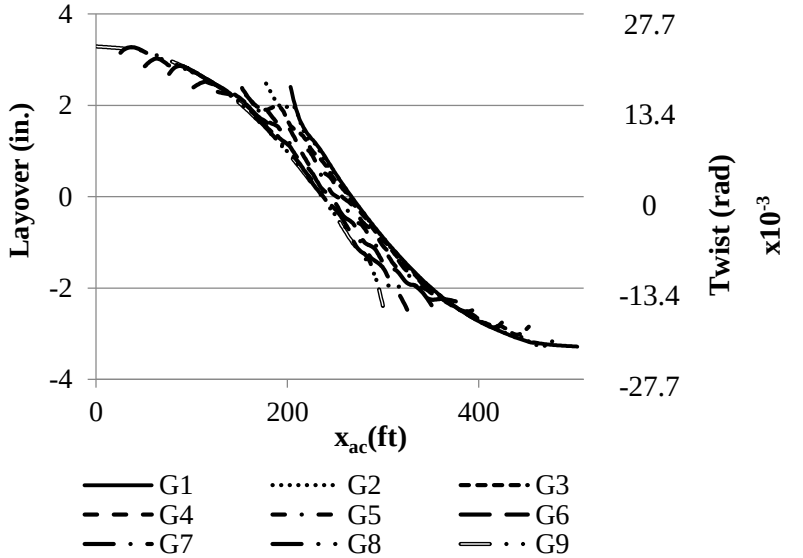

Figure 104. SDL girder layovers and twists of Bridge (J1) NISSS54 with TDLF detailing based on LGA cambers.

6.6.1.4 Cross-Frame Forces

For straight bridges with parallel skew, both the average and the maximum CF forces in the completed bridge are small under SDL for SDLF detailing, and they are small under TDL for TDLF detailing. The effects of SDLF and TDLF detailing approximately cancel the CF DL effects, when the SDLF and TDLF detailing is based on cambers obtained from LGA girder deflections. If the bridge design is based on LGA, it is common that the CFs are detailed based on LGA cambers. It is emphasized that the recommendation of this research is that the engineer should not mix the methods of analysis being applied to a given bridge. That is, if a RA is employed for the overall bridge design (i.e., grid analysis or 3D FEA), the cambers should be calculated based on the RA. This recommendation is due to the high chance of significant errors entering into the solutions when the results from LGA and from RA are mixed (e.g., improperly using the LGA result for the total girder cambers when the bridge is detailed for SDLF, which will result in substantial girder elevation errors), as well as other reasons discussed in Section 6.2.3.

From Tables 34 and 35, it can be observed that the average and maximum CF forces are relatively small under the targeted conditions. However, the actual CF forces generally are not zero under the targeted condition for reasons discussed in Section 6.2.2. The following can be observed from the above tables:

- Under SDL/SDLF, the largest F2/F1 ratio of the average of the CF member forces (in each bridge) is 0.48. This ratio corresponds to the bridge with the next to the largest skew index of all the bridges studied, (I2) NISSS14. The CF forces are substantially reduced by the improved framing arrangement in this particular bridge. The above ratio is close to zero for nearly all of the other bridges studied. The next largest value is 0.25.

- Under SDL/SDLF, the largest F2/F1 ratio of the maximum CF member force (in each bridge) is 0.31. This ratio corresponds to Bridge (J2) NISSS54.
- Under TDL/TDLF, the largest F3/F1 ratio of the average of the CF member forces (in each bridge) is 0.48. These values are greater than or equal to 0.12 for all but one of the other bridges studied. The larger ratios correspond to cases with smaller NLF CF forces.
- Under TDL, the largest F3/F1 ratio of the maximum CF member force (in each bridge) is again 0.31. Many of the other bridges have similar maximum values.

The SDLF maximum fit-up forces for the straight skewed bridges shown in Table 16 (Section 5.2) are slightly larger than their maximum forces in the completed bridge under SDL shown in Table 35. This is because the critical CFs are installed at intermediate erection stages for which the bridge configuration and boundary conditions were not the same as the final bridge configuration that the CFs were detailed for. For instance, in the case of bridge cases (J1) and (J2) NISSS54, field splices and shoring towers are required due to the span length. A minimum number of CFs were installed before making the splice connection to keep the girders stable. Figure 105 shows the frequency distribution of the changes in the CF chord forces due to SDLF and TDLF detailing for Bridge (J1) NISSS54. Figure 106 shows this frequency distribution for the CF diagonal forces in this bridge. From these figures, it can be observed that nearly all of the CF members (both chords and diagonals) have internal forces that are decreased due to SDLF and TDLF detailing. The maximum negative percent change in the CF forces, normalized by the member yield load, are 21.6 % for SDLF detailing and 37.9 % for TDLF detailing.

Table 34. Average magnitude of the CF member forces in each of the straight bridges with parallel skew studied in this research (F1, F2, and F3 are the average CF forces with NLF, SDLF, and TDLF detailing based on LGA cambers, respectively. The largest F2/F1 and F2-F1 under SDL and F3/F1 and F3-F1 under TDL are highlighted by dark shading).

Load Cond.	Bridge	NLF	SDLF			TDLF		
		F1 (kip)	F2 (kip)	F2/F1	F2 – F1 (kip)	F3 (kip)	F3/F1	F3 – F1 (kip)
SDL	(I1) NISSS14	8.8	1.7	0.19	-7.1	26.2	2.98	17.4
	(I2) NISSS14	3.3	1.6	**0.48**	-1.7	15.4	4.67	12.1
	(J1) NISSS54	19.5	1.0	0.05	**-18.5**	20.3	1.04	0.8
	(J2) NISSS54	5.7	1.4	0.25	-4.3	9.2	1.61	3.5
	(K1) EICSS12	1.4	0.0	0.00	-1.4	4.6	3.29	3.2
	(K2) EICSS12	0.9	0.0	0.00	-0.9	2.8	3.11	1.9
	(K3) EICSS12	1.0	0.0	0.00	-1.0	3.2	3.20	2.2
	(L) NICSS16	1.4	0.1	0.07	-1.3	6.0	4.29	4.6
	(M1) EICSS2	4.4	0.0	0.00	-4.4	8.7	1.98	4.3
	(M2) EICSS2	2.0	0.0	0.00	-2.0	4.2	2.10	2.2
TDL	(I1) NISSS14	37.8	28.4	0.75	-9.4	6.5	0.17	-31.3
	(I2) NISSS14	13.9	11.1	0.80	-2.8	6.7	**0.48**	-7.2
	(J1) NISSS54	42.9	22.5	0.52	-20.4	2.0	0.05	**-40.9**
	(J2) NISSS54	13.5	7.7	0.57	-5.8	3.4	0.25	-10.1
	(K1) EICSS12	6.0	4.6	0.77	-1.4	1.5	0.25	-4.5
	(K2) EICSS12	3.5	2.7	0.77	-0.8	1.1	0.31	-2.4
	(K3) EICSS12	4.2	3.2	0.76	-1.0	1.1	0.26	-3.1
	(L) NICSS16	7.5	6.0	0.80	-1.5	1.0	0.13	-6.5
	(M1) EICSS2	13.1	8.8	0.67	-4.3	1.6	0.12	-11.5
	(M2) EICSS2	7.0	5.2	0.74	-1.8	2.2	0.31	-4.8

Table 35. Maximum magnitude of the CF member forces in each of the straight bridges with parallel skew studied in this research (F1, F2, and F3 are the maximum CF forces with NLF, SDLF, and TDLF detailing based on LGA cambers, respectively. The largest F2/F1 and F2-F1 under SDL and F3/F1 and F3-F1 under TDL are highlighted by dark shading).

Load Cond.	Bridge	NLF	SDLF			TDLF		
		F1 (kip)	F2 (kip)	F2/F1	F2 – F1 (kip)	F3 (kip)	F3/F1	F3 – F1 (kip)
SDL	(I1) NISSS14	33.5	5.6	0.17	-27.9	93.1	2.78	59.6
	(I2) NISSS14	29.7	6.5	0.22	-23.2	103.9	3.50	74.2
	(J1) NISSS54	162.4	6.4	0.04	**-156.0**	145.5	0.90	-16.9
	(J2) NISSS54	25.4	8.0	**0.31**	-17.4	35.2	1.39	9.8
	(K1) EICSS12	4.2	0.2	0.05	-4.0	13.8	3.29	9.6
	(K2) EICSS12	3.2	0.0	0.00	-3.2	10.0	3.13	6.8
	(K3) EICSS12	5.0	0.1	0.02	-4.9	15.2	3.04	10.2
	(L) NICSS16	12.0	0.7	0.06	-11.3	51.4	4.28	39.4
	(M1) EICSS2	42.1	0.6	0.01	-41.5	80.0	1.90	37.9
	(M2) EICSS2	20.6	0.6	0.03	-20.0	43.5	2.11	22.9
TDL	(I1) NISSS14	144.4	109.4	0.76	-35.0	22.9	0.16	-121.5
	(I2) NISSS14	130.7	101.8	0.79	-28.9	30.1	0.23	-100.6
	(J1) NISSS54	354.0	181.9	0.51	-172.1	8.8	0.02	**-345.2**
	(J2) NISSS54	58.5	31.2	0.53	-27.3	18.1	**0.31**	-40.4
	(K1) EICSS12	17.7	13.6	0.77	-4.1	4.1	0.23	-13.6
	(K2) EICSS12	13.7	10.6	0.77	-3.1	3.4	0.25	-10.3
	(K3) EICSS12	20.5	15.4	0.75	-5.1	3.5	0.17	-17.0
	(L) NICSS16	63.5	51.0	0.80	-12.5	7.1	0.11	-56.4
	(M1) EICSS2	122.7	80.5	0.66	-42.2	5.4	0.04	-117.3
	(M2) EICSS2	69.8	49.3	0.71	-20.5	11.7	0.17	-58.1

Figure 107 shows the frequency distribution for the CF chords and Figure 108 shows this frequency distribution for the CF diagonal forces in all the straight bridges with parallel skew considered in this research. Table 36 shows a summary of the percent change in the CF forces, normalized by the member yield load, due to SDLF or TDLF detailing in all the straight bridges with parallel skew. It can be observed that SDLF and TDLF detailing have substantial beneficial (subtractive) effects on the CF DL forces. The CF forces are close to but not ideally zero under the targeted conditions for various reasons explained above. In addition, the magnitude of the influence of the DLF detailing on the chord forces is somewhat larger than on the diagonal forces for straight skewed bridges, which is the opposite of the trend for CF member forces for curved-radially supported bridges. Furthermore, in the case of straight skewed bridges, these influences tend to involve a significant reduction in the CF forces.

The statistics for the percent change in the individual CF member forces relative the member yield load, due to SDLF and TDLF detailing, indicate a wide range (dispersion) of individual CF member force effects. However, the predominant tendency is a reduction of the CF member forces in parallel-skew straight bridges due to SDLF and TDLF detailing.

Figure 110 shows an estimate of the CF member forces under the SDL, assuming SDLF detailing, obtained by scaling the NLF RA forces for all the cross-frame members by 0.35. One can observe that the absolute maximum CF force values from Figure 109 are estimated conservatively.

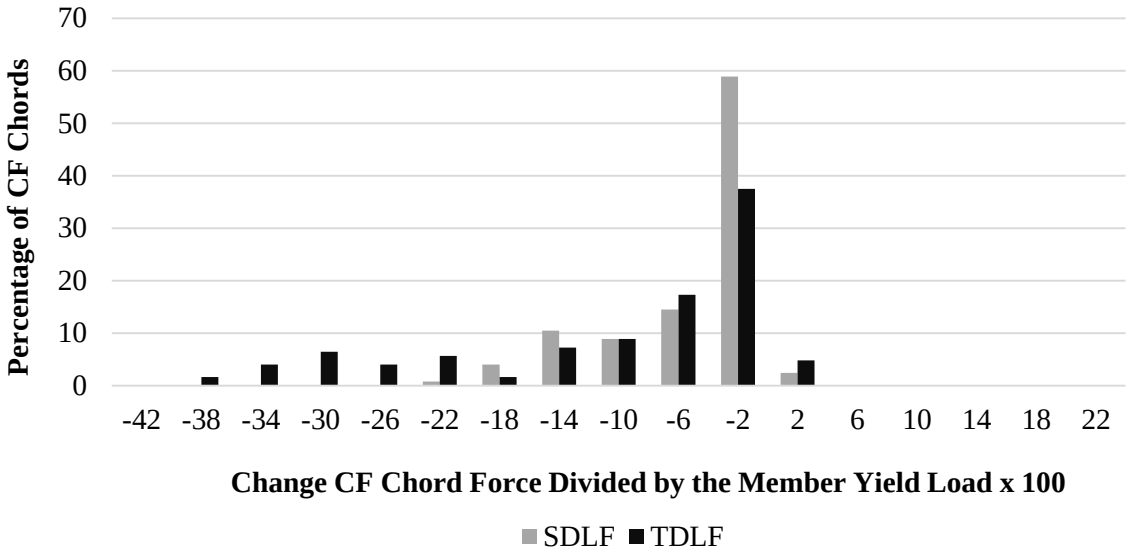

Figure 105. Frequency distribution for the change in the magnitude of the CF chord forces, normalized by the member yield load, due to SDLF and TDLF detailing using LGA cambers, Bridge (J1) NISSS54.

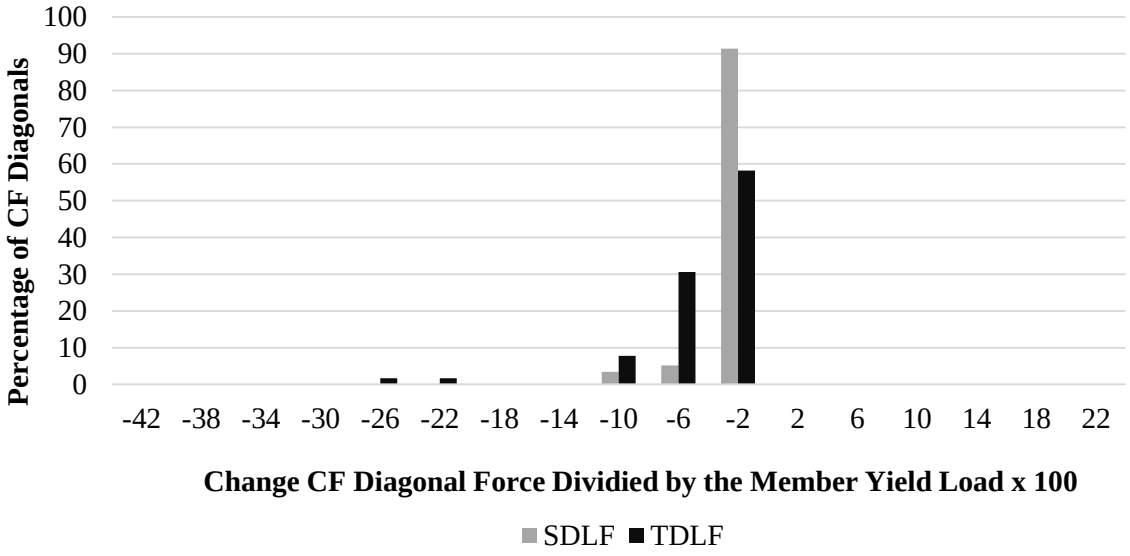

Figure 106. Frequency distribution for the change in the magnitude of the CF diagonal forces, normalized by the member yield load, due to SDLF and TDLF detailing using LGA cambers, Bridge (J1) NISSS54.

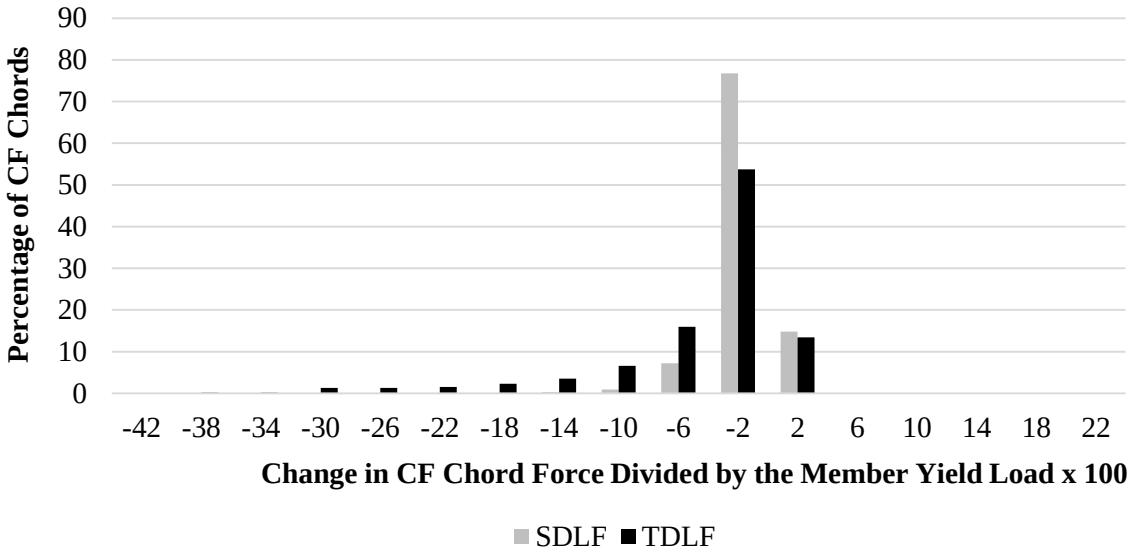

Figure 107. Frequency distribution for the change in the magnitude of the CF chord forces, normalized by the member yield load, due to SDLF and TDLF detailing using LGA cambers, all the straight bridges with parallel skew studied in this research.

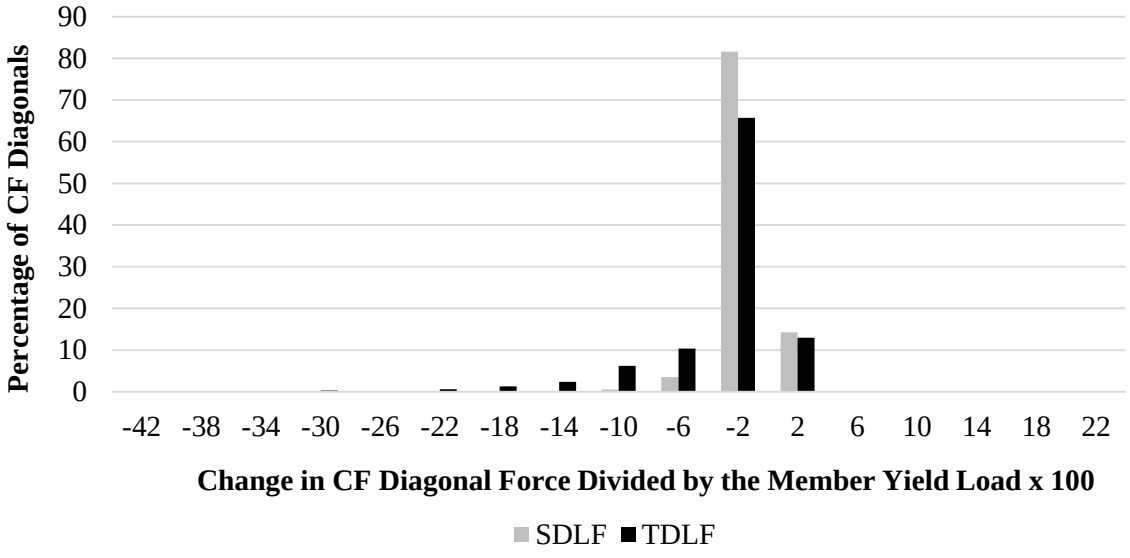

Figure 108. Frequency distribution for the change in the magnitude of the CF diagonal forces, normalized by the member yield load, due to SDLF and TDLF detailing using LGA cambers, all the straight bridges with parallel skew studied in this research.

Table 36. Summary statistics for the percent change in the magnitude of the CF forces divided by the member yield load (change in member force divided by the member yield load x 100), due to SDLF or TDLF detailing using LGA cambers, all the straight bridges with parallel skew studied in this research.

	Chords		Diagonals	
	SDLF	TDLF	SDLF	TDLF
Average	-1.63	-4.85	-0.97	-2.88
Median	-0.65	-2.34	-0.47	-1.47
Max	0.78	3.33	0.99	4.36
Min	-21.6	-37.9	-11.7	-28.9
COV	51.2	34.2	52.4	42.9

However, the actual distribution of the CF forces from Figure 109 is predicted poorly. The poor prediction of the CF force distribution is not of any significant consequence though since all the CF forces are relatively small. Since Figure 110 simply shows all the NLF RA CF forces scaled by 0.35, it can be concluded that the distribution of the non-zero CF forces under SDL associated with NLF detailing is very different from the distribution of the reduced (smaller) CF forces under SDL associated with SDLF detailing.

Figure 111 shows the difference between the magnitude of the DLF RA forces and the CF forces under SDL, assuming SDLF detailing, estimated by scaling the NLF RA forces, divided by the CF member yield loads. One can observe that the largest under-prediction of the DLF RA results is $0.01P_y$ for several of the top chord members, while the largest over-prediction is $-0.025P_y$ using the recommended estimate on Bridge (I2) NISSS14. Figure 112 shows the same results as Figure 111, but under TDL and assuming TDLF detailing. The maximum under-prediction is $0.05P_y$ and the largest over-prediction is $-0.115P_y$ for this case.

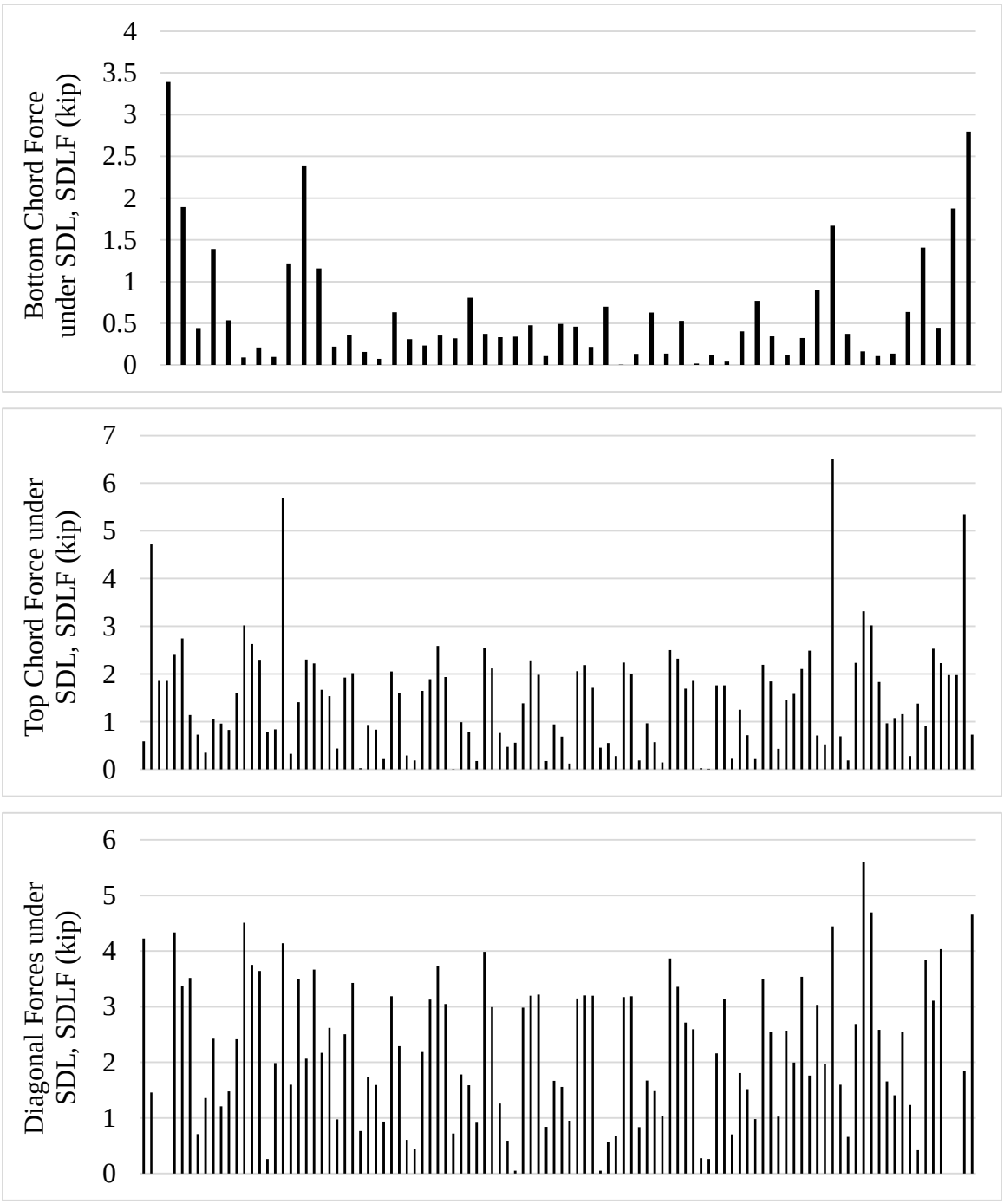

Figure 109. Magnitude of CF member forces from DLF RA, Bridge (I2) NISSS14 under SDL, SDLF detailing based on LGA cambers.

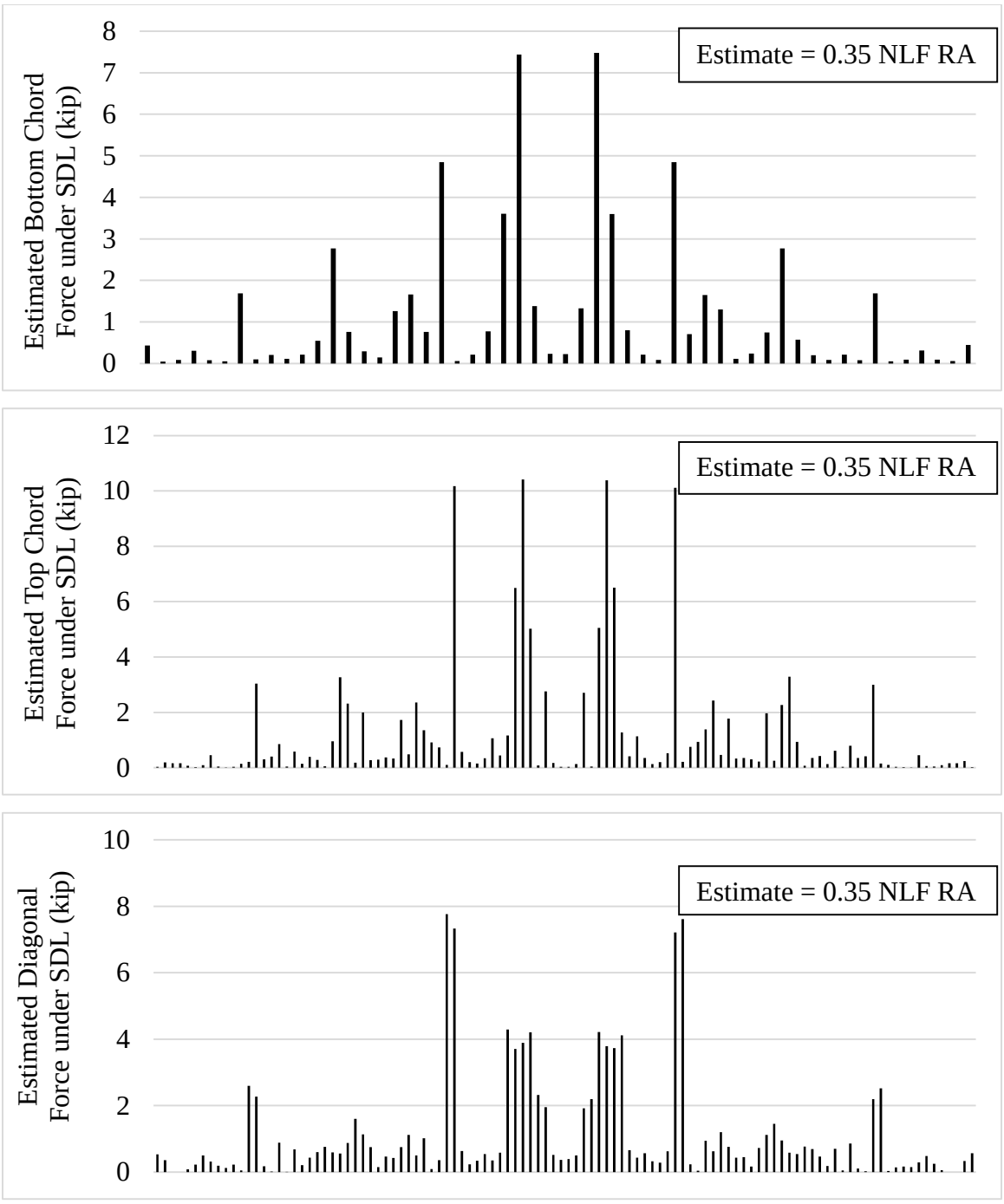

Figure 110. Estimated magnitude of CF member forces based on scaling of NLF RA results, assuming SDLF detailing, Bridge (I2) NISSS14 under SDL.

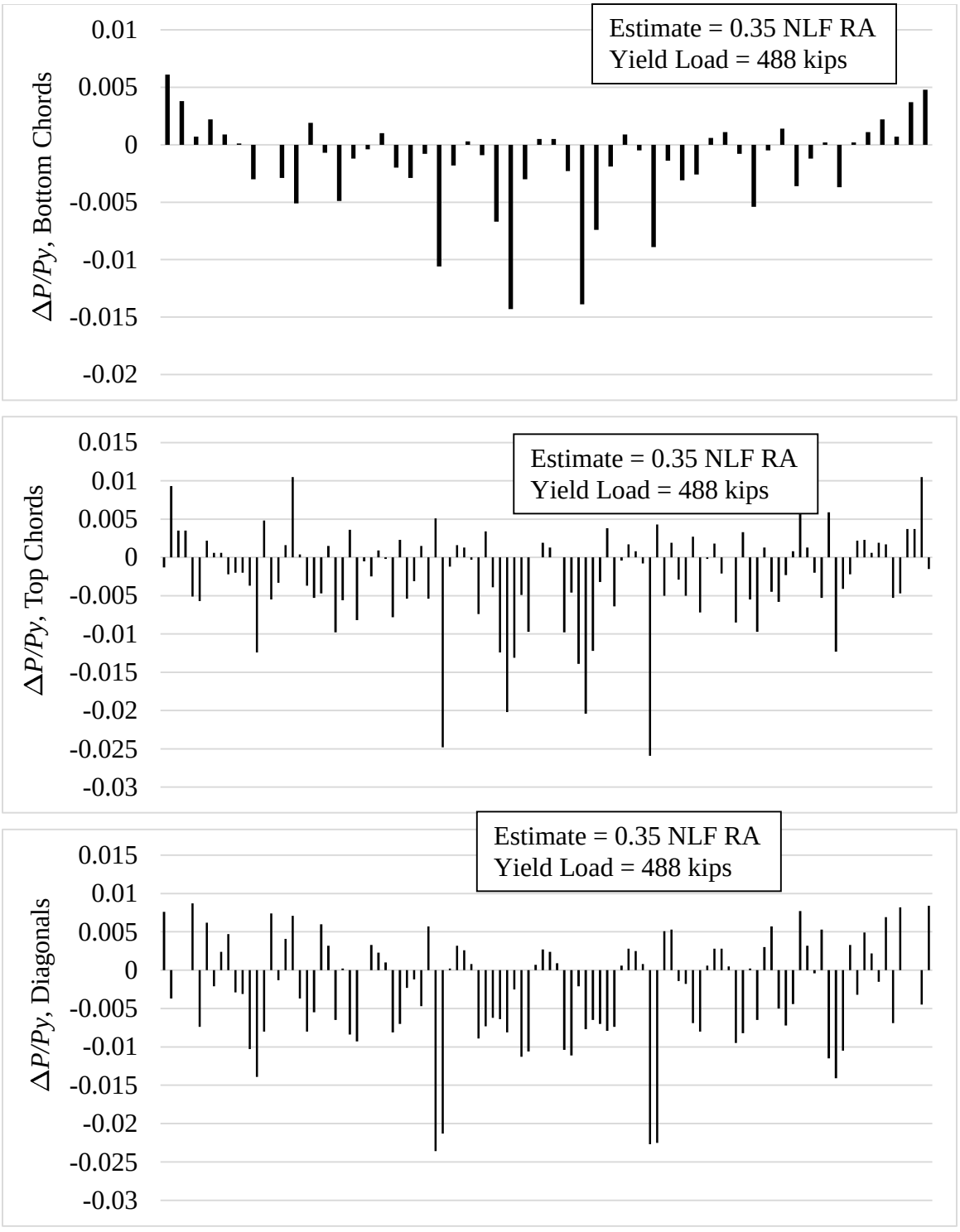

Figure 111. Difference between the magnitude of the DLF RA forces and the values estimated by scaling the NLF RA results, divided by the member yield load ($\Delta P/P_y$), Bridge (I2) NISSS14 under SDL, SDLF detailing based on LGA cambers.

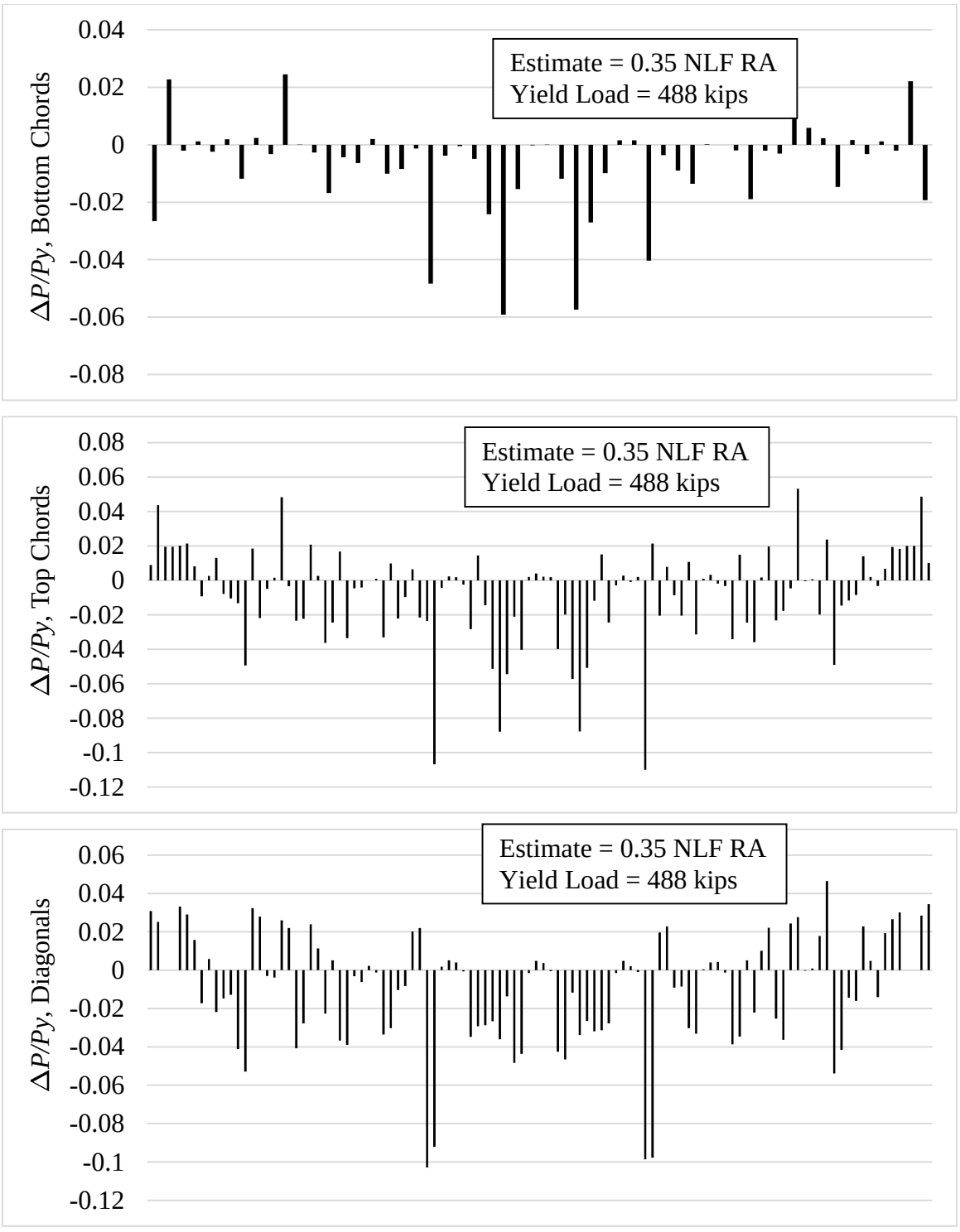

Figure 112. Difference between the magnitude of the DLF RA forces and the values estimated by scaling the NLF RA results, divided by the member yield load ($\Delta P/P_y$), Bridge (I2) NISSS14 under TDL, TDLF detailing based on LGA cambers.

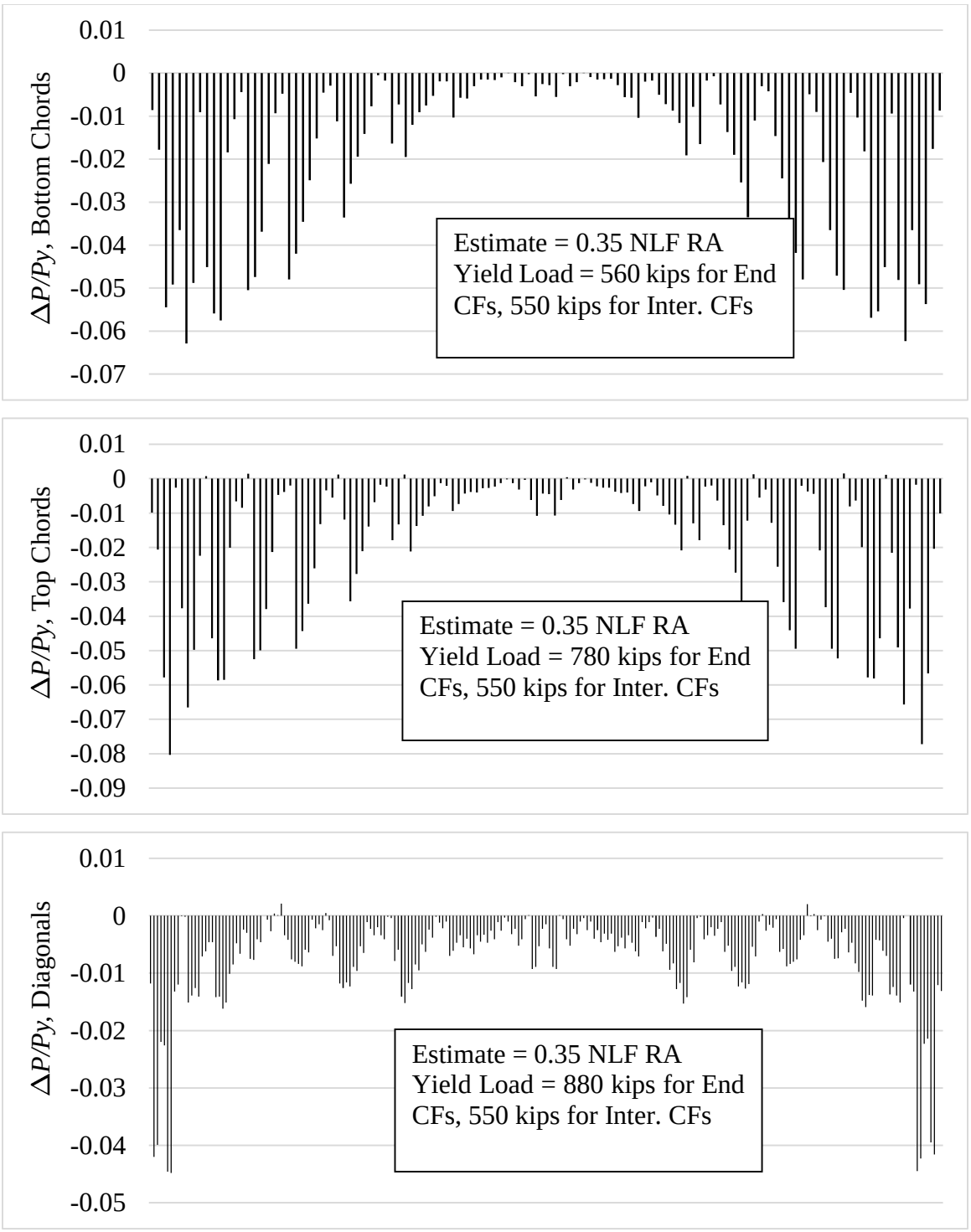

Figure 113. Difference between the magnitude of the DLF RA forces and the values estimated by scaling the NLF RA results, divided by the member yield load ($\Delta P/P_y$), Bridge (J1) NISSS54 under SDL, SDLF detailing based on LGA cambers.

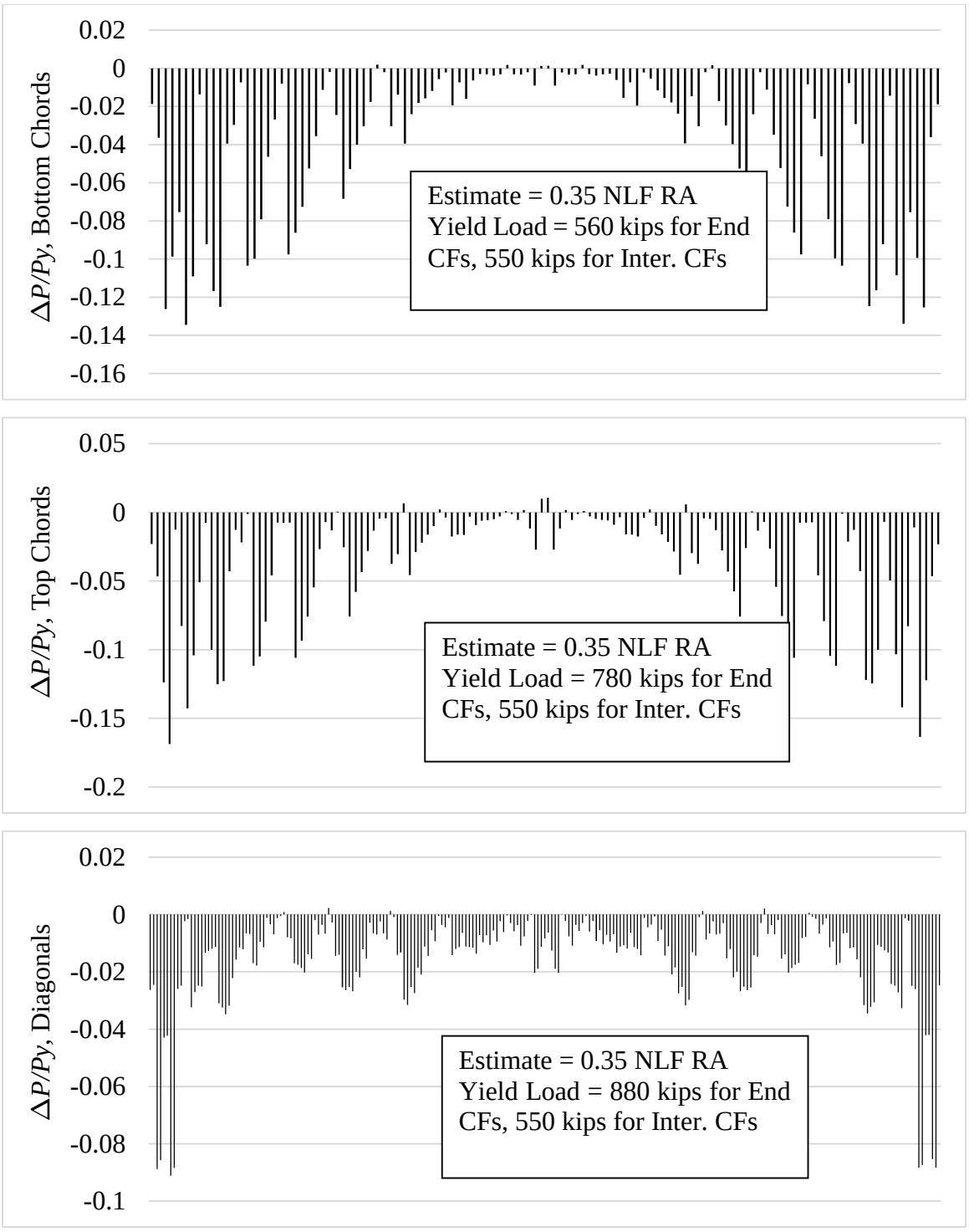

Figure 114. Difference between the magnitude of the DLF RA forces and the values estimated by scaling the NLF RA results, divided by the member yield load ($\Delta P/P_y$), Bridge (J1) NISSS54 under TDL, TDLF detailing based on LGA cambers.

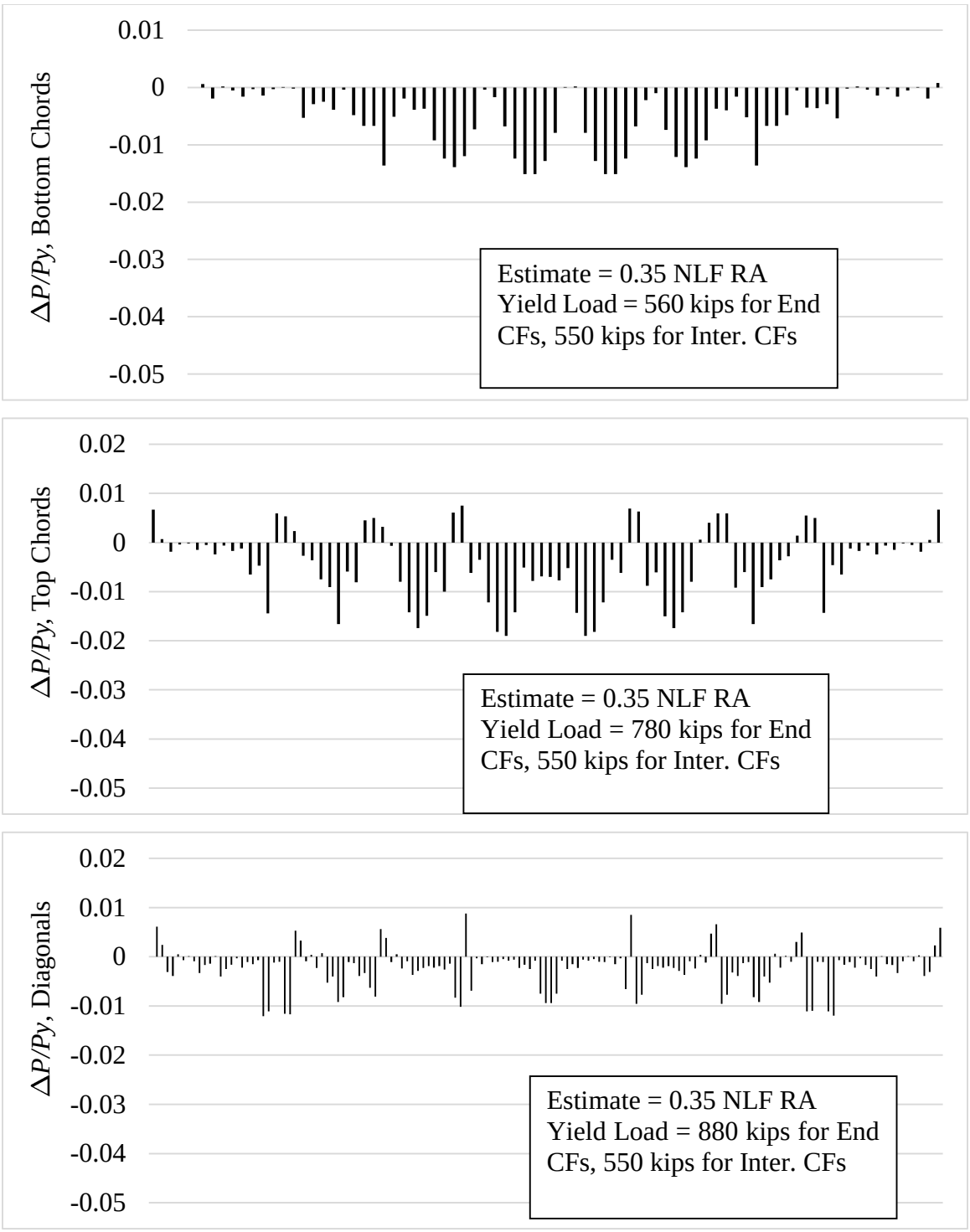

Figure 115. Difference between the magnitude of the DLF RA forces and the values estimated by scaling the NLF RA results, divided by the member yield load ($\Delta P/P_y$), Bridge (J2) NISSS54 under SDL, SDLF detailing based on LGA cambers.

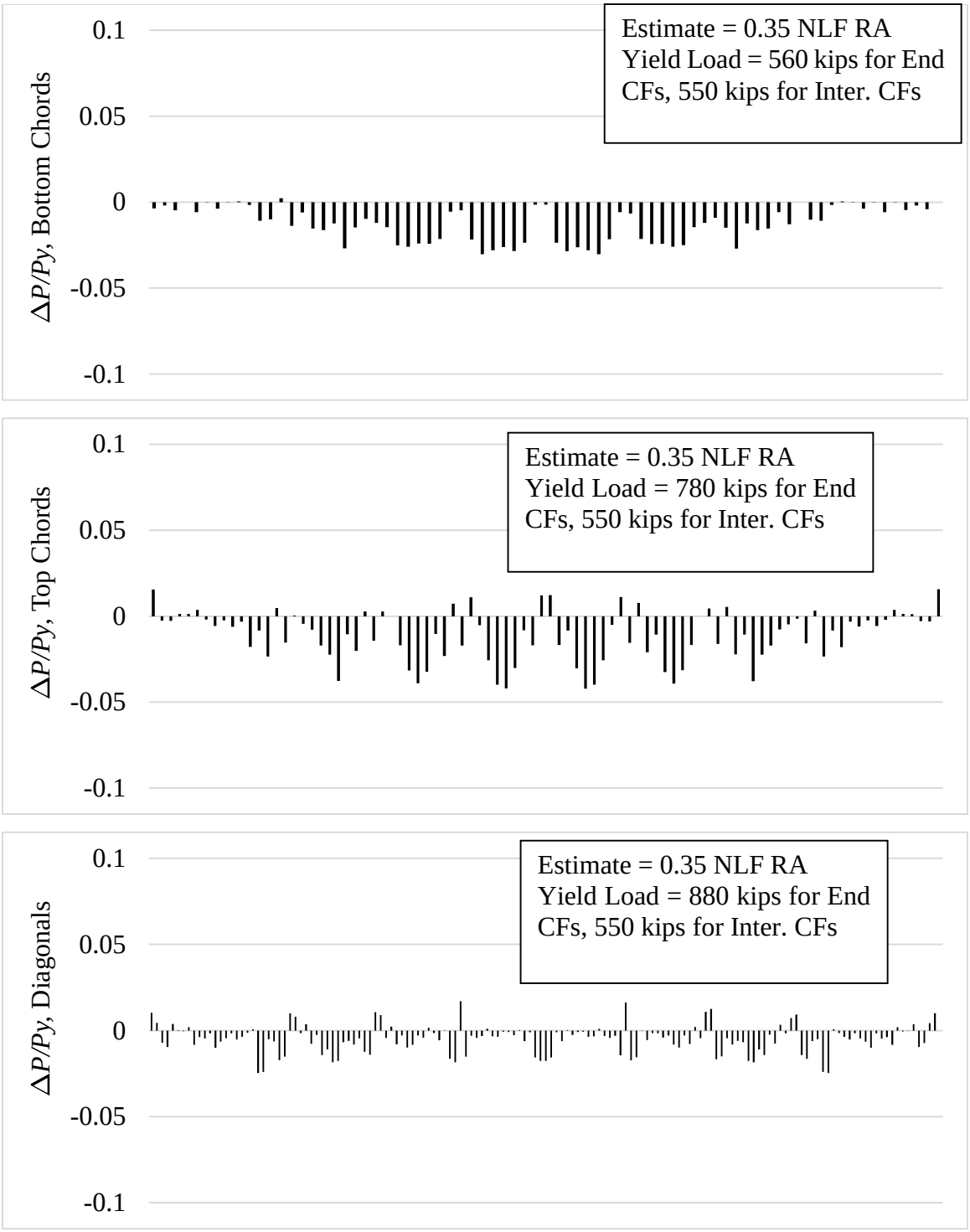

Figure 116. Difference between the magnitude of the DLF RA forces and the values estimated by scaling the NLF RA results, divided by the member yield load ($\Delta P/P_y$), Bridge (J2) NISSS54 under TDL, TDLF detailing based on LGA cambers.

Figures 113 and 114 show comparable plots to Figures 111and 112 for Bridge (J1) NISSS54. Figures 115 and 116 do the same for Bridge (J2) NISSS54. For Bridge (J1), the largest under-prediction is $0.002P_y$ for SDL/SDLF and $0.001P_y$ for TDL/TDLF, whereas the largest over-prediction is $-0.08P_y$ for SDL/SDLF and $-0.17P_y$ for TDL/TLDF. For Bridge (J2), the largest under-prediction is $0.008P_y$ for SDL/SDLF and $0.017P_y$ for TDL/TDLF, while the largest over-prediction is $-0.019P_y$ for SDL/SDLF and $0.042P_y$ for TDL/TDLF.

Similar to the estimate recommended for curved radially-supported bridges in Section 6.5.1.4, the largest under-prediction is less than $0.05P_y$ for all the cases considered, given the CF member sizes selected in the original bridge designs.

6.6.1.5 Girder Stresses

For straight bridges with parallel skew, the SDLF and TDLF detailing effects based on LGA cambers tend to increase the major-axis bending stresses in the interior girders and decrease these stresses in the fascia girders. This behavior is shown in Figure 117through Figure 120 for bridges (J1) NISSS54 and (I1) NISSS14, respectively. This increase or decrease is significant in these bridge cases, which have substantial nuisance transverse stiffness and uplift at some of the bearings.

The girder flange lateral bending stresses are theoretically zero under SDL for SDLF detailing and under TDL for TDLF detailing based on LGA cambers, and they are generally significant under TDL if NLF detailing is used (shown in Figure 121 through Figure 125 for bridge cases (I1) and (J1), respectively). However, the stresses are actually non-zero

under SDL for SDLF detailing and under TDL for TDLF detailing due to a number of factors, as discussed in Section 6.2.2.

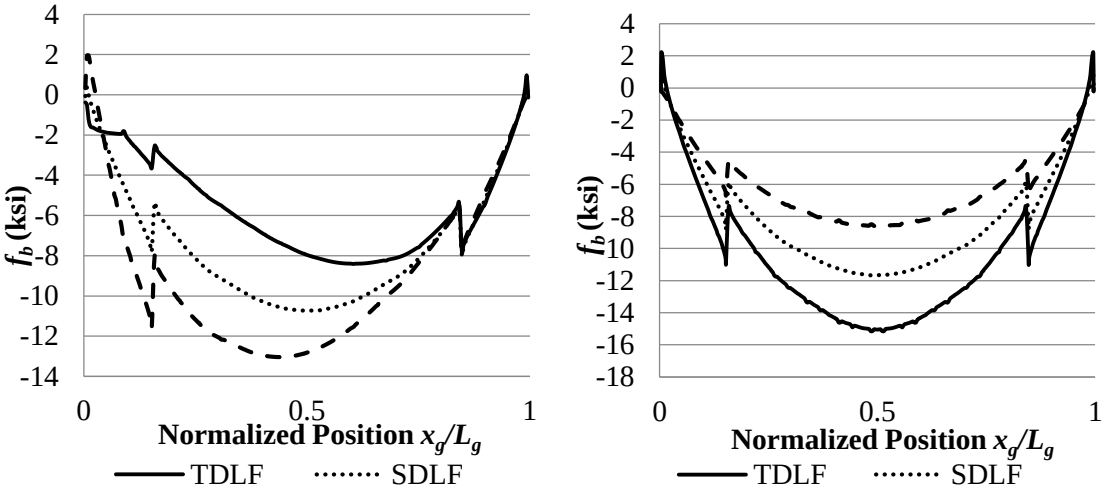

Figure 117. Top flange major-axis bending stresses in Bridge (J1) NISSS54 fascia girder (left) and innermost girder (right) under SDL with detailing based on LGA cambers.

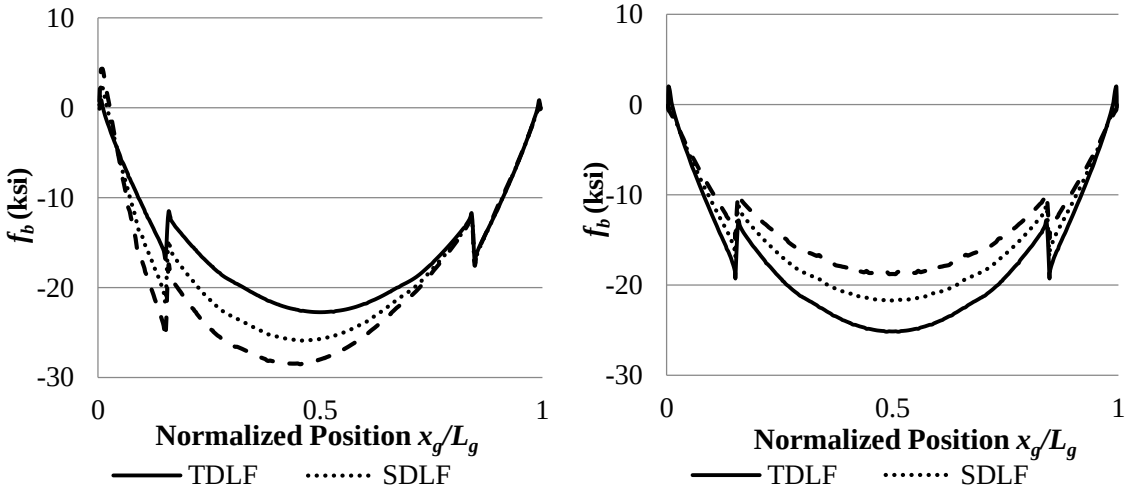

Figure 118. Top flange major-axis bending stresses in Bridge (J1) NISSS54 fascia girder (left) and innermost girder (right) under TDL with detailing based on LGA cambers.

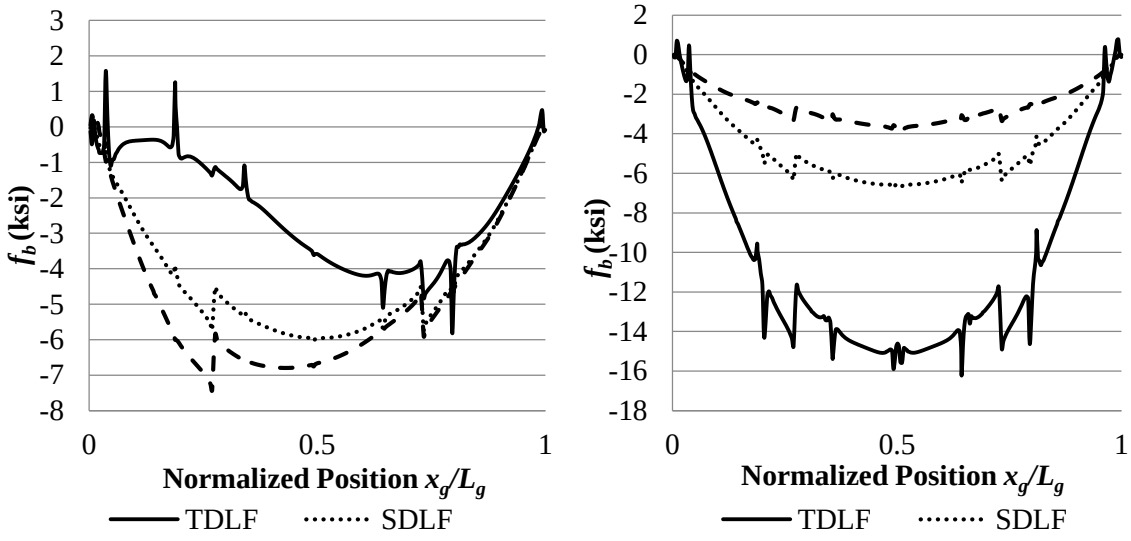

Figure 119. Top flange major-axis bending stresses in Bridge (I1) NISSS14 fascia girder (left) and innermost girder (right) under SDL with detailing based on LGA cambers.

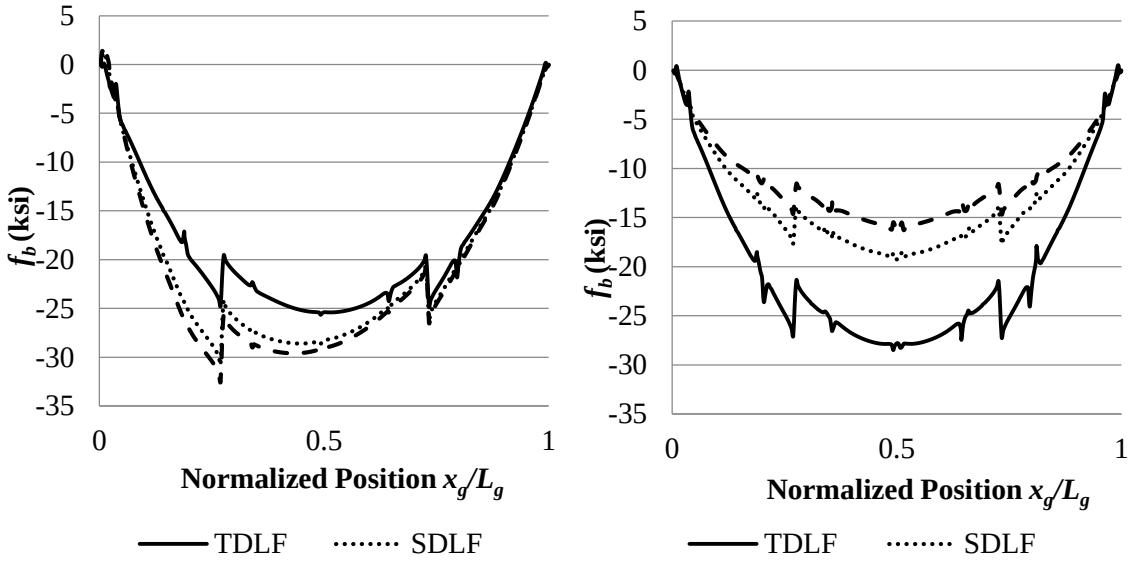

Figure 120. Top flange major-axis bending stresses in Bridge (I1) NISSS14 fascia girder (left) and innermost girder (right) under TDL with detailing based on LGA cambers.

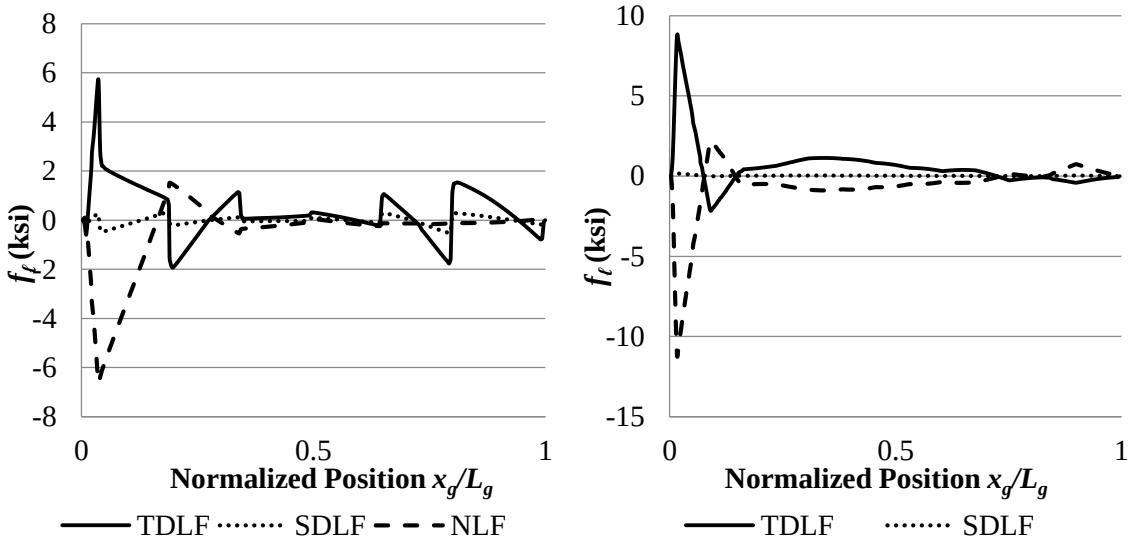

Figure 121. Top flange lateral bending stresses in fascia girder under SDL with detailing based on LGA cambers, in Bridge (I1) NISSS14 (left) and in bridge in Bridge (J1) NISSS54 (right).

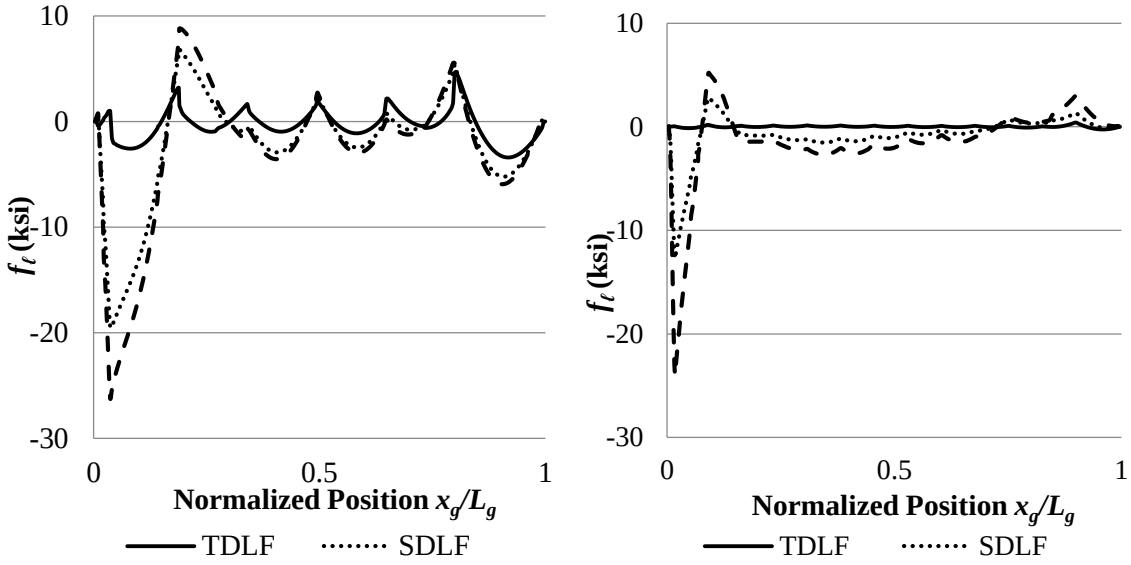

Figure 122. Top flange lateral bending stresses in fascia girder under TDL with detailing based on LGA cambers, in Bridge (I1) NISSS14 (left) and in bridge in Bridge (J1) NISSS54 (right).

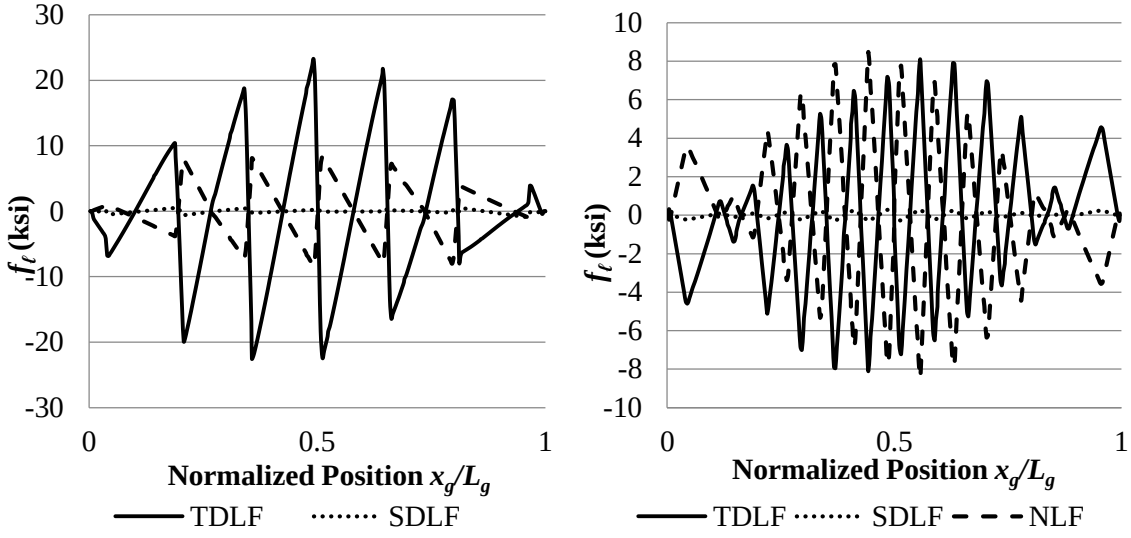

Figure 123. Top flange lateral bending stresses innermost girder under SDL with detailing based on LGA cambers in Bridge (I1) NISSS14 (left) and in bridge in Bridge (J1) NISSS54 (right).

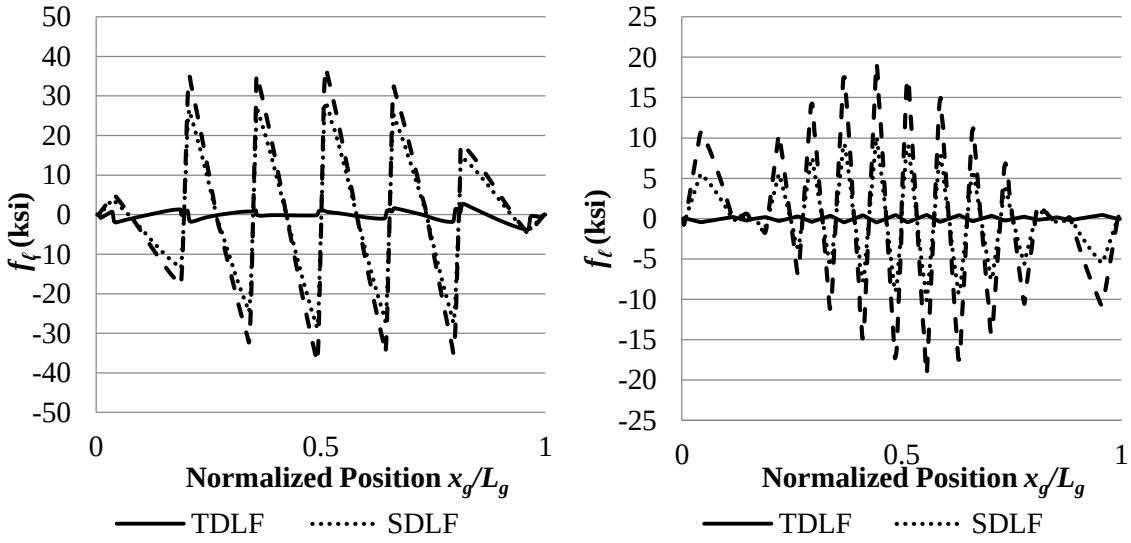

Figure 124. Top flange lateral bending stresses innermost girder under TDL with detailing based on LGA cambers in Bridge (I1) NISSS14 (left) and in bridge in Bridge (J1) NISSS54 (right).

From Figure 125, one can observe that, for straight bridges with parallel skew, the girder flange lateral bending stresses under SDL with TDLF detailing are approximately

equal in magnitude but opposite in sign to the flange lateral bending stresses under TDL with SDLF detailing. With SDLF detailing, the flange lateral bending stresses are theoretically zero under SDL. The flange lateral bending stresses with SDLF detailing under TDL are theoretically equal to the flange lateral bending stresses due to the CDL from 3D FEA. With TDLF detailing based on LGA cambers, the flange lateral bending stresses are theoretically zero under TDL. The flange lateral bending stresses with TDLF detailing under SDL are theoretically equal to the negative of the flange lateral bending stresses due to the CDL from 3D FEA.

Tables 37 and 38 show the maximum magnitude of the girder stresses for NLF, SDLF and TDLF detailing based on LGA cambers for the critical fascia girder and the innermost girder, respectively, in the straight bridges with parallel skew studied in this research. The following can be observed:

- SDLF and TDLF detailing with LGA cambers imposes the LGA responses on the girders in the targeted DL condition.
- In bridges where the framing arrangement is improved to reduce the "nuisance" transverse stiffness effects, the girders in the bridge 3D system deflect in a fashion closer to that of the LGA model, and the changes in the major-axis bending stresses due to the DLF detailing are smaller.

Table 37. Maximum magnitudes of major-axis bending stresses and top flange lateral bending stresses of the critical fascia girder in the straight skewed bridges studied in this research with the CFs detailed based on LGA cambers (f_{b1}, f_{b2} and f_{b3} are the maximum major-axis bending stresses, and $f_{\ell 1}$, $f_{\ell 2}$ and $f_{\ell 3}$ are the maximum girder flange lateral bending stresses for NLF, SDLF, and TDLF detailing, respectively; the largest f_{b2}/f_{b1}, $f_{\ell 2}/f_{\ell 1}$ under SDL for SDLF and f_{b3}/f_{b1} and $f_{\ell 3}/f_{\ell 1}$ under TDL for TDLF are highlighted by dark shading).

Load Cond.	Bridge	NLF		SDLF				TDLF			
		f_{b1} (ksi)	$f_{\ell 1}$ (ksi)	f_{b2} (ksi)	$\frac{f_{b2}}{f_{b1}}$	$f_{\ell 2}$ (ksi)	$\frac{f_{\ell 2}}{f_{\ell 1}}$	f_{b3} (ksi)	$\frac{f_{b3}}{f_{b1}}$	$f_{\ell 3}$ (ksi)	$\frac{f_{\ell 3}}{f_{\ell 1}}$
SDL	(I1) NISSS14	7.4	6.6	6.0	0.81	0.5	0.08	5.8	0.78	5.7	0.86
	(I2) NISSS14	6.8	2.5	6.2	0.91	1.2	**0.48**	4.5	0.66	7.3	2.92
	(J1) NISSS54	13.1	11.2	10.7	0.82	0.2	0.02	8.1	0.62	8.8	0.79
	(J2) NISSS54	12.0	4.1	10.7	0.89	0.3	0.07	8.5	0.71	3.2	0.78
	(K1) EICSS12	4.1	1.2	3.6	0.88	0.0	0.00	3.3	0.80	4.0	3.33
	(K2) EICSS12	3.9	0.8	3.6	0.92	0.0	0.00	3.4	0.87	2.9	3.63
	(K3) EICSS12	3.9	0.2	3.5	0.90	0.0	0.00	3.2	0.82	0.6	3.00
	(L) NICSS16	3.7	0.7	3.4	0.92	0.0	0.00	2.5	0.68	2.2	3.14
	(M1) EICSS2	7.7	0.9	7.4	0.96	0.0	0.00	7.6	0.99	1.9	2.11
	(M2) EICSS2	7.4	0.5	7.3	0.99	0.0	0.00	7.0	0.95	0.9	1.80

Table 37 (Continued). Maximum magnitudes of major-axis bending stresses and top flange lateral bending stresses of the critical fascia girder in the straight bridges with parallel skew studied in this research with the CFs detailed based on LGA cambers (f_{b1}, f_{b2} and f_{b3} are the maximum major-axis bending stresses, and $f_{\ell 1}$, $f_{\ell 2}$ and $f_{\ell 3}$ are the maximum girder flange lateral bending stresses for NLF, SDLF, and TDLF detailing, respectively; the largest f_{b2}/f_{b1}, $f_{\ell 2}/f_{\ell 1}$ under SDL for SDLF and f_{b3}/f_{b1} and $f_{\ell 3}/f_{\ell 1}$ under TDL for TDLF are highlighted by dark shading).

Load Cond.	Bridge	NLF		SDLF				TDLF			
		f_{b1} (ksi)	$f_{\ell 1}$ (ksi)	f_{b2} (ksi)	$\frac{f_{b2}}{f_{b1}}$	$f_{\ell 2}$ (ksi)	$\frac{f_{\ell 2}}{f_{\ell 1}}$	f_{b3} (ksi)	$\frac{f_{b3}}{f_{b1}}$	$f_{\ell 3}$ (ksi)	$\frac{f_{\ell 3}}{f_{\ell 1}}$
TDL	(I1) NISSS14	32.5	26.2	30.8	0.95	19.5	0.74	25.7	0.79	4.7	0.18
	(I2) NISSS14	29.6	7.5	28.8	0.97	5.9	0.79	26.1	0.88	4.4	0.59
	(J1) NISSS54	28.5	24	25.9	0.91	12.7	0.53	22.7	0.80	0.4	0.02
	(J2) NISSS54	26.9	6.5	25.3	0.94	3.3	0.51	22.8	0.85	0.7	0.11
	(K1) EICSS12	17.6	5.1	17.1	0.97	3.9	0.76	15.2	0.86	1.1	0.22
	(K2) EICSS12	17.1	3.2	16.7	0.98	2.5	0.78	15.2	0.89	1.0	0.31
	(K3) EICSS12	17.1	1.6	16.7	0.98	1.4	0.88	15.3	0.89	1.7	**1.06**
	(L) NICSS16	19.2	4.0	18.8	0.98	3.8	0.95	16.8	0.88	2.7	0.68
	(M1) EICSS2	23.7	2.6	23.3	0.98	1.7	0.65	22.9	**0.97**	1.0	0.38
	(M2) EICSS2	24.1	4.2	23.8	**0.99**	3.0	0.71	23.2	0.96	1.1	0.26

Table 38. Maximum magnitudes of major-axis bending stresses and top flange lateral bending stresses of the innermost girder in the straight bridges with parallel skew studied in this research with CFs detailed based on LGA cambers (f_{b1}, f_{b2} and f_{b3} are the maximum major-axis bending stresses, and $f_{\ell 1}$, $f_{\ell 2}$ and $f_{\ell 3}$ are the maximum girder flange lateral bending stresses for NLF, SDLF, and TDLF detailing, respectively; the largest f_{b2}/f_{b1}, $f_{\ell 2}/f_{\ell 1}$ under SDL for SDLF and f_{b3}/f_{b1} and $f_{\ell 3}/f_{\ell 1}$ under TDL for TDLF are highlighted by dark shading).

Load Cond.	Bridge	NLF		SDLF				TDLF			
		f_{b1} (ksi)	$f_{\ell 1}$ (ksi)	f_{b2} (ksi)	$\frac{f_{b2}}{f_{b1}}$	$f_{\ell 2}$ (ksi)	$\frac{f_{\ell 2}}{f_{\ell 1}}$	f_{b3} (ksi)	$\frac{f_{b3}}{f_{b1}}$	$f_{\ell 3}$ (ksi)	$\frac{f_{\ell 3}}{f_{\ell 1}}$
SDL	(I1) NISSS14	3.8	8.5	6.7	**1.76**	0.9	0.11	16.2	**4.26**	23.2	2.73
	(I2) NISSS14	5.5	12.5	6.3	1.15	0.6	0.05	10.4	1.89	41.1	3.29
	(J1) NISSS54	8.6	8.5	11.7	1.36	0.3	0.04	15.2	1.77	8.1	0.95
	(J2) NISSS54	10.1	7.5	10.9	1.08	0.5	0.07	11.8	1.17	10.5	1.40
	(K1) EICSS12	3.6	0.6	3.7	1.03	0.1	0.17	5.0	1.39	1.9	3.17
	(K2) EICSS12	3.7	0.5	3.7	1.00	0.1	**0.20**	3.8	1.03	1.6	3.20
	(K3) EICSS12	3.6	1.5	3.8	1.06	0.0	0.00	4.4	1.22	0.5	0.33
	(L) NICSS16	3.6	5.5	3.4	0.94	0.3	0.05	3.2	0.89	24.0	**4.36**
	(M1) EICSS2	6.1	0.6	7.1	1.16	0.0	0.00	9.1	1.49	1.1	1.83
	(M2) EICSS2	6.9	2.0	7.0	1.01	0.0	0.00	7.2	1.04	4.3	2.15

Table 38 (Continued). Maximum magnitudes of major-axis bending stresses and top flange lateral bending stresses of the innermost girder in the straight bridges with parallel skew studied in this research with CFs detailed based on LGA cambers (f_{b1}, f_{b2} and f_{b3} are the maximum major-axis bending stresses, and $f_{\ell 1}$, $f_{\ell 2}$ and $f_{\ell 3}$ are the maximum girder flange lateral bending stresses for NLF, SDLF, and TDLF detailing, respectively; the largest f_{b2}/f_{b1}, $f_{\ell 2}/f_{\ell 1}$ under SDL for SDLF and f_{b3}/f_{b1} and $f_{\ell 3}/f_{\ell 1}$ under TDL for TDLF are highlighted by dark shading).

Load Cond.	Bridge	NLF		SDLF				TDLF			
		f_{b1} (ksi)	$f_{\ell 1}$ (ksi)	f_{b2} (ksi)	$\frac{f_{b2}}{f_{b1}}$	$f_{\ell 2}$ (ksi)	$\frac{f_{\ell 2}}{f_{\ell 1}}$	f_{b3} (ksi)	$\frac{f_{b3}}{f_{b1}}$	$f_{\ell 3}$ (ksi)	$\frac{f_{\ell 3}}{f_{\ell 1}}$
TDL	(I1) NISSS14	16.5	37.2	19.3	**1.17**	28.4	0.76	28.5	**1.73**	3.8	0.10
	(I2) NISSS14	24.8	61.6	25.5	1.03	48.0	0.78	27.7	1.12	2.5	0.04
	(J1) NISSS54	18.8	19.3	21.7	1.15	10.1	0.52	25.2	1.34	0.5	0.03
	(J2) NISSS54	22.8	19.8	23.5	1.03	10.6	0.54	24.3	1.07	0.8	0.04
	(K1) EICSS12	14.5	2.5	14.8	1.02	2.0	0.80	15.8	1.09	0.8	0.32
	(K2) EICSS12	16.0	2.5	16.0	1.00	1.9	0.76	15.9	0.99	0.9	**0.36**
	(K3) EICSS12	15.1	6.3	15.2	1.01	4.7	0.75	15.8	1.05	0.7	0.11
	(L) NICSS16	18.5	30.9	18.4	0.99	24.7	0.80	18.1	0.98	0.3	0.01
	(M1) EICSS2	19.4	1.7	20.3	1.05	1.1	0.65	22.3	1.15	0.1	0.06
	(M2) EICSS2	21.7	7.2	21.7	1.00	5.2	0.72	21.8	1.00	1.8	0.25

- If DLF detailing is conducted using LGA cambers on a straight skewed bridge, it is not acceptable in general to simply build a 3D model of the bridge and turn gravity on.
- A 3D FEA or accurate RA that correctly incorporates the initial lack-of-fit effects from the DLF detailing will produce accurate results.
- It is possible for the engineer to combine results from LGA of the targeted DL condition with accurate RA solutions for all the other responses, but the chances for costly errors are high.
- Regardless of the method of detailing, straight skewed bridges respond as 3D systems once the girders are interconnected.

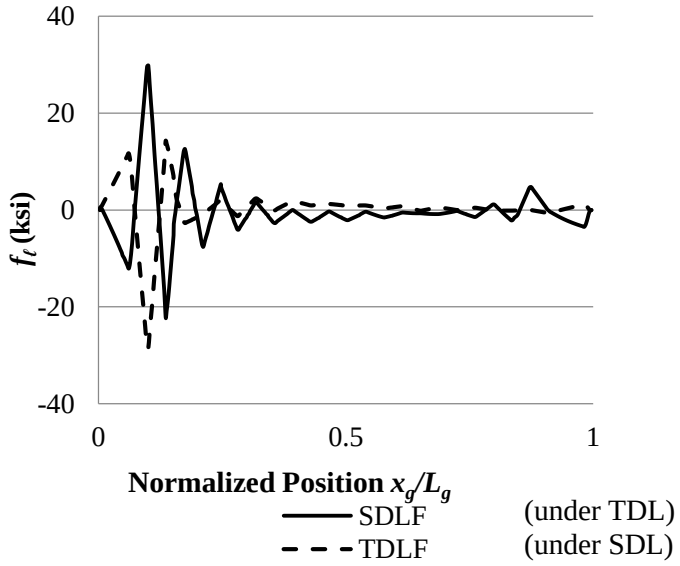

Figure 125. Top flange lateral bending stresses in Bridge (J1) NISSS54 interior girder adjacent to a fascia girder under TDL with SDLF detailing and under SDL with TDLF detailing (SDLF and TDLF detailing based on LGA cambers).

6.6.1.6 Vertical Reactions

In straight bridges with parallel skew, the skew effects tend to twist the girders such that they layover in the direction towards the acute corner of the bearing lines. With NLF detailing, the vertical reactions tend to be larger on the girders near the acute corner and smaller on the girders near the obtuse corner along each of the skewed bearing lines, except that the reaction for the fascia girders can be opposite to this trend. Table 39 shows the corresponding results for Bridge (J1) NISSS54. In this bridge case, because of the severe nuisance transverse stiffness along the short direction between the obtuse corners of the span, the fascia girder reactions at the obtuse corners are substantially larger than the other reactions if NLF detailing is used. SDLF and TDLF detailing based on LGA cambers substantially reduce these large reactions.

With SDLF and TDLF detailing based on LGA cambers, the girders in straight skewed bridges behave as line girders under the targeted load condition. The vertical reactions can be calculated accurately with LGA for each of the girders in this condition – SDL for SLDF and TDL for TDLF, but they cannot be calculated accurately with LGA in any other condition. This statement of course applies to all the other bridge DL responses as well. The reactions for SDLF under TDL can be calculated as the sum of the LGA SDL reactions and NLF RA CDL reactions. The reactions for TDLF under SDL can be calculated as the sum of the LGA TDL reactions and the negative of the NLF RA CDL reactions.

Table 39. Bridge (J1) NISSS54 vertical reactions (kips) (G1 and G9 are fascia girders, bearing locations experiencing uplift are highlighted by dark shading), detailing based on LGA cambers.

Girder	Detailing Method	SDL Support 1	SDL Support 2	TDL Support 1	TDL Support 2
G1	NLF	387	145	833	329
	SDLF	138	145	588	323
	TDLF	**Uplift**	140	304	314
G2	NLF	61	171	133	367
	SDLF	160	157	231	353
	TDLF	100	145	345	341
G3	NLF	121	174	267	375
	SDLF	157	157	302	359
	TDLF	233	139	343	343
G4	NLF	94	127	202	279
	SDLF	159	158	270	309
	TDLF	232	192	345	344
G5	NLF	109	109	238	238
	SDLF	158	158	288	288
	TDLF	209	209	344	344
G6	NLF	127	94	279	201
	SDLF	158	159	309	269
	TDLF	192	233	344	345
G7	NLF	174	121	375	267
	SDLF	157	158	360	302
	TDLF	139	233	343	343
G8	NLF	170	63	366	139
	SDLF	157	160	353	234
	TDLF	145	98	342	347
G9	NLF	146	384	330	828
	SDLF	144	137	323	584
	TDLF	139	**Uplift**	313	302

From Table 40, it can be observed that the largest maximum absolute and percentage increases in the TDL reactions are 98 kips and 74 % respectively, due to SDLF detailing based on LGA cambers, for the straight bridges with parallel skew considered in this research. This occurs in Bridge (J1) which has substantial nuisance transverse stiffness. The maximum absolute and percentage increases in the TDL reactions are 212 kips and 159 % respectively, also in this bridge, due to TDLF detailing based on LGA cambers.

From Table 40, it can also be observed that the largest maximum absolute and percentage decreases in the TDL reactions are 245 kips and 29 % respectively, due to SDLF detailing based on LGA cambers, for the straight bridges with parallel skew considered in this research. This occurs in Bridge (J1) which has substantial nuisance transverse stiffness. The maximum absolute and percentage decreases in the TDL reactions are 529 kips and 64 % respectively, also in this bridge, due to TDLF detailing based on LGA cambers. It is evident from Tables 39 and 40 that with TDLF detailing based on LGA cambers, uplift may occur at the obtuse corner on the fascia girder bearings, particularly during the erection of the steel. This uplift force is exacerbated with longer spans and sharper skews. In addition, uplift at the supports is more likely to occur with contiguous framing arrangements and staggered framing arrangements with small stagger distances and small offsets from the skewed bearing lines (i.e., when the bridge has highly stiff transverse load paths). These issues are relieved by the recommended CF framing arrangements discussed in Chapter 7. Bridge (J2) is an illustration of these framing arrangement recommendations. This bridge substantially reduces the maximum absolute and percentage decreases in the TDL reactions to 75 kips and 19%, respectively due to TDLF. However, for SDLF, the

maximum absolute and percentage decreases in the TDL reactions are only 33 kips and 8%.

Table 40. Summary of maximum absolute and percentage increases and decreases in the TDL vertical reactions at the girder bearings, due to SDLF and TDLF detailing based on LGA cambers, in the straight skewed bridges (the largest of these maximum absolute and percentage increases decreases are highlighted by dark shading).

Bridge	SDLF				TDLF			
	Decreases		Increases		Decreases		Increases	
	Max (kips)	Max %	Max (kips)	Max %	Max (kips)	Max %	Max (kips)	Max %
(I1) NISSS14	-27	-12	12	16	-182	-50	48	65
(I2) NISSS14	-11	-7	9	11	-50	-29	41	51
(J1) NISSS54	**-245**	**-29**	**98**	**74**	**-529**	**-64**	**212**	**159**
(J2) NISSS54	-33	-8	16	5	-75	-19	35	12
(K1) EICSS12	-1	-2	1	1	-6	-9	4	6
(K2) EICSS12	-1	-2	1	1	-6	-7	3	5
(K3) EICSS12	-1	-2	1	1	-4	-7	3	5
(L) NICSS16	-5	-5	3	5	-25	-27	16	29
(M1) EICSS2	-45	-8	67	28	-139	-23	205	85
(M2) EICSS2	-28	-5	22	6	-88	-16	67	18

6.6.2 Summary and Recommendations – Straight Bridges with Parallel Skew and Cambers Set Based on LGA

The influence of SDLF and TDLF detailing on the responses in completed straight bridge systems with parallel skew and girder cambers calculated based on LGA may be summarized as follows. Recommendations pertaining to these quantitative results are highlighted in bold italicized text.

General

- Straight bridges with a difference in the skew angles at the ends of all the spans less than or equal to $\Delta\theta = 20^{o}$ may be considered as parallel skew bridges.
- The use of LGA for setting the girder cambers in sharply skewed straight bridges is generally discouraged based on the considerations discussed in Section 6.2.3.

Girder Elevations

- The use of LGA to calculate the vertical displacements associated with the CDL, for SDLF, or associated with the TDL, for NLF, results in measurable elevation errors. For the most extreme bridge case considered in this research, (I1) NISSS14, the largest deviation from the targeted elevations under TDL is 2.7 inches for SDLF detailing and 3.5 inches for NLF detailing when LGA is used for all of the vertical deflection calculations. Bridge (J1) NISSS54 has corresponding deviations from the targeted elevations under TDL of 2.0 inches for SDLF and 3.5 inches for NLF.
- The largest deviation from the targeted elevations under TDL is 0.3 inches, corresponding to Bridge (J2) NISSS54, when TDLF detailing based on LGA cambers is employed. These deviations from the targeted elevations are due to the incidental effects discussed earlier in Section 6.2.2.

- ***Based on these findings, it is recommended that LGA alone should not be utilized for calculation of the girder total cambers in straight bridges with parallel skew, unless TDLF detailing is employed.***
- If the girder total camber for SDLF is calculated based on the SDL camber from LGA plus the negative of the CDL deflections from RA, then the largest deviation from the targeted elevations under TDL is reduced to 0.4 inches for the most extreme case considered in this research, Bridge (J1) NISSS54.
- ***Based on these findings, it is recommended that, if LGA is used for calculating the girder cambers in straight bridges with parallel skew, the girder TDL cambers should be calculated as follows:***
    - ***For TDLF, the negative of the girder TDL vertical deflections obtained from the LGA.***
    - ***For SDLF, the negative of the girder SDL vertical deflections obtained from the LGA plus the negative of the CDL vertical deflections obtained from a NLF RA.***

Girder Layovers

- All the straight bridges with parallel skew considered in this research exhibit practically zero layover under TDL, for TDLF, when the TDL camber is based on LGA.
- All the straight bridges with parallel skew considered in this research exhibit practically zero layover under SDL, for SDLF, when the SDL camber is based on LGA.
- The calculated girder non-zero layovers under the SDL for TDLF, and under the TDL for SDLF, are very close to the theoretical values.
- ***It is recommended that the girder layovers may be assumed to be negligible in the targeted DL condition in straight bridges with parallel skew when the CFs are***

detailed using the above recommended procedures with LGA. The fascia girders should be checked separately for twist rotation between the CF locations due to eccentric overhang bracket loads.

- ***For straight bridges with parallel skew, detailed for SDLF using the above recommended procedures with LGA, the girder layovers under the TDL may be estimated as the CDL layovers obtained from a NLF RA.***
- ***For straight bridges with parallel skew, detailed for TDLF using the above recommended procedures with LGA, the girder layovers under the SDL may be estimated as the negative of the CDL layovers obtained from a NLF RA.***

Cross-Frame Forces

- Under SDL, the largest ratio of the average of the CF member forces for SDLF detailing (in each bridge) to the corresponding forces for NLF detailing is 0.48 (in straight bridges with parallel skew, when the CFs are detailed using the above recommended procedures with LGA). This ratio corresponds to the bridge with the next to the largest skew index of all the bridges studied, (I2) NISSS14. The CF forces are substantially reduced by an improved framing arrangement (and are thus relatively small) in this particular bridge. The above ratio is close to zero for nearly all of the other bridges studied. The next largest value is 0.25.
- Under SDL, the largest ratio of the maximum CF member force (in each bridge) for SDLF detailing to the corresponding force for NLF detailing is 0.31. That is, the beneficial locked-in force is 1.0 – 0.31 = 0.69 of the CF force corresponding to NLF detailing for this member.

- Under TDL, the largest ratio of the average of the CF member forces for TDLF detailing (in each bridge) to the corresponding forces for NLF detailing is 0.48. These values are greater than or equal to 0.12 for all but one of the other bridges studied. The larger ratios correspond to cases with smaller NLF CF forces.
- Under TDL, the largest ratio of the maximum CF member force for TDLF detailing to that for NLF detailing, is again 0.31. Many of the other bridges have similar maximum values. That is, the beneficial locked-in force is 1.0 – 0.31 = 0.69 of the CF force corresponding to NLF detailing for this member.
- The statistics for the percent change in the individual CF member forces relative the member yield load due to SDLF and TDLF detailing indicate a wide range (dispersion) of individual CF member force effects, but a predominant tendency for reduction of the CF member forces in parallel-skew straight bridges due to SDLF and TDLF detailing.
- There is a substantial reduction in the maximum CF member forces, particularly for bridges with a nuisance transverse stiffness problem, by the use of SDLF and TDLF detailing. The reduction due to TDLF is as large as 345 kip under the TDL in the most extreme case, Bridge (J1) NISSS54. Using the recommended improved framing arrangements, as shown for Bridge (J2) NISSS54, results in a further significant reduction in the overall magnitude of the CF forces.
- ***In lieu of a DLF RA, it is recommended that a net load factor of (γ_p – 0.65) be used for determination of the factored SDL CF forces in straight I-girder bridges with parallel skew, when the CFs are detailed for SDLF using the above recommended procedures with LGA. This net load factor is to be applied to the results from a NLF RA for the SDL. It should be noted that these SDL CF forces must be added to the***

factored CDL CF forces from a NLF RA to obtain the total factored DL CF forces. The factor of 0.65 is a slightly conservative estimate of the above SLDF locked-in force ratio of 1.0 – 0.31 = 0.69.

- ***In lieu of a DLF RA, it is recommended that a net load factor of (γ_p – 0.65) be used for determination of the factored TDL CF forces in straight I-girder bridges with parallel skew, when the CFs are detailed for TDLF using the above recommended procedures with LGA. This net load factor is to be applied to the results from a NLF RA for the TDL. The factored CF forces under the SDL may be estimated by subtracting the factored CDL CF forces obtained by a NLF RA from the above factored TDLF forces.*** The factor of 0.65 is a conservative estimate of the above TDLF locked-in force ratio of 1.0 – 0.31 = 0.69. In cases where additional uncertainties and variabilities associated with TDLF are anticipated, such as incidental participation of deck forms and early concrete stiffness in the structural resistance, and/or larger potential play in the CF connections due to the larger CF forces associated with TDLF, it is suggested that a value between 0.65 and 0.50 may be used for the above locked-in force estimate based on the judgment of the engineer of record. This suggested reduction is based on the judgement of the research. The current research did not perform any specific investigations of the above effects.
- The maximum difference in the magnitude of the individual CF member forces from a DLF RA and (1 – 0.65 = 0.35) of the estimated values from a NLF RA, normalized by the member yield load, is 1.1 and 4.8 %, and the average difference is -0.5 and -1.4 %

for SDLF under SDL and TDLF under TDL, respectively, for the straight parallel skew bridges studied in this research and girder cambers based on LGA.

Girder Stresses

- For SDLF detailing, the largest girder flange lateral bending stress (f_ℓ) under SDL is 1.2 ksi for all the straight parallel-skew bridges studied when the CFs are detailed based on LGA using the above recommended procedures. This stress is theoretically equal to zero. The above stress occurs in the fascia girders of Bridge (I2) NISSS14 and is 48 % of the corresponding f_ℓ for NLF detailing. The next largest f_ℓ in the straight parallel-skew bridges studied, under SDL for SDLF, is 0.9 ksi (11 % of the corresponding f_ℓ for NLF detailing) and occurs in an interior girder of Bridge (I1) NSSS14. All the other bridge maximum girder f_ℓ values, under SDL for SLDF, are 0.6 ksi or smaller.
- For TDLF detailing, the largest girder f_ℓ under the TDL is 4.7 ksi for all the straight parallel-skew bridges studied when the CFs are detailed based on LGA using the above recommended procedures. This stress is theoretically equal to zero if the overhang eccentric bracket loads are not included in the structural analysis; however these loads are included in the TDLF-TDL values presented in this research. The above stress occurs in the fascia girders of (I1) NISSS14 and is 18 % of the corresponding f_ℓ for NLF detailing. The next largest girder $f_\ell$values in the straight parallel-skew bridges studied, under TDL for TDLF, are 4.4 ksi in the fascia girders of (I2) NISSS14 (59 % of the corresponding f_ℓ for NLF detailing), 2.7 ksi in the fascia girders of Bridge (L) NICSS16 (68 % of the corresponding f_ℓ for NLF detailing), 3.8 ksi in an interior girder of (I1) NISSS14 (10 % of the corresponding f_ℓ for NLF detailing), and 2.5 ksi in an interior girder of (I2) NISSS14 (4 % of the corresponding f_ℓ for NLF detailing). All of

the other maximum girder f_ℓ values are less than 2 ksi in all the straight parallel-skew bridges studied in this work.

- For all the bridges studied in this research, the use of an assumed locked-in f_ℓ of 0.65 of the f_ℓ from a NLF RA gives an accurate to conservative estimate of the f_ℓ values determined from a DLF RA.

- ***In lieu of a DLF RA, for straight bridges with parallel skew and with the CFs detailed for SDLF using the above recommended procedures with LGA, it is recommended that the above procedures for calculation of the CF forces also be used for determining the girder f_ℓ values.***

- For both SDLF and TDLF, the changes in the girder major-axis bending stresses (f_b) due to the effects of the CF detailing using the LGA cambers are substantial. The recommended framing arrangements that relieve nuisance transverse stiffness effects dramatically reduce the magnitude of these changes. In these cases, the deflections of the 3D bridge system obtained from NLF RA are much closer to the deflections obtained from LGA.

- The above substantive change in the girder major-axis bending stresses is because, for the targeted SDL or TDL condition, the lack-of-fit due to the DLF detailing with LGA cambers actually modifies the vertical displacements of the girders in the 3D system to the displacements associated with the LGA. This behavior is captured by a DLF RA, but is neglected by a NLF RA.

- The solution for f_b from a NLF RA can be substantially in error in sharply skewed bridges when the DLF detailing is based on LGA cambers.

- LGA gives accurate f_b values for the targeted DL condition – SDL for SDLF and TDL for TDLF.
- ***In lieu of a DLF RA, for straight bridges with parallel skew and with the CFs detailed using the above recommended procedures with LGA, it is recommended that the girder f_b values in the targeted DL condition be taken as the values from the LGA.***
- ***In lieu of a DLF RA, for straight bridges with parallel skew and with the CFs detailed for SDLF using the above procedures with LGA, the girder f_b values under the TDL may be estimated by adding the CDL f_b values obtained from a NLF RA to the SDL f_b values obtained from LGA.***
- ***In lieu of a DLF RA, for straight bridges with parallel skew and with the CFs detailed for TDLF using the above recommended procedures with LGA, the girder f_b values under SDL may be estimated by subtracting the CDL f_b values obtained from a NLF RA from the TDL f_b values obtained from LGA.***
- The above procedures for calculating the girder f_b values differ from the recommended procedures for calculating the CF forces and the girder f_ℓ values. The CF force and f_ℓ procedures are more conservative based on the recognition that although the theoretical CF forces and girder flange lateral bending stresses are zero in the targeted DL condition, various incidental effects can result in measurable non-zero values for these forces and stresses.

Vertical Reactions

- The results for the girder reactions largely parallel the above results for the girder major-axis bending stresses.
- ***In lieu of a DLF RA, for straight bridges with parallel skew and with the CFs detailed using the above recommended procedures with LGA, it is recommended that the girder reactions in the targeted DL condition be taken as the values from the LGA.***
- ***In lieu of a DLF RA, for straight bridges with parallel skew and with the CFs detailed for SDLF using the above recommended procedures with LGA, the girder reactions under the TDL may be estimated by adding the CDL reactions obtained from a NLF RA to the SDL reactions obtained from LGA.***
- ***In lieu of a DLF RA, for straight bridges with parallel skew and with the CFs detailed for TDLF using the above recommended procedures with LGA, the girder reactions under SDL may be estimated by subtracting the CDL reactions obtained from a NLF RA from the TDL reactions obtained from LGA.***

The above recommendations are considered applicable for straight bridges with parallel skew up to 70^{o} and spans up to 300 ft. These limits are different from those listed in the tables for recommended fit conditions discussed in Section 11.1. The limits here are aimed at ensuring sufficient accuracy of the structural analysis whereas the limits discussed in Section 11.1 address broader questions of ensuring reliable fit-up of the structural steel.

For bridges that exceed these limits, it is recommended that DLF RA be considered. Chapter 3 explains the details of several procedures for conducting a DLF RA.

6.7 Straight Bridges with Parallel Skew and Cambers Set Based on NLF RA

Straight bridges with a difference in the skew angles at the ends of all the spans less than or equal to $\Delta\theta = 20^o$ may be considered as parallel skew bridges. This section studies a limited number straight bridges with parallel skew and cambers set based on NLF RA. These bridge cases are (I1) and (I2) NISSS14 and (J1) and (J2) NISSS54. These are the critical cases of all the straight parallel-skew bridges studied in this research. Section 6.7.1 provides quantitative results on the influence of SDLF and TDLF detailing on bridge responses in these bridges with cambers set based on NLF RA. The influence of SDLF and TDLF is discussed on the responses in the following order: girder vertical displacements, girder elevations, girder layovers, CF forces, girder stresses, and vertical reactions. Section 6.7.2 then summarizes the influences on the key bridge responses, and provides recommendations for handling these effects. The recommendations are highlighted in bold italicized text.

6.7.1 Quantitative Results

6.7.1.1 Girder Vertical Displacements

For straight bridges with parallel skew and cambers set based on NLF RA, SDLF and TDLF detailing tend to reduce the vertical displacement of the fascia girders and increase the vertical displacement of the interior girders. The increase or decrease in the vertical displacements when the cambers are based on NLF RA is not as significant as when the cambers are based on LGA. This is because when the cambers are set based on NLF RA, the resulting targeted DL elevations are essentially the "natural" deflected elevations of the girders under the targeted DL in the 3D structural system. As such, the girders are subjected predominantly just to twist rotations to move them from their deflected out-of-plumb

geometry in the 3D system to their approximately plumb targeted DL geometry, via the DLF detailing effects. The girder twisting is accomplished with relative ease when the straight girders are in this "natural" deflected geometry.

Figure 126 shows the fascia and middle girder TDL vertical displacements in Bridge (J1) NISSS54 if the CFs are detailed for TDLF based on the cambers calculated from NLF RA (calculated using the common practice of constructing a model of the full bridge system and "turning gravity on.") In this case, the fascia girder displacements are practically unaffected by the CF detailing, while the displacements on the middle girder are only slightly affected. The maximum displacement difference between TDLF and NLF is 0.83 inches on the middle girder.

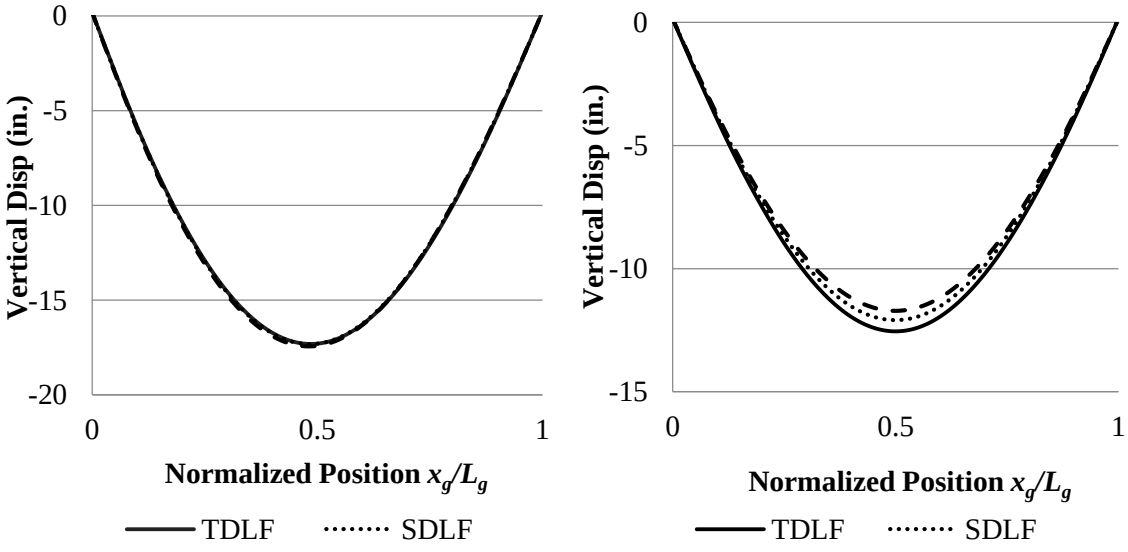

Figure 126. Bridge (J1) NISSS54 fascia girder (left) and middle girder (right) vertical displacements under TDL with the CFs detailed based on NLF RA cambers.

6.7.1.2 Girder Vertical Elevations

The girder cambers for the straight parallel-skew bridges in this section are based on NLF RA. The vertical elevations under TDL for NLF detailing are zero (assuming no

superelevation, etc., as a simplification). Figures 127 and 128 show the results for the girder TDL elevations in Bridge (I1) NISSS14 and (J1) NISSS54, respectively, with all of the calculations conducted by NLF RA. The deviations from the targeted deviations in bridge cases (I1) and (J1) are larger than bridge cases (I2) and (J2) since (I1) and (J1) have substantially larger nuisance transverse stiffness. As one might expect, the elevations are the exact "zero" values for NLF detailing, since the bridge responds in this case as if the gravity loads were simply "turned on." The vertical elevations deviate slightly from the targeted zero values for SDLF detailing, and the deviations are somewhat larger for the case of TDLF detailing. Bridge (J1) exhibits a maximum deviation of 0.8 inches from the targeted DL elevations for TDLF. Bridge (I1) exhibits a maximum deviation of 1.4 inches from the targeted DL elevations for TDLF.

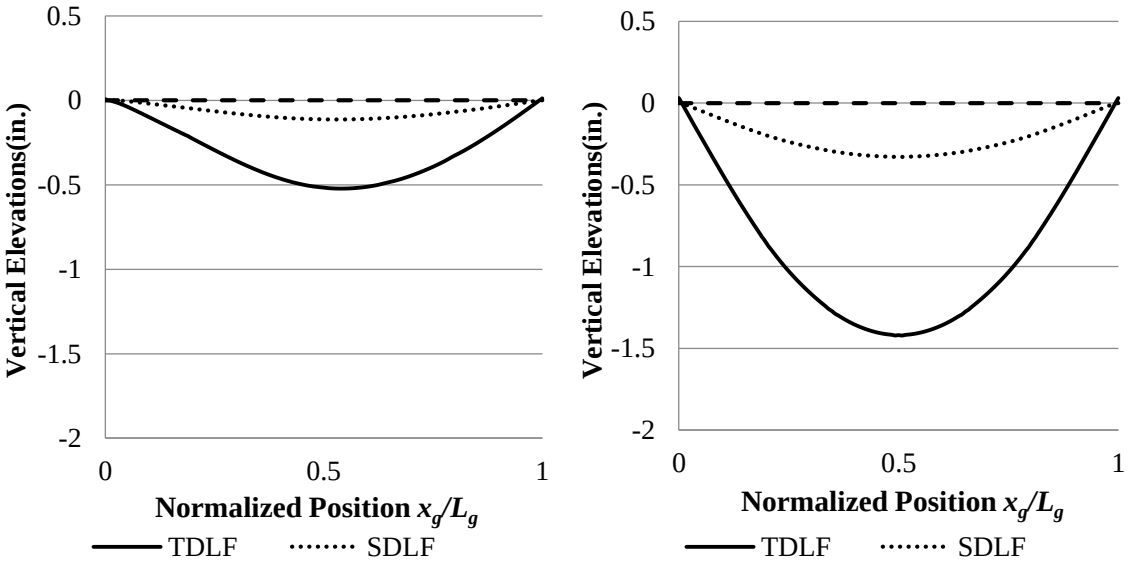

Figure 127. Bridge (I1) NISSS14 fascia girder (left) and middle girder (right) vertical elevations under TDL with the CF detailed based on 3D FEA and the girder TDL cambers based entirely on 3D FEA

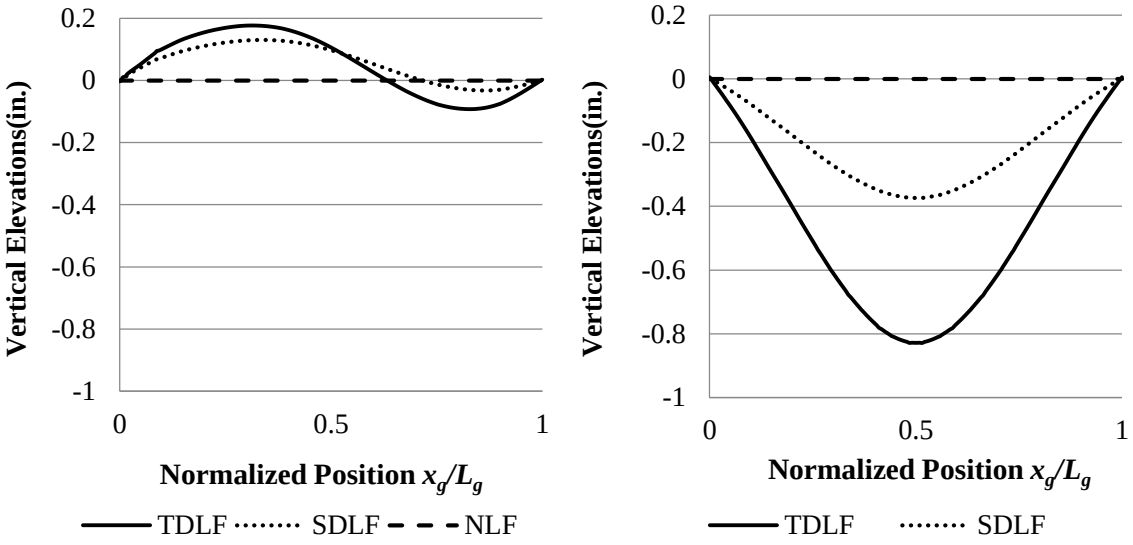

Figure 128. Bridge (J1) NISSS54 fascia girder (left) and middle girder (right) vertical elevations under TDL with the CF detailed based on 3D FEA and the girder TDL cambers based entirely on 3D FEA

6.7.1.3 Girder Layovers

In straight skewed bridges, SDLF and TDLF detailing based on RA cambers still gives approximately plumb webs under the targeted condition. However, the layovers are no longer theoretically zero under the targeted condition. This is due to the overall elastic deformations of the CFs and the elastic torsional deformations of the girders in the structural system. There is only one set of cambers and corresponding CF drops that gives theoretically exactly plumb webs for straight skewed bridges – the LGA cambers.

Figure 129 shows the fascia girder layovers under TDL for Bridge (J1) NISSS54 based on NLF RA. Table 41 shows the maximum girder layovers and twists in the critical straight parallel-skewed Bridge (I2) NISSS14. This bridge has the largest layovers in the straight parallel-skewed bridge cases based on NLF RA cambers studied in this section.

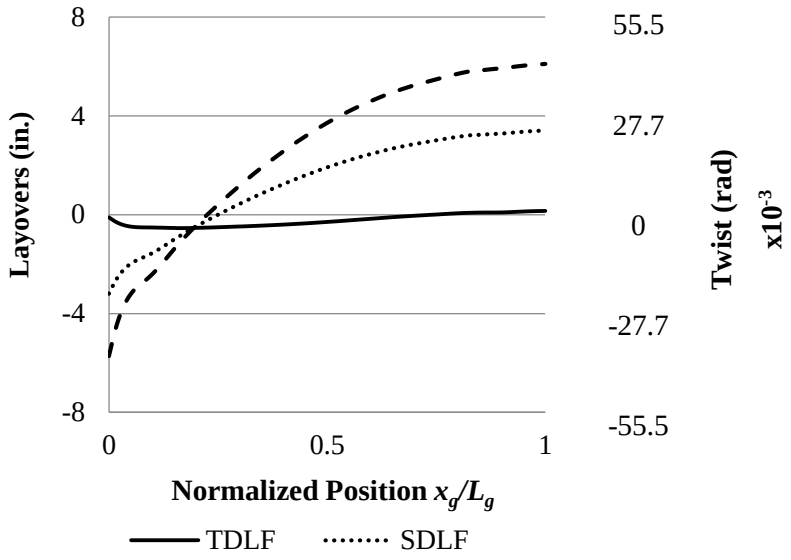

Figure 129. TDL fascia girder layovers Bridge (J1) NISSS54 for detailing based on NLF RA.

Table 41. Maximum magnitudes of girder layovers and twists in the critical straight parallel-skewed Bridge (I2) NISSS14 with CFs detailed entirely based on NLF RA cambers. (LO1, LO2, and LO3 are maximum girder layovers with NLF, SDLF, and TDLF detailing, respectively. ϕ1, ϕ2, and ϕ3 are maximum girder twists with NLF, SDLF, and TDLF detailing, respectively).

Load Cond.	Girder Depth (in.)	NLF		SDLF		TDLF	
		LO1 (in.)	ϕ1 (rad) x10^{-3}	LO2 (in.)	ϕ2 (rad) x10^{-3}	LO3 (in.)	ϕ3 (rad) x10^{-3}
SDL	72	0.7	9.7	0.1	1.4	2.6	36.1
TDL	"	3.2	44.4	2.6	36.1	0.6	8.3

6.7.1.4 Cross-Frame Forces

In straight skewed bridges, SDLF and TDLF detailing based on RA cambers gives small CF forces under the targeted condition. However, the CF forces are no longer theoretically zero under the targeted condition due to the overall elastic deformations of the CFs and the elastic torsional deformations of the girders in the structural system. Table 42 shows the average and maximum magnitude of the CF forces for the critical bridge

cases (J1) and (J2) NISSS54. There is clearly a substantial reduction in the average of the CF member forces as well as in the maximum CF member force due to SDLF and TDLF with RA cambers for the straight parallel skew bridges considered in this research, in cases where the CF member forces are relatively large due to nuisance transverse stiffness effects. However, for the alternate framing plans where the CF forces are significantly reduced, the effect of SLDF or TDLF detailing with RA cambers on the CF forces is relatively erratic.

It is apparent that given the reductions in the cross-frame forces due to the improved framing arrangement in Bridge (J2), the incidental effects discussed in Section 6.2.2 combined with the influence of the elastic deformations of the CFs and elastic torsional deformations of the girders within the 3D bridge system has a substantial influence on these smaller CF forces for SDLF. As a result, under SDL, the largest ratio of the average of the CF member forces for SDLF detailing with RA cambers to the corresponding average force for NLF detailing is 1.28 in Table 30. As such, the estimation of the CF forces from DLF RA as simply 1.0 of the NLF RA results is considered below for SDL/SDLF. Under TDL, the largest ratio of the maximum CF member force for TDLF detailing with RA cambers to the corresponding force for NLF detailing is 0.55, corresponding to Bridge (J2). Therefore, the estimation of the CF forces from DLF RA as 0.6 of the NLF RA results is considered below for TDL/TLDF.

Figure 130 shows the actual distribution of the CF forces under the SDL in Bridge (J2) NISSS54, including the locked-in force effects from SDLF detailing with NLF RA cambers. The presentation of the CF forces in these plots, as well as the plots in the subsequent figures is similar to that Section 6.5.1.4. The reader is referred to this previous

section for an explanation of these details. One can observe that the largest of the CF member forces in Figure 130 is approximately 31 kips.

Table 42. Average and maximum magnitude of the CF member forces in the critical bridge cases (J1) and (J2) NISSS54 (F1, F2, and F3 are the average and maximum CF forces with NLF, SDLF, and TDLF detailing based on NLF RA cambers, respectively). The largest F2/F1 ratio under SDL for SDLF and F3/F1 ratio under TDL for TDLF are highlighted by dark shading.

	Load Cond.	Bridge	NLF	SDLF		TDLF	
			F1 (kip)	F2 (kip)	F2/F1	F3 (kip)	F3/F1
Avg	SDL	(I2) NISSS14	3.3	2.3	0.70	10.8	3.27
		(J1) NISSS54	19.4	7.4	0.38	13.9	0.72
		(J2) NISSS54	5.7	7.3	**1.28**	8.9	1.56
	TDL	(I2) NISSS14	13.9	12.5	0.90	9.5	**0.68**
		(J1) NISSS54	42.9	29.2	0.68	16.3	0.38
		(J2) NISSS54	13.5	13.4	0.99	6.4	0.47
Max	SDL	(I2) NISSS14	29.8	15.1	0.51	45.2	
		(J1) NISSS54	162.4	31.8	0.20	252.6	1.56
		(J2) NISSS54	25.4	30.9	**1.22**	20.8	0.82
	TDL	(I2) NISSS14	130.8	116.0	0.89	63.6	
		(J1) NISSS54	354	155.8	0.44	73.6	0.21
		(J2) NISSS54	58.5	38.9	0.66	32.3	**0.55**

Figure 131 shows an estimate of the CF member forces under SDL, assuming SDLF detailing, estimated as 1.0 of the NLF RA member forces. One can observe that the maximum chord forces are slightly over-estimated – the maximum DLF RA chord force is 19.5 kips whereas the prediction from the NLF RA is 25.4 kips. However, maximum diagonal forces are somewhat under-estimated – the maximum DLF RA diagonal force is 30.9 kips while the prediction from the NLF RA is 18.9 kips. However, this difference is judged to be acceptable given the small magnitude of the forces, and given the further considerations discussed below. Similar to the results discussed for straight skewed

bridges and LGA cambers in Section 6.6.1.4, the pattern of the NLF RA CF forces is very different from that of the DLF RA forces though.

Figure 132 shows the difference between the magnitude of the DLF RA forces and the CF forces under SDL, assuming SDLF detailing, estimated by 1.0 of the NLF RA forces, divided by the CF member yield loads. One can observe that the largest under-prediction of the DLF RA results is $0.045P_y$ for several of the diagonals, while the largest over-prediction is $-0.062P_y$ on several diagonals using the suggested estimate on Bridge (J2) NISSS54. Figure 133 shows the same results as Figure 132, but under TDL and assuming TDLF detailing. The maximum under-prediction is $0.0016P_y$ and the largest over-prediction is $-0.059P_y$ for this case.

Figures 134 and 135 show comparable results to Figures 132 and 133 for the other critical Bridge (I2) NISSS14. For this bridge, the largest under-prediction is $0.011P_y$ for SDL/SDLF and $0.051P_y$ for TDL/TDLF, whereas the largest over-prediction is $-0.032P_y$ for SDL/SDLF and $-0.052P_y$ for TDL/TLDF. Similar to the previous estimates, the largest under-prediction approximately $0.05P_y$ for all the cases considered, given the CF member sizes selected in the original bridge designs.

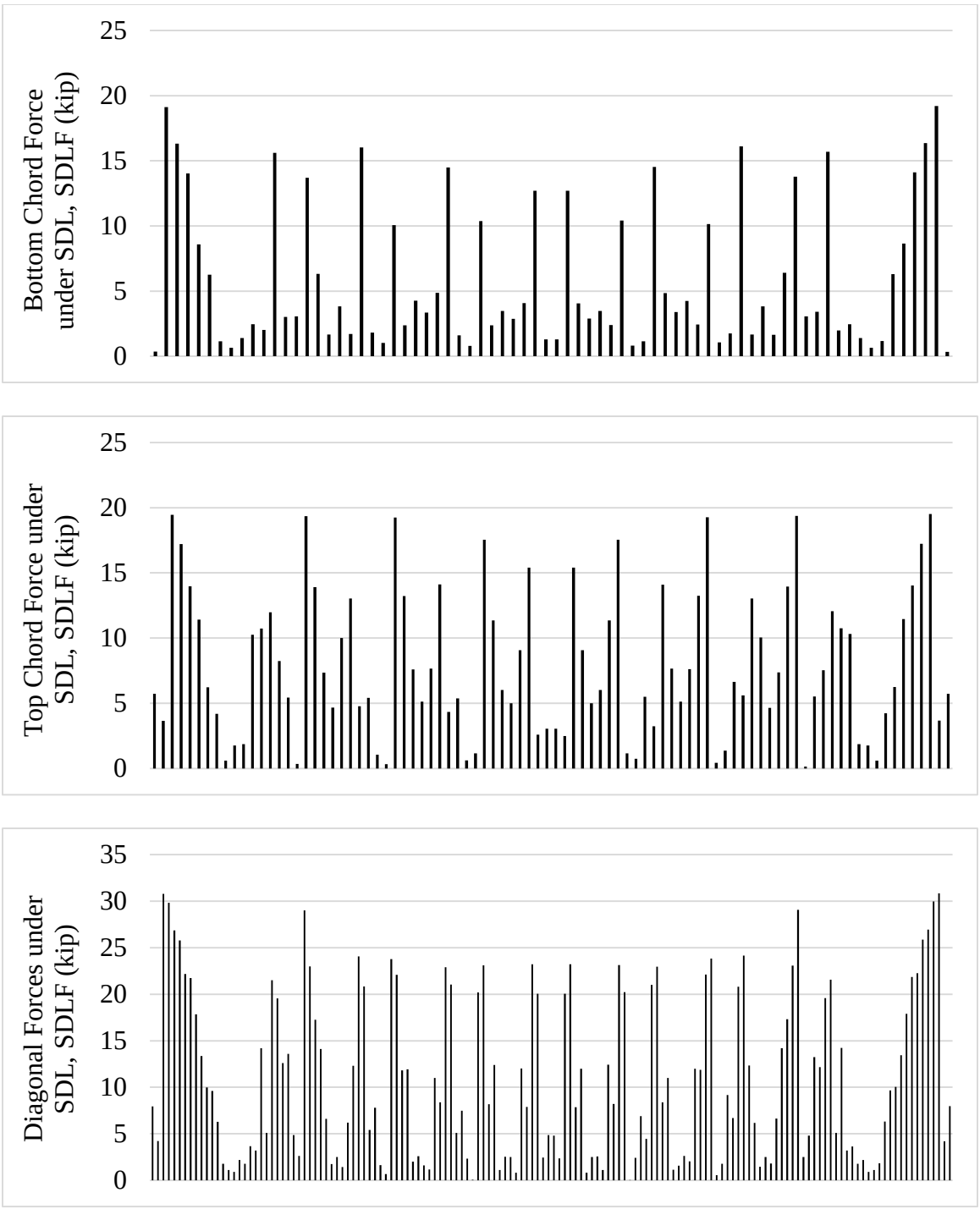

Figure 130. Magnitude of CF member forces from DLF RA, Bridge (J2) NISSS54 under SDL, SDLF detailing based on NLF RA cambers.

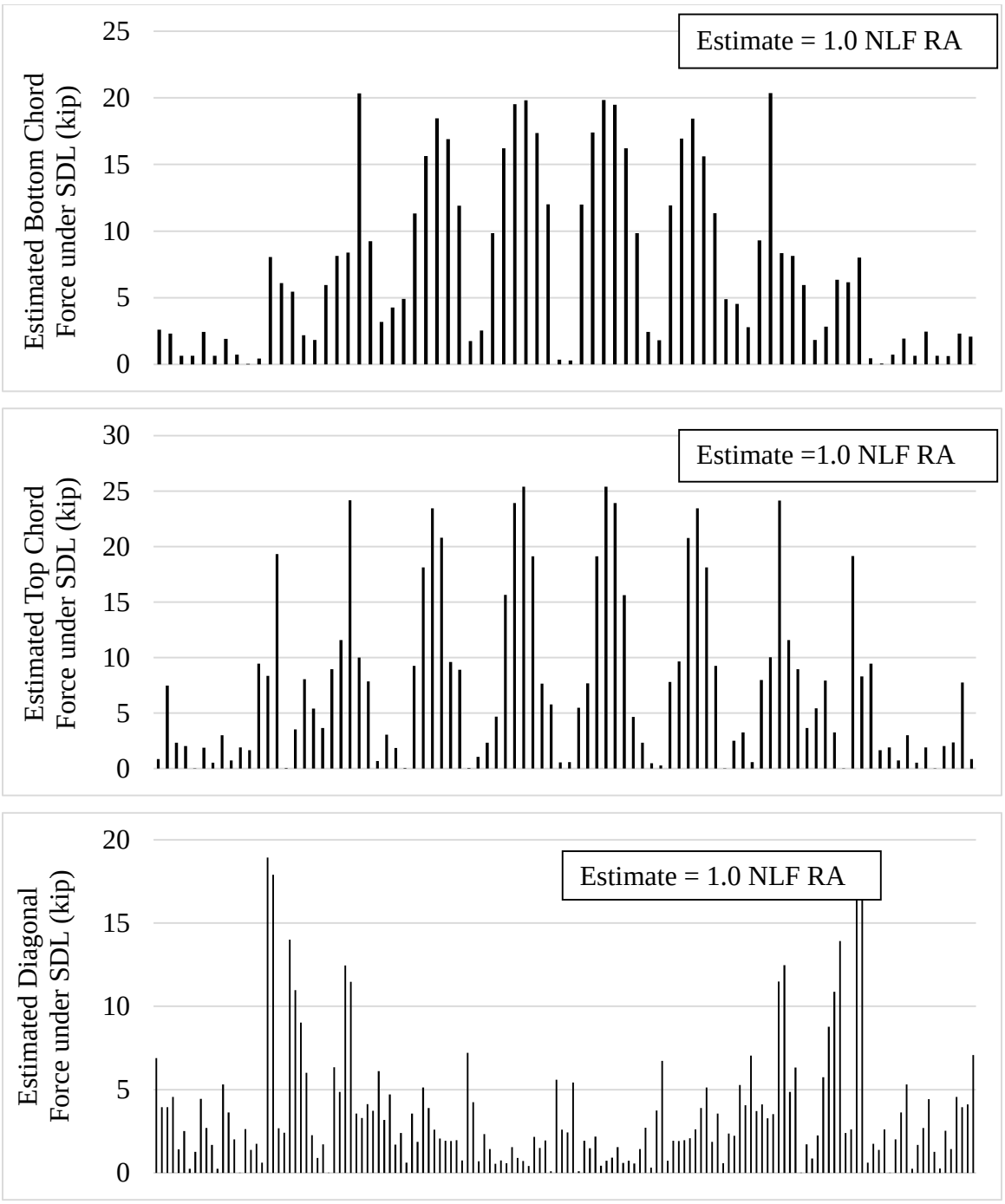

Figure 131. Estimated magnitude of CF member forces based on scaling of NLF RA results, assuming SDLF detailing, Bridge (J2) NISSS54 under SDL.

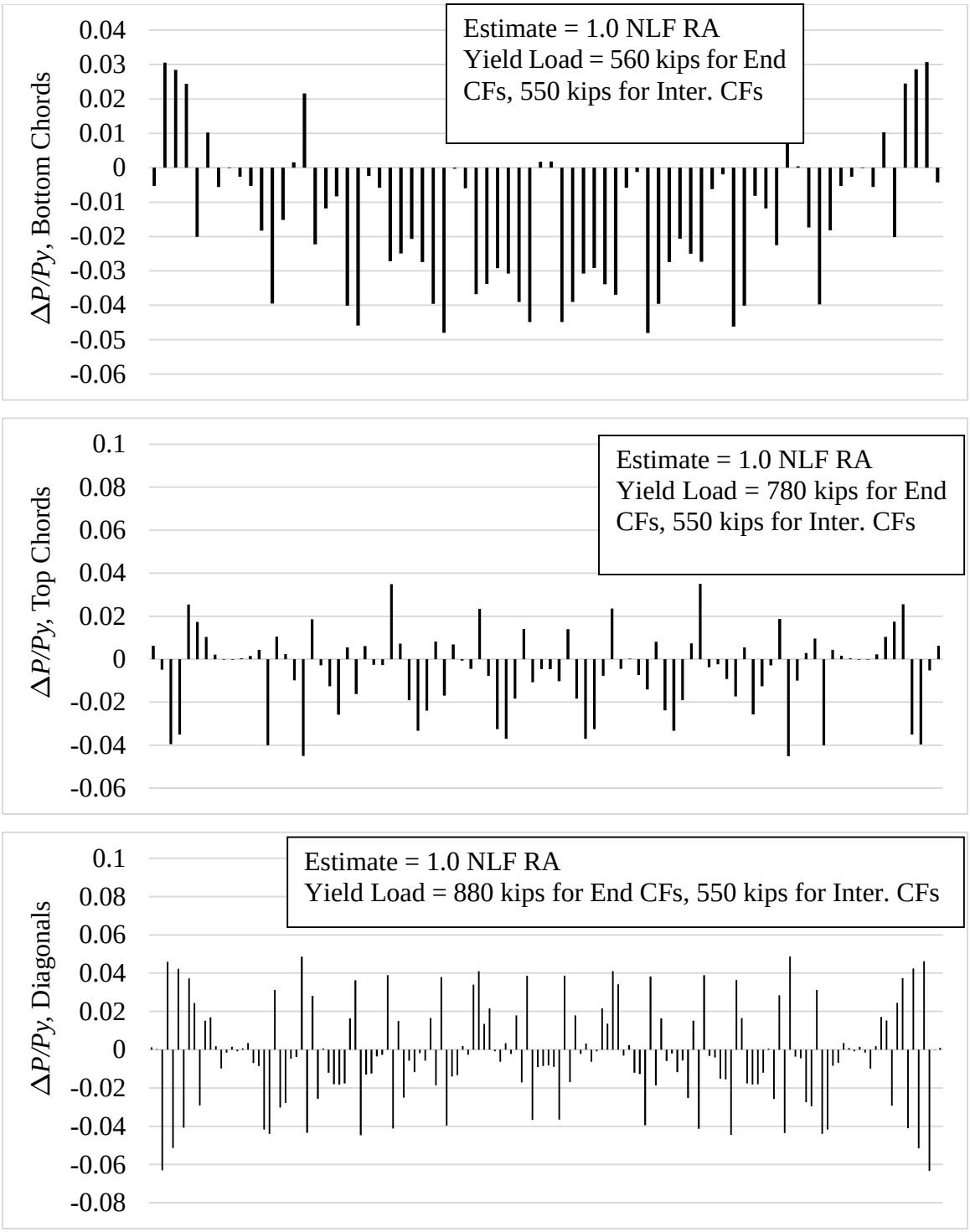

Figure 132. Difference between the magnitude of the DLF RA forces and the values estimated by scaling the NLF RA results, divided by the member yield load ($\Delta P/P_y$), Bridge (J2) NISSS54 under SDL with SDLF detailing based on NLF RA cambers.

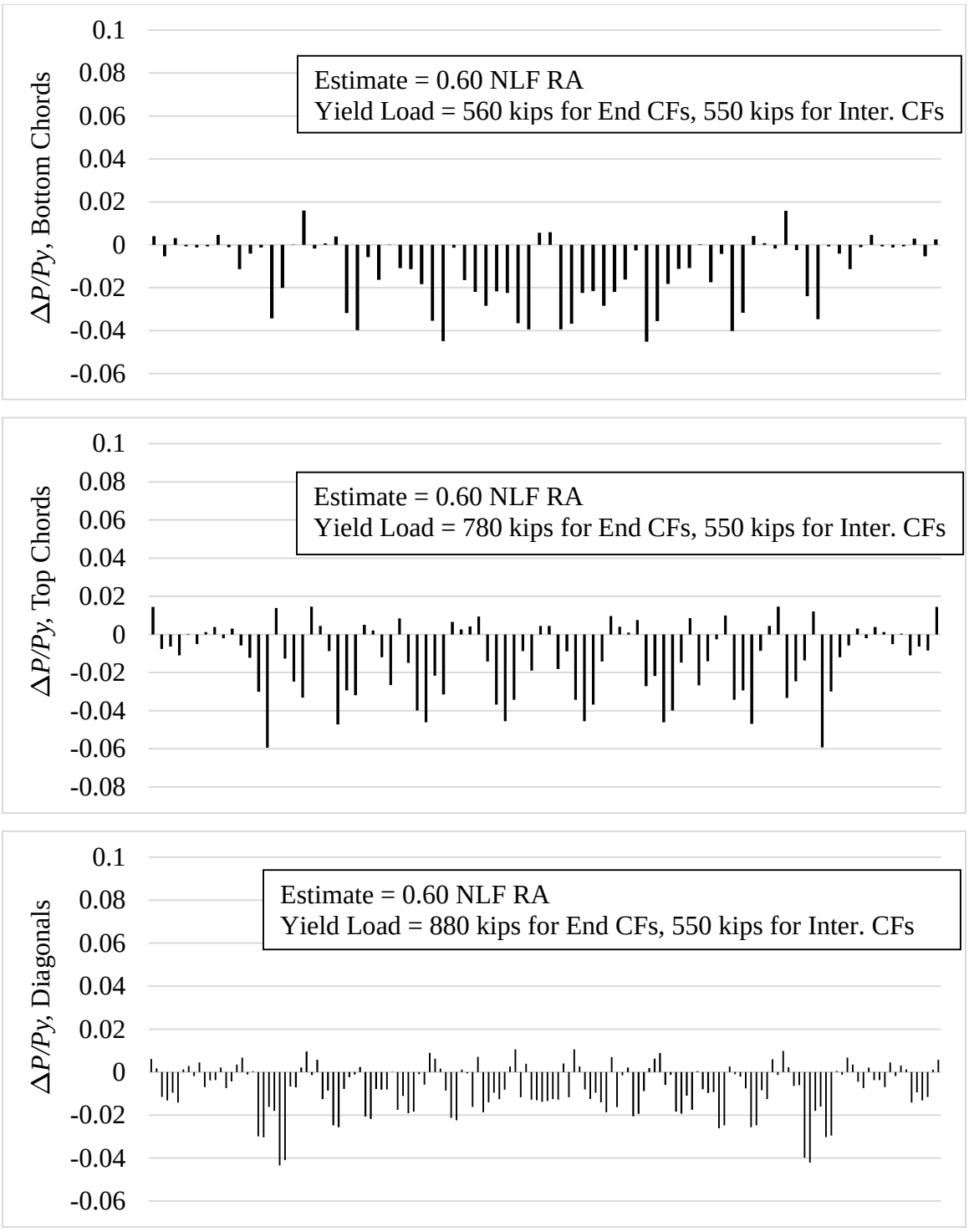

Figure 133. Difference between the magnitude of the DLF RA forces and the values estimated by scaling the NLF RA results, divided by the member yield load ($\Delta P/P_y$), Bridge (J2) NISSS54 under TDL with TDLF detailing based on NLF RA cambers.

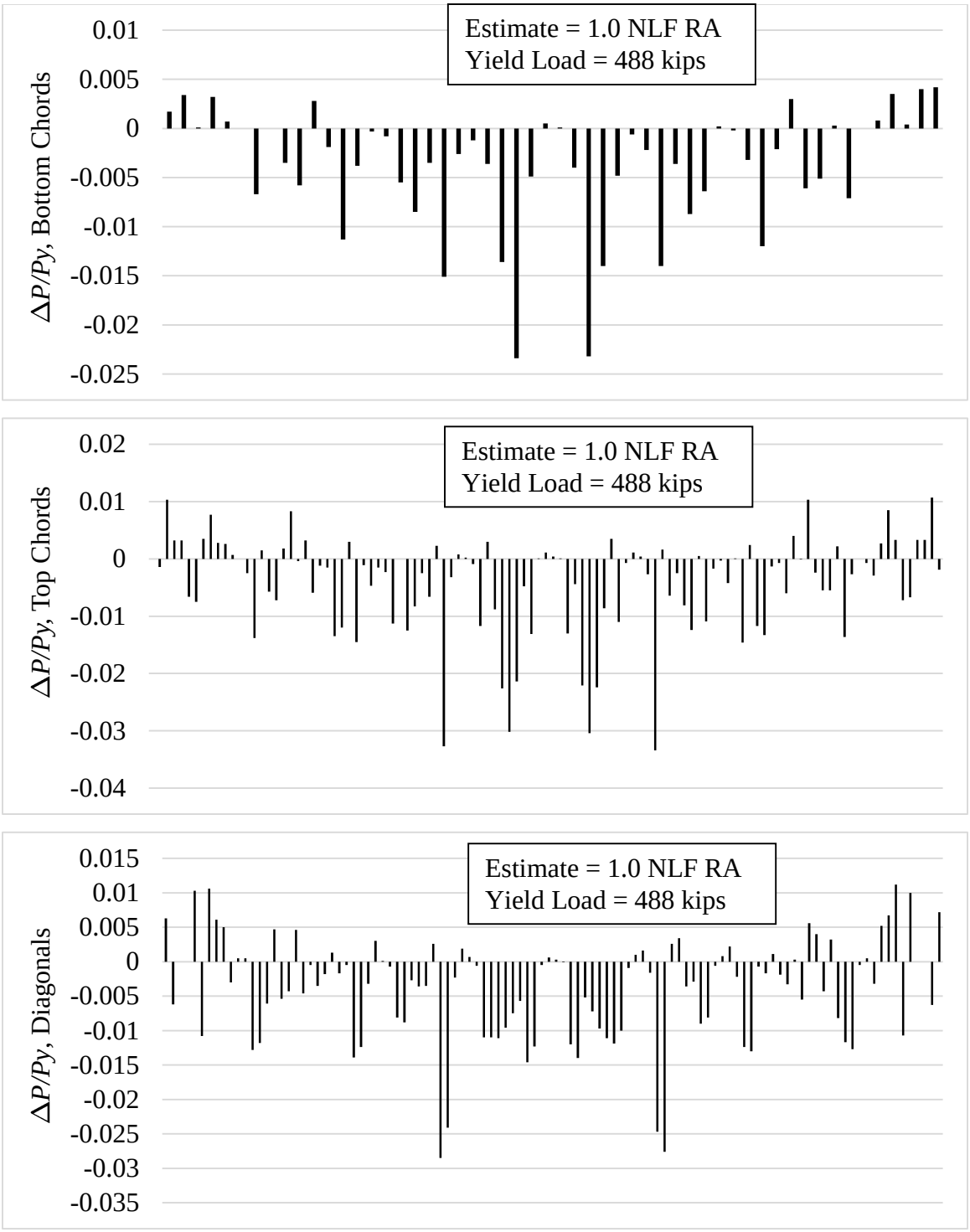

Figure 134. Difference between the magnitude of the DLF RA forces and the values estimated by scaling the NLF RA results, divided by the member yield load ($\Delta P/P_y$), Bridge (I2) NISSS14 under SDL with SDLF detailing based on NLF RA cambers.

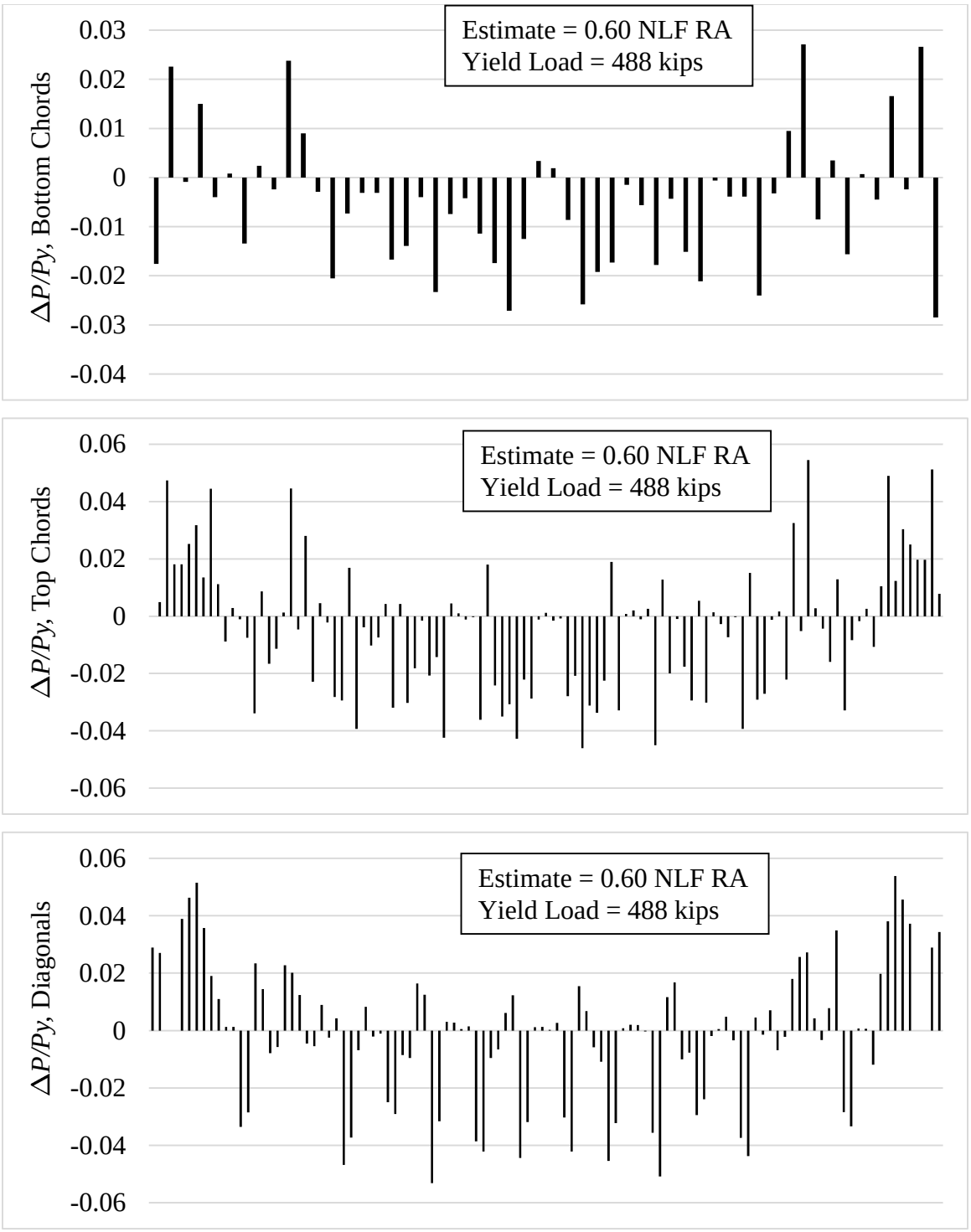

Figure 135. Difference between the magnitude of the DLF RA forces and the values estimated by scaling the NLF RA results, divided by the member yield load ($\Delta P/P_y$), Bridge (I2) NISSS14 under TDL with TDLF detailing based on NLF RA cambers.

6.7.1.5 Girder Stresses

In straight bridges with parallel skew, SDLF and TDLF detailing based on RA cambers gives small girder flange lateral bending stresses under the targeted condition. However, the girder flange lateral bending stresses are no longer theoretically zero under the targeted condition due to the overall elastic deformations of the CFs and the elastic torsional deformations of the girders in the structural system. From Table 43 and Figures 136 to 139, it can be seen that SDLF and TDLF based on NLF RA cambers give some reduction in the flange lateral bending stresses under the targeted condition relative to the NLF values. The largest ratio of the flange lateral bending stress under SDL with SDLF detailing is 49 % (4.2 ksi), corresponding to Bridge (I1). The largest corresponding value under TDL with TDLF detailing is 73 % (5.5 ksi), corresponding to Bridge (I2). However, the largest absolute flange lateral bending stresses are 4.9 ksi (39 % of the corresponding NLF RA stress, $f_{\ell 1}$) for SDL/SDLF and 22.7 ksi (37 % of $f_{\ell 1}$) for TDL/TDLF.

Figure 140 to Figure 143 show the variation in the fascia girder and innermost girder major-axis bending stresses for the different detailing methods for the most critical bridges with respect to this consideration, Bridges (I1) and (J1). For the straight parallel-skew bridges studied in this research, the largest percentage increase in any of the girder major-axis bending stresses under the TDL, due to the effect of SDLF and TDLF detailing based on NLF RA cambers, is 7 % (1.2 ksi)) and 28 % (4.7 ksi), respectively. Both of these changes in stress occur on the innermost girder on Bridge (I1) NISSS14. These changes in stress are a larger fraction of the total stress under the SDL condition.

Table 43. Maximum magnitudes of top flange lateral bending stresses of the critical fascia girder and innermost girder in the straight bridges with parallel skew studied in this research with the CFs detailed based on NLF RA cambers ($f_{\ell 1}$ is the maximum girder flange lateral bending stresses with NLF. f_{ℓ} is the maximum girder flange lateral bending stresses with SDLF under SDL and TDLF under TDL. The largest $\frac{f_{\ell}}{f_{\ell 1}}$ under SDL and TDL are highlighted by dark shading).

Load	Bridge	Fascia Girder			Innermost Girder		
		$f_{\ell 1}$ (ksi)	f_{ℓ} (ksi)	$\frac{f_{\ell}}{f_{\ell 1}}$	$f_{\ell 1}$ (ksi)	f_{ℓ} (ksi)	$\frac{f_{\ell}}{f_{\ell 1}}$
SDL	(I1) NISSS14	6.4	1.1	0.17	8.5	4.2	**0.49**
	(I2) NISSS14	2.4	1.0	**0.45**	12.5	4.9	0.39
	(J1) NISSS54	10.5	2.0	0.20	8.5	3.5	0.42
	(J2) NISSS54	3.9	1.3	0.33	7.5	1.2	0.16
TDL	(I1) NISSS14	25.5	7.1	0.27	37.6	18.4	**0.49**
	(I2) NISSS14	7.3	5.5	**0.73**	61.3	22.7	0.37
	(J1) NISSS54	22.6	4.6	0.20	19.3	8.0	0.41
	(J2) NISSS54	6.2	1.7	0.27	19.7	3.5	0.18

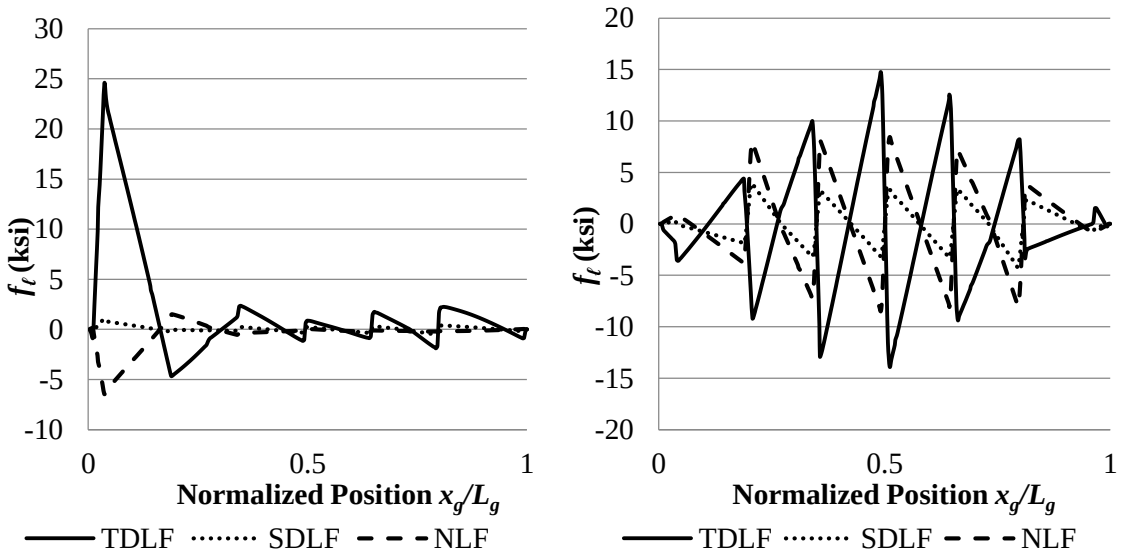

Figure 136. Top flange lateral bending stresses in Bridge (I1) NISSS14 fascia girder (left) and interior girder (right) under SDL with detailing based on NLF RA cambers.

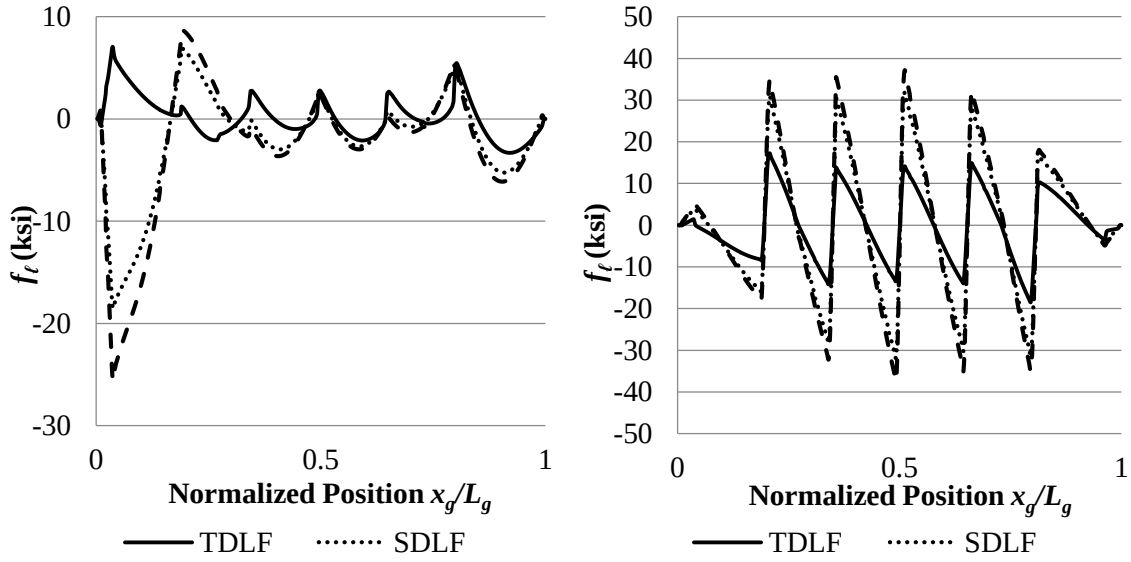

Figure 137. Top flange lateral bending stresses in Bridge (I1) NISSS14 fascia girder (left) and interior girder (right) under TDL with detailing based on NLF RA cambers.

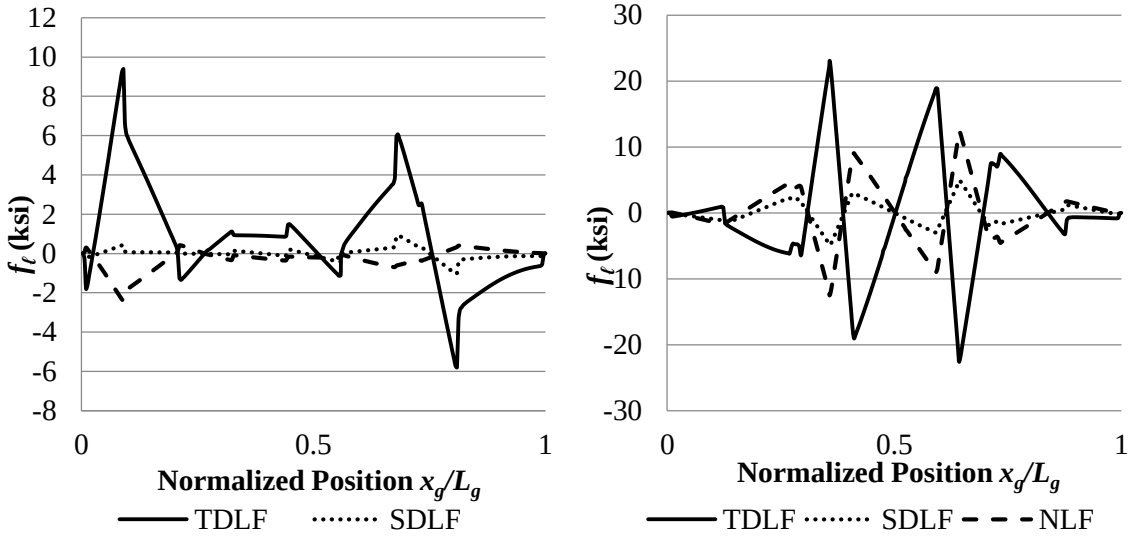

Figure 138. Top flange lateral bending stresses in Bridge (I2) NISSS14 fascia girder (left) and interior girder (right) under SDL with detailing based on NLF RA cambers.

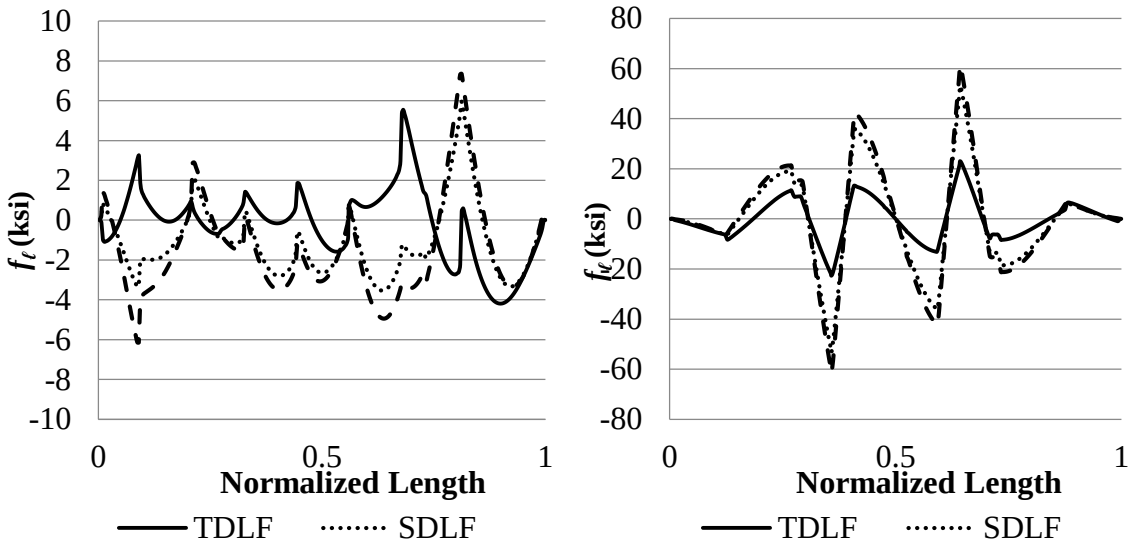

Figure 139. Top flange lateral bending stresses in Bridge (I2) NISSS14 fascia girder (left) and interior girder (right) under TDL with detailing based on NLF RA cambers.

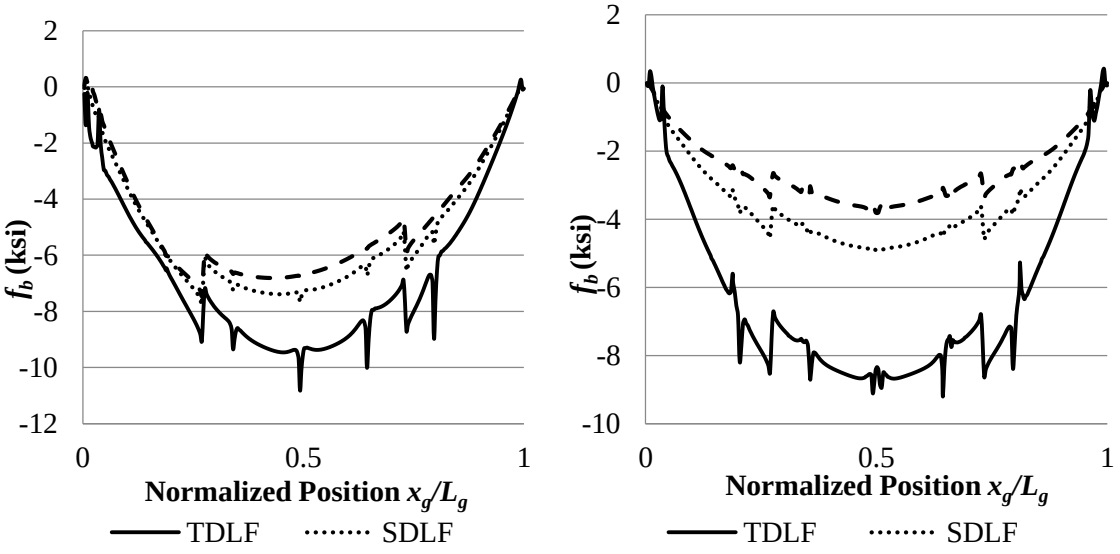

Figure 140. Top flange major-axis bending stresses in Bridge (I1) NISSS14 fascia girder (left) and innermost girder (right) under SDL with detailing based on NLF RA cambers.

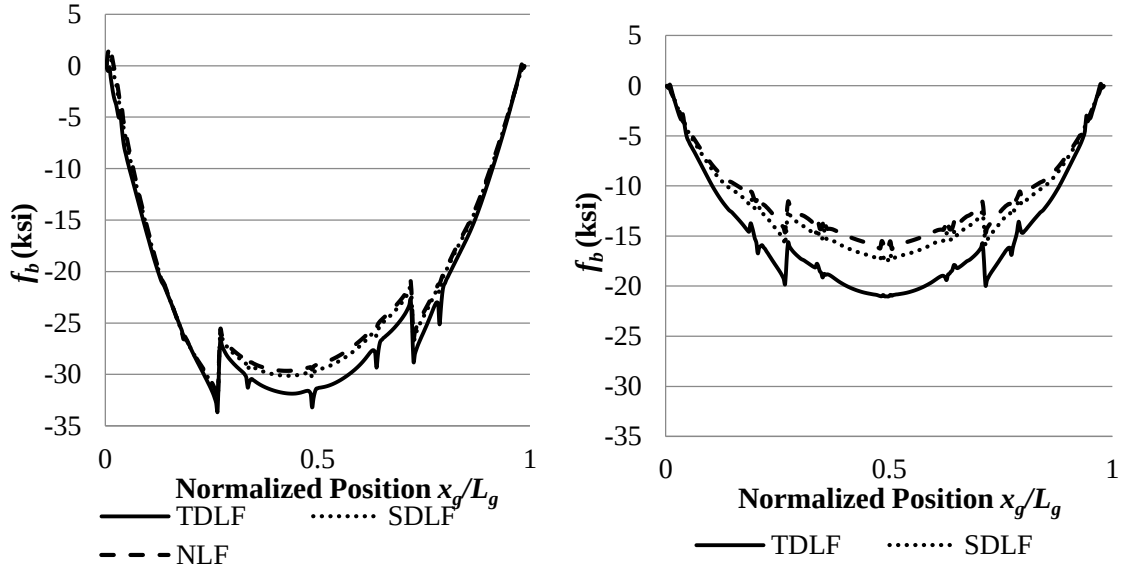

Figure 141. Top flange major-axis bending stresses in Bridge (I1) NISSS14 fascia girder (left) and innermost girder (right) under TDL with detailing based on NLF RA cambers.

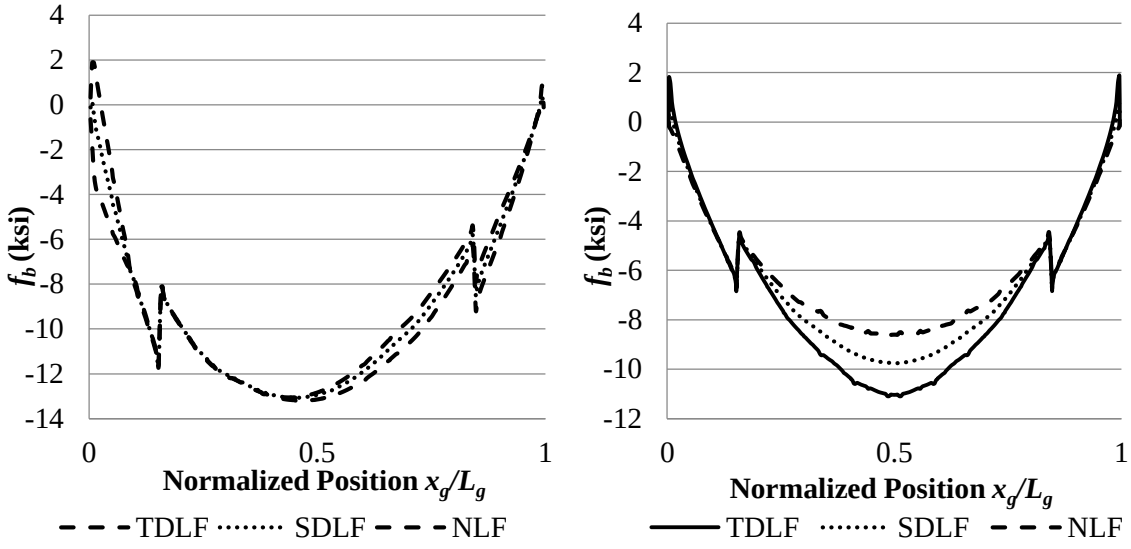

Figure 142. Top flange major-axis bending stresses in Bridge (J1) NISSS54 fascia girder (left) and innermost girder (right) under SDL with detailing based on NLF RA cambers.

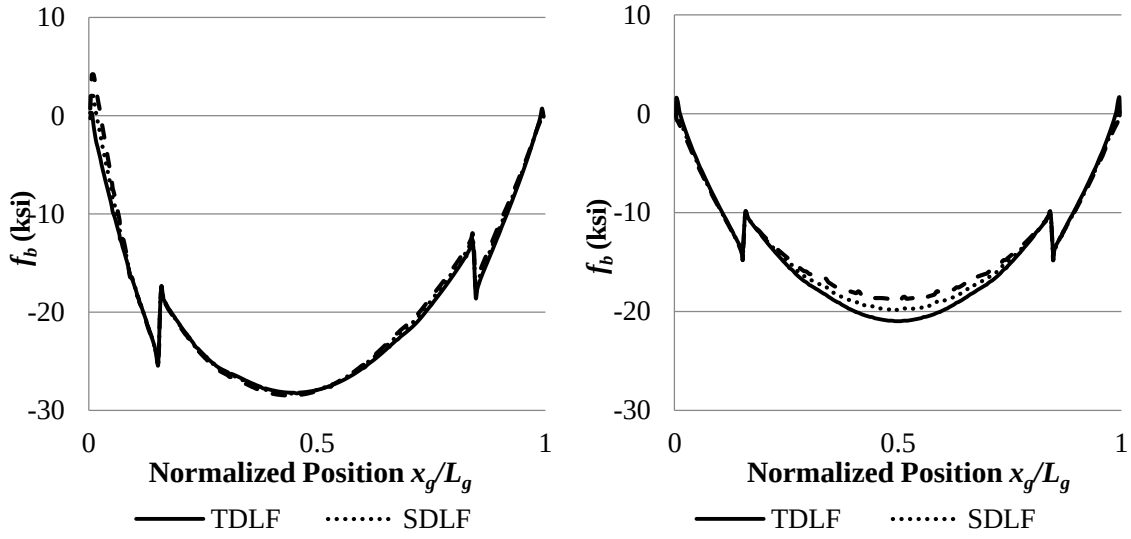

Figure 143. Top flange major-axis bending stresses in Bridge (J1) NISSS54 fascia girder (left) and innermost girder (right) under TDL with detailing based on NLF RA cambers.

6.7.1.6 Vertical Reactions

In straight parallel-skew bridges, the use of NLF RA cambers for DLF detailing tends to give smaller differences between the fascia girder and interior girder reactions along each of the skewed bearing lines compared to the use of DLF detailing with LGA cambers. This reduces the tendency for uplift at the obtuse corners of the bridge plan. This behavior is related to the fact that the girder vertical displacements are changed substantially by the DLF detailing when LGA cambers are used, whereas there is little change in the girder vertical displacements due to DLF detailing with RA cambers. Table 44 shows the SDL and TDL vertical reactions for Bridge (J1) with cambers set based on NLF RA. Under SDL with TDLF detailing based on the RA cambers, the smallest reaction is 14 kips at the obtuse corners of the bridge plan whereas uplift is encountered for this scenario. Application of the rules for CF framing arrangements recommended in this research also tends to alleviate uplift at the obtuse corners. Bridge (J2) NISSS54 and Bridge (I2) NISSS14 follow these recommendations.

Bridge (J1) NISSS54 has a severe nuisance stiffness problem. With the use of RA cambers, the largest increase in the TDL reactions is 71 % (94 kips) due to SDLF detailing and 163 % (216 kips) due to TDLF detailing for this bridge. These increases occur at the bearing on girder G2 near the corresponding obtuse corner of the span. The largest decrease in the TDL reactions is 20 % (168 kips) due to SDLF detailing and 44 % (370 kips) due to TDLF detailing. These decreases occur at the bearing on G1 at the corresponding obtuse corner of the span. The reactions at the opposite obtuse corner are essentially the same. It can be observed that for this severe case, a DLF RA is required to accurately predict the reactions. The use of LGA SDL reactions plus NLF RA CDL can be used to give a

conservative estimate of SDLF under TDL reactions. The use of LGA TDL reactions can be used to give a conservative estimate of TDLF under TDL reactions.

The largest increase in the TDL reactions is 4 % due to SDLF detailing and 9 % due to TDLF detailing for Bridge (J2). The largest decrease in the TDL reactions is 6 % due to SDLF detailing and 14 % due to TDLF detailing for Bridge (J2). For bridge (J2), which follows the framing recommendations in this research, the change in the reactions due to SDLF and TDLF can be neglected.

Table 44. Bridge (J1) NISSS54 vertical reactions (kips) (G1 and G9 are fascia girders), detailing based on NLF RA cambers.

Girder	Detailing Method	SDL Support 1	SDL Support 2	TDL Support 1	TDL Support 2
G1	NLF	384	146	828	332
	SDLF	219	154	666	334
	TDLF	14	161	463	337
G2	NLF	63	170	138	367
	SDLF	155	168	227	363
	TDLF	276	168	350	363
G3	NLF	122	173	270	372
	SDLF	161	157	308	358
	TDLF	206	137	350	340
G4	NLF	94	127	200	279
	SDLF	121	128	231	279
	TDLF	153	127	267	275
G5	NLF	109	109	238	238
	SDLF	127	127	257	256
	TDLF	147	147	277	277
G6	NLF	127	94	279	199
	SDLF	128	121	279	231
	TDLF	127	154	275	268
G7	NLF	173	122	372	271
	SDLF	157	161	358	308
	TDLF	138	209	341	353
G8	NLF	170	64	367	141
	SDLF	168	156	363	231
	TDLF	169	272	363	348
G9	NLF	146	382	332	825
	SDLF	153	217	334	662
	TDLF	161	14	337	462

Table 45. Summary of maximum absolute and percentage increases and decreases in the TDL vertical reactions at the girder bearings, due to SDLF and TDLF detailing based on LGA cambers, in the straight parallel-skewed bridges (the largest of these maximum absolute and percentage increases are highlighted by dark shading).

Bridge	SDLF				TDLF			
	Decreases		Increases		Decreases		Increases	
	Max (kips)	Max %	Max (kips)	Max %	Max (kips)	Max %	Max (kips)	Max %
(I1) NISSS14	-16	-7	7	10	-66	-29	31	42
(I2) NISSS14	-5	-3	4	5	-23	-13	19	24
(J1) NISSS54	**-168**	**-20**	**94**	**71**	**-370**	**-44**	**216**	**163**
(J2) NISSS54	-23	-6	12	4	-54	-14	29	9

6.7.2 Summary and Recommendations – Straight Bridges with Parallel Skew and Cambers Set Based on NLF RA

The influence of SDLF and TDLF detailing on the responses in completed straight bridge systems with non-parallel skew and girder cambers calculated based on LGA may be summarized as follows. Recommendations pertaining to these quantitative results are highlighted in bold italicized text.

General

- The use of LGA for setting the girder cambers in sharply skewed straight bridges is generally discouraged based on the considerations discussed in Section 6.2.3.
- Straight bridges with a difference in the skew angles at the ends of all the spans less than or equal to $\Delta\theta = 20^{o}$ may be considered as parallel skew bridges. Section 6.6 applies in these cases.

- With LGA cambers, the responses of straight non-parallel skew bridges are close to the ideal theoretical values (i.e., in the targeted DL conditions, zero layover, CF forces, and girder flange lateral bending stresses, and girder major-axis bending stresses and vertical reactions equal to the values from LGA).

The following discussions focus predominantly on the TDL results with TDLF detailing based on LGA cambers, using the Bridge (H1) EISSS57 as an extreme example.

Girder Elevations

- For Bridge (H1) EISSS57, the maximum deviation from the targeted elevations is 0.03 inches under the TDL with TDLF based on the LGA cambers.
- For this bridge, the maximum deviation from the targeted elevations is 0.63 inches if the LGA results are used for all the camber calculations and the bridge is detailed for SDLF.
- ***It is recommended that LGA alone should not be utilized for calculation of the girder total cambers in straight bridges with parallel or non-parallel skew, unless TDLF detailing is employed.***
- ***It is recommended that, if LGA is used for calculating the girder cambers in straight bridges with parallel or non-parallel skew, the girder TDL cambers should be calculated as follows:***
    - ***For TDLF, the negative of the girder TDL vertical deflections obtained from the LGA.***
    - ***For SDLF, the negative of the girder SDL vertical deflections obtained from the LGA plus the negative of the CDL vertical deflections obtained from a NLF RA.***

- Although the above error in the targeted elevations is tolerable for Bridge (H1), the recommendations developed for parallel skew are extended to the non-parallel skew cases to maintain simplicity and consistency.

Girder Layovers

- For Bridge (H1) EISSS57, the maximum girder layover under the TDL, with TDLF detailing based on LGA cambers, is 0.1 inches (0.001 rad).
- ***It is recommended that the girder layovers may be assumed to be negligible in the targeted DL condition in straight bridges with parallel or non-parallel skew when the CFs are detailed using the above recommended procedures with LGA. The fascia girders should be checked separately for twist rotation between the CF locations due to eccentric overhang bracket loads.***
- ***For straight bridges with parallel or non-parallel skew, detailed for SDLF using the above recommended procedures with LGA, the girder layovers under the TDL may be estimated as the CDL layovers obtained from a NLF RA.***
- ***For straight bridges with parallel or non-parallel skew, detailed for TDLF using the above recommended procedures with LGA, the girder layovers under the SDL may be estimated as the negative of the CDL layovers obtained from a NLF RA.***

Cross-Frame Forces

- Under SDL in Bridge (H1) EISSS57, the largest ratio of the average of the CF member forces for SDLF detailing to the corresponding forces for NLF detailing is 0.07 for SDLF based on LGA cambers.

- Under SDL in Bridge (H1) EISSS57, the largest ratio of the maximum CF member force for SDLF detailing to the corresponding force for NLF detailing is 0.26 for SDLF based on LGA cambers. That is, the beneficial locked-in force is 1.0 – 0.26 = 0.74 of the CF force corresponding to NLF detailing for this member.
- Under TDL in this bridge, the largest ratio of the average of the CF member forces for TDLF detailing to the corresponding forces for NLF detailing is 0.14 for TDLF based on LGA cambers.
- Under TDL in this bridge, the largest ratio of the maximum CF member force for TDLF detailing to the corresponding force for NLF detailing is 0.37 for TDLF based on LGA cambers. That is, the beneficial locked-in force is 1.0 – 0.37 = 0.63 of the CF force corresponding to NLF detailing for this member.
- ***In lieu of a DLF RA, it is recommended that a net load factor of (γ_p – 0.65) be used for determination of the factored SDL CF forces in straight I-girder bridges with parallel or non-parallel skew, when the CFs are detailed for SDLF using the recommended procedures with LGA. This net load factor is to be applied to the results from a NLF RA for the SDL. It should be noted that these SDL CF forces must be added to the factored CDL CF forces from a NLF RA to obtain the total factored DL CF forces.*** The factor of 0.65 is a slightly conservative estimate of the maximum SLDF locked-in force ratio of 1.0 – 0.26 = 0.74, selected to be consistent with the recommendations for straight parallel-skew bridges.
- ***In lieu of a DLF RA, it is recommended that a net load factor of (γ_p – 0.65) be used for determination of the factored TDL CF forces in straight I-girder bridges with parallel or non-parallel skew, when the CFs are detailed for TDLF using the***

recommended procedures with LGA. This net load factor is to be applied to the results from a NLF RA for the TDL. The factored CF forces under the SDL may be estimated by subtracting the factored CDL CF forces obtained by a NLF RA from the above factored TDLF forces. The factor of 0.65 is an estimate of the TDLF locked-in force of 1.0 – 0.37 = 0.63, selected to be consistent with the recommendations for straight parallel-skew bridges. In cases where additional uncertainties and variabilities associated with TDLF are anticipated, due to incidental participation of deck forms, early concrete stiffness gain, and/or larger potential play in the CF connections due to the larger CF forces associated with TDLF, it is suggested that a value between 0.65 and 0.50 may be used for the above locked-in force estimate based on the judgment of the engineer of record. This suggested reduction is based on the judgement of the research. The current research did not perform any specific investigations of the above effects.

- The maximum difference in the magnitude of the individual CF member forces from a DLF RA and (1 – 0.65 = 0.35) of the estimated values from a NLF RA, normalized by the member yield load, is 1.1 and 4.8 %, and the average difference is -0.5 and -1.4 % for SDLF under SDL and TDLF under TDL, respectively, for the straight bridges with non-parallel skew studied in this research and girder cambers based on LGA.
- The maximum difference in the magnitude of the individual CF member forces from a DLF RA and (1 – 0.65 = 0.35) of the estimated values from a NLF RA, normalized by the member yield load, is 1.1 and 3.1 %, and the average difference is -0.5 and -1.0 % for SDLF under SDL and TDLF under TDL, respectively, for the straight bridges studied in this research with non-parallel skew and girder cambers based on LGA.

Girder Stresses

- For Bridge (H1) EISSS57, the largest maximum girder flange lateral bending stress (f_ℓ), under the TDL for TDLF based on LGA cambers, is 0.8 ksi, 80 % of the corresponding maximum girder NLF value. This f_ℓ occurs on the longest fascia girder in the bridge. The next largest maximum girder f_ℓ is 0.4 ksi, on the shortest fascia girder under the TDL for TLDF based on LGA cambers, and is 8 % of the corresponding maximum girder NLF value. The largest maximum girder f_ℓ based on the assumption of NLF detailing is 8.4 ksi, and occurs on the interior Girder 3 in this bridge. The maximum f_ℓ on Girder 3 is reduced to 0.1 ksi (1 % of the above NLF value) by the use of TDLF detailing based on the LGA cambers.
- For all the bridges studied in this research, the use of an assumed locked-in f_ℓ of 0.65 of the f_ℓ from a NLF RA gives an accurate to conservative estimate of the f_ℓ values determined from a DLF RA.
- ***In lieu of a DLF RA, for straight bridges with non-parallel skew and with the CFs detailed for SDLF using the recommended procedures with LGA, it is recommended that the corresponding procedures for calculation of the CF forces proposed for parallel-skew bridges also be used for determining the girder f_ℓ values.***
- In (H1) EISSS57, the largest increase in the girder major-axis bending stresses under the TDL, due to the effect of SDLF detailing based on LGA cambers, is 1.5 ksi (6 %). The largest increase in any of the girder major-axis bending stresses under the TDL, due to the effect of TDLF detailing based on LGA cambers, is 2.9 ksi (13 %). The

largest increase occurs in the long fascia Girder G7, but a slightly smaller increase appears in the short fascia Girder G1.

- The LGA solution gives accurate f_b values for the targeted DL condition – SDL for SDLF and TDL for TDLF.
- ***In lieu of a DLF RA, for straight bridges with non-parallel skew and with the CFs detailed using the above recommended procedures with LGA, it is recommended that the girder f_b values in the targeted DL condition be taken as the values from the LGA.***
- ***In lieu of a DLF RA, for straight bridges with non-parallel skew and with the CFs detailed for SDLF using the recommended procedures with LGA, the girder f_b values under the TDL may be estimated by adding the CDL f_b values obtained from a NLF RA to the SDL f_b values obtained from LGA.***
- ***In lieu of a DLF RA, for straight bridges with non-parallel skew and with the CFs detailed for TDLF using the recommended procedures with LGA, the girder f_b values under SDL may be estimated by subtracting the CDL f_b values obtained from a NLF RA from the TDL f_b values obtained from LGA.***

Vertical Reactions

- When LGA cambers are used with (H1) EISSS57, the results for the girder reactions parallel the above results for the girder major-axis bending stresses, except that the changes in the reactions are affected more significantly.
- The recommendations for improved CF framing arrangements from this research have a measurable effect in reducing the changes in the bearing reactions due to DLF.

- ***In lieu of a DLF RA, for straight bridges with non-parallel skew and with the CFs detailed using the recommended procedures with LGA, it is recommended that the girder reactions in the targeted DL condition be taken as the values from the LGA.***
- ***In lieu of a DLF RA, for straight bridges with non-parallel skew and with the CFs detailed for SDLF using the recommended procedures with LGA, the girder reactions under the TDL may be estimated by adding the CDL reactions obtained from a NLF RA to the SDL reactions obtained from LGA.***
- ***In lieu of a DLF RA, for straight bridges with non-parallel skew and with the CFs detailed for TDLF using the recommended procedures with LGA, the girder reactions under SDL may be estimated by subtracting the CDL reactions obtained from a NLF RA from the TDL reactions obtained from LGA.***

The above recommendations are considered applicable for straight bridges with non-parallel skew, skew angles up to 70^{o}, and spans up to 300 ft.

For bridges that exceed these limits, it is recommended that DLF RA be considered. Chapter 3 explains the details of several procedures for conducting a DLF RA.

6.8 Straight Bridges with Non-Parallel Skew and Cambers Set Based on LGA

Straight bridges with a difference in the skew angles at the ends of all the spans less than $\Delta\theta = 20^{o}$ may be considered as parallel skew bridges, and are addressed in Sections 6.6 and 6.7. With LGA cambers, the responses of straight non-parallel skew bridges are close to the ideal theoretical values (i.e., in the targeted DL conditions, zero layover, CF forces, and girder flange lateral bending stresses, and girder major-axis bending stresses and vertical reactions equal to the values from LGA). The following discussions focus

predominantly on the TDL results with TDLF detailing based on LGA cambers, using the Bridge (H1) EISSS57 as an extreme example.

Section 6.8.1 provides quantitative results on the influence of SDLF and TDLF detailing with cambers set based on LGA. The influence of SDLF and TDLF is discussed on the responses in the following order: girder vertical displacements, girder elevations, girder layovers, CF forces, girder stresses, and vertical reactions. Section 6.8.2 then summarizes the influences on the key bridge responses, and provides recommendations for handling these effects. The recommendations are highlighted in bold italicized text.

6.8.1 Quantitative Results

6.8.1.1 Girder Vertical Displacements

For straight non-parallel skewed bridges, SDLF and TDLF detailing tend to increase the vertical displacement of the longer fascia girder and reduce the vertical displacement of the other girders. The increase or decrease in the vertical displacements, for bridges with a high skew index, is significant when the detailing is based on Line Girder Analysis (LGA) cambers as shown in Figure 144 for Bridge (H1) EISSS57. The maximum TDL displacement difference between the result for TDLF and NLF detailing is 0.82 inches on the innermost girder and 1.26 inches on the fascia girder in (H1) EISSS57. This occurs due to the fact that when the CFs are detailed for TDLF, the effect of the TDLF detailing is to force the girders to deflect in the manner calculated by LGA under the TDL condition. However this effect is accomplished only under this targeted TDL condition. Similarly, when the CFs are detailed for SDLF, the effect of the SDLF detailing is to force the girders to deflect in the manner calculated by LGA under the SDL condition (but only under this condition).

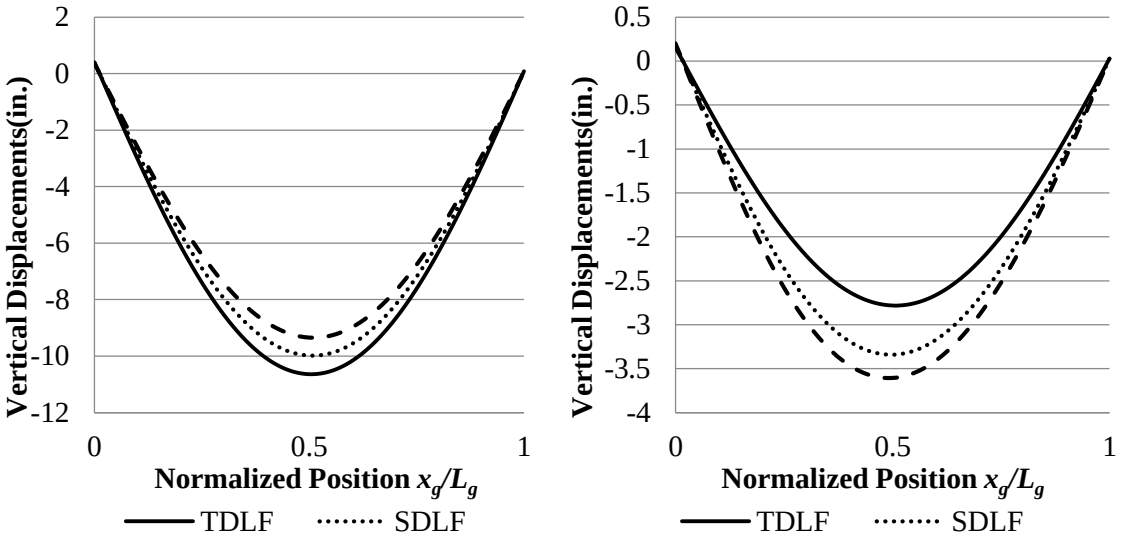

Figure 144. Bridge (H1) EISSS57 critical fascia girder (left) and middle girder (right) vertical displacements under TDL with the CFs detailed based on LGA cambers.

6.8.1.2 Girder Elevations

As noted previously, when straight skewed bridges are designed using LGA, the CFs are commonly detailed based on LGA cambers. The TDL LGA girder cambers are taken as the negative of the TDL girder vertical deflections calculated from a LGA. With TDLF detailing, the corresponding TDL girder elevations are theoretically zero (neglecting superelevation, etc.). Similarly, the SDL LGA cambers are taken as the negative of the SDL girder displacements calculated from a LGA. The actual responses corresponding to the above are always slightly different from the above theoretical ideals due to various factors that are not accounted for in the CF detailing, as discussed in Section 6.2.2. However, the use of LGA cambers gives the closest capture of these ideals.

In addition, it is essential to recognize that the above findings apply ONLY to the targeted DL conditions. For example, if one uses solely a LGA to determine the TDL girder deflections for a bridge that has been detailed for SDLF, the calculated elevations can be

significantly in error. The correct calculation of the girder deflections in this case, if the SDLF detailing is based on LGA cambers, is to sum the girder SDL deflections obtained from a LGA with the CDL deflections obtained from a RA.

Figure 145 shows the vertical elevations for the critical fascia girder of Bridge (H1) EISSS57, under TDL, if the CFs are detailed based on LGA and the girder TDL cambers are set *entirely* based on LGA. One can observe that the elevations match accurately with the targeted zero final elevations for TDLF in this situation. However, these good results apply *ONLY* to the use of TDLF for this TDL condition. If NLF detailing is used, and if the girder cambers are set based on the LGA results for the TDL, the girder final elevations can be substantially in error from the targeted elevations. These errors are equal to the differences between the LGA girder deflections and the 3D FEA girder deflections. If SDLF detailing is used, and if the girder cambers are set based on the LGA results for the TDL, the elevation errors will be smaller. However, these errors can still be substantial, equal to the differences between the LGA girder deflections and the 3D FEA girder deflections under the CDL.

Nevertheless, for the extreme Bridge (H1) NISSS57, the largest error in the girder vertical elevations caused by using LGA results for all the girder deflections is only 1.3 inches, which is considered to be small enough to be addressed within the selection of the girder concrete haunch depths. The above deviation from the ideal elevation by 1.3 inches corresponds to NLF detailing and the use of the LGA total cambers.

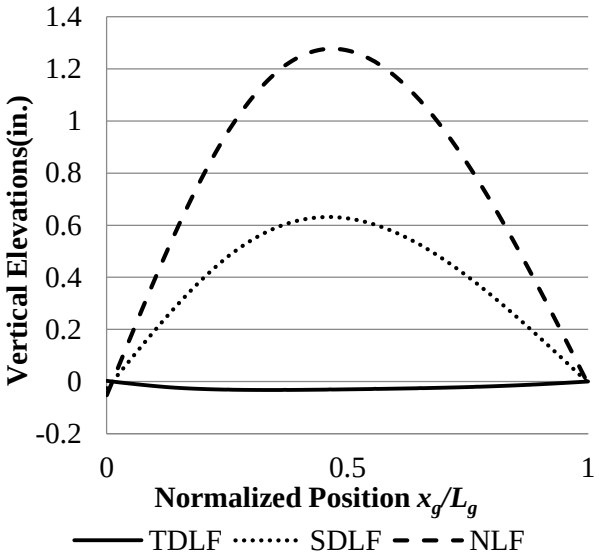

Figure 145. Bridge (H1) EISSS57 critical fascia girder vertical elevations under TDL with the CF detailed based on LGA cambers.

6.8.1.3 Girder Layovers

For straight bridges with non-parallel skew, the CFs theoretically fit to the girders under SDL with zero force, when the CFs are detailed for SDLF using LGA. In this case, the girders are nearly ideally plumb under SDL with SDLF detailing based on LGA for Bridge (H1) EISSS57 (see Figure 146). Similarly, the girders are nearly ideally plumb under TDL with TDLF detailing based on LGA.

From Figure 146 one can observe that, for this straight non-parallel skew bridge, the layovers under SDL with TDLF detailing are approximately equal in magnitude but opposite in sign to the layovers under TDL with SDLF detailing. With SDLF detailing, the layovers are theoretically zero under SDL (when LGA cambers are employed). The layovers with SDLF detailing under TDL are approximately equal to the layovers due to the CDL determined from a NLF RA. With TDLF detailing, the layovers are theoretically zero under TDL. The layovers with TDLF detailing under SDL are thus theoretically equal

in magnitude but opposite in sign to the layovers due to the CDL determined from a NLF RA.

It should be emphasized that LGA can be a very erroneous predictor of the CDL displacements. This is because the girders are interconnected by their CFs and are thus behaving as a three-dimensional structural system under the action of the CDLs.

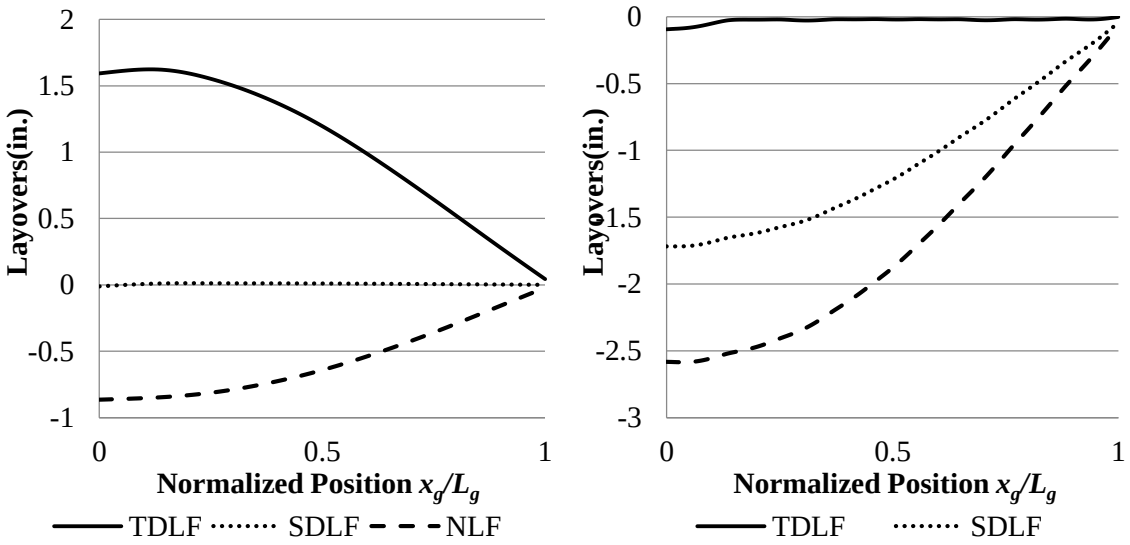

Figure 146. Fascia girder layovers of Bridge (H1) EISSS57 under SDL (left) and under TDL (right) with cambers based on LGA.

6.8.1.4 Cross-Frame Forces

For straight bridges with non-parallel skew and girder cambers based on LGA, both the average and the maximum CF forces in the completed bridge are small under SDL for SDLF detailing, and they are small under TDL for TDLF detailing. The effects of SDLF and TDLF detailing approximately cancel the CF DL effects, when the SDLF and TDLF detailing is based on cambers obtained from LGA girder deflections. When a straight skewed bridge is designed using LGA, the CFs are detailed commonly based on LGA cambers. It is emphasized that the recommendation of this research is that the engineer

should not mix the methods of analysis being applied to a given bridge. That is, if a RA is employed for the overall bridge design (i.e., grid analysis or 3D FEA), the cambers should be calculated based on the RA. This recommendation is due to the high chance of significant errors entering into the solutions when the results from LGA and from RA are mixed (e.g., improperly using the LGA result for the total girder cambers when the bridge is detailed for SDLF, which can result in substantial girder elevation errors) as well as other reasons discussed in Section 6.2.3. The CF forces are theoretically zero under the targeted DL condition. However, the actual CF forces generally are not zero under the targeted condition for reasons discussed in Section 6.2.2.

Table 46. Average magnitude of the CF member forces in straight non-parallel skewed Bridge (H1) EISSS57 (F1, F2, and F3 are the average CF forces with NLF, SDLF, and TDLF detailing based on LGA cambers, respectively).

Load Cond.	NLF	SDLF			TDLF		
	F1 (kip)	F2 (kip)	F2/F1	F2 – F1 (kip)	F3 (kip)	F3/F1	F3 – F1 (kip)
SDL	4.6	0.3	0.07	-4.3	6.2	1.35	1.6
TDL	12.1	7.7	0.64	-4.4	1.7	0.14	-10.4

Table 47. Maximum magnitude of the CF member forces in straight non-parallel skewed Bridge (H1) EISSS57 (F1, F2, and F3 are the maximum CF forces with NLF, SDLF, and TDLF detailing based on LGA cambers, respectively).

Load Cond.	NLF	SDLF			TDLF		
	F1 (kip)	F2 (kip)	F2/F1	F2 – F1 (kip)	F3 (kip)	F3/F1	F3 – F1 (kip)
SDL	19.2	5.0	0.26	-14.2	27.3	1.42	8.1
TDL	48.9	30.5	0.62	-18.4	18.1	0.37	-30.8

The following can be observed:

- Under SDL, the largest F2/F1 ratio of the average of the CF member forces is 0.07.

- Under SDL, the largest F2/F1 ratio of the maximum CF member force is 0.26.
- Under TDL, the largest F3/F1 ratio of the average of the CF member forces is 0.14.
- Under TDL, the largest F3/F1 ratio of the maximum CF member force) is 0.37.

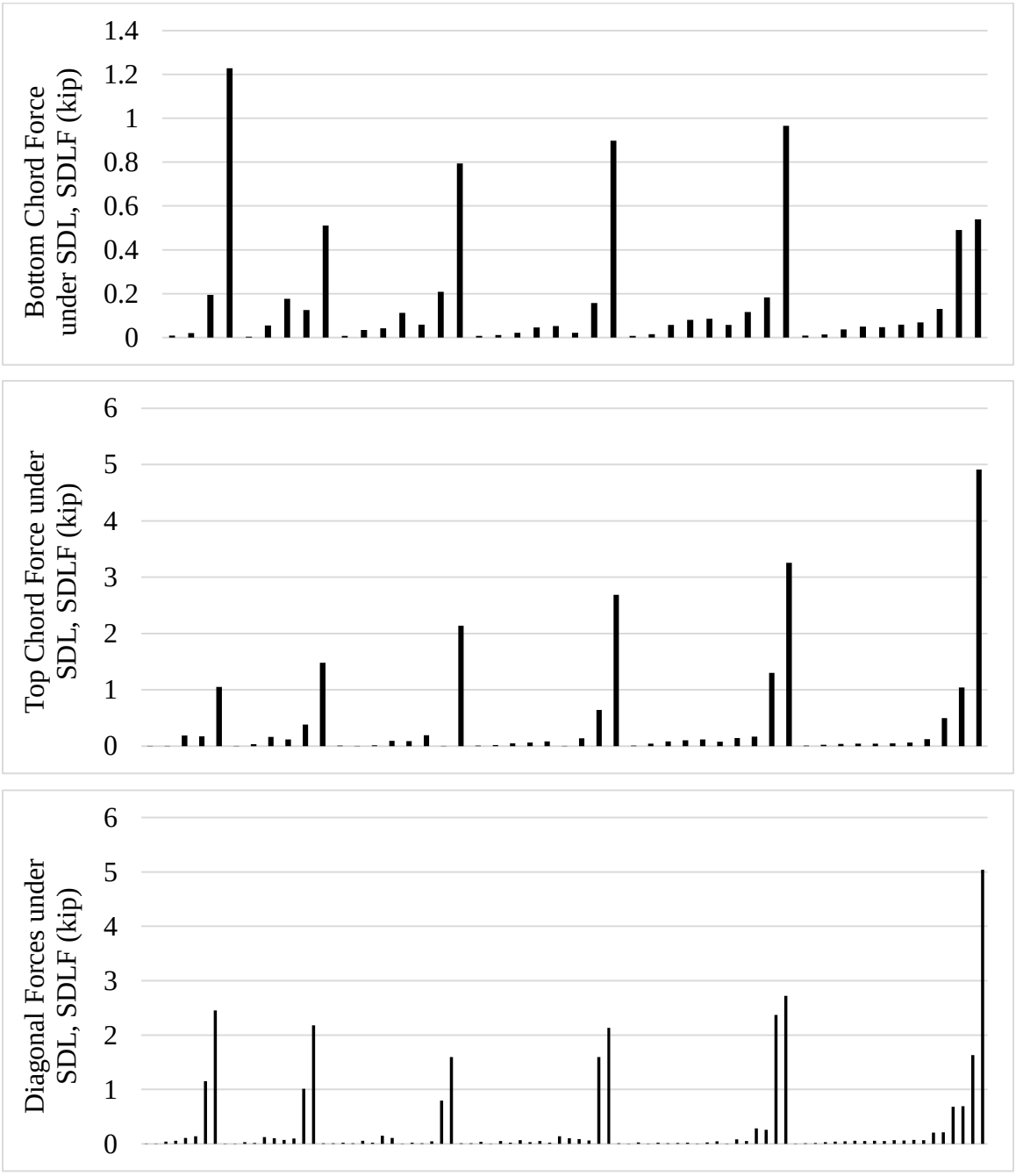

Figure 147. Magnitude of CF member forces from DLF RA, Bridge (H1) EISSS57 under SDL, SDLF detailing based on LGA cambers.

Figure 148 shows an estimate of the CF forces under the SDL, assuming SDLF detailing, obtained by scaling the NLF RA forces for all the cross-frame members by 0.35. This is the scale factor recommended in Section 6.6.2 for both SDL/SDLF and TDL/TDLF estimates in straight parallel skew bridges. One can observe that the absolute maximum CF force values from Figure 147 are estimated accurately to conservatively. However, the actual distribution of the CF forces from Figure 147 is predicted poorly. The poor prediction of the CF force distribution is not of any significant consequence though since all the CF forces are relatively small. Since Figure 148 simply shows all the NLF RA CF forces scaled by 0.35, it can be concluded that the distribution of the non-zero CF forces under SDL associated with NLF detailing is very different from the distribution of the reduced (smaller) CF forces under SDL associated with SDLF detailing.

Figure 149 shows the difference between the magnitude of the DLF RA forces and the CF forces under SDL, assuming SDLF detailing, estimated by scaling the NLF RA forces, divided by the CF member yield loads. The plots in this figure are similar those for the curved radially-supported bridges shown previously. One can observe that the largest under-prediction of the DLF RA results is $0.009P_y$ for one of the chords of the cross-frame connected to the longer fascia girder at the upper-right non-skewed corner of the bridge plan. The largest over-prediction is $-0.028P_y$ using the recommended estimate. Figure 150 shows the same results, but under TDL and assuming TDLF detailing. The maximum under-prediction is $0.027P_y$ and the largest over-prediction is $-0.065P_y$ for this case.

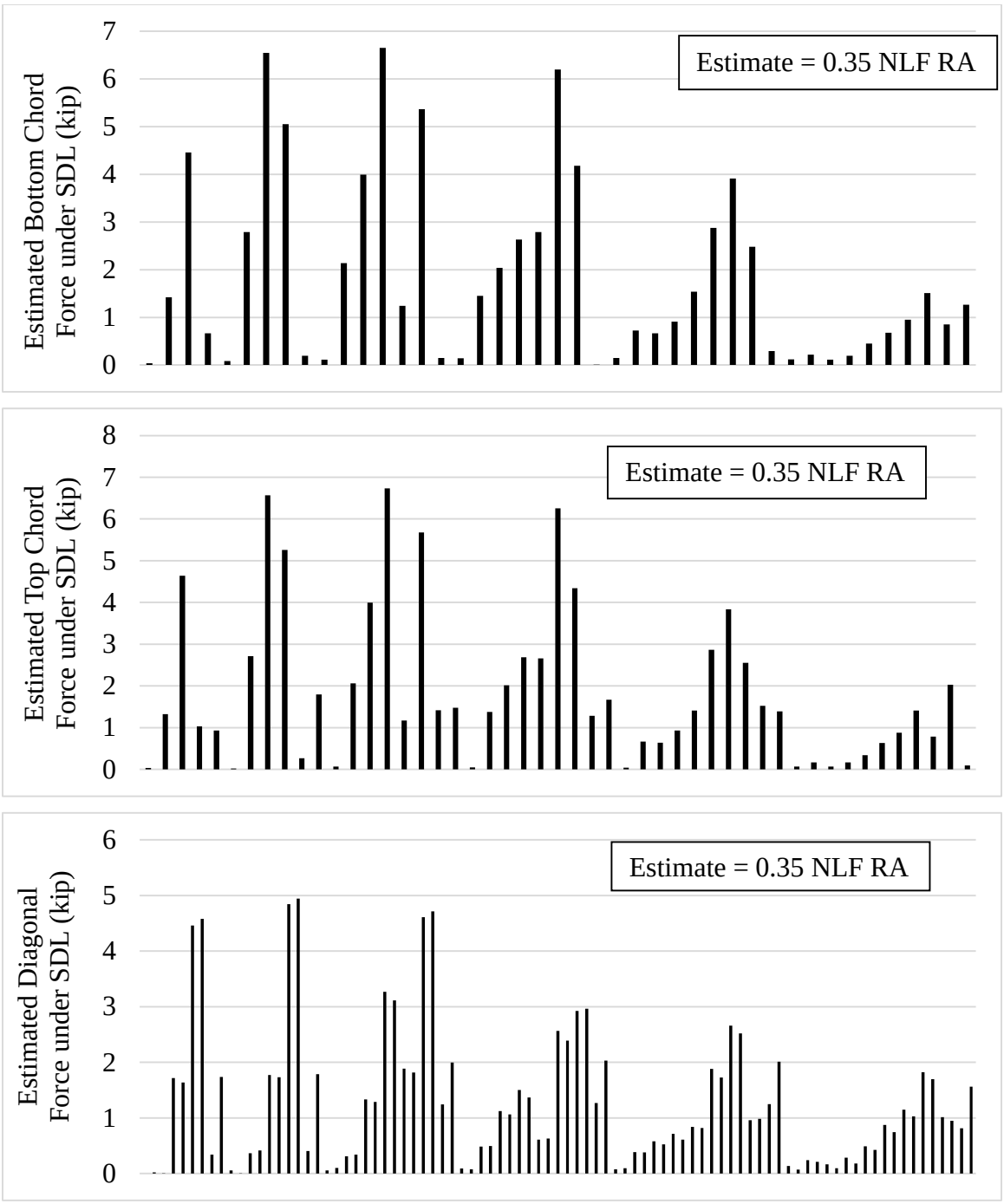

Figure 148. Estimated magnitude of CF member forces based on scaling of NLF RA results, assuming SDLF detailing, Bridge (H1) EISSS57 under SDL.

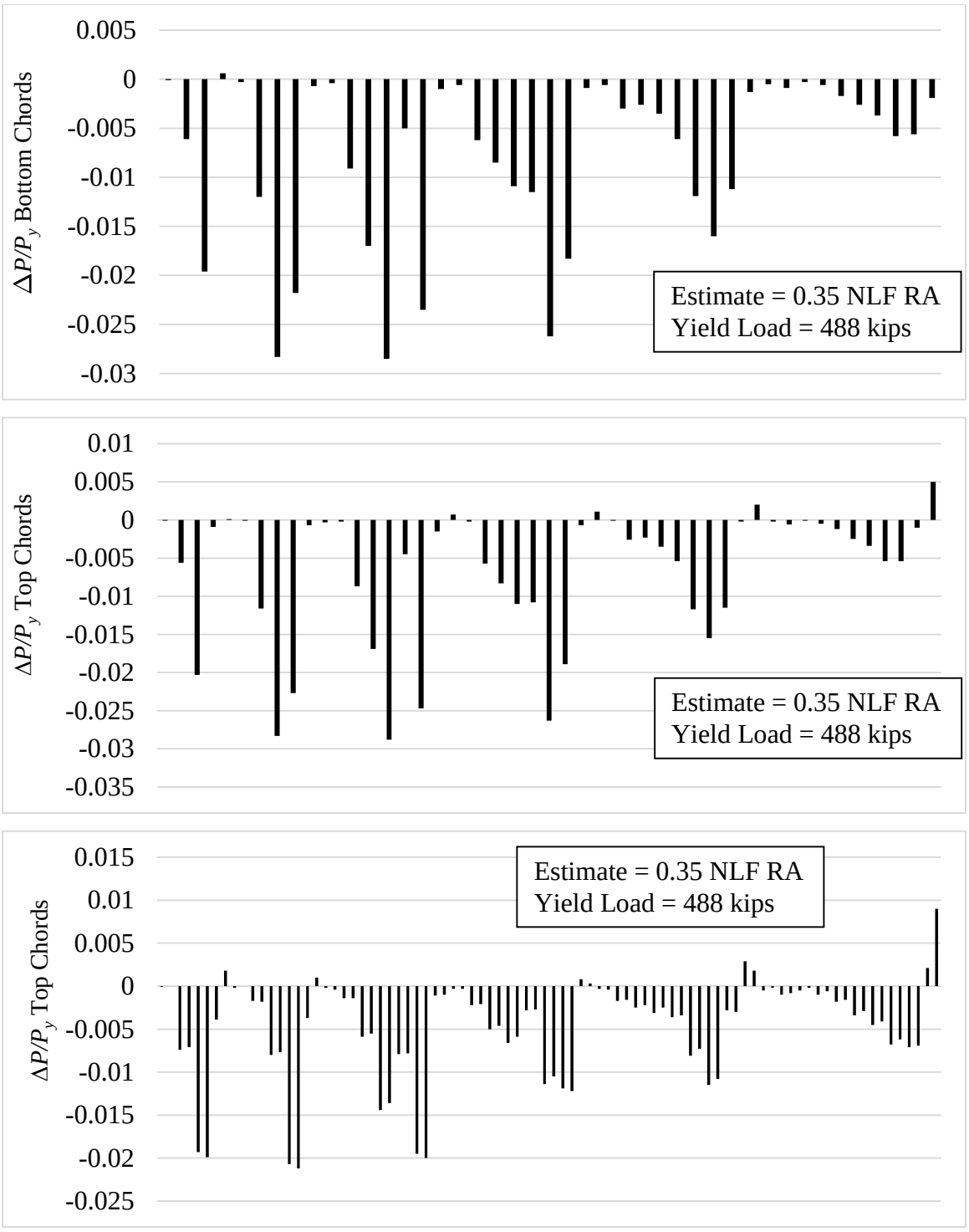

Figure 149. Difference between the magnitude of the DLF RA forces and the values estimated by scaling the NLF RA results, divided by the member yield load ($\Delta P/P_y$), Bridge (H1) EISSS57 under SDL, SDLF detailing based on LGA cambers.

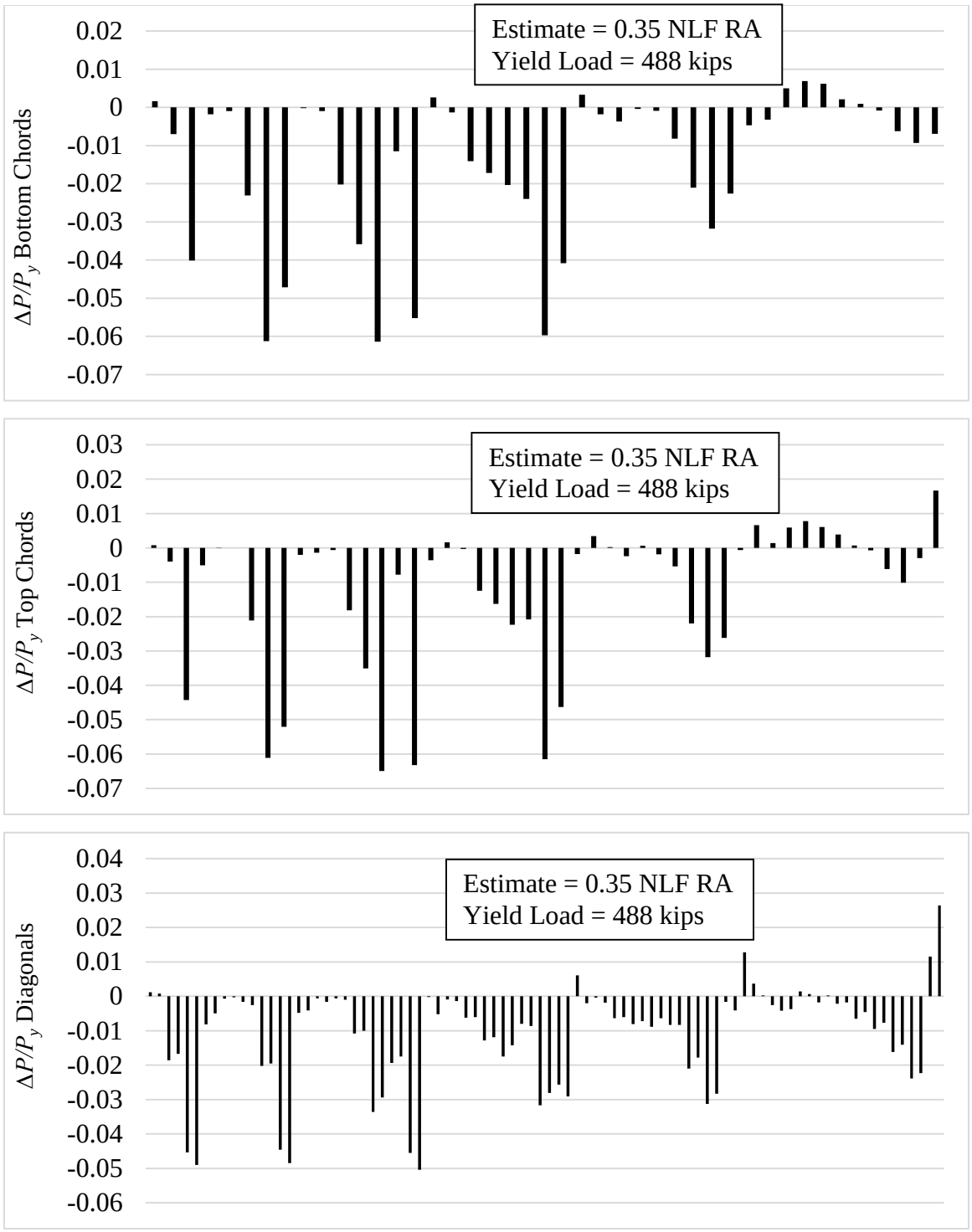

Figure 150. Difference between the magnitude of the DLF RA forces and the values estimated by scaling the NLF RA results, divided by the member yield load ($\Delta P/P_y$), Bridge (H1) EISSS57 under TDL, TDLF detailing based on LGA cambers.

6.8.1.5 Girder Stresses

For straight bridges with non-parallel skew, the SDLF and TDLF detailing effects based on LGA cambers tend to increase the major-axis bending stresses on the longer fascia girders and decrease these stresses in the other girders. This behavior is shown in Figures 151 and 152 for Bridge (H1) EISSS57.

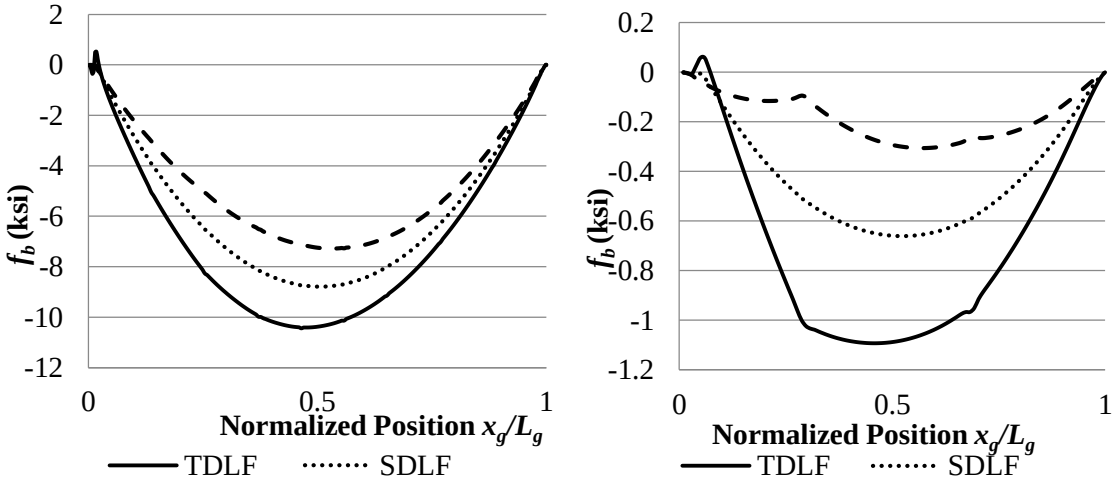

Figure 151. Top flange f_b in Bridge (H1) EISSS57 longer fascia girder (left) and short fascia girder (right) under SDL with detailing based on LGA cambers.

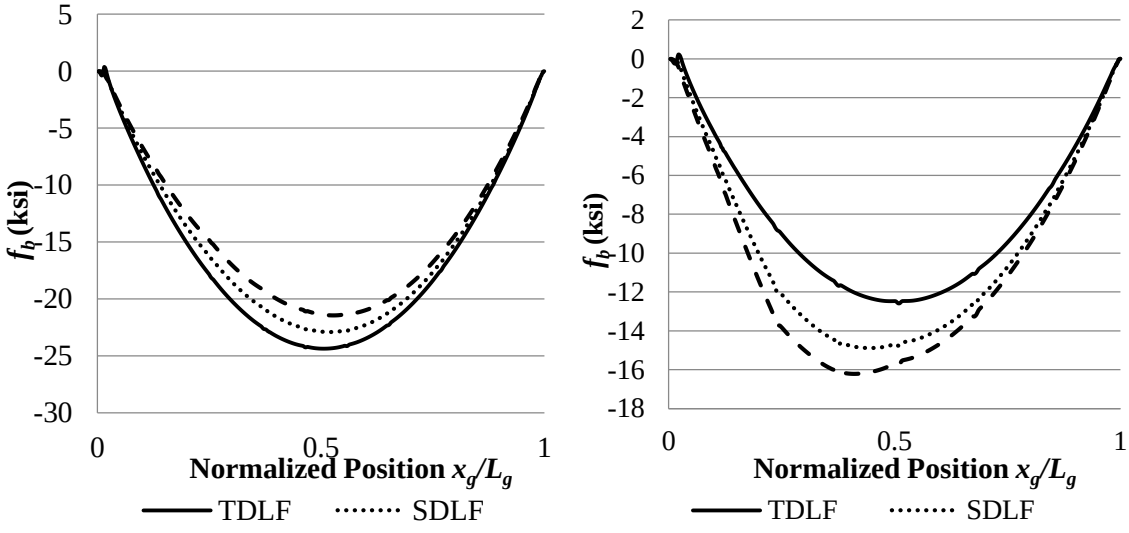

Figure 152. Top flange f_b in Bridge (H1) EISSS57 longer fascia girder (left) and short fascia girder (right) under TDL with detailing based on LGA cambers.

The girder flange lateral bending stresses are theoretically zero under SDL for SDLF detailing and under TDL for TDLF detailing based on LGA cambers, and they are generally significant under TDL if NLF detailing is used. However, the stresses are actually non-zero under SDL for SDLF detailing and under TDL for TDLF detailing due to a number of factors discussed in Section 6.2.2.

From Figure 154, one can observe that, for straight bridges with non-parallel skew, the girder flange lateral bending stresses under SDL with TDLF detailing are approximately equal in magnitude but opposite in sign to the flange lateral bending stresses under TDL with SDLF detailing. With SDLF detailing, the flange lateral bending stresses are theoretically zero under SDL. The flange lateral bending stresses with SDLF detailing under TDL are theoretically equal to the flange lateral bending stresses due to the CDL from 3D FEA. With TDLF detailing, the flange lateral bending stresses are theoretically zero under TDL. The flange lateral bending stresses with TDLF detailing under SDL are theoretically equal to the negative of the flange lateral bending stresses due to the CDL from 3D FEA.

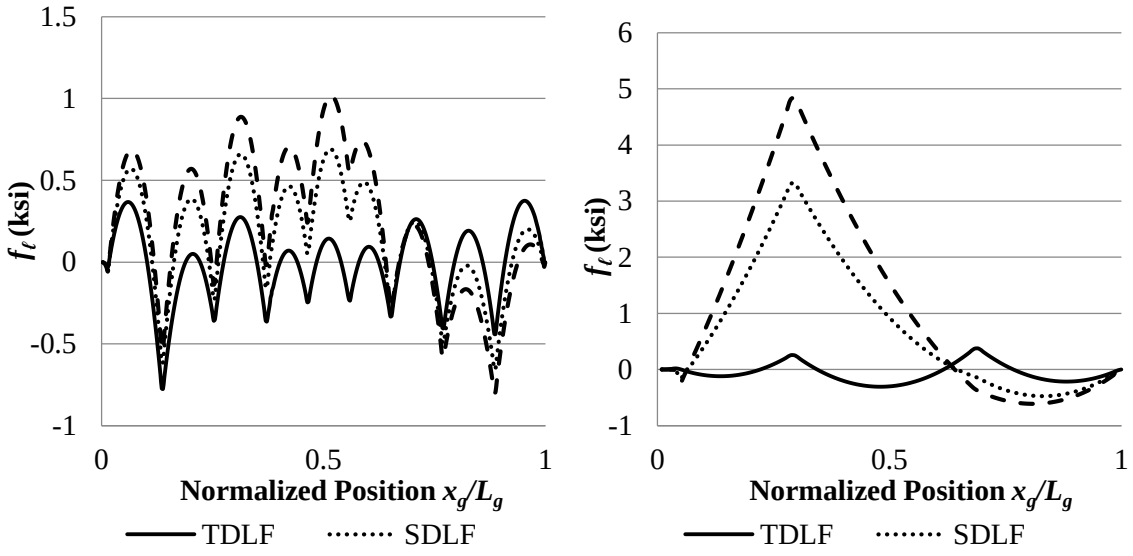

Figure 153. Top flange f_ℓ in Bridge (H1) EISSS57 longer fascia girder (left) and shorter fascia girder (right) under TDL with detailing based on LGA cambers.

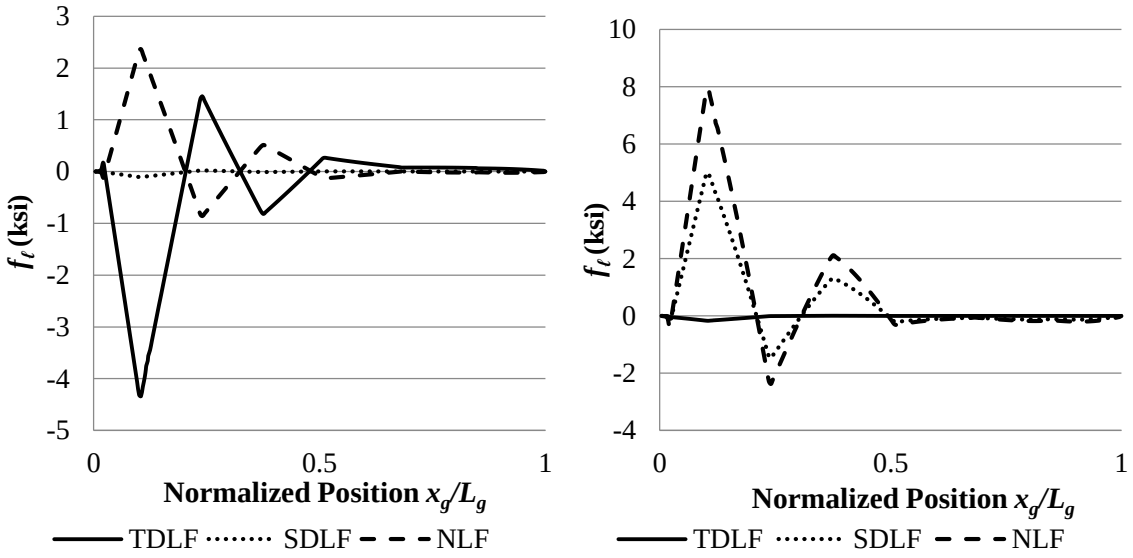

Figure 154. Top flange f_ℓ in Bridge (H1) EISSS57 middle girder under SDL (left) and under TDL (right) with detailing based on LGA cambers.

6.8.1.6 Vertical Reactions

With SDLF and TDLF detailing based on LGA cambers, the girders in straight skewed bridges behave as line girders under the targeted load condition. The vertical reactions can be calculated accurately with LGA for each of the girders in this condition – SDL for SLDF and TDL for TDLF, but that cannot be calculated accurately with LGA in any other condition. This statement of course applies to all the other bridge DL responses as well.

From Table 48, the maximum absolute and percentage increases in the TDL vertical reactions are 11 kips and 34%, respectively, due to SDLF detailing based on LGA cambers, in Bridge (H1). This maximum increase occurs at the shorter fascia Girder G1 bearing on the skewed bearing line. The maximum absolute and percentage increase in the TDL vertical reactions are 27 kips (81%) due to TDLF detailing based on LGA cambers. This maximum occurs at the same bearing. The maximum absolute and percentage decreases in the TDL vertical reactions are 9 kips and 8%, respectively, due to SDLF detailing based on LGA cambers, in Bridge (H1). The maximum absolute and percentage decreases in the TDL vertical reactions are 31 kips (20%) due to TDLF detailing based on LGA cambers. The changes in the vertical reactions in bridge (H2) is not as significant as in bridge (H1).

With SDLF and TDLF detailing based on LGA cambers, the girders in straight skewed bridges behave as line girders under the targeted load condition. The vertical reactions can be calculated accurately with LGA for each of the girders in this condition – SDL for SLDF and TDL for TDLF, but they cannot be calculated accurately with LGA in any other condition. This statement of course applies to all the other bridge DL responses as well. The reactions for SDLF under TDL can be calculated as the sum of the LGA SDL reactions

and NLF RA CDL reactions. The reactions for TDLF under SDL can be calculated as the sum of the LGA TDL reactions and the negative of the NLF RA CDL reactions.

Table 48. Bridge (H1) EISSS57 vertical reactions (kips) (G1 and G7 are fascia girders), detailing based on LGA cambers.

Girder	Detailing Method	SDL Support 1	SDL Support 2	TDL Support 1	TDL Support 2
G1	NLF	8	10	32	42
	SDLF	19	15	43	47
	TDLF	33	22	59	53
G2	NLF	28	33	99	113
	SDLF	29	24	100	104
	TDLF	30	12	101	93
G3	NLF	30	38	95	124
	SDLF	36	32	102	117
	TDLF	51	26	118	112
G4	NLF	55	44	156	136
	SDLF	44	40	146	132
	TDLF	22	27	125	119
G5	NLF	58	46	163	139
	SDLF	50	46	155	138
	TDLF	37	45	143	137
G6	NLF	59	48	164	140
	SDLF	56	52	161	143
	TDLF	56	64	161	155
G7	NLF	52	53	151	154
	SDLF	62	60	159	160
	TDLF	73	65	169	165

Table 49. Summary of maximum absolute and percentage increases and decreases in the TDL vertical reactions at the girder bearings, due to SDLF and TDLF detailing based on LGA cambers, in the straight bridges with non-parallel skew (the largest of these maximum absolute and percentage increases are highlighted by dark shading).

Bridge	SDLF				TDLF			
	Decreases		Increases		Decreases		Increases	
	Max (kips)	Max %	Max (kips)	Max %	Max (kips)	Max %	Max (kips)	Max %
(H1) EISSS57	**-9**	**-8**	**11**	**34**	**-31**	**-20**	**27**	**81**
(H2) EISSS57	-5	-5	9	24	-21	-15	21	56

6.8.2 Summary and Recommendations – Straight Bridges with Non-Parallel Skew and Cambers Set Based on LGA

The influence of SDLF and TDLF detailing on the responses in completed straight bridge systems with non-parallel skew and girder cambers calculated based on LGA may be summarized as follows. Recommendations pertaining to these quantitative results are highlighted in bold italicized text.

General

- The use of LGA for setting the girder cambers in sharply skewed straight bridges is generally discouraged based on the considerations discussed in Section 6.2.3.
- Straight bridges with a difference in the skew angles at the ends of all the spans less than or equal to $\Delta\theta = 20^{o}$ may be considered as parallel skew bridges. Section 6.6 applies in these cases.
- With LGA cambers, the responses of straight non-parallel skew bridges are close to the ideal theoretical values (i.e., in the targeted DL conditions, zero layover, CF forces, and

girder flange lateral bending stresses, and girder major-axis bending stresses and vertical reactions equal to the values from LGA).

- The following discussions focus predominantly on the TDL results with TDLF detailing based on LGA cambers, using the Bridge (H1) EISSS57 as an extreme example.

Girder Elevations

- For Bridge (H1) EISSS57, the maximum deviation from the targeted elevations is 0.03 inches under the TDL with TDLF based on the LGA cambers.
- ***It is recommended that LGA alone should not be utilized for calculation of the girder total cambers in straight bridges with parallel or non-parallel skew, unless TDLF detailing is employed.***
- ***It is recommended that, if LGA is used for calculating the girder cambers in straight bridges with parallel or non-parallel skew, the girder TDL cambers should be calculated as follows:***
    - ***For TDLF, the negative of the girder TDL vertical deflections obtained from the LGA.***
    - ***For SDLF, the negative of the girder SDL vertical deflections obtained from the LGA plus the negative of the CDL vertical deflections obtained from a NLF RA.***

Girder Layovers

- For Bridge (H1) EISSS57, the maximum girder layover under the TDL, with TDLF detailing based on LGA cambers, is 0.1 inches (0.001 rad).

- ***It is recommended that the girder layovers may be assumed to be negligible in the targeted DL condition in straight bridges with parallel or non-parallel skew when the CFs are detailed using the above recommended procedures with LGA. The fascia girders should be checked separately for twist rotation between the CF locations due to eccentric overhang bracket loads.***
- ***For straight bridges with parallel or non-parallel skew, detailed for SDLF using the above recommended procedures with LGA, the girder layovers under the TDL may be estimated as the CDL layovers obtained from a NLF RA.***
- ***For straight bridges with parallel or non-parallel skew, detailed for TDLF using the above recommended procedures with LGA, the girder layovers under the SDL may be estimated as the negative of the CDL layovers obtained from a NLF RA.***

Cross-Frame Forces

- Under SDL in Bridge (H1) NISSS57, the largest ratio of the average of the CF member forces for SDLF detailing to the corresponding forces for NLF detailing is 0.07 for SDLF based on LGA cambers.
- Under SDL in Bridge (H1) NISSS57, the largest ratio of the maximum CF member force for SDLF detailing to the corresponding force for NLF detailing is 0.26 for SDLF based on LGA cambers. That is, the beneficial locked-in force is 1.0 – 0.26 = 0.74 of the CF force corresponding to NLF detailing for this member.
- Under TDL in Bridge (H1) NISSS57, the largest ratio of the average of the CF member forces for TDLF detailing to the corresponding forces for NLF detailing is 0.14 for TDLF based on LGA cambers.

- Under TDL in Bridge (H1) NISSS57, the largest ratio of the maximum CF member force for TDLF detailing to the corresponding force for NLF detailing is 0.37 for TDLF based on LGA cambers. That is, the beneficial locked-in force is 1.0 – 0.37 = 0.63 of the CF force corresponding to NLF detailing for this member.
- ***In lieu of a DLF RA, it is recommended that a net load factor of (γ_p – 0.65) be used for determination of the factored SDL CF forces in straight I-girder bridges with parallel or non-parallel skew, when the CFs are detailed for SDLF using the recommended procedures with LGA. This net load factor is to be applied to the results from a NLF RA for the SDL. It should be noted that these SDL CF forces must be added to the factored CDL CF forces from a NLF RA to obtain the total factored DL CF forces.*** The factor of 0.65 is a slightly conservative estimate of the maximum SLDF locked-in force ratio of 1.0 – 0.26 = 0.74, selected to be consistent with the recommendations for straight parallel-skew bridges.
- ***In lieu of a DLF RA, it is recommended that a net load factor of (γ_p – 0.65) be used for determination of the factored TDL CF forces in straight I-girder bridges with parallel or non-parallel skew, when the CFs are detailed for TDLF using the recommended procedures with LGA. This net load factor is to be applied to the results from a NLF RA for the TDL. The factored CF forces under the SDL may be estimated by subtracting the factored CDL CF forces obtained by a NLF RA from the above factored TDLF forces.*** The factor of 0.65 is an estimate of the TDLF locked-in force of 1.0 – 0.37 = 0.63, selected to be consistent with the recommendations for straight parallel-skew bridges. In cases where additional uncertainties and variabilities associated with TDLF are anticipated, such as incidental participation of deck forms

and early concrete stiffness in the structural resistance, and/or larger potential play in the CF connections due to the larger CF forces associated with TDLF, it is suggested that a value between 0.65 and 0.50 may be used for the above locked-in force estimate based on the judgment of the engineer of record. This suggested reduction is based on the judgement of the research. The current research did not perform any specific investigations of the above effects.

- The maximum difference in the magnitude of the individual CF member forces from a DLF RA and (1 – 0.65 = 0.35) of the estimated values from a NLF RA, normalized by the member yield load, is 1.1 and 4.8 %, and the average difference is -0.5 and -1.4 % for SDLF under SDL and TDLF under TDL, respectively, for the straight bridges with non-parallel skew studied in this research and girder cambers based on LGA.
- The maximum difference in the magnitude of the individual CF member forces from a DLF RA and (1 – 0.65 = 0.35) of the estimated values from a NLF RA, normalized by the member yield load, is 1.1 and 3.1 %, and the average difference is -0.5 and -1.0 % for SDLF under SDL and TDLF under TDL, respectively, for the straight bridges studied in this research with non-parallel skew and girder cambers based on LGA.

Girder Stresses

- For Bridge (H1) EISSS57, the largest maximum girder flange lateral bending stress (f_ℓ), under the TDL for TDLF based on LGA cambers, is 0.8 ksi, 80 % of the corresponding maximum girder NLF value. This f_ℓ occurs on the longest fascia girder in the bridge. The next largest maximum girder f_ℓ is 0.4 ksi, on the shortest fascia girder under the TDL for TLDF based on LGA cambers, and is 8 % of the corresponding maximum girder NLF value. The largest maximum girder f_ℓ based on the assumption

of NLF detailing is 8.4 ksi, and occurs on the interior Girder 3 in this bridge. The maximum f_ℓ on Girder 3 is reduced to 0.1 ksi (1 % of the above NLF value) by the use of TDLF detailing based on the LGA cambers.

- For all the bridges studied in this research, the use of an assumed locked-in f_ℓ of 0.65 of the f_ℓ from a NLF RA gives an accurate to conservative estimate of the f_ℓ values determined from a DLF RA.
- ***In lieu of a DLF RA, for straight bridges with non-parallel skew and with the CFs detailed for SDLF using the recommended procedures with LGA, it is recommended that the corresponding procedures for calculation of the CF forces proposed for parallel-skew bridges also be used for determining the girder f_ℓ values.***
- In (H1) NISSS57, the largest increase in any of the girder major-axis bending stresses under the TDL, due to the effect of SDLF detailing based on LGA cambers, is 1.5 ksi (6%). The largest increase in any of the girder major-axis bending stresses under the TDL, due to the effect of TDLF detailing based on LGA cambers, is 2.9 ksi (13%). The largest increase occurs in the long fascia Girder G7, but a slightly smaller increase appears in the short fascia Girder G1.
- The LGA solution gives accurate f_b values for the targeted DL condition – SDL for SDLF and TDL for TDLF.
- ***In lieu of a DLF RA, for straight bridges with non-parallel skew and with the CFs detailed using the above recommended procedures with LGA, it is recommended that the girder f_b values in the targeted DL condition be taken as the values from the LGA.***
- ***In lieu of a DLF RA, for straight bridges with non-parallel skew and with the CFs detailed for SDLF using the recommended procedures with LGA, the girder f_b values***

under the TDL may be estimated by adding the CDL f_b values obtained from a NLF RA to the SDL f_b values obtained from LGA.

- ***In lieu of a DLF RA, for straight bridges with non-parallel skew and with the CFs detailed for TDLF using the recommended procedures with LGA, the girder f_b values under SDL may be estimated by subtracting the CDL f_b values obtained from a NLF RA from the TDL f_b values obtained from LGA.***

Vertical Reactions

- When LGA cambers are used with (H1) NISSS57, the results for the girder reactions parallel the above results for the girder major-axis bending stresses, except that the largest increases in the reactions are affected more significantly.
- For (H1) NISSS57, when the cambers are determined from LGA, the largest increase in the reactions is 34 % due to SDLF detailing and 81 % due to TDLF detailing for the critical Bridge (H1) EISSS57 relative to the NLF RA solution.
- ***In lieu of a DLF RA, for straight bridges with non-parallel skew and with the CFs detailed using the recommended procedures with LGA, it is recommended that the girder reactions in the targeted DL condition be taken as the values from the LGA.***
- ***In lieu of a DLF RA, for straight bridges with non-parallel skew and with the CFs detailed for SDLF using the recommended procedures with LGA, the girder reactions under the TDL may be estimated by adding the CDL reactions obtained from a NLF RA to the SDL reactions obtained from LGA.***
- ***In lieu of a DLF RA, for straight bridges with non-parallel skew and with the CFs detailed for TDLF using the recommended procedures with LGA, the girder***

reactions under SDL may be estimated by subtracting the CDL reactions obtained from a NLF RA from the TDL reactions obtained from LGA.

The above recommendations are considered applicable for straight bridges with non-parallel skew, skew angles up to 70^{o}, and spans up to 300 ft.

For bridges that exceed these limits, it is recommended that DLF RA be considered. Chapter 3 explains the details of several procedures for conducting a DLF RA.

6.9 Straight Bridges with Non-Parallel Skew and Cambers Set Based on NLF RA

Straight bridges with a difference in the skew angles at the ends of all the spans less than equal to $\Delta\theta = 20^{o}$ may be considered as parallel skew bridges, and are addressed in Sections 6.6 and 6.7. The following discussions focus predominantly on the TDL results with TDLF detailing based on NLF RA cambers, using the Bridge (H1) EISSS57 as an extreme example. In (H1) EISSS57, the pattern of the RA cambers is very similar to the pattern of the LGA cambers, but the RA cambers are smaller in magnitude than the LGA cambers.

Section 6.9.1 provides quantitative results on the influence of SDLF and TDLF detailing with cambers set based on NLF RA. The influence of SDLF and TDLF is discussed on the responses in the following order: girder vertical displacements, girder elevations, girder layovers, CF forces, girder stresses, and vertical reactions. Section 6.9.2 then summarizes the influences on the key bridge responses, and provides recommendations for handling these effects. The recommendations are highlighted in bold italicized text.

6.9.1 Quantitative Results

6.9.1.1 Girder Vertical Displacements

For straight bridges with non-parallel skew based on NLF RA, SDLF and TDLF detailing tend to increase the vertical displacement of the longer fascia girder and reduce the vertical displacements of the other girders. The increase or decrease in the vertical displacements when the cambers are based on NLF RA is not as significant as when the cambers are based on LGA. This is because when the cambers are set based on NLF RA, the resulting targeted DL elevations are essentially the "natural" deflected elevations of the girders under the targeted DL in the 3D structural system. As such, the girders are subjected predominantly just to twist rotations to move them from their deflected out-of-plumb geometry in the 3D system to their approximately plumb targeted DL geometry, via the DLF detailing effects. The girder twisting is accomplished with relative ease when the straight girders are in this "natural" deflected geometry.

Figure 155 shows the fascia and middle interior girder TDL vertical displacements in Bridge (H1) EISSS57 if the CFs are detailed for TDLF based on the cambers calculated from NLF RA (calculated using the common practice of constructing a model of the full bridge system and "turning gravity on"). In this case, both the fascia and interior girder displacements are practically unaffected by the CF detailing. The maximum displacement difference between TDLF and NLF is 0.39 inches on the longer fascia girder.

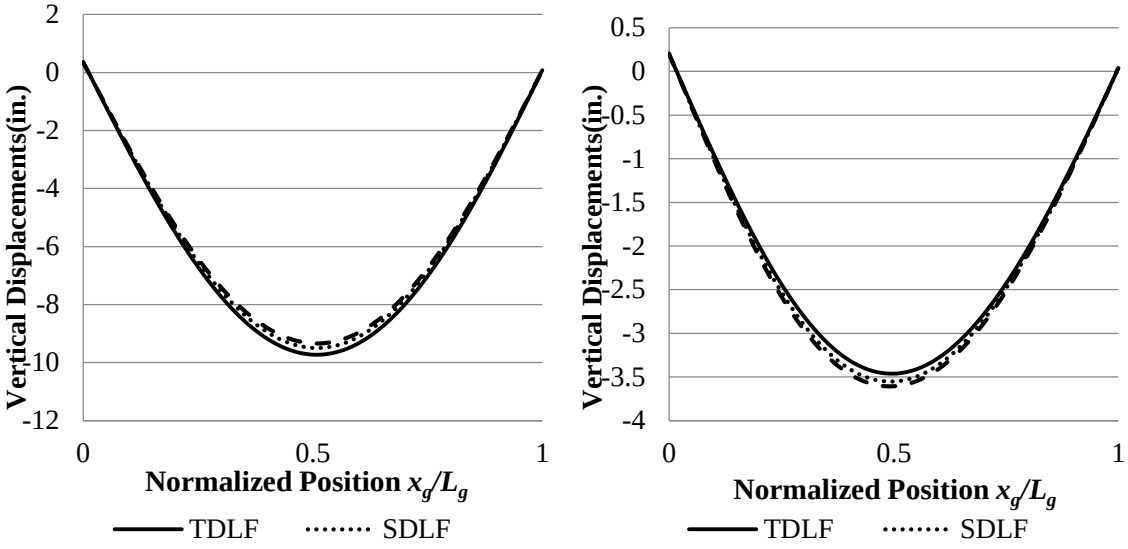

Figure 155. Bridge (H1) EISSS57 critical fascia girder (left) and middle girder (right) vertical displacements under TDL with the CFs detailed based on NLF RA cambers.

6.9.1.2 Girder Elevations

The girder cambers are based on NLF RA in this section. The vertical elevations under TDL for NLF detailing are theoretically zero (assuming no superelevation, etc., as a simplification). Figure 156 shows the results for the girder TDL elevations in Bridge (H1) EISSS57, with all of the calculations conducted by NLF RA. One can observe that, as one might expect, the elevations are the exact "zero" values for NLF detailing, since the bridge responds in this case as if the gravity loads were simply "turned on." The vertical elevations deviate slightly from the targeted zero values for SDLF detailing, and the deviations are somewhat larger for the case of TDLF detailing. Bridge (H1) exhibits a maximum deviation of 0.4 inches from the targeted DL elevations with TDLF detailing.

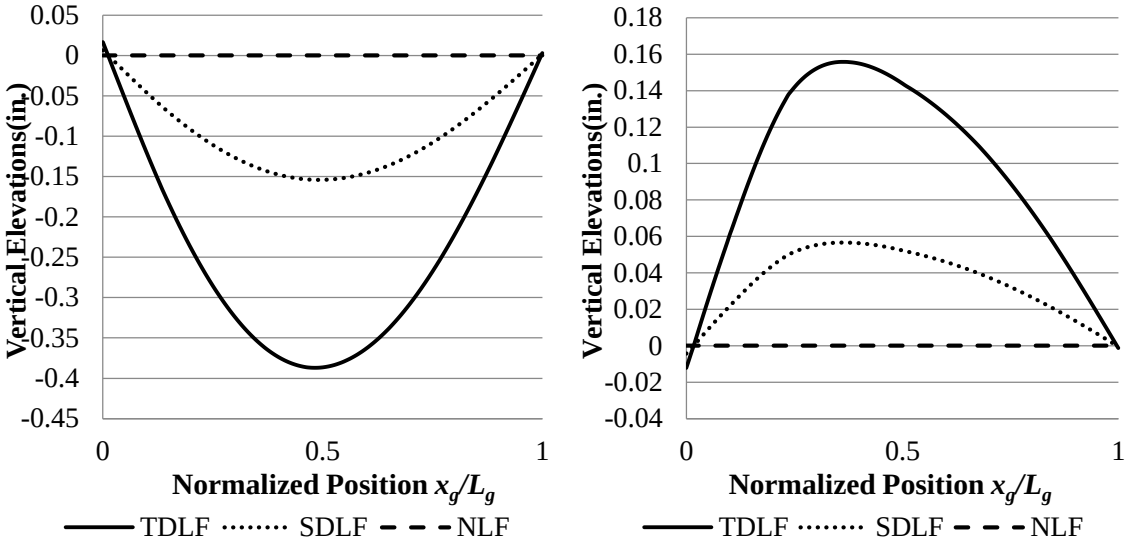

Figure 156. Bridge (H1) EISSS57 longer fascia girder (left) and middle girder (right) vertical elevations under TDL with the CF detailed based on NLF RA and the girder TDL cambers based entirely on NLF RA

6.9.1.3 Girder Layovers

In straight skewed bridges, SDLF and TDLF detailing based on RA cambers still gives approximately plumb webs under the targeted condition. However, the layovers are no longer theoretically zero under the targeted condition. This is due to the overall elastic deformations of the CFs and the elastic torsional deformations of the girders in the structural system. There is only one set of cambers and corresponding CF drops that gives theoretically exactly plumb webs for straight skewed bridges – the LGA cambers.

Figure 157 shows the longer fascia girder layover under TDL for Bridge (H1) EISSS57 based on NLF RA. One can observe that the layovers with TDLF detailing based on NLF RA are approximately zero under TDL.

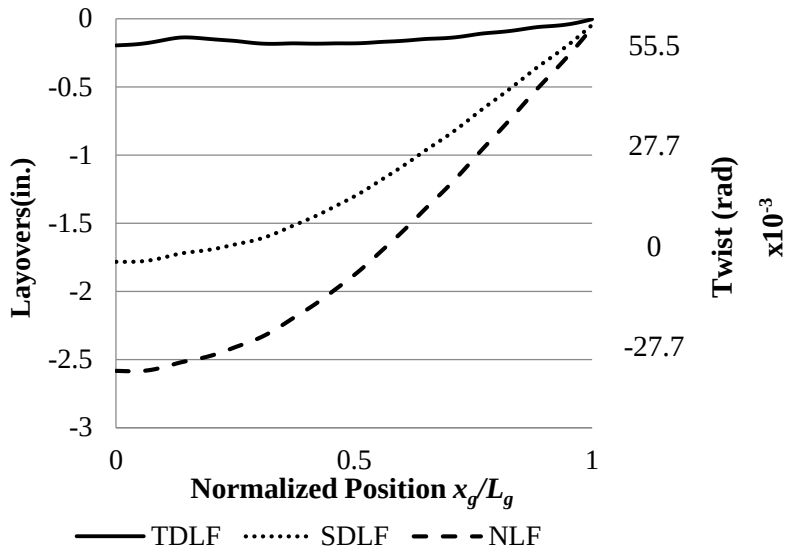

Figure 157. Longer fascia girder layover under the TDL for Bridge (H1) EISSS57 with detailing based on NLF RA.

6.9.1.4 Cross-Frame Forces

In straight non-parallel skewed bridges, SDLF and TDLF detailing based on RA cambers gives small CF forces under the targeted condition. However, the CF forces are not theoretically zero under the targeted condition due to the overall elastic deformations of the CFs and the elastic torsional deformations of the girders in the structural system, for reasons discussed in Section 6.2.2.

Tables 50 and 51 report the average magnitude of the CF member forces and the maximum magnitude of these forces in Bridge (H1) EISSS57. The following can be observed from these tables:

- Under SDL, the largest F2/F1 ratio of the average of the CF member forces is 0.61.
- Under SDL, the largest F2/F1 ratio of the maximum CF member force is 0.62.
- Under TDL, the largest F3/F1 ratio of the average of the CF member forces is 0.62.
- Under TDL, the largest F3/F1 ratio of the maximum CF member force is 0.65.

Table 50. Average magnitude of the CF member forces in straight non-parallel skewed bridge EISSS57 (F1, F2, and F3 are the average CF forces with NLF, SDLF, and TDLF detailing based on NLF RA cambers, respectively).

Load Cond.	NLF	SDLF			TDLF		
	F1 (kip)	F2 (kip)	F2/F1	F2 – F1 (kip)	F3 (kip)	F3/F1	F3 – F1 (kip)
SDL	4.6	2.8	0.61	-1.8	2.6	0.57	-2.0
TDL	12.1	10.2	0.83	-1.9	7.5	0.62	-4.6

Table 51. Maximum magnitude of the CF member forces in straight non-parallel skewed bridge EISSS57 (F1, F2, and F3 are the maximum CF forces with NLF, SDLF, and TDLF detailing based on NLF RA cambers, respectively).

Load Cond.	NLF	SDLF			TDLF		
	F1 (kip)	F2 (kip)	F2/F1	F2 – F1 (kip)	F3 (kip)	F3/F1	F3 – F1 (kip)
SDL	19.2	12.0	0.62	-7.2	12.1	0.63	-7.1
TDL	48.8	42.5	0.87	-6.3	31.7	0.65	-17.1

Figure 158 shows the actual distribution of the CF forces under the SDL in Bridge (H1) EISSS57, including the locked-in force effects from SDLF detailing with NLF RA cambers. The presentation of the CF forces in these plots, as well as the plots in the subsequent figures is similar to Section 6.5.1.4. The reader is referred to this previous section for an explanation of these details. One can observe that the largest of the CF member forces in Figure 158 is only 12.0 kips.

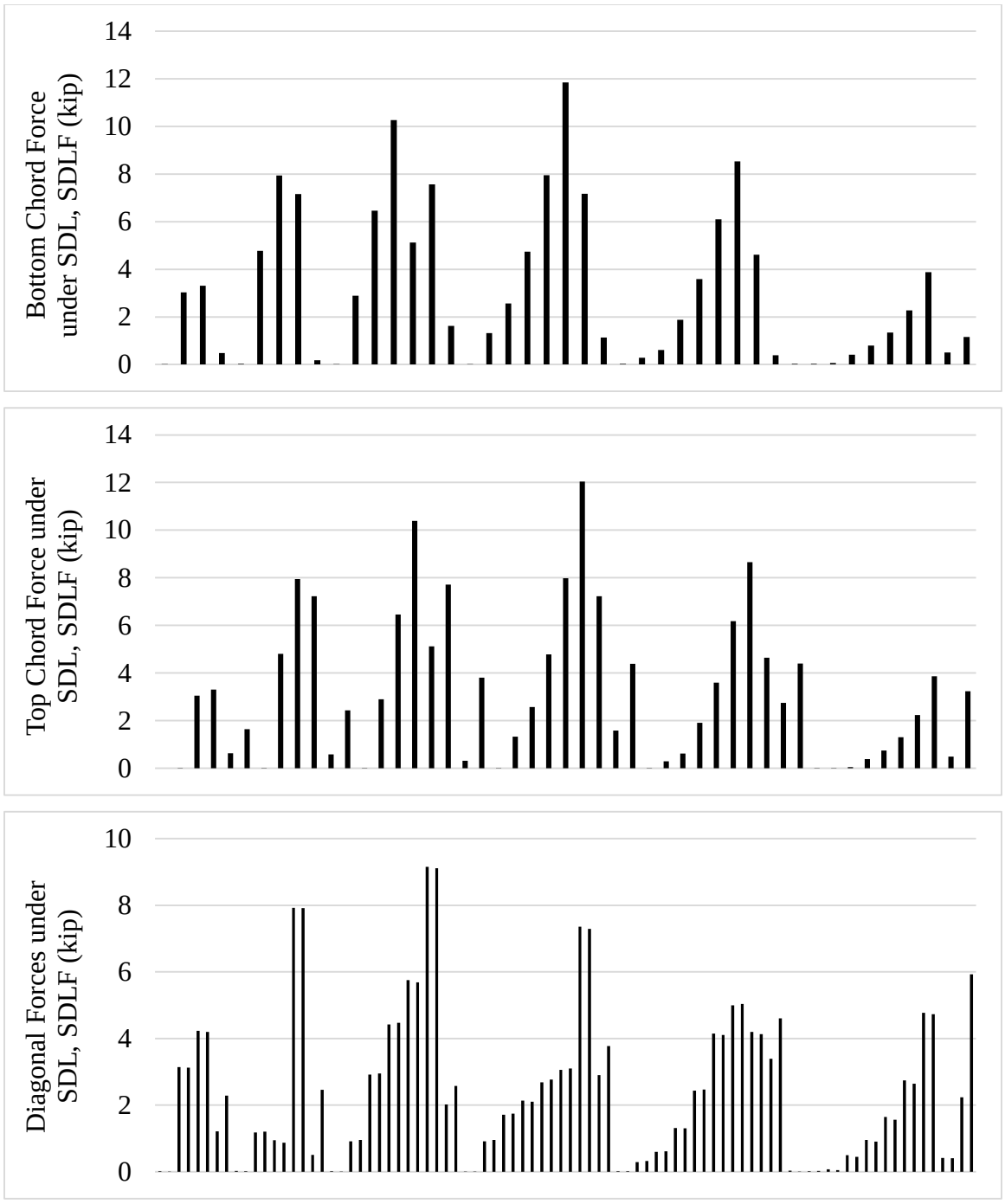

Figure 158. Magnitude of CF member forces from DLF RA, Bridge (H1) EISSS57 under SDL, SDLF detailing based on NLF RA cambers.

Figure 159 shows an estimate of the CF forces under the SDL, assuming SDLF detailing, obtained by scaling the NLF RA forces for all the cross-frame members by 1.0. This is the scale factor recommended in Section 6.7.2 for both SDL/SDLF and TDL/TDLF estimates in straight parallel skew bridges. One can observe that almost all of the CF force values from Figure 158 are estimated accurately to conservatively. However, the actual distribution of the CF forces from Figure 158 is predicted poorly. The poor prediction of the CF force distribution is not of any significant consequence though since all the CF forces are relatively small. Since Figure 159 simply shows all the NLF RA CF forces scaled by 1.0, it can be concluded that the distribution of the non-zero CF forces under SDL associated with NLF detailing is very different from the distribution of the reduced (smaller) CF forces under SDL associated with SDLF detailing. Figure 160 shows the difference between the magnitude of the DLF RA forces and the CF forces under SDL, assuming SDLF detailing, estimated by scaling the NLF RA forces, divided by the CF member yield loads. One can observe that the largest under-prediction of the DLF RA results is $0.007P_y$ for one of the chords of the cross-frame. The largest over-prediction is -0.0454 using the recommended estimate. Figure 161 shows the same results, but under TDL and assuming TDLF detailing. The maximum under-prediction is 0.0409 and the largest over-prediction is -0.0506 for this case.

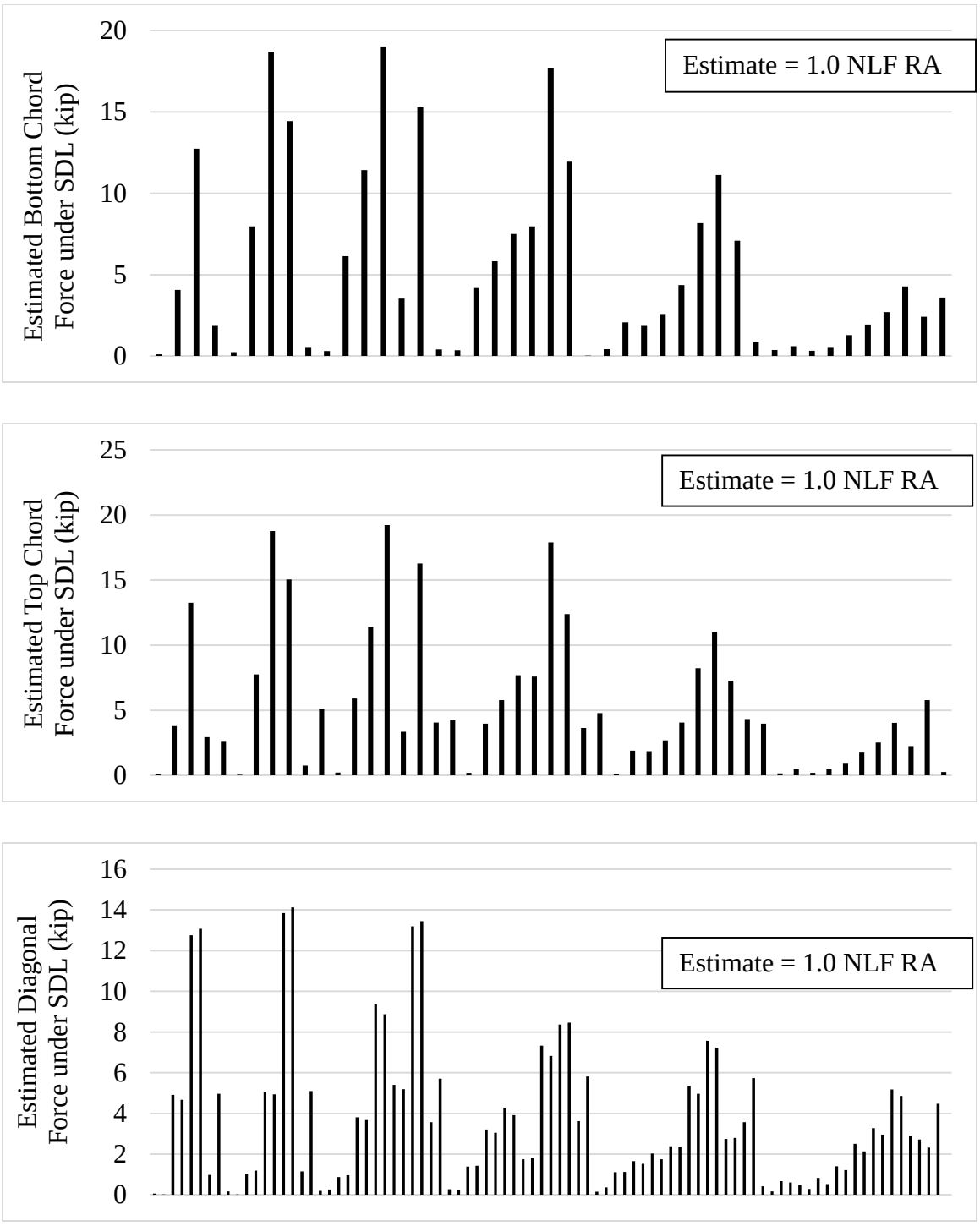

Figure 159. Estimated magnitude of CF member forces based on scaling of NLF RA results, assuming SDLF detailing, Bridge (H1) EISSS57 under SDL.

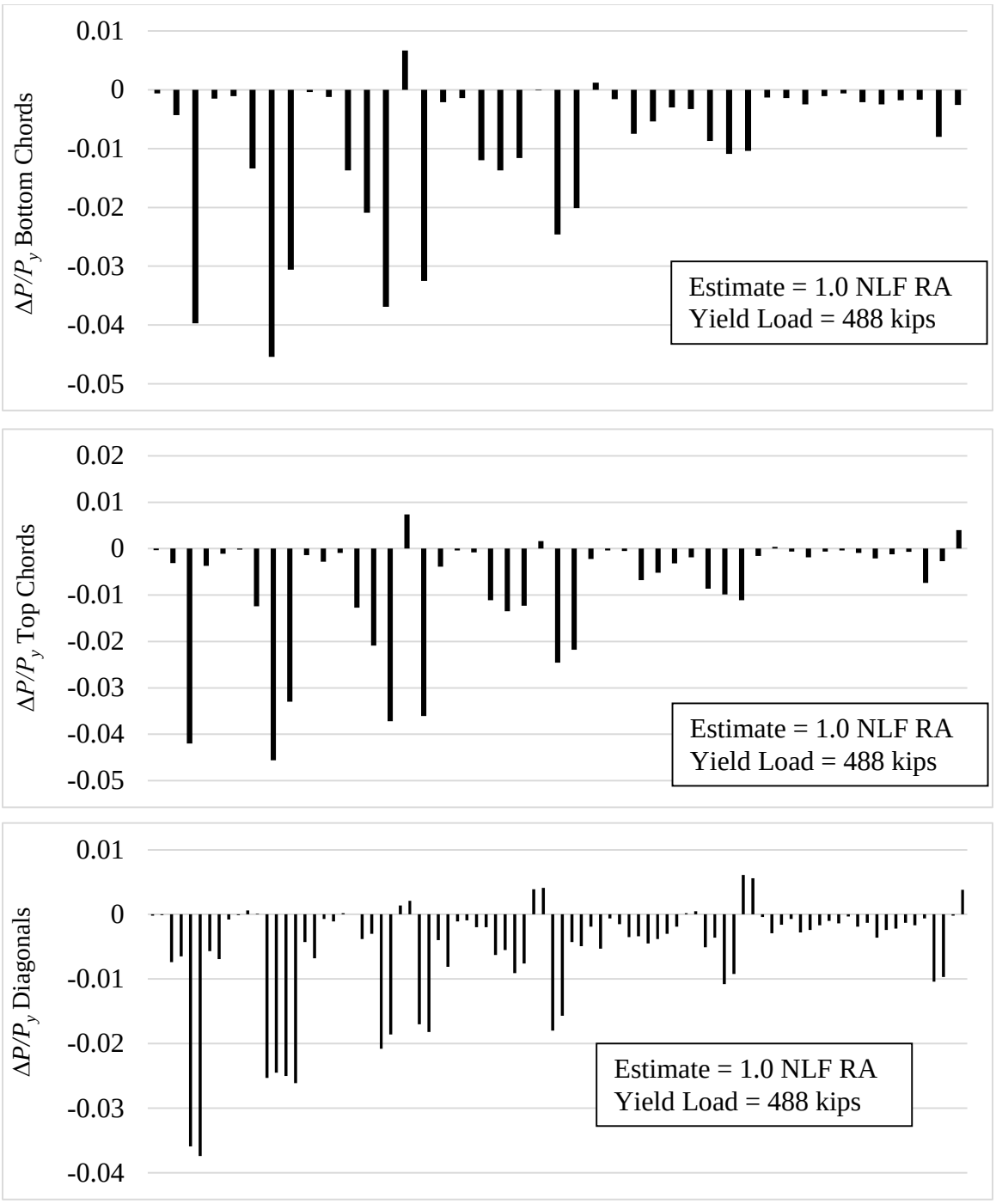

Figure 160. Difference between the magnitude of the DLF RA forces and the values estimated by scaling the NLF RA results, divided by the member yield load (ΔP/Py), Bridge (H1) EISSS57 under SDL, SDLF detailing based on NLF RA cambers.

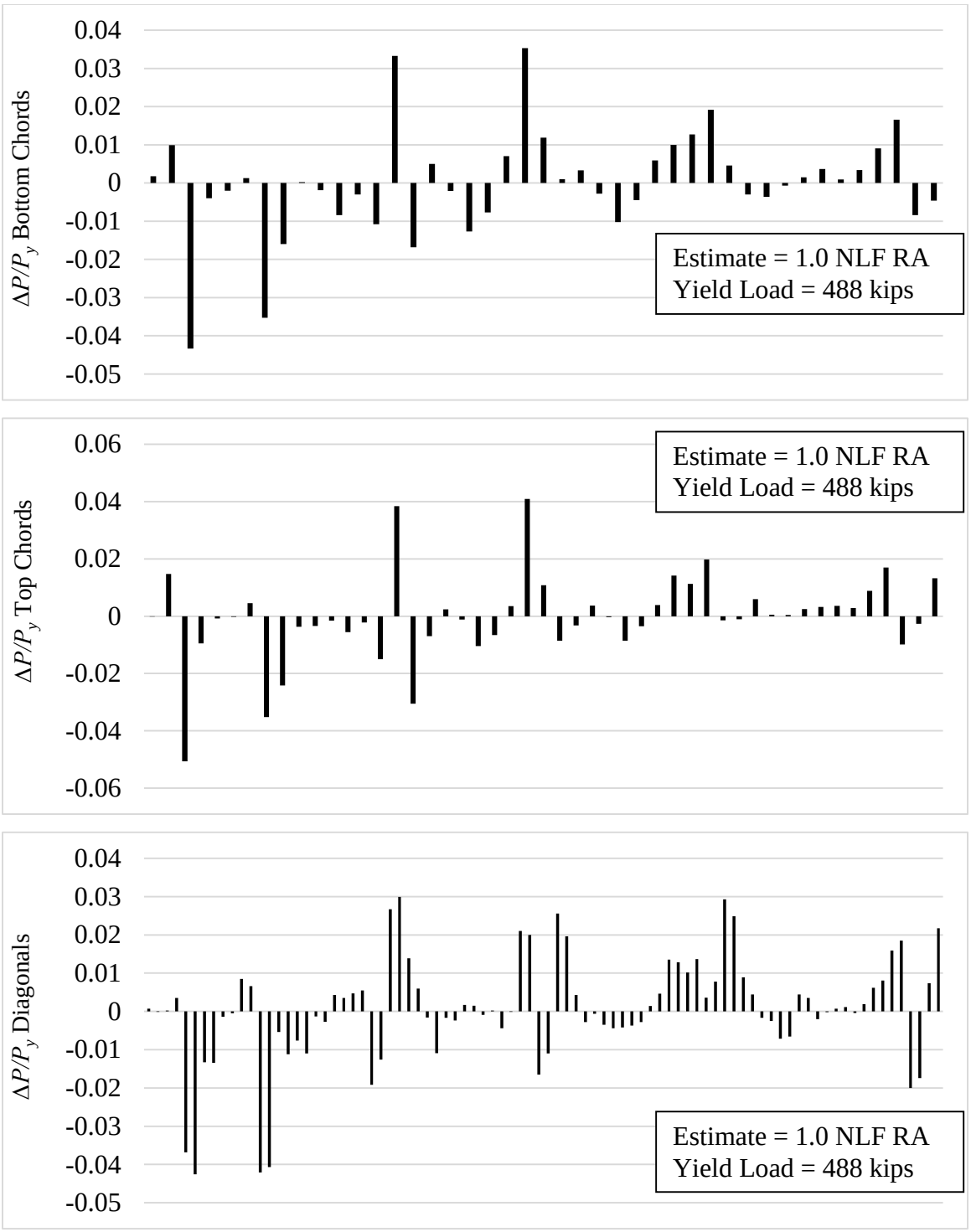

Figure 161. Difference between the magnitude of the DLF RA forces and the values estimated by scaling the NLF RA results, divided by the member yield load (ΔP/Py), Bridge (H1) EISSS57 under TDL, TDLF detailing based on NLF RA cambers.

6.9.1.5 Girder Stresses

For straight bridges with non-parallel skew, the SDLF and TDLF detailing effects based on NLF RA cambers tend to increase the major-axis bending stresses in the longer fascia girder and decrease these stresses in the other girders. This behavior is shown in Figure 163 for Bridge (H1) EISSS57. These changes in the major-axis bending stresses are negligible for Bridge (H1).

The girder flange lateral bending stresses are small under SDL for SDLF detailing and under TDL for TDLF detailing based on RA cambers, and they are generally significant under TDL if NLF detailing is used. This behavior is shown in Figure 165 for Bridge (H1) under the TDL.

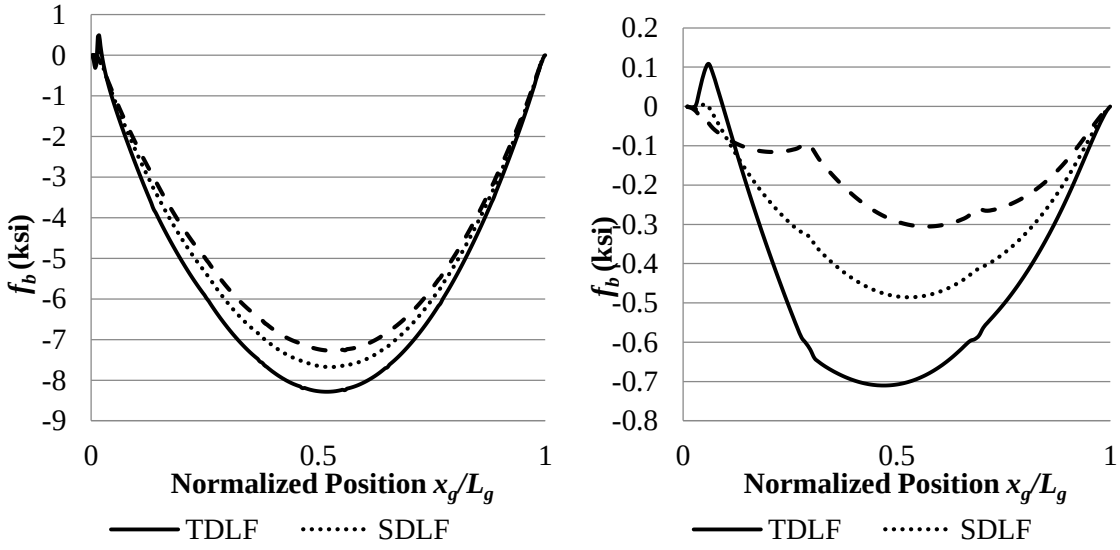

Figure 162. Top flange f_b in Bridge (H1) EISSS57 longer fascia girder (left) and short fascia girder (right) under SDL with detailing based on NLF RA cambers.

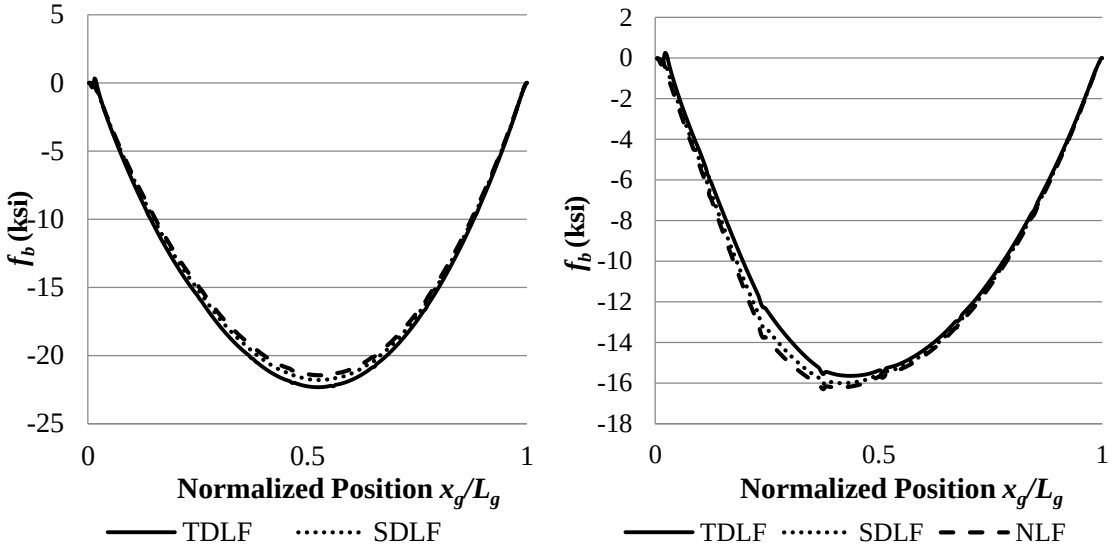

Figure 163. Top flange f_b in Bridge (H1) EISSS57 longer fascia girder (left) and short fascia girder (right) under TDL with detailing based on NLF RA cambers.

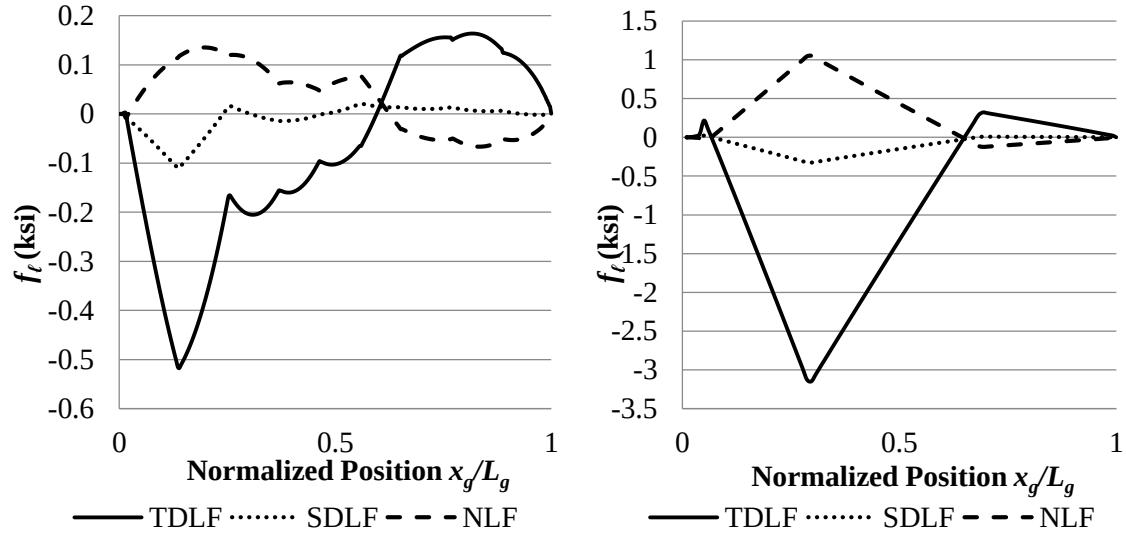

Figure 164. Top flange f_ℓ in Bridge (H1) EISSS57 longer fascia girder (left) and short fascia girder (right) under SDL with detailing based on NLF RA cambers.

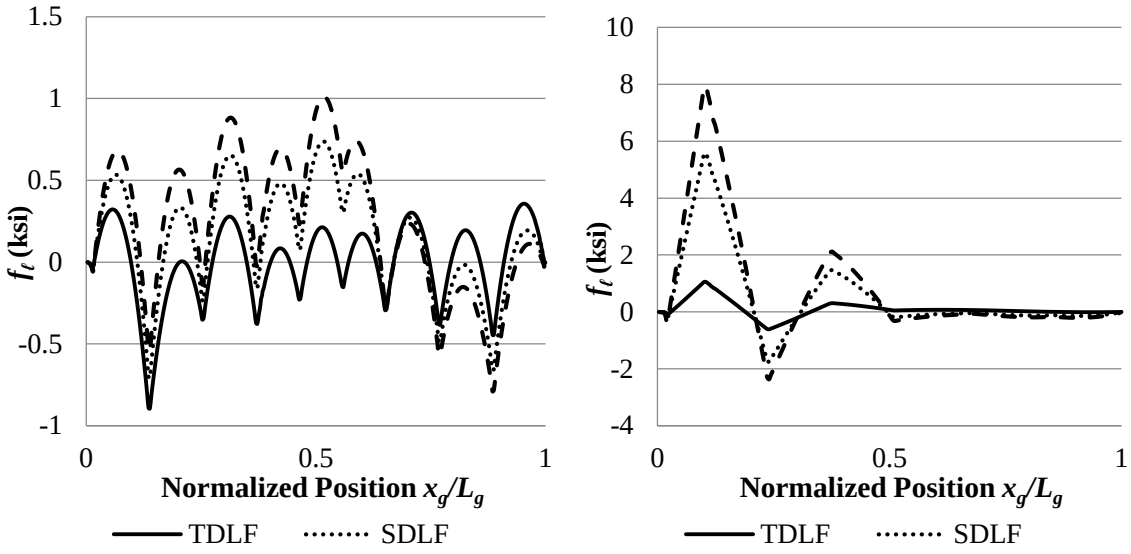

Figure 165. Top flange f_ℓ in Bridge (H1) EISSS57 longer fascia girder (left) and short fascia girder (right) under TDL with detailing based on NLF RA cambers.

6.9.1.6 Vertical Reactions

Table 52 shows the vertical reactions for Bridge (H1) with cambers set based on NLF RA. From Tables 52 and 53, the largest increase in the reactions under TDL is 5 kips (23 %) due to SDLF detailing and 19 kips (58 %) due to TDLF detailing for Bridge (H1). This maximum occurs at the shorter fascia Girder G1 bearing on the skewed bearing line. The reactions on the shorter fascia Girder G1 are somewhat smaller for this case, where the girder cambers are based on NLF RA, compared to the results in Table 48, where the girder cambers are based on LGA. This is behavior is related to the fact that the girder vertical displacements are changed substantially by the DLF detailing when LGA cambers are used, whereas there is little change in the girder vertical displacements due to DLF detailing with RA cambers. The largest decrease in the reactions under TDL is 6 kips (5 %) due to SDLF detailing and 15 kips (12 %) due to TDLF detailing for Bridge (H1). It can be observed that for this severe case, a DLF RA is required to accurately predict the reactions. The use

of LGA SDL reactions plus NLF RA CDL can be used to give a conservative estimate of SDLF under TDL reactions. The use of LGA TDL reactions can be used to give a conservative estimate of TDLF under TDL reactions. In addition, for bridge (H2), which follows the framing recommendations in this research, the change in the reactions due to SDLF and TDLF can be neglected.

Table 52. Bridge (H1) EISSS7 vertical reactions (kips) (G1 and G7 are fascia girders), detailing based on NLF RA cambers.

Girder	Detailing Method	SDL Support 1	SDL Support 2	TDL Support 1	TDL Support 2
G1	NLF	8	10	32	42
	SDLF	15	13	40	44
	TDLF	26	15	51	47
G2	NLF	28	33	99	113
	SDLF	26	27	97	107
	TDLF	23	19	94	99
G3	NLF	30	38	95	124
	SDLF	30	36	96	122
	TDLF	33	34	99	119
G4	NLF	55	45	156	136
	SDLF	51	44	153	136
	TDLF	45	42	147	133
G5	NLF	58	46	163	139
	SDLF	56	47	161	139
	TDLF	53	47	158	139
G6	NLF	59	48	164	140
	SDLF	59	49	164	141
	TDLF	60	52	164	143
G7	NLF	52	54	151	154
	SDLF	54	56	152	156
	TDLF	58	59	154	159

Table 53. Summary of maximum absolute and percentage increases and decreases in the TDL vertical reactions at the girder bearings, due to SDLF and TDLF detailing based on NLF RA cambers, in the straight bridges with non-parallel skew (the largest of these maximum absolute and percentage increases are highlighted by dark shading).

Bridge	SDLF				TDLF			
	Decreases		Increases		Decreases		Increases	
	Max (kips)	Max %	Max (kips)	Max %	Max (kips)	Max %	Max (kips)	Max %
(H1) EISSS57	**-6**	**-5**	**5**	**23**	**-15**	**-13**	**19**	**58**
(H2) EISSS57	-3	-4	5	7	-7	-11	4	12

6.9.2 Summary and Recommendations – Straight Bridges with Non-Parallel Skew and Cambers Set Based on NLF RA

The influence of SDLF and TDLF detailing on the responses in completed straight bridge systems with non-parallel skew and girder cambers calculated based on NLF RA may be summarized as follows. Recommendations pertaining to these quantitative results are highlighted in bold italicized text.

General

- Straight bridges with a difference in the skew angles at the ends of all the spans less than or equal to $\Delta\theta = 20^{o}$ may be considered as parallel skew bridges. Section 6.7 applies in these cases.
- The following discussions focus predominantly on the TDL results with TDLF detailing based on NLF RA cambers, using the Bridge (H1) EISSS57 as an extreme example.

- In (H1) EISSS57, the pattern of the RA cambers is very similar to the pattern of the LGA cambers, but the RA cambers are smaller in magnitude than the LGA cambers.

Girder Elevations

- The maximum deviation from the targeted elevations is 0.4 inches under the TDL with TDLF based on NLF RA cambers.
- ***It is recommended that NLF RA is sufficient for calculation of the girder cambers in straight bridges with non-parallel skew. There is no need to consider any change in the girder vertical displacements and elevations due to the change in the internal forces, and the change in the vertical deflections in the structural system, associated with the DLF detailing.***

Girder Layovers

- The maximum girder layover under the TDL with TDLF detailing based on NLF RA cambers is 0.2 inches (0.002 rad).
- ***It is recommended that the girder layovers may be assumed to be negligible in the targeted DL condition in straight bridges with non-parallel skew in which the cambers are set based on NLF RA. There is no need to consider any change in the girder layovers due to the change in the internal forces, and the change in the elastic deformations in the system, associated with the DLF detailing. The fascia girders should be checked separately for twist rotation between the CF locations due to eccentric overhang bracket loads.***
- ***For straight parallel-skew bridges detailed for SDLF, the girder layovers under the TDL may be estimated as the CDL layovers obtained from a NLF RA.***

- ***For straight parallel-skew bridges detailed for TDLF, the girder layovers under the SDL may be estimated as the negative of the CDL layovers obtained from a NLF RA.***

Cross-Frame Forces

- Under SDL in Bridge (H1) EISSS57, the largest ratio of the average of the CF member forces for SDLF detailing to the corresponding forces for NLF detailing is 0.61 for SDLF based on NLF RA cambers.
- Under SDL in Bridge (H1) EISSS57, the largest ratio of the maximum CF member force for SDLF detailing to the corresponding force for NLF detailing is 0.62 for SLDF based on NLF RA cambers. That is, the beneficial locked-in force is 1.0 – 0.62 = 0.38 of the CF force corresponding to NLF detailing for this member.
- Under TDL in this bridge, the largest ratio of the average of the CF member forces for TDLF detailing to the corresponding forces for NLF detailing is 0.62 for TDLF based on NLF RA cambers.
- Under TDL in this bridge, the largest ratio of the maximum CF member force for TDLF detailing to the corresponding force for NLF detailing is 0.65 for TLDF based on NLF RA cambers. That is, the beneficial locked-in force is 1.0 – 0.65 = 0.35 of the CF force corresponding to NLF detailing for this member.
- ***Based on the above results, in lieu of a DLF RA, it is recommended that the locked-in forces due to SDLF detailing with RA cambers should be neglected and the NLF RA results should be used directly estimate the CF forces in straight bridges with parallel or non-parallel skew detailed for SDLF based on RA cambers.*** This recommendation is generally conservative, but is selected to be consistent with the recommendations for straight parallel-skew bridges.

- ***In lieu of a DLF RA, it is recommended that a net load factor of (γ_p – 0.4) be used for determination of the factored TDL CF forces in straight I-girder bridges with parallel skew, when the CFs are detailed for TDLF using a NLF RA. This net load factor is to be applied to the results from a NLF RA for the TDL. The factored CF forces under the SDL may be estimated by subtracting the factored CDL CF forces obtained via a NLF RA from the above factored TDL forces.*** The factor of 0.4 is an estimate of the TDLF locked-in force of 1.0 – 0.65 = 0.35, selected to be consistent with the recommendations for straight parallel-skew bridges, and intended to account for additional uncertainties and variabilities associated with TDLF. In cases where additional uncertainties and variabilities associated with TDLF are anticipated, such as incidental participation of deck forms and early concrete stiffness in the structural resistance, and/or larger potential play in the CF connections due to the larger CF forces associated with TDLF, it is suggested that a value between 0.4 and 0.3 may be used for the above locked-in force estimate based on the judgment of the engineer of record.
- For SDLF under SDL, the maximum difference in the magnitude of the individual CF member forces from a DLF RA and the estimated values from a NLF RA, normalized by the member yield load, is 0.74 %, and the average difference is –0.71 %, for the straight bridges studied in this research with parallel skew and girder cambers based on RA.
- For TDLF under TDL, the maximum difference in the magnitude of the individual CF member forces from a DLF RA and (1 – 0.4 = 0.6) of the estimated values from a NLF RA, normalized by the member yield load, is 4.1 %, and the average difference is 0.0

%, for the straight bridges studied in this research with parallel skew and girder cambers based on RA.

Girder Stresses

- The largest maximum girder flange lateral bending stress (f_ℓ) in (H1) EISSS57, under the TDL for TDLF based on LGA cambers, is 0.9 ksi, 90 % of the corresponding maximum girder NLF value. This f_ℓ occurs on the longest fascia girder in the bridge. The next largest maximum girder f_ℓ is 0.4 ksi, on the shortest fascia girder under the TDL for TLDF based on LGA cambers, and is 8 % of the corresponding maximum girder NLF value. The largest maximum girder f_ℓ based on the assumption of NLF detailing is 8.4 ksi, and occurs on the interior Girder 3 in this bridge. The maximum f_ℓ on Girder 3 is reduced to 0.4 ksi (5 % of the above NLF value) by the use of TDLF detailing based on the LGA cambers.
- For all the straight non-parallel skew bridges studied in this research, the use of an assumed locked-in f_ℓ of 0.35 of the f_ℓ from a NLF RA gives an accurate to conservative estimate of the f_ℓ values determined from a DLF RA.
- ***In lieu of a DLF RA, for straight bridges with parallel or non-parallel skew and with the CFs detailed for SDLF or TDLF using a NLF RA, it is recommended that the above procedures for calculation of the CF forces also be used for determining the girder f_ℓ values.***
- In (H1) EISSS57, the largest increase in any of the girder major-axis bending stresses under the TDL, due to the effect of SDLF detailing based on NLF RA cambers, is 0.5 ksi (2 %). The largest increase in any of the girder major-axis bending stresses under the TDL, due to the effect of TDLF detailing based on NLF RA cambers, is 0.9 ksi (4

%). The largest increase occurs in the long fascia Girder G7, but a slightly smaller increase occurs in the short fascia Girder G1.

- ***Based on the above results, it is recommended that for straight bridges with non-parallel skew and with the girder cambers set based on a NLF RA, the DLF effects on the girder f_b values may be neglected for SDLF detailing as long as the recommendations for the CF framing arrangements specified in this research are followed.***
- ***It is recommended that for straight bridges with non-parallel skew and with the girder cambers set based on a NLF RA, the DLF effects on the girder f_b values may be neglected for TDLF detailing as long as:***

  1) The recommendations for the CF framing arrangements specified in this research are followed, and

  2) The skew index is less than or equal to approximately 1.0.

  That is, in cases that satisfy the above requirements, the girder f_b values may be obtained from a NLF RA (which does not consider of the lack-of-fit from the detailing of the CFs).

- ***For straight bridges with non-parallel skew that do not satisfy the above requirements, and when the CFs are detailed based on a NLF RA, it is recommended that the girder major-axis bending stresses be determined from a DLF RA.***
- The above requirements are conservative compared to the results for (H1) EISSS57. They are specified to be the same as the corresponding requirements for straight bridges with parallel skew, to simplify the rules and to avoid potential unconservative errors for bridges that fall near the boundaries between parallel and non-parallel skew.

Vertical Reactions

- The results for the girder reactions largely parallel the above results for the girder major-axis bending stresses.
- For (H2) EISSS57, which follows the recommended practices to avoid nuisance transverse stiffness effects, when the cambers are determined from NLF RA, the largest increase in the reactions under the TDL is 7 % due to SDLF detailing and 12 % due to TDLF detailing, relative to the NLF RA solution. For these cases, the maximum increase in the reaction is only 5 kip.
- For (H2), EISSS57, when the cambers are determined from NLF RA, the largest decrease in the reactions under TDL is -4 % due to SDLF detailing and -11 % due to TDLF detailing, relative to the NLF RA solution. For these cases, the maximum decrease in the reaction is only 7 kip.
- ***Based on the above results, it is recommended that for straight bridges with parallel and non-parallel skew and with the girder cambers set based on a NLF RA, the DLF effects on the girder reactions may be neglected for SDLF detailing as long as the recommendations for the CF framing arrangements specified in this research are followed.***
- ***Additional requirements are recommended for TDLF based on NLF RA cambers. It is recommended that for straight bridges with parallel and non-parallel skew and with girder cambers set based on a NLF RA, the DLF effects on the girder reactions may be neglected for TDLF detailing as long as:***
  1) ***The recommendations for the CF framing arrangements specified in this research are followed, and***

2) The skew index is less than or equal to approximately 1.0.

That is, in cases that satisfy the above requirements, the girder reactions may be obtained from a NLF RA (which does not consider of the lack-of-fit from the detailing of the CFs).

- The above requirements are conservative for Bridge (H2), but are specified to be consistent with the recommendations for parallel skew bridges and to cover cases that may be on the boundary in the definitions of when a bridge may be considered as parallel versus non-parallel skew. .
- ***For straight bridges with parallel and non-parallel skew that do not satisfy the above requirements, it is recommended that the girder reactions be determined from a DLF RA.***

The above recommendations are considered applicable for straight bridges with non-parallel skew, skew angles up to 70^{o}, and spans up to 300 ft. For bridges that exceed these limits, it is recommended that DLF RA be considered. Chapter 3 explains the details of several procedures for conducting a DLF RA.

6.10 Curved and Skewed Bridges with Cambers Set Based on NLF RA

In the limit that the skew becomes small, taken as $\theta \leq 20^{o}$, the curved radially-supported bridge recommendations are considered to apply. Therefore, Section 6.5 should be consulted for these cases. In the limit that the horizontal curvature becomes small, taken as

$L_s/R \leq 0.03$, the straight bridge recommendations are considered to apply. Sections 3.4.6 through 3.4.9 address these cases. Section 6.10.1 provides quantitative results on the influence of SDLF and TDLF detailing on bridge responses in curved and skewed bridges with cambers set based on NLF RA. The influence of SDLF and TDLF is discussed on the responses in the following order: girder vertical displacements, girder elevations, girder layovers, CF forces, girder stresses, and vertical reactions. Section 6.10.2 then summarizes the influences on the key bridge responses, and provides recommendations for handling these effects. The recommendations are highlighted in bold italicized text.

6.10.1 Quantitative Results

6.10.1.1 Girder Vertical Displacements

For curved and skewed bridges, SDLF and TDLF detailing tend to increase the vertical displacements of all the girders when the skew orientation makes the inside girder longer, as in Bridge (N) NISCS14 as shown in Figure 166 and Table 54. When the skew orientation makes the outside girder longer, as in Bridge (O1) NISCS15, SDLF and TDLF detailing tend to reduce the vertical displacements of all the girders. SDLF and TDLF detailing effects also reduce the vertical displacements in continuous-span curved and skewed bridges as shown in Table 54 for bridge cases (S), (T1), (T2), (U1), and (U2). From this table, the largest change in the maximum TDL vertical displacement is 4.4 inches for SDLF detailing and 7.4 inches for TDLF detailing. These maximums occur in Bridge (R1) NISCS39 which has L_s = 300 ft and the skew makes the outside girder longer. Bridge cases (R1) and (R2) are very extreme, and (R2) is essentially unbuildable. With the exception of (R1) and (R2), the largest change in the maximum TDL vertical displacement is 0.9 inches for SDLF detailing and 2.1 inches for TDLF detailing.

One should note that Table 54 reports the absolute maximum downward displacement in the bridge. As such, the data in this table is useful for understanding the overall trends in the behavior of the bridges, but not necessarily the changes that occur in individual girders. In some of the cases for the bridges considered in this research, the location of the maximum displacement can change substantially as a function of the CF detailing method.

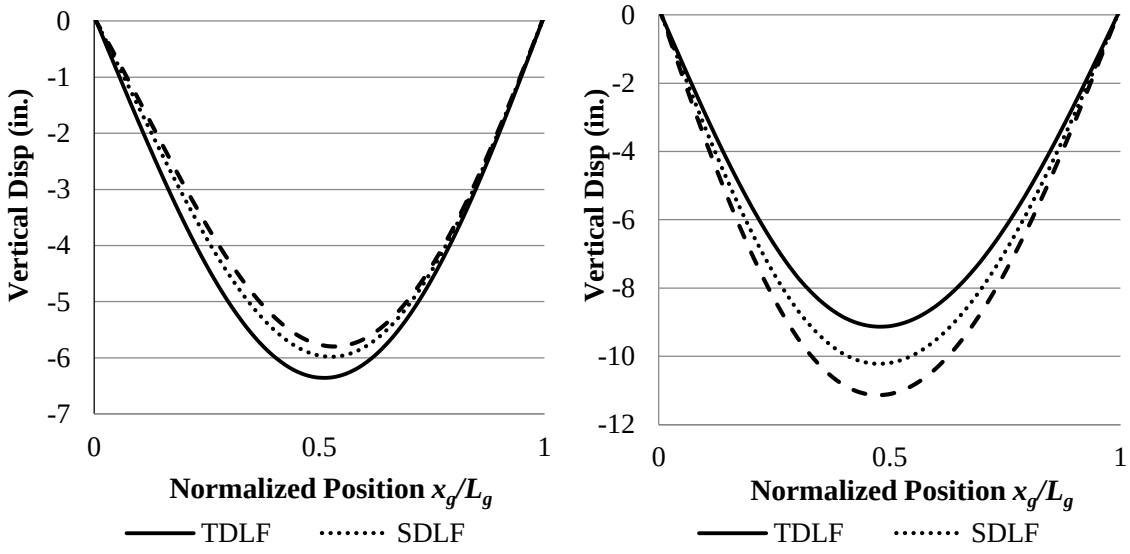

Figure 166. TDL vertical displacement of Bridge (N) NISCS14 longer fascia girder (left) and Bridge (O1) NISCS15 longer fascia girder (right).

Table 54. Maximum TDL vertical displacements and changes in maximum TDL vertical displacements relative to NLF detailing for the curved and skewed bridges studied in this research. (Excluding bridges (R1) and (R2), the largest changes by SDLF and TDLF under TDL are highlighted by dark shading).

Bridge	NLF	SDLF		TDLF	
	Disp. (in.)	Disp. (in.)	Change (in.)	Disp. (in.)	Change (in.)
(N) NISCS14	-5.8	-6	-0.2	-6.4	-0.6
(O1) NISCS15	-11.1	-10.2	0.9	-9.1	2
(O2) NISCS15	-9.4	-8.8	0.6	-8.2	1.2
(P) EISCS3	-6.6	-6.3	0.3	-6	0.6
(Q1) NISCS38	-13	-13.6	-0.6	-14.3	-1.3
(Q2) NISCS38	-12.8	-13.3	-0.5	-13.9	-1.1
(R1) NISCS39	-26.2	-21.8	4.4	-18.8	7.4
(R2) NISCS39	-24.3	-20.9	3.4	-18.7	5.6
(S) XICCS7	-4.9	-4.8	0.1	-4.5	0.4
(T1) EICCS27	-28.6	-28	0.6	-26.9	1.7
(T2) EICCS27	-27.3	-26.6	**0.7**	-25.2	**2.1**
(U1) EICCS28	-23.9	-23.5	0.4	-23.2	0.7
(U2) EICCS28	-25.8	-24.9	0.9	-24.3	1.5

6.10.1.2 Girder Elevations

As noted previously, for curved and skewed bridges, all of the camber calculations are conducted using NLF RA in this research. For curved and skewed bridges, the girder cambers with the CFs detailed for NLF are exactly the same magnitude but opposite in sign to the RA girder vertical deflections. The corresponding vertical elevations under TDL for NLF detailing are zero (assuming no superelevation, etc., as a simplification). The SDLF and TDLF detailing effects reduce or increase the vertical displacements depending on the skew orientation as discussed above. As a result, the vertical elevations with SDLF and TDLF detailing under TDL are below the targeted elevations for bridges with a longer inside girder, such as Bridge (N) NISCS14 (Figure 167). The vertical elevations with SDLF

and TDLF detailing under TDL are above the targeted elevations for bridges with a longer outside fascia girder, such as Bridge (O1) NISCS15.

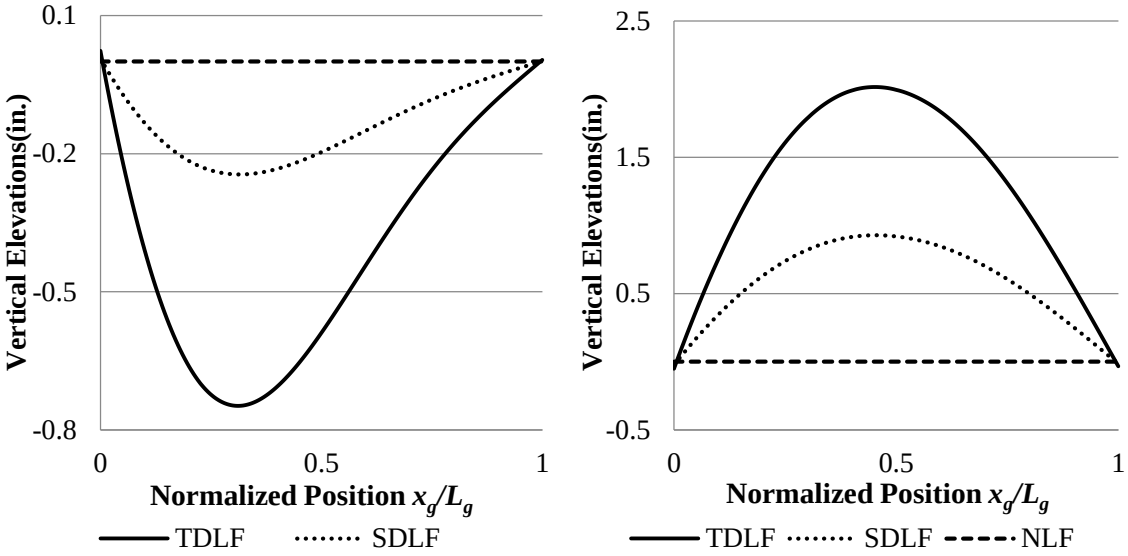

Figure 167. Bridge (N) NISCS14 longer fascia girder (left) and Bridge (O1) NISCS15 longer fascia girder (right) final elevations under TDL.

The deviation from the targeted vertical elevations, when the bridge is detailed for SDLF or TDLF detailing, is equal to the displacement caused by the SDLF and TDLF detailing effects alone. Considering the complete set of curved and skewed bridges studied in this research, from Table 55, the largest deviations from the targeted elevation under TDL are 7.4 inches for TDLF detailing and 4.4 inches for SDLF detailing (Bridge (R1) NISCS39 which has a span length of 300ft and outside girder length of 341 ft). The use of SDLF detailing or TDLF detailing is not recommended for such a case. With the exception of (R1) and (R2) NISCS39, the largest deviations from the targeted/expected elevations are 1.2 in for SDLF and 2.1 in for TDLF.

Table 55. Maximum final elevation deviations under from the zero elevation line, for the curved and skewed bridges studied in this research (Excluding bridges (R1) and (R2), the largest final girder elevations with SDLF and TDLF detailing under TDL are highlighted by dark shading).

Bridge	NLF (in.)	SDLF (in.)	TDLF (in.)
(N) NISCS14	0.0	0.2	0.6
(O1) NISCS15	0.0	0.9	2.0
(O2) NISCS15	0.0	0.6	1.2
(P) EISCS3	0.0	0.3	0.6
(Q1) NISCS38	0.0	0.6	1.3
(Q2) NISCS38	0.0	0.5	1.1
(R1) NISCS39	0.0	4.4	7.4
(R2) NISCS39	0.0	3.4	5.6
(S) XICCS7	0.0	0.1	0.4
(T1) EICCS27	0.0	0.6	1.7
(T2) EICCS27	0.0	**0.7**	**2.1**
(U1) EICCS28	0.0	1.2	2.1
(U2) EICCS28	0.0	0.9	1.5

6.10.1.3 Girder Layovers

For curved and skewed bridges, when the skew is substantial and makes the inside girder longer as in the case of Bridge (N) NISCS14, the girders and the bridge cross-section both tend to roll largely towards the inside of the curve under the action of the DL (see the layovers and twists with NLF detailing in Figures 168 and 169). The portion of the bridge near the right radial bearing line rolls towards the outside of the curve due to the horizontal curvature effects. However, the skew effects cause the girders to twist towards the inside of the curve, which is opposite from the direction that the girders in a similar curved radially-supported bridge would tend to roll under DL. As a result, the layovers are reduced near mid-span. The layovers are largest at the left-hand skewed bearing line. The girder on

the inside of the curve in Bridge (N), which is longer than the girder on the outside of the curve in this bridge, has the largest layover of all the girders, -1.03 inches The SDLF and TDLF detailing effects largely twist the girders towards the outside of the curve, which is the direction opposite to the predominant direction of the bridge twist rotations. With TDLF detailing, the largest layover is -0.3 in, which occurs on the inside girder.

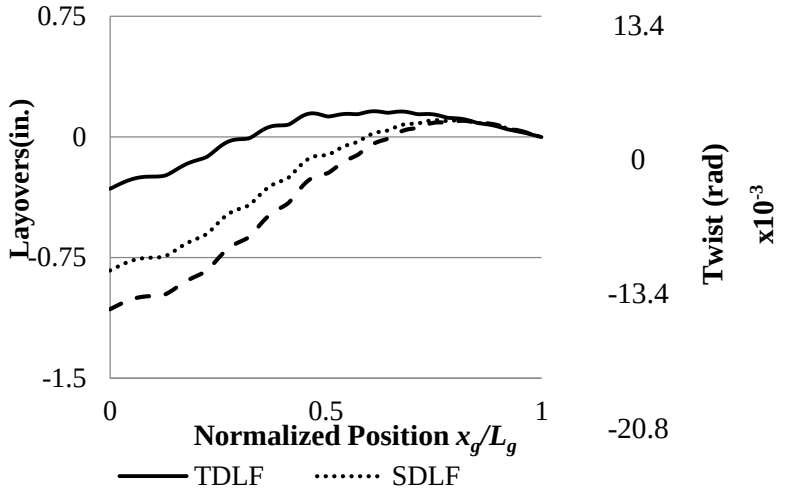

Figure 168. TDL layovers and twists of the girder on the inside of the curve in Bridge (N) NISCS14 (Positive layovers indicate rolling towards the outside of the curve).

When the skew makes the outside girder longer as in the case of Bridge (O1) NISCS15, the girders and the bridge cross-section both tend to roll substantially towards the outside of the curve under the action of the DL, which is the same direction that a similar curved radially-supported bridge cross-section tends to roll under DL (see the layovers and twists with NLF detailing in Figures 170 and 171). As a result, the girder layovers are amplified. The outside girder of Bridge (O1), which is the longer fascia girder, has the largest layovers of all the girders, 2.0 inches for NLF. The largest layovers occur near mid-span. The girder on the outside of the curve has a layover of 0.9 inches at the left-hand skewed bearing line. The SDLF and TDLF detailing effects twist the girders towards the inside of the curve,

which is the direction opposite to the predominant direction of the bridge twist rotations. With TDLF detailing, the largest layover is -0.4 in, which occurs on the inside girder.

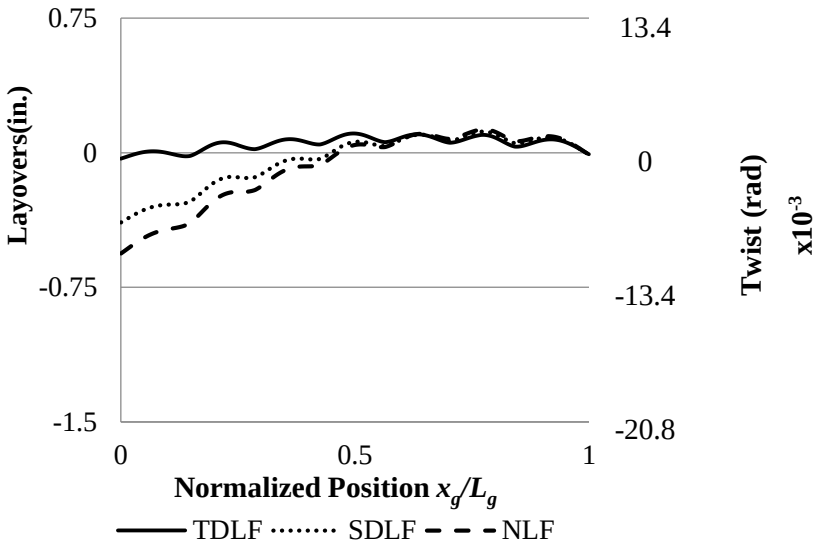

Figure 169. TDL layovers and twists of the girder on the outside of the curve in Bridge (N) NISCS14 (Positive layovers indicate rolling towards the outside of the curve).

Considering the complete set of curved and skewed bridges studied in this research, the largest girder layovers are 0.5 inches (0.056 rad) under SDL for SDLF detailing and 1.7 inches (0.0189 rad) under TDL for TDLF detailing (see Table 56). The large 1.7 inches layover occurs at the skewed bearing line at one of the interior piers in Bridge (T2) EICCS27, which has a maximum span of 279 ft and a maximum skew angle of 70 degrees. The framing arrangement of Bridge (T2) uses skewed bearing line CFs at the interior pier and intermediate CFs that are offset from the skewed bearing line. This framing arrangement alleviates the nuisance transverse stiffness issues that cause large forces in the CF members. However, due to this flexibility, there is some layover of the girders, especially at the skewed bearing lines.

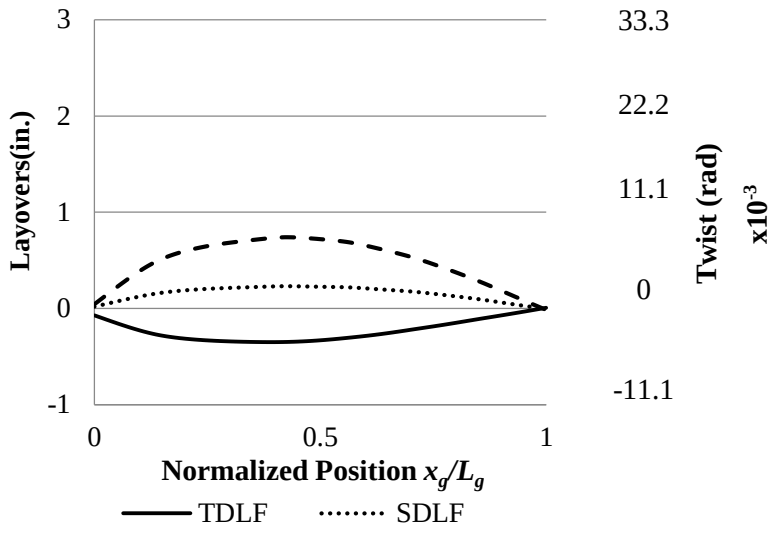

Figure 170. TDL layovers and twists of the girder on the inside of the curve in Bridge (O1) NISCS15 (Positive layovers indicate rolling towards the outside of the curve).

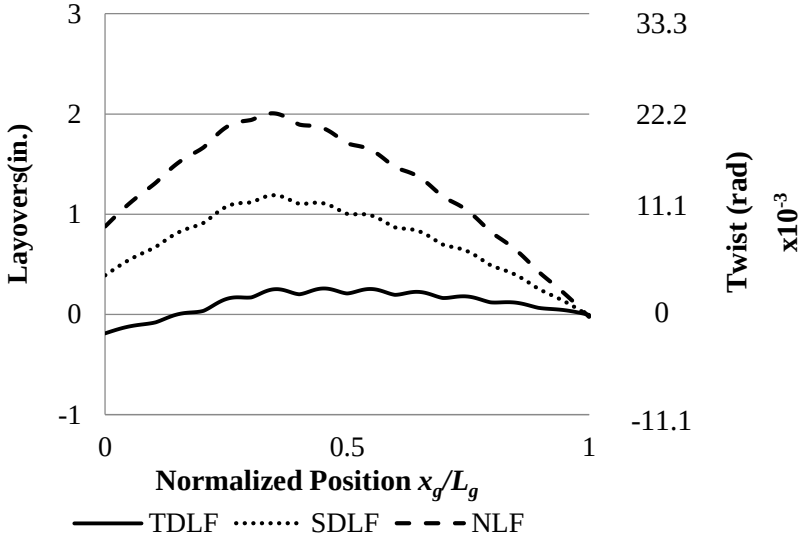

Figure 171. TDL layovers and twists of the girder on the outside of the curve in Bridge (O1) NISCS15 (Positive layovers indicate rolling towards the outside of the curve).

Table 56. Maximum magnitudes of girder layovers and twists in the curved and skewed bridges studied in this research (LO1, LO2, and LO3 are the maximum girder layovers with NLF, SDLF, and TDLF detailing, respectively. $\phi 1$, $\phi 2$, and $\phi 3$ are the maximum girder twists with NLF, SDLF, and TDLF detailing, respectively. The largest girder layovers and twists with SDLF under SDL and TDLF under TDL are highlighted by dark shading).

Load Cond.	Bridge	Girder Depth (in.)	NLF		SDLF		TDLF	
			LO1 (in.)	$\phi 1$ (rad) x10^{-3}	LO2 (in.)	$\phi 2$ (rad) x10^{-3}	LO3 (in.)	$\phi 3$ (rad) x10^{-3}
SDL	(N) NISCS14	72	0.3	4.2	0.1	1.4	0.4	5.6
	(O1) NISCS15	90	0.9	10.0	0.2	2.2	0.9	10.0
	(O2) NISCS15	"	0.6	6.7	0.1	1.1	0.7	7.8
	(P) EISCS3	68	0.4	5.9	0.1	1.5	0.6	8.8
	(Q1) NISCS38	156	1.5	9.6	0.4	2.6	1.1	7.1
	(Q2) NISCS38	"	1.5	9.6	0.3	1.9	1.2	7.7
	(R1) NISCS39	180	3.2	17.8	0.5	2.8	2.8	15.6
	(R2) NISCS39	"	3	16.7	0.4	2.2	2.2	12.2
	(S) XICCS7	92	0.3	3.3	0.1	1.1	0.8	8.7
	(T1) EICCS27	90	1.1	12.2	0.1	1.1	2.9	32.2
	(T2) EICCS27	"	1.2	13.3	**0.5**	**5.6**	3	33.3
	(U1) EICCS28	120	2.2	18.3	0.4	3.3	1.3	10.8
	(U2) EICCS28	"	2.5	20.8	0.4	3.3	1.7	14.2
TDL	(N) NISCS14	72	1.1	15.3	0.8	11.1	0.3	4.2
	(O1) NISCS15	90	2.0	22.2	1.2	13.3	0.4	4.4
	(O2) NISCS15	"	1.3	14.4	0.8	8.9	0.3	3.3
	(P) EISCS3	68	1.0	14.7	0.6	8.8	0.2	2.9
	(Q1) NISCS38	156	3.3	21.2	2.1	13.5	0.8	5.1
	(Q2) NISCS38	"	3.2	20.5	2	12.8	0.7	4.5
	(R1) NISCS39	180	5.6	31.1	2.3	12.8	1.2	6.7
	(R2) NISCS39	"	5.1	28.3	2.1	11.7	0.9	5.0
	(S) XICCS7	92	1.2	13.0	0.9	9.8	0.7	7.6
	(T1) EICCS27	90	4.4	48.9	3.4	37.8	0.6	6.7
	(T2) EICCS27	"	4.4	48.9	3.2	35.6	**1.7**	**18.9**
	(U1) EICCS28	120	4.0	33.3	2.1	17.5	0.6	5.0
	(U2) EICCS28	"	4.5	37.5	2.3	19.2	0.5	4.2

6.10.1.4 Cross-Frame Forces

The effects of the detailing methods on the DL CF forces in the completed bridge system are influenced in complex ways by the different combinations of skew and curvature. SDLF and TDLF detailing methods can either increase or decrease the CF forces depending on the combination of the skew index, I_s, and the tightness of the curvature L_s/R. In Table 57, F1, F2, and F3 are CF forces for NLF, SDLF and TDLF detailing respectively. Table 57 reports the average and maximum CF member forces under TDL. The most important points from these this table are:

- The F2/F1 and F3/F1 ratios for both the average and the maximum CF member forces are often slightly smaller than 1.0.
- The only ratio greater than 1.1 is highlighted in the table. This case is a continuous-span bridge.
- The orientation of the skew has a significant influence on the CF forces in completed curved and skewed bridges. When the skew orientation makes the inside girder longer, the skew causes girder twist rotations that are in the opposite direction from those due to the horizontal curvature. As a result, the average and maximum CF forces were significantly reduced as illustrated in the case of bridges (N) NISCS14, (P) EISCS3, and (Q1) and (Q2) NISCS38.
- When the skew orientation makes the outside girder longer, the skew causes girder twist rotations that are in the same direction as those due to the horizontal curvature, resulting in a significant increase in the average and maximum CF forces as illustrated in the case of bridges (O) NISCS15 and (R1) and (R2) NISCS39.

- For curved and skewed continuous-span bridges, the skew can make the outside fascia girder longer in one span and shorter in another span. The middle spans of bridge cases (S) XICCS7, (T1) and (T2) EICCS27 and (U1) and (U2) EICCS28 all have a parallel skew in their middle spans. The effects of the skew orientation in continuous-span bridges tend to cause the average and maximum CFs forces to be greater in the span where the skew orientation makes the outside fascia girder longer than in the span where the skew orientation makes the outside fascia girder shorter.
- SDLF and TDLF detailing increase the forces for about half of the CFs and decrease CF forces for about the other half by about the same percentage, normalized by the member yield load. Thus, SDLF and TDLF detailing do not significantly change the average CF forces.
- Changes in the CF forces due to SDLF detailing tend to be small in curved bridges that do not have sharp skew, tight curvature, and long spans, and
- Changes in the CF member forces due to TDLF detailing can be significant in cases with tight curvature, sharp skew, and long spans.

Table 57. Average and maximum magnitudes of the CF chord forces in each of the curved and skewed bridges studied in this research (F1, F2, and F3 are the average or maximum CF forces with NLF, SDLF, and TDLF detailing, respectively; the largest F2/F1 ratio under SDL and F3/F1 ratio under TDL are highlighted).

	Bridge	SDL			TDL		
		NLF	SDLF		NLF	TDLF	
		F1 (kip)	F2 (kip)	F2/F1	F1(kip)	F3 (kip)	F3/F1
Avg	(N) NISCS14	7.7	6.6	0.86	24.1	20.7	0.86
	(O1) NISCS15	48.7	44.5	0.91	99.6	90.2	0.91
	(O2) NISCS15	47.4	42.8	0.90	95.9	86.0	0.90
	(P) EISCS3	10.1	8.3	0.82	22.2	18.2	0.82
	(Q1) NISCS38	14.6	11.5	0.79	28.6	22.9	0.80
	(Q2) NISCS38	15.1	11.8	0.78	29.6	24.0	0.81
	(R1) NISCS39	72.0	65.4	0.91	129.2	103.4	0.80
	(R2) NISCS39	80.0	69.4	0.87	138.6	109.9	0.79
	(S) XICCS7	1.9	1.8	0.95	8.1	7.5	0.93
	(T1) EICCS27	13.4	5.9	0.44	48.6	22.2	0.46
	(T2) EICCS27	3.1	3.3	**1.06**	12.1	11.7	**0.97**
	(U1) EICCS28	22.4	15.4	0.69	41.9	26.5	0.63
	(U2) EICCS28	16.1	12.3	0.76	30.2	21.0	0.70
Max	(N) NISCS14	24.3	17.9	0.74	77.0	70.5	0.92
	(O1) NISCS15	222.7	195.0	0.88	471.8	405.3	0.86
	(O2) NISCS15	159.7	103.9	0.65	317.9	215.1	0.68
	(P) EISCS3	34.8	36.5	1.05	80.2	81.9	**1.02**
	(Q1) NISCS38	45.6	38.5	0.84	89.9	75.5	0.84
	(Q2) NISCS38	66.5	39.0	0.59	137.8	106.4	0.77
	(R1) NISCS39	391.7	276.1	0.70	678.0	525.7	0.78
	(R2) NISCS39	450.2	185.6	0.41	769.5	287.7	0.37
	(S) XICCS7	9.9	7.4	0.75	43.8	30.5	0.70
	(T1) EICCS27	52.7	22.3	0.42	203.1	84.7	0.42
	(T2) EICCS27	16.8	19.7	**1.17**	74.2	67.5	0.91
	(U1) EICCS28	152.1	69.8	0.46	271.7	122.7	0.45
	(U2) EICCS28	99.6	80.4	0.81	176.1	134.9	0.77
	(N) NISCS14	7.7	6.6	0.86	24.1	20.7	0.86
	(O1) NISCS15	48.7	44.5	0.91	99.6	90.2	0.91
	(O2) NISCS15	47.4	42.8	0.90	95.9	86.0	0.90

Table 58. Average and maximum magnitudes of the CF diagonal forces in each of the curved and skewed bridges studied in this research (F1, F2, and F3 are the average or maximum CF forces with NLF, SDLF, and TDLF detailing, respectively; the largest F2/F1 ratio under SDL and F3/F1 ratio under TDL are highlighted).

	Bridge	SDL			TDL		
		NLF	SDLF		NLF	TDLF	
		F1 (kip)	F2 (kip)	F2/F1	F1(kip)	F3 (kip)	F3/F1
Avg	(N) NISCS14	7.1	7.1	1.00	21.7	21.7	1.00
	(O1) NISCS15	15.8	15.0	0.95	35.7	34.0	0.95
	(O2) NISCS15	13.7	12.4	0.91	30.5	28.1	0.92
	(P) EISCS3	5.7	5.1	0.89	13.8	12.3	0.89
	(Q1) NISCS38	13.3	13.0	0.98	28.0	27.3	0.98
	(Q2) NISCS38	15.4	14.9	0.97	32.6	31.4	0.96
	(R1) NISCS39	33.6	30.7	0.91	60.8	52.0	0.86
	(R2) NISCS39	34.1	27.4	0.80	61.2	47.0	0.77
	(S) XICCS7	2.6	2.2	0.85	11.0	9.7	0.88
	(T1) EICCS27	9.5	4.7	0.49	35.9	17.9	0.50
	(T2) EICCS27	5.3	6.7	**1.26**	20.8	23.4	**1.13**
	(U1) EICCS28	12.8	9.5	0.74	24.8	17.9	0.72
	(U2) EICCS28	10.2	8.8	0.86	20.3	17.3	0.85
Max	(N) NISCS14	17.0	15.6	0.92	54.4	49.6	0.91
	(O1) NISCS15	74.6	74.2	0.99	158.7	165.6	1.04
	(O2) NISCS15	73.0	46.2	0.63	145.8	92.4	0.63
	(P) EISCS3	25.5	13.0	0.51	55.0	27.9	0.51
	(Q1) NISCS38	34.9	29.0	0.83	57.9	60.9	1.05
	(Q2) NISCS38	34.6	34.9	1.01	73.2	74.1	1.01
	(R1) NISCS39	132.2	123.7	0.94	224.3	211.7	0.94
	(R2) NISCS39	235.2	89.5	0.38	392.7	141.3	0.36
	(S) XICCS7	13.0	12.8	0.98	52.2	50.2	0.96
	(T1) EICCS27	51.5	18.4	0.36	189.7	73.2	0.39
	(T2) EICCS27	18.6	29.1	**1.56**	77.7	97.7	**1.26**
	(U1) EICCS28	79.7	43.0	0.54	144.4	65.5	0.45
	(U2) EICCS28	51.2	38.6	0.75	93.5	67.0	0.72
	(N) NISCS14	7.1	7.1	1.00	21.7	21.7	1.00
	(O1) NISCS15	15.8	15.0	0.95	35.7	34.0	0.95
	(O2) NISCS15	13.7	12.4	0.91	30.5	28.1	0.92

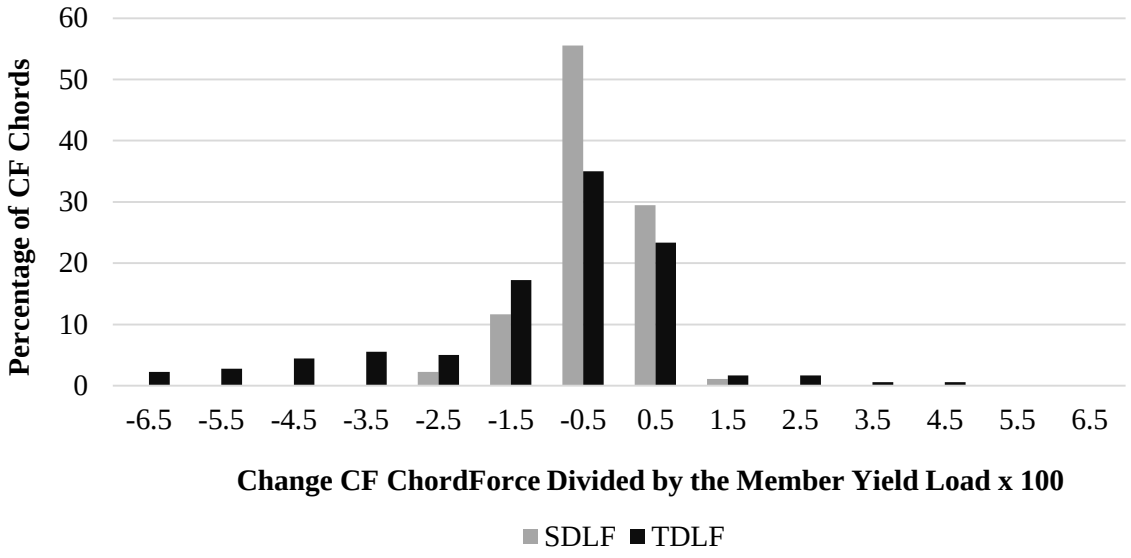

Figure 172. Frequency distribution for the change in the magnitude of the CF chord forces, normalized by the member yield load, due to SDLF and TDLF detailing in Bridge (N) NISCS14.

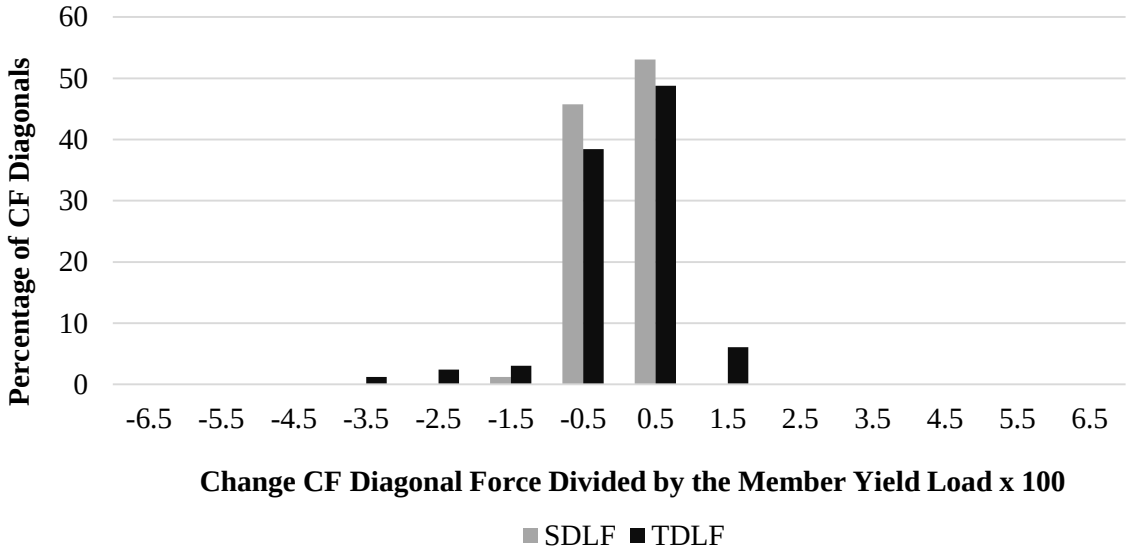

Figure 173. Frequency distribution for the change in the magnitude of the CF diagonal forces, normalized by the member yield load, due to SDLF and TDLF detailing in Bridge (N) NISCS14.

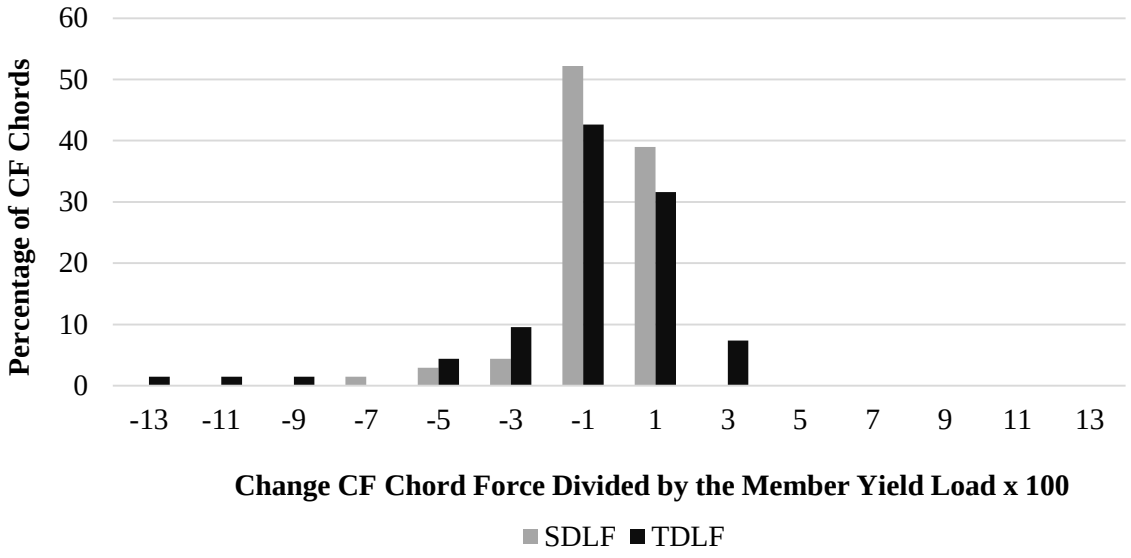

Figure 174. Frequency distribution for the change in the magnitude of the CF chord forces, normalized by the member yield load, due to SDLF and TDLF detailing in Bridge (O) NISCS15.

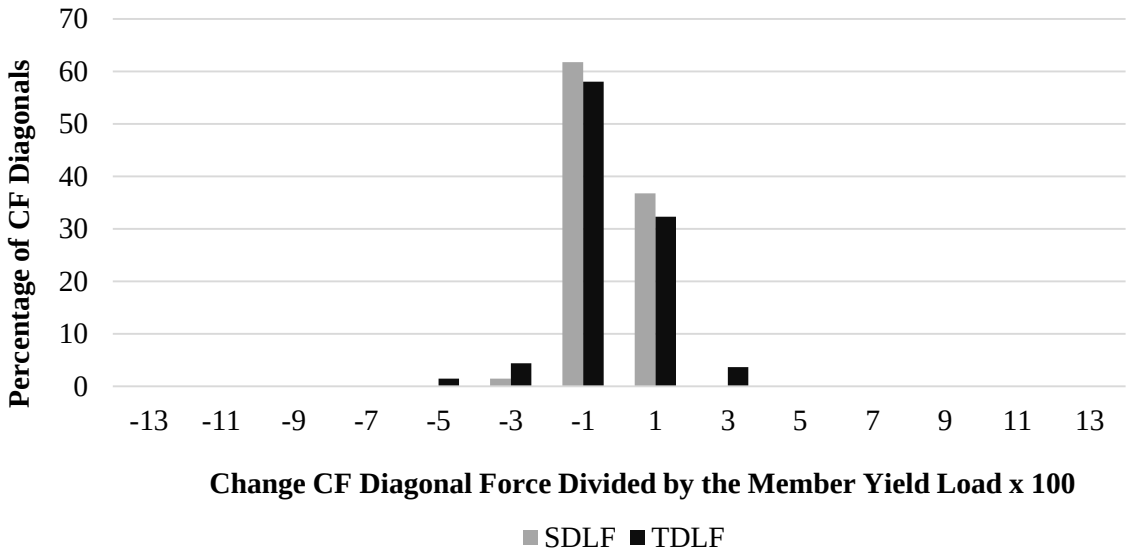

Figure 175. Frequency distribution for the change in the magnitude of the CF diagonal forces, normalized by the member yield load, due to SDLF and TDLF detailing in Bridge (O) NISCS15.

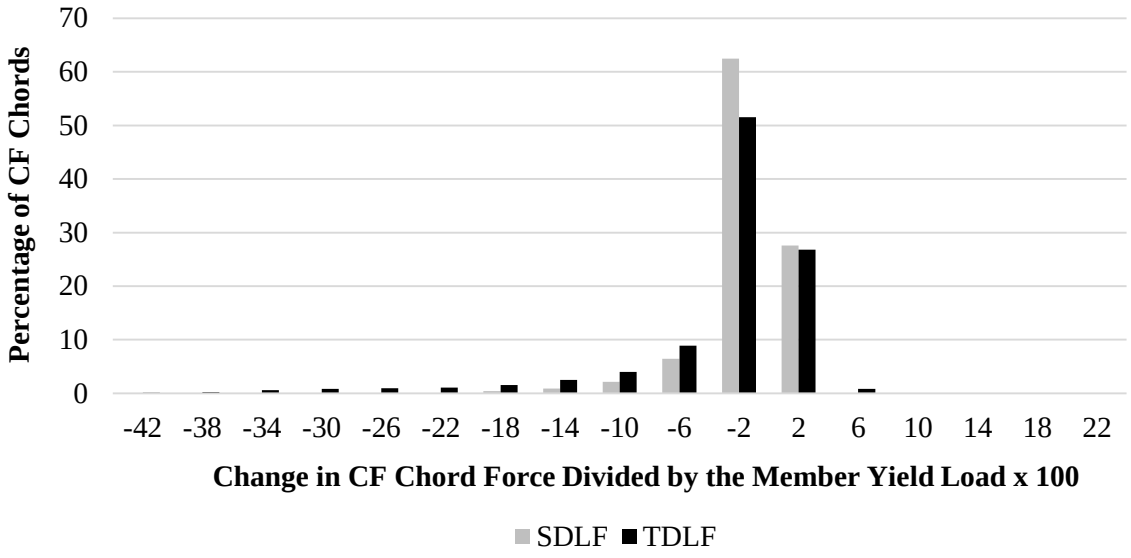

Figure 176. Frequency distribution for the change in the magnitude of the CF chord forces, normalized by the member yield load, due to SDLF and TDLF detailing in the all curved and skewed bridges.

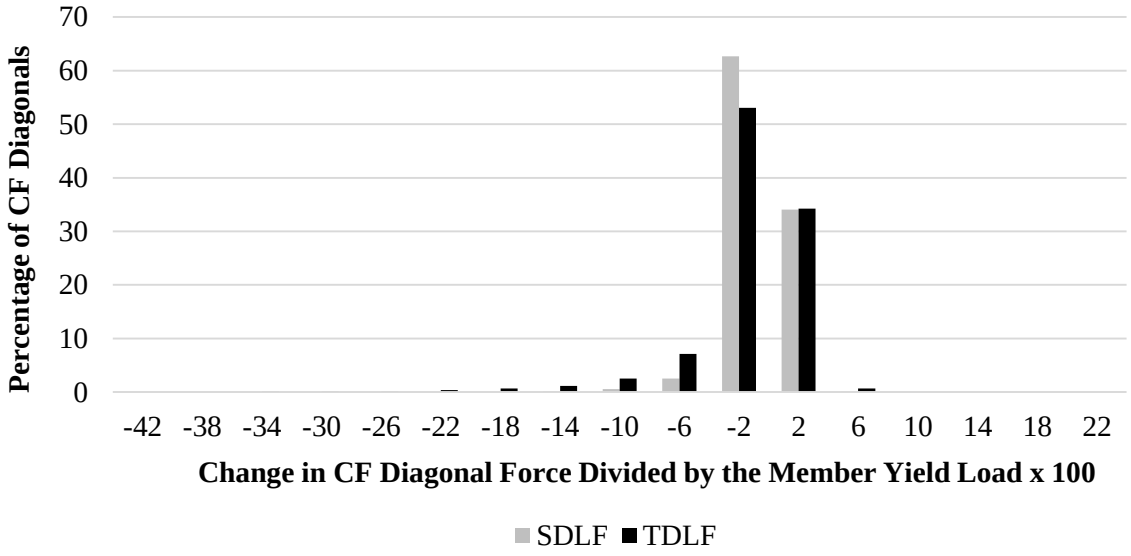

Figure 177. Frequency distribution for the change in the magnitude of the CF diagonal forces, normalized by the member yield load, due to SDLF and TDLF detailing in the all curved and skewed bridges. Figure 179 shows an estimate of the CF forces under the SDL, assuming SDLF detailing, obtained by scaling the NLF RA forces by 1.0 for the cross-frame chords and by 2.0 for the cross-frame diagonals. This is the scale factor

recommended in Section 6.5.2 for both SDL/SDLF and TDL/TDLF estimates in curved radially-supported bridges. One can observe that almost all of the CF force values from Figure 179 are estimated accurately to conservatively. However, the actual distribution of the CF forces from Figure 178 is predicted poorly. The poor prediction of the CF force distribution is not of any significant consequence though since all the CF forces are relatively small. Since Figure 179 simply shows all the NLF RA CF forces scaled by 1.0 for the chords and by 2.0 for the diagonals, it can be concluded that the distribution of the non-zero CF forces under SDL associated with NLF detailing is very different from the distribution of the reduced (smaller) CF forces under SDL associated with SDLF detailing.

Table 59. Summary statistics of the percent change in the magnitude of the CF forces divided by the member yield load (change in member force divided by the member yield load x 100), due to SDLF or TDLF detailing in all the curved and skewed bridges.

	Chords		Diagonals	
	SDLF	TDLF	SDLF	TDLF
Average	-1.14	-2.78	-0.43	-0.87
Median	-0.37	-0.85	-0.15	-0.34
Max	4.68	15.5	6.53	22.0
Min	-25.3	-42.2	-13.9	-39.1
COV	-12.5	-20.2	-7.81	-10.7

Figure 178 shows the actual distribution of the CF forces under the SDL in Bridge (Q1) EISSS57, including the locked-in force effects from SDLF detailing with NLF RA cambers. One can observe that the largest of the CF member forces in Figure 178 is 38.5 kips.

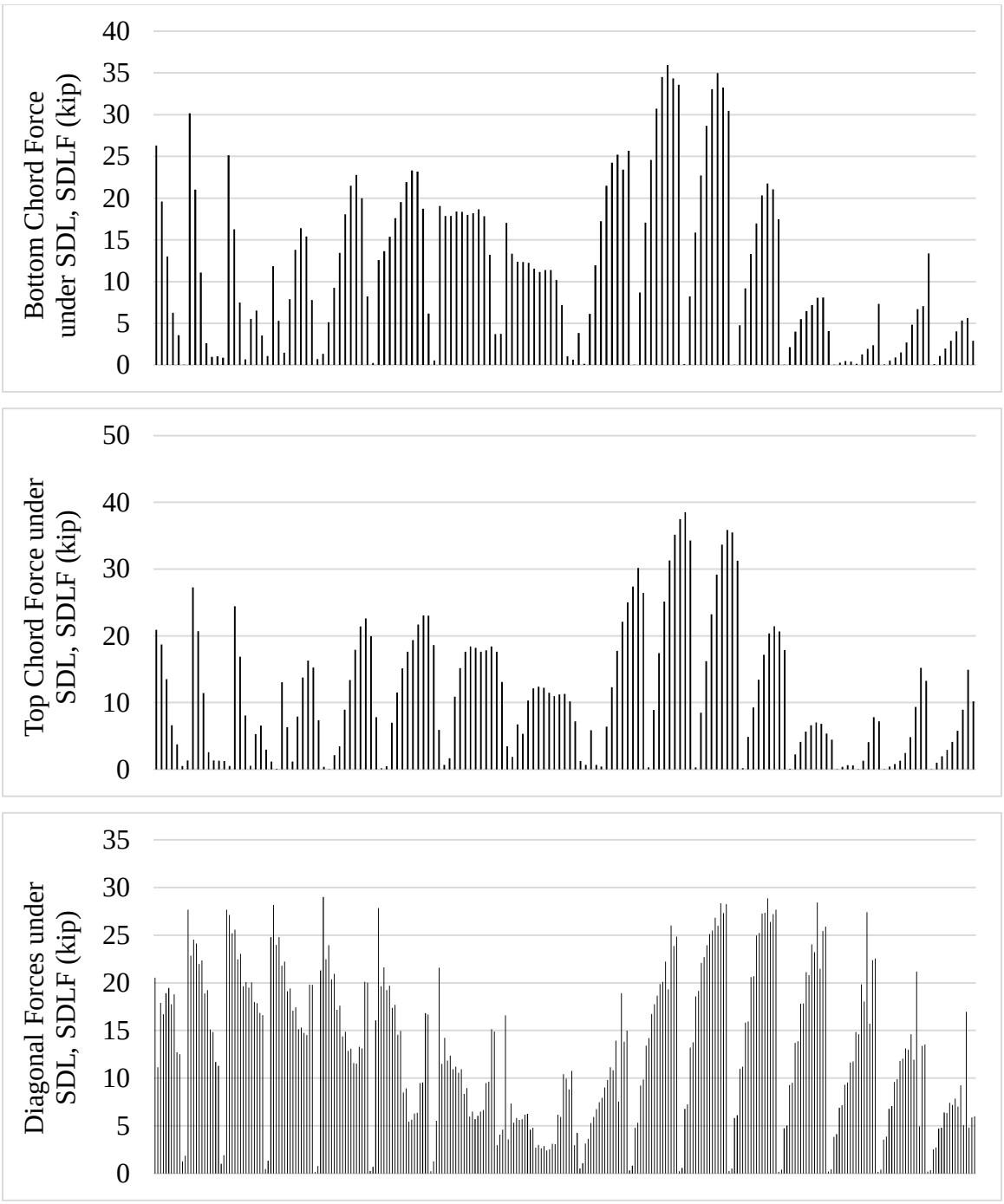

Figure 178. Magnitude of CF member forces from DLF RA, Bridge (Q1) NISCS38 under SDL, SDLF detailing.

Figure 180 shows the difference between the magnitude of the DLF RA forces and the CF forces under SDL, assuming SDLF detailing, estimated by scaling the NLF RA forces,

divided by the CF member yield loads for Bridge (Q1). The plots in this figure are similar those for the curved radially-supported bridges shown previously. One can observe that the largest under-prediction of the DLF RA results is $0.0191P_y$ for one of the chords of the cross-frame. The largest over-prediction is -0.07 using the recommended estimate. Figure 181 shows the same results as Figure 180 for Bridge (Q1), but under TDL and assuming TDLF detailing. The maximum under-prediction is 0.0393 and the largest over-prediction is -0.2243 for this case.

Figures 182 and 183 shows the same results as Figures 180 and 181 but for Bridge (Q2). The maximum under-prediction is 0.0199 and the largest over-prediction is -0.1283 for SDLF under SDL. The maximum under-prediction is 0.0439 and the largest over-prediction is -0.0416 for TDLF under TDL.

Figures 184 and 185 shows the same results as Figures 180 and 181 but for Bridge (P). The maximum under-prediction is 0.0034 and the largest over-prediction is -0.0416 for SDLF under SDL. The maximum under-prediction is 0.0085 and the largest over-prediction is -0.2134 for TDLF under TDL.

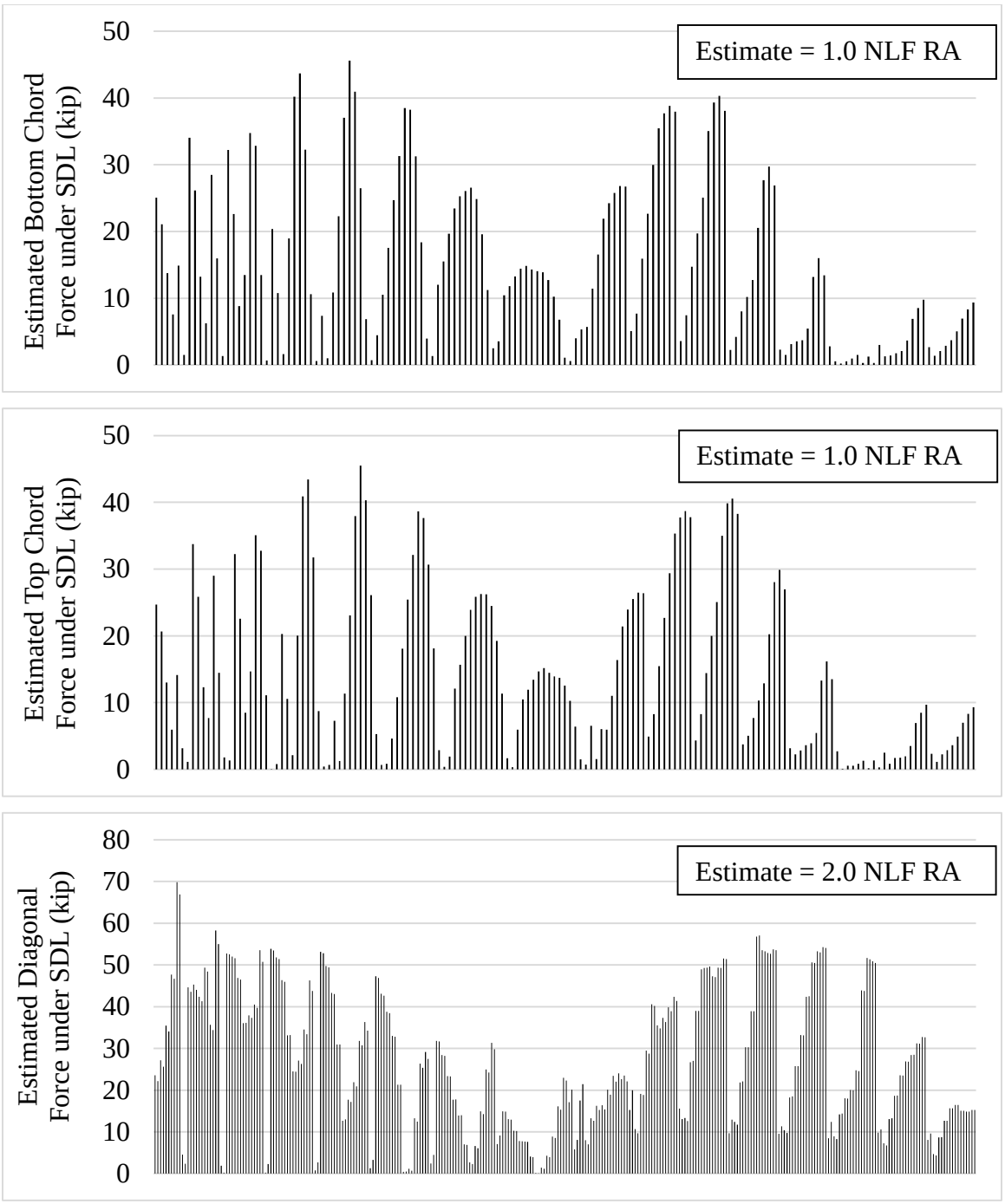

Figure 179. Estimated magnitude of CF member forces based on scaling of NLF RA results, assuming SDLF detailing, Bridge (Q1) NISCS38 under SDL.

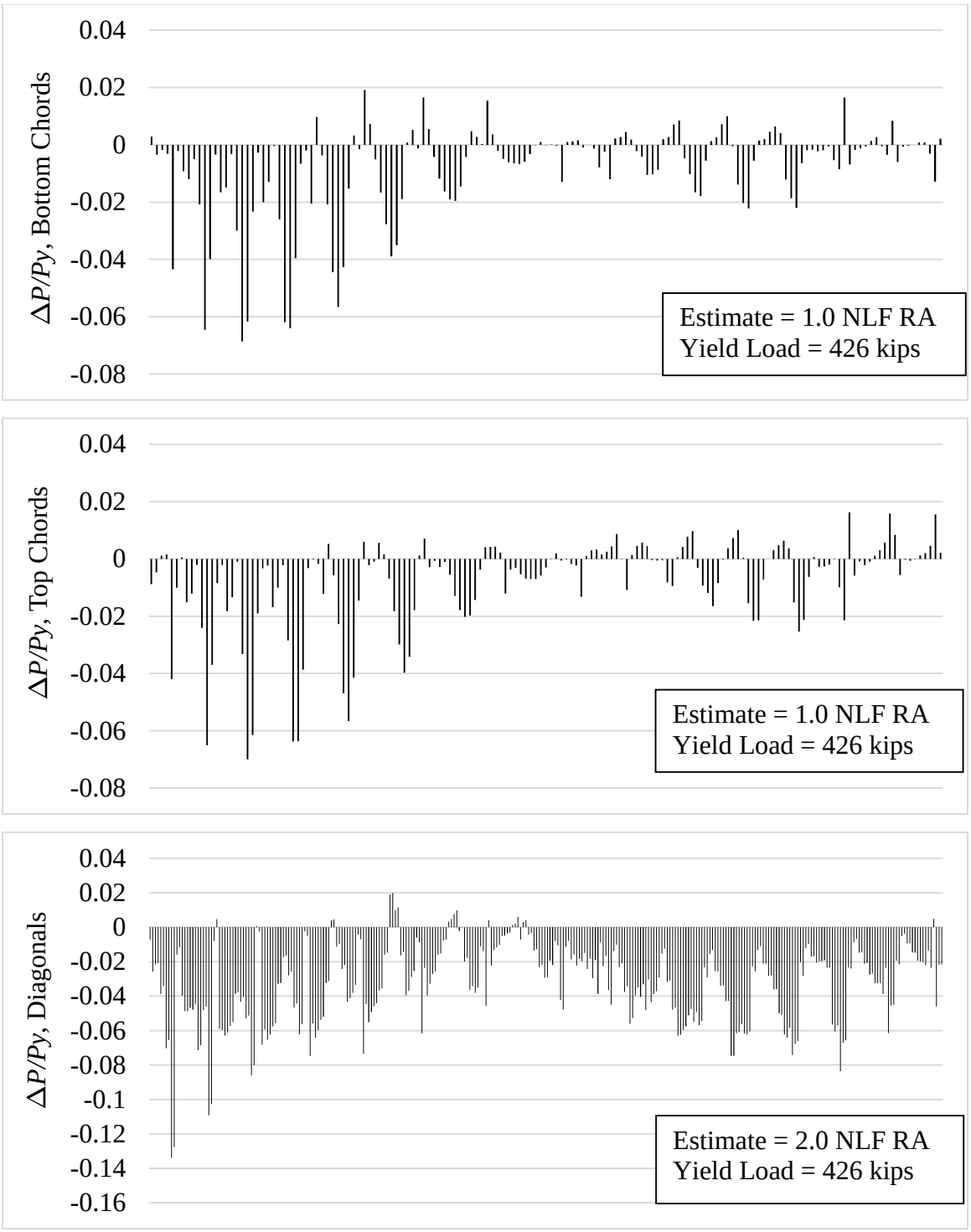

Figure 180. Difference between the magnitude of the DLF RA forces and the values estimated by scaling the NLF RA results, divided by the member yield load ($\Delta P/P_y$), Bridge (Q1) NISCS38 under SDL with SDLF detailing based on NLF RA cambers.

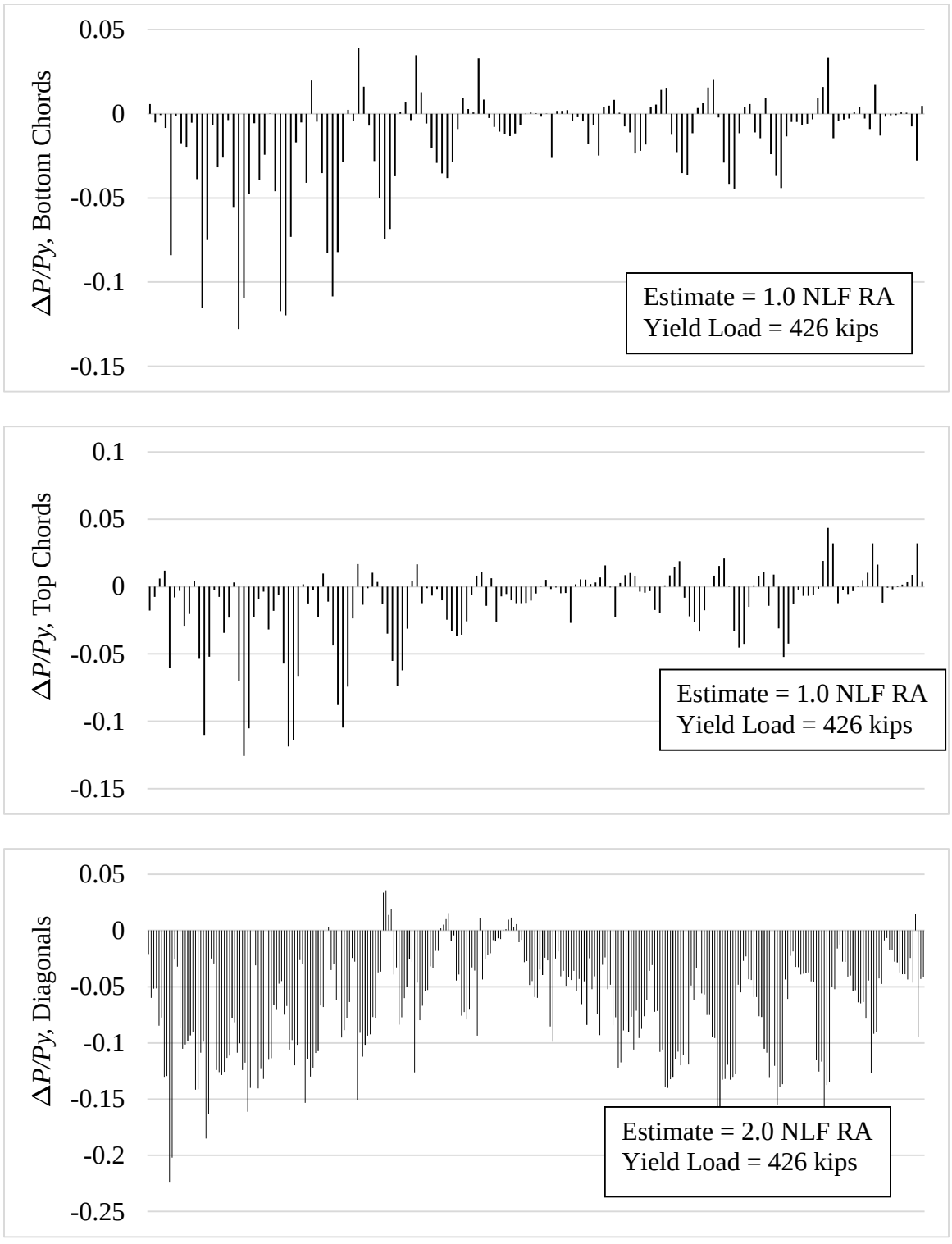

Figure 181. Difference between the magnitude of the DLF RA forces and the values estimated by scaling the NLF RA results, divided by the member yield load ($\Delta P/P_y$), Bridge (Q1) NISCS38 under TDL with TDLF detailing based on NLF RA cambers.

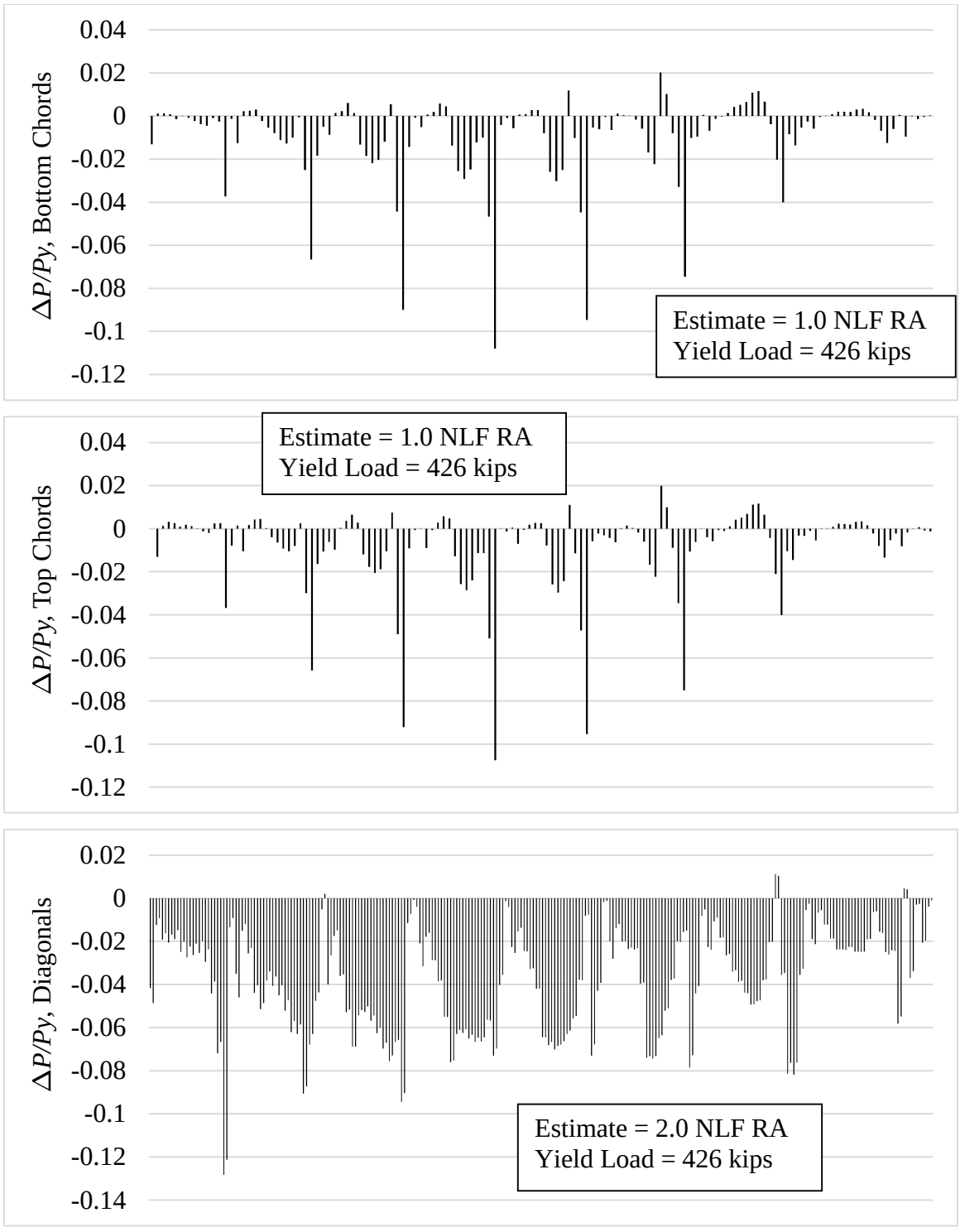

Figure 182. Difference between the magnitude of the DLF RA forces and the values estimated by scaling the NLF RA results, divided by the member yield load ($\Delta P/P_y$), Bridge (Q2) NISCS38 under SDL with SDLF detailing based on NLF RA cambers.

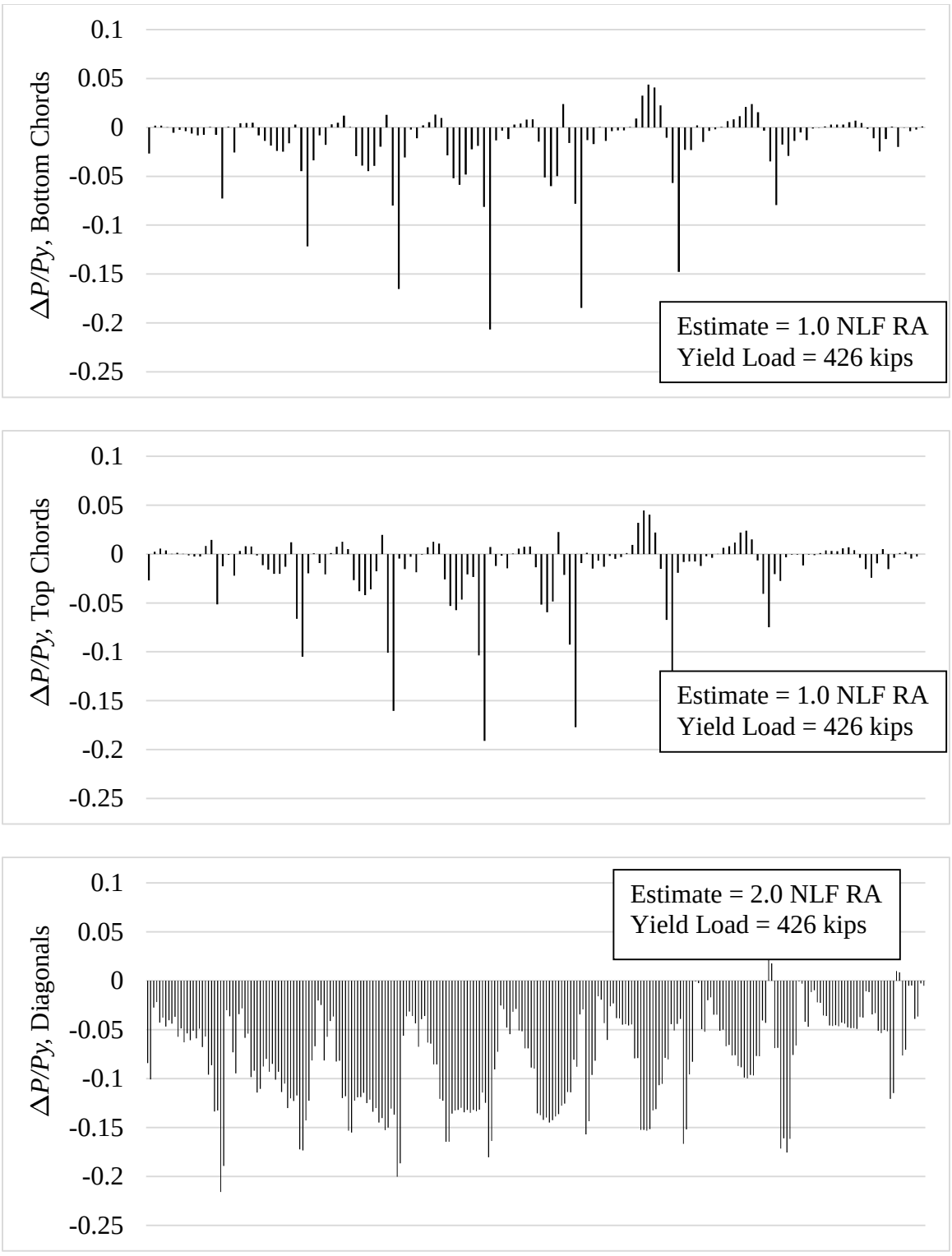

Figure 183. Difference between the magnitude of the DLF RA forces and the values estimated by scaling the NLF RA results, divided by the member yield load ($\Delta P/P_y$), Bridge (Q2) NISCS38 under TDL with TDLF detailing based on NLF RA cambers.

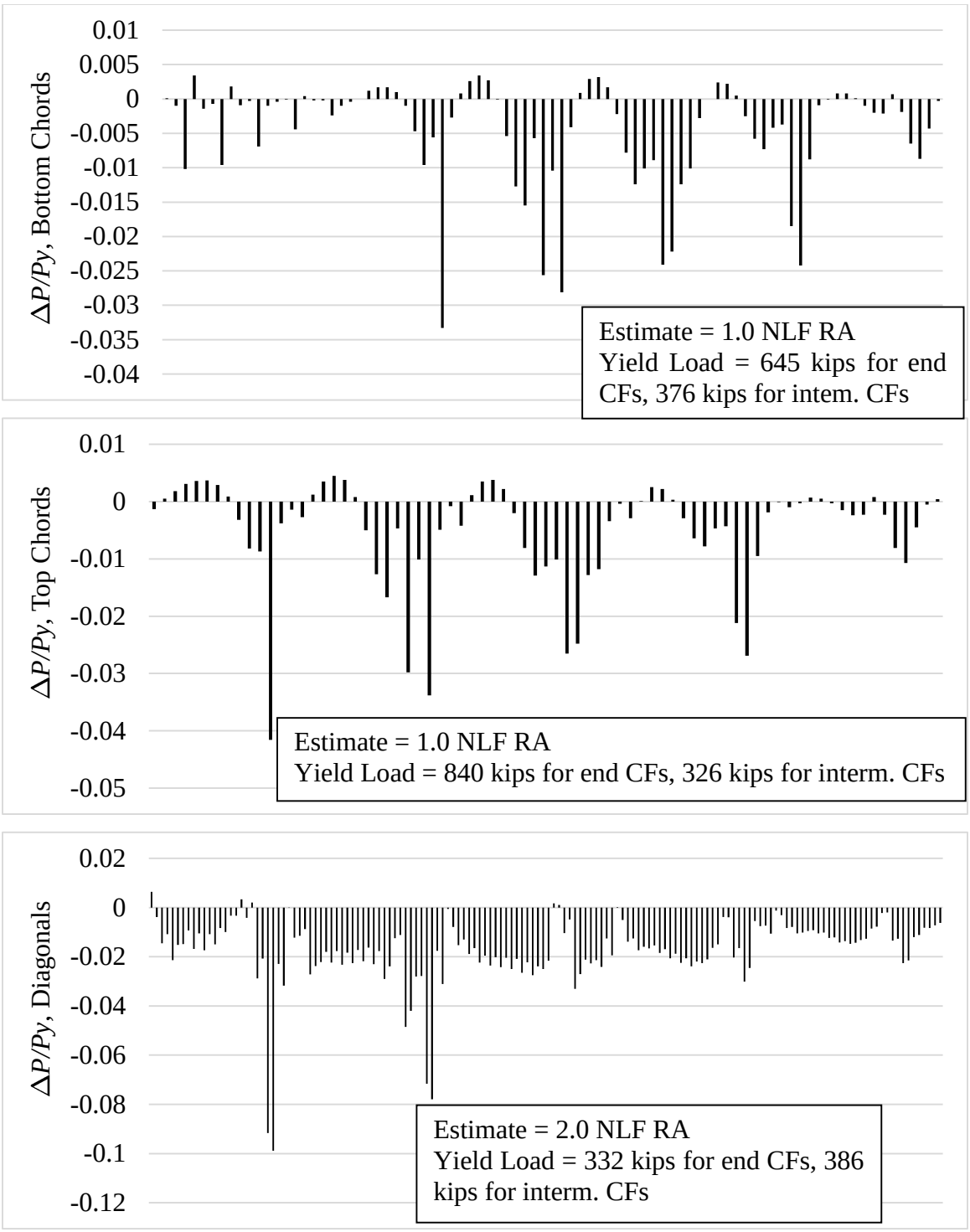

Figure 184. Difference between the magnitude of the DLF RA forces and the values estimated by scaling the NLF RA results, divided by the member yield load ($\Delta P/P_y$), Bridge (P) EISCS3 under SDL with SDLF detailing based on NLF RA cambers.

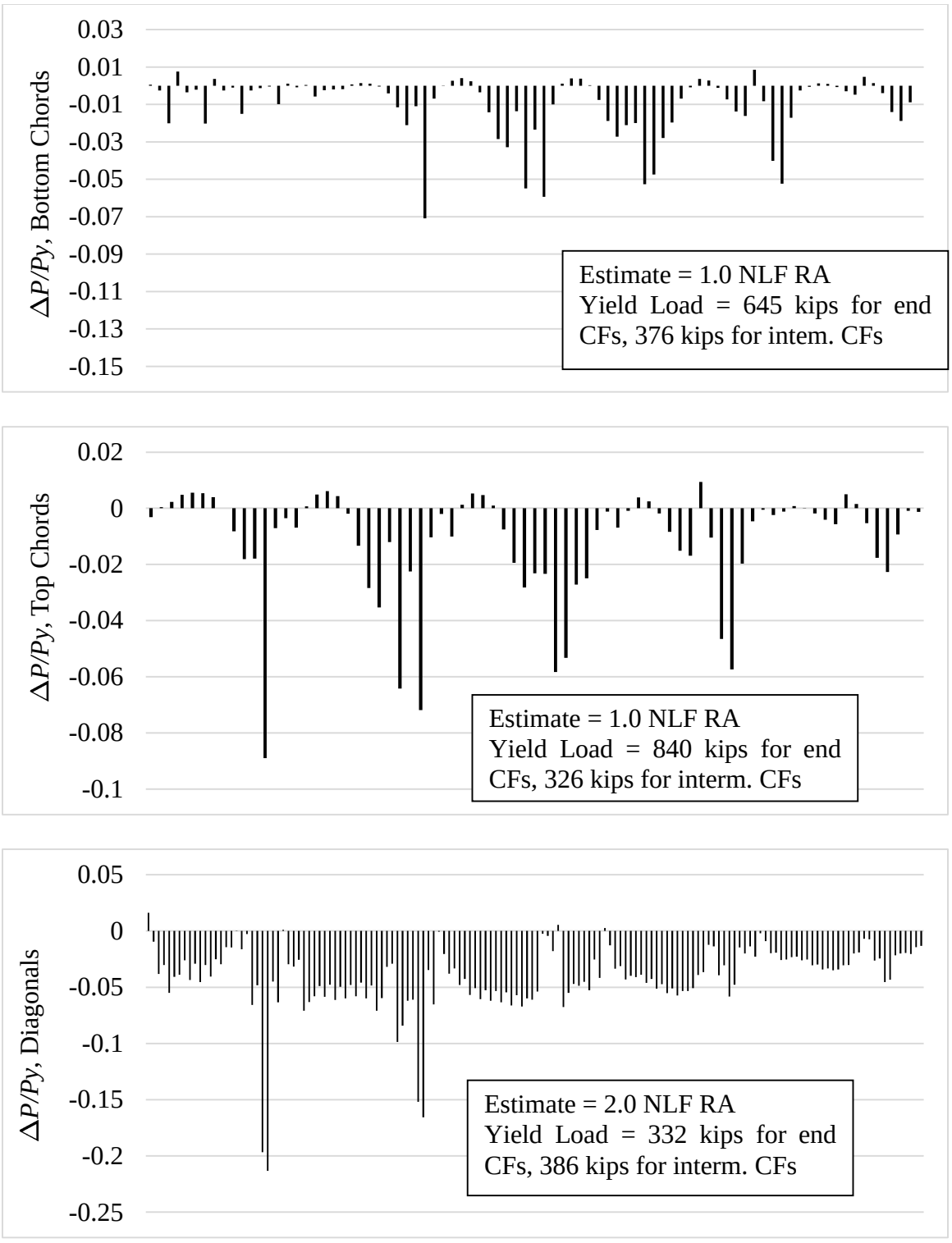

Figure 185. Difference between the magnitude of the DLF RA forces and the values estimated by scaling the NLF RA results, divided by the member yield load ($\Delta P/P_y$), Bridge (P) EISCS3 under TDL with TDLF detailing based on NLF RA cambers.

6.10.1.5 Girder Stresses

For curved bridges with or without skew, the girder on the outside of the curve typically tends to have the largest girder major-axis bending stresses and flange lateral bending stresses. The skew orientation of Bridge (N) NISCS14 decreases the maximum vertical displacement and maximum layover of the outside girder of Bridge (N) NISCS14. The skew orientation of Bridge (O1) NISCS15 increases the maximum vertical displacement and maximum layover of the outside girder of Bridge (O1) NISCS15. However, from Figure 186 to Figure 189, the skew orientations of bridge cases (N) and (O1) have negligible influence on the maximum major-axis bending stresses and flange lateral bending stresses on the outside girder.

Considering all the curved and skewed bridge cases studied in this research, from Tables 60 and 61, the largest increases in the major-axis bending stresses under TDL are nine and 16 % for SDLF and TDLF, respectively. The largest increases in the flange lateral bending stresses under TDL are 14 and 31 % for SDLF and TDLF, respectively.

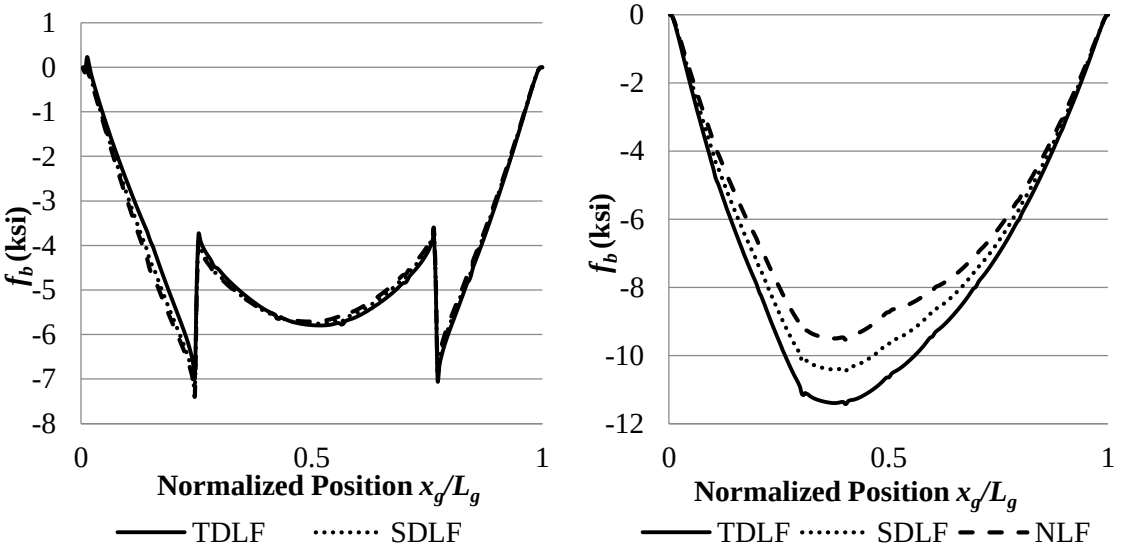

Figure 186. SDL top flange major-axis bending stresses of the outside girder for Bridge (N) NISCS14(left) and Bridge (O1) NISCS15 (right).

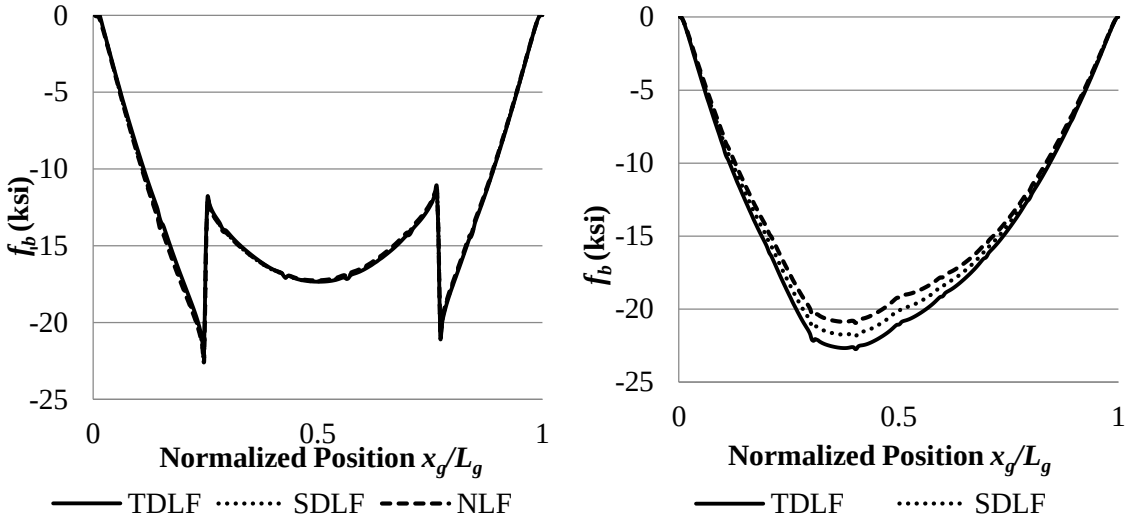

Figure 187. TDL top flange major-axis bending stresses of the outside girder for Bridge (N) NISCS14(left) and Bridge (O1) NISCS15 (right).

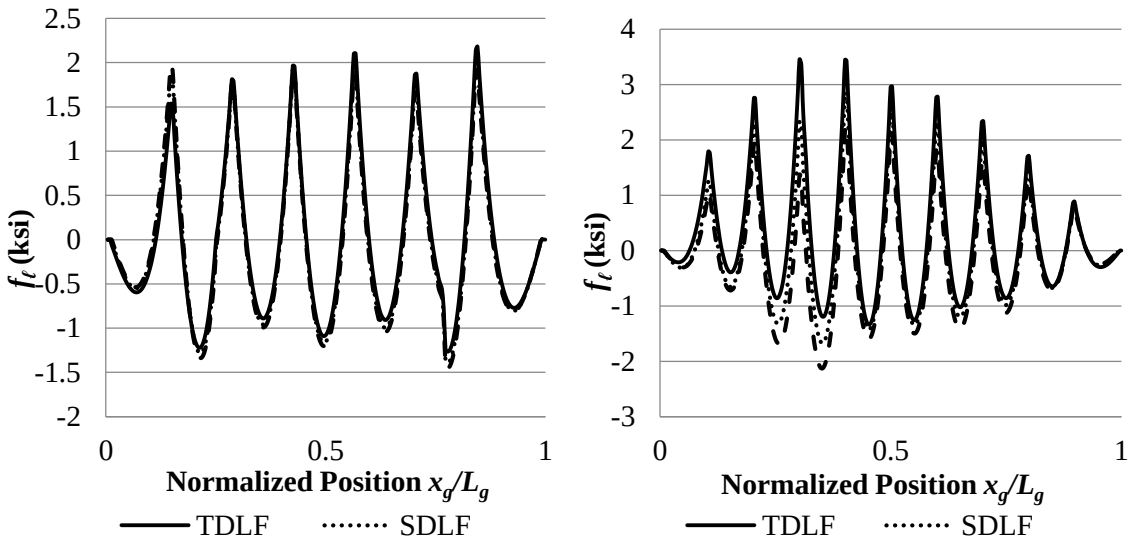

Figure 188. SDL top flange lateral bending stresses of the outside girder for Bridge (N) NISCS14 (left) and Bridge (O1) NISCS15 (right).

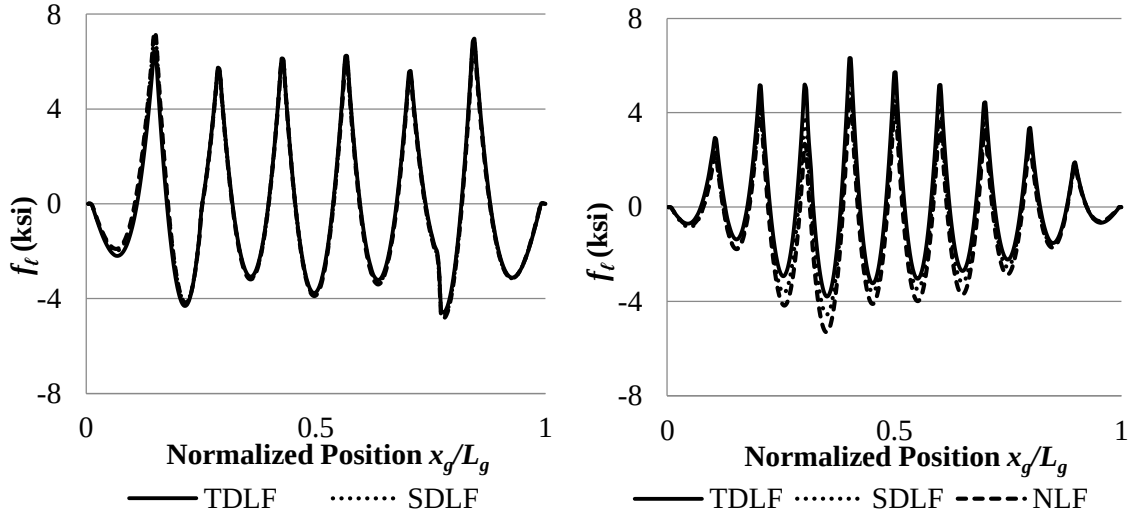

Figure 189. TDL top flange lateral bending stresses of the outside girder for Bridge (N) NISCS14 (left) and Bridge (O1) NISCS15 (right).

Table 60. Maximum magnitudes of major-axis bending stresses and top flange lateral bending stresses under TDL on the girder on the outside of the curve in the curved and skewed bridges studied in this research. (f_{b1}, f_{b2} and f_{b3} are the maximum major-axis bending stresses, and $f_{\ell 1}$, $f_{\ell 2}$ and $f_{\ell 3}$ are the maximum girder flange lateral bending stresses for NLF, SDLF, and TDLF detailing, respectively; the largest f_{b2}/f_{b1}, $f_{\ell 2}/f_{\ell 1}$ under SDL for SDLF and f_{b3}/f_{b1} and $f_{\ell 3}/f_{\ell 1}$ under TDL for TDLF are highlighted by dark shading).

Bridge	SDL						TDL					
	NLF		SDLF				NLF		TDLF			
	f_{b1} (ksi)	$f_{\ell 1}$ (ksi)	f_{b2} (ksi)	$\frac{f_{b2}}{f_{b1}}$	$f_{\ell 2}$ (ksi)	$\frac{f_{\ell 2}}{f_{\ell 1}}$	f_{b1} (ksi)	$f_{\ell 1}$ (ksi)	f_{b3} (ksi)	$\frac{f_{b3}}{f_{b1}}$	$f_{\ell 3}$ (ksi)	$\frac{f_{\ell 3}}{f_{\ell 1}}$
(N) NISCS14	7.4	2.0	7.3	0.99	2.0	1.00	22.5	7.2	22.1	0.98	7	0.97
(O1) NISCS15	9.5	2.2	10.4	1.09	2.8	1.27	21.0	5.3	22.7	1.08	6.3	1.19
(O2) NISCS15	8.6	2.0	9.3	1.08	2.5	1.25	18.7	4.2	20.1	1.07	5.5	**1.31**
(P) EISCS3	8.9	1.7	9.2	1.03	1.5	0.88	21.0	4.1	21.6	1.03	3.8	0.93
(Q1) NISCS38	12.0	1.0	12.5	1.04	0.9	0.90	24.4	2.8	25.2	1.03	1.9	0.68
(Q2) NISCS38	12.2	1.2	12.7	1.04	1.1	0.92	24.8	3.2	25.6	1.03	2.3	0.72
(R1) NISCS39	16.9	4.1	17.7	1.05	1.8	0.44	29.4	10.8	29.8	1.01	3.7	0.34
(R2) NISCS39	17.3	3.8	17.3	1.00	1.4	0.37	29.7	9.5	28.8	0.97	2.8	0.29
(S) XICCS7	3.9	0.9	4.1	1.05	1.1	1.22	16.9	5.1	17.5	1.04	5.4	1.06
(T1) EICCS27	12.4	1.1	12.7	1.02	1.3	1.18	43.2	7.9	43.6	1.01	7.2	0.91
(T2) EICCS27	12.5	1.1	12.4	0.99	3.7	**3.36**	44.3	8.5	42.7	0.96	9.6	1.13
(U1) EICCS28	12.2	2.0	14.3	**1.17**	1.8	0.90	22.2	5.2	25.8	**1.16**	3.5	0.67
(U2) EICCS28	13.8	2.1	14.5	1.05	1.2	0.57	24.6	5.7	26.2	1.07	3.2	0.56

Table 61. Maximum magnitudes of major-axis bending stresses and top flange lateral bending stresses under TDL on the girder on the inside of the curve in the curved and skewed bridges studied in this research. (f_{b1}, f_{b2} and f_{b3} are the maximum major-axis bending stresses, and $f_{\ell 1}$, $f_{\ell 2}$ and $f_{\ell 3}$ are the maximum girder flange lateral bending stresses for NLF, SDLF, and TDLF detailing, respectively; the largest f_{b2}/f_{b1}, $f_{\ell 2}/f_{\ell 1}$ under SDL for SDLF and f_{b3}/f_{b1} and $f_{\ell 3}/f_{\ell 1}$ under TDL for TDLF are highlighted by dark shading).

Bridge	SDL						TDL					
	NLF		SDLF				NLF		TDLF			
	f_{b1} (ksi)	$f_{\ell 1}$ (ksi)	f_{b2} (ksi)	$\frac{f_{b2}}{f_{b1}}$	$f_{\ell 2}$ (ksi)	$\frac{f_{\ell 2}}{f_{\ell 1}}$	f_{b1} (ksi)	$f_{\ell 1}$ (ksi)	f_{b3} (ksi)	$\frac{f_{b3}}{f_{b1}}$	$f_{\ell 3}$ (ksi)	$\frac{f_{\ell 3}}{f_{\ell 1}}$
(N) NISCS14	4.5	1.4	4.1	0.91	1.2	0.86	13.8	4.3	12.5	0.91	3.7	0.86
(O1) NISCS15	2.2	2.0	1.1	0.50	0.4	0.20	2.6	5.9	1	0.38	1	0.17
(O2) NISCS15	2.3	3.1	1.6	0.70	0.5	0.16	3.7	7.3	1.5	0.41	0.8	0.11
(P) EISCS3	3.6	1.0	2.9	0.81	0.5	0.50	9.5	2.7	8	0.84	1.1	0.41
(Q1) NISCS38	8.3	1.1	7.6	0.92	0.7	0.64	17.8	2.9	16.5	0.93	1.5	0.52
(Q2) NISCS38	8.1	1.5	7.6	0.94	1.1	0.73	17.7	3.7	16.6	0.94	2.3	0.62
(R1) NISCS39	2.4	7.9	2.0	0.83	0.5	0.06	5.0	20.0	2.3	0.46	2.2	0.11
(R2) NISCS39	4.8	10.2	3.7	0.77	0.6	0.06	7.7	22.1	4.7	0.61	0.9	0.04
(S) XICCS7	4.5	1.9	4.7	**1.04**	1.4	0.74	20.0	8.3	20.8	**1.04**	6.4	0.77
(T1) EICCS27	11.7	1.3	11.3	0.97	1.3	1.00	40.8	5.9	39	0.96	4.1	0.69
(T2) EICCS27	10.2	1.6	9.8	0.96	2.2	**1.38**	35.0	7.5	32.9	0.94	8.1	**1.08**
(U1) EICCS28	5.3	1.9	4.9	0.92	1.3	0.68	13.2	5.5	12.5	0.95	2.9	0.53
(U2) EICCS28	5.1	4.7	4.8	0.94	0.9	0.19	12.9	11.1	12	0.93	2.2	0.20

6.10.1.6 Vertical Reactions

In curved and skewed bridges, when the skew makes the inside girder longer as in Bridge (N) NISCS14, the skew effects tend to counteract the curvature effects. In addition, larger DL is applied to the inside girder, which is the longer girder. As a result, the overall DL tends to distribute more equally to each of the girders (shown in Table 62 for Bridge (N)). SDLF and TDLF detailing effects have negligible changes in the vertical reactions in this case.

In curved and skewed bridges, when the skew makes the outside girder longer as in Bridge (O1) NISCS15, the skew effects tend to be additive with the curvature effects. In addition, larger DL is applied to the girder on the outside of the curve, which is the longer girder. The loads tend to shift from the inside to the outside of the bridge cross-section, resulting in higher vertical reactions in the outside girder and lower vertical reactions in the inside girder of the curve. This behavior is exhibited by Bridge (O1) in Table 63. The inside girder in Bridge (O1), Girder 9, experiences uplift at the skewed bearing line (highlighted as "Uplift" in the table). SDLF and TDLF detailing effects twist the girders in the direction opposite to that which the girders tend to roll under the DL. The detailing effects increase the reactions in both the inside and outside girders due to complex 3D behaviors. For Bridge (O1) NISCS15, the reactions at the skewed bearing line on Girder 1 under TDL are increased by 12 kips by SDLF detailing and 26 kips by TDLF detailing. The support at the skewed bearing line on Girder 9 experiences uplift with NLF detailing. The reactions at the skewed bearing line on Girder 9 under TDL are 18 kips with SDLF detailing and 39 kips with TDLF detailing. However, the reactions on Girder 4 under TDL, an interior girder, are decreased by 5 kips with SDLF detailing and 7 kips with TDLF

detailing. The total net change in vertical reactions at all bearings is zero when SDLF or TDLF detailing is employed.

Of the other curved and skewed bridge cases studied in this research, bridge cases (O2) NISCS15, (R1) and (R2) NISCS39, and (U1) EICCS28 experienced uplift at the bearing on the inside girder at the obtuse corner of the bridge plan. The skew orientation of these bridge cases make the outside girder longer (the outside girder is longer in one end span for continuous-span Bridge (U1)). It is important to note that uplift is exacerbated by longer spans, sharper skews, tighter curvature, and contiguous framing arrangements.

From Table 64, the largest maximum absolute and percentage increases in the vertical reactions are 152 kips and 554 % respectively, due to SDLF, for the curved and skewed bridges considered in this research. The largest maximum absolute and percentage increases are 298 kips and 983 % respectively due to TDLF detailing. These maximums occur in bridge cases (U1) and (U2).

Table 62. Bridge (N) NISCS14 vertical reactions (kips), where the skew increases the length of the girder on the inside of the curve (G1 and G9 are the girders on the outside and the inside of the curve, respectively).

Girder	Detailing Method	SDL Support 1	SDL Support 2	TDL Support 1	TDL Support 2
G1	NLF	56	53	172	164
	SDLF	53	53	170	165
	TDLF	49	54	165	165
G2	NLF	53	49	165	153
	SDLF	51	49	163	152
	TDLF	46	49	158	152
G3	NLF	50	45	157	142
	SDLF	52	45	159	142
	TDLF	57	46	164	143
G4	NLF	51	40	162	125
	SDLF	51	39	162	124
	TDLF	50	37	161	123
G5	NLF	44	37	140	116
	SDLF	46	37	142	116
	TDLF	51	39	147	118
G6	NLF	46	35	144	109
	SDLF	48	36	146	111
	TDLF	52	38	151	113
G7	NLF	51	44	154	133
	SDLF	52	44	154	133
	TDLF	53	45	156	134
G8	NLF	45	40	134	120
	SDLF	44	39	132	120
	TDLF	40	38	128	119
G9	NLF	31	34	95	103
	SDLF	30	33	94	102
	TDLF	29	30	93	98

Table 63. Bridge (O1) NISCS15 vertical reactions (kips) where the skew increases the length of the girder on the outside of the curve (G1 and G9 are the girders on the outside and inside of the curve, respectively. The bearing locations experiencing uplift are highlighted by dark shading).

Girder	Detailing Method	SDL Support 1	SDL Support 2	TDL Support 1	TDL Support 2
G1	NLF	170	133	369	287
	SDLF	183	138	381	292
	TDLF	199	143	395	297
G2	NLF	131	124	280	271
	SDLF	132	126	280	274
	TDLF	128	130	281	275
G3	NLF	71	120	162	265
	SDLF	62	120	153	263
	TDLF	55	115	140	264
G4	NLF	64	77	150	177
	SDLF	59	73	145	174
	TDLF	53	72	143	169
G5	NLF	51	73	126	168
	SDLF	45	69	120	164
	TDLF	38	65	112	161
G6	NLF	39	64	104	150
	SDLF	35	60	100	147
	TDLF	33	56	96	145
G7	NLF	39	38	86	92
	SDLF	26	36	80	91
	TDLF	21	34	78	88
G8	NLF	7	5	74	57
	SDLF	23	10	75	57
	TDLF	19	14	70	58
G9	NLF	**Uplift**	**Uplift**	**Uplift**	11
	SDLF	9	**Uplift**	18	14
	TDLF	29	**Uplift**	39	17

Table 64. Summary of maximum percentage increase in the vertical reaction at each of the girder bearings due to SDLF and TDLF detailing in the curved and skewed bridges (Largest increases highlighted by dark shading).

Bridge	SDLF under SDL		TDLF under TDL	
	Change (kips)	Percentage Change	Change (kips)	Percentage Change
(N) NISCS14	5	2	7	5
(O1) NISCS15	246	16	6	55
(O2) NISCS15	62	15	38	61
(P) EISCS3	35	6	13	26
(Q1) NISCS38	8	12	23	7
(Q2) NISCS38	8	16	28	7
(R1) NISCS39	39	54	137	159
(R2) NISCS39	24	6	24	33
(S) XICCS7	4	3	18	4
(T1) EICCS27	191	48	165	143
(T2) EICCS27	6	9	14	7
(U1) EICCS28	**155**	**154**	**298**	132
(U2) EICCS28	45	92	130	**983**

6.10.2 Summary and Recommendations – Curved and Skewed Bridges with Cambers Set Based on NLF RA

The influence of SDLF and TDLF detailing on the responses in the completed curved and skewed bridge systems studied in this research may be summarized as follows. Recommendations pertaining to these quantitative results are highlighted in bold italicized text.

General

- In the limit that the skew becomes small, taken as $\theta \leq 20^o$, the curved radially-supported bridge recommendations are considered to apply. Therefore, Section 6.5 should be consulted for these cases.
- In the limit that the horizontal curvature becomes small, taken as $L_s/R \leq 0.03$, the straight bridge recommendations are considered to apply.

Girder Elevations

- The elevations are slightly low for the most extreme curved and skewed bridges considered when the skew makes the inside girder shorter.
- The elevations are slightly high for the most extreme curved and skewed bridges considered when the skew makes the outside girder longer.
- With the exception of (R1) and (R2) NISCS39, which are so extreme that (R2) is essentially unbuildable, the largest deviations from the targeted/expected elevations (calculated without considering the DLF effects) are 1.2 inches for SDLF and 2.1 inches for TDLF.
- ***It is recommended that NLF RA is sufficient for calculation of the cambers in curved radially-supported bridges. This recommendation is identical to the recommendations for general curved radially-supported and straight skewed bridges.***

Girder Layovers

- The maximum layover under SDL for SDLF is 0.5 inches (0.0056 rad) for the bridges studied.

- The maximum layover under TDL for TDLF is 1.7 inches (0.0189 rad) for the bridges studied.
- These nonzero layovers are largely due to elastic deformations of the CFs and the elastic torsional deformations of the girders in the three-dimensional bridge systems.
- ***It is recommended that the girder layovers may be assumed to be negligible in the targeted DL condition in curved and skewed bridges. There is no need to consider any change in the girder layovers due to the change in the internal forces, and the change in the elastic deformations in the system, associated with the DLF detailing. The fascia girders should be checked separately for twist rotation between the CF locations due to eccentric overhang bracket loads.***
- ***For curved and skewed bridges detailed for SDLF, the girder layovers under the TDL may be estimated as the CDL layovers obtained from a NLF RA.***
- ***For curved and skewed bridges detailed for TDLF, the girder layovers under the SDL may be estimated as the negative of the CDL layovers obtained from a NLF RA.***
- ***This recommendations are identical to the recommendations for general curved radially-supported and for general straight skewed bridges.***

Cross-Frame Forces

- Not considering bridge (T2) EICCS27, the average of the CF chord forces under SDL decreases for SDLF detailing in the bridges studied. In addition, the average of the CF chord forces under TDL decreases for TDLF detailing in the bridges studied. Bridge (T2) has an extremely large skew index and an improved arrangement of the CFs that greatly reduces its CF forces. The improvement (reduction) in the overall CF force

magnitudes coincides with larger elastic girder torsional deformations, which results in changes in the force distributions in the structural system, including the distributions associated with the TDLF detailing effects.

- Not considering bridge (T2) EICCS27, the largest increase in the maximum of the CF chord forces under SDL is 5 % (1.7 kip) for SDLF detailing in the bridges studied. The largest increase in the maximum of the CF member forces under TDL is 2 % (1.7 kip) for TDLF detailing. Both of these increases occur in bridge (P) EISCS3.
- Not considering bridge (T2) EICCS27, the average of the CF diagonal forces under SDL either remains unchanged (bridge (N) NISCS14) or decreases for SDLF detailing in the bridges studied. In addition, the average of the CF diagonal forces under TDL either remains unchanged (bridge (N) NISCS14) or decreases for TDLF detailing in the bridges studied.
- Not considering bridge (T2) EICCS27, the largest increase in the maximum of the CF diagonal forces under SDL is 1 % (0.3 kip) for SDLF detailing in the bridges studied. This increase occurs in bridge (Q1) NISCS38.The largest increase in the maximum of the CF member forces under TDL is 5 % (kip) for TDLF detailing. This increase occurs in bridge (Q2) NISCS38.
- For the bridges studied, the overall statistics for the percent change in the individual CF member forces relative the member yield load due to SDLF and TDLF detailing indicate a wide range (dispersion) of individual CF member force effects, but a predominant tendency for reduction of the CF member forces (relative to the values associated with the assumption of NLF detailing) due to SDLF and TDLF detailing. The reductions in the CF member forces tend to not be as large as in the straight skewed

bridges. This is due to the overall influence of the effects associated with horizontal curvature, which are opposite to the effects associated with support skew.

- It is observed that the combination of the skew effects and the horizontal curvature effects tends to reduce the influence of DLF detailing on the CF forces from the values associated with the recommendations for curved radially-supported bridges in all cases.
- ***Based on the above observations, it is recommended that, in lieu of a DLF RA, the CF member forces in curved and skewed I-girder bridges may be calculated conservatively by using the recommendations for curved radially-supported bridges.***
- With the use of the above scale factors, the maximum difference between the magnitudes of the individual DLF RA CF member forces versus the scaled NLF RA results, normalized by the member yield load, is reduced to 4.4 and 9.0 %, and the corresponding average difference is reduced to -1.9 and -4.3 % for SDLF under SDL and TDLF under TDL, respectively, for the curved radially-supported bridges studied in this research, excluding bridge (T2)

Girder Stresses

- For the curved and skewed bridges studied in this research:
  - The largest increase in the maximum major-axis bending stress on any of the girders, under TDL for SDLF (relative to the response from NLF RA), is 9 % (2.0 ksi).
  - The largest increase in the maximum major-axis bending stress on any of the girders, under TDL for TDLF (relative to the response from NLF RA), is 16 % (3.6 ksi).

- The largest increase in the maximum flange lateral bending stress on any of the girders, under TDL for SDLF (relative to the response from NLF RA), is 14 % (0.6 ksi).
- The largest increase in the flange lateral bending stress on any of the girders, under TDL for TDLF (relative to the response from NLF RA), is 31 % (1.3 ksi).

- ***It is recommended that, in lieu of a DLF RA, the girder f_b and f_ℓ values in curved and skewed I-girder bridges may be calculated conservatively by using the recommendations for curved radially-supported bridges.***

Vertical Reactions

- Horizontally curved and skewed bridges where the outside girder is made longer by the skew of the bearing lines are apt to see uplift at an obtuse corner of the bridge plan.
- For simply-supported bridges that have both a tight horizontal curvature and sharp skew, DLF detailing tends to relieve potential uplift conditions at lightly loaded bearings that are most vulnerable to uplift. Therefore, as an approximate estimate for simply-supported bridges, if uplift is not encountered at any of the bearings in a NLF RA, it should be sufficient to assume that uplift will not be a problem in the bridge if it is detailed for SDLF or TDLF.
- DLF detailing increases the reactions on some of the girders and decreases them on others. The net total change in the vertical reactions is zero.
- In the simple-span curved and skewed bridges studied where the length of the girder on the outside of the curve is increased by the skew (Bridges (O1) and (O2) NISCS15 and (R1) and (R2) NISCS39), the reactions tend to be very small or negative at the

girder on the inside of the curve (negative reactions mean uplift, based on the assumption that a tie-down device is employed). In these cases, both SDLF and TDLF reduce the uplift and redistribute the reactions substantially.

- In the simple-span curved and skewed bridges considered in this research, where the length of the girder on the inside of the curve is increased by the skew (Bridges (N) NISCS14, (P) EISCS3, and (Q1) and (Q2) NISCS38), the largest increase in the reactions is 16 % (8 kip) under SDL for SDLF and 26 % (13 kip) under TDL for TDLF.
- In the extreme simple-span curved and skewed Bridge (O1) NISCS15, where the length of the girder on the outside of the curve is increased substantially by the skew, the largest increase in the reactions is 16 % (8 kip) and 54 % (39 kip) for SDLF under SDL and TDLF under TDL, respectively.
- In the continuous-span curved and skewed bridges, the influence of DLF detailing on the reactions can be substantial in certain cases, as much as 155 kip (154 %) under SDL for SLDF and 298 kip (132 %) under TDL for TDLF (neglecting the very large percentage change for bridge (U2) EICCS28, due to the fact that some of the reactions from the NLF RA are relatively small.
- ***In lieu of a DLF RA, it is recommended that the influence of SDLF detailing on the girder reactions in curved and skewed simply-supported bridges, where the length of the girder on the inside of the curve is increased by the skew, may be addressed by scaling the SDL reactions from a NLF RA by the multiplier 1.20.***
- ***In lieu of a DLF RA, it is recommended that the influence of SDLF detailing on the SDL girder reactions in curved and skewed simply-supported bridges, where the***

length of the girder on the outside of the curve is increased by the skew, may be addressed by scaling the SDL reactions from a NLF RA by the multiplier 1.60.

- ***For all other cases, it is recommended that a DLF RA should be conducted to determine the girder reactions in curved and skewed I-girder bridges.***
- ***For SDLF detailing, the TDL reactions can be computed as the sum of the above SDL reactions and CDL reactions.***
- ***In simple spans, if uplift is not experienced for NLF, it is likely that uplift would not occur for SDLF and TDLF. This is because SDLF and TDLF tend to increase the vertical reactions bearing that are most vulnerable to uplift.***

The above recommendations are considered applicable for curved and skewed bridges with L_s/R up to 0.5, skews up to 70^o, and spans up to 300 ft. These limits are different from those listed in the tables for recommended fit conditions discussed in Section 11.1. The limits here are aimed at ensuring sufficient accuracy of the structural analysis whereas the limits discussed in Section 11.1 address broader questions of ensuring reliable fit-up of the structural steel. For bridges that exceed these limits, it is recommended that DLF RA be considered. Chapter 3 explains the details of several procedures for conducting a DLF RA.

CHAPTER 7

INLFUENCE OF FRAMING ARRANGEMENTS ON FIT RESPONSES

The cross-frame framing arrangement can have a significant effect on the overall bridge behavior as well as the fit-up forces. In a number of the bridges studied in this research, specific improvements in the cross-frame framing arrangements were possible based on the NCHRP Report 725 research and other recent developments and findings. These improvements relate particularly to the alleviation of significant nuisance transverse stiffness paths associated with skew and the application of the considerations discussed in this section.

7.1. Provide Generous Offsets between Intermediate Cross-Frames and Skewed Supports and Avoid Large Discrepancies in Girder Unbraced Lengths to the Extent Practicable at Skewed Bearing Lines

NCHRP Report 725 recommends the use of an offset of the intermediate cross-frames from the skewed bearing line cross-frames that is the larger of $1.5D$ or $0.4L_b$ wherever practicable, where D is the girder web depth and L_b is the next or adjacent interior unbraced length. The provision of this offset locates cross-frames where girder differential displacements between the cross-frame ends are significantly reduced, leading to lower cross-frame forces. This offset has been incorporated in AASHTO LRFD Article C6.7.4.2.

Upon applying these rules to the suite of bridges selected for this research, it is apparent that the above 1.5D rule is overly punitive and difficult to implement in longer-span highly-skewed bridges. This is because $1.5D$ is commonly a larger fraction of the other unbraced lengths for longer-span bridges, where the typical unbraced lengths of 30 ft or less are a smaller fraction of the overall span length. As such, the unbraced length on the fascia

girders at the acute corners of the spans tended to be too long. However, the other characteristic of the longer-span straight skewed bridges is that their flanges tend to be a smaller fraction of the overall girder depths. This is a "natural" occurrence in the designs, since the unbraced lengths, L_b, are also a smaller fraction of the span lengths. The flange width is the predominant dimension that influences the girder warping and lateral bending stiffnesses, and therefore influences the tendency to develop large transverse nuisance stiffness due to small offsets (and stagger distances). The research found that a length of $4b_f$, where b_f is the largest girder flange width within the unbraced lengths on either side of the first cross-frame, serves as a better minimum limit that should always be met to ensure that offsets (and stagger distances) actually serve their intended purpose.

For bridges with sharply skewed bearing lines, the max($4b_f$, $0.4L_b$) offset rule still result in a large L_b on the fascia girder near the acute corners of sharply skewed spans. The AASHTO Standard Specifications formerly recommended a maximum unbraced length of 25 ft. This has been replaced in the AASHTO LRFD Specifications by the requirement for a rational analysis to assess the cross-frame spacing. However, cross-frame spacings larger than 30 ft are relatively rare in straight I-girder bridges, and are not permitted for curved I-girder bridges. If the overhang loads do not cause excessive twisting of the fascia girder, then unbraced lengths slightly larger than 30 ft can be accommodated easily in many cases at the simply-supported ends of a straight-girder bridge. However, the negative moments at in interior pier can require increases in the size of the fascia girder at an acute corner to handle the lateral torsional buckling limit state. To solve the above issues of either the torsional rotations due to overhang loads or the lateral torsional buckling resistance, the first intermediate cross-frames from the bearing lines may be skewed to reduce the

unbraced length on the fascia girder at this location. A skew angle of approximately one-half the skew angle of the bearing line is suggested. Figure 190 demonstrates this application skewed intermediate cross-frames by showing a portion of the framing arrangement of a continuous-span bridge

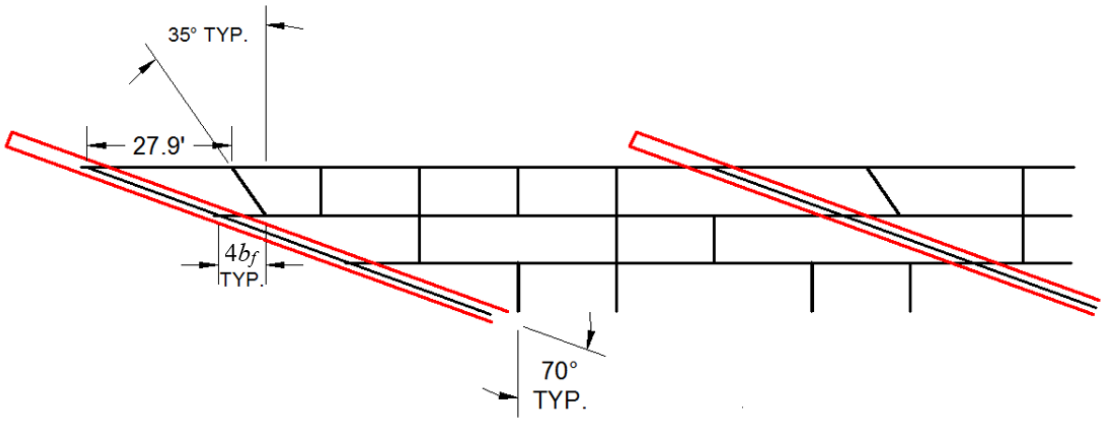

Figure 190. Use of skewed intermediate cross-frames adjacent the skewed bearing lines (not recommended).

The most important points of the framing arrangement shown in Figure 190 are:

- It maintains the minimum offset of the larger of $4b_f$ and $0.4L_b$ while also providing an acceptable unbraced length on the fascia girders, where b_f is the largest girder flange width within the unbraced lengths on either side of the first cross-frame and L_b is the next or adjacent interior unbraced length. This research recommends that the traditional recommendation of an offset of $1.5D$ in the AASHTO LRFD Article C6.7.4.2 be modified to $4b_f$. An engineer who understands approximately what b_f/D values will be needed for a given type of bridge structure can still convert the $4b_f$ requirement into a related fraction of the girder web depth, if desired.

- The skewed intermediate cross-frame also experiences smaller differential vertical deflections at its ends than if it were framed normal to the girders. This reduction in vertical differential deflections leads to a substantial reduction in nuisance transverse stiffness.

- Although the intermediate cross-frame skew results in some coupling between the girder major-axis bending and twisting rotations, this effect is not as severe as in the bearing line cross-frames since the skew angle is only about half that of the bearing line.

- Skewing the above intermediate cross-frame actually provides an additional "degree of freedom" (dof) of low stiffness that may facilitate the installation of the skewed cross-frame – the rotation of the cross-frame about its axis and the rotation of the girder about its longitudinal axis both have relatively low stiffness compared to the other deformations in the region of the acute corner. By skewing the intermediate cross-frame, these two flexible rotational dofs have components that are additive to one another, rather than these rotations being orthogonal to one another.

It should be noted that the use of skewed intermediate cross-frames may result in a potential increase in the fabrication costs for the skewed connection plate detail. Therefore, the scheme shown in Figure 190 is not generally recommended. To avoid using skewed intermediate cross-frames at the acute corners of the spans in such cases, it is instead recommended that the first cross-frame in the exterior bays adjacent to the skewed bearing lines be framed perpendicular to the girders with a small offset from the bearing on the

interior girder as shown in Figure 191, and that the diagonal members of this cross-frame be removed to reduce the resulting nuisance transverse stiffness. The cross-frames highlighted by an oval and labeled on this plan view as “CO” (for “chords only”) do not contain any diagonals. This allows for a small offset of these cross-frames relative to the skewed bearing lines without inducing large cross-frame forces from nuisance transverse stiffness effects, while reducing the large unbraced length on the adjacent girder at the acute corner of the bridge plan. This scheme may be considered as a variant of the lean-on bracing concept, discussed further in Section 7.4.

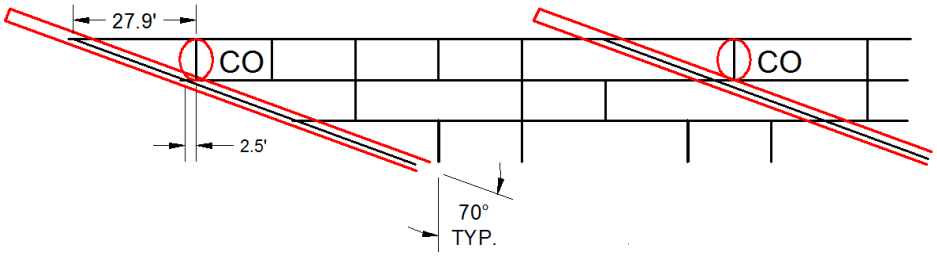

Figure 191. Demonstration of the use of intermediate cross-frames with chord only adjacent to the skewed bearing lines (recommended).

7.2. Provide Bearing-Line Cross-Frames at Interior Piers in Continuous-Span Bridges and Avoid Framing of Intermediate Cross-Frames Directly Into Bearing Locations

Figure 13 shows the Bridge (M1) EICSS2 framing arrangement with intermediate cross-frames connected directly into the bearings at the interior piers where bearing-line cross-frames are also provided. This framing arrangement causes substantial nuisance transverse stiffness. The enforcement of compatible deformations is difficult for this type of framing arrangement, leading potentially to large required external fit-up forces during erection and large internal forces in the cross-frames in the vicinity of the piers.

One option to avoid this problem on continuous-span bridges is to offset the intermediate cross-frames relative to the skewed bearing line at the interior piers, as discussed above in Section 7.1. Alternately, this problem can be avoided by not using any skewed bearing line cross-frames at the pier, but instead providing an intermediate cross-frame normal to the girder on one or both sides of each bearing. These two alternative framing arrangements are shown for bridge cases (K2) and (K3) EICSS12, respectively. It is important to note that at least one cross-frame must be connected to the girder at or near each bearing. This is necessary to transfer lateral loads to the bearing, if the bearing is laterally restrained, as well as to provide bracing to the girder at this location.

Nevertheless, for cross-frames framing directly into the bearing locations at an interior pier in a continuous-span bridge, the girder vertical displacement is zero on the side connected at the bearing location and non-zero on the other side. As such, framing any intermediate cross-frame directly into a bearing tends to cause substantial nuisance transverse stiffness.

When the span ratio is balanced, the major-axis bending rotations at the interior piers are minimal. The pier cross-sections act approximately as if they were fixed points. NCHRP Report 725 shows that at a skewed bearing line $\phi_z = \phi_x \tan\theta$ where ϕ_x is the major-axis bending rotation, ϕ_z is the twist rotation, and θ is the skew angle (zero for zero skew). Since ϕ_x is minimal at the interior piers in balanced spans, the twist rotations ϕ_z are also minimal. The use of skewed bearing line cross-frames to transfer lateral loads to the restrained bearings and provide bracing to the girder at the interior pier, along with a liberal offset of the first intermediate cross-frames on each side of the interior pier, generally

results in a greater reduction of overall nuisance transverse stiffness and lower forces in the interior skewed bearing line cross-frames.

Table 65 compares the average and maximum cross-frame forces under SDL and TDL for bridge cases (K2) and (K3) EICCS12. The framing arrangement of bridge case (K2) gives smaller average and maximum cross-frame forces under both SDL and TDL, for all three detailing methods, compared to the framing arrangement of bridge case (K3). In continuous-span cases, the use of skewed bearing line cross-frames at the interior piers, with ample offsetting of the intermediate cross-frames from the bearing line, generally gives much lower cross-frames forces than the use of intermediate cross-frames framing into the bearing locations, as discussed previously. The use of skewed bearing lines cross-frames at the interior piers along with liberal offsetting of the intermediate cross-frames, as in bridge case (K2), is recommended.

If L_s/R is small and the skew is sharp in a continuous-span curved and skewed bridge, the structure tends to behave more like a straight skewed bridge. In this case, it can be beneficial to stagger the cross-frames near a skewed interior bearing line. It is recommended that cross-frames should always be used between the girders along the skewed bearing lines. Bridge cases (S) XICCS7 and T2 (EICCS27) are examples of this type of case.

Table 65. Average and maximum cross-frame forces under SDL and TDL for bridge cases (K2) and (K3) EICCS12. The (K2) and (K3) columns show the values for bridge cases (K2) and (K3), respectively.

Summary	Load Condition	NLF (kip)		SDLF (kip)		TDLF (kip)	
		(K2)	(K3)	(K2)	(K3)	(K2)	(K3)
Average	SDL	0.9	1.0	0.0	0.0	2.8	3.2
	TDL	3.5	4.2	2.7	3.2	1.1	1.1
Maximum	SDL	3.2	5.0	0.0	0.1	10.0	15.2
	TDL	13.7	20.5	10.6	15.4	3.4	3.5

7.3. For Straight Skewed Bridges, Stagger the Intermediate Cross-Frames in Discrete Increments such that the Staggers Closely Parallel the Skew as the Skewed Bearing Lines are Approached

It is common practice to allow skewed intermediate cross-frames where the support lines are skewed by less than or equal to 20 degrees from normal. However, where the support lines are skewed more than 20 degrees from normal, AASHTO requires that the cross-frames be framed orthogonal to the girders. In this case, it may be advantageous to place the intermediate cross-frames oriented normal to the girders in discontinuous lines, to selectively remove certain cross-frames, and/or to stagger the cross-frames in adjacent bays between the girders, in such a manner that the transverse stiffness of the bridge is reduced. This is particularly important in the vicinity of skewed supports. Removal of highly stressed cross-frames, particularly in the vicinity of the obtuse corners of a span, interrupts and reduces the stiffness of the corresponding transverse load path by forcing load transfer via girder flange lateral bending. This practice is usually beneficial as long as the unbraced lengths between the cross-frame locations satisfy the flange resistance requirements of the design specifications.

The above practices tend to decrease the cross-frame forces and increase the girder flange lateral bending. However, in certain cases involving excessively stiff transverse load paths, the cross-frame forces may be decreased to the extent that the associated flange lateral bending stresses are also reduced. Where the flange sizes are increased due to the additional flange lateral bending, this increase often is not significant. In fact, the increased cost resulting from the increased flange sizes is often much less than the increased cost of providing a larger number of cross-frames as well as larger cross-frames and larger connections.

This research recommends framing of the cross-frames within straight skewed spans using arrangements such as those shown in Bridge (J2), Bridge (K2), Figure 192 (a variation of Bridge (H2)), and Figure 193 (a variation of Bridge (M2)) to both dramatically reduce the number of cross-frames required within the bridge as well as to reduce the overall transverse stiffness effects.

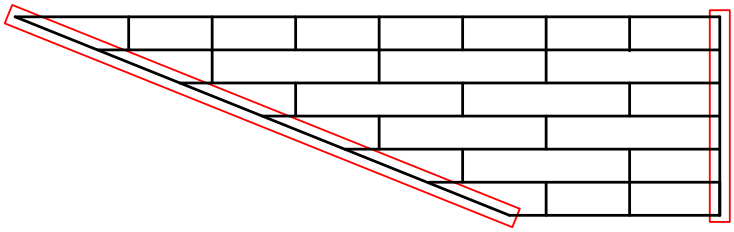

Figure 192. Beneficial Staggered Cross-Frame Framing Arrangement for a Straight Bridge with Non-Parallel Skew

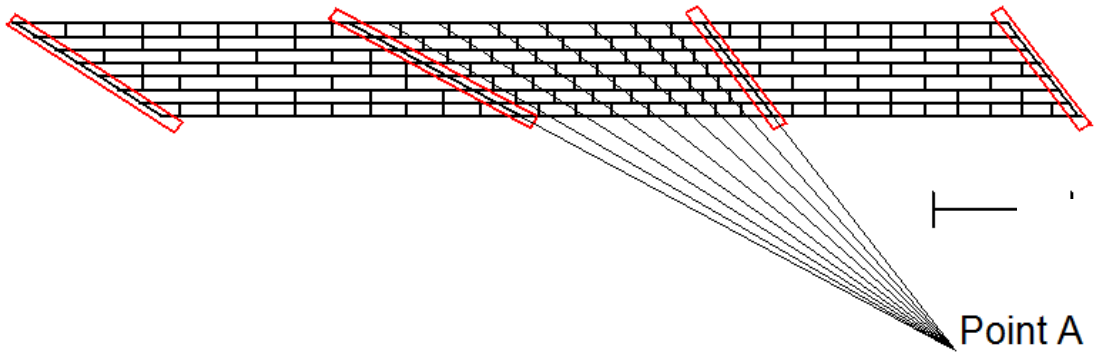

Figure 193. Additional alternative framing arrangement for bridge EISSS2.

The recommended practices, and their influence on the bridge responses, can be illustrated using Bridges (J1) and Bridge (J2). Bridge (J1) has a 300 ft span length, a 74 ft width between its fascia girders, and a 70^{o} skew of its abutment bearing lines. Due to its long span and high skew index, this bridge is particularly sensitive to any variation in attributes that affect erection fit-up. In addition, Bridge (J1) NISSS54 has small stagger distances between its cross-frames and small offsets of the intermediate cross-frames from the skewed bearing lines, resulting in large nuisance transverse stiffness.

Sanchez (2011) showed that the cross-frame forces in straight skewed bridges can be reduced substantially by framing the intermediate cross-frames parallel to the skew, in parallel skew bridges, and by "fanning" the cross-frames between the skew angles of the bearing lines in non-parallel skew bridges. However, the extensive use of skewed intermediate cross-frames leads to various other problems, particularly when the skew angles are large. One simple variation on the scheme suggested by Sanchez is to place the cross-frames perpendicular to the girders in a staggered arrangement, but position a common "work point" on the different cross-frames parallel to the skew or fanned approximately between the skew angles at the ends of the span. This research provides a

basic example of this approach using Bridge (J2) NISSS54. The particulars of this framing arrangement are as follows:

- The cross-frames adjacent to the skewed bearing lines are placed at the same offset distance relative to these lines, satisfying the offset recommendations in Section 7.1.
- The other intermediate cross-frames are placed at a constant spacing along the span length to satisfy the flange resistance requirements of the design specifications.
- In addition, every other cross-frame is intentionally omitted within the bays between the interior girders of the bridge plan. This relaxes the large transverse stiffness that would otherwise be developed in the short diagonal direction between the obtuse corners of the span.
- Furthermore, the smallest unbraced lengths or stagger distances between intermediate cross-frame locations within the bridge spans are larger than $4b_f$ and $0.4L_b$. The use of stagger distances smaller than $4b_f$ tends to result in the associated cross-frames working more like a contiguous cross-frame line rather than a discontinuous one.

Eleven intermediate cross-frames are attached between the fascia girders and the first interior girder on each side of the bridge. However, every other cross-frame is omitted within the interior of the bridge plan. This results in 30 fewer intermediate cross-frames than if all of the cross-frame lines were framed contiguously. However, since the cross-frames are staggered, there is no reduction in the unbraced length of the girders. The reduction of cross-frames is even greater, (a reduction of 42 cross-frames), compared to

the staggered arrangement of Bridge (J1). The cross-frame framing arrangement of Bridge (J2) results in a substantial reduction in the large cross-frame forces as shown in Table 66.

Table 66. Average and maximum cross-frame forces under SDL and TDL for bridge cases (J1) and (J2) NISSS54. The (J1) and (J2) columns show the values for bridge cases (J1) and (J2), respectively.

Summary	Load Condition	NLF (kip)		SDLF (kip)		TDLF (kip)	
		(J1)	(J2)	(J1)	(J2)	(J1)	(J2)
Average	SDL	19.5	5.7	1.0	1.4	20.3	9.2
	TDL	42.9	13.5	22.5	7.7	2.0	3.4
Maximum	SDL	162.4	25.4	6.4	8.0	145.5	35.2
	TDL	354.0	58.5	181.9	31.2	8.8	18.1

Figure 192 shows a similar concept on a straight bridge with an extreme non-parallel skew. The essential consideration, when intentionally omitting cross-frames between the interior girders, is that a cross-frame must be provided on at least one side of a girder at each location where a brace point is desired. In some situations, additional cross-frames may be retained to provide additional lateral stiffness for bracing or for other purposes; however, the alternating removal of the internal cross-frames is sufficient and is the preferred option in most cases. The framing arrangement in Figure 192 results in lower average cross-frame forces and maximum cross-frame forces compared to the framing arrangement of Bridge (H1).

Figure 25 shows an alternative beneficial framing concept on a straight bridge with a parallel skew. In Figure 25, the cross-frames adjacent to the bearing lines are all placed at the same offset distance relative to the skewed bearing lines, satisfying the above offset recommendations. The other intermediate cross-frames are placed at a constant spacing along the span length to satisfy the flange resistance requirements of the design

specifications. In addition, the stagger distances between intermediate cross-frame locations within the bridge spans is set at a value greater than $4b_f$ and $0.4L_b$, This arrangement relaxes the large transverse stiffness that would otherwise be developed in the short diagonal direction between the obtuse corners of the spans. Additional discussion of this framing arrangement is provided in Section 7.4.

Figure 193 shows a continuous-span straight skewed I-girder bridge with different skew angles at the bearing lines. Within the end spans of this bridge, the normal cross-frames adjacent to the bearing lines are all placed at the same offset distance relative to the skewed bearing lines, satisfying the above offset recommendations, except that a number of these cross-frames are intentionally omitted. This is necessary to satisfy the offset recommendations in the right-hand end span, which has smaller parallel skew. In a few locations, two adjacent cross-frames are intentionally omitted, progressing along the length of the span within a given bay between the interior girders. A cross-frame is framed into every girder on at least one side at each location where a braced point is desired. Within the center span, where the bearing lines are non-parallel but both have significant skew, the cross-frames are arranged in a "fanned" pattern from one bearing line to the next. The lighter-weight lines, which pass through work points at the mid-length of the cross-frames in the center span, all intersect at Point A. This arrangement can be shown to be one of the best options to mitigate the transverse stiffness load paths in this type of span.

7.4. Comparison of Recommended Staggered Cross-Frame Arrangement to Lean-On Arrangement of Cross-Frames in Straight Skewed Bridges

The lean-on cross-frame system has been studied extensively in research on straight parallel skew bridges (Romage 2008; Zhou 2006). In this structural system, the diagonals are left out of a large number of the cross-frames. Only the top and bottom chords are installed, providing a load path to resist the torsional rotation of all the girders connected along contiguous cross-frame lines by one or only a few cross-frames on each line (Helwig and Yura 2012). This basically provides a "shear release," removing the restraint of the differential displacements between the girders throughout much of the bridge plan.

This research studied Bridge (K1) EICSS12, which has a lean-on cross-frame system and has been studied extensively by Romage (2008). The cross-frames shown with an X on the plan have diagonals, whereas all the other intermediate cross-frames have only top and bottom chords. The following discussion summarizes a few key considerations in developing a lean-on cross-frame arrangement.

Along skewed bearing lines, cross-frames with diagonals are needed to transfer the lateral loads to the laterally restrained bearings. The cross-frame diagonals are removed at intermediate cross-frame locations having large differential vertical deflections. The remaining top and bottom chords do not develop any significant forces from girder relative vertical deflections. Cross-frames that contain diagonals are placed as far from the support as possible. It is critical that each cross-frame line has at least one cross-frame with diagonals to provide restraint of the girder torsional rotations along that line. There are no diagonals in the first cross-frame line connected to the fascia girders at the acute corners. Only top and bottom chords are needed at these locations since the short girder segments

between the bearing line and these cross-frames are adequate to effectively brace the girders.

Along each girder pair, at least one cross-frame is needed for stability during the steel erection. To facilitate erection and increase stability, at least two cross-frames with diagonals are provided between each girder pair. It is best that each cross-frame line has a pair of cross-frames with diagonals (Zhou 2006). Zhou also recommends keeping the cross-frame lines contiguous and spreading the cross-frames with diagonals across the width of the bridge for both stability and constructability purposes. Some additional cross-frames with diagonals are provided to limit the differential vertical displacements between the girders.

One attribute of the lean-on cross-frame system that may limit its usefulness in general is the fact that the bearing line cross-frames at skewed abutments impose a significant twist on the girders at their ends, due to the compatibility of the girder and cross-frame rotations at these locations. If contiguous cross-frame lines are framed into the girders close to these bearing locations, the cross-frame containing the diagonals still may provide substantial restraint of this twisting of the ends of the girders. The staggered cross-frame systems discussed in Section 7.3 soften the system "flexurally" by relying on the lateral bending stiffness of the girders between the cross-frame locations. This research studied the efficacy of the "shear release" provided by the lean-on framing systems, as in Bridge (K1), versus the "flexural softening" of the system in the transverse direction via the staggered arrangement of the cross-frames, as in Bridge (K2) (see Table 67). The staggered cross-frame arrangement in Bridge (K2) gives lower average and maximum cross-frame forces for all the three detailing methods than the framing arrangement of Bridge (K1). It is

important to note that from Section 5.2, Bridge (K1) gives smaller erection fit-up forces than Bridge (K2). However, the difference in the fit-up forces is small.

Table 67. Average and maximum cross-frame forces under SDL and TDL for bridge cases (K1) and (K2) EICCS12.

Summary	Load Condition	NLF (kip)		SDLF (kip)		TDLF (kip)	
		(K1)	(K2)	(K1)	(K2)	(K1)	(K2)
Average	SDL	1.4	0.9	0.0	0.0	4.6	2.8
	TDL	6.0	3.5	4.6	2.7	1.5	1.1
Maximum	SDL	4.2	3.2	0.2	0.0	13.8	10.0
	TDL	17.7	13.7	13.6	10.6	4.1	3.4

A designer might be concerned that the shear release provided by the lean-on framing arrangement could allow excessive differential vertical deflections between the girders, resulting in large deviations in the final elevations. In fact, this is one of the design considerations discussed by Zhou (2006). From Figure 194, with SDLF detailing, the maximum deviations in the final elevations are 0.61 inches and 0.54 inches for bridge cases (K1) and (K2), respectively. (The variable x_{ac} in the plots is the position along the length of the bridge relative to the bearing at the acute corner at the starting end of the bridge.) The differences in the deviations of the final elevations are negligible between bridge cases (K1) and (K2). It can be concluded that the lean-on and the recommended staggered cross-frame framing systems are comparable in terms of achieving the desired results of mitigating nuisance transverse stiffness effects while providing lateral bracing and some degree of interconnection to the girders.

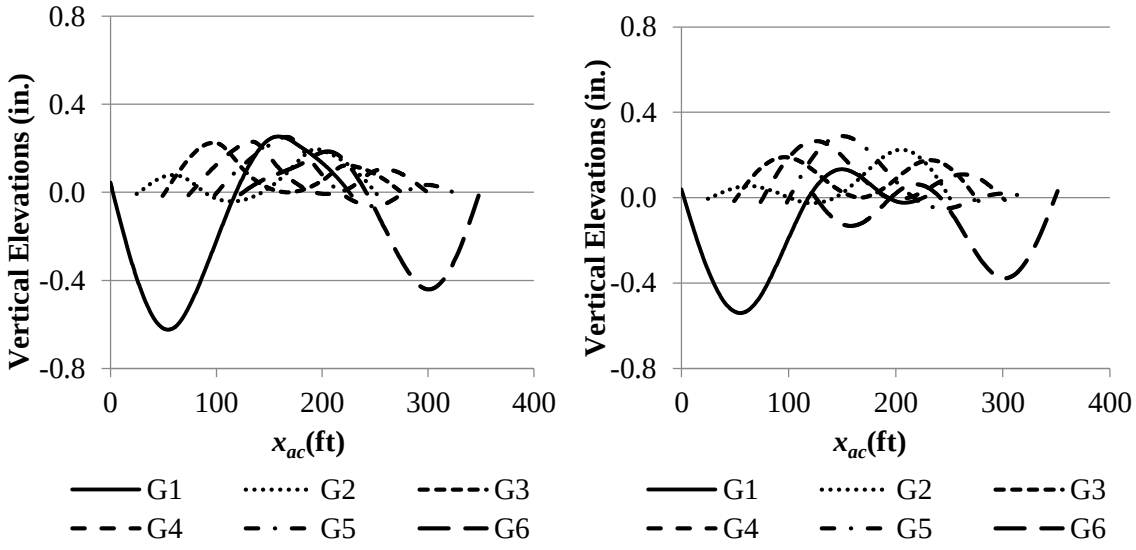

Figure 194. Final vertical elevations with SDLF detailing, based on LGA cambers, of bridge cases (K1) (left) and (K2) (right) EICSS12.

7.5. Use Contiguous Cross-Frames within the Main Portion of the Span in Curved and Skewed Bridges

For curved and skewed spans, omitting cross-frames in the vicinity of skewed bearing lines, can help to alleviate uplift at critical bearing locations; however, this is typically at the expense of larger cross-frame forces and larger bridge deflections compared to the use of contiguous intermediate cross-frame lines with the recommended offset provided at the skewed bearing lines. Contiguous cross-frame lines are necessary within the span of curved I-girder bridges to develop the width of the bridge structural system for resistance of the overall torsional effects. As such, the use of discontinuous cross-frame lines near a skewed bearing line in these bridge types involves competing considerations. Cross-frames can be omitted to alleviate uplift considerations at certain bearings, and potentially to relieve excessive cross-frame forces due to transverse stiffness effects in certain cases; for instance, if the horizontal curvature is relatively small and the skew is significant. However, removal of too many cross-frames may result in a larger than desired increase in

the cross-frame forces and bridge system deflections due to the horizontal curvature effects when the bridge is significantly curved.

Table 68 illustrates the above competing considerations by showing various responses for bridge cases (O1) NISCS15 (staggered framing arrangement) and (O2) NISCS15 (contiguous framing arrangement).

Table 68. Comparisons of various bridge responses under SDL and TDL conditions with NLF detailing for bridge cases (O1) (staggered framing arrangement) and (O2) NISCS15 (contiguous framing arrangement).

Summary	Load Condition	Bridge (O1) NISCS15 (Staggered CFs)	Bridge (O2) NISCS15 (Contiguous CFs)
Maximum Layovers (in.)	SDL	0.9	0.6
	TDL	2.0	1.3
Maximum Vertical Disp. (in.)	SDL	-5.1	-4.3
	TDL	-11.1	-9.4
Average CF Forces (kip)	SDL	32.3	30.6
	TDL	67.6	63.3
Tie-Down Forces (kip)	SDL	11	3
	TDL	52	77
f_ℓ **(ksi)**	SDL	9.5	8.6
	TDL	12.8	7.3

CHAPTER 8

INLFUENCE OF ERECTION SCHEMES ON FIT RESPONSES

As the spans become larger, the curvature becomes tighter, and/or the skews become sharper, determining an effective erection scheme is critical to ensure that a curved and/or skewed bridge is constructible and the maximum fit-up forces are maintained in a reasonable range. In some cases, site constraints such as waterway (Bridge (E) EICCR11), and availability, capacity, and allowed erection duration and location of cranes and shoring towers, can dictate the erection schemes.

8.1. General Aspects of Erection Schemes

Girder field sections can be lifted during the erection of the steel using various schemes including:

(1) Lifting solely at the center of gravity of the field section,

(2) Lifting the field section at two locations, but with crane cables attached directly, and

(3) Lifting the field section at two locations separated by a spreader beam. The cables are attached to the spreader beam ends and to single lifting point.

The above lifting schemes are illustrated in Figure 195, adapted from Davidson (1996), are discussed further below:

- Lifting Scheme 1 tends to allow curved girder field sections to roll excessively.

- Lifting Scheme 2 induces forces in the girder sections due to the inclined cables. With Scheme 2, additional minor- and major-axis bending is induced in the curved girder field section.

- Lifting Scheme 3 is used as the main method of lifting girder field sections in this research. The lifting locations should be located at approximately 0.25 of the field section length from the ends of the field section for straight girders. For curved girders, the lifting points are determined using the UT-Lift software (Ferguson Laboratory, 2014) to ensure stability and minimize the girder torsional rotations. For most of the curved bridge cases analyzed in this research, the lifting points are between 0.2L and 0.25L. For a number of cases, the girder field sections are too long and heavy for a single lifting crane. In these cases, two lifting cranes with cables attached directly to the lifting points were used for moderately long field sections, and two lifting cranes with spreader beams were used for significantly long field sections.

It is important to recognize the following mechanics of the lifting crane and spreader beam behavior:

- The girder pick points are “hung” from the ends of the spreader beam.

- The assembly involving the spreader beam and the diagonal cables works essentially as a rigid pin-connected truss as long as the cables are in tension. If the cables go into compression, they go slack and the assembly does not provide any restraint to the bridge.

- The triangular assembly is restrained vertically at its top, but is free to move laterally in any direction at all of its joints.

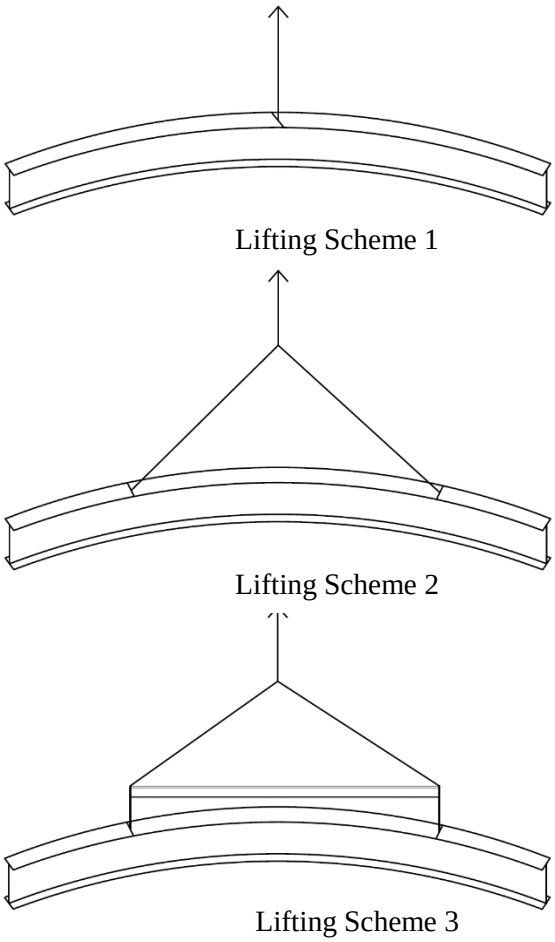

Figure 195. Various lifting schemes of girder field sections, adapted from Davidson (1996).

- The vertical forces transmitted to the field section at the ends of the spreader beam must be equal. This is because equilibrium must be maintained between the vertical loads transmitted to the triangular assembly at the ends of the spreader beam and the single total vertical crane reaction applied at the top of the triangular assembly. The pick points on the field section are free to move vertically relative to one another to obtain this balance of the forces.

- The average elevation of the hold points at the ends of the spreader beams is controlled by the specified elevation at the top of the triangular assembly. Although it is possible that the physical crane may pull laterally on this assembly by a minor amount, these actions are assumed to be negligible in this research.

Often, a holding crane is needed during the early stages of steel erection to reduce deflections, ensure stability, and facilitate the fit-up of girders and cross-frames, especially in curved bridges. The following are considerations regarding holding cranes:

- The holding crane is often attached near the middle of the span.
- For curved bridges, the holding crane should be on girder at the outside of the curve.
- In bridges with tight curvature, the holding crane may need to be retained on the outside girder until multiple girders of the bridge cross-section have been installed.
- When the erection is from the inside to the outside of the curve, the holding crane should be placed on the inside girder adjacent to the girder that is being installed.

Shoring towers are often needed in the construction of long-span bridges and curved bridges. Multiple field splices may be required within longer spans. Shoring towers help limit deflections and facilitate the installation of field splices and cross-frames. The shoring towers should be used across the full width of the bridge cross-section to best facilitate the erection. The number of shoring towers and cranes is selected generally to provide for a feasible, safe, and economical erection. Furthermore, tie-downs typically are provided for the girders at the shoring tower locations and/or the permanent supports to ensure girder stability before and after the splices are made within the spans.

The elevations of holding cranes, lifting cranes, and shoring towers need to be specified for the evaluation of the erection scheme. When the pick points on the girders displace upward relative to the pick points on the crane cables, the cables go slack and do not provide any restraint to the bridge. When the contact points on the girder displace upward, the shoring towers and/or permanent supports do not provide any support to the girder unless tie-downs are provided. In addition, one should note that the lifting and holding cranes do not provide lateral restraint to the girders.

The critical stages for fit-up often are stages that have the highest differential deflections between the girders. This is largely because high differential deflections are indicative of the potential for development of large internal forces between the girders, either in the final constructed geometry or during the erection of the steel. Fit-up potentially can be the most difficult for the last girders installed in the bridge cross-section, and for drop-in segments installed in continuous spans.

8.2. Influence of Erection Schemes in Curved Radially-Supported Bridges

For curved bridges, cranes and/or temporary supports are critical for stabilizing the partially completed systems, as well as for erecting the girders and cross-frames. Individual curved girders and narrow partially-erected curved bridge units have little stability on their own. The bridge cross-section generally over-rotates until all of its girders are installed.

For most of the curved radially-supported bridges studied in this research, the bridges are erected from the outside to the inside of the curve. This is for the following reasons:

- The girder on the inside of the curve on the portion of the bridge cross-section that has been completed deflects less than the outside girder.

- The girder that is being installed is supported by a lifting crane, and thus its deflections are typically small.
- Erecting from the outside to the inside of the curve requires smaller fit-up forces due to the smaller differential displacements between the inside girder and the girder being installed.
- Erecting from the outside to the inside of the curve, if possible, avoids the need to lift the outside girder on the partially completed bridge cross-section to achieve fit-up with the next girder being installed on the outside of the curve, which is typically the case when the bridge is erected from the inside to the outside of the curve.
- For highly curved bridges such as most of the curved bridges considered in this study, the crane and temporary support requirements for erection from the inside to the outside of the curve can be significantly greater than for erection from the outside to the inside of the curve.

In many cases, when a bridge is highly curved, a holding crane will be required on the girder on the outside of the curve until a number of the girders in the bridge cross-section have been installed. The erection schemes employed in this research install the bearing line cross-frames immediately after the girder was placed on its supports, to help provide torsional stability to the girder. Then the remaining intermediate cross-frames are sequentially installed.

Figure 196 shows a representative erection scheme for bridge (A) EISCR1, proceeding from the outside to the inside of the curve. The bold lines indicate the girders and cross-frames that are already installed at a given stage. The triangles show the locations of the crane holding or lifting points. Where one symbol is shown on a girder, that point is a pick

point for the holding crane. Where two symbols are shown on a girder, these points are the pick points for the lifting crane. These points are attached to the ends of a spreader beam in the erection schemes employed in this research. The stages and sub-stages are designated by the stage number followed by a dash and the sub-stage number. The stage number corresponds to the installation of a field section and cross-frames that connect the field section to the adjacent portion of the bridge that is already erected. The substage number indicates the order of the cross-frame that is being installed within a stage. For example, stage 2-3 indicates sub-stage 3 of stage 2. Stage 2-3 involves the installation of the third cross-frame from the left bearing line between Girder 1 (G1) and Girder 2 (G2).

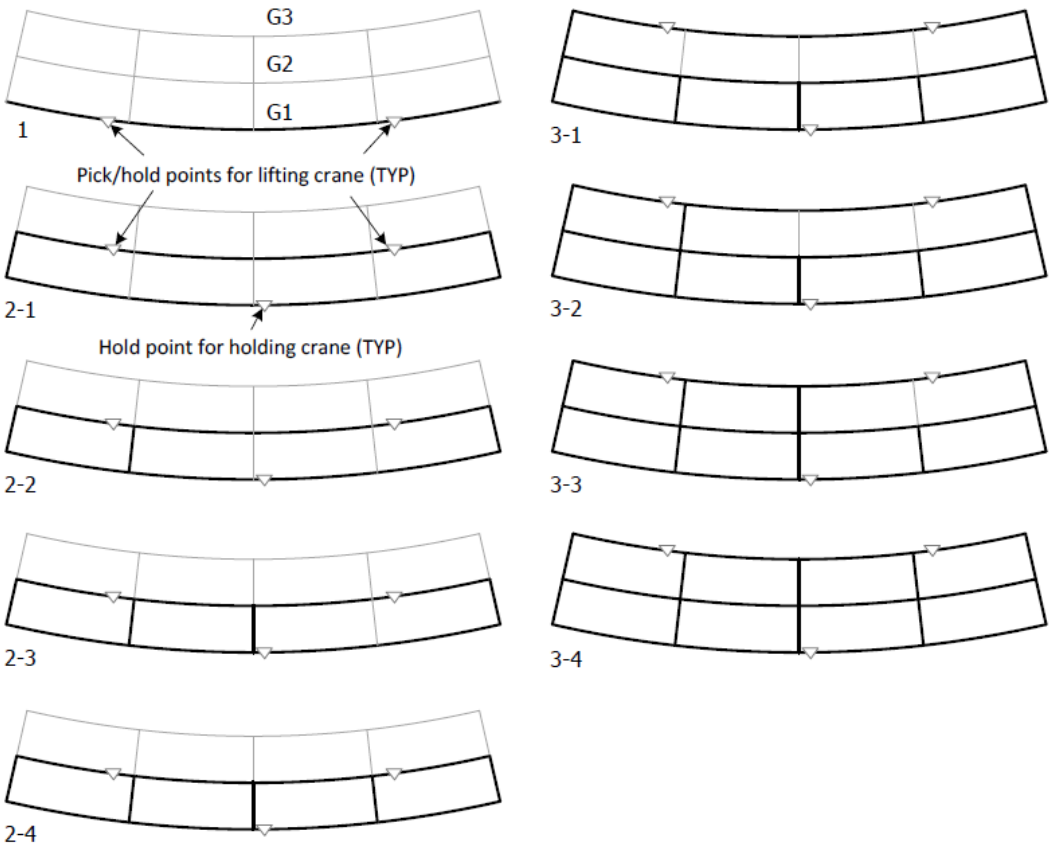

Figure 196. Bridge (A) EISCR1 erection scheme, from the outside to the inside.

8.2.1. Influence of Manipulation of Temporary Support Elevations by the Erector

This section discusses the influence of the manipulation of temporary support elevations in curved radially-supported bridges by presenting the calculated results for the critical (maximum) external fit-up forces of bridge (A) EISCR1. As discussed in Chapter 5, the cross-frame fit-up forces are defined as the local forces that need to be developed at the top and bottom chord cross-frame connections to the latest girder that is being installed into the bridge. From Figure 196, this is girder G2 for Stage 2 and this is girder G3 for Stage 3 on bridge (A) EISCR1. It is assumed that the cross-frames are first attached to the adjacent girder in the partially-completed bridge, and then the cross-frame connections are made successively to the "latest" girder. Since V-type cross-frames are used in Bridge (A) EISCR1, it is assumed that the top-chord connection corresponding to the cross-frame diagonal is made first, and that this is followed by the connection to the bottom chord.

The fit-up forces can be sensitive to the holding elevations of the holding and lifting cranes, particularly in curved bridges. In addition, there are various nonlinear effects that impact the fit-up forces, i.e., boundary or contact/noncontact nonlinearities, crane cables going slack, etc. It is recommended that the crane holding elevations can be varied relative to the base NL girder elevations as a starting point, to minimize the fit-up forces. In the study below, it is desired to calculate the minimum fit-up force as a function of the crane holding elevations corresponding to the installation of each of the cross-frames, and then to determine the maximum value of these minimum cross-frame fit-up forces throughout the overall erection sequence.

Table 69 lists the various elevations considered for the holding and lifting cranes for the erection of bridge (A) EISCR1, as well as the critical sub-stage in each of the main

stages 2 and 3 of its erection sequence. Actually, a number of additional crane holding elevations were studied; however, only the ones shown in Table 69 are presented to simplify the discussions.

Sub-stage 3 is the critical stage, requiring the largest fit-up forces for both of the main stages and for all of the crane holding elevations in Bridge (A) EISCR1, regardless of the detailing method. One can observe that this sub-stage corresponds to the installation of the cross-frame at the mid-span of the bridge. This finding is certainly logical, since the largest differential displacements between the girders tend to occur at the mid-span in bridge (A) EISCR1.

Table 69. Bridge (A) EISCR1 erection critical sub-stages

Crane Elevation Designation	**Holding Elevations**	**Stage**	
		2	**3**
A	Holding Crane: NL; Lifting Crane: NL	2-3	3-3
B	Holding Crane: SDL; Lifting Crane: SDL	2-3	3-3
C	Holding Crane: NL; Lifting Crane: NL + 40 % * SDL Camber (upward)	2-3	3-3
D	Holding Crane: NL; Lifting Crane: NL + 80 % SDL Camber (upward)	2-3	3-3
E	Holding Crane: NL; Lifting Crane: NL – 40 % SDL Camber (downward)	2-3	3-3
F	Holding Crane: NL; Lifting Crane: NL + 160 % SDL Camber (upward)	2-3	3-3

* The % values indicate the percentage of the SDL camber displacement at the hold points.

Table 70 shows the vertical and horizontal components of the calculated fit-up forces for the critical sub-stage 3 for each of the cross-frame detailing methods and for each of the most important combinations of holding and lifting crane holding elevations considered in this work. The most important points from Table 70 are as follows:

- The sub-stages are further designated as 2-3A, 2-3B, 3-3A and 3-3B to distinguish between the forces for each of the sub-stages of the connection of the critical cross-frame to the girders.
- Sub-stages A and B are the first and second connections between the cross-frames and the girders. The forces labeled as V1 and H1 in the table are the forces in the first connection between the cross-frame and the "latest" girder at the top chord of the critical cross-frame. The forces labeled as V2 and H2 are the forces in the second connection between the cross-frame and the "latest" girder at the bottom chord of the critical cross-frame.
- It should be noted that the cells marked as "NA" in the table for the sub-stages 2-3A and 3-3A correspond to the state where the second connection has not yet been made. Therefore, the forces V2 and H2 are in fact zero at this state or sub-stage.
- Furthermore, it should be noted that the forces V1 and H1 for sub-stages 2-3B and 3-3B are strictly *not* actual external fit-up forces. For these sub-stages, V1 and H1 are simply the internal connection forces developed at the top chord of the cross-frame when the bottom chord connection is made.
- The forces shown in Table 70 are the forces applied from the cross-frame to the girder that is being installed. Therefore, if the vertical force is positive, the cross-frame is having to push up on the girder to make the connection. Hence, if the lifting crane elevation is raised in this case, the vertical connection force will tend to be reduced. Conversely, if the vertical force is negative, the cross-frame is having to push down on the girder to make the connection. Hence, if the lifting crane

elevation is lowered, the vertical connection force will tend to be reduced in this case.

Table 71 parallels Table 70, but shows just the single vector force resultants of V1 and H1, and V2 and H2, at the cross-frame connections to the girder that is being installed into the bridge. These resultants are designated as F1 and F2. For each row in Table 71, corresponding to a given cross-frame detailing method and a particular critical sub-stage, it is assumed that the crane operator(s) would vary the crane holding elevations to minimize the vertical component of the fit-up force (shown as V1 and V2 in Table 70). This would be achieved in the field during the erection essentially by the crane operator following the directions of the iron workers to raise or lower the holding points to aid them in aligning the holes for the connection of the cross-frame to the "latest" girder that is being installed.

The resulting minimum fit-up force resultants F1 and F2 for each row of Table 71 are listed in Table 72. For instance, corresponding to Sub-stage 2-3A and NLF detailing, the minimum fit-up force is obtained by positioning the holding and lifting crane elevations both at the NL elevation of the girders. This results in a minimum fit-up force F1 of 0.4 kips. However, for Sub-stage 2-3A and SDLF detailing, the minimum fit-up force F1 (equal to 1.1 kips) is obtained by positioning the holding crane at the NL elevation, but raising the lifting crane hold location by 160 % of the SDL camber. As indicated by the comments in the right-most column of Table 72, girder G2 is lifted off of both its supports at this sub-stage. In addition, one can observe from Table 70 that V1 has become slightly negative and the fit-up force is dominated by the horizontal components H1 when the lifting crane is raised to this elevation. Therefore, F1 = 1.1 kips is a reasonable estimate of the minimum possible fit-up force for SDLF detailing at this critical sub-stage.

It should be noted that the elevations of the holding points of the lifting crane are varied in the above by varying the elevation at the top of the lifting crane. This in effect varies the average elevation of the hold points at the ends of the spreader beam. The actual elevations of these hold points are not equal to one another; these elevations "adjust" to the deflections of the bridge system such that the forces in the two inclined cables remain the same.

For Sub-stage 2-3A and TDLF detailing, the minimum fit-up force resultant shown in Table 72 is again obtained when the holding crane hold point is located at the NL girder elevation on G1 and the average lifting crane hold elevations are located at 160 % of the SDL Camber above the NL girder elevation on G3. Actually, for this case, it is possible that the fit-up force resultant can be reduced further by increasing the average elevation of the lifting crane hold points by an additional amount. By inspecting Table 70, one can ascertain that the force V1 is still positive, equal to 7.3 kips, and that this force still dominates the connection force resultant at Sub-stage 2-3A, for TDLF detailing. However, Girder G2 is already lifted substantially off of its supports by this operation, and the subsequent evaluations of F2 indicate significantly larger fit-up forces for TDLF detailing than the resultant for F1 = 7.7 kips shown in Table A3-6 for Sub-stage 2-3A and TDLF detailing.

Table 70. Bridge (A) EISCR1 critical fit-up forces applied to the girder being installed (kip).

Sub-Stage	Detailing Method	Holding Elevations											
		Crane Elevation A				Crane Elevation B				Crane Elevation C			
		V1	H1	V2	H2	V1	H1	V2	H2	V1	H1	V2	H2
2-3A	NLF	-0.2	0.4	--	--	6.5	0.3	--	--	-0.7	0.5	--	--
	SDLF	2.3	0.9	--	--	8.5	0.7	--	--	1.7	0.9	--	--
	TDLF	9.8	2.7	--	--	14.5	1.9	--	--	9.1	2.4	--	--
2-3B	NLF	0.4	1.7	-0.0	-1.8	6.8	1.6	-0.1	-1.7	-0.2	2	-0.0	-2
	SDLF	5.2	7.2	1.2	-7.3	10.5	5.3	1.1	-5.4	4.1	5.9	1.2	-6
	TDLF	18.5	21.8	5.0	-21.7	21.8	16.7	5.0	-16.6	18.5	21.8	5	-21.7
3-3A	NLF	-2.8	0.3	--	--	4.9	-0.1	--	--	-3.3	0.3	--	--
	SDLF	0.3	0.6	--	--	6.6	0.4	--	--	-0.2	0.6	--	--
	TDLF	9.9	1.5	--	--	10.3	1.4	--	--	9.2	1.5	--	--
3-3B	NLF	-2.4	2.3	-0.0	-2.3	4.7	-0.2	-0.1	0.2	-3	1.9	-0.0	-1.9
	SDLF	2.3	6.6	1.0	-6.6	8.2	4.7	1.0	-4.8	1.6	6.0	1.1	-6.0
	TDLF	15	18.7	4.2	-18.6	15.9	17.3	4.2	-17.2	15	18.7	4.2	-18.6

Notes:

(1) Sub-stage “A” = first connection of cross-frame and girder
(2) Sub-stage “B” = second connection of cross-frame and girder
(3) For crane elevation definition see Table 18
(4) V1, H1 = vertical and horizontal components of the forces in the first connection, or internal connection forces developed at the location of the first connection when the second connection is made.
(5) V2, H2 = vertical and horizontal components of the forces in the second connection
(6) Cells marked with “--" correspond to the state where the second connection has not yet been made

Table 20 (Continued). Bridge (A) EISCR1 critical fit-up forces applied to the girder being installed (kip).

Sub-Stage	Detailing Method	Holding Elevations											
		Crane Elevation D				Crane Elevation E				Crane Elevation F			
		V1	H1	V2	H2	V1	H1	V2	H2	V1	H1	V2	H2
2-3A	NLF	-1.3	0.5	--	--	0.6	0.7	--	--	-2.5	0.6	--	--
	SDLF	1.1	1.0	--	--	3.1	1.3	--	--	-0.1	1.1	--	--
	TDLF	8.5	2.4	--	--	10.2	2.9	--	--	7.3	2.5	--	--
2-3B	NLF	-0.7	2.3	-0.0	-2.3	1.9	4.2	-0.1	-4.3	-1.7	2.8	0.0	-2.8
	SDLF	3.6	6.2	1.2	-6.2	6.8	9.8	1.1	-9.9	2.6	6.7	1.2	-6.8
	TDLF	17.0	19.2	5.0	-19.1	18.5	21.8	5.0	-21.7	15.7	19.0	5.1	-18.9
3-3A	NLF	-3.5	0.3	--	--	-2.3	0.4	--	--	-3.7	0.3	--	--
	SDLF	-0.8	0.5	--	--	0.9	0.7	--	--	-1.2	0.5	--	--
	TDLF	8.6	1.4	--	--	9.9	1.5	--	--	7.4	1.3	--	--
3-3B	NLF	-3.3	1.8	0.1	-1.7	-1.8	2.7	0.0	-2.7	-3.5	1.9	0.1	-1.9
	SDLF	0.9	5.6	1.1	-5.6	3.0	7.1	1.1	-7.1	0.1	5.2	1.1	-5.1
	TDLF	15	18.7	4.2	-18.6	15.0	18.7	4.2	-18.6	13.8	17.8	4.2	-17.7

Table 71. Bridge (A) EISCR1 critical fit-up force resultants applied to the girder being installed (kip).

Stage	Detailing Method	Holding Elevations											
		Crane Elevation A		Crane Elevation B		Crane Elevation C		Crane Elevation D		Crane Elevation E		Crane Elevation F	
		F1	F2	F1	F2	F1	F2	F1	F2	F1	F2	F1	F2
2-3A	NLF	0.4	--	6.5	--	0.9	--	1.4	--	0.9	--	2.6	--
	SDLF	2.5	--	8.5	--	1.9	--	1.5	--	3.4	--	1.1	--
	TDLF	10.2	--	14.6	--	9.4	--	8.8	--	10.6	--	7.7	--
2-3B	NLF	1.7	1.8	7.0	1.7	2.0	2.0	2.4	2.3	4.6	4.3	3.3	2.8
	SDLF	8.9	7.4	11.8	5.5	7.2	6.1	7.2	6.3	11.9	10.0	7.2	6.9
	TDLF	28.6	22.3	27.5	17.3	28.6	22.3	25.6	19.7	28.6	22.3	24.6	19.6
3-3A	NLF	2.8	--	4.9	--	3.3	--	3.5	--	2.3	--	3.7	--
	SDLF	0.7	--	6.6	--	0.6	--	0.9	--	1.1	--	1.3	--
	TDLF	10.0	--	10.4	--	9.3	--	8.7	--	10.0	--	7.5	--
3-3B	NLF	3.3	2.3	4.7	0.2	3.6	1.9	3.8	1.7	3.2	2.7	4.0	1.9
	SDLF	7.0	6.7	9.5	4.9	6.2	6.1	5.7	5.7	7.7	7.2	5.2	5.2
	TDLF	24.0	19.1	23.5	17.7	24.0	19.1	24.0	19.1	24.0	19.1	22.5	18.2

Table 72. Bridge (A) EISCR1 critical fit-up force resultants applied to the girder being installed (kip).

Stage	Detailing Method	Minimum Fit-Up Forces as a Function of the Crane Elevations		Comments on Configuration Pertaining to the Minimum Fit-Up Force
		F1	F2	
2-3A	NLF	0.4	--	Lift-off at G2 supports
	SDLF	1.1	--	Lift-off at G2 supports
	TDLF	7.7	--	Lift-off at G2 supports
2-3B	NLF	--	1.7	Slack cables on lifting crane (G2)
	SDLF	--	5.5	Slack cables on lifting crane (G2)
	TDLF	--	17.3	Slack cables on lifting crane (G2)
3-3A	NLF	2.3	--	Lift-off at G3 supports
	SDLF	0.6	--	Lift-off at G3 supports
	TDLF	7.5	--	Slack cables on lifting crane (G3)
3-3B	NLF	--	0.2	No slack cables or lift-off
	SDLF	--	4.9	Slack cables on lifting crane (G3) and on holding crane (G1)
	TDLF	--	17.7	

The largest of the minimum fit-up forces F2, for SDLF detailing, is obtained as 5.5 kips in Sub-Stage 2-3B. For TDLF detailing, the largest of the minimum fit-up forces F2 is obtained as 17.7 kips in Sub-Stage 3-3B. In both cases, these minimum forces are obtained by lowering both the holding crane as well as the lifting crane to the girder SDL elevations. The corresponding required fit-up forces at the other critical sub-stages 3-3B and 2-3B for these cases are only slightly smaller. Also, these force resultants are dominated by the horizontal components H2, and therefore, the overall fit-up force resultant is effectively minimized in terms of the holding crane elevations in these cases.

The total overall maximums of the above minimum fit-up force resultants, as a function of the crane holding elevations are summarized in Table 73. One can observe that the NLF,

SDLF, and TDLF maximum fit-up forces are 3.3, 7.4, and 22.3 kips, respectively, for the case of the NL holding elevations. By iteratively considering the holding and lifting cranes at various positions, the maximum fit-up forces were reduced to 2.3, 5.5, and 17.7 kips for NLF, SDLF, and TDLF detailing, respectively. One can observe that these changes are reasonably small in magnitude, for this bridge; however, they are certainly measurable and a potentially significant percentage of the fit-up forces.

Table 73. Bridge (A) EISCR1 maximums of the minimum fit-up force resultants F_{max} as a function of the crane position (kip) and maximum fit-up force resultants $F_{no\text{-}load}$ with the crane at NL elevations (kip).

Detailing Method	F1	F2	F_{max}	$F_{no\text{-}load}$
NLF	2.3	1.7	2.3	3.3
SDLF	1.1	5.5	5.5	7.4
TDLF	7.7	17.7	17.7	22.3

Although the erector will often make minor elevation adjustments in the field to facilitate fit-up, iteratively adjusting the crane and shoring elevations to minimize the calculated fit-up forces was not feasible within the scope of this research. This sort of practice certainly would not be feasible as part of any ordinary erection engineering calculations either.

The fit-up forces on the other curved radially-supported bridge cases investigated in this research are conducted with the crane and shoring tower supports all placed at the NL elevations. The NL elevations always serve as a useful starting point for the selection of crane or shoring tower support elevations for curved radially-supported bridges (straight skewed bridges are different, as discussed subsequently). The fit-up forces in curved radially-supported bridges generally can be reduced somewhat by manipulating the elevations upward and/or downward from these positions; however, performing any sort

of engineering calculations to estimate the impact of "jimmying" the various support elevations around generally would be cost prohibitive.

8.2.2. Influence of Erection from the Inside to the Outside of the Curve

Depending on a number of factors such as site constraints, erectors may decide to erect from the inside to the outside of the curve. Bridge (B) NISCR2 Erection Scheme 2A (see Figure 54) is an example of this type of erection. The fit-up forces for all three detailing methods are prohibitive as explained below:

- The partially-completed bridge cross-section over-rotates.
- As the next girder is installed on the outside of the curve, it is held by the lifting crane basically at its NL elevation. The girder being installed is adjacent to the outside girder on the partially-completed bridge cross-section. The vertical deflections in the girder on the outside of the curve in the partially-completed bridge cross-section are relatively high, causing high differential vertical displacements between this girder and the girder that is being installed. These large displacements lead to high cross-frame fit-up forces.

The large cross-frame fit-up forces shown for Erection Scheme 2A in Table 15 (84.4 kip for NLF, 82.5 kip for SDLF, and 80.2 kip for TDLF) indicate that this is not a feasible erection scheme. It is necessary to add additional vertical support on the outside girder of the partially completed bridge cross-section, to reduce its vertical deflections. One cannot resolve the vertical displacement incompatibility by effectively lifting the partially-completed bridge via the local equipment that is intended only to install the cross-frames. Erection Scheme 2B does this by placing an additional holding crane on the outside girder of the partially completed bridge cross-section.

The additional holding crane for Erection Scheme 2B adds cost to the erection but reduces the fit-up forces for all the detailing methods. The NLF and TDLF fit-up forces for Erection Scheme 2B are reduced to 40.4 kip and 50.5 kip, respectively, which are close to the 40 kip threshold where fit-up is considered to be difficult.

Interestingly, the SDLF fit-up force for Erection Scheme 2B is only 19.4 kips, which is below the 40 kip threshold. This is the only case of the curved radially-supported bridges studied, other than Erection Scheme 2A of this bridge, in which the maximum fit-up forces are smaller for SDLF than for NLF. The reason for this behavior is that the displacement incompatibility between the cross-frames and their connection points on the girder being installed happens to be smaller for SDLF detailing, given the configuration of the geometry and the support points at the critical stage.

8.3. Influence of Erection Schemes in Straight Skewed Bridges

The potential fit-up considerations for straight skewed bridges are somewhat different than those discussed above for curved radially-supported bridges. A number of considerations for straight skewed simply-supported spans are as follows:

- For short straight skewed simply-supported spans that do not require a field splice within the span, and therefore would rarely require shoring towers, the cross-frames can be installed sequentially from one abutment to the other after each girder is lifted onto its vertical supports.
- Tie downs can be provided at the supports as necessary to maintain lateral-torsional stability of the girders.
- For long spans that require a field splice within the span (because the field sections otherwise become too heavy), and often may require shoring towers, it is best to

install only a few cross-frames or struts before the field splice is made, and to install the remaining cross-frames after the field splice is completed. The intent is to install the majority of the cross-frames after all the girders have been erected, so that the girders are deflected close to their SDL elevation profiles. For SDLF detailing, the cross-frames are detailed to fit ideally to the final girder SDL profiles, and therefore, allowing the girders to deflect to a position close to this profile should clearly facilitate fit-up.

- If any temporary supports are still being employed when the cross-frames are being installed, positioning the temporary supports at the final girder SDL elevations is often a good starting point to alleviate potential large fit-up forces.
- Typically, cranes are only used to lift the girders into place and are not critical to the erection of straight skewed bridges constructed in the above ways. This is in contrast to the curved bridge cases discussed in Section 8.2.
- When the cross-frames are detailed for SDLF, their installation using the above type of erection scheme results in the lowest level of fit-up forces.

For continuous-span straight skewed bridges, the erection schemes with the greatest ease of fit-up are typically similar to those for the simply-supported bridges described above. However, it is impractical for the erector to install each girder in all the spans, one at a time throughout the bridge length, to achieve the girder SDL elevation profiles. The erector would have to move back and forth along the entire bridge length to do this. Instead, all the girders are typically erected in each span before moving to the next span. In these bridge types, a good option is to:

- Install only a minimal number of cross-frames to keep the bridge stable until all the girders are erected.
- Once all the girders in all spans have been erected, install the remaining cross-frames span-by-span.

This scheme limits the crane movement along the length of the bridge while keeping the bridge stable and the SDLF fit-up forces relatively small. In addition, this procedure also appears to provide the best option to mitigate large fit-up forces in straight skewed bridges detailed for TDLF detailing. However, for longer spans with sharp skew, the largest fit-up forces associated with TDLF can be problematic in some cases.

Figure 197 shows a representative erection scheme for the straight skewed bridge (J1) NISSS54 at its Stage 3. The stage designation follows the scheme discussed in Section 8.2. Due to the bridge's 300 ft. span, a shoring tower is needed to facilitate the splice connection from Stage 3-1 to Stage 3-4. The shoring tower support is only on the girder that is being installed, and is shown by the square symbol within the span in the plan view. Only the end cross-frames and a few top and bottom flange struts are installed between the girders during these stages. After Stage 3-3, the shoring tower is removed and the remaining cross-frames are installed sequentially.

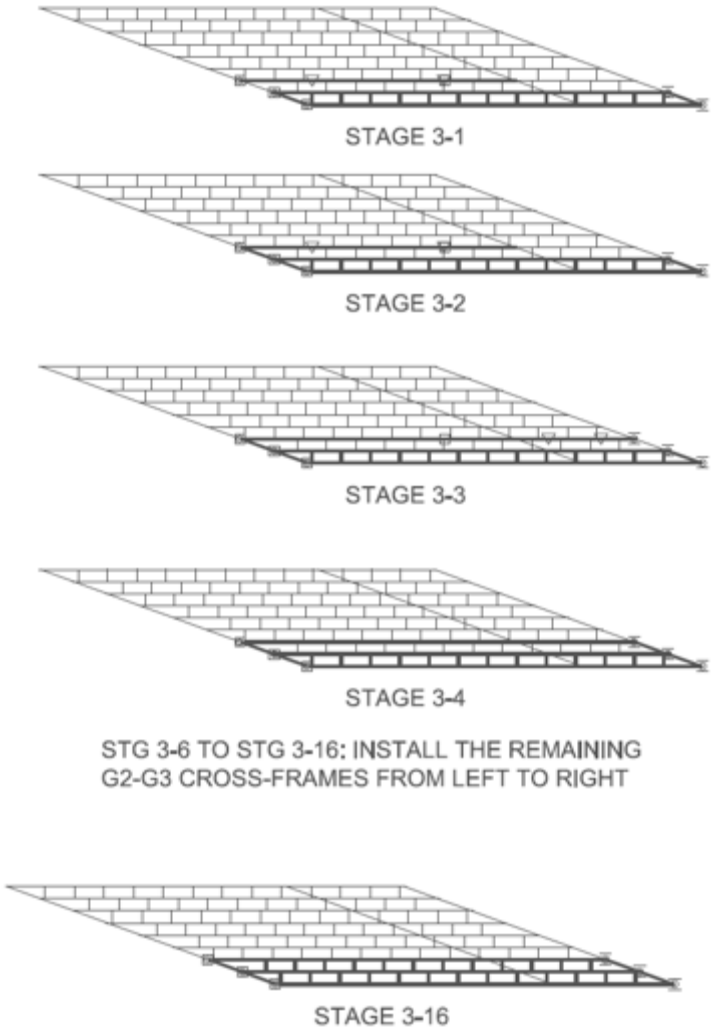

Figure 197. Bridge (J1) NISSS54 erection scheme of stage 3.

8.4. Influence of Erection Schemes in Curved and Skewed Bridges

For the curved and skewed bridges studied in this research, the holding crane, lifting crane and shoring tower elevations are located at the no-load elevations. As discussed in Section 8.2.1, the fit-up forces in curved bridges can be reduced by varying the crane and shoring tower elevations from the no-load elevations. However, it is shown that the reduction in fit-up forces is not significant. Also, iteratively adjusting the crane and shoring tower elevations to minimize the fit-up forces is not practical in general erection

engineering practice. In addition, it was concluded that this was not feasible within the scope of this research. With that said, in some cases, it can be very beneficial for the steel erection personnel to install cross-frames at positions where the deflected geometries are reasonably compatible, and for the crane operator to incrementally raise or lower a girder that is being installed after successive insertions of cross-frames, to in effect "button up" the cross-frames between the girder that is being installed and the structural steel that is already in place.

From the studies of multiple erection schemes on bridge (O1) and (O2) with the maximum fit-up forces as shown in Table 17 and the studies of the erection schemes of the other curved and skewed bridge cases, one can conclude the following:

- When shoring towers are employed, generally it is advisable that they span across the full bridge cross-section to limit the overall deflections in extreme curved and skewed cases.
- Among many other factors, the number of shoring towers required to facilitate fit-up in highly curved and skewed bridges is a function of the span length and the number of field sections and number of spans.
- For continuous-span cases, when erecting the subsequent spans, leaving the shoring towers in place through the entire erection and subsequent spans helps to reduce the overall deflections, which can facilitate fit-up.
- Similar to the recommended practice for curved radially-supported bridges, the erection scheme for curved and skewed bridges should also be from the outside to inside on tightly curved bridges, whenever practicable, to reduce the maximum fit-up forces.

- The cross-frames ideally should be installed sequentially from the radial bearing line (if there is a radial bearing line) to the skewed bearing line. Installing the cross-frames in this way reduces the deflection incompatibilities when installing the cross-frames near the skewed end of the span.

CHAPTER 9

DETAILED EVALUATION OF STRAIGHT SKEWED BRIDGE RESPONSES ASSOCIATED WITH THE USE OF LGA VERSUS 3D FEA CAMBER

It is common for girder camber profiles to be calculated from a 1D Line Girder Analysis (LGA) for some bridges, 2D Grid analysis for others, and in some cases from a 3D Finite Element Analysis (FEA). For a highly skewed I-girder bridge, the differences in the cambers obtained from LGA versus the other two methods can be substantial. An engineer may rightfully question whether these camber differences can have a significant influence on the intended fit behavior. This section addresses the influence of these differences and explains the mechanics behind the findings.

Bridge (J2) NISSS54 is used to demonstrate the influence of camber calculations in straight skewed bridges. This bridge has a 300 ft simple span, 9 girders spaced at 9.25 ft, and an 80 ft wide deck. Both bearing lines are skewed at 70 degrees. Due to its severe skew, relatively wide deck, and long span length, this bridge is one of several straight skewed bridges with the greatest potential for fit-up difficulty considered in this research. The fascia and interior girders are identical. All the girder webs are 12 ft deep and 1 in. thick. The girder flange thicknesses are stepped at four locations.

To simplify the discussion, only cambers based on LGA and 3D FEA are discussed in this section. The cambers calculated from a 2D Grid analysis are practically the same as those calculated from 3D FEA if the 2D Grid analysis employs the improvements recommended by NCHRP Report 725 for I-girder bridges. The detailed procedures for the 3D FEA and LGA calculations conducted in this section are outlined in Section 2.1. It is

important to note that the concrete deck weight is modeled on the noncomposite I-girders as distributed line loads applied at the centerlines of the top flanges. This weight is calculated based on the tributary widths between the girders and from the deck overhangs.

Table 74 shows the girder plate lengths and the girder flange dimensions for Bridge (J2) NISSS54. The intermediate cross-frames are X-type, framed perpendicular to the girders and with L6x6x1 sections used for all their members. The end cross-frames at the abutments are inverted V-type and utilize WT6x53 sections for their chords and WT9x38 sections for their diagonals. The intermediate cross-frames are placed in a staggered pattern with work points positioned along the same angle as the bearing lines. The framing arrangement of bridge (J2) NISSS54, as discussed in Section 7.3, mitigates the effects of nuisance transverse stiffness associated with the bridge's severe skew.

Table 74. Bridge (J2) NISSS54 girder plate lengths and girder flange dimensions.

Length (ft)	Top flange		Bottom flange	
	Width (in.)	Thickness (in.)	Width (in.)	Thickness (in.)
45	28	1.25	30	1.25
45	28	2	30	2.25
120	28	2	30	2.75
45	28	2	30	2.25
45	28	1.25	30	1.25

9.1. SDLF Behavior using Line Girder Analysis Cambers

The practice of SDLF detailing using the cambers obtained from a Line Girder Analysis (LGA) theoretically gives exactly plumb girder webs, zero cross-frame forces, and zero flange lateral bending stresses under the targeted dead load, in this case SDL. This fact is explained below by two hypothetical erection sequences.

9.1.1. Erection Sequence 1

In straight skewed bridges, the girders deflect only vertically under their self-weight and the self-weight of the cross-frames, as long as the cross-frames are not connected to the girders in a manner such that they are engaged and can transfer internal shears and moments. Therefore, if all the girders are theoretically placed on their vertical supports, just the top chords of all the cross-frames are attached to the girders (such that there is no shear and moment transfer via the cross-frames), and the girders are allowed to deflect under the full steel self-weight, the resulting girder vertical deflections are exactly equal to the SDL deflections obtained from a LGA.

If the SDL cambers are set based on the above deflections, and the cross-frames are then detailed for SDLF using these cambers, then the cross-frames will fit exactly to the girders in the above SDL geometry. In other words, for the structure in the above hypothetical deflected geometry under the steel self-weight, the cross-frame connections match up perfectly with the corresponding positions on the girders. Therefore, the connections to the girders can be completed without any forcing. These statements apply to all straight I-girder bridges with either parallel skew or non-parallel skew. However, they do not apply to curved I-girder bridges.

All the cross-frames are assumed inactive and the girders deflect only in the plane of their webs in a LGA. The girders deflect independently of each other under the dead loads in this analysis. Figure 198 shows the girder vertical deflections due to SDL in the Bridge (J2) NISSS54 bridge, calculated by LGA. The SDL and TDL camber profiles on the engineering drawings are taken simply as the inverse of the vertical deflections under SDL or TDL, respectively.

One can observe that all the girder vertical deflections are nearly identical in Figure 198. This is because the girders are all of the same size and length, such that the SDL is the same for all the interior girders. The SDL applied to the fascia girders is only slightly less since the cross-frames connect to only one side of the fascia girders. The cross-frame weights, applied as concentrated nodal loads to the fascia girders, are one-half of those applied to the interior girders.

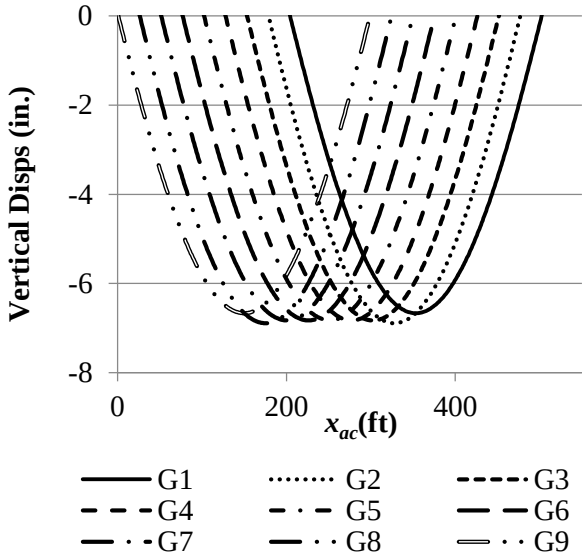

Figure 198. Bridge (J2) NISSS54 girder vertical displacements due to SDL calculated by LGA.

Table 75 shows the maximum girder layovers, the maximum cross-frame stresses, and the maximum flange lateral bending stresses for NISSS54 under SDL, including SDLF effects based on the LGA cambers. The girder layovers and internal stresses closely match the theoretical ideal zero values. The reason for the minor deviation from zero is because the secondary bending actions induced by the connections of inverted-V cross-frames at the skewed bearing lines are not accounted for in the process of detailing the cross-frames. Another reason is the intermediate connection plates. They are not placed symmetrically

along the web of each girder due to the staggered cross-frame pattern. Because of the weight and stiffness of the connection plates, the girder lateral deflections under self-weight, before the cross-frames are connected to the girders, are very slightly non-zero.

Table 75. Bridge (J2) NISSS54 maximum responses (girder layovers and twists, cross-frame (CF) stresses, and flange lateral bending stresses (f_ℓ)) under SDL, including SDLF effects based on LGA cambers

Layover (in.)	**Twist (rad)x10^{-3}**	**CF stress (ksi)**	**f_ℓ (ksi)**
0.077	0.53	0.46	0.46

Due to stability considerations, bridge (J2) NISSS54 would not be erected in the hypothetical fashion explained above, where all the girders are allowed to deflect under the full steel self-weight without any cross-frame connections. It would be erected in stages (such as the stages shown in Figure 197) in which individual girders or girder pairs would be placed and the cross-frames would be connected to the erected girders successively after each of the girder lines or girder pairs are placed. However, based on common engineering analysis assumptions discussed below, the final bridge responses in the completed bridge system under the SDL are independent of the specific erection sequence.

Once the cross-frames are connected to the girders, the interconnected girders deflect as a three-dimensional system under subsequent dead loads. The cross-frames brace the girders, but they also serve as an additional transverse load path in the system. As a result, the girders deflect vertically and simultaneously twist under the subsequent dead loads. This behavior of straight skewed bridges is different from the behavior of a straight bridge with zero skew. In a straight bridge with zero skew, the girders deflect predominantly only in a vertical fashion. This is because there are no significant differential deflections

between the girders and there is no interaction between the girders and the displacements of the bearing line cross-frames. However, in a straight skewed bridge, such as (J2) NISSS54, there are substantial non-zero differential deflections between the girders at each of the cross-frames, since the cross-frames connect to different positions within the span of each of the girders. In addition, to maintain compatibility between the cross-frames and the girders along the skewed abutment bearing lines, the girders have to twist substantially at the skewed abutments.

9.1.2. Behavior Independent of Erection Sequence

Regardless of the sequence in which the bridge is erected, if the SDL cambers are calculated from LGA, and the cross-frames are detailed for SDLF using these cambers, the girder layovers and internal stresses in the completed bridge system under the SDL are theoretically equal to the above ideal values. This is because as long as:

(1) All the bridge components are kept elastic,

(2) The influence of the girder splice and cross-frame-to-girder connection tolerances is assumed to be negligible, and

(3) There are no effects such as friction providing unintended restraint at the supports, the bridge is what is referred to in structural mechanics as a conservative elastic structural system.

Within these limits, the response of the structure for any given erection stage is independent of the erection sequence up to that point. In mechanics terms, the bridge is a conservative elastic system and the behavior at any given erection stage is unique and path independent.

9.1.3. Erection Sequence 2

To further understand the fit behavior, bridge (J2) NISSS54 responses can be examined assuming that all the cross-frames are connected to the girders first, before the dead loads are applied to the bridge, and then the SDL is "turned on." For SDLF detailing, the cross-frames are fabricated to fit to the girder connection work points in a conceptual geometry in which the girders are plumb when the girders are subjected to their SDL deflections. As such, the cross-frames do not fit up with the girders in the reference no-load geometry. This initial lack-of-fit between the cross-frames and the girders in the reference no-load geometry induces girder layovers (i.e., relative lateral displacements of the top and bottom flanges) in the opposite direction from the layovers due to the SDL. These SDLF detailing effects on the girder layovers are shown in Figure 199. Similarly, the SDLF detailing effects cause girder flange lateral bending stresses as shown in Figure 202.

When the SDL is subsequently applied to the bridge in the above conceptual scenario, the girders deflect vertically and twist under the application of the SDL to the three-dimensional structural system, as discussed above. Figures 200 and 203 show the girder layovers and flange lateral bending stresses, respectively, due to the SDL. The girder layovers and flange lateral stresses due to the SDL (not including the SDLF detailing effects) are substantial. This is due to the compatibility between the girders and the heavily skewed bearing line cross-frames as well as the differential deflections between the girders within the span.

One can observe that the layovers in Figure 199 due to the SDLF locked-in forces based on the LGA cambers, are approximately equal in magnitude and opposite in direction to the layovers in Figure 200 due to the SDL. That is, these two sets of layovers effectively

cancel one another. As such, the girder flanges are essentially straight in the final SDL condition as shown in Figure 201 (the layover shown in this figure is the summation of those from Figures 199 and 200). Since the girder flanges are essentially straight, their lateral bending is approximately zero in the final SDL condition as shown in Figure 204 (the summation of Figures 203 and 204). Furthermore, since the girder flange lateral bending is effectively zero, the cross-frame forces are all essentially zero under the SDL condition as well.

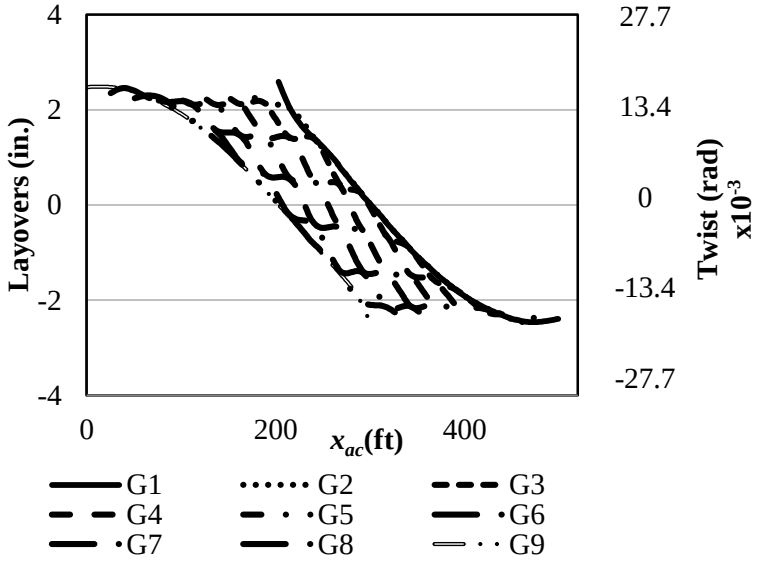

Figure 199. Bridge (J2) NISSS54 girder layovers and twists due to SDLF detailing effects based on LGA cambers.

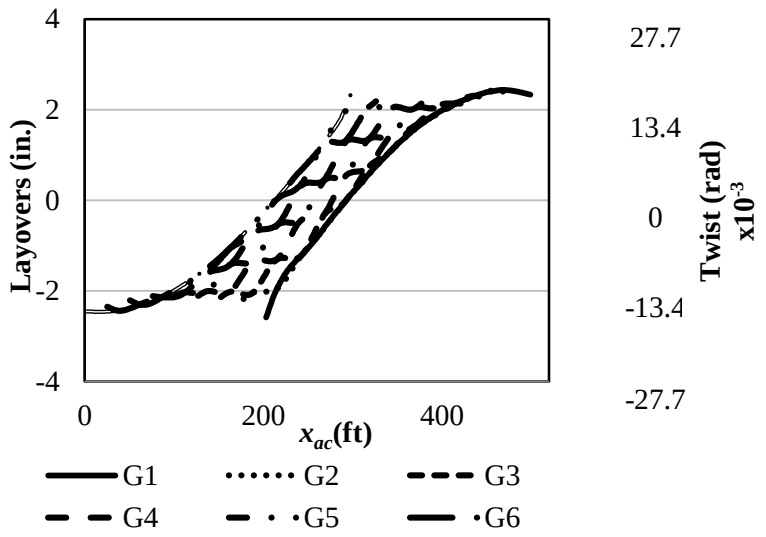

Figure 200. Bridge (J2) NISSS54 girder layovers and twists due to SDL.

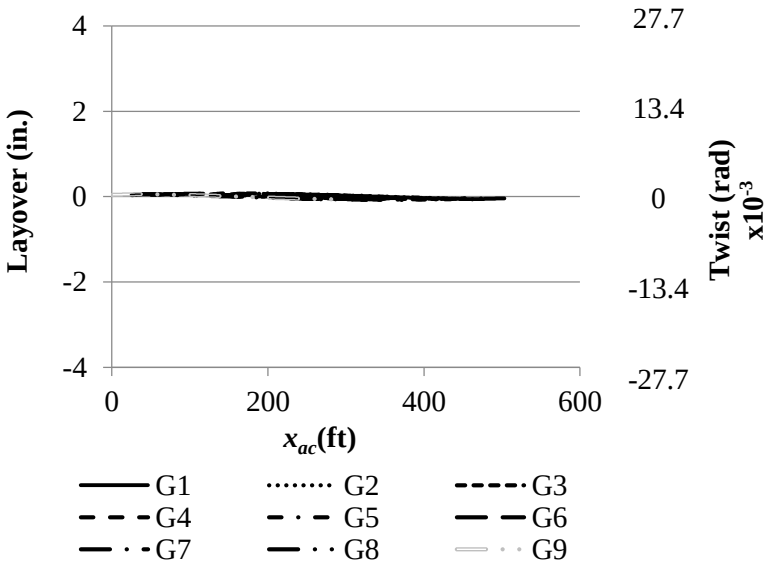

Figure 201. Bridge (J2) NISSS54 girder layovers and twists under SDL including SDLF detailing effects based on LGA cambers.

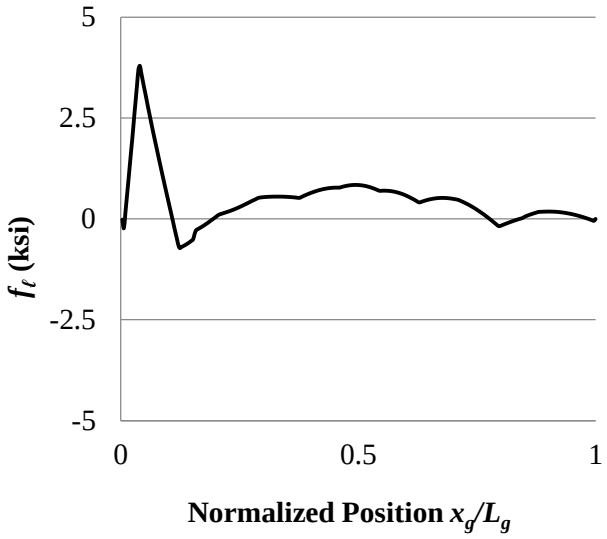

Figure 202. Bridge (J2) G1 top flange lateral bending stresses due to SDLF detailing effects based on LGA cambers.

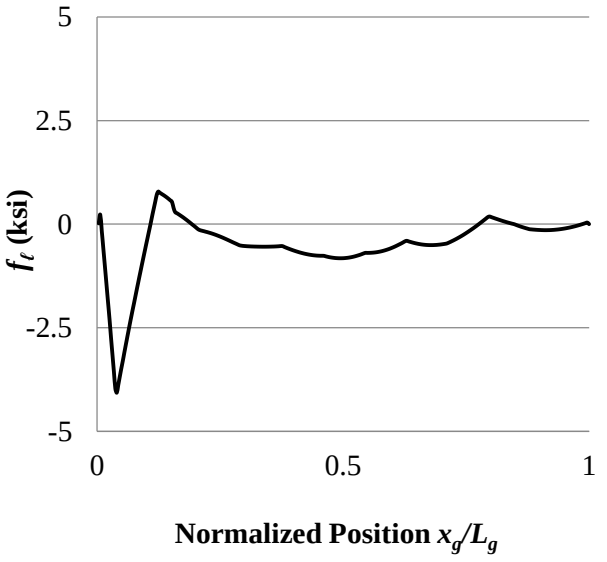

Figure 203. Bridge (J2) G1 top flange lateral bending stresses due to SDL.

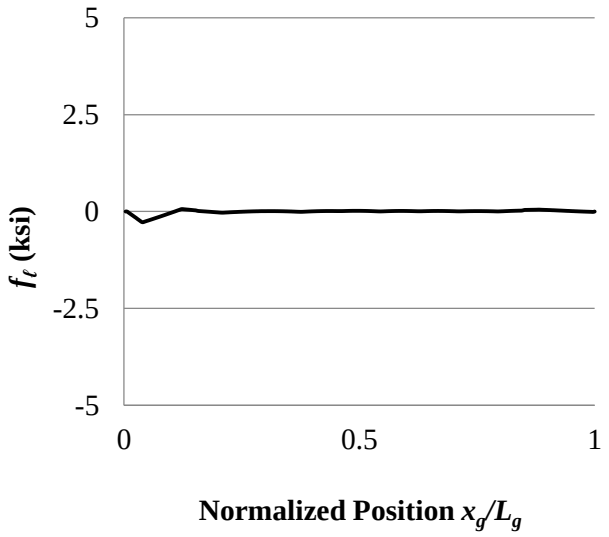

Figure 204. Bridge (J2) G1 top flange lateral bending stresses due to SDL including SDLF effects based on LGA cambers.

In addition, the SDLF detailing effects based on LGA cambers cause significant girder vertical displacements as shown in Figure 205. Figure 206 shows the NISSS54 girder vertical deflections due to SDL when the bridge deflects as a system. The vertical deflections are much smaller near the center of the bridge width in the three-dimensional structural system. This is due to the substantial transverse load path between the obtuse corners of the bridge, developed via the cross-frames. Figure 207 shows the SDL girder deviations from target elevations using LGA cambers. These elevations are equal to the summation of:

- The negative of the LGA vertical displacements (Figure 198)
- The vertical displacements due to SDLF detailing effects based on LGA cambers (Figure 205). And
- The vertical displacements due to SDL when the bridge deflects as a system (Figure 206).

As explained in Section 9.1.1, when the detailing is SDLF based on LGA cambers, the girder deviations from target elevations, girder layovers, and flange lateral bending stresses are theoretically zero under SDL condition. However, the solutions shown in Figures 201, 204, and 207 are slightly non-zero due to modeling attributes discussed in Section 9.1.1. It should also be noted that due to additional vertical displacements due to SDLF detailing effects based on LGA cambers, the girder deviations from target elevations are approximately zero despite the large differences between the SDL LGA cambers and the vertical displacements due to SDL.

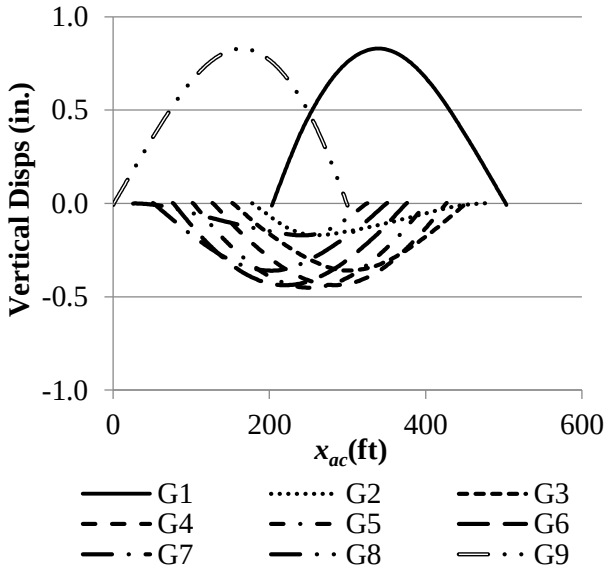

Figure 205. Bridge (J2) girder displacements under due to SDLF detailing effects based on the LGA cambers.

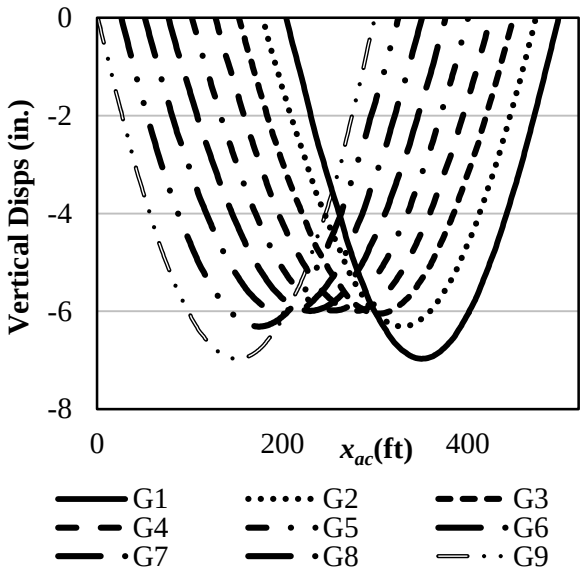

Figure 206. Bridge (J2) NISSS54 girder vertical displacements due to SDL when the bridge deflects as a system.

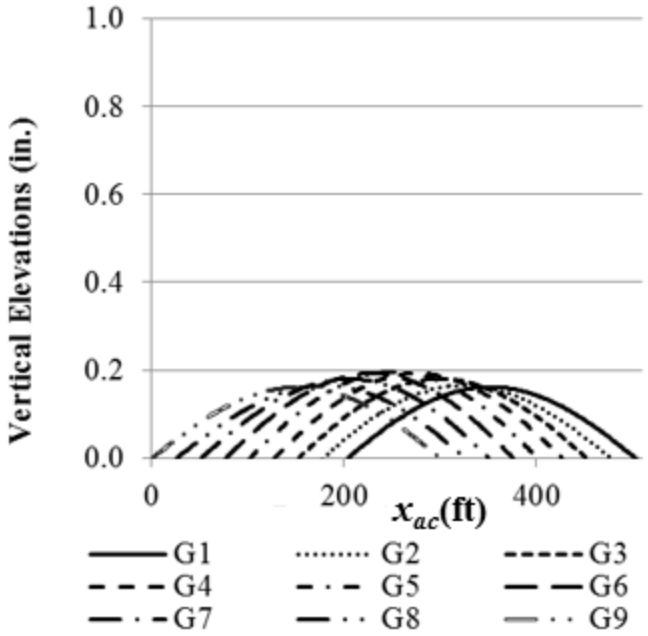

Figure 207. Bridge (J2) girder deviations from target elevations under SDL for SDLF detailing based on the LGA cambers.

Figures 208 and 209 show the major-axis bending stresses due to SDLF detailing effects based on LGA cambers and due to SDL, respectively. Since the vertical displacements caused by SDLF detailing effects based on LGA cambers are significant (Figure 205), the corresponding major-axis bending stresses are also significant. Figure 210 (the summation of Figures 208 and 209) shows major-axis bending stresses under SDL including the SDLF detailing effects.

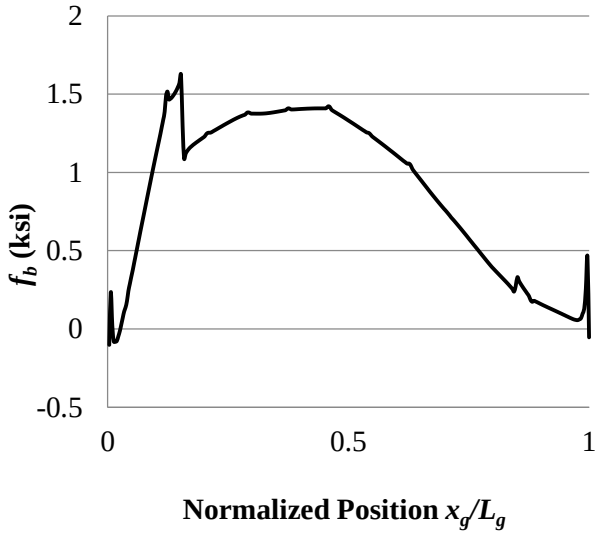

Figure 208. Bridge (J2) G1 top flange major-axis bending stresses due to SDLF detailing effects based on LGA cambers.

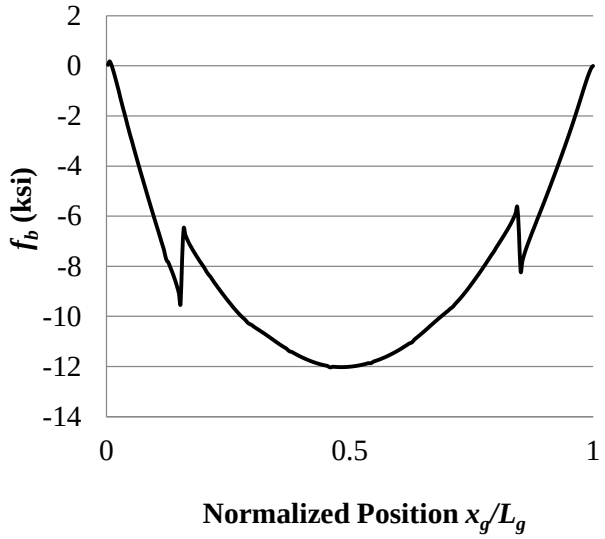

Figure 209. Bridge (J2) G1 top flange major-axis bending stresses due to SDL when the bridge deflects as a system.

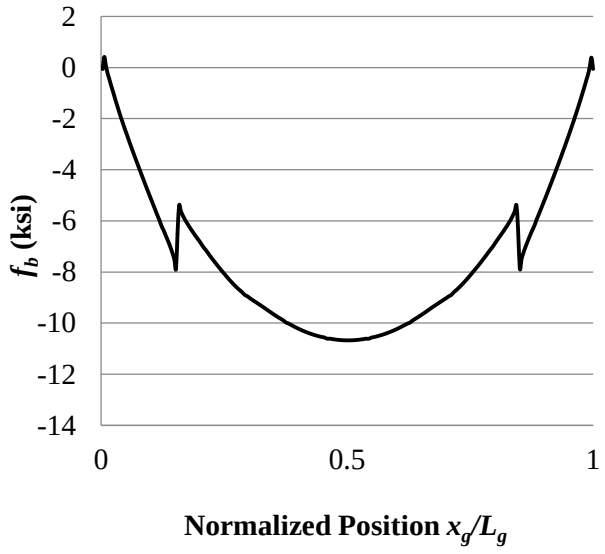

Figure 210. Bridge (J2) G1 top flange major-axis bending stresses due to SDL including SDLF effects based on LGA cambers.

9.1.4. Summary

One can view the above behavior as a beneficial effect of lack-of-fit between the cross-frames and the girders in the reference no-load bridge geometry. The lack-of-fit effects cancel the SDL effects, theoretically resulting in plumb girders, zero lateral bending, zero girder deviations from target elevations, and zero cross-frame forces in the SDL condition. Alternatively, one can consider the earlier hypothetical erection scenario, in which the cross-frames fit to the girders in their ideal SDL deflected geometry without any forcing, if the girders and cross-frames are all placed first without engaging the cross-frames in resisting any internal forces. Both idealized sequences, or any other erection sequence, produce the same result, since under the previously stated assumptions, the bridge is a conservative elastic structural system.

9.2. SDLF Behavior using 3D FEA Cambers

The common current structural practice, when using 2D Grid or 3D FEA, is to build a model of the structure and then simply "turn the gravity load on." This practice captures the behavior of the bridge if the cross-frames could be fully connected to all the girders, in a no-load (e.g., a shored) condition, without any forcing (i.e., cross-frames detailed for NLF), followed by removal of the shoring. This practice does not account for the actual behavior of the bridge if the girders and cross-frames could be placed first and allowed to deflect under the steel self-weight, followed by connection of the cross-frames fabricated for SDLF to the girders in their SDL condition without any forcing. Furthermore, it does not account for any other erection scenario with detailing of the cross-frames for anything other than NLF. In fact, one should recall that given the previously stated assumptions, the bridge is a conservative elastic structural system; hence, the erection sequence does not

influence the completed state of the bridge. However, the fit method, for instance SDLF versus NLF, certainly does influence the response. Also, the SDL deflections assumed in setting the cambers definitely influence the completed state of the bridge.

For the parallel skew bridge (J2) NISSS54, the differences in the cambers obtained from LGA (negative of the vertical displacements Figure 198) versus 3D FEA (negative of vertical displacements in Figure 206) are substantial. When the cross-frames are detailed for SDLF based on 3D FEA cambers, due to beneficial lack-of-fit effects generated by the cross-frame detailing, the girders tend to be close to plumb, and the cross-frame forces and girder flange lateral bending stresses will be relatively small. However, these quantities will generally differ from the targeted ideal zero values. This fact is further explained below.

In the context of a conceptual model in which the cross-frames are connected to the girders first, including the SDLF detailing effects, and then the SDL is subsequently applied (recall that the sequencing of these steps has no influence on the final result since the response is path independent within the limits of the previously stated assumptions), SDLF detailing based on the 3D FEA based cambers (referred to as just the 3D FEA cambers for simplicity) induces layovers (Figure 211) in the girders in the opposite direction from those due to the SDL (Figure 200). However, these layovers are opposite but not exactly equal to the layovers caused by the SDL.

Figure 212 demonstrates this point by showing the final layover of the girders under the SDL, when SDLF based on the 3D FEA cambers is used. The maximum girder layover in this case is 0.26 in. These results show that, for practical engineering purposes, these 12

ft. deep girder webs can be considered plumb. However, strictly speaking, they are not exactly plumb.

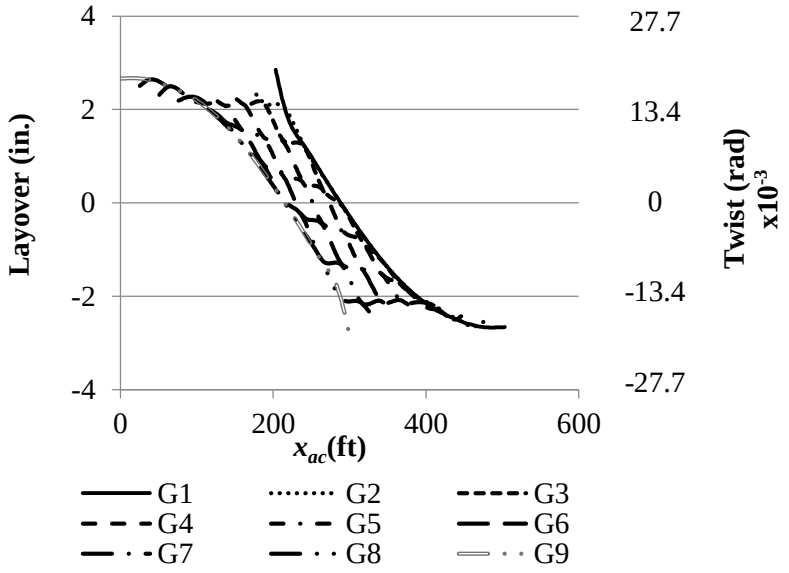

Figure 211. Bridge (J2) NISSS54 girder layovers and twists due to SDLF detailing effects based on 3D FEA cambers.

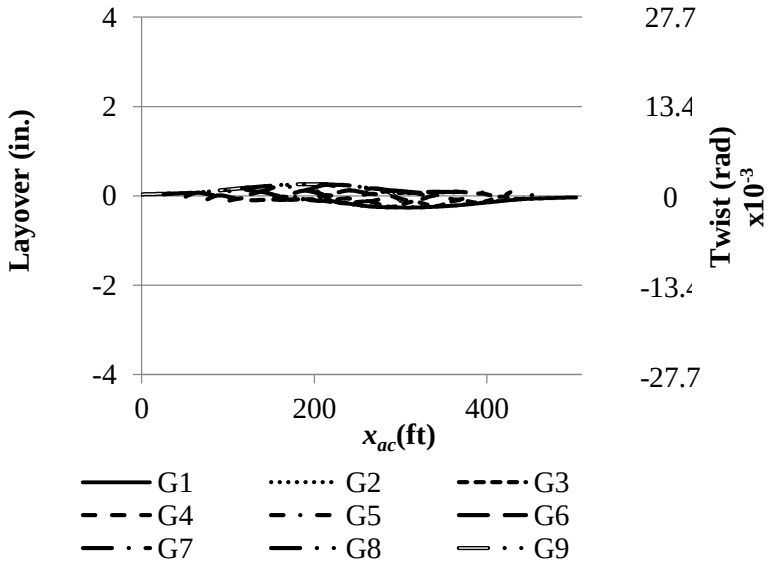

Figure 212. Bridge (J2) NISSS54 girder layovers and twists under SDL including the effects of SDLF detailing based on the 3D FEA cambers.

Since the girders are not exactly plumb under SDL, for SDLF based on the 3D FEA cambers, the associated cross-frame axial forces and girder flange lateral bending stresses are not exactly zero either. However, these stresses are relatively small (maximum cross-frame stress magnitude of 2.81 ksi). Figure 213 shows the flange lateral bending stresses due to SDLF detailing effects based on 3D FEA cambers. Theses stresses are slightly larger than those induced by SDLF detailing effects based on LGA cambers (Figure 202). Figure 214 shows the flange lateral bending stresses under SDL including SDLF detailing effects based on 3D FEA cambers. It can be seen that theses stresses are close to zero and slightly larger those under SDL including SDLF detailing effects based on LGA cambers (Figure 204).

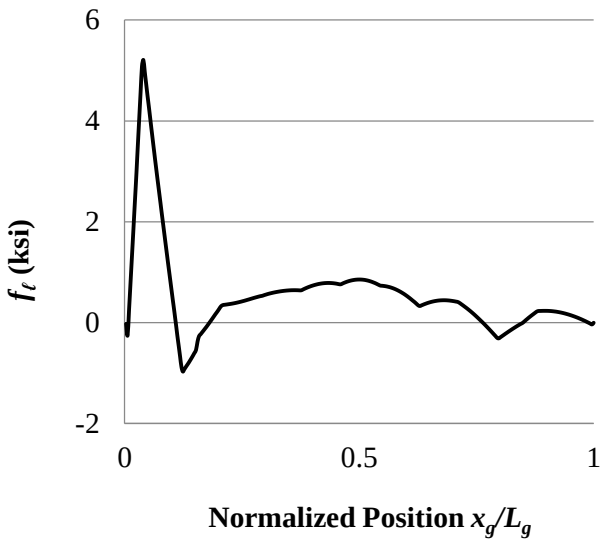

Figure 213. Bridge (J2) G1 top flange lateral bending stress due to SDLF detailing effects based on 3D FEA cambers.

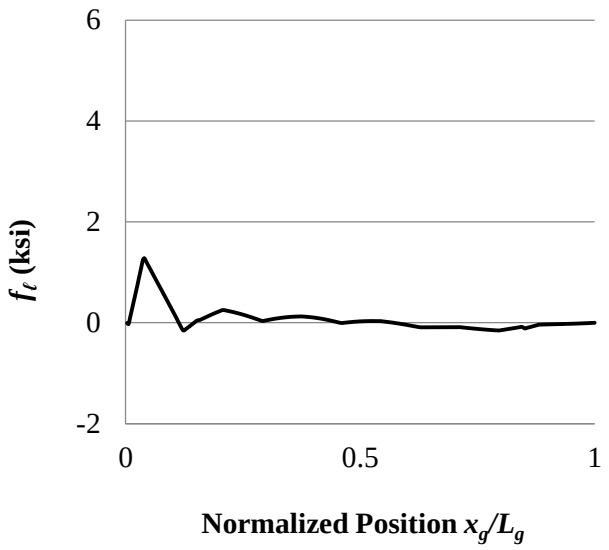

Figure 214. Bridge (J2) G1 top flange lateral bending stress under SDL including the effects of SDLF based on the 3D FEA cambers.

Although it can be seen from Figures 198 and 206 that the SDL cambers calculated from LGA and 3D FEA are substantially different, the final bridge geometries and internal stresses are very similar under the targeted dead load condition.

As noted previously, the SDL girder elevations due to SDLF detailing based on the LGA cambers closely match with the ideal targeted elevations. This is because if the girders were allowed to deflect under SDL before all the cross-frames were connected to the girders, the resulting girder vertical deflections would be exactly equal to the SDL deflections obtained from a LGA.

The SDL girder elevation due to SDLF based on the 3D FEA cambers deviate slightly from the ideal targeted elevations under the SDL. The girder deviations from target elevations under the SDL condition, due to SDLF based on 3D FEA cambers, can be considered as the summation of three independent components:

- The 3D FEA cambers (negative the SDL vertical displacements in Figure 206).
- The change in elevations due to SDLF effects from the 3D FEA cambers (Figure 215). And
- The system vertical deflections due to the SDL effects alone (Figure 206).

Therefore, the girder deviations from target elevations in this scenario (Figure 216) are exactly equal the change in elevations due to the SDLF effects from 3D FEA cambers (Figure 215). It can be observed that maximum deviations from the ideal zero elevation change line are +0.53 and -0.11 in.

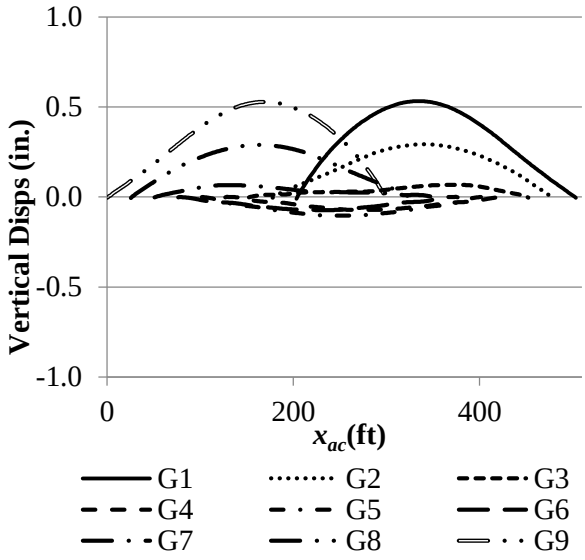

Figure 215. Bridge (J2) girder vertical displacements due to SDLF detailing effects based on the 3D FEA cambers.

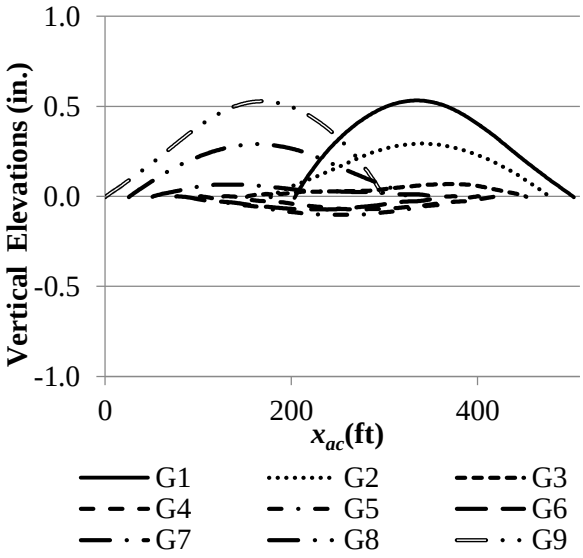

Figure 216. Bridge (J2) girder deviations from target elevations under SDL including SDLF detailing effects based on the 3D FEA cambers.

Figure 217 shows the major-axis bending stresses due to SDLF detailing effects based on 3D FEA cambers. One can see that these major-axis bending stresses are less than those when the SDLF detailing is based on LGA cambers (Figure 208). Figure 218 (summation of Figures 217 and 209) shows major-axis bending stresses under SDL including the SDLF detailing effects based on 3D FEA cambers.

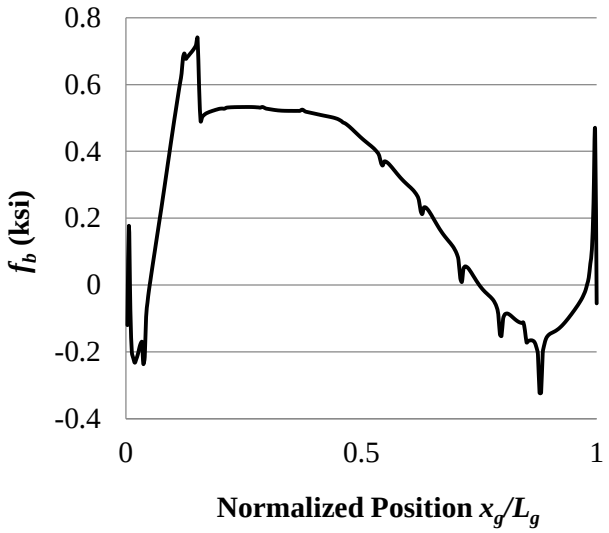

Figure 217. Bridge (J2) G1 top flange major-axis bending stress due to SDLF detailing effects based on the 3D FEA cambers.

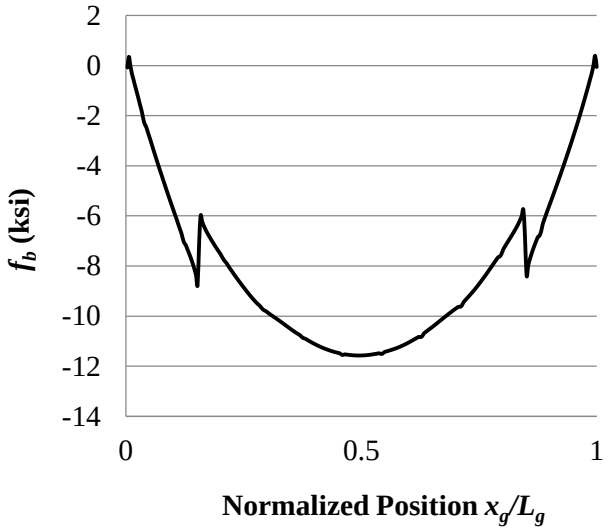

Figure 218. Bridge (J2) G1 top flange major-axis bending stress under SDL including the effects of SDLF based on the 3D FEA cambers.

9.3. TDLF Behavior

Similar conclusions to the above can be drawn for TDLF detailing. The final bridge geometries and internal stresses are very similar for TDLF regardless of whether the cambers are calculated by LGA, 2D-gird analysis, or 3D FEA. This is because the behavior of a skewed I-girder bridge is very similar under both SDL and TDL within the context of the assumption that the volume of the deck concrete is small enough such that the deck can be placed entirely in one stage and the concrete dead weight must be resisted entirely by the noncomposite steel structural system (or alternately, if the influence of staged deck placement is assumed to be negligible). The concrete weight is calculated based on the tributary deck widths and is applied as vertical line loads at the tops of the girders.

Figure 219 shows the girder TDL vertical displacements calculated by LGA and 3D FEA for Bridge (J2) NISSS54. One can observe that:

- All the girder vertical displacements calculated by LGA are nearly identical. This is because the girders are all of the same size and length, such that the TDL is the same for all the interior girders. The TDL applied to the fascia girders is only slightly less since the cross-frames connect to only one side of the fascia girders and the deck overhangs are not large.
- The TDL vertical displacements calculated by 3D FEA are much smaller near the center of the bridge width in the three-dimensional structural system. This is due to the substantial transverse load path between the obtuse corners of the bridge, developed via the cross-frames.

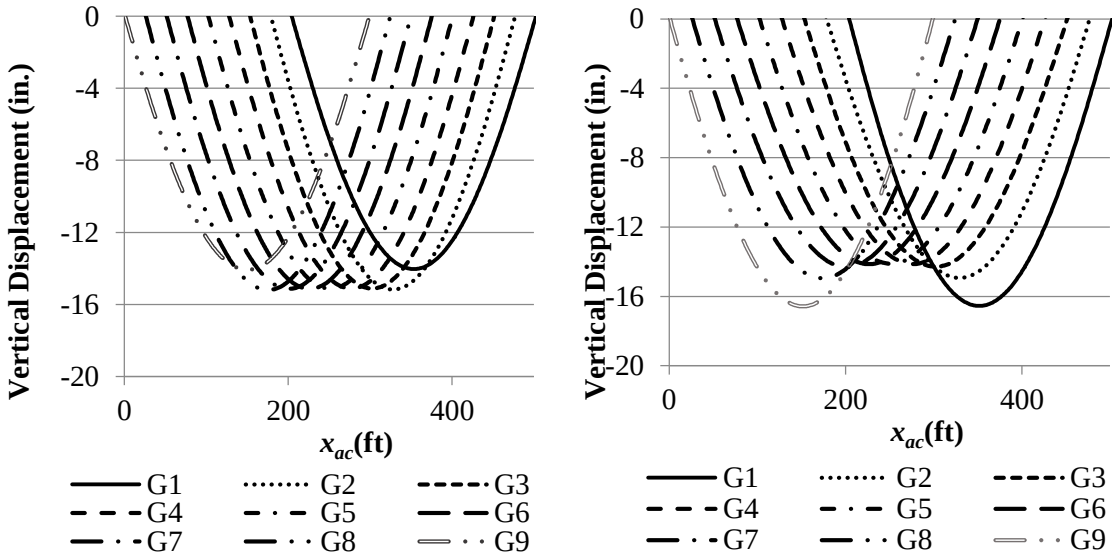

Figure 219. Bridge (J2) girder vertical displacements due to TDL calculated by (a) LGA and (b) 3D FEA.

The TDLF detailing effects based on the LGA and 3D FEA cambers cause the girder vertical displacements shown in Figure 220. Figure 221 shows the final TDL girder elevations. When the cambers are from LGA, the final elevations are equal to the summation of:

1) The LGA TDL cambers (the negative of the TDL vertical displacements calculated by LGA, shown in Figure 219a),
2) The vertical displacements due to TDLF detailing effects based on LGA cambers (shown in Figure 220a), and
3) The vertical displacements of the three-dimensional bridge system due to the TDL (Figure 219b).

Theoretically, when LGA cambers are used, the final girder elevations are zero under TDL condition. However, the solutions shown in Figure 221a are slightly non-zero. This is due

to the incidental effects as well as the fact that eccentric overhang bracket loads are included in the TDL solution of Figure 219b. It should also be noted that due to the additional significant vertical displacements due to the TDLF detailing effects based on the LGA cambers (Figure 220a), these final elevations are approximately zero despite the large differences between the TDL LGA cambers (which are the negative of the LGA vertical displacements as shown in Figure 219a) and the vertical displacements due to the TDL (Figure 219b).

When the cambers are based on 3D FEA, the final elevations are equal to the summation of:

1) The 3D FEA cambers (the negative the TDL vertical displacements calculated by 3D FEA, shown in Figure 219b),
2) The change in elevations due to TDLF detailing effects from the 3D FEA cambers (shown in Figure 220b), and
3) The system vertical deflections due to the TDL effects alone (Figure 219b).

Therefore, the final girder elevations (Figure 221b) are exactly equal the change in elevations due to the TDLF detailing effects from 3D FEA cambers shown in Figure 220b.

One can observe that the layovers in Figure 222a due to the TDLF locked-in forces based on the LGA cambers, are effectively equal in magnitude and opposite in direction to the layovers in Figure 223 due to the TDL. That is, these two sets of layovers approximately cancel one another. As such, the girder flanges are completely straight in the final TDL condition, as shown in Figure 224a.

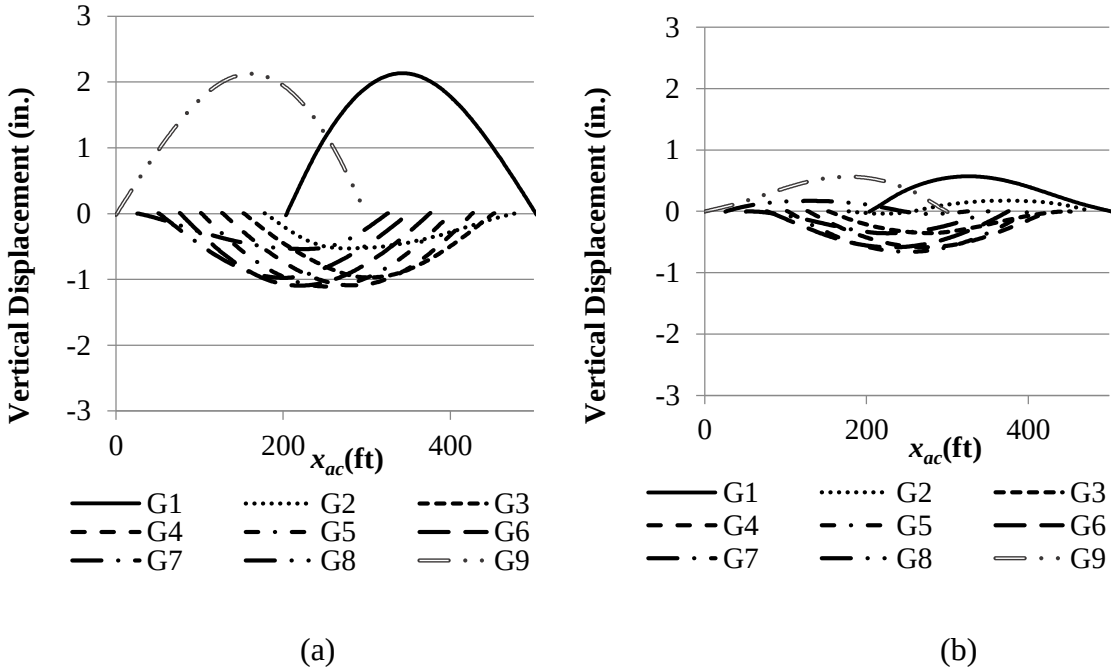

Figure 220. Bridge (J2) girder vertical displacements due to TDLF detailing effects based on the (a) LGA cambers and (b) 3D FEA cambers.

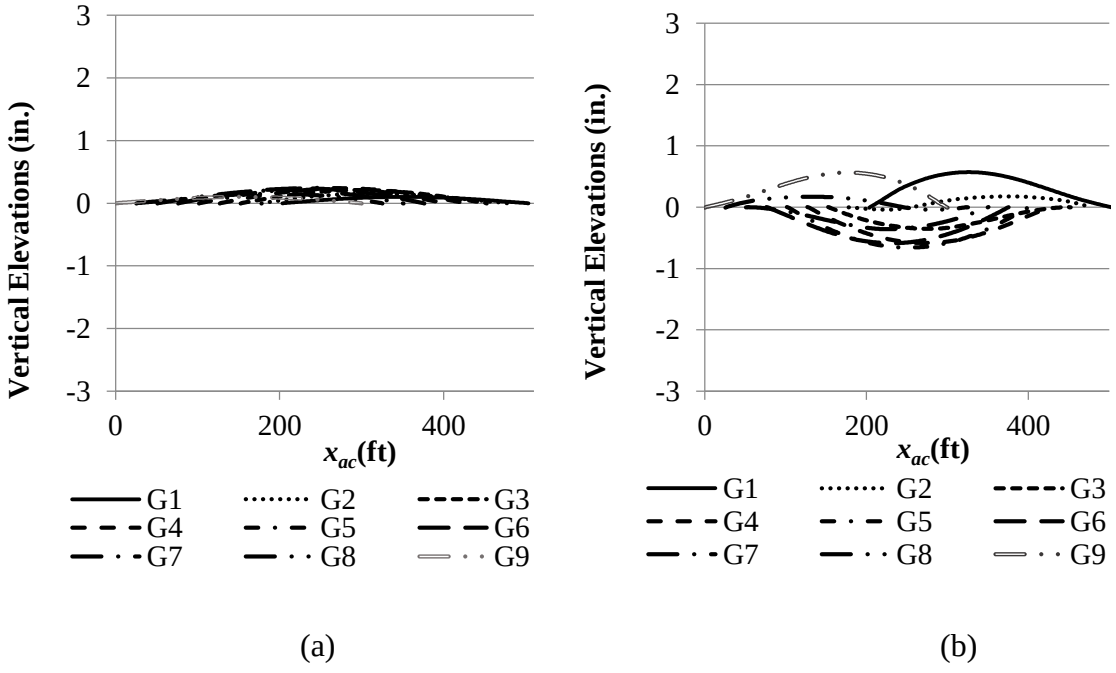

Figure 221. Bridge (J2) final girder elevations under TDL including TDLF detailing effects based on the (a) LGA cambers and (b) 3D FEA cambers.

The TDLF detailing effects based on the 3D FEA based cambers induce the girder layovers (Figure 222b) that are in the opposite direction from those due to the TDL (Figure 223). However, these layovers are not exactly equal the layovers caused by the TDL. This is because the LGA based camber is the only vertical camber that produces the targeted ideal results in a straight skewed I-girder bridge. Figure 224b demonstrates this point by showing the final layover under the TDL, when TDLF based on the 3D FEA cambers is used. The maximum girder layover in this case is 0.71 inches. These results show that, for practical engineering purposes, these 12 ft. deep girder webs can be considered plumb. However, strictly speaking, they are not exactly plumb.

Since the girder flanges are effectively straight in the targeted DL condition, when LGA cambers are employed, the flange lateral bending stresses are effectively zero in the final TDL condition as shown in Figure 227a. When the cambers are based on 3D FEA, the TDL girder layovers are small, but non-zero. Again, the LGA based camber is the only vertical camber that produces the targeted ideal in a straight skewed I-girder bridge. The final TDL flange lateral bending stresses, based on 3D FEA girder cambers, are shown in Figure 227b.

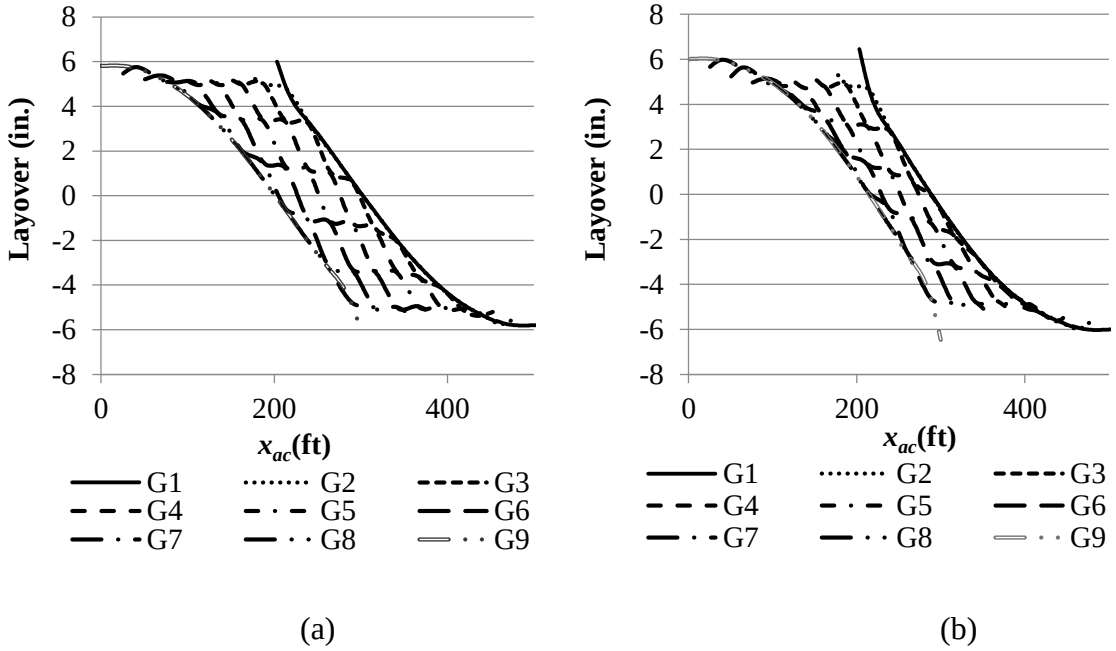

Figure 222. Bridge (J2) girder layovers due to TDLF detailing effects based on the (a) LGA cambers and (b) 3D FEA cambers.

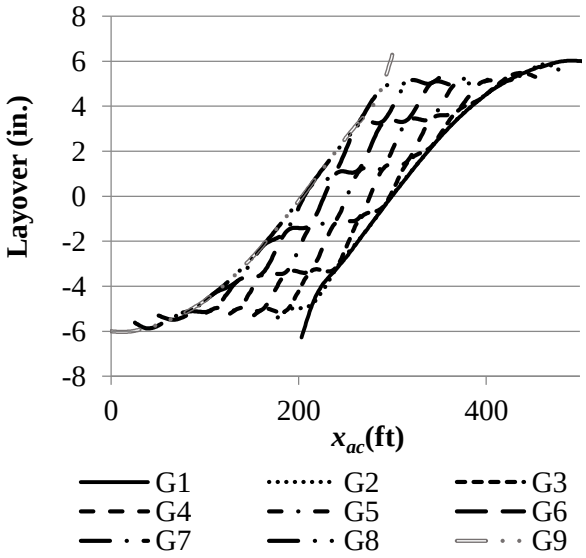

Figure 223. Bridge (J2) girder layovers due to TDL calculated by NLF 3D FEA.

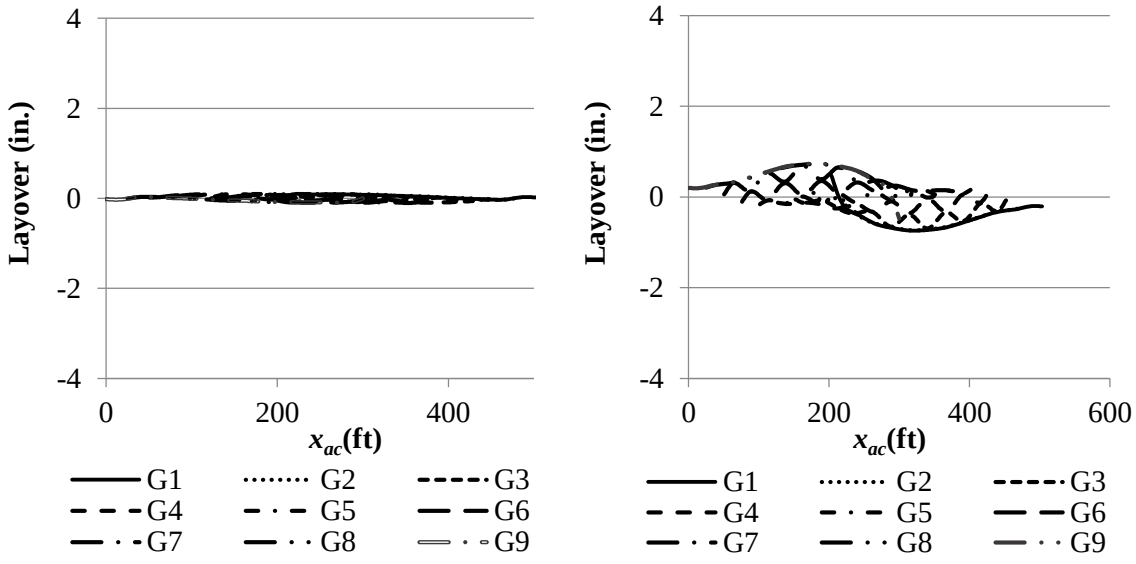

Figure 224. Bridge (J2) girder layovers under TDL including TDLF detailing effects based on the (a) LGA cambers and (b) 3D FEA cambers.

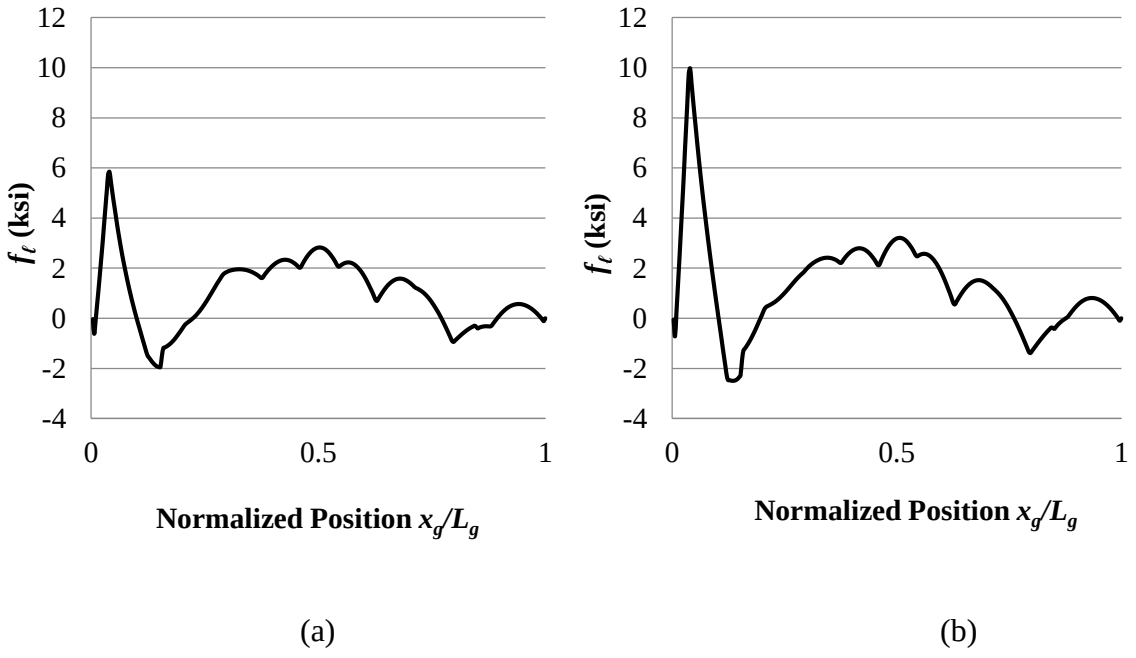

Figure 225. Bridge (J2) G1 top flange lateral bending due to TDLF detailing effects based on the (a) LGA cambers and (b) 3D FEA cambers.

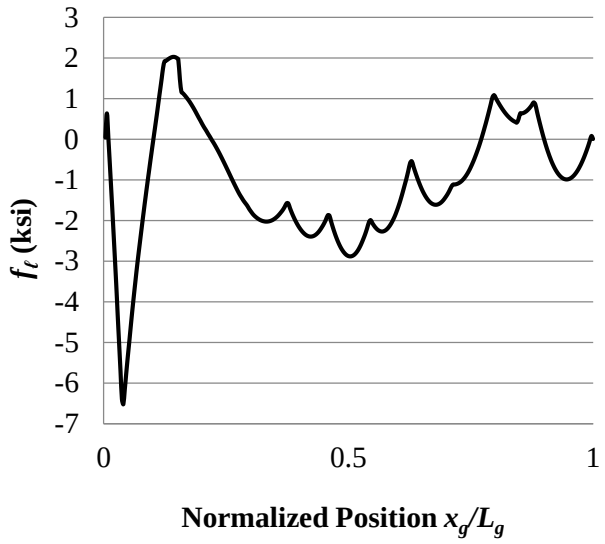

Figure 226. Bridge (J2) G1 top flange lateral bending stresses due to TDL calculated by 3D FEA.

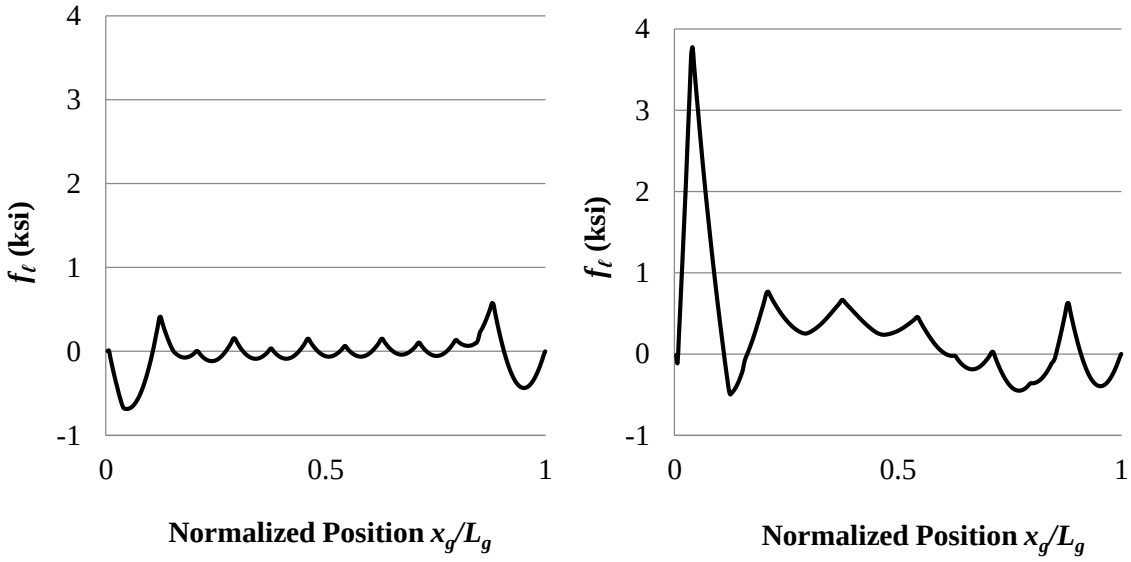

Figure 227. Bridge (J2) G1 top flange lateral bending stresses under TDL including TDLF detailing effects based on the (a) LGA cambers and (b) 3D FEA cambers.

Figure 228 shows the girder major-axis bending stresses due to TDLF detailing effects based on LGA cambers and 3D FEA cambers. Since the vertical displacements caused by

the TDLF detailing effects are larger when the cambers are from LGA than when the cambers are from 3D FEA, the corresponding major-axis bending stresses are also larger. Figure 229 shows the major-axis bending stresses under the TDL in the three-dimensional bridge system, calculated by creating the bridge model and then "turning gravity on." Figure 230 shows major-axis bending stresses under TDL including the TDLF detailing effects based on LGA cambers and 3D FEA cambers. The LGA based results shown in Figure 230a are a close match to the girder major-axis bending stresses from the LGA. The TDLF detailing effects shown in Figure 228a modify the stresses from Figure 229, producing these LGA major-axis bending stresses. The girder major-axis bending stresses shown in Figure 230b, obtained with TDLF detailing based on the 3D FEA cambers, are slightly different.

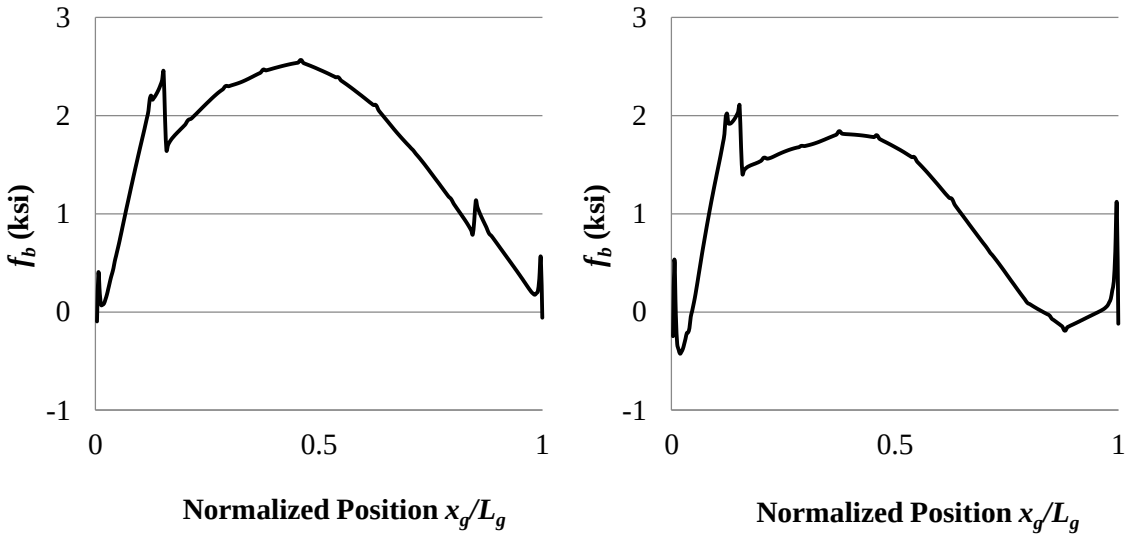

(a) (b)

Figure 228. Bridge (J2) G1 top flange major-axis bending stresses due to TDLF detailing effects based on the (a) LGA cambers and (b) 3D FEA cambers.

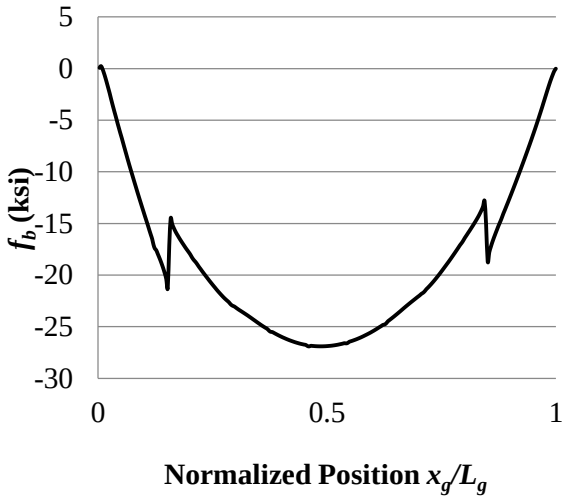

Figure 229. Bridge (J2) G1 top flange major-axis bending stresses due to TDL calculated by 3D FEA.

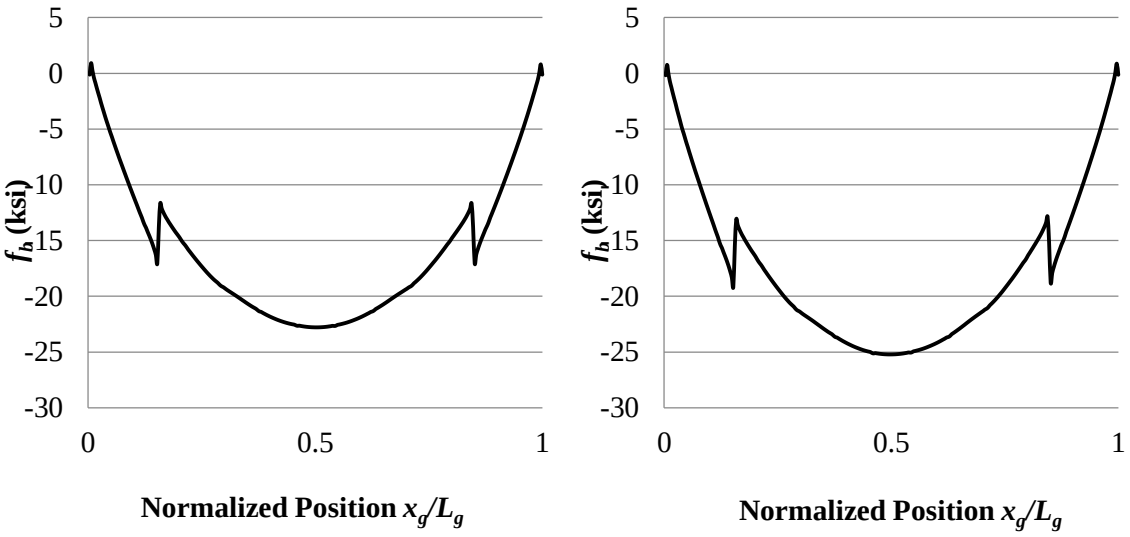

Figure 230. Bridge (J2) G1 top flange major-axis bending stresses under TDL including TDLF detailing effects based on the (a) LGA cambers and (b) 3D FEA cambers.

9.4 Summary

The camber profiles calculated from LGA and 3D FEA for a straight sharply-skewed bridge can be substantially different. However, the final bridge geometries and responses obtained with either SDLF or TDLF detailing are very similar. The use of cambers from LGA gives the closest match to the ideal zero girder layovers and flange lateral bending stresses under the targeted dead load conditions while the use of 3D FEA cambers gives girder layovers and internal stresses that are small, but non-zero, compared to the overall dead load responses under the targeted conditions. The final girder elevations due to TDLF detailing based on the LGA cambers closely match with the ideal targeted girder elevations under TDL. However, the final girder elevations due to TDLF based on the 3D FEA cambers deviate only slightly from the ideal targeted elevations under TDL. Based on the studies synthesized in Chapter 6, it can be concluded that the 3D FEA results are close enough to matching the ideal values such that it is sufficient to use 3D FEA (or other accurate RA) cambers for detailing of straight skewed bridges.

CHAPTER 10

SENSITIVITIES OF THE COMPLETED BRIDGE RESPONSES TO VARIOUS FACTORS

This section discusses the sensitivities of the completed bridge responses to girder over-camber, variations in the deck thickness, and variations in the cross-frame stiffness in bridges detailed for a SDLF or a TDLF. The straight skewed bridge (J2) NISSS54 is used as a representative extreme case to investigate these sensitivities.

The cross-frame drops for SDLF or TDLF detailing are set by subtracting the corresponding SDL or TDL camber profiles from the fully-cambered girder elevations, or in other words, by applying the SDL or TDL deflections to the fully-cambered girder elevations. As a result, the girder layovers and the internal stresses potentially can be affected significantly by any tolerances associated with the physical cambering of the girders.

SDLF and TDLF detailing rely on the dead load cambers provided on the engineering drawings. For dead load fit detailing, the girders are theoretically plumb under the targeted dead load condition, in a straight skewed I-girder bridge, if the girders are cambered exactly according to the specified LGA cambers. Any deviations from the specified cambers make the ideal girder layovers and internal stresses nonzero. The larger the deviations of the actual from the specified cambers, the more the girder layover and internal stresses are affected.

Fabricators generally impose positive tolerances on the girder camber profiles. The negative camber tolerance specified in the AASHTO/AWS D1.5 Bridge Welding Code (AWS, 2010) is zero. Fabricated girders that are under-cambered may be rejected. The

positive camber tolerance at the mid-span is +1.5 in for spans that are greater than 100 ft. (AWS, 2010). For other positions along the span, the positive camber tolerance varies parabolically between 1.5 in. at mid-span and 0 in. at the supports (although the Bridge Welding Code indicates a separate tolerance on the camber at interior supports of $\pm$ 1/8 in).

It is expected that for a bridge such as (J2) NISSS54, the fabricator would typically use a positive over-camber within the middle of the above range. The impact of this practice is investigated below by assuming LGA cambers and scaling the Bridge (J2) NISSS54 camber profiles by the factors (1 + *T* / *C*), where *T* is the maximum over-camber at the girder mid-span and *C* is the specified girder camber at its mid-span. For example, for the fascia girder G1, the specified TDL camber at mid-span is C = 14.08 in. Therefore, the G1 camber is scaled by the factor (1 + *T*/14.08). The maximum over-camber at the girder mid-span *T* is taken as 0.5., 1.0., and 1.5 in. The parameter *T* is assumed to be the same for all the girders in this base study (the effect of deviations in the over-camber between girders is discussed below). Figure 231 shows the corresponding maximum layovers, cross-frame stresses and girder flange lateral bending stresses under TDL in Bridge (J2) NISSS54 for TDLF detailing. As discussed previously, all of these quantities are theoretically equal to zero for this case, with the exception of effects due to factors such as eccentric overhang bracket loads, etc. (see Section 6.4.2). Figure 232 shows a comparable result for this bridge corresponding to the SDL condition and SDLF detailing. Although the above AWS camber tolerances strictly apply only to the full or TDL camber of the girders, Figure 232 shows the results if there are deviations of 0.5, 1.0 and 1.5 inches in the SDL camber. These deviations can occur simply due to over-camber of the girders relative to their proper full (total) cambers, i.e., the negative of the SDL deflection from the LGA plus the negative of

the girder deflections due to the concrete dead load, determined from an accurate refined analysis.

Interestingly, the maximum responses increase in a nearly linear fashion with increases in the camber tolerance in Figures 231 and 232. This is because the material is assumed to be linear elastic and the geometric nonlinearity in the bridge structural system is very minor under the targeted dead load conditions.

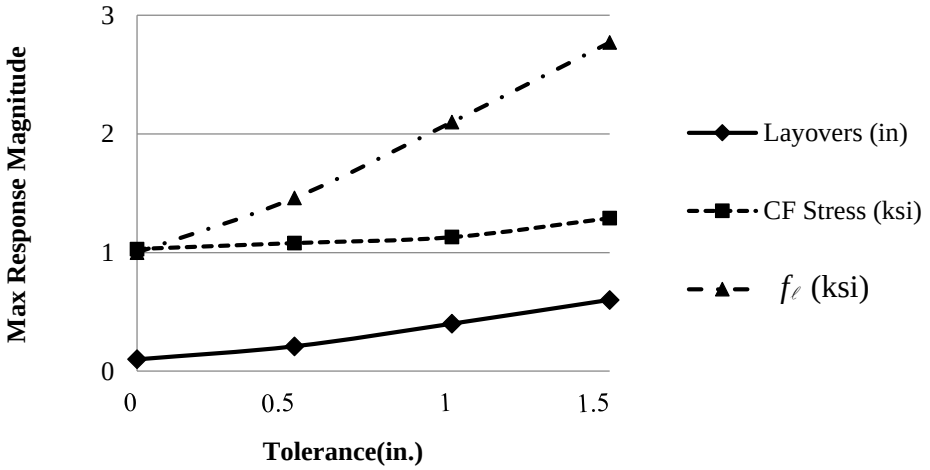

Figure 231. Bridge (J2) NISSS54 maximum responses under TDL, for TDLF detailing based on LGA cambers, versus the camber tolerance.

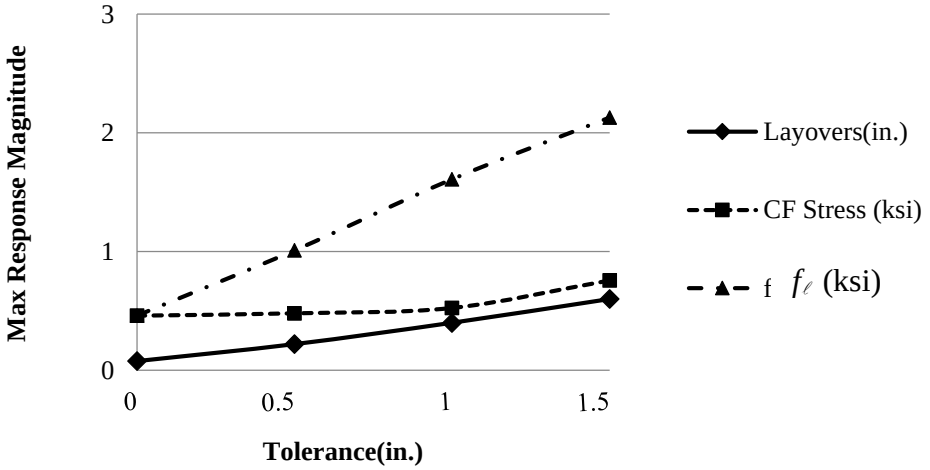

Figure 232. Bridge (J2) NISSS54 maximum responses under SDL, for SDLF detailing based on LGA cambers, versus the camber tolerance.

The camber tolerances have similar effects on the responses for TDLF or SDLF detailing based on the 3D FEA cambers. Any deviations from the specified cambers change the final girder layovers and internal stresses. These increases are nearly a linear function of the camber tolerance values since the nonlinearity in the structural system is minor.

Another tolerance that can have an important influence on the response is the concrete deck thickness tolerance. For TDLF detailing, the cross-frames are detailed such that, ideally, the girders are plumb under TDL. Changes in the deck thickness cause a change in the concrete weight. An increase in the concrete weight leads to a nearly linear increase in the bridge responses. Figure 233 shows the maximum responses under TDL, for TDLF detailing based on LGA cambers, versus the deck thickness tolerance. The corresponding responses for TDLF based on 3D FEA cambers are similar and are not shown for the sake of brevity.

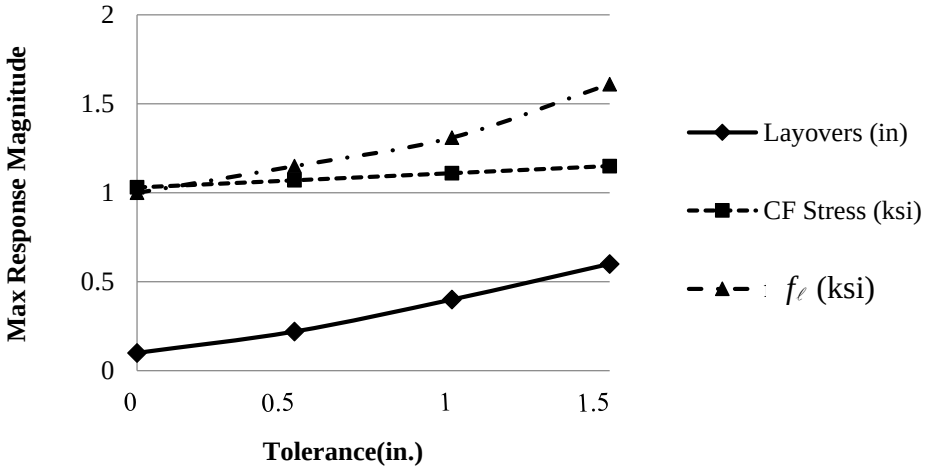

Figure 233. Bridge (J2) NISSS54 maximum responses under TDL, for TDLF detailing based on LGA cambers, versus the deck thickness tolerance.

It is important to note that while the above potential increases in the above cambers and deck thicknesses lead to measurable changes in the bridge responses, these changes are relatively small compared to the overall bridge responses.

One other sensitivity that can have an important influence on the response is the assumed axial stiffness of cross-frame members in the bridge model. In the main studies of this research, the axial stiffness of the single-angle and flange-connected tee-section cross-frame members is taken as 0.65 of the nominal EA/L to account for the additional flexibility associated with the eccentric one-sided connections at the member ends, as specified in (AASHTO, 2015). The influence of variations of the axial stiffness of the cross-frame members on the bridge responses is investigated below by varying the elastic modulus of the cross-frames for bridge (J2) NISSS54. The intermediate cross-frames are single-angle members and the bearing line cross-frames are flange-connected tee-section members in this bridge.

Figures 234, 235, and 236 show the maximum layovers, cross-frame stresses, and girder flange lateral bending stresses, respectively, under TDL, for TDLF detailing based on LGA cambers, versus the cross-frame elastic modulus. One can observe that the maximum layovers, cross-frame stresses, and flange lateral bending stresses are practically unchanged for TDLF detailing. This is because the cross-frame forces, and therefore the cross-frame deformations, are close to zero under TDL for TDLF detailing. As long as the cross-frame members have sufficient strength, they respond in essentially the same manner, for this scenario, regardless of their stiffness.

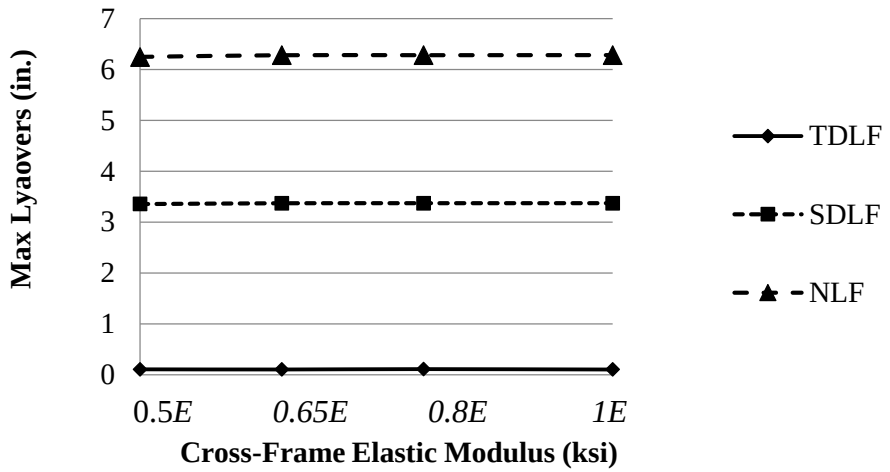

Figure 234. Bridge (J2) NISSS54 maximum layovers under TDL, for TDLF detailing based on LGA cambers, versus the cross-frame elastic modulus.

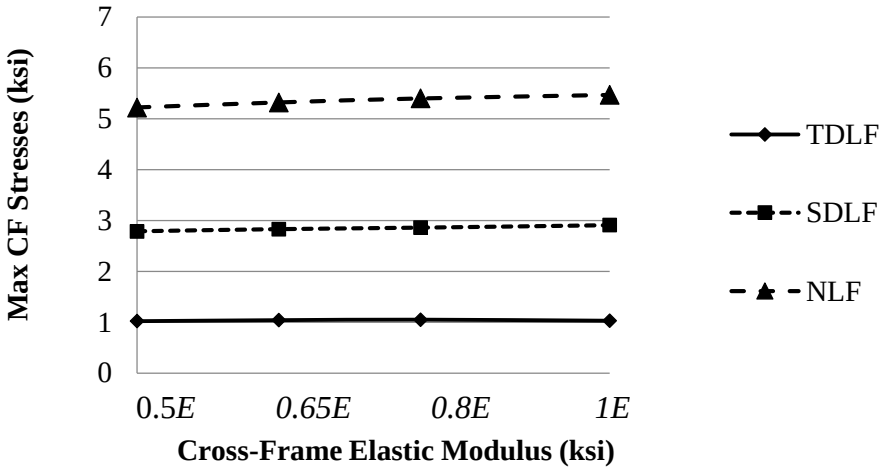

Figure 235. Bridge (J2) NISSS54 maximum cross-frame stresses under TDL, for TDLF detailing based on LGA cambers, versus the cross-frame elastic modulus.

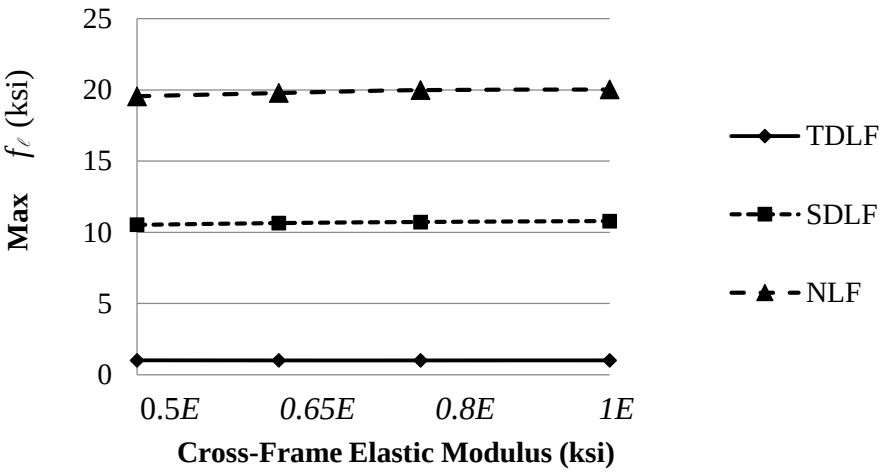

Figure 236. Bridge (J2) NISSS54 maximum flange lateral bending stresses under TDL, for TDLF detailing based on LGA cambers, versus the cross-frame elastic modulus.

Conversely, for SDLF or NLF detailing, the cross-frame members are subjected to significant internal forces under TDL. Under this scenario, increasing the stiffness of the cross-frames reduces the cross-frame deformations associated with these forces, and thus increases the cross-frame stresses and girder flange lateral bending stresses as shown in Figures 235 and 236. However, the changes in the cross-frame stresses and girder flange lateral bending stresses are relatively small given the variation in the cross-frame stiffnesses considered. In addition, since the cross-frames are effectively rigid in their plane, the girder layovers are effectively unchanged with respect to variation in the stiffness of the cross-frames as shown in Figure 234.

CHAPTER 11

CONCLUSIONS AND RECOMMENDATIONS

11.1. Key Findings

This section presents key findings from this research. Section 11.1.1 discusses recommended estimates of factored dead load bridge responses. Section 11.2.3 presents findings on including cross-frame detailing method effects directly in the structural analysis. Section 11.1.3 discusses recommendations for fit conditions. Sections 11.1.4 concludes with recommended framing arrangements.

11.1.1 Recommended Estimates of Factored Dead Load Bridge Responses

From a technical viewpoint, there is no reason why lack-of-fit effects should not and cannot be included in any refined analysis of a bridge structural system. The handling of these effects is very similar to the calculation of the effects of temperature change. The associated concepts are very straightforward and simple at the fundamental level associated with their implementation within a structural analysis. These concepts are taught in nearly every undergraduate strength of materials and introductory structural analysis class. The corresponding detailed effects of the basic lack-of-fit on the internal forces and stresses in I-girder bridge structures is relatively complex. This complexity is best addressed by including the lack-of-fit effects in the structural analysis. Nevertheless, at the present time (2015), inclusion of the lack-of-fit effects from SDLF or TDLF detailing is not well supported in professional analysis and design software. An engineer who wishes to include these effects typically must to a significant amount of calculations external to the software, then input information such as, for example, pseudo temperature increases or decreases in

the cross-frame members that produce the same initial strains as the initial lack-of-fit displacements. Until this situation is improved, and for simple sanity checking of the results from these types of analysis calculations when they are performed, the basic estimates recommended in Table 76.

The first column of Table 76 lists the primary responses that need to be calculated for the design of the structural components in a curved and/or skewed I-girder bridge. The second through fourth columns list recommended calculations of the factored DL responses including the consideration of the SDLF and/or TDLF detailing effects as appropriate for curved radially-supported, straight skewed, and curved and skewed I-girder bridges.

In curved I-girder bridges, the locked-in force effects from SDLF and TDLF detailing tend to be additive with the corresponding DL effects. The additional forces associated with TDLF detailing tend to be prohibitive for highly-curved I-girder bridges, and thus TDLF detailing of these types of structures is strongly discouraged. Therefore, Table 76 does not address estimates for curved bridges detailed for TDLF. The following procedures do not address the effects due to the bracket loads supporting the eccentric deck overhangs during deck construction. These effects may be estimated separately as described in AASHTO LRFD Article C6.10.3.4 and combined as appropriate with the other dead load effects discussed below.

Table 76. Recommended estimates of factored dead load bridge responses for curved and/or skewed bridges in their final constructed condition, in lieu of including lack-of-fit directly within the structural analysis.

Responses	(1) Curved Radially-Supported	(2) Straight Skewed	(3) Curved and Skewed
CF Forces	γ_p (2.0 SDL + ADL*) for SDLF†, except γ_p (SDL + ADL) for chords of X-Type CFs	γ_p TDL for SDLF, ($\gamma_p - 0.4$) TDL for TDLF	Same as (1)
Flange lateral bending	γ_p (1.2 SDL + ADL*) for SDLF†	($\gamma_p - 0.5$) SDL + γ_p ADL* for SDLF ($\gamma_p - 0.4$) TDL for TDLF	Same as (1)
Major-axis bending	γ_p TDL for SDLF†	γ_p TDL for SDLF‡ γ_p TDL for TDLF§	Same as (1)
Vertical Reactions	γ_p TDL for SDLF† For simply supported bridges, DLF tends to increase the smallest reactions at the girders on the inside of the curve¶	γ_p TDL for SDLF‡\\ γ_p TDL for TDLF§\\ For simply-supported bridges the tendency for uplift on the girder bearings at the obtuse corners of the bridge plan is lessened by the use of DLF detailing based on RA cambers (compared to the use of LGA cambers)	For simply-supported bridges¶**: Worst-case maximum reactions††: • γ_p (1.2 SDL + ADL) for SDLF†, when the length of girder on the inside of the curve is increased by the skew • γ_p (1.6 SDL + ADL) for SDLF†, when the length of girder on the outside of the curve is increased by the skew

* ADL = Additional Dead Load

†TDLF detailing is strongly discouraged for curved bridges with $L_s/R > 0.03$ ±, where L_s is the span length along the centerline of the bridge.

‡ Contingent on the use of discontinuous CF lines with $L_b \geq \max(4b_f, 0.4L_{b.adj})$ for all unbraced lengths within the span, where b_f is the largest girder flange width within on either side of a given CF, and $L_{b.adj}$ is the smallest adjacent unbraced length.

§ Contingent on $I_s \leq 1.0$ ± and $L_b \geq \max(4b_f, 0.4L_{b.adj})$.

¶ The influence of DLF detailing on the reactions for curved continuous-span bridges is relatively complex; If potential uplift and/or increases in the reactions are a concern, a Dead Load Fit Refined Analysis (DLF RA) is recommended.

\\ If potential uplift at obtuse corners of the bridge plan is a concern, the uplift condition can be estimated conservatively by using LGA for the targeted DL condition and NLF RA for additional dead and/or live loads.

** In curved and skewed I-girder bridges, the CF lines need to be contiguous out within the spans to develop the width of the structural system; in some cases, this requirement can exacerbate potential uplift conditions at obtuse corners of the bridge plan that are on the inside of the curve.

†† If potential uplift at obtuse corners of the bridge plan is a concern, a DLF RA should be considered.

For curved I-girder bridges, with or without skew and with a maximum L_s/R greater than 0.03 $\pm$, the additional locked-in force effects may be accounted for approximately by multiplying the unfactored SDL cross-frame forces by the factor 2.0 and the unfactored SDL flange lateral bending stresses by the factor 1.2 prior to applying the AASHTO LRFD DL factor γ_p. For X-type cross-frames, SDLF detailing has a substantial effect only on the cross-frame diagonal forces; therefore, the above factor of 2.0 need only be applied to the diagonal forces for these types of cross-frames. This research shows that these factors provide a reasonable coarse approximation of the SDLF detailing effects for a range of curved bridges with L_s/R ranging from 0.2 to 0.5. The smaller increase in the flange lateral bending stresses is due to the attribute that the ratio of the locked-in effects from SDLF detailing to the effects from the horizontal curvature generally tend to be smaller for the flange lateral bending stresses than for the cross-frame forces. For a bridge where the factored SDL cross-frame forces are one-half of the factored TDL forces, and the factored TDL forces are one-half of the total factored forces for design, the total factored cross-frame forces are increased by a factor of 1.25. For bridges with smaller L_s/R, the horizontal curvature effects are smaller, and hence the scaled SDL cross-frame forces and girder flange lateral bending stresses are smaller.

Table 76 shows that the girder major-axis bending stresses and vertical reactions in curved radially-supported I-girder bridges may be estimated sufficiently from a refined analysis that does not include the consideration of the initial lack-of-fit from the SDLF detailing of the cross-frames. One caveat associated with this recommendation, shown as a footnote to the table, is that the influence of DLF detailing on the reactions for curved continuous-span bridges is relatively complex. In cases where potential uplift and/or

increase in the reactions are a concern in these types of bridges, it is recommended that a refined analysis that includes the consideration of the initial lack-of-fit displacements should be considered. This type of analysis is referred to as a Dead Load Fit Refined Analysis (DLF RA) in the table.

The third column of Table 76 lists recommended calculations of the factored DL responses for straight skewed I-girder bridges, including the consideration of the SDLF and/or TDLF detailing effects as appropriate. For straight skewed I-girder bridges detailed for SDLF, direct calculation of the influence of DLF detailing on the girder vertical reactions and major-axis bending stresses should be considered. For straight skewed I-girder bridges detailed for TDLF, the skew index, I_s, should be less than 1.0 $\pm$ in order to avoid potential significant impacts from nuisance transverse stiffness on the girder reactions and major-axis bending stresses.

For straight skewed I-girder bridges that are detailed for TDLF, the TDL cross-frame forces and flange lateral bending stresses, when determined from a refined analysis not including the influence of DLF detailing, may be reduced to account for the corresponding locked-in forces introduced into the structural system during the steel erection. In this case, a net reduced load factor of ($\gamma_p - 0.4$) may be applied to the unfactored TDL cross-frame forces and flange lateral bending stresses, where γ_p is the required AASHTO LRFD factor on DL and 0.4 is an estimated lower-bound estimate of the internal locked-in force effect (AASHTO LRFD multiplies the locked-in force effects by a load factor of 1.0). It should be noted that larger beneficial locked-in force effects can be calculated in many situations by performing a direct DLF RA. In straight skewed bridges detailed for a TDLF, the engineer should also check the cross-frame forces and the flange lateral bending stresses

for the fit-up force effects during the steel erection. These effects may be estimated as the negative of the corresponding unfactored concrete dead load force effects, which should then be multiplied by γ_p.

This research recommends that the AASHTO LRFD load factor, γ_p, should be applied directly to the DC cross-frame forces for straight skewed bridges detailed for SDLF. Significant cross-frame force reductions are achievable in straight skewed bridges detailed for SDLF; however, in the most extreme cases studied by this research, incidental and elastic deformation effects in the structural system lead to negligible corresponding locked-in force effects in the cross-frames for SDLF. This research found that the SDLF locked-in force effects on the girder flange lateral bending stresses may be estimated conservatively as 0.5 of the f_ℓ values determined from a refined analysis not considering the initial lack-of-fit (i.e., a NLF RA). Therefore, Table 76 recommends a net reduced load factor of ($\gamma_p - 0.5$) on the SDL for these bridges. The overall influence of this beneficial effect is relatively small, since the SDL stresses are often a fraction of the overall required design stresses, plus these stresses are multiplied by 1/3 in the application of the AASHTO LRFD one-third rule for the strength design. Therefore, a simpler conservative approximation would be to use the same approach as recommended for the cross-frames for SDLF of straight skewed bridges, i.e., simply factor the SDL f_ℓ values obtained from a NLF RA by γ_p, neglecting the beneficial locked-in force effects from the SDLF detailing. It should be emphasized that the best estimate of the internal force reductions, when either SDLF or TDLF is employed, is obtained by calculation of the locked-in force effects directly within the structural analysis.

The fourth column of Table 76 lists recommended calculations of the factored DL responses for curved and skewed I-girder bridges. This research found that the cross-frame forces and the girder flange lateral bending and major-axis bending stresses can be estimated conservatively for curved and skewed bridges by applying the same recommendations discussed above for curved radially-supported bridges. Unfortunately, the accurate estimation the girder reactions is rather difficult in curved and skewed I-girder bridges. Therefore, if potential uplift and/or increases in the reactions are a concern in these types of bridges, it is recommended that a DLF RA be considered.

All of the above recommendations are based on the use of the girder deflections determined from an accurate refined analysis for setting the girder cambers, and the associated cross-frame drops and corresponding connection plate rotational orientations for SDLF or TLDF detailing. For straight skewed I-girder bridges designed using Line Girder Analysis (LGA), the LGA cambers may be used for detailing of the cross-frames. However, various limitations associated with doing so should be recognized. Section 6.2.3 details these considerations. In short, the use of LGA girder deflections for SDLF or TDLF detailing of the cross-frames in straight skewed bridges theoretically imposes (or allows) the girders to respond under the targeted DL condition (SDL for SDLF or TDL for TDLF) precisely in the manner assumed within the LGA. This means that, theoretically, the girders all deflect independently of one another, only in the vertical direction, and the cross-frame forces and girder flange lateral bending stresses are effectively zero. As discussed in detail in Section 6.2.2, various incidental effects can result in these theoretical or ideal conditions not being exactly achieved. Nevertheless, the cross-frame force and flange lateral bending stress reductions associated with the use of LGA cambers tend to be

substantial. This research provides a lower-bound estimate of the beneficial locked-in force effects as 0.65 of the corresponding responses obtained from a NLF RA. That is, one can expect these forces and stresses to be reduced to values less than or equal to 35 % of the calculated NLF RA responses.

Of course, if LGA is used for the design of a straight skewed I-girder bridge, the structural analysis does not provide any information regarding the corresponding cross-frame forces and girder flange lateral bending stresses. It is important to note that the above theoretical results associated with SDLF or TDLF based on LGA girder deflections occur ONLY in the targeted DL condition. The DL results for any other loading, aside from the approximations associated with live load distribution factors, completely miss the fact that the girders, the cross-frames and the composite bridge deck respond as a three-dimensional system

11.1.2 Procedures for Including Cross-Frame Detailing Effects Directly in the Structural Analysis

For curved and skewed bridges, there can be major advantages in terms of reduction of the cross-frame forces and girder flange lateral bending stresses from the SDLF or TDLF detailing and the behavior emanating from the skew effects. However, in curved radially-supported bridges, the locked-in forces emanating from the horizontal curvature and SDLF or TDLF detailing effects tend to be additive with the internal dead load forces. It is possible to account for beneficial reductions or the increases in the cross-frame forces and girder flange lateral bending stresses by using the most accurate and direct method to calculate the locked-in force effects due to SDLF and TDLF detailing - including the initial strains or stresses due to the initial lack-of-fit directly in the structural analysis. Any

software that is capable of modeling thermal loading or fixed-end force effects has the ability to include the initial strains due to the initial lack-of-fit. In addition, although TDLF detailing is strongly discouraged for horizontally curved I-girder bridges, it is important to have a method to assess the additive TDLF effects in curved bridges that are detailed in this way.

The initial strains can be obtained in refined analysis software by imposing the vertical deflections associated with the girder dead load cambers. Conducting the displacement analysis in refined analysis software to obtain the initial strains due to detailing methods can be time consuming and not all bridge software is capable of running such an analysis. A tool, GT-LOFT, was developed as part of this research to facilitate the calculation of the cross-frame initial strains associated with their detailing. A thorough discussion of the calculation of the initial strains via GT-LOFT, with examples, is provided in Chapter 3.

11.1.3 Recommended Fit Conditions

The quantitative data from this research supports the fit condition recommendations of the NSBA guidelines documents (NSBA 2014) and (NSBA 2015), which are summarized in Tables 77 and 78 below. These tables subdivide I-girder bridges into several classifications based on simple quantifications of the magnitudes of their horizontal curvature and/or skew. It is suggested that bridges with L/R less than or equal to 0.03 in all of their spans may be considered effectively as straight bridges when making decisions about the fit condition. In addition, it is suggested that bridges that have a maximum skew angle less than or equal to 20 (with an angle of zero indicating zero skew) may be considered effectively as non-skewed with regard to fit decisions. The top rows of Table 77 indicate that any fit condition is acceptable for bridges that satisfy both of these limits.

The limits are shown with the qualification "+/ – " to emphasize that there is no dramatic shift in the responses when the limits are crossed, but that they are approximate values where a shift in the fit decision should be considered.

Table 77. Recommended fit conditions for straight bridges (including horizontally curved bridges with L/R in all spans ≤ 0.03 +/-), from NSBA (2014) and (2015).

Square Bridges and Skewed Bridges up to 20 deg +/- Skew			
	Recommended	***Acceptable***	***Avoid***
Any span length	Any		None
Skewed Bridges with Skew > 20 deg +/- and $I_s \leq 0.30$ +/-			
	Recommended	***Acceptable***	***Avoid***
Any span length	TDLF or SDLF		NLF
Skewed Bridges with Skew > 20 deg +/- and $I_s > 0.30$ +/-			
	Recommended	***Acceptable***	***Avoid***
Span lengths up to 200 ft +/-	SDLF	TDLF	NLF
Span lengths greater than 200 ft +/-	SDLF		TDLF & NLF

Table 78. Recommended fit conditions for horizontally curved bridges ($(L/R)_{max} > 0.03$ +/-), from NSBA (2014) and (2015).

Radial or Skewed Supports			
	Recommended	***Acceptable***	***Avoid***
Span lengths greater than 250 ft +/- and $L/R > 0.1$ +/-	NLF	SDLF	TDLF
All other cases	SDLF	NLF	TDLF

The remainder of Table 77 addresses the recommended fit condition for bridges that have significant skew but are effectively straight when it comes to a decision about the fit condition. The middle recommendation in Table 77 pertains to bridges in which the skew index I_s (Eq. (1)) is less than or equal to 0.30. In these cases, the influence of the skew is generally such that either TDLF or SDLF detailing should be acceptable. However, NLF is not recommended for bridges where any of the skew angles θ are larger than 20 degrees. The last two rows of Table 77 pertain to straight I-girder bridges with $I_s > 0.30$. For these

types of bridges, SDLF is recommended in all cases, and TDLF is considered acceptable up to approximately 200 ft span lengths. For straight I-girder bridges with span lengths larger than 200 ft, skew greater than 20^o and $I_s > 0.30$ it is considered wise to avoid TDLF.

When SDLF and TDLF detailing are used for straight skewed bridges, it is recommended that the engineer should account for the beneficial reduction of the cross-frame forces and flange lateral bending stresses due to the locked-in force effects introduced into the structure during the erection.

Table 78 addresses the recommended fit condition for horizontally curved I-girder bridges. This table suggests that if the bridge has any span lengths greater than 250 ft +/- in combination with $L/R > 0.1$ +/-, NLF should be considered. Otherwise, SDLF is recommended. In these cases, the engineer can safely neglect the additive locked-in force effects introduced into the system during the erection. These recommendations apply irrespective of any skew of the bearing lines. Lastly, Table 78 recommends that TDLF should be avoided in all cases for bridges that are classified as horizontally curved with respect to the consideration of the fit condition.

11.1.4 Recommended Framing Arrangements

In addition, this research recommends that the cross-frames can be staggered within the bridge spans as shown in Figures 237, 238, and 239 to both dramatically reduce the number of cross-frames required in the bridge as well as to reduce overall transverse nuisance stiffness effects. (One should note that staggering of the cross-frames tends to increase the flange lateral bending stresses, and therefore increases the girder flange sizes; however, this increase in flange size often not significant. The increased flange size and cost is often much less than the cost of larger cross members and connections.)

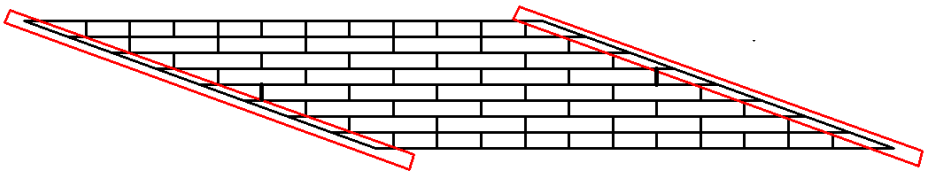

Figure 237. Recommended staggered framing arrangements for straight parallel-skewed bridges.

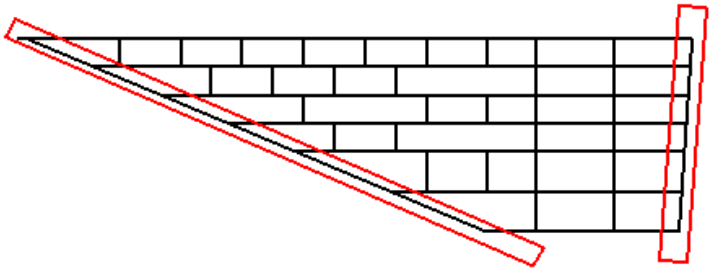

Figure 238. Recommended staggered framing arrangements for straight skewed bridges with only one bearing line having a substantial skew angle.

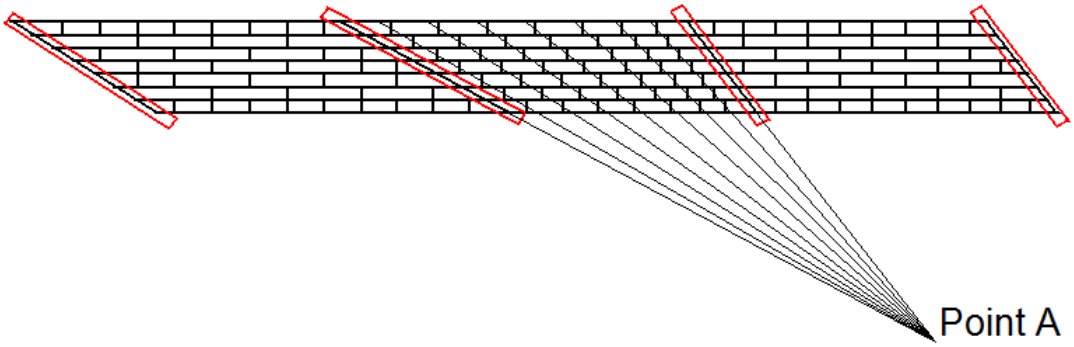

Figure 239. Recommended staggered framing arrangements for straight skewed bridges with different skew angles of the bearing lines.

11.2. Further Research Needs

This research has proposed improved design, detailing and erection guidelines to ensure fit-up of skewed and/or curved steel I-girder bridges. These guidelines provide a clear understanding of the implications of various framing arrangements, cross-frame detailing methods, and erection procedures on the ease of fit-up during the steel erection, achievement of the targeted constructed geometry, and generation of locked-in stresses in the cross-frames and girders. Nevertheless, the following areas merit further study:

11.2.1 Early Concrete Deck Stiffness and Strength

Cross-frame detailing methods can have a significant influence on the bridge responses in the completed bridge as well as during construction. The detailing methods are significantly influenced by the camber calculations as the cross-frame detailing is set based on the camber profiles. In continuous-span bridges, the construction often involves staged deck placement. The portion of the deck that has already been placed contributes to the stiffness of the bridge. In the current research, this contribution to stiffness of concrete was neglected, leading to an over-estimate of TDL cambers. More extensive coupled field and analytical evaluation of the effects of early concrete deck stiffness and strength gains, including the influence of staged concrete deck placement would be valuable to better quantify the effects of TDLF detailing on the completed bridge as well as during construction. Prior research addressing this consideration has been limited to only a few bridges and a few parameters of the concrete mix design and methods of construction. A more comprehensive understanding of the actual early-age behavior during and after placement of concrete decks is needed.

11.2.2 Further Cross-Frame Analysis and Design Improvements

With the increasing utilization of skew and curvature in steel I-girder bridges, requirements for cross-frames to be designed as primary members in horizontally curved bridges, and the improvements in refined analysis methods, the need for more detailed analysis and improved design of diaphragms and cross-frames arises. Areas that need to be researched to achieve improvements in cross-frame analysis and design include, but are not limited to: (1) Improved fatigue design of cross-frames using accurate refined analysis, (2) Improved consideration of girder stability bracing requirements, (3) Improved accounting for the true stiffness of cross-frames in refined analysis methods, and (4) Simplified design of tee (WT) section struts. These topics are discussed in more detail below:

11.2.2.1 Improved Fatigue Design of Cross-Frames Using Accurate Refined Analysis

A 0.75 factor on the RA CF stress range, under the loads of two vehicle traveling in two separate transverse positions, is suggested by the AASHTO *LRFD Bridge Design Specifications*, C6.6.1.2.1. It is apparent that this suggestion is based mostly on engineering judgment. Some of the problems due to this suggestion are:

- The current provisions for fatigue loading are based upon longitudinal member behavior. Cross-frame are transverse members and may not be applicable to these provisions.
- The fatigue truck configuration for transverse members such as cross-frames is not clear.

11.2.2.2 Improved Consideration of Girder Stability Bracing Requirements

Provisions for girder stability bracing strength and stiffness are available in the AISC (2010) Specifications and from other sources such as Helwig and Yura (2012) and Yura (2001). These provisions are straightforward and are useful in many cases for the design of cross-frames for steel I-girder bridges. However, these provisions have a number of limits of applicability for common structural conditions in I-girder bridges. Specifically, improvements and extensions are needed in following areas:

- The current stability bracing provisions and research studies to date have not fully addressed the stability bracing requirements within the negative moment regions of composite continuous-span I-girders, particularly regarding the beneficial effects from the concrete deck stiffness in combination with the torsional and/or lateral bracing from cross-frames and other bridge components.

- The current stability bracing provisions focus largely on the stiffness and strength demands placed on bracing components in situations where the I-girders being braced are nominally straight, but with unavoidable geometric imperfections, and where the I-girders are acting as isolated members in supporting the loads rather than as part of a complex three-dimensional structural system. The calculated bracing demands are essentially due to second-order effects associated with the member internal forces and the initial member imperfections out of the plane of the web in this idealized isolated configuration. The true cross-frame forces in curved and/or skewed I-girder bridges actually may be impacted by only a small extent due to stability bracing effects in many situations. Research is needed to determine when second-order effects such as those addressed by the current stability bracing provisions are important and how to best

incorporate the consideration of these effects in appropriate simplified design criteria for all types of I-girder bridge geometries.

11.2.2.3 Improved accounting for the true stiffness of cross-frames in refined analysis methods.

Single angle and flange-connected tee section struts in cross-frame members are typically subjected to eccentric axial loading, due to their connection to gusset plates and/or girder connection plates as discussed in Section 2.1. As discussed in this section, this research has followed the recommendation from AASHTO LRFD Article 5.6.3.3.4 in reducing the axial stiffness of these types of members by the scale factor 0.65. Chapter 10 provides analysis results for a straight severely skewed bridge which indicate that the cross-frame stresses and the bridge deflections are insensitive to the specific values of this cross-frame stiffness. In addition, the authors observe that the bridge responses are relatively insensitive to the cross-frame properties in the benchmark examples discussed in Chapter 3. However, the studies in these sections involve only two bridges. In some straight skewed bridges having extreme nuisance stiffness effects, and in some horizontally curved bridge geometries (possibly wide horizontally curved bridges where the cross-frames framing in the radial direction do not act essentially as rigid components compared to the I-girders) the bridge responses may sensitive to the specific cross-frame stiffness values.

Recent research by Battistini et al. (2014) has provided equations for a variable stiffness reduction factor, for different types of cross-frames composed of single angle members, that can be applied in lieu of the simpler 0.65 factor recommended by AASHTO. Bridge system sensitivity analyses should be conducted to gage the importance of using these more accurate stiffness reduction factors. In addition, additional appropriate factors should be

evaluated and studied for specific cases involving flange-connected tee (WT) section cross-frame members.

11.2.2.4 Simplified design of tee (WT) section struts.

Streamlined procedures are currently available in AISC (2010) and in the AASHTO LRFD Specifications for the design of single angle cross-frame members subjected to eccentric axial loading via their connections to gussets or girder connection plates. These procedures are based on the use of a modified effective length factor that accounts for the angle geometric properties, the eccentric axial loading, and the common nature of the restraints provided by the end connections (White 2012). Similar procedures are not available at present for tee sections; instead, designers must check WT cross-frame members as general eccentrically-loaded singly-symmetric beam-columns, including the corresponding relatively complex evaluation of the strength of these member types under pure axial compression and under pure flexure about an axis parallel to the flange. It would be desirable to have a streamlined design procedure for these types of members similar to that for single angles. The challenges involved include the fact that tee section members loaded as cross-frame members commonly have enhanced beam-column resistances. This is due to the nature of their single symmetry as well as the nature of the eccentric loading. This enhanced resistance is not commonly recognized with the current AISC (2010) and AASHTO LRFD beam-column strength equations. The challenge will be largely whether these enhanced resistances can be recognized within new simplified calculation procedures.

11.2.3 Implementation and Validation of Analysis Methods for Handling of Lack-of-Fit in Professional Bridge Design Software

It is possible to directly calculate the internal "locked-in forces" associated with SDLF or TDLF detailing directly within either a 2D grid or 3D Finite Element Analysis. Resulting "Dead Load Fit Refined Analysis" (DLF RA) procedures provide a much more accurate characterization of the beneficial (subtractive) and non-beneficial (additive) locked-in internal forces and stresses due to these cross-frame detailing methods. Their implementation and adoption in steel I-girder bridge design practice can lead to significant economies. The handling of these effects is very similar to the calculation of the effects of temperature change. The associated concepts are very straightforward and simple at the fundamental level associated with their implementation within a structural analysis. These concepts are taught in nearly every undergraduate strength of materials and introductory structural analysis class. The corresponding detailed effects of the basic lack-of-fit on the internal forces and stresses in I-girder bridge structures is relatively complex. This complexity is best addressed by including the lack-of-fit effects in the structural analysis.

Nevertheless, at the present time (2015), inclusion of the lack-of-fit effects from SDLF or TDLF detailing is not well supported in professional analysis and design software. An engineer who wishes to include these effects typically must to a significant amount of calculations external to the software, then input information such as, for example, pseudo temperature increases or decreases in the cross-frame members that produce the same initial strains as the initial lack-of-fit displacements. Software providers should implement the types of procedures discussed in Chapter 3. These procedures should then be thoroughly tested and their benefits demonstrated in practical curved and skewed I-girder bridge design.

APPENDIX A

3D FEA RESULTS OF BRIDGE NISSS4 INLCUDING THE INITIAL STRAINS CALCULATED BY GT-LOFT

This appendix provides more detailed analytical results for straight skewed bridge NISSS4 used an example of using GT-LOFT to determine the initial strains associated with No Load Fit (NLF), Steel Dead Load Fit (SDLF) and Total Dead Load Fit (TDLF) detailing methods. This bridge has a span length of 150 ft and severe skew angles of 70 degrees. For illustration purposes, all girders have the same prismatic section (1.125 in. x 16 in. top flanges and 2 in. x 18 in. bottom flanges). The intermediate cross-frames are X type, and the end cross-frames are K type. All cross-frame members are L6x6x1.

These results are with SDLF and TDLF detailing effects included via the initial strains calculated by GT-LOFT. Since the nonlinearity effects in bridge NISSS4 are insignificant, the responses are approximately the same with engineering and log strains. Thus, this appendix shows only the responses with the initial engineering strains.

The initial strains for SDLF and TDLF detailing calculated by GT-LOFT are comparable to the initial strains for SDLF and TDLF detailing calculated by an accurate refined analysis. There are small but negligible difference in the initial strains calculated by GT-LOFT and an accurate refined analysis. The responses of bridge NISSS4 are comparable using the initial strains from GT-LOFT and the initial strains from an accurate refined analysis.

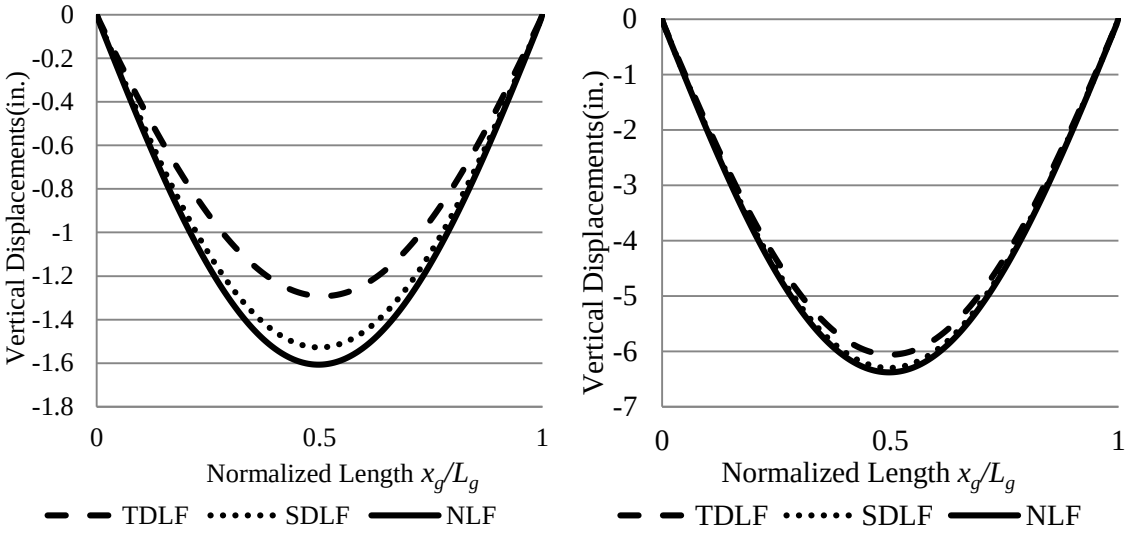

Figure A-1. NISSS4 G1 SDL and TDL 3D FEA vertical displacements

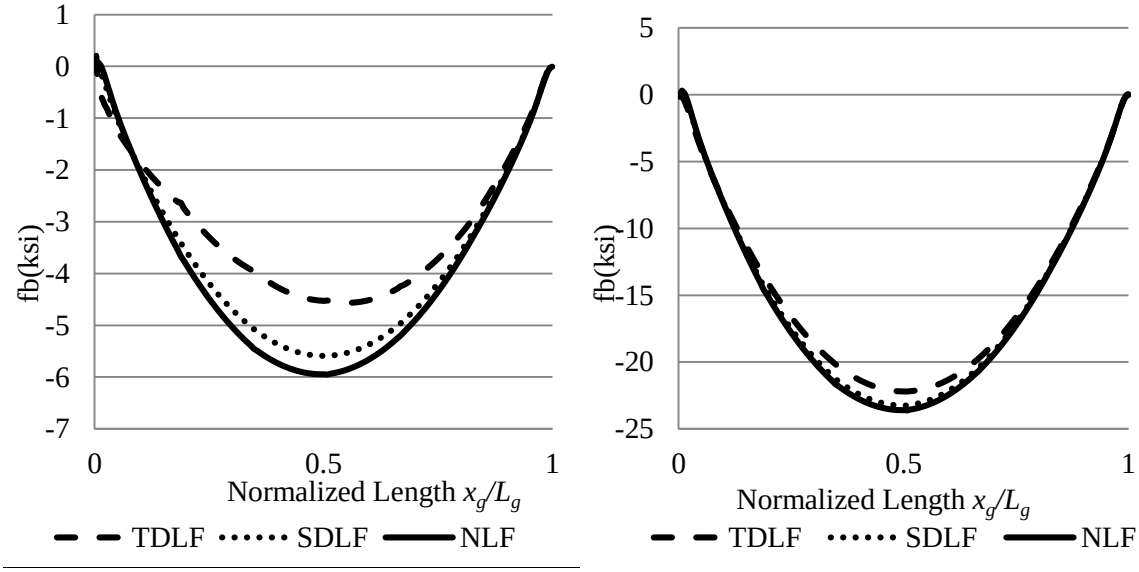

Figure A-2. NISSS4 G1 SDL and TDL 3D FEA top flange major-axis bending stresses

Table A-1. NISSS4 3D FEA maximum axial forces in CF diagonals under SDL (kips)

CF	Detailing Method	CF Location		
		G1-G2	G2-G3	G3-G4
1	NLF	1.3	0.2	0.4
	SDLF	0.8	0.1	0.8
	TDLF	7.0	0.4	1.7
2	NLF	0.4	0.5	1.2
	SDLF	0.3	0.6	0.5
	TDLF	2.7	3.4	4.2
3	NLF	1.9	0.8	0.6
	SDLF	0.5	0.6	0.5
	TDLF	6.1	2.4	1.4
4	NLF	1.5	0.5	1.1
	SDLF	0.5	0.5	0.5
	TDLF	3.0	0.4	1.9
5	NLF	1.1	0.8	1.4
	SDLF	0.5	0.6	0.5
	TDLF	2.2	2.3	2.9
6	NLF	0.6	0.6	1.9
	SDLF	0.4	0.5	0.5
	TDLF	1.6	3.5	6.0
7	NLF	0.9	0.8	0.7
	SDLF	0.5	0.2	0.3
	TDLF	3.4	2.0	4.1
8	NLF	0.1	NA	1.6
	SDLF	0.7	NA	0.6
	TDLF	2.8	NA	7.1

Table A-2. NISSS4 3D FEA maximum axial forces in CF diagonals under TDL (kips

CF	Detailing Method	CF Location		
		G1-G2	G2-G3	G3-G4
1	NLF	5.1	0.9	1.8
	SDLF	3.0	0.8	2.1
	TDLF	3.2	0.5	3.1
2	NLF	1.5	1.7	4.5
	SDLF	1.4	1.2	3.9
	TDLF	2.2	2.2	2.9
3	NLF	7.4	3.2	2.2
	SDLF	5.8	2.6	2.1
	TDLF	0.5	1.6	0.4
4	NLF	5.7	1.7	4.3
	SDLF	4.7	1.8	3.7
	TDLF	1.6	1.7	1.7
5	NLF	4.4	3.2	5.6
	SDLF	3.7	2.6	4.7
	TDLF	1.5	1.6	1.6
6	NLF	2.3	2.1	7.3
	SDLF	2.1	1.6	5.6
	TDLF	0.3	2.0	0.6
7	NLF	3.5	3.3	2.8
	SDLF	3.0	2.6	2.3
	TDLF	2.9	0.7	2.1
8	NLF	0.3	NA	6.2
	SDLF	0.5	NA	4.1
	TDLF	2.6	NA	2.5

APPENDIX B

3D FEA RESULTS OF BRIDGE (B) NISCR2 INLCUDING THE INITIAL STRAINS CALCULATED BY GT-LOFT

This appendix provides more detailed analytical results for curved radially-supported bridge (B) NISCR2 used an example of using GT-LOFT to determine the initial strains associated with No Load Fit (NLF), Steel Dead Load Fit (SDLF) and Total Dead Load Fit (TDLF) detailing methods. This bridge has a span length of 150 ft and centerline radius of curvature of 438 ft. All of the girders have four section changes. The intermediate cross-frames are X type, and the end cross-frame are K type. All cross-frame members are L6x6x3/4

These results are with SDLF and TDLF detailing effects included via the initial strains calculated by GT-LOFT. Since the nonlinearity effects in bridge NSICR2 are insignificant, the responses are approximately the same with engineering and log strains. Thus, this appendix shows only the responses with the initial engineering strains.

The initial strains for SDLF and TDLF detailing calculated by GT-LOFT are comparable to the initial strains for SDLF and TDLF detailing calculated by an accurate refined analysis. There are small but negligible difference in the initial strains calculated by GT-LOFT and an accurate refined analysis. The responses of bridge NISCR2 are comparable using the initial strains from GT-LOFT and the initial strains from an accurate refined analysis.

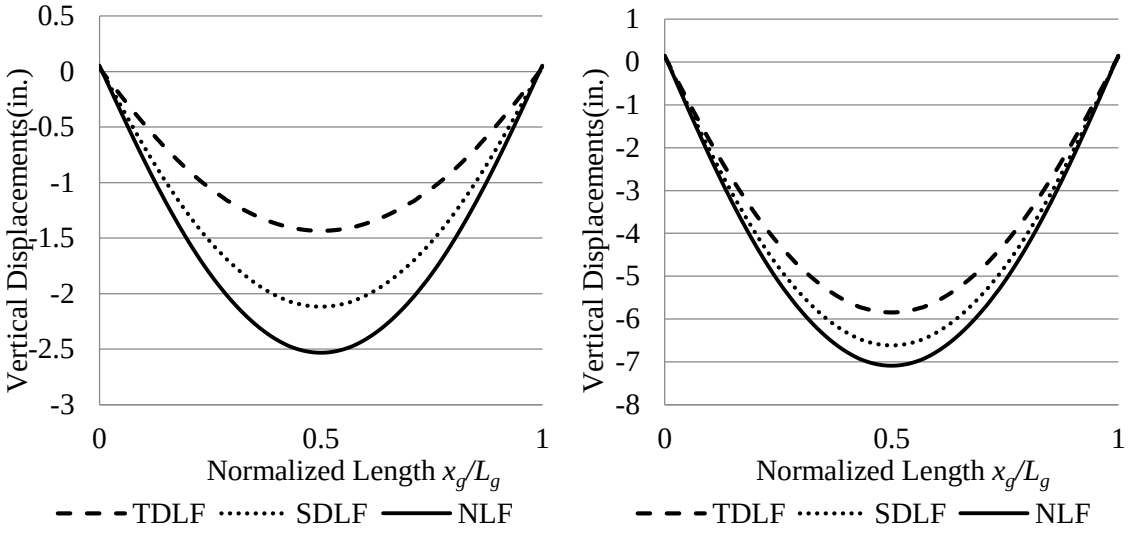

Figure B-1. (B) NISCR2 G1 SDL and TDL 3D FEA vertical displacements

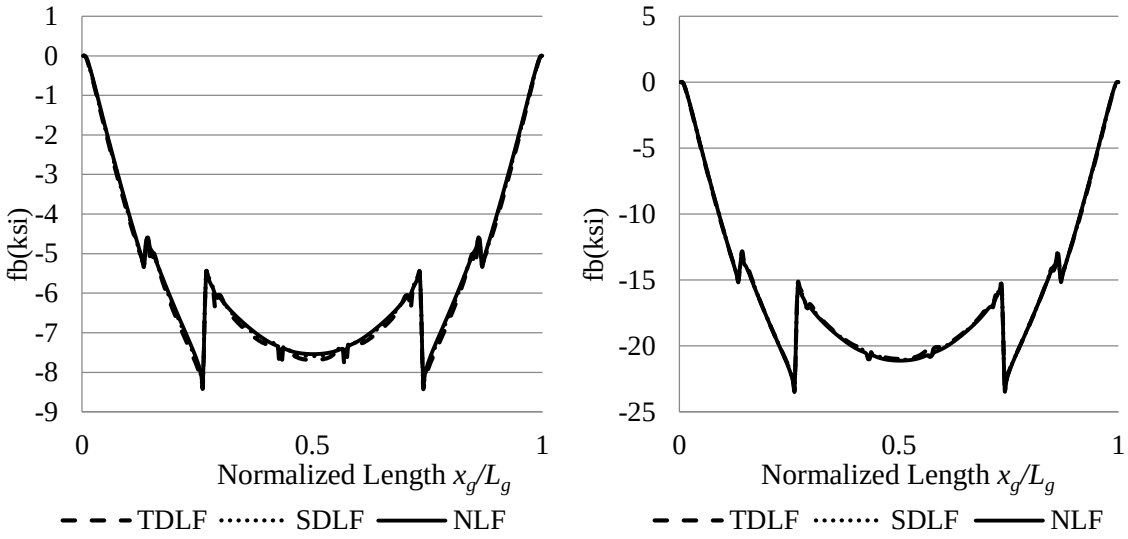

Figure B-2. (B) NISCR2 G1 SDL and TDL 3D FEA top flange major-axis bending stresses.

Table B-1. (B) NISCR2 3D FEA maximum axial forces in CF diagonals (kips)

CF	Detailing Method	Load Type & CF Location					
		SDL G1-G2	SDL G2-G3	SDL G3-G4	TDL G1-G2	TDL G2-G3	TDL G3-G4
1	NLF	1.1	0.9	0.7	4.0	3.2	2.4
	SDLF	1.0	0.6	0.3	3.8	2.9	1.9
	TDLF	1.0	0.0	-0.2	3.8	2.1	1.2
2	NLF	4.2	5.2	4.0	12.1	16.6	11.3
	SDLF	10.3	11.6	9.8	18.3	23.0	17.1
	TDLF	18.1	19.8	17.2	26.3	31.2	24.5
3	NLF	7.4	9.9	6.7	21.4	31.0	19.9
	SDLF	18.9	21.4	17.8	32.8	42.3	30.7
	TDLF	30.9	33.9	29.9	44.5	54.3	42.5
4	NLF	8.6	11.6	8.1	25.4	36.1	24.2
	SDLF	23.6	26.6	22.2	40.0	50.7	37.9
	TDLF	37.7	41.8	36.3	53.6	65.3	51.5
5	NLF	8.6	11.6	8.1	25.4	36.1	24.1
	SDLF	23.6	26.6	22.2	40.0	50.7	37.9
	TDLF	37.7	41.8	36.3	53.6	65.3	51.5
6	NLF	7.4	9.9	6.7	21.5	31.0	19.8
	SDLF	18.9	21.4	17.7	32.8	42.3	30.6
	TDLF	30.9	33.8	29.8	44.5	54.3	42.4
7	NLF	4.3	5.2	3.9	12.5	16.4	10.8
	SDLF	10.3	11.5	9.7	18.6	22.7	16.7
	TDLF	17.9	19.8	17.3	26.3	31.0	24.3
8	NLF	0.8	0.0	0.1	2.8	0.1	-0.2
	SDLF	0.9	0.3	0.2	3.0	0.5	0.0
	TDLF	0.4	1.2	0.5	2.7	1.7	0.7

APPENDIX C

2D-GRID RESULTS OF BRIDGE NISSS4 INLCUDING THE INITIAL FIXED-END FORCES CALCULATED BY GT-LOFT

This appendix provides more detailed analytical results for straight skewed bridge NISSS4 used an example of using GT-LOFT to determine the initial fixed-end forces associated with No Load Fit (NLF), Steel Dead Load Fit (SDLF) and Total Dead Load Fit (TDLF) detailing methods. This bridge has a span length of 150 ft and severe skew angles of 70 degrees. For illustration purposes, all girders have the same prismatic section (1.125 in. x 16 in. top flanges and 2 in. x 18 in. bottom flanges). The intermediate cross-frames are X type, and the end cross-frames are K type. All cross-frame members are L6x6x1.

Table C-1. NISSS4 girder properties

Girder	Length (ft)	Area (in^2)	I_y (in^4)	I_z (in^4)	J (in^4)	J_{new} (in^4)
G1	150	99	1357	88213	61	4906,610@5,188
G2	150	99	1357	88213	61	376,(3166,1652)@4,3166,610,4906
G3	150	99	1357	88213	61	4906,610,(3166,1652)@4,3166,376
G4	150	99	1357	88213	61	188,610@5,4906

Table C-2. NISSS4 cross-frame properties (Timoshenko Approach)

CFs	Length (in)	Area (Chords Only) (in^2)	Shear Area (in^2)	I_y (Chords Only) (in^4)	$I_{z\_equiv.}$ (in^4)	J (Chords Only) (in^4)
End	96	22	3.40	71	21142	7.4
Interm.	281	22	17.63	71	21142	7.4

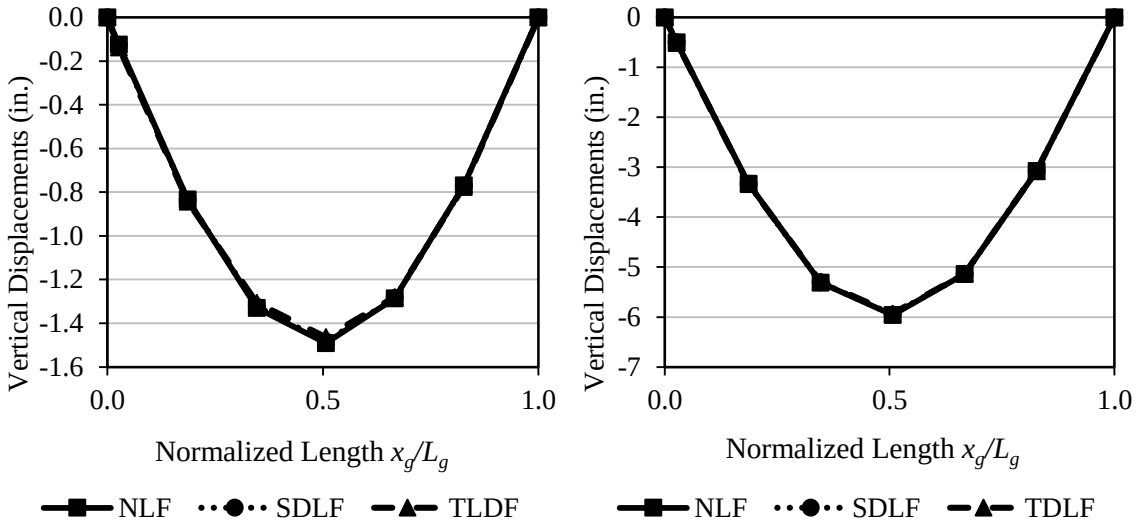

Figure C-1. NISSS4 G1 SDL and TDL 2D-Grid vertical displacements

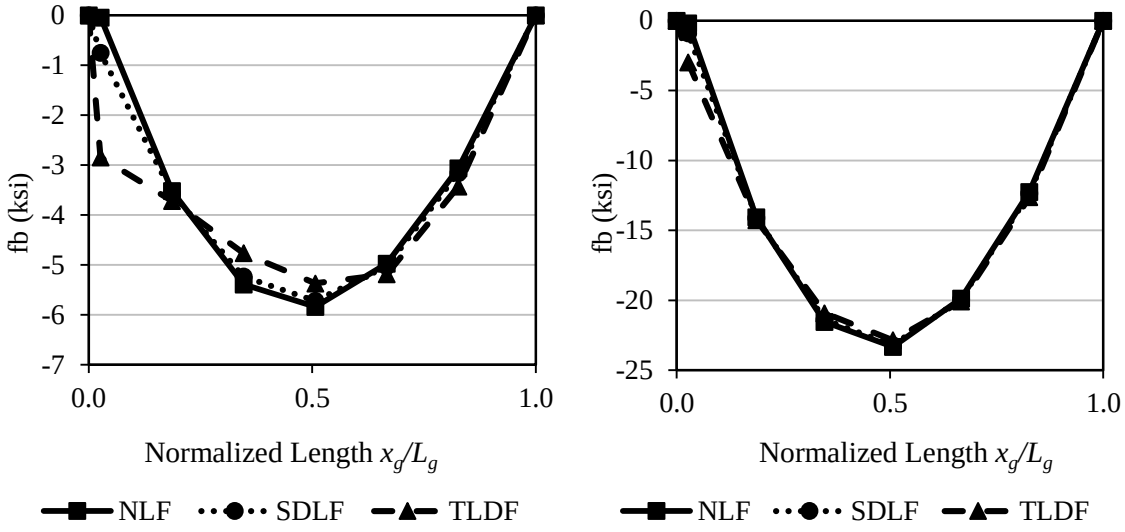

Figure C-2. NISSS4 G1 SDL and TDL 2D-Grid major-axis bending stresses

Table C-3. NISSS4 CF equivalent element forces and moment under SDL

CF	Detailing Method	G1-G2			G2-G3			G3-G4		
		V (kip)	M1 (kip*in)	M2 (kip*in)	V (kip)	M1 (kip*in)	M2 (kip*in)	V (kip)	M1 (kip*in)	M2 (kip*in)
1	NLF	4.7	1363	-35	-0.4	86	-205	-0.7	-199	7
	SDLF	-1.2	-337	-10	-0.7	-24	-163	-0.6	-164	-7
	TDLF	-18.9	-5380	63	-1.4	-351	-34	-0.4	-56	-48
2	NLF	-0.3	-400	370	0.4	-102	140	2.0	165	25
	SDLF	0.5	110	-65	0.8	54	24	1.1	109	0
	TDLF	2.8	1624	-1357	2.0	516	-322	-1.4	-57	-73
3	NLF	3.0	12	278	-0.5	-242	196	0.8	52	27
	SDLF	-0.1	3	-9	0.5	28	24	-0.2	-20	1
	TDLF	-9.3	-25	-865	3.6	829	-487	-3.2	-233	-77
4	NLF	1.9	-6	185	0.0	-211	211	-1.0	-118	18
	SDLF	0.1	1	11	0.0	4	5	-0.2	-23	0
	TDLF	-5.0	23	-507	0.0	602	598	2.1	258	-54
5	NLF	1.0	-18	118	0.5	-196	242	-1.9	-185	6
	SDLF	0.1	1	-12	-0.5	14	34	-0.2	15	1
	TDLF	-2.6	-52	303	-3.4	-527	854	4.9	-491	24
6	NLF	-0.8	-27	-52	-0.4	-140	102	-3.0	-278	-12
	SDLF	0.1	1	-12	-0.7	14	56	0.2	-19	1
	TDLF	2.9	-75	-201	-1.7	-362	524	9.7	-901	-31
7	NLF	-2.0	-25	-165	0.4	205	-86	0.3	-370	400
	SDLF	-1.2	0	112	0.7	-167	-17	0.1	-67	58
	TDLF	1.3	-74	-48	1.3	-50	-327	-0.6	-1363	1417
8	NLF	0.7	-7	199	NA	NA	NA	-4.7	35	-1363
	SDLF	0.6	-7	-167	NA	NA	NA	0.7	-16	-182
	TDLF	0.4	-47	-70	NA	NA	NA	16.8	41	-4765

Table C-4. NISSS4 CF equivalent element forces and moment under TDL

CF	Detailing Method	G1-G2			G2-G3			G3-G4		
		V (kip)	M1 (kip*in)	M2 (kip*in)	V (kip)	M1 (kip*in)	M2 (kip*in)	V (kip)	M1 (kip*in)	M2 (kip*in)
1	NLF	18.9	5448	-138	-1.7	345	-819	-2.7	-795	27
	SDLF	12.9	3748	-114	-1.9	235	-777	-2.7	-760	13
	TDLF	-4.8	-1295	-41	-2.6	-93	-649	-2.4	-651	-28
2	NLF	-1.3	-1598	1478	1.6	-407	560	7.9	658	99
	SDLF	-0.5	-1088	1043	2.0	-251	443	7.1	603	75
	TDLF	1.8	425	-249	3.2	210	97	4.6	436	2
3	NLF	12.1	50	1113	-1.9	-969	782	3.3	207	107
	SDLF	9.0	40	825	-0.9	-699	611	2.2	135	81
	TDLF	-0.2	12	-30	2.1	103	100	-0.8	-78	3
4	NLF	7.5	-25	741	0.0	-843	843	-4.1	-471	73
	SDLF	5.7	-18	567	0.0	636	637	-3.3	-376	55
	TDLF	0.6	4	49	0.0	21	26	-1.0	-96	1
5	NLF	4.1	-73	471	1.9	-782	969	-7.5	-741	25
	SDLF	3.2	56	-365	1.0	600	-693	-5.8	571	-18
	TDLF	0.5	3	-50	-2.0	59	128	-0.7	64	5
6	NLF	-3.3	-107	-207	-1.6	-560	407	-12.1	-1113	-50
	SDLF	-2.3	81	143	-1.9	433	-249	-8.9	816	39
	TDLF	0.4	5	-46	-2.9	58	219	0.6	-67	6
7	NLF	-7.9	-99	-658	1.7	819	-345	1.3	-1478	1598
	SDLF	-7.1	74	605	1.9	-781	241	1.0	1041	-1140
	TDLF	-4.6	0	445	2.6	-664	-68	0.4	-255	218
8	NLF	2.7	-27	795	NA	NA	NA	-18.9	138	-5448
	SDLF	2.7	13	-763	NA	NA	NA	-13.5	-120	3903
	TDLF	2.5	-27	-666	NA	NA	NA	2.6	-63	-680

APPENDIX D

2D-GRID RESULTS OF BRIDGE (B) NISCR2 INLCUDING THE INITIAL FIXED-END FORCES CALCULATED BY GT-LOFT

This appendix provides more detailed analytical results for curved radially-supported bridge (B) NISCR2 used an example of using GT-LOFT to determine the initial fixed-end forces with No Load Fit (NLF), Steel Dead Load Fit (SDLF) and Total Dead Load Fit (TDLF) detailing methods. This bridge has a span length of 150 ft and centerline radius of curvature of 438 ft. All of the girders have four section changes. The intermediate cross-frames are X type, and the end cross-frame are K type. All cross-frame members are L6x6x3/4.

Table D-1. (B) NISCR2 girder properties

Girder	Length (ft)	Area (in^2)	I_y (in^4)	I_z (in^4)	J (in^4)	J_{new} (in^4)
G1	154	118,142, 179@3, 142,118	2721,4041, 5805@3, 4041,2721	134110,175235, 244786@3, 175235,134110	36,95, 250@3, 95,36	515,2657, 4193@3, 2657,515
G2	151	118,142, 179@3, 142,118	2721,4041, 5805@3, 4041,2721	134110,175235, 244786@3, 175235,134110	36,95, 250@3, 95,36	515,2657, 4193@3, 2657,515
G3	149	97,103, 130@3, 103,97	1820,2108, 3305@3, 2108,1820	110049,119713, 169730@3, 119713,110049	21,29, 93@3, 29,21	386,1590, 2492@3, 1590,386
G4	146	97,103, 130@3, 103,97	1820,2108, 3305@3, 2108,1820	110049,119713, 169730@3, 119713,110049	21,29, 93@3, 29,21	386,1590, 2492@3, 1590,386

Table D-2. NISCR2 cross-frame properties (Timoshenko Approach)

CFs	Length (in)	Area (Chords Only) (in^2)	Shear Area (in^2)	I_y (Chords Only) (in^4)	$I_{z\_equiv.}$ (in^4)	J (Chords Only) (in^4)
End	96	17	7.99	56.2	21928	3.2
Interm.	96	17	15.28	56.2	21928	3.2

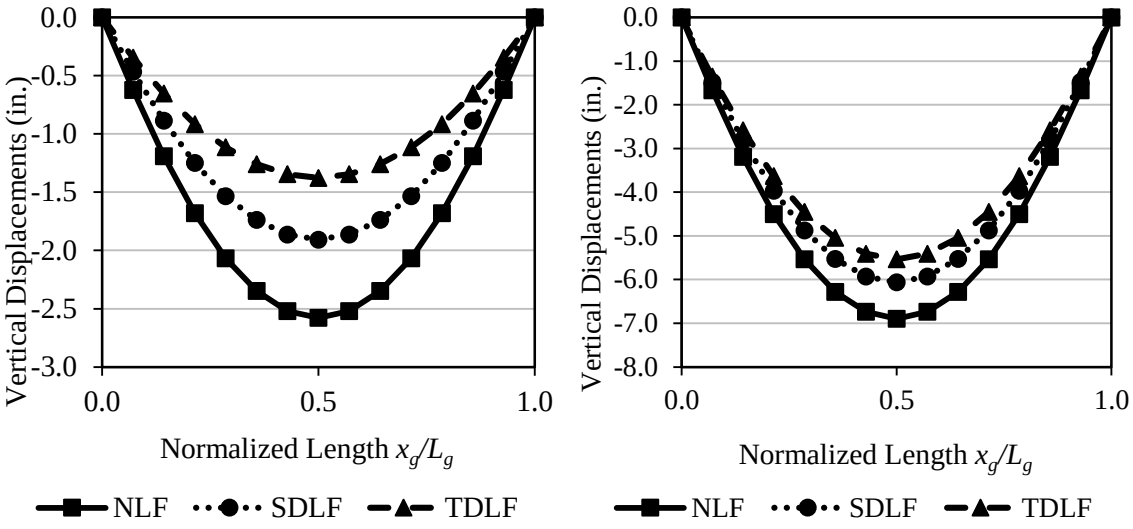

Figure D-1. (B) NISCR2 G1 SDL and TDL 2D-Grid vertical displacements

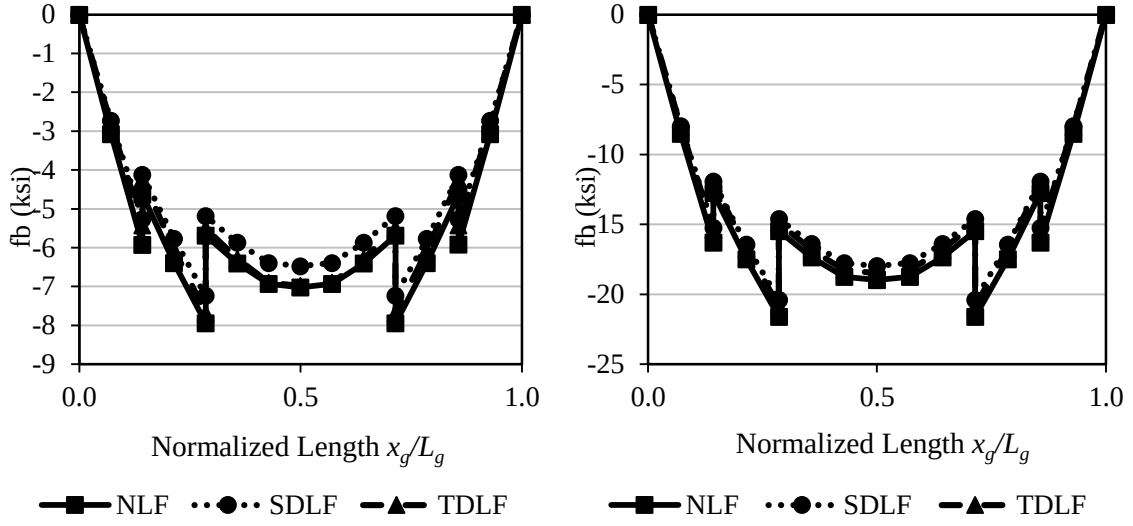

Figure D-2. (B) NISCR2 G1 SDL and TDL 2D-Grid major-axis bending stresses

Table D-3. (B) NISCR2 CF equivalent element forces and moment under SDL

CF	Detailing Method	G1-G2			G2-G3			G3-G4		
		V (kip)	M1 (kip*in)	M2 (kip*in)	V (kip)	M1 (kip*in)	M2 (kip*in)	V (kip)	M1 (kip*in)	M2 (kip*in)
1	NLF	4.7	1363	-35	-0.4	86	-205	-0.7	-199	7
	SDLF	-1.2	-337	-10	-0.7	-24	-163	-0.6	-164	-7
	TDLF	-18.9	-5380	63	-1.4	-351	-34	-0.4	-56	-48
2	NLF	-0.3	-400	370	0.4	-102	140	2.0	165	25
	SDLF	0.5	110	-65	0.8	54	24	1.1	109	0
	TDLF	2.8	1624	-1357	2.0	516	-322	-1.4	-57	-73
3	NLF	3.0	12	278	-0.5	-242	196	0.8	52	27
	SDLF	-0.1	3	-9	0.5	28	24	-0.2	-20	1
	TDLF	-9.3	-25	-865	3.6	829	-487	-3.2	-233	-77
4	NLF	1.9	-6	185	0.0	-211	211	-1.0	-118	18
	SDLF	0.1	1	11	0.0	4	5	-0.2	-23	0
	TDLF	-5.0	23	-507	0.0	602	598	2.1	258	-54
5	NLF	1.0	-18	118	0.5	-196	242	-1.9	-185	6
	SDLF	0.1	1	-12	-0.5	14	34	-0.2	15	1
	TDLF	-2.6	-52	303	-3.4	-527	854	4.9	-491	24
6	NLF	-0.8	-27	-52	-0.4	-140	102	-3.0	-278	-12
	SDLF	0.1	1	-12	-0.7	14	56	0.2	-19	1
	TDLF	2.9	-75	-201	-1.7	-362	524	9.7	-901	-31
7	NLF	-2.0	-25	-165	0.4	205	-86	0.3	-370	400
	SDLF	-1.2	0	112	0.7	-167	-17	0.1	-67	58
	TDLF	1.3	-74	-48	1.3	-50	-327	-0.6	-1363	1417
8	NLF	0.7	-7	199	NA	NA	NA	-4.7	35	-1363
	SDLF	0.6	-7	-167	NA	NA	NA	0.7	-16	-182
	TDLF	0.4	-47	-70	NA	NA	NA	16.8	41	-4765

Table D-4. (B) NISCR2 CF equivalent element forces and moment under TDL

CF	Detailing Method	G1-G2			G2-G3			G3-G4		
		V (kip)	M1 (kip*in)	M2 (kip*in)	V (kip)	M1 (kip*in)	M2 (kip*in)	V (kip)	M1 (kip*in)	M2 (kip*in)
1	NLF	18.9	5448	-138	-1.7	345	-819	-2.7	-795	27
	SDLF	12.9	3748	-114	-1.9	235	-777	-2.7	-760	13
	TDLF	-4.8	-1295	-41	-2.6	-93	-649	-2.4	-651	-28
2	NLF	-1.3	-1598	1478	1.6	-407	560	7.9	658	99
	SDLF	-0.5	-1088	1043	2.0	-251	443	7.1	603	75
	TDLF	1.8	425	-249	3.2	210	97	4.6	436	2
3	NLF	12.1	50	1113	-1.9	-969	782	3.3	207	107
	SDLF	9.0	40	825	-0.9	-699	611	2.2	135	81
	TDLF	-0.2	12	-30	2.1	103	100	-0.8	-78	3
4	NLF	7.5	-25	741	0.0	-843	843	-4.1	-471	73
	SDLF	5.7	-18	567	0.0	636	637	-3.3	-376	55
	TDLF	0.6	4	49	0.0	21	26	-1.0	-96	1
5	NLF	4.1	-73	471	1.9	-782	969	-7.5	-741	25
	SDLF	3.2	56	-365	1.0	600	-693	-5.8	571	-18
	TDLF	0.5	3	-50	-2.0	59	128	-0.7	64	5
6	NLF	-3.3	-107	-207	-1.6	-560	407	-12.1	-1113	-50
	SDLF	-2.3	81	143	-1.9	433	-249	-8.9	816	39
	TDLF	0.4	5	-46	-2.9	58	219	0.6	-67	6
7	NLF	-7.9	-99	-658	1.7	819	-345	1.3	-1478	1598
	SDLF	-7.1	74	605	1.9	-781	241	1.0	1041	-1140
	TDLF	-4.6	0	445	2.6	-664	-68	0.4	-255	218
8	NLF	2.7	-27	795	NA	NA	NA	-18.9	138	-5448
	SDLF	2.7	13	-763	NA	NA	NA	-13.5	-120	3903
	TDLF	2.5	-27	-666	NA	NA	NA	2.6	-63	-680

REFERENCES

AASHTO/NSBA (2011). *Guidelines for the Analysis of Steel Girder Bridges*, G13.1, AASHTO/NSBA Steel Bridge Collaboration, American Association of State Highway and Transportation Officials, Washington, D.C. and National Steel Bridge Alliance, Chicago, IL.

AASHTO (2015). AASHTO LRFD *Bridge Design Specifications*, 7th Edition with 2015 Interims, American Association of State Highway and Transportation Officials, Washington, DC.

AWS (2010). Bridge Welding Code, American Welding Society, Miami, FL.

Battistini, A., Wang, W., Donahue, S., Helwig, T., Engelhardt, M. and Frank, K. (2014). "Improved Cross-Frame Details for Steel Bridges," Report No. FHWA/TX-13/0-6564-1, Center for Transportation Research, University of Texas, Austin, TX, 411 pp.

Chavel, B.W, and Earls, C. (2003). "Deflection of Horizontally Curved I-Girder Bridge Members Under Construction," Report No. CE/ST 28, Department of Civil Engineering, University of Pittsburgh, Pittsburgh, PA, 261 pp.

Chavel, B.W., and Earls, C.J. (2006a). "Construction of a Horizontally Curved Steel I-Girder Bridge. Part I: Erection Sequence." Journal of Bridge Engineering, 11(1), ASCE, 81-90.

Chavel, B.W., and Earls, C.J. (2006b). "Construction of a Horizontally Curved Steel I-Girder Bridge. Part II: Inconsistent Detailing." Journal of Bridge Engineering, 11(1), ASCE, 91-98.

Chavel, B.W. (2008). "Construction and Detailing Methods of Horizontally Curved Steel I-Girder Bridges," Ph.D. Dissertation, Swanson School of Engineering, University of Pittsburgh, Pittsburgh, PA, 357 pp.

Dassault Systemes (2014). Abaqus Unified FEA, Complete solutions for realistic simulation, ABAQUS 6.13. http://www.3ds.com/products-services/simulia/portfolio/abaqus/latest-release/.

Davidson, J.S., (1996), "Nominal Bending and Shear Strength of Horizontally Curved Steel I-Girder Bridges," Ph.D. Dissertation, Auburn University, Auburn, Alabama.

Domalik, D. E, Linzell, D. G, and Shura, J. F, (2005a). "Design and Field Monitoring of a Horizontally Curved Steel Plate Girder Bridge," HDR Bridgeline, Vol.14, No.1.

Domalik, D. E, Shura, J. F, and Linzell, D. G, (2005b). "The Design and Field Monitoring of a Horizontally Curved Steel Plate Girder Bridge," in Proc., 84th Annual Meeting of the Transportation Research Board.

Ferguson Laboratory (2014). "Software Developed at FSEL, UT Lift 1.3," https://fsel.engr.utexas.edu/software/ (October 12, 2014).

Jung, S.-K. and White, D.W. (2008). "Inelastic Strength Behavior of Horizontally Curved Composite I-Girder Bridge Structural Systems," Report to Federal Highway Administration, January, 667 pp.

Helwig, T.A. and Yura, J.A. (2012). "Bracing System Design," *Steel Bridge Design Handbook*, Publication No. FHWA-IF-12-052, Vol. 13, November. 90 pp.

Howell, T. and Earls, C. (2007). "Curved Steel I-Girder Bridge Response during Construction Loading: Effects of Web Plumbness."J. Bridge Eng., 12(4), 485–493.

McGuire, W., Gallagher, R., and Ziemian, R. (2000). "Matrix Structural Analysis." Second Edition, John Wiley & Sons, Inc.

NHI (2011). "Analysis and Design of Skewed and Curved Steel Bridges with LRFD, Reference Manual", NHI Course No. 130095, Publication No. FHWA-NHI-10-087, National Highway Institute, Federal Highway Administration, 1476 pp.

Nguyen, T.V., and White, D.W. 2014. "Impact of Camber Calculation, Camber and Deck Thickness Tolerance, and Framing Arrangement on Fit Responses in Straight Skewed I-Girder Bridges," Proceedings of the NSBA World Steel Bridge Symposium, Toronto, Ontario, Canada, available from the National Steel Bridge Alliance, Chicago, IL, March 26-28.

NSBA Technical Subcommittee (2014). "Skewed and Curved I-Girder Bridge Fit – Stand Alone Summary" AASHTO/NSBA Steel Bridge Collaboration, August 20, 6 pp.

NSBA Technical Subcommittee (2015). "Skewed and Curved I-Girder Bridge Fit," Guidelines Document, AASHTO/NSBA Steel Bridge Collaboration, November.

Ozgur, C. (2011). "Influence of Cross-Frame Detailing on Curved and Skewed Steel I-Girder Bridges," Ph.D. Dissertation, School of Civil and Environmental Engineering, Georgia Institute of Technology, Atlanta, GA, 398 pp.

Romage, M.L. (2008). "Field Measurements on Lean-On-Bracing for Steel Girder Bridges with Skewed Supports," M.S. thesis, University of Texas, Austin, TX.

Yura, J. (2001). "Fundamentals of Beam Bracing," *Engineering Journal*, American Institute of Steel Construction, 38(1), 11-26.

Sanchez, T.A. (2011), "Influence of Bracing Systems on the Behavior of Steel Curved and/or Skewed I-Girder Bridges during Construction," Ph.D. Dissertation, School of Civil and Environmental Engineering, Georgia Institute of Technology, Atlanta, GA, 335 pp.

White, D.W. (2012). "Structural Behavior of Steel," *Structural Steel Design Handbook*, Publication No. FHWA-IF-12-052 – Vol. 4, November, 267 pp.

Zhou, C. (2006). "Utilizing Lean-On Cross-Frame Bracing for Steel Bridges," Ph.D. dissertation, University of Houston, Houston, TX.